Graduate Texts in Physics

Daniel Grumiller
Mohammad Mehdi Sheikh-Jabbari

# Black Hole Physics

## From Collapse to Evaporation

Springer

# Graduate Texts in Physics

*Graduate Texts in Physics* publishes core learning/teaching material for graduate- and advanced-level undergraduate courses on topics of current and emerging fields within physics, both pure and applied. These textbooks serve students at the MS- or PhD-level and their instructors as comprehensive sources of principles, definitions, derivations, experiments and applications (as relevant) for their mastery and teaching, respectively. International in scope and relevance, the textbooks correspond to course syllabi sufficiently to serve as required reading. Their didactic style, comprehensiveness and coverage of fundamental material also make them suitable as introductions or references for scientists entering, or requiring timely knowledge of, a research field.

Daniel Grumiller ·
Mohammad Mehdi Sheikh-Jabbari

# Black Hole Physics

## From Collapse to Evaporation

Springer

Daniel Grumiller
Institute for Theoretical Physics
TU Wien
Vienna, Austria

Mohammad Mehdi Sheikh-Jabbari
School of Physics
Institute for Research in Fundamental Sciences
Tehran, Iran

ISSN 1868-4513 ISSN 1868-4521 (electronic)
Graduate Texts in Physics
ISBN 978-3-031-10342-1 ISBN 978-3-031-10343-8 (eBook)
https://doi.org/10.1007/978-3-031-10343-8



This Springer imprint is published by the registered company Springer Nature Switzerland AG
The registered company address is: Gewerbestrasse 11, 6330 Cham, Switzerland

*Mohammad Mehdi Sheikh-Jabbari dedicates this book to his wife Yasaman Farzan for all her support and encouragement*

*Daniel Grumiller dedicates this book to his parents Ingo Grumiller, Wilfried Raunikar, and Helga Weule for passing on their curiosity about Life, the Universe, and Everything*

# Foreword

The study of black holes arguably began in 1783 with John Michell. At the time, Michell was the rector of St. Michael's church in the Yorkshire village of Thornhill. Prior to this, he had been educated and become a fellow of Queens' College Cambridge and also had been Woodward professor of geology in Cambridge. However, fellows of Cambridge colleges at the time were required to be celibate and so he migrated on marriage, as many at the time did, to the church. His clerical duties were sufficiently light that he was able to continue his scientific studies. In the Proceedings of the Royal Society, he laid out the possibility that there were stars that could not be seen. His reasoning was entirely Newtonian. He was able to calculate the escape velocity of a particle from the surface of a massive body. He knew that light had large, but finite, velocity as had been shown in the previous century by Rømer. His conclusion was that if a star was sufficiently condensed, then it would be invisible. Supposing that the star had mass $M$, then if its radius $R$ was such that

$$R < \frac{2G_{\mathrm{N}}M}{c^2}$$

where $G_{\mathrm{N}}$ is Newton's gravitational constant and $c$ is the speed of light, then it would be invisible. Remarkably, the same formula holds in general relativity. Some 14 years later in 1796, Pierre Laplace, working independently, published a similar result from the other side of the English Channel.

It was not until Einstein proposed the general theory of relativity that matters progressed. As soon as his theory became known, Karl Schwarzschild found in 1915 the exact solution of Einstein's field equations that bears his name. His solution is a spacetime metric that contains a black hole. For a long time, there were discussions about whether the horizon was singular or not, and whether the spacetime singularity at the center of the black hole was unphysical. Despite the uncertainty about whether the Schwarzschild metric was physically acceptable, in 1939 J. Robert Oppenheimer and Hartman Snyder showed that, under certain circumstances, a star could collapse to form a black hole. Nevertheless, considerable skepticism about the possible existence of black holes remained until the early 1970s.

A revolution in our understanding of general relativity and black holes, in particular, started in the late 1950s driven by John Archibald Wheeler in Princeton. He seems to have been motivated by attempts to understand the final state of stars and also began to formulate a quantum theory of gravity. This started a period of great excitement. Two key events were that Roger Penrose proved the first singularity theorem in 1965. He showed that if a trapped surface formed, then a spacetime singularity must exist. This result removed one of the possible stumbling blocks in understanding black holes. In Oppenheimer–Snyder collapse, one does form a spacetime singularity, but such a thing might have been a consequence of assuming exact spherical symmetry, something which cannot happen in nature. Penrose's result showed that singularities would form without making any assumptions about spatial symmetry. Also in 1965, Roy Kerr found the spacetime metric that describes the most general stationary black hole in an asymptotically flat spacetime. These results triggered a flurry of key results in classical general relativity. They led to an understanding of the astrophysics of black holes. The discovery of black hole X-ray sources as stellar remnants, quasars, the black holes in the centers of galaxies as conclusively proved by the recent results of the event horizon telescope, and the production and detection of gravitational waves in collisions involving black holes have removed any uncertainty about their existence.

However, there are still challenges. Hawking showed that black holes emit radiation that appears to be thermal. This was perhaps the first successful result in quantum gravity and it has generated an enormous follow-up literature. The deepest puzzle is the information paradox. Quantum mechanical information appears to be destroyed as a black hole evaporates away. Most of us believe that this cannot happen, largely because of the incredible successes that quantum mechanics has. Nevertheless, the subject is still open, and there are many that believe that information is destroyed. There has been a lot of recent progress and in particular, the beginning of our understanding of holography, the discovery of soft hair, and the application of rigorous quantum information theory is helping an exploration of this problem.

This book provides an excellent introduction to all of these topics. It is really the first to attempt such a synthesis and provides a valuable compendium of information on black holes for students of all ages and researchers of all flavors. The collection of problems at the end of each chapter encourages enthusiasts to gain a mastery of the subject and undoubtedly will help lead to much-needed further insights into one of the biggest mysteries in fundamental physics today.

London, England Malcolm Perry

# Preface

Black holes are predictions of Albert Einstein's theory of general relativity and have been the focus of intense studies for over a century, as they provide a rich source of theoretical and experimental challenges. Black holes entail some of the deepest puzzles on the road toward quantum gravity and engendered seminal theoretical discoveries, such as thermodynamical properties of black holes, their role in the holographic principle, and the recent merger of geometrical and quantum information concepts. Black holes, by their very definition, are hard to detect directly. Recent technological advancements have led to novel methods of detection through gravitational waves and by observing their shadows. The 2020 physics Nobel prize awarded "for the discovery that black hole formation is a robust prediction of the general theory of relativity" is a testimony of the importance of black holes.

In this book, we elucidate the theoretical concepts of black hole physics and discuss some of the main phenomenological signatures and prospects in recent and future black hole observations. The scope is narrow in the sense that everything we present is in one way or another related to black holes; at the same time, our scope is ambitiously broad, since we cover ground including observational challenges, geometrical tools, thermodynamics, particle creation, holography, and quantum information. The principal goal of this book is to provide the reader with an up-to-date status of black hole physics.

This book is mainly intended for three groups:

1. graduate-level physics students who intend to start their research career in the field of black holes;
2. postdocs who recently changed their research focus toward black holes and want to get up-to-date on recent and current research topics;
3. advanced researchers who want to teach (or learn) basic and advanced aspects of black hole physics and the associated mathematical tools.

The main style we pursue is hands-on, which in particular means that there will be numerous exercises as an integral part of the learning experience conveyed by our book. We assume the reader is familiar with the basics of general relativity and with standard undergraduate physics, like special relativity, thermodynamics, quantum mechanics, and statistical mechanics. Moreover, we assume familiarity with the basics of quantum field theory on Minkowski space. Apart from these, we have tried to cover the required material in the main text accompanied by appendices. We mainly focus on established knowledge, but also give a taste of current trends and issues of dispute. Since the research field of black holes is a rapidly advancing area on theoretical, numerical, and observational fronts, topics that are only partially addressed and understood by the time of publication of this book may well become a part of established physics in just a few years.

We cover all topics and areas that we consider essentials of black hole physics. However, as always there are several inclusions and exclusions of topics that some readers may find questionable. While our choices naturally are influenced by our field of research, theoretical aspects of black holes, we aspire to give a broad and fair overview of all aspects of black hole physics. We have strived to

1. make this a self-contained book on black holes,
2. cover basic, advanced, and expert topics suitable for a 1-year course,
3. provide many exercises and (hints for) solutions, and
4. guide the reader through current research topics.

While covering a wide range of topics, we avoid being overly encyclopedic; we do not intend to give a full literature review on all topics and discuss only the most essential points. At the end of each chapter, we provide suggestions for further reading. Finally and importantly, each chapter comes with a set of problems that are an integral part of the book. There are two types of problems: (1) Exercises meant to engage the reader with the analysis and discussions of the chapter by filling in the gaps of calculations and proofs. (2) Problems that are extensions of the analysis of the chapter. They are interesting and relevant, but we did not find them crucial enough to be added to the main text.

## How to Read and Use This Book

We provide now a rough guideline for how to use this book. Graduate students who read this book on their own should attempt to solve at least half of the exercises at the end of each chapter, as a cross-check whether they have digested the material in the main text. If you are such a student and have already some experience with black holes, you may skip reading some of the earlier chapters, but you should still try to complete the exercises just to make sure that you know what you thought you knew. If you have no experience with black holes whatsoever, then just start reading Chap. 1 and proceed from there.

Postdocs reading this book may want to skip ahead to their main focus of interest, which is likely to be in the second half of the book, Chaps. 6–10. Still, we recommend that you have a look at some of the exercises in the first five chapters. Essentially, the same is true for more advanced researchers who want to learn about advanced aspects of black hole physics.

If you plan to use this book as a tool for teaching, then our main recommendation is to drop stuff that you find less relevant and to schedule at least one year (better: two years) if you plan to teach the content of the whole book. Depending on the amount of time you have available, here are some reasonable options. If you are aiming for a one-semester introductory course (about 25 h of lectures), you can cover the content of the first five chapters, essentially in the order in which they appear in this book, ending with black hole thermodynamics as a segue to a more advanced course. If you have two semesters available, you can also cover material from Chaps. 6–10, but not all of them and not necessarily in the order they appear in the book. Some reasonable options are (1) Teach the content of Chap. 6; skip Chap. 7; continue with the first two sections of Chap. 8; follow up with the material you prefer from the remainder of Chap. 8 and Chap. 9; conclude with your version of Sect. 10.3. (2) Start with the first three sections of Chap. 7 and teach relevant concepts about quantum gravity and holography using either gravity in three dimensions, dilaton gravity in two dimensions, or both; then present the material of Chaps. 6 and 8–10 from this lower-dimensional perspective. (3) Assuming the audience is familiar with string theory, you can start with the last two sections of Chap. 7 and then continue with Chaps. 8–10. Finally, if you have two years available, then you can reserve the first semester as an introduction to general relativity with a bias toward black holes (Jim Hartle's way of teaching works well in this context: you can discuss geodesics and classical tests of the Schwarzschild metric before you even introduce Riemannian geometry—so you start out with the "geometry tells matter how to move" aspect of gravity and only later continue with the "matter tells geometry how to curve" aspect); from the book you could cover just the first two chapters, Chap. 4 and Appendices A and F; in the second semester, you can then cover Chaps. 3, 5, and 6 and Appendix D (Appendices C, G, and E are optional, depending on the precise scope of your lectures; they can also be presented as part of the third semester); in the third semester, you could focus on Chap. 7, gravity in diverse dimensions, and then pursue the presentation of Chaps. 8–10 from this lower-dimensional perspective (the advantage of this is that you can teach rather advanced concepts including holography and quantum information aspects of black holes with a relatively moderate but powerful set of technical tools); in the fourth semester, you can guide the students to current research topics, using whichever combination of chapters you find suitable for that purpose (the precise selection will depend largely on your own research interests and what you consider as promising).

The rest of this book is organized as follows. The first five chapters of this book address classical aspects of black holes. The next five chapters discuss semi-classical and quantum aspects of black holes. The appendices are self-contained summaries or technical elaborations and in particular, Appendix J collects hints and solutions to some selected exercises. Below is a more detailed account of the content of all the chapters and appendices, in their order of appearance.

In Chap. 1, we give an introduction and review some historical aspects of black hole physics.

Chapter 2 starts with the most basic black hole solution, the Schwarzschild metric, and discusses 4-dimensional black hole solutions of increasing complexity as well as their basic properties.

Chapter 3 provides definitions of concepts like horizon and singularity and discusses classic theorems like uniqueness, singularity, and topology theorems.

The information imprinted on particles and/or fields probing black holes in the classical setting is the subject of Chap. 4, as well as the formation of black holes through particle collision and collapse of matter fields and the linear and non-linear stability of black holes. A crucial result derived from these classical considerations is that black holes are labeled by their charges.

Chapter 5 reviews a general formulation to precisely define these charges and concludes that in physical processes involving black holes, these charges obey the laws of thermodynamics, once we identify the temperature and chemical potentials associated with them.

Semiclassical aspects, in which the gravity theory and the black hole solution are considered classically while probes are treated using quantum field theory, lead to interesting results like Hawking radiation and black hole evaporation, which is the topic of Chap. 6. While this semiclassical analysis confirms the thermodynamical picture, it raises puzzles that still await a satisfactory understanding. The latter brings us closer to the forefront of the current research on theoretical aspects of black hole physics.

Chapter 7 deals with gravity theories and their black hole solutions in lower and higher dimensions. The first seven chapters of this book are very well-established material; the chapters afterward involve formulations, concepts, and results that have been developed in the last three decades or so and in parts include topics of the ongoing research.

Chapter 8 introduces the holographic principle and discusses several aspects of black hole holography.

Chapter 9 is devoted to quantum aspects of black holes beyond the semiclassical approximation and includes proposals for counting or identification of black hole microstates.

Chapter 10 provides a summary and an outlook on current and future research endeavors.

Appendix A summarizes variational identities.

Appendix B defines *p*-forms.

Appendix C reviews the Cartan formulation of geometry.

Appendix D discusses the Teukolsky equation.

Appendix E gives basics of quantum field theory in curved spacetime.

Appendix F provides the Hamiltonian formulation of general relativity, including boundary aspects.

Appendix G focuses on the covariant phase space method.

Appendix H provides derivations of basic equations in the membrane paradigm.

Appendix I displays string theory low energy effective actions in the supergravity approximation.

Appendix J contains hints and solutions to some selected exercises.

The references in our bibliography are ordered by their first appearance in the book; to help the reader locate these references, we have provided all page numbers where they are quoted.

We hope the reader enjoys our book and has fun solving the exercises. We appreciate corrections of typos/mistakes sent by e-mail to jabbari@theory.ipm.ac.ir or to grumil@hep.itp.tuwien.ac.at.

Tehran, Iran — Mohammad Mehdi Sheikh-Jabbari
Vienna, Austria — Daniel Grumiller

# Acknowledgements

We thank our numerous undergraduate, graduate, and Ph.D. students who have taken lectures on black hole physics during the past decade, and who improved the quality of these lectures and the exercises through their incessant questions and feedback. We are grateful to Michael Peskin for his useful comments on the template and very early draft of the book. We thank Florian Ecker, Roberto Emparan, Martin Laihartinger, Hooman Neshat, Johann Oberleitner, Fabian Pichler, Vahid Taghiloo, Raphaela Wutte, and M. H. Vahidinia for pointing out necessary improvements in this book, including the exercises.

Daniel Grumiller thanks, in particular, Rene Meyer, who was among the first students (back in 2004/2005) to witness the first installment of black hole lectures, as well as Stefan Prohazka, Max Riegler, and Sebastian Singer, who compiled the first edition of black hole lecture notes (back in 2009). His black hole research group at TU Wien is supported since 2009 by the Austrian Science Fund (FWF) through numerous grants.

Mohammad Mehdi Sheikh-Jabbari thanks A. Mollabashi, M. R. Mohammadi-Mozaffar, Saeedeh Sadeghian, Ali Seraj, and especially Kamal Hajian for their comments on the black hole lectures I gave at IPM, Tehran in the last few years and for their collaborations on research work which was quite useful in developing some parts of this book. I would also like to thank Sadik N. Deger, Mahdi Godazgar, Joan Simon, Vahid Taghiloo, Mohammad H. Vahidinia, Hossein Yavartanoo, and Céline Zwikel for the comments and corrections on the earlier draft of the book. During this period, I have benefited from grants from the Iranian National Elites Foundation, SarAmadan grants, and particularly acknowledge the INSF junior research chair in black hole physics (INSF grant No 950124). I would like to especially thank the Abdus Salam ICTP, especially its directors Fernando Quevedo and Atish Dabholkar, and its HECAP section for the warm hospitality during my one-year sabbatical leave (June 2019–June 2020) which provided me with the opportunity to devote quality time in writing this book.

# Contents

# Acronyms

| | |
|---|---|
| ADM | Arnowitt–Deser–Misner |
| AdS | Anti-de Sitter |
| ANEC | Averaged Null Energy Condition |
| BH | Bekenstein–Hawking |
| BMS | Bondi–van der Burgh–Metzner–Sachs |
| BTZ | Bañados–Teitelboim–Zanelli |
| CCC | Cosmic Censorship Conjecture |
| CFT | Conformal Field Theory |
| CPSF | Covariant Phase Space Formalism |
| CS | Chern–Simons |
| CTC | Closed timelike curve |
| DEC | Dominant Energy Condition |
| dS | de Sitter |
| EEP | Einstein Equivalence Principle |
| EF | Eddington–Finkelstein |
| EFT | Effective Field Theory |
| EHT | Event Horizon Telescope |
| EOM | Equations of motion |
| EP | Equivalence Principle |
| *fido* | Fiducial observer |
| FLRW | Friedmann–Lemaître–Robertson–Walker |
| GR | General Relativity |
| GW | Gravitational Wave(s) |
| HEP | High Energy Physics |
| IR | Infrared |
| ISCO | Innermost Stable Circular Orbit |
| JT | Jackiw–Teitelboim |
| KK | Kaluza–Klein |
| KN | Kerr–Newman |
| LEFT | Low Energy Effective Theory |
| LIGO | Laser Interferometer Gravitational-wave Observatory |
| MP | Myers–Perry |
| NEC | Null Energy Condition |
| NHEK | Near-horizon extremal Kerr |

| | |
|---|---|
| NUT | Newman–Unti–Tamburino |
| PBH | Primordial Black Hole |
| PW | Parikh–Wilczek |
| QFT | Quantum Field Theory |
| QG | Quantum Gravity |
| QNEC | Quantum Null Energy Condition |
| QNM | Quasi-normal mode |
| RN | Reissner–Nordström |
| RT | Ryu–Takayanagi |
| SEC | Strong Energy Condition |
| SEP | Strong Equivalence Principle |
| SPSM | Solution phase space method |
| TOV | Tolman–Oppenheimer–Volkoff |
| UV | Ultraviolet |
| WEC | Weak Energy Condition |
| WEP | Weak Equivalence Principle |

# Notations and Conventions

| | |
|---|---|
| $-, +, \ldots, +$ | Metric signature |
| $\mu, \nu, \lambda, \ldots$ | Spacetime indices |
| $i, j, k, \ldots$ | Space indices |
| $g_{\mu\nu}$ | Metric tensor |
| $\Gamma^{\lambda}{}_{\mu\nu}$ | Chirstoffel connection |
| $\mathcal{L}_\xi$ | Lie derivative along vector field $\xi$ |
| $R^{\mu}{}_{\nu\alpha\beta} = \partial_\alpha \Gamma^{\mu}{}_{\nu\beta} + \ldots$ | Riemann curvature |
| $R_{\mu\nu} = R^{\lambda}{}_{\mu\lambda\nu} = \partial_\lambda \Gamma^{\lambda}{}_{\mu\nu} + \ldots$ | Sign convention for Ricci |
| $B_{(\mu\nu)} := \frac{1}{2}(B_{\mu\nu} + B_{\nu\mu})$ | Symmetrization |
| $B_{[\mu\nu]} := \frac{1}{2}(B_{\mu\nu} - B_{\nu\mu})$ | Antisymmetrization |
| $I$ | Actions |
| $L$ | Lagrangians |
| $\mathcal{L}$ | Lagrange densities |
| $\approx$ | On-shell equalities |
| $:=$ | Definitions |
| $O(r^n)$ | Order $r^n$ and smaller |
| $o(r^n)$ | Smaller than order $r^n$ |
| $\Omega_D = \frac{2\pi^{(D+1)/2}}{\Gamma((D+1)/2)}$ | Unit sphere volume |
| $\hbar = c = k_B = 1$; we usually keep $G_{\mathrm{N}}$ | Conversion factors |

Our sign conventions are compatible with the textbooks by Misner, Thorne, and Wheeler [1], Wald [2], Schutz [3], Hartle [4], Carroll [5], Poisson [6], Cheng [7], Padmanabhan [8], Straumann [9], and Zee [10] but differ from the textbooks by Weinberg [11], d'Inverno [12], Rindler [13], and Hobson, Efstathiou and Lasenby [14].

# List of Figures

# 1 Introduction

**Abstract**

This chapter sets the stage for this book by giving an overview of the research field of black holes. We start with a brief review of the formulation of general relativity (GR) in Sect. 1.1. We then provide a historic summary of black holes, both from theoretical and observational perspectives in Sect. 1.2. We discuss the core collapse of typical stars to black holes at the end of the star's lifetime in Sect. 1.3. Besides their observational richness, black holes give rise to several profound theoretical questions, particularly in the context of QG. We summarize different schools of thought developed to address them in Sect. 1.4.

## 1.1 Essentials of General Relativity

The possibility of objects like black holes was considered already in 1783 by the country parson John Michell using Newtonian gravity. He pondered what would happen if the escape velocity of a star would exceed the speed of light. Both ingredients—Newtonian gravity and the speed of light measured by Ole Rømer—became available just about a century earlier, so the time seemed ripe for Michell's musings. Indeed, Pierre-Simon Laplace also mentioned the possibility of black holes about a decade later. See [15] for more historical details on the origin of black holes.

Despite their possible existence in Newtonian gravity, it was only within Einstein's GR that black holes appeared as ubiquitous solutions, finding a prominent place therein. This is why we start with a quick review of GR. This section is not a substitute for a proper GR course and is mainly meant to set the stage, clarify our conventions, and remind the reader of relevant aspects of GR.



D. Grumiller and M. M. Sheikh-Jabbari, *Black Hole Physics*, Graduate Texts in Physics,
https://doi.org/10.1007/978-3-031-10343-8_1

### 1.1.1 Equivalence Principle and Geodesics

Einstein's GR may be thought of either as an extension of special relativity to include frames that are just locally inertial or as a way to modify Newtonian gravity to make it compatible with special relativity. GR is based on the Equivalence Principle (EP), which has different inequivalent formulations. Here, we briefly mention the three most common ones, adopting the terminology of [16]: there is the Weak Equivalence Principle (WEP), the Einstein Equivalence Principle (EEP), and the Strong Equivalence Principle (SEP). For a more complete discussion on the statements of the EPs and their experimental tests, we refer the reader to [17–20].

The WEP posits the equivalence of gravitational and inertial mass, applicable already in Newtonian gravity. A consequence of the WEP is that all point particles of different masses follow the same trajectory in a given external gravitational field. The WEP dates back to before Newton and was formulated first by Galilei; it is hence also called the Galilean or Newtonian EP. A direct consequence of the WEP is that the gravitational field may be (locally) replaced by acceleration, which hints that a particle trajectory, in the absence of other forces, should be a geometric quantity. This is so because forces for which the mass cancels in Newton's axiom $F = ma$ are known as fictitious forces, like centrifugal or Coriolis force. They can be eliminated by changing the reference frame, which implies that the description of fictitious forces is possible entirely in terms of geometry. Einstein assumed the WEP to be also true in relativistic systems.

The EEP states that the outcome of any *local non-gravitational* experiment in a freely falling laboratory is independent of the velocity and position of the laboratory in spacetime. That is, all physical observables associated with non-gravitational local physical processes should be the same for generic observers with arbitrary velocity and acceleration.

The SEP stipulates that *all* laws of physics in the context of special relativity (with the same values for physical constants and parameters in those laws) should be *locally* valid. Here, locally means in any sufficiently small free-falling region of spacetime, for any point/event in the spacetime. So, the difference between EEP and SEP is that the latter includes also gravitational interactions. The SEP requires that the internal dynamics in a self-gravitating system under free-fall in an external gravitational field should not depend on the external field strength.

In a mathematical formulation, spacetime is naturally described through differential geometry on manifolds with Minkowski signature. Accordingly, all the geometric information is encoded in the metric tensor $g_{\mu\nu}$ and the connection $\Gamma^{\mu}{}_{\alpha\beta}$ as functions of some coordinates $x^{\mu}$ for a given patch of the spacetime. Greek indices are always spacetime indices and they can either refer to an explicit coordinate system or be intended as abstract indices.

Physical theories generically deal with particles, fields, and their interactions. Particles are mathematically described through their trajectories in spacetime, which we parametrize as $x^{\mu} = x^{\mu}(\lambda)$ with some affine parameter $\lambda$. Particles generically source the fields and are affected by the fields through the forces exerted on them. Fields are described by various tensor fields. In GR the metric $g_{\mu\nu}(x^{\alpha})$ is the dynamical field. The EPs have important implications for the dynamics of particles and fields as well as their interactions.

The EEP implies that free particles follow geodesics,

$$\boxed{\frac{\mathrm{d}^2x^\mu}{\mathrm{d}\lambda^2} + \Gamma^\mu{}_{\alpha\beta}\frac{\mathrm{d}x^\alpha}{\mathrm{d}\lambda}\frac{\mathrm{d}x^\beta}{\mathrm{d}\lambda} = 0\,.} \tag{1.1}$$

The affine parameter $\lambda$ parametrizes the geodesic trajectory, $x^\mu = x^\mu(\lambda)$. The EEP then fixes the symmetric part of the connection to be the Christoffel symbol of the second kind.

$$\Gamma^\mu{}_{\alpha\beta} + \Gamma^\mu{}_{\beta\alpha} = g^{\mu\nu}\left(\partial_\alpha g_{\beta\nu} + \partial_\beta g_{\alpha\nu} - \partial_\nu g_{\alpha\beta}\right). \tag{1.2}$$

Here, $g^{\mu\nu}$ denotes the inverse metric, and $g^{\mu\alpha}g_{\alpha\nu} = \delta^\mu_\nu$ and $\partial_\mu = \partial/\partial x^\mu$ are partial derivatives. The above can be recast as the metric compatibility condition, $\nabla_\alpha g_{\mu\nu} = 0$, where $\nabla_\alpha$ denotes the covariant derivative.

The EEP is made manifest in the geodesic equation through the fact that there always exists a so-called normal coordinate system in which the Christoffel symbols vanish locally. The geodesic equation (1.1) implies that the norm of the velocity vector $\mathrm{d}x^\mu/\mathrm{d}\lambda$ is an invariant along the geodesic. Therefore, depending on the sign of $|\mathrm{d}x^\mu/\mathrm{d}\lambda|^2$, there are three classes: timelike, lightlike (null), and spacelike geodesics. In our conventions, these are respectively associated with negative, zero, and positive norms of the velocity vector. Relativistic causality implies that physical particles must follow causal curves, i.e. curves whose tangent vector along the path is timelike or null. Thus, for most applications, the interesting geodesics are causal ones.

The EEP and SEP have implications for the dynamics of fields. While not necessary, it is usually assumed that the dynamics of fields is provided by an action where the equations of motion (EOM) are obtained by a variational principle. That is, requiring vanishing variation of the action for arbitrary field variations yields the field equations.[1] Given an action for a generic tensor field, the SEP implies that the action should be minimally coupled to gravity and should be invariant under general coordinate transformations, also known as diffeomorphisms. Minimal coupling means that in normal coordinates the action reduces to the one we have in special relativity where the field theory is defined in Minkowski spacetime. Starting with a diffeomorphism invariant action and recalling that the fields and their variations are tensors, the variational principle implies that the field equations are tensor equations, so their components transform covariantly under diffeomorphisms. General coordinate invariance of the action is a weaker condition than imposing the EEP.

[1] In general, varying an action yields bulk field equations plus boundary EOM. Having a well-defined variational principle amounts to choosing appropriate boundary conditions for the fields and their variations that guarantee that the boundary EOM hold. Typically, there can be several inequivalent choices of boundary conditions for a given bulk theory, e.g. Dirichlet, Neumann, Robin, or mixed boundary conditions. As discussed in Chap. 6, in Einstein gravity usually the Gibbons–Hawking–York boundary term [8,21,22] is employed, as it guarantees Dirichlet boundary conditions for the metric.

Unless explicitly mentioned otherwise, in this book we assume the SEP. Requiring the SEP implies that the Lagrangian for gravity should be a local scalar function made from invariants of the Riemann tensor or its covariant derivatives. The SEP by itself does not uniquely fix the gravity action. One may then add other physical requirements to fix or at least restrict the gravity action. An efficient paradigm borrowed from effective field theories (EFTs) is the derivative expansion. The main assumption here is that the true field theory may not be known, but if tested at sufficiently low energies only a few terms contribute to the essential dynamics, namely those with the lowest number of derivatives. Applying this paradigm to gravity compatible with the SEP yields a gravitational action of the form $I[g_{\mu\nu}] \sim \int \mathrm{d}^4x\sqrt{-g}\,\big(R - 2\Lambda + \dots\big)$ where the ellipsis denotes terms with at least four derivatives on the metric and possible boundary terms. The action is normalized such that the Ricci scalar $R$ has a conventional factor of unity in the integrand (see below for the overall normalization of the action). This part is known as the Einstein–Hilbert action, but we will also refer to the full action as such. The only term with fewer derivatives than the Ricci scalar is the cosmological constant $\Lambda$. This action is the core of Einstein gravity.

### 1.1.2 Einstein Gravity

The bulk action including Einstein gravity plus matter fields in usual conventions is

$$I = I_{\text{grav}} + I_{\text{matter}} = \frac{1}{16\pi G_{\text{N}}}\int_{\mathcal{M}} \mathrm{d}^4x\sqrt{-g}\,\big(R - 2\Lambda\big) + \int_{\mathcal{M}} \mathrm{d}^4x\sqrt{-g}\,\mathcal{L}(\Phi_I) \tag{1.3}$$

where $G_{\text{N}}$ is Newton's constant, $\mathcal{M}$ is the spacetime manifold, $g = \det g_{\mu\nu}$, and $\Phi_I$ denotes summarily matter fields. Variation of this action yields Einstein's field equations

$$\boxed{G_{\mu\nu} + \Lambda g_{\mu\nu} = 8\pi G_{\text{N}}\, T_{\mu\nu}} \tag{1.4}$$

where

$$G_{\mu\nu} := \frac{1}{\sqrt{-g}}\,\frac{\delta(\sqrt{-g}R)}{\delta g^{\mu\nu}} = R_{\mu\nu} - \frac{1}{2}\,g_{\mu\nu}R \qquad\qquad T_{\mu\nu} := -\frac{2}{\sqrt{-g}}\,\frac{\delta I_{\text{matter}}}{\delta g^{\mu\nu}}\,. \tag{1.5}$$

Einstein's equations (1.4) are supplemented by the EOM for the matter fields $\Phi_I$.

$$\frac{\delta I_{\text{matter}}}{\delta \Phi_I} = 0. \tag{1.6}$$

Einstein's theory is classically *background-independent* in the sense that the spacetime manifold $\mathcal{M}$ in which the gravitational and all the other fields reside is a solution to the same field equations and not specified as an external background. The metaphor often used in this context is that the 'stage becomes an actor', where

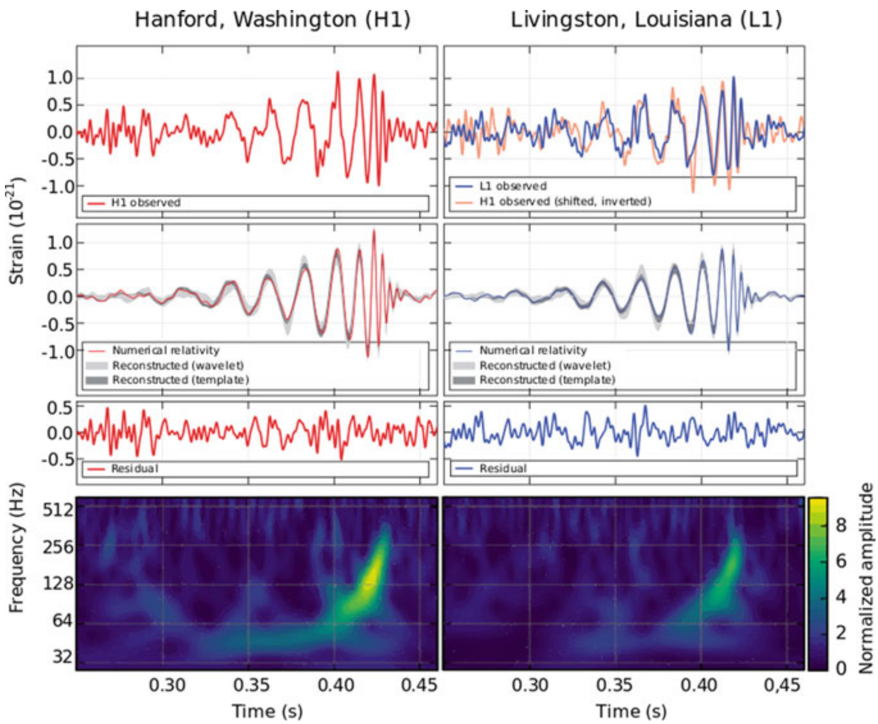


**Fig. 1.1** First observation of GWs by LIGO. Depicted is the GW-form, both measured and fitted from theory, corresponding to the merger of two black holes with about 29 and 36 solar masses, resulting in a final black hole of about 62 solar masses, with 3 solar masses radiated away through GWs. *Source* [23]

'stage' refers to spacetime and 'actor' to the interacting fields. In Einstein's gravity, the spacetime metric itself is an interacting field.

Einstein's field equations (1.4) are ten coupled second order, non-linear, partial differential equations. Already the two-body problem is prohibitively difficult to solve, as opposed to Newtonian gravity, where the two-body problem is a first-semester physics exercise. And yet, we need to solve the two-body problem to decipher gravitational wave (GW) data from black hole mergers like in Fig. 1.1. Moreover, the non-linearity of the equations makes the relation between sources $T_{\mu\nu}$ and fields $g_{\mu\nu}$ highly non-trivial, as compared to linear theories like Maxwell's. In essence, this non-linearity is the reason why we have black hole solutions. It also makes a full classification of solutions (with given asymptotic behavior and known matter content $\Phi_I$) quite non-trivial and hence interesting.

Given the non-linearity of the Einstein equations (1.4), it is not manifest that they provide a well-posed initial value problem, also known as a Cauchy problem. By this, it is meant that initial data are provided for the metric, the matter fields, and their momenta on some constant time slice of spacetime. Having a well-posed Cauchy evolution means that the Einstein equations define deterministic dynamics. Due to their non-linear nature, the Einstein equations can yield solutions that have singular loci or so-called Cauchy horizons (to be defined and discussed in Chap. 3). At singularities and beyond Cauchy horizons, there is no well-defined Cauchy evolution and hence the dynamics ceases to be deterministic.

## 1.2 Brief Review of Black Hole History

The history of black holes within Einstein's gravity may be divided into two episodes, with the separation point being in the mid-1960s. The first five decades ($\sim$1916–1967) were a time of slow but steady progress regarding black holes, which picked up speed in the 1960s. Around 1967, the term 'black hole' was popularized by John Wheeler after his audience got tired of repeatedly hearing the expression 'gravitationally completely collapsed object' [24]. A few years earlier Roy Kerr had found a class of solutions describing rotating black holes [25]. This, and other discoveries in the 1960s, established two main branches of black hole research in the second episode of black hole history.

One of them can be summarized as 'black holes in the sky'. It started in the late 1960s and has greatly evolved with the advancement of cosmological, astrophysical, and GW observations, largely due to rapid technological innovations. In the typical cycle of most technologies, paraphrased as 'the discovery of today is the tool of tomorrow and the background of the day after', we have barely reached tomorrow in 2022 when it comes to black holes. The main upshot of this research branch is that the observational evidence for black holes from accretion disk physics, microlensing, observations of Keplerian orbits around supermassive black holes, GW observations of black hole mergers, and imaging of black hole shadows is so overwhelming that there is little room for doubt about their existence. See Fig. 1.2 for the first image of a black hole shadow.

The second, purely theoretical, branch started slightly later in the 1970s with seminal discoveries by Jacob Bekenstein and Stephen Hawking, who kicked off the study of thermodynamical, semiclassical, and quantum effects in black hole physics. While this story is still mostly in the discovery phase and thus few statements can be made on which all respectable researchers would agree, one aspect of black holes seems uncontroversial: they appear to be a key system to understand on our road toward the elusive theory of QG. This is what makes them so striking for theoretical research.

### 1.2.1 First Five Decades: Finding Solutions and Classic Analyses

Constructing exact solutions to Einstein's equations (1.4) has been an important part of the research work carried out in this era. What is now known as Schwarzschild black hole was the first non-trivial exact solution to the vacuum Einstein equations $R_{\mu\nu} = 0$. Karl Schwarzschild found his solution at the end of 1915, less than two weeks after Einstein's groundbreaking work on GR [27], and published it in 1916. The same solution with a simpler and more direct derivation was independently

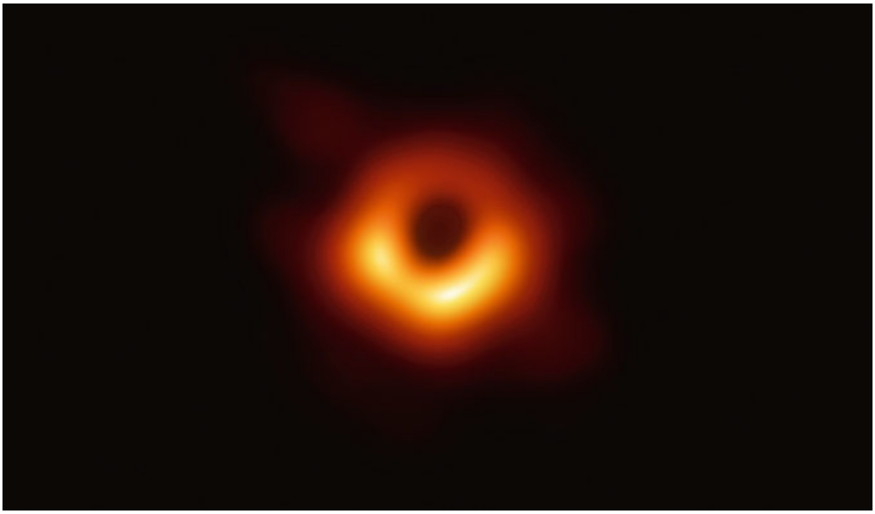

**Fig. 1.2** Imaging of the shadow of the black hole Messier 87 [26]

found by Johannes Droste [28]; see [29] for more historical remarks. It took a long time to fully understand this solution. As we will discuss in the coming chapters, this solution has two specific loci, a horizon, and a curvature singularity. The length scale associated with the horizon can be determined through dimensional reasoning. The only way to combine mass $M$ and Newton's constant $G_{\mathrm{N}}$ into a length (in units where the vacuum speed of light equals unity) is $r \sim MG_{\mathrm{N}}$. Inserting as an example the mass of the sun $M = M_{\odot} \sim 2 \cdot 10^{30}\,\mathrm{kg}$ yields a length scale of about $2\,\mathrm{km}$. Somewhat unexpectedly, this is not some astronomical number but rather a typical walking distance. The physical reason for this apparent scale disparity between an astronomical mass and an everyday-life distance is that gravity is an extremely weak force, which is either incidental or something profound [30].

That the horizon is not a singularity (as thought initially) but still a special place became apparent through works of many in the course of several decades, among them Ludwig Flamm (1916) [31], Paul Painlevé (1921) [32], Allvar Gullstrand (1922) [33], Arthur Eddington (1924) [34], Georges Lemaître (1932) [35], Howard Robertson (1938) [36], John Synge (1950) [37], David Finkelstein (1958) [38], George Szekeres (1960) [39], Martin Kruskal (1960) [40], Roger Penrose (1965) [41–43], and Werner Israel (1966) [44]. Each of them introduced a different coordinate system to make manifest and stress-specific features of the Schwarzschild solution. As implied by the EEP and its manifestation through general covariance, the physics is independent of the choice of the coordinate system. Nonetheless, a lesson learned from all these efforts is that the choice of an appropriate coordinate system can have an important role in revealing various features of a given spacetime.

The efforts for understanding the Schwarzschild solution led to the realization that in general there could be causally disconnected regions of spacetime, separated by a null hypersurface dubbed ‘horizon’. Horizons can be formed by the evolution of spacetime [41,45]; they may be observer-dependent; there are local and global concepts of horizons. All these different possibilities will be discussed and clarified in the coming chapters. However, for the sake of the introductory discussion in this chapter, we adopt a rough definition of black holes as spacetimes with a horizon, where by horizon we mean a null hypersurface that acts like a semi-permeable membrane through which things can fall in but cannot come out. As we shall mention below, this defining property of black holes needs to be revised once quantum effects are considered.

Historically, the next black hole solution was the one found by Hans Reissner and Gunnar Nordström (RN) in 1916 [46,47]. It describes electrically charged static, spherically symmetric black holes. While Schwarzschild needed only a few weeks to find the black hole solution named after him and RN followed soon afterward, it took a couple of decades until Roy Kerr constructed a non-static, non-spherically symmetric, rotating black hole solution [25]. In the same year, Frank Tangherlini generalized the Schwarzschild solution to any dimension [48]. These discoveries were soon followed by the charged rotating Kerr–Newman (KN) solution in 1965 [49]. These efforts of the 1960s were completed by proofs of various theorems, in particular uniqueness, no-hair, singularity, and topology theorems. Among other things, these theorems established the pragmatic insight that Kerr black holes are the most general exact solution of Einstein's equations (1.4) that most astrophysicists need to care about. Moreover, they showed that singularities hidden inside black holes are not artifacts of some special assumptions, but rather generic aspects of black hole spacetimes.

In the late 1960s, the stability of black hole solutions was investigated, perhaps as a way to remedy the singularity forming as a result of gravitational collapse. The first steps in this direction were made by Roger Penrose with two main conclusions: (1) Through the Penrose process (also known as the superradiance effect or black hole mining) [50,51], one can extract energy and angular momentum from rotating black holes. (2) Penrose's Cosmic Censorship Conjecture (CCC) states that a 'naked singularity' (meaning one that is not screened by a horizon) either cannot be formed or is unreachable for any physical observer as long as they do not jump beyond a horizon [45,52,53]. In the 1980s, the non-linear stability of flat space was proven by Demetrios Christodoulou and Sergiu Klainerman [54,55]. Proof of non-linear stability of Schwarzschild black hole came later in 2021 [56].

In parallel but closely related developments, it was established that black holes can dynamically form within GR through the gravitational collapse of ordinary matter, starting from seminal work by Subrahmanyan Chandrasekhar and by Richard Tolman, Robert Oppenheimer, and George Volkoff (TOV). In particular, as we will review in Sect. 1.3, usual stars, if heavy enough, can evolve into black holes. Therefore, black holes with masses of the order of typical stars, like a few times the mass of our Sun, should be ubiquitous in the sky, which provided a good motivation to believe in their existence even during the first five decades, when there were no observational hints of black holes yet.

### 1.2.2 Black Holes Through Observations

That black holes, with their unusual theoretical properties, could be objects found in the sky received a great boost with the discovery of neutron stars (pulsars) in the late 1960s. The first strong candidate for a black hole, Cygnus X-1, was discovered in 1972 through X-ray emission from a binary star system by Charles T. Bolton and by Louise Webster and Paul Murdin [57,58]. These X-ray binaries usually consist of a heavy star (typically a black hole) which gradually accretes mass from a lighter companion star. About a year later, it was largely accepted that the black hole hypothesis provided the simplest explanation of the X-ray spectrum observed, though there remained some lingering doubts for a while about whether or not Cygnus X-1 contains a black hole. In the meantime, dozens of black holes have been discovered through X-ray spectra from binary systems; see e.g. [59].

In 1994, Charles Townes and colleagues [60,61] observed highly rotating ionized neon gas around the center of our galaxy in Sagittarius A*. They attributed their observation to a supermassive black hole of mass around a few million $M_{\odot}$. Since then, a lot of further evidence gathered for this hypothesis. It is very much hoped that a more direct image of the shadow of this black hole can be generated using the Event Horizon Telescope (EHT) based on radio astronomy [62] in the coming years.

Astronomical black hole hunts are usually done in three different channels:

(1) X-ray astronomy, in particular by Chandra X-ray observatory [63] looking for accreting stars in binaries.
(2) Radio astronomy, in particular by the EHT and its upgrades [62].
(3) GW detection, by the Laser Interferometer Gravitational-wave Observatory (LIGO) [64] and Virgo (and their upgrades) [65], and other upcoming GW detection experiments.

These different channels are apt for observing different mass ranges. The EHT is suited to observe supermassive black holes of the order of several million to several billion $M_{\odot}$. While started in 2006, it published its and *the* first black hole image from the center of the Messier 87 galaxy in 2019 [26]. The GW detection technique is more suitable to record mergers of binary objects of masses from about a few $M_{\odot}$ to a few hundred $M_{\odot}$. X-ray astronomy could be used for a wider range of masses including solar mass to supermassive objects. There are proposals to use gravitational microlensing as a method to detect black holes; see, for example, [66–68]. While a promising proposal, it has not yet produced confirmed observations.

The X-ray astronomy and GW observatories have produced a catalog of a few hundred black hole candidates with a mass range of a few to a few billion solar masses. It is a thriving area of research. and this list is improved and enlarged essentially day by day. While there is a consensus that what we see in observations does correspond to the black holes in our theoretical setting (GR), some have entertained the idea that the theory has compact massive solutions (e.g. gravastars [69–71]) which to a good extent have similar observational signatures to black holes. More precise

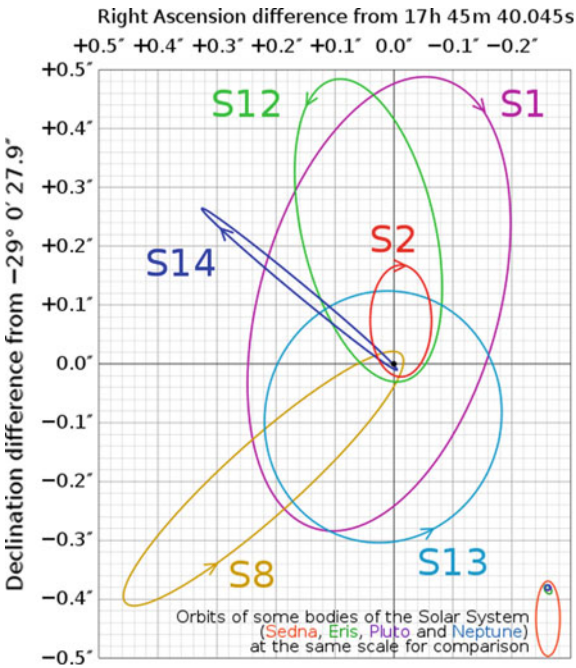


**Fig. 1.3** Measured Kepler orbits of stars around black hole Sagittarius A*. Image by cmglee on wikipedia. Original source: [72]

GW detection experiments and/or more precise EHT images will provide a more definitive answer.

The status of black hole observations is summarized in Table 1.1, ordered by mass ranges. The most common black hole type is stellar, generated through the gravitational collapse of stars, as discussed in Sect. 1.3. Not only are these black holes abundant, as expected from the conclusions above, but there is also an abundance of observational data from accretion disks surrounding black holes and GW emission from stellar black hole mergers.

Heavier black holes are labeled either as 'intermediate' or 'supermassive'. The latter are located at centers of galaxies, including Sagittarius A* in our Milky Way. While believed to be abundant, observational evidence for them is more scarce. The best evidence for the black hole at the center of the Milky Way is from stars on Kepler orbits around the black hole (see Fig. 1.3). The best evidence for an extragalactic supermassive black hole is the observation of the shadow of the Messier 87 black hole (see Fig. 1.2). There are very few observations of intermediate black holes through GW emission from mergers of two heavy stellar black holes.

Lighter black holes fall into three categories, 'primordial', 'mesoscopic', and 'microscopic'. Primordial black holes (PBHs) could be generated in the early universe and if lucky, we could observe them through Hawking radiation or microlensing. This has not happened so far, which places some bounds on their abundance. PBHs have also been proposed as dark matter candidates [73–75]. Mesoscopic black holes in principle could also be generated in the early universe, but are so light that they would have Hawking evaporated by now, meaning that it is harder to place

**Table 1.1** Black hole zoology from high to small mass

| Black hole type | Mass range | Status | Some observation methods |
|---|---|---|---|
| Supermassive | $\geq 10^5\ M_\odot$ | Handful observations | Kepler orbits, black hole shadow |
| Intermediate | $10^2$–$10^5\ M_\odot$ | Few observations | GWs from heavy mergers |
| Stellar | 3–100 $M_\odot$ | Numerous observations | Accretion disks, GWs from mergers |
| Primordial | $10^{11}$ kg–$10^{31}$ kg | Not observed | Hawking radiation, microlensing |
| Mesoscopic | $10^{-8}$ kg–$10^{11}$ kg | No data | ? |
| Microscopic | $\lesssim 10^{-8}$ kg | Not observed | Large Hadron Collider |

bounds on them from data. Microscopic black holes are of the order of the Planck mass (and in certain speculative theories can even be lighter than that). These are very short-lived and the Large Hadron Collider provides exclusion bounds on their existence.

### 1.2.3 Black Holes as Thermodynamical Systems

The information buildup of the 1960s implied that black holes are not strange solutions of GR that should somehow be bypassed or dismissed, but on the contrary, they should be taken as real physical objects to be properly understood. In particular, one may ask what are the implications of the presence of black holes, horizons, and singularities for other areas of physics. A serious exploration of this class of questions was started in the 1970s by John Wheeler and his coworkers on the one side and Penrose, Hawking, and collaborators on the other side. While there have been some very good technical and conceptual advancements, some questions unveiled in the 1970s are still occupying us today.

In the early 1970s, triggered by some questions from his Ph.D. advisor Wheeler, Bekenstein noted that black holes should have an entropy [76] to save the second law of thermodynamics. The key gedankenexperiment is to throw some entropic substance (originally a cup of lukewarm tea) into the black hole to hide its entropy behind the black hole horizon; if black holes did not have an entropy, the second law of thermodynamics would be violated. However, if black holes do have an entropy related to their size there is not necessarily a contradiction, since throwing something into a black hole increases its mass and thus its size. More specifically, Bekenstein proposed a black hole entropy proportional to the area of the horizon, partly motivated by Hawking's area theorem that resembles the second law of thermodynamics, with area playing the role of entropy. All four laws of thermodynamics have corresponding black hole mechanics statements [77], but it was not immediately obvious whether one should take this analogy seriously and conclude that black holes behave like thermal systems.

Initially, Bekenstein's conjecture appeared to contradict basic aspects of black hole physics or thermodynamics: if black holes had entropy, the four laws of black hole mechanics dictate that they also should have a temperature that scales like surface gravity. However, any substance with temperature must radiate, and black holes, almost by definition, should not radiate. The contradiction was resolved by Hawking, who studied the behavior of quantum fields external to the horizon. Quantizing under these external conditions revealed that the horizon is no longer a one-way road semiclassically; there is quantum leakage to the outside. This leakage is of the form of usual black body radiation with a Planck spectrum giving a temperature proportional to surface gravity. This radiation is commonly known as Hawking radiation [78,79].

Quite remarkably, the thermodynamical and quantum mechanical considerations led to results confirming each other. The four laws of black hole mechanics do not just resemble the laws of thermodynamics, they are *identical* to them. The surface gravity, the gravitational acceleration of a free-falling observer at the surface of the horizon (up to a factor of $1/(2\pi)$), is indeed the temperature of the Hawking radiation. The entropy does scale like the area, with a precise numerical factor of $1/(4G_{\rm N})$, thus confirming Bekenstein's proposal. The Bekenstein–Hawking (BH) entropy

$$S_{\rm BH} = \frac{\text{area}}{4G_{\rm N}} \tag{1.7}$$

is the first milestone in this line of research. Note that (1.7) is written in natural units where Boltzmann constant $k_{\rm B}$, Planck constant $\hbar$, and vacuum speed of light $c$ are set to 1. See Exercises 1.2 and 1.3 for more discussion on these units.

The fact that thermodynamical and quantum mechanical considerations confirm each other could be pointing to a deep feature of quantum theory or QG that is not yet fully understood and formulated. But it shows already the conceptual importance that black holes play in our attempts to bring together GR with quantum mechanics. Actually, given the scarcity of observational data regarding QG, the BH law (1.7) is often used as a template for falsification. The basic logic is as follows. Suppose you have constructed your favorite theory of QG (perhaps in some suitable limit, e.g. of large black holes). One of the first questions you should address is: can you predict the BH law (1.7) with the correct prefactor? If not, you should dismiss your construction as unphysical, since it is practically guaranteed to be incorrect. This argumentation shows the amount of trust we have in the BH result (1.7) and its usefulness in QG research.

The 1970s brought great conceptual advances and completely changed the picture physicists had about black holes. But, as Hawking famously noted in the late 1970s, these results engender deeper conceptual questions about the unitarity of the evolution of quantum systems involving black holes, the information puzzle (also known as information paradox or information loss problem) [80]. The short version of this puzzle is that black holes can be generated from pure quantum states, such as a bunch of laser beams pointing to a common center.[2] After the black hole formation process has settled down, the black hole will emit Hawking radiation and eventually evaporates. Thus, the final state is thermal and consists of the outgoing Hawking quanta. From this, one may conclude that one has a conversion of a pure initial state into a mixed final state, which is impossible in a unitary quantum theory. So the issue at stake here is unitarity, and the first question of the information loss problem is whether or not the information is lost in evaporating black holes in principle or just for practical purposes. The latter happens also in many macroscopic quantum systems, such as a bunch of laser beams pointing to a piece of coal, thereby heating it up.

The last four–five decades allowed us to sharpen the questions revolving around black hole evaporation and the information puzzle. One important step came through the work of William Unruh [81] who established that surface gravity = temperature is compatible with the EP. Explicitly, any accelerated observer should describe physics at a non-zero temperature. Another conceptual step was taken through the work of many, in particular, Gerard 't Hooft [82] and Leonard Susskind [83], by the introduction of stretched horizon/brick wall and black hole complementarity [83, 84]. The main point of black hole complementarity is to claim that the EP and quantum theory are compatible with each other and that physical information available to the observers outside the horizon is complete without the need for adding the information from the inside, while at the same time an infalling observer has access to (some of) the information falling through the horizon.

A supplementary viewpoint to black hole complementarity puts more focus on the thermodynamical aspects of black holes. Thanks to Ludwig Boltzmann's insights, we should expect a statistical mechanics explanation of black hole entropy. So it is worthwhile to ask whether it is indeed true that black holes have an underlying microscopic description, and if they do, can we identify and count the black hole microstates? Finally, even if we succeed in this endeavor, does the counting agree with the BH law (1.7), at least in the semiclassical limit? Having a statistical mechanics description of black holes is not only an important result in its own right, but it may allow concluding that black holes behave like other statistical mechanics systems, such as the laser-coal example above. This in turn could lead to the conclusion that there is only information loss for practical purposes, but not in principle.

In the early 1990s, 't Hooft [85] and Susskind [86] proposed the holographic principle, which is inspired by the BH law (1.7) and the simple observation that the area scales in the same way as the volume in one lower dimension. The holographic principle postulates that QG in $D+1$ spacetime dimensions is equivalent to ordinary quantum field theory (QFT) without gravity in $D$ spacetime dimensions. If correct, this is probably one of the most astounding conceptual outcomes of theoretical black hole research.

[2] This is not the most practical way to generate a black hole, but for this kind of argumentation gedankenexperiments are usually sufficient to point out the key issues.

In the mid-1990s, Andrew Strominger and Cumrun Vafa [87] presented a method to count black hole microstates of certain supersymmetric black holes at zero temperature within superstring theory, the most prominent candidate of QG. At that time, it was quite a surprise that superstring theory knows about the BH law (1.7), and encouraged by this result many researchers concluded that string theory could be on the right track. However, despite great successes, generalizations, and elaborations since the seminal Strominger–Vafa paper, their counting does not directly shed light on the information puzzle, as supersymmetric black holes do not Hawking-radiate.

In 1997, Juan Maldacena proposed a new duality in superstring theory, known as Anti-de Sitter/Conformal Field Theory (AdS/CFT) correspondence [88]. It provides a concrete realization of the holographic principle by identifying which gravity theory (type IIB superstring theory on $\mathrm{AdS}_5 \times S^5$) is dual to which QFT (maximally supersymmetric Yang–Mills theory in four spacetime dimensions). Moreover, it allowed concrete tests by calculating observables on gravity and field theory sides and comparing them, using the holographic dictionary established by Steven Gubser, Igor Klebanov, and Alexander Polyakov [89] and by Edward Witten [90]. Besides more practical applications to describe strongly coupled QFTs or strongly correlated condensed matter systems, the main job of AdS/CFT is to teach us about QG by providing us with tools for concrete calculations that in turn enable us to answer sharp questions on black holes, their microstates, and their evaporation. It is hard to exaggerate the impact of AdS/CFT on QG research since it provides a non-perturbative definition of QG in terms of its QFT dual, which does not involve gravity.

After the turn of the millennium for a while, the information puzzle was considered to be solved by AdS/CFT, in the sense that the CFT dual was unitary by construction and thus information cannot be lost. However, it still would be nice to understand how precisely information is not lost from the gravity perspective, and also whether one can understand on the CFT side why semiclassically information appears to be lost.

These issues reentered the lightcone of numerous researchers after black hole complementarity was challenged in the work of Ahmed Almheiri, Donald Marolf, Joseph Polchinski, and James Sully [91]; see also [92]. They concluded that the three main assumptions of black hole complementarity—unitary time evolution, SEP, and linear quantum mechanics—were incompatible with each other and one had to give up at least one of them. Further, they suggested giving up the SEP at the scale of the horizon, which practically means that an observer falling into a black hole would be killed by a firewall near the horizon. As of today, there is no universally accepted resolution of the firewall paradox, though there are intriguing proposals within AdS/CFT that do not require a firewall and that maintain the SEP; see, for example, [93,94] and references therein.

Attempts in addressing the black hole information puzzle may be roughly put into three different classes of ideas: (1) The information puzzle arises in the semiclassical approximation and can be resolved within the same regime. Relatedly, black hole microstates of (sufficiently big and hot) black holes can be constructed in the same approximation. (2) The information puzzle and the construction of black hole microstates are inherently quantum problems and a full theory of QG is essential to understand them. (3) Information is lost.

All three viewpoints have their advocates and are active areas of research. While the jury is still out on this issue, it is fair to say that option (3) is a minority viewpoint.

## 1.3 Gravitational Collapse in Stars

Since the early days of GR, the evolution of stars was studied. Typically, one models the stellar matter by a perfect fluid (with pressure $P$, energy density $\rho$, and some barotropic equation of state, $P = P(\rho)$) and studies its dynamics governed by Einstein's equation (1.4). This model yields the TOV equation [95,96] for the spherical symmetric matter. The free ingredient in the TOV model is the equation of state, which carries the information about the interactions of matter in the star. It changes in different phases of stellar evolution.

If heavier than 8–9 $M_{\odot}$, a star can reach a supernova phase in its evolution, where the outer layers of the star are expelled, leaving behind a remnant that is typically a neutron star or a black hole. For details on the end of the life of stars, see [97–99].

### 1.3.1 Core Collapse Supernova and Black Hole Formation

As a star evolves, it gradually uses up its light element nuclear fuel and there is a buildup of iron nuclei in the core of the star. Iron is very stable and cannot enter into nuclear reactions. Even in the absence of thermal pressure, which follows from the absence of nuclear reactions, the core remains stable if sufficiently light, since the gravitational attraction of its constituents can then be balanced by the Fermi degeneracy pressure of the electrons. When and if the mass of the iron core reaches the Chandrasekhar mass, $M \approx 1.4M_{\odot}$, the Fermi degeneracy pressure of electrons in the core cannot withstand the attraction of the gravitational force and the core implodes. This provides enough energy and pressure to disintegrate the iron nuclei in the core so that the protons and neutrons are set free. More importantly, it also provides thermal energy to protons and electrons and results in the de-leptonization process through inverse $\beta$-decay: protons capture electrons and produce neutrons and electron neutrinos. Neutrinos are only weakly interacting and therefore emitted from the core, carrying away energy in the process. Thus, in the end, nearly no leptons remain in the core. The de-leptonization process happens on short time scales, of about $10^{-4}$ s.

In the absence of the Fermi degeneracy pressure of electrons, the core compresses under its gravitational self-attraction. This sends shock-waves through the outer layers of the star. The core itself is heated up and light particles, in particular neutrinos, are produced thermally within the core. The thermal neutrinos again diffuse out, further reducing its energy (by about 10%), opening the way for further squeeze and shock-waves to the outer layers. The outer layers explode in a supernova, and what remains is a very compact object with a mass around the Chandrasekhar mass. The whole process of de-leptonization to the supernova takes only a few hours.

Depending on the precise mass of that very compact object, distinct possibilities arise. If its mass is less [3] than 2–3$M_\odot$, then generically it consists mostly of neutrons (since neutrinos are emitted, and electrons and protons converted into neutrons) and is kept stable due to a balance of gravitational attraction and the Fermi degeneracy pressure of neutrons. Reality is a bit more complicated than this simple picture where the whole core is converted into neutrons, and in fact, the four fundamental forces (electromagnetic, weak, strong, and gravitational) play a role in the stability of compact stars; see [105] for lecture notes. Since we want to stick to the essence of the discussion, let us pretend that the final result of this process is a neutron star. The newly born neutron star is usually observed as a pulsar.

If the mass of the remaining very compact object is bigger than $3M_\odot$, the degeneracy pressure cannot withstand gravitational attraction and instead of a neutron star we get a black hole. Black holes are hence theoretical predictions of GR that are expected to be quite abundant in our universe.

### 1.3.2 Estimating the Chandrasekhar Mass

To discuss the gravitational collapse of a star, we need a model of stellar evolution. The evolution of real stars is a complicated problem and many aspects of it are still a matter of research. Here, we give a very simple account to give the essence of the derivation of the Chandrasekhar mass. The details of the derivation may be followed through in Exercise 1.4. For a more thorough discussion and analysis, we refer the reader to [51,102,103].

Consider a star, a compact spherical body of mass $M$ and radius $R$. The total energy of the system is given by

$$E(R) = E_{\mathrm{kin}} + E_{\mathrm{grav}} \tag{1.8}$$

[3] The precise number depends on the precise composition of the compact star and requires to specify the equation of state. The theoretical upper bound on neutron stars with known interactions obtained through the TOV model using the latest data from various astrophysical sources is $2.16M_\odot$ [100], while the heaviest confirmed observation of a neutron star so far is $2.14M_\odot$ [101] and the lightest observed neutron star has $1.1M_\odot$ [102]. By comparison, the lightest confirmed stellar-mass black hole has a mass around $5M_\odot$ [103]. So theoretically, it is possible to have slightly lighter black holes than observed so far. Allowing for more exotic stars, like quark stars [104] or stars made out of other exotic types of matter, one may have pulsars heavier than $2.16M_\odot$. Finding the precise boundary between compact stars and black holes as well as determining the composition of the former are active research areas that are of interest both observationally and theoretically. On the theory side, it touches upon the frontiers of particle physics in a regime where the four fundamental interactions, including GR effects, are important.

where

$$E_{\text{kin}} \simeq \frac{\mathcal{K}_p}{R^p} \qquad E_{\text{grav}} = -\alpha \frac{GM^2}{R}, \tag{1.9}$$

with $\alpha$ being a positive numeric coefficient.[4] The coefficient $\mathcal{K}_p$ and value of $p$ depend on the details of the internal dynamics of the star. In a rough account, one can distinguish three different stages in the evolution of a usual star:

(1) The normal phase, when the gravitational pressure of the star is balanced by its thermal pressure. In this phase, $p = 3$ and $\mathcal{K}_3 = \frac{3}{2} \cdot \frac{3MT}{4\pi}$ where $T$ is the temperature of the star.
(2) When the usual nuclear fusion reactions of the star are more or less over and its gravitational attraction is balanced by the degeneracy pressure of non-relativistic electrons. In this case, $p = 2$ and $\mathcal{K}_2 \sim \frac{3}{5}(9\pi/4)^{2/3} \cdot \frac{1}{2m_e} \cdot (M/m_N)^{5/3}$ where $m_e, m_N$ are respectively the electron and nucleon masses (i.e. masses of protons and neutrons, which roughly are the same).
(3) The last stage, when the kinetic energy is dominated by the degeneracy pressure of neutrons. In this case, $p = 1$ and $\mathcal{K}_1 \sim \frac{1}{4}(3\pi M/(4m_N))^{4/3}$.

Go through Exercises 1.4, 1.5, and 1.6 for more discussions.

When $p > 1$, $E(R)$ in (1.8) has a minimum at $R_{\text{star}}$, where $R_{\text{star}}^{p-1} = p\mathcal{K}_p/(\alpha G_{\text{N}} M^2)$, at which the star settles down. The $p = 1$ case during the last stage is very special: there is no minimum and if $\mathcal{K}_1 < \alpha G_{\text{N}} M^2$ there is nothing to stop the gravitational collapse. There is hence a phase transition at the critical mass, the Chandrasekhar mass

$$M_{\text{C}} = \gamma m_N \left(\frac{M_{\text{Pl}}}{m_N}\right)^3 \tag{1.10}$$

where $\gamma$ is a numerical coefficient, $M_{\text{Pl}}$ is the Planck mass (cf. Exercise 1.2), and $m_N$ is the nucleon mass. To compute the coefficient $\gamma$, one should not only determine $\alpha$ more carefully but also examine how relativistic our fermions are. For this detailed analysis, we refer interested readers to [51, 102, 103]. The final result is $\gamma \sim 0.8$ and $M_{\text{C}} = 1.4 M_\odot$. One of the remarkable features of the Chandrasekhar mass $M_{\text{C}}$ (1.10) is that it only contains one physical parameter, the neutron mass $m_N$, and the three constants of nature, $c$, $\hbar$, $G_{\text{N}}$, which appear through the Planck mass (see Exercise 1.2); $M_{\text{C}}$ only depends on microphysics. Despite the fact that this was computed for electron degeneracy pressure, $M_{\text{C}}$ in (1.10) is independent of $m_e$.

To summarize this part, if we start with core masses below the Chandrasekhar limit (1.10), $M_{\text{core}} < M_{\text{C}}$, the star stabilizes and the electrons at the Fermi surface are sub-relativistic. If we start with $M_{\text{core}} > M_{\text{C}}$, the electron degeneracy pressure cannot withstand the gravitational force and the system collapses. The final outcome depending on $M$ can either be a neutron star or a black hole. A detailed computation,

[4] Assuming uniform density $\alpha = 5/3$, but in real situations the density has a radial profile, which effectively changes $\alpha$. The specific value of $\alpha$ does not change our qualitative analysis here.

which involves also GR effects (see Exercise 1.6 to see why), indicates that we typically get a neutron star for $M < 3M_\odot$ and for $M > 3M_\odot$ a black hole. This is of course assuming having a matter made from known particles and interactions (within the Standard Model of particle physics). Other exotic types of matter may give other values, for example, see [104,106,107].

The message to take away from this part is that black holes are produced abundantly in our universe through gravitational collapse, as a consequence of the dynamics of ordinary matter with known physics.

## 1.4 Different Schools of Thought on Black Holes

The field of black hole physics has received a lot of attention, especially in recent years, in part due to fantastic progress in observations involving black holes. In this somewhat philosophical section, we mainly focus on theoretical aspects of black hole physics and just briefly touch upon the exciting and intense research associated with observational aspects. There are several conceptually distinct ways to think about black holes, and all of them have their merits and limits. We group these approaches loosely together into three schools of thought, defined in the remainder of this section. Here, we mainly focus on what these schools have offered for black hole physics, and not for (quantum) gravity in general.

These schools are not mutually exclusive, but serve to highlight different aspects of the same physical entities, namely black holes. They also influence the way some researchers think about unresolved issues in black hole physics, including the information loss puzzle and QG. We shall say more about these open issues and speculations in later chapters.

### 1.4.1 GR School

The motto of this school is 'everything is geometry and symmetries'. Its main guiding principle is the EP and its main framework GR as a theory of spacetime.

As mentioned in Sects. 1.2.1 and 1.2.3, one may consider black holes primarily as objects in classical GR and try to study and explore questions regarding black holes which come about and can be studied in this setting. We call this attitude the *GR school*, whose focus is mostly on geometrical aspects of gravity.

Questions studied within the GR school may be put in two categories according to the main set of techniques being used to analyze them, namely analytical and numerical gravity. Examples for the first category are to develop exact solution techniques, to prove various theorems about black holes and spacetimes containing them, including singularity, area, no-hair, uniqueness, positive mass theorems, and the four laws of black hole mechanics, to show the stability of solutions, and to venture into theories beyond GR, like GR in dimensions different from four or modified gravity theories. Many classic textbooks adopt this viewpoint; see, for example, [108,109]. Examples of the second category include black hole formation

[110], black hole collision and GW emission from black hole binaries [111], accretion disk simulations [112], and the development of new numerical solution techniques in GR; see, for example, [113].

A particular GR school aspect that we highlight, influenced by ongoing current research, is the concept of asymptotic/boundary symmetries. Their precise definition will be given in later chapters, but the concept can easily be explained at this stage already. In the presence of actual or asymptotic boundaries, some of the coordinate transformations that preserve the boundary and fall-off conditions need not be a pure gauge. Rather, the state of the system can be changed. A simple example is a black hole with Poincaré symmetries at the asymptotically flat boundary. A boost, while formally merely a change of coordinates, changes the state of the black hole for an asymptotic observer as compared to the black hole at rest. Similar remarks apply to some more complicated coordinate transformations that can produce new physical states, depending on the precise structure of the boundary. Sometimes, the excitations associated with these states are referred to as 'boundary gravitons', 'edge modes', or 'boundary degrees of freedom'. The existence of boundary degrees of freedom has led to the 'soft hair' proposal [114] which associates new degrees of freedom to the black hole horizon.

The classification of consistent boundary conditions (including a precise specification of what 'consistent' is supposed to mean) and their associated asymptotic symmetries is an ongoing research endeavor. One of the early surprises that came out of this line of research was that gravity in asymptotically flat spacetimes at large distances from the sources is not merely special relativity with Poincaré symmetries; instead, in the ground-breaking work Bondi, van der Burgh, Metzner, and Sachs [115,116] showed that there is an infinite enhancement of Poincaré symmetries by so-called 'supertranslations', which are angle-dependent translations of the retarded time along the celestial lightcone. The recent realization that these enhanced symmetries have a HEP interpretation in terms of Ward identities for soft scattering processes [117] and the so-called celestial holography, see, for example, [118], shows that the GR school is not independent of the HEP school of thought.

### 1.4.2 HEP School

The motto of this school is 'everything is particles and fields'. Its main guiding principles are unitarity and locality, and its main framework is QFT.

The High Energy Physics (HEP) school of thought was first developed in the 1950s and 60s by early attempts to quantize GR [119–122]; see [123] for some of the history. The outcome of these early attempts was non-renormalizability of GR [124,125], which initially was thought to be an obstacle to having a theory of QG. By now the perspective has shifted. It is understood that GR can be quantized perturbatively like any other EFT; see [126]. It is not too hard to calculate loop corrections to some observables like the Newton potential [127,128], but it will be quite a challenge to measure them. This is why QG is mostly a theory-driven research field, and this is true regardless of the precise ultraviolet (UV) completion of GR.

An essential aspect of the HEP school is to view GR primarily as a theory describing massless spin-2 particles with gauge symmetries

$$h_{\mu\nu} \to h_{\mu\nu} + \nabla_\mu \xi_\nu + \nabla_\nu \xi_\mu \tag{1.11}$$

much like we think about Maxwell's theory as a theory describing massless spin-1 particles with gauge symmetries

$$A_\mu \to A_\mu + \nabla_\mu \xi \; . \tag{1.12}$$

The geometric aspects are then somewhat incidental within this school and emerge as an effective concept at low energies. This approach is particularly suitable when there is a clear split of the full metric into background and fluctuations, $g_{\mu\nu} = \bar{g}_{\mu\nu} + h_{\mu\nu}$, such as in the treatment of GWs, scattering processes, primordial fluctuations in the early universe, black hole perturbations, and the Hawking effect.

Even if one just starts with a quadratic action involving a massless spin-2 field, one can iteratively add cubic, quartic, and higher-order vertices, and at least in the infrared (IR) limit the resulting theory uniquely turns out to be GR [129]. In this sense, the GR and HEP schools imply each other, and there is certainly no contradiction between them; there is only a slight shift of emphasis. Some textbooks that adopt the HEP viewpoint are [11, 130].

Black holes are not small perturbations of the vacuum state, so following the HEP school, one has to work a bit harder to even formulate what a black hole is if one does not want to resort to geometric notions such as horizons. Classically, black holes can be understood as solitons that correspond to thermal states. Perturbative excitations above these solitons then have an interpretation as GWs (gravitons) emitted from black holes, black hole perturbations, or Hawking quanta. How to define black holes quantum mechanically is unclear, both from a HEP and a GR perspective. This is part of the reason why black holes are a key system to be understood on our way toward QG.

For the classical theory, the question of whether one should adopt the GR or the HEP viewpoint is merely a matter of taste and practicality. There is, however, a strong difference in how researchers may think about semiclassical and quantum aspects of black holes and QG, depending on how strongly they adopt either of these viewpoints. We shall address these issues in more detail in the remainder of the book.

### 1.4.3 Quantum Information School

The motto of this school is ‘everything is information and entanglement’. Its main tool is entanglement and various measures associated with it, and its framework is the quantum information theory.

The last school is the most recent one. Its basic philosophy is to put quantum theory first and then apply it to some questions arising in the context of black holes. The logic behind this philosophy is the premise that ultimately our world is described by quantum mechanics, and while we are certainly entitled to use the stationary phase approximation to describe classical trajectories, we should perhaps refrain from doing so when encountering some puzzles in the (semi-)classical limit. Moreover, whatever QG might be, there is no guarantee it has a simple description in terms of the language commonly used within the GR or HEP schools.

In the context of black hole physics, there are at least two issues where the argument in the previous paragraph applies. One is the information loss problem, which exhibits an apparent clash between GR and quantum aspects. The other is the singularity at the center of the black hole, where the GR description breaks down. An overview of the sort of questions addressed within this school can be found in these lecture notes [131].

We shall come back to this school in later chapters. Our focus will be on selected achievements and quantum information aspects related to black holes and not so much on the variety of approaches to QG.

## Further Reading

Some classic GR textbooks are [8,10,11,108,109,132,133]. Some textbooks dedicated specifically to black holes are [51,133–138]. A historically important article on black holes in Physics Today is [139]. A black hole roadmap to future black hole observations is available here [140]. Some black hole books for a broader public are [141–144] and for first-year postgraduate students [145,146]. The scientific background concerning the 2020 physics Nobel prize to Roger Penrose, Reinhard Genzel, and Andrea Ghez is available online at
https://www.nobelprize.org/uploads/2020/10/advanced-physicsprize2020.pdf.

## Exercises

**1.1 Speed of light and Newton gravity.**

For the pre-history of black holes, there were two essential discoveries in the late seventeenth century, the finiteness of the speed of light and Newton's gravity law. In this first exercise, we revisit both.

(1) Use Rømer's observation that the eclipses of Jupiter's moon Io were delayed maximally by 16.5 min when the Earth was farthest away from Jupiter, together with the radius of Earth's orbit $1.5 \cdot 10^{11}$ m, to estimate the speed of light.

(2) Derive Newton's gravitational inverse square law from the three Kepler laws (I. Planetary orbits are elliptic with the Sun at one of the two foci; II. A line segment between Sun and planet sweeps out the same area in a given amount of time; III. The square of the orbital period is proportional to the cube of the semi-major axis of the orbit).

**1.2 Natural units, Planck length, and Planck mass.**

In HEP, it is common to choose units of length and time such that the vacuum speed of light $c$ and Planck's constant $\hbar$ are equal to one. These are called HEP natural units. In HEP natural units, mass, momentum, and energy all have the same dimension, while length has a dimension of inverse mass; masses of elementary particles are typically measured in electron-volt (eV).

(1) What is the mass of electrons ($m_e \sim 10^{-30}$ kg) and nucleons ($m_N \sim 10^{-27}$ kg) in eV?

(2) Show that in HEP natural units, Newton's constant $G_{\rm N}$ is a quantity of dimension length squared, or inverse mass squared. Let us define the Planck mass $M_{\rm Pl}$ and Planck length $\ell_{\rm Pl}$ in natural units as

$$M_{\rm Pl}^{-2} = \ell_{\rm Pl}{}^2 := G_{\rm N} \,. \tag{1.13}$$

Starting from $G_{\rm N} = 6.67 \times 10^{11}\ {\rm m}^3/({\rm kg} \cdot {\rm s}^2)$, compute the Planck mass in units of giga-electron-volt (GeV) and in kilograms. Compare the Planck mass with the mass of a nucleon. Compute the Planck length in meters.

(3) There is another natural set of units often used by the classical GR community, obtained by setting $c$ and $G_{\rm N}$ equal to one. In these GR natural units, mass, energy, and length have the same units. What is Planck's constant $\hbar$ in GR natural units?

Note: For the field of black hole physics, one may use a combined natural unit system where $c$, $\hbar$, and $G_{\rm N}$ are set to one. In this book, we will mainly use the HEP natural units and make $G_{\rm N}$ explicit throughout. In all cases, we set Boltzmann's constant to unity so that temperature has units of energy and entropy is dimensionless.

**1.3 More on black hole entropy.**

The purpose of this exercise is to become more familiar with the dimensional analysis described in the previous exercise.

(1) Consider a black hole of mass $M$ (e.g. a Schwarzschild black hole) and recall that in our theory, we only have Newton's constant $G_{\rm N}$, speed of light $c$, and Planck's constant $\hbar$. Construct a quantity of dimension length that is linear in $G_{\rm N}$ and $M$. Call this horizon radius $r_h$. Next, suppose the horizon is a sphere and compute the horizon area $A_h$.

(2) Define the black hole entropy $S_{\rm BH}$ as a dimensionless quantity proportional to the horizon area, cf. (1.7). Show that this information is enough to attach the appropriate powers of conversions factors $G_{\rm N}$, $c$, $\hbar$ to write $S_{\rm BH}$ in units of Boltzmann constant $k_{\rm B}$ up to a dimensionless numerical constant.

(3) The black hole mass $M$ has units of energy. Use naively the first law of thermodynamics, $M = T S_{\rm BH}$, and the expression $S_{\rm BH}$ for black hole entropy (1.7) to compute a characteristic temperature scale associated with a black hole of mass $M$. Check in particular the temperature associated with a black hole of the mass of our sun, $M = M_\odot \approx 2 \cdot 10^{30}$ kg.

**1.4 More on stellar evolution and derivation of the Chandrasekhar mass.**

As pointed out in Sect. 1.3.2, in a rough modeling, one can distinguish three different phases in the evolution of a star that undergoes core collapse supernova. The energy of the system is given in (1.8) and (1.9). In this exercise, we intend to give a taste of the computation of $\mathcal{K}_p$ factors in each phase.

(1) *Thermal pressure phase.* Consider a neutral gas of nucleons and electrons at a given temperature $T$. For a usual star, particles are generically non-relativistic, and it is a reasonable approximation to ignore interactions except for gravity, which is well described by Newtonian gravity. The thermal pressure of this gas is $P \sim nT$, where $n$ is the number density of particles. Show that kinetic energy scales as

$$E_{\text{kin}} \simeq \frac{3}{2 \cdot \frac{4\pi}{3}} \frac{MT}{R^3} . \tag{1.14}$$

(2) *Non-relativistic electron degeneracy pressure phase.* Once the nuclear fuel of the star is depleted, the temperature first drops and gravity squeezes the star. As a result, the star heats up again due to the reduction in gravitational energy, but can also radiate off its energy through photons. This phase is slow and can go on for billions of years. Nonetheless, the star core does not collapse to zero radius due to the Pauli exclusion principle, so the core is supported by the degeneracy pressure of the electrons, which for this part of the exercise are assumed to behave non-relativistically. Show that the kinetic energy scales as

$$E_{\text{kin}}(R) = \frac{\mathcal{K}_2}{R^2} \qquad \mathcal{K}_2 \sim \frac{3}{5} \left(\frac{9\pi}{4}\right)^{2/3} \cdot \frac{1}{2m_e} \cdot \left(\frac{M}{m_N}\right)^{5/3} . \tag{1.15}$$

Using (1.15), compute the radius of the core and show that its radius scales as

$$R_{\text{star}} \sim \frac{1}{G_{\text{N}} m_e m_N} \left(\frac{m_N}{M}\right)^{1/3} \frac{1}{m_N} . \tag{1.16}$$

(3) *Relativistic electron degeneracy pressure phase.* The star radius $R_{\text{star}}$ decreases with the star mass $M$. In the process of reaching $R_{\text{star}}$, electrons can become relativistic and one should revisit (1.15). Repeat the analysis yielding (1.15) for the case where the electrons at the Fermi surface are relativistic, i.e. $P_{\text{F}} \simeq \mathcal{E}_{\text{F}}$. Show that kinetic energy scales as

$$E_{\text{kin}}(R) = \frac{\mathcal{K}_1}{R} \qquad \mathcal{K}_1 = \frac{1}{4} \left(\frac{3\pi M}{4m_N}\right)^{4/3} . \tag{1.17}$$

**1.5 Checking basic assumptions about stars.**
In our analysis at the beginning of Sect. 1.3.2 and also in part of the previous Exercise 1.4, we assumed the validity of the non-relativistic and Newtonian approximation and ignored forces other than gravity. Here, we explore these assumptions/approximations more closely. Consider in this exercise a star with solar mass $M = M_\odot$ as a ball of radius $R$ of hot gas at temperature $T \sim 10^6$ Kelvin, and for simplicity assume that this mass is mainly due to hydrogen atoms, or a plasma of protons and electrons.

(1) Using (1.8) and (1.9), compute the star radius $R$ as a function of its mass and temperature.

(2) Estimate the velocity of electrons and protons. Compare this velocity with the speed of light.

(3) Considering that we have a homogeneous neutral gas of electrons and protons, argue that contributions of electromagnetic interactions to the pressure of the gas are negligible.

(4) What is the numerical value of the thermal pressure of this gas?

(5) Compute the escape velocity for electrons from the surface of the star and compare it with the typical speed of the particles there.

(6) Consider the phase when the star is supported by the degeneracy pressure of electrons. Estimate the value of the Fermi energy of electrons, $\mathcal{E}_F \equiv P_F^2/(2m_e)$ for a White Dwarf. (A White Dwarf is a stellar object that is supported by the degeneracy pressure of electrons, has a mass of about $M_\odot$, and a radius about a hundredth of the Sun.) Show that $\mathcal{E}_F \sim 0.3\,\text{MeV}$ and calculate the associated Lorentz boost factor. How good/bad is the non-relativistic approximation?

(7) Compute the numeric value of $R_{\text{star}}$ (1.16).

(8) Calculate the Fermi momentum $P_F$ at $R_{\text{star}}$ as a function of the mass.

(9) To estimate GR corrections, note that they are given by powers of $g = G_N M/R$; Newtonian gravity is exact to first order $g$, while GR effects are of higher order, at least $g^2$. What is the value for $g$ (in natural units) for our Sun?

(10) Is there a range of mass $M$ and radius $R$ (for any $T$) where GR corrections are large enough to modify the result by at least 1%?

**1.6 Neutron stars.**

Neutron stars are very condensed objects, essentially gigantic nuclei, where all four fundamental interactions come into play. In this exercise, we make a crude approximation and assume the neutron star to be fully supported by the neutron degeneracy pressure and use the Newtonian approximation for gravity.

(1) Convince yourself that (and explain why) the critical mass beyond which a neutron star collapses is of the order of the Chandrasekhar mass $M_C$.

(2) The radius of a neutron star $R_{\text{NS}}$ may be estimated by $R_{\text{NS}} = R_{\text{star}}(M = M_C, m_e \to m_n)$, where $m_n$ is the neutron mass, with $R_{\text{star}}$ given in (1.16). What is the numerical value (in kilometers) for a neutron star of mass $M_C$?

(3) What is the Fermi energy $\mathcal{E}_F$ of neutrons for non-relativistic or relativistic neutrons?

(4) Compare the neutron star Fermi energy with the binding energy of the iron nucleus and with the binding energy of quarks within a neutron. Do your results justify the name ‘neutron star’?

(5) Neutrons have a magnetic dipole moment. Assuming the neutron star to be a collection of neutrons of aligned spins and dipole moments, compute the spin and magnetic field of the star at its surface.

(6) Check whether GR corrections are significant for a neutron star.

**1.7 Black hole entropy versus stellar entropy.**

Consider a black hole and a star of five solar masses, $M \sim 10^{31}$ kg.

(1) Compute the black hole radius $r_h$ (cf. Exercise 1.3) and the black hole entropy $S_{\text{BH}}$ (1.7).

(2) Compare the latter with the entropy of a star, assuming it scales extensively, i.e. with the stellar volume.

(3) For which order of magnitude of the mass $M$ would black hole and stellar entropies coincide?

# 2 Black Hole Solutions and Basic Properties

**Abstract**

In this chapter, we review classic black hole solutions, starting with Schwarzschild and its basic properties, including isometries and ADM charge, in Sect. 2.1. In Sect. 2.2, we analyze particle probes and geodesics in a Schwarzschild background. The maximal extension, near horizon, and causal structure, captured by Carter–Penrose diagrams, is presented in Sect. 2.3. Thereafter, we generalize from Schwarzschild black holes to Reissner–Nordström (Sect. 2.4), Kerr (Sect. 2.5), Kottler and Kerr (A)dS (Sect. 2.6), Plebanski–Demianski (Sect. 2.7), and Vaydia (Sect. 2.8).

## 2.1 Schwarzschild Metric, Basic Facts, and Analyses

As reviewed in the previous chapter, the Schwarzschild geometry was the first non-trivial exact solution to the Einstein equations (1.4) for vanishing cosmological constant and matter. The Schwarzschild metric is the most general spherically symmetric solution of the vacuum Einstein equations $R_{\mu\nu} = 0$. In Schwarzschild coordinates, it reads

$$\mathrm{d}s^2 = -f(r)\,\mathrm{d}t^2 + \frac{\mathrm{d}r^2}{f(r)} + r^2\mathrm{d}\Omega^2 \tag{2.1}$$

where

$$\mathrm{d}\Omega^2 = \mathrm{d}\theta^2 + \sin^2\theta\,\mathrm{d}\phi^2 \qquad\qquad f(r) = 1 - \frac{2G_{\text{N}}M}{r}\,. \tag{2.2}$$

The coordinates are interpreted as time $t \in \mathbb{R}$, radius $r \in (0, \infty)$, polar angle $\theta \in [0, \pi]$, and azimuthal angle $\phi \sim \phi + 2\pi$. This is a one-parameter family of solutions, specified by the non-negative mass parameter $M$. It is the GR analog of the Coulomb solution of Maxwell's theory. While it describes also black holes, it should be stressed that the Schwarzschild solution is the correct exterior solution to any spherically symmetric gravitational source.



D. Grumiller and M. M. Sheikh-Jabbari, *Black Hole Physics*, Graduate Texts in Physics,
https://doi.org/10.1007/978-3-031-10343-8_2

### 2.1.1 Symmetries and Killing Vectors

The metric (2.1) is invariant under time-reversal $t \to -t$, time translations, $t \to t + t_0$, $t_0 \in \mathbb{R}$, and spherical rotations. These properties can be stated covariantly using the language of Killing vectors and isometries of the metric.

While we assume the reader is familiar with these concepts, let us still remind ourselves what an isometry and a Killing vector are. Given some vector field(s) $\xi_{(n)}$ (where $n$ is some counting index), they generate isometries if the Lie variation of the metric along them vanishes.

$$\mathcal{L}_{\xi_{(n)}} g_{\mu\nu} := \xi^\lambda_{(n)} \partial_\lambda g_{\mu\nu} + g_{\mu\lambda} \partial_\nu \xi^\lambda_{(n)} + g_{\nu\lambda} \partial_\mu \xi^\lambda_{(n)} = 0 \quad \Leftrightarrow \quad \nabla_\mu \xi_{(n)\,\nu} + \nabla_\nu \xi_{(n)\,\mu} = 0. \tag{2.3}$$

Vector fields with these properties are called Killing vectors. The equation on the right in (2.3) is the Killing equation.

The Schwarzschild isometries are generated by four real Killing vector fields

$$\xi_{(0)} = \partial_t \qquad \xi_{(1)} = \partial_\phi \qquad \xi_{(2)} + i\xi_{(3)} = e^{i\phi}\big(\partial_\theta + i \cot\theta\, \partial_\phi\big)\,. \tag{2.4}$$

The total isometry group is $\mathbb{R} \times SO(3)$, i.e. the Schwarzschild solution has time translation symmetry and is spherically symmetric. The Killing vector $\xi_{(0)}$ is timelike for $r > 2G_{\text{N}}M$, becomes null at $r = 2G_{\text{N}}M$, and is spacelike for $r < 2G_{\text{N}}M$. The spherical Killing vectors $\xi_{(i)}$ are spacelike in the whole range of coordinates. The Killing vectors $\xi_{(0)}$ and $\xi_{(1)}$ are examples of coordinate Killing vectors, meaning that the isometries generated by them are manifest in the Schwarzschild metric (2.1), (2.2) by inspection, since all metric coefficients are independent of $t$ and $\phi$.

**> Stationary, static, axisymmetric, and circular spacetimes**

Geometries with an asymptotically timelike Killing vector field are called *stationary*. The timelike Killing vector may become spacelike or null in the interior of the geometry, as it happens for the Schwarzschild case discussed above. For stationary spacetimes, one can choose a time coordinate $t$ such that the timelike Killing vector becomes the coordinate Killing vector $\partial_t$.

If a stationary geometry is also time-reversal symmetric, it is called *static*. For static spacetimes, one can adopt a coordinate system in which $\partial_t$ is the timelike Killing vector and that time-reversal is given by $t \to -t$. See Exercise 2.3 for more details. The Schwarzschild geometry (2.1) is hence a static solution.

Stationary and axisymmetric spacetimes which have two Killing vectors $\xi_t = \partial_t, \xi_\phi = \partial_\phi$ are called *circular* if in appropriate coordinate system they have another double reflection symmetry $(t, \phi) \to (-t, -\phi)$; see Exercise 2.4 for more.

### 2.1.2 Flamm Diagram

To get the first visual sense of the Schwarzschild geometry, one may look at some of its 2- or 3-dimensional sections. Given that the Schwarzschild solution is spherically symmetric, a natural choice is to suppress the angular part and study the 2-dimensional Lorentzian part spanned by the coordinates $t$ and $r$. We shall do this later in the form of various diagrams, including Carter–Penrose diagrams.

Here, we consider instead a constant time slice (which time we take is irrelevant due to staticity) at some fixed value of the polar angle, say, $\theta = \pi/2$,

$$\mathrm{d}s^2 = \frac{\mathrm{d}r^2}{1-\frac{r_h}{r}} + r^2\mathrm{d}\phi^2 \qquad\qquad r_h := 2G_{\mathrm{N}}M \tag{2.5}$$

which may be embedded into a 3-dimensional flat space for visualization. Let $(r, \phi, z)$ span a flat space in cylindrical coordinates and consider the 2-dimensional surface $z = z(r)$ in it such that

$$z = 2\sqrt{r_h}\sqrt{r - r_h}\,. \tag{2.6}$$

Then the induced metric on the surface is the same as (2.5). Equation (2.6) defines a parabola, the rotated version of which is depicted in Fig. 2.1. This rotational paraboloid covers the region $r \geq r_h$ and gives a vague sense of curvature in the Schwarzschild geometry. However, as we shall see below, physically relevant aspects of the causal structure are better captured by Carter–Penrose diagrams, so let us move on.

### 2.1.3 Singularities, Asymptotic, and Near Horizon Behavior

The Schwarzschild solution is asymptotically flat, in the sense $\lim_{r\to\infty} f(r) = 1$. As we will discuss in the coming chapters in more detail, the notion of asymptotic flatness should be defined more precisely, specifying how each of the metric components falls off. For example, if the flat Minkowski metric in the spherical coordinates is denoted by $\bar{g}_{\mu\nu}$ and its inverse by $\bar{g}^{\mu\nu}$, one may ask how different components of $h^{\mu}{}_{\nu} = \bar{g}^{\mu\alpha}(g_{\nu\alpha} - \bar{g}_{\nu\alpha})$ approach zero at large $r$. In the case of the Schwarzschild solution, the leading large $r$ terms are

$$h^t{}_t = -h^r{}_r = -\frac{2G_{\mathrm{N}}M}{r} + O(r^{-2})\,. \tag{2.7}$$

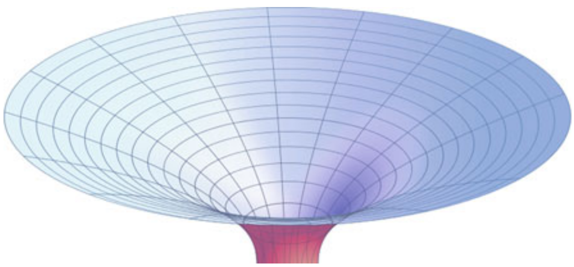

**Fig. 2.1** Flamm diagram showing a constant time slice of the Schwarzschild black hole at fixed polar angle

We will argue below that for asymptotically flat static solutions, the quantity $-\frac{r}{2G_{\mathrm{N}}}h^t{}_t$ may be identified with the physical mass associated with the solution. Alternatively, one could provide a notion of asymptotic flatness based on how Riemann curvature approaches zero asymptotically. The metric- and curvature-based notions of asymptotic flatness can differ; see the opening of Chap. 3.

The metric (2.1) has three singular loci: $r = \infty$, $r = r_h = 2G_{\mathrm{N}}M$ and $r = 0$. To establish whether these loci are genuine singularities or singularities that arise merely as a consequence of the chosen coordinates, one should focus on coordinate-independent quantities, such as scalar invariants of the Riemann tensor. If at least one of the scalar invariants of the Riemann tensor is singular, the locus where this happens is called 'curvature singularity'. See [147] and references therein for a classification of all possible curvature invariants.

The singularity at $r = \infty$ is the usual behavior of Minkowski space in spherical coordinates and is not associated with strong curvature effects. The fact that the metric and distances blow up at $r = \infty$ is a manifestation of the asymptotic region of the spacetime.

Regarding the other two singular loci, consider the Kretschmann scalar,

$$R^{\mu\nu\alpha\beta}R_{\mu\nu\alpha\beta} = \frac{12r_h^2}{r^6}. \tag{2.8}$$

The Kretschmann scalar is finite at $r = r_h$ and tends to $+\infty$ at $r = 0$. This shows that there is a singularity at $r = 0$, and it indicates that there might not be anything genuinely singular about the locus $r = r_h$. We refer to the locus $r = r_h$ as 'horizon' and will discuss some of its properties in Sect. 2.3.3. A more precise definition of a horizon will be provided in Sect. 3.1 in the next chapter.

To check the smoothness of the geometry near the horizon $r \approx r_h$, we expand the metric around it by first introducing a new radial coordinate

$$r = r_h + \frac{1}{4r_h}\rho^2 \tag{2.9}$$

and then keeping only the leading powers of this new coordinate $\rho$

$$\mathrm{d}s^2 = \big(-\kappa^2\rho^2\mathrm{d}t^2 + \mathrm{d}\rho^2 + (2G_{\mathrm{N}}M)^2\mathrm{d}\Omega^2\big)\big(1 + \mathcal{O}(\rho^2)\big) \tag{2.10}$$

with so-called surface gravity (for a proper definition, see the next chapter)

$$\kappa = \frac{1}{4G_{\mathrm{N}}M}. \tag{2.11}$$

Neglecting higher-order terms, the above metric is a direct product of 2-dimensional Minkowski space (spanned by $t$ and $\rho$) and a Euclidean 2-sphere. Minkowski space appears here in Rindler coordinates, which is the coordinate system used by an observer accelerated with uniform acceleration $\kappa$. While the higher-order terms in

$\rho$ are essential to make (2.10) a vacuum solution, to demonstrate smoothness of the geometry at $r = r_h$ only the displayed terms are relevant.

So far we have not gained much, since the metric (2.10) still is singular at $\rho = 0$. To eliminate this singularity, we change coordinates $T = \rho \sinh(\kappa t)$ and $X = \rho \cosh(\kappa t)$, in terms of which the metric above reads

$$\mathrm{d}s^2 = -\mathrm{d}T^2 + \mathrm{d}X^2 + (2G_\mathrm{N} M)^2\, \mathrm{d}\Omega^2 + \cdots \tag{2.12}$$

where the ellipsis denotes subleading terms. General $\rho =$ const. lines are hyperbolas since $X^2 - T^2 = \rho^2$. The locus $\rho = 0$ corresponds to the degenerate hyperbola $T^2 = X^2$, consisting of two intersecting 45°-lines. The metric (2.12) has clearly no singular behavior at $\rho = 0$. This finally proves by construction that the singularity in the Schwarzschild metric (2.1) with (2.2) at $r = r_h = 2G_\mathrm{N} M$ is merely an artifact of the coordinates used.

### 2.1.4 ADM Mass and Angular Momentum

There are various ways to define mass and angular momentum associated with a background geometry, some of which we shall discuss at length in later chapters. Perhaps the simplest one is the Arnowitt–Deser–Misner (ADM) method [148, 149]. The ADM prescription works well for stationary asymptotic flat geometries which have the following general asymptotic form

$$\mathrm{d}s^2 = -\mathrm{d}t^2 + \mathrm{d}r^2 + r^2 \mathrm{d}\Omega^2 + \frac{2G_\mathrm{N} M_\mathrm{ADM}}{r}\mathrm{d}t^2 - \frac{2G_\mathrm{N} J_\mathrm{ADM}}{r}\sin^2\theta\, \mathrm{d}t\mathrm{d}\phi + \cdots \tag{2.13}$$

where the ellipsis denotes subleading terms that vanish sufficiently fast for $r \to \infty$. Different components of the metric may have different subleading behavior, depending on the solution. ADM mass and angular momentum are defined as

$$M_\mathrm{ADM} := \frac{1}{2G_\mathrm{N}} \lim_{r\to\infty} (g_{tt} + 1) r \qquad\qquad J_\mathrm{ADM} := -\frac{1}{G_\mathrm{N}} \lim_{r\to\infty} \frac{r\, g_{t\varphi}}{\sin^2\theta}\,. \tag{2.14}$$

The sign in the definition of the ADM angular momentum $J_\mathrm{ADM}$ is conventional.

The ADM prescription may seem a bit ad hoc, but it can be put in a more robust setting through the $3+1$ ADM decomposition [150]; see Exercise 2.6. In Chap. 5, we provide some other, more covariant, definitions for black hole mass, angular momentum, and other charges, which reduce to the ADM ones for the asymptotic flat cases. For the Schwarzschild solution, the mass parameter $M$ coincides with the ADM mass. We shall often refer to it as 'black hole mass'.

### 2.1.5 Infinite Redshift Surface

The coordinate $t$ is the time as measured by the asymptotic observer, who almost sees Minkowski space. Suppose such an observer measures a time interval $\Delta t$. The clock of an observer sitting at some fixed finite value of $r_0$ measures time intervals $\Delta t_0$ with a redshift factor relative to the asymptotic observer, $\Delta t_0 = \sqrt{f(r)}\,\Delta t$. This gravitational redshift is a direct consequence of the EP. For instance, the ratio between the frequencies of an emitter at $r = r_A$ and a receiver at $r = r_B$ is given by the inverse of the associated redshift factors of time intervals, $\sqrt{f(r_B)}/\sqrt{f(r_A)}$. In particular, if the receiver is the asymptotic observer, $f(r_B \to \infty) = 1$, the frequency they observe is redshifted, $\omega_B = \omega_A\sqrt{f(r_A)}$, since $f(r) < 1$ for finite $r$. If the emitter is close to $r = r_h$ the redshift factor tends to zero. That is, a very large frequency (or energy) emitted from the $r \approx r_h$ region will correspond to a small frequency (or energy) at asymptotic infinity.

Above, we compared two fiducial observers (*fido*s) at two constant radii. One may compare a free-fall observer to a *fido* at the same radius or two free-fall observers at different radii. The EEP implies that a free-fall observer should locally see a flat space, though in a frame boosted with respect to the asymptotic observer. Thus, she should measure frequencies and energies as the asymptotic observer does with a Doppler shift. The frequencies measured by two free-fall observers $A, B$ with two boost factors with respect to the asymptotic observer $\gamma_A, \gamma_B$ are related as $\gamma_A^{-1}\omega_A = \gamma_B^{-1}\omega_B$.

Therefore, the free-fall observer will receive signals of increasing frequencies as she moves toward $r = 3r_h$ and decreasing frequencies in the region $r_h < r < 3r_h$, so that at $r = r_h$ she measures the same frequency as the asymptotic observer has sent. Similarly, one may compare a free-fall and a *fido* at the same radius. See Exercise 2.10 for more quantitative analysis.

## 2.2 Particle Probes and Geodesics

One of the slogans by Wheeler is ‘geometry tells matter how to move’. More precisely, given some metric one can determine the movement of free-fall test particles in that geometry. The key assumption, contained in the word ‘test particle’, is that we probe spacetime in such a way that we can neglect the backreactions of the probe. For instance, we could send a spaceship on a free-fall trajectory orbiting a planet or consider a small planet orbiting a star, or a star orbiting a galaxy; however, the test particle assumption becomes inadequate when the probe-approximation no longer is good, such as for black hole binary systems where both partners have comparable masses, or for probes that are too extended so that the point particle approximation no longer is accurate.

The test particles can be massive or massless. In the absence of non-gravitational forces, the EEP states that their trajectories follow timelike or null geodesics, respectively.

Consider a geodesic path $\gamma$ parameterized by $x^\mu(\lambda)$ described by the geodesic equation (1.1). In the presence of symmetries, it is often simpler to start from the geodesic action

$$I_{\text{particle}} = \int_\gamma \mathrm{d}\lambda\, \mathcal{L}_{\text{particle}} \qquad \mathcal{L}_{\text{particle}} = \sqrt{|g_{\mu\nu}\dot{x}^\mu \dot{x}^\nu|} \tag{2.15}$$

rather than calculating all the Christoffel symbols required for (1.1). Here, $\dot{x}^\mu = \frac{\mathrm{d}x^\mu}{\mathrm{d}\lambda}$ is the velocity with respect to the geodesic parameter $\lambda$. The geodesic length is $I_{\text{particle}}$. The action (2.15) enjoys 1-dimensional diffeomorphism invariance, $\lambda \to f(\lambda)$, along the particle worldline (see Exercises 2.7 and 2.8 for more discussion). On solutions of EOM $\mathcal{L}_{\text{particle}} = \text{const}$. Therefore, one may choose an affine parameterization such that

$$g_{\mu\nu}\dot{x}^\mu \dot{x}^\nu = \sigma \tag{2.16}$$

where $\sigma = +1$ ($\sigma = 0$) [$\sigma = -1$] for spacelike (null) [timelike] geodesics. Unless mentioned otherwise, we always adopt this parameterization.

Let us now focus on geodesics of the Schwarzschild solution (2.1), (2.2). To simplify matters, we start by searching for constants of motion. Among the four Killing vectors (2.4) there are two mutually commuting ones, $\partial_t$ and $\partial_\phi$. Applying Noether's theorem to (2.15) for Schwarzschild background yields two conserved charges associated with these Killing vectors, respectively, called $E$ and $J$ [cf. (2.123) in Exercise 2.8]; the latter is the angular momentum per unit mass of the test particle and the former is related but not identical to the total energy. The third one, $\sigma$, comes from reparametrization invariance along the geodesic and was already implemented in (2.16). The spherical $SO(3)$ symmetry of the action implies that motion in the Schwarzschild geometry is always planar. This symmetry can be exploited to rotate this plane into the equator so that any geodesic curve has a constant polar angle $\theta = \pi/2$.

We then have three variables $(t, r, \phi)$ and three independent constants of motion $(\sigma, E, J)$

$$-f(r)\dot{t}^2 + \frac{\dot{r}^2}{f(r)} + r^2\dot{\phi}^2 = \sigma \tag{2.17a}$$

$$f(r)\dot{t} = E \tag{2.17b}$$

$$r^2\dot{\phi} = J \tag{2.17c}$$

where $f(r) = 1 - \frac{r_h}{r}$. This mechanics problem is integrable, since we have the same number of first order variables as constants of motion. Solving the last two equations for $\dot{t}$, $\dot{\phi}$ and inserting into the first one obtains

$$\dot{r}^2 + J^2\frac{f(r)}{r^2} - \sigma f(r) = E^2\,. \tag{2.18}$$

One may also define the so-called path equation, by taking $u = 1/r(\phi)$,

$$u'^2 + u^2 f(u) - \frac{\sigma}{J^2} f(u) = \frac{E^2}{J^2} \tag{2.19}$$

where $u' = \mathrm{d}u/\mathrm{d}\phi = -\dot{r}/J$. Solving the path equation yields generalized Kepler orbits (which includes general relativistic effects) for the motion of test particles around spherically symmetric mass distributions.

Inserting (2.2) into (2.18) for $\sigma = -1$ yields the energy conservation relation

$$\frac{\dot{r}^2}{2} - \frac{G_{\mathrm{N}} M}{r} + \frac{J^2}{2r^2} - \frac{J^2 G_{\mathrm{N}} M}{r^3} = \frac{E^2 - 1}{2} \tag{2.20}$$

where the first term is the radial kinetic energy (per mass unit), the second term the Newton potential, the third term the centrifugal potential, and the fourth term the GR correction; Newtonian gravity would lead to the same equation as above, except for the fourth term, which is absent there. The right-hand side is a constant of motion, the total energy (per mass unit). The precise form of the second term a posteriori justifies calling $M$ 'mass parameter', as this is exactly its role in Newtonian gravity. Let us explore now null and timelike geodesics in some detail.

### 2.2.1 Null Geodesics

For $\sigma = 0$, the energy conservation equation (2.18) and the path equation (2.19) become

$$\frac{\dot{r}^2}{2} + \frac{J^2}{2r^2} - \frac{J^2 G_{\mathrm{N}} M}{r^3} = \frac{E^2}{2} \qquad\qquad u'^2 + u^2(1 - 2G_{\mathrm{N}} M u) = \frac{E^2}{J^2} \tag{2.21}$$

with the latter only depending on the ratio $E/J$. To get physical intuition, it is useful to interpret the energy conservation equation (2.21) mechanically in terms of a particle moving in a 1-dimensional effective potential so that energy conservation reads

$$\frac{\dot{r}^2}{2} + V_{\mathrm{eff}}(r) = E_{\mathrm{eff}} = \text{const.} \tag{2.22}$$

with

$$V_{\mathrm{eff}}(r) = \frac{J^2}{2r^2} - \frac{J^2 G_{\mathrm{N}} M}{r^3} \tag{2.23}$$

and $E_{\mathrm{eff}} = \frac{E^2}{2}$. The potential (2.23) is plotted in Fig. 2.2. One can imagine placing a ball somewhere in the potential and then easily visualize how the trajectory of this ball will be. For instance, placing a ball at rest to the right of the maximum will lead to the ball rolling off to infinity, corresponding to a trajectory where the corresponding light ray escapes the black hole; by contrast, placing a ball to the left of the maximum

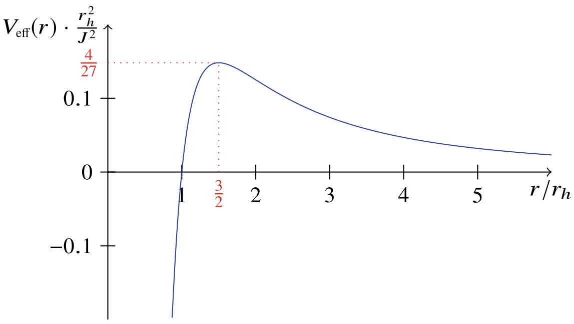


**Fig. 2.2** Effective potential (2.23) (divided by $J^2$). We set $2G_{\text{N}}M = 1$ so that $r$ and $V_{\text{eff}}(r)/J^2$ are given in units of $r_h$. The presence of a maximum shows there is an unstable circular orbit, the photon-sphere. The absence of a minimum shows there are no stable circular orbits. The fact the potential tends to $-\infty$ at small $r$ means that light rays can be captured by the black hole even when they do not travel radially toward its center, thereby anticipating black hole shadows

means it will roll quickly toward the center, corresponding to a light ray captured by the black hole.

We discuss now different classes of geodesics quantitatively.

## > Radial geodesics

For vanishing angular momentum, $J = 0$, (2.17) for $\sigma = 0$ yield

$$\dot{r} = \pm\left(1 - \frac{2G_{\text{N}}M}{r}\right)\dot{t}\,. \tag{2.24}$$

Integration yields

$$t = \pm r_* := \pm \int_{r_0}^{r} \frac{\mathrm{d}\tilde{r}}{f(\tilde{r})} = \pm\left[r - r_0 + r_h \ln \frac{r - r_h}{r_0 - r_h}\right]. \tag{2.25}$$

One may use $r_*$ as a new radial coordinate instead of $r$ in terms of which radial null geodesics take the simple form $t \pm r_*$ =constant. This is called the Regge–Wheeler coordinate. As (2.25) shows, $r_*$ is defined in the region $r > r_h$ (or $r < r_h$) if $r_0 > r_h$ (or $r_0 < r_h$). For large $r$, the Regge–Wheeler coordinate coincides almost with the Schwarzschild radial coordinate, $r_* \simeq r$, while for the region $r \sim r_h$ the Regge–Wheeler radial coordinate is dominated by the log piece. To emphasize the log behavior and the ensuing very slow change in $r_*$ compared to the time coordinate $t$, $r_*$ is also called tortoise coordinate.

A physical consequence of the slow-down inherent to the tortoise coordinate is that an asymptotic observer will never see stuff falling through $r = r_h$; instead, everything is frozen (and, as we discussed, infinitely red-shifted) at that radius.

Radial geodesics are useful mostly for theoretical purposes. For black hole observations, generic geodesics are more relevant, in particular for observations from accretion disk physics, where rays of electromagnetic waves are emitted in a diverse frequency range from radio to X- and $\gamma$-rays. Before dropping all assumptions, we consider another important special case.

### Circular null orbits and photon-sphere

Circular paths require $u'' = u' = 0$, which happens at $r = 3r_h/2$ and for $J/E = 3\sqrt{3}r_h/2$. This radial value is referred to as 'photon-sphere'.

Any path with $J/E < 3\sqrt{3}r_h/2$ will eventually end passing the horizon $r = r_h$ and falling into the black hole. For $J/E > 3\sqrt{3}r_h/2$, the paths are not closed and always remain in $r > 3r_h/2$ region.

This means that orbits on the photon-sphere are unstable. Kicking a photon on such a circular orbit around the black hole will either lead to its escape to infinity or its capture by the black hole.

---

After the two important special cases above, we now consider generic solutions to (2.21). A detailed analysis is left as an exercise (Exercise 2.12). Here we summarize the main results.

### Generic orbits, deflection of light, and lensing

The trajectories of light rays at a given dimensionless impact parameter $b^{-1} := \frac{Er_h}{J}$ are governed by (2.19) which may be written as

$$\hat{u}'^2 + \left(\hat{u}^3 - \hat{u}^2\right) = \frac{1}{b^2} - \frac{4}{27}, \qquad \hat{u} := \frac{2}{3} - r_h u = \frac{2}{3} - \frac{r_h}{r}. \tag{2.26}$$

If $b > \frac{3\sqrt{3}}{2}$ and we start in the $\hat{u} > 0$ region (corresponding to $r > 3r_h/2$), the trajectory has a minimum $r$ for which $\hat{u}' = 0$ and happens at $\hat{u}^3_{\text{min}} - \hat{u}^2_{\text{min}} = 1/b^2 - 4/27$. These are deflected light trajectories and are typical light paths around a black hole. The light flying around a black hole would be lensed and as a result, objects seen from behind a black hole (or any gravity source) are perceived as bigger than they are.

If $b > \frac{3\sqrt{3}}{2}$ and we start in the $\hat{u} < 0$ region (corresponding to $r < 3r_h/2$), the trajectories fall into the black hole and end up in $r < r_h$ region.

As we decrease the impact factor $b$, the deflection angle increases and if the light ray becomes closer than the photon-sphere $r = 3r_h/2$ to the black hole it would be trapped. If $b < \frac{3\sqrt{3}}{2}$ (low impact parameters), the light ray always passes through the horizon and falls into the black hole.

---

### 2.2.2 Timelike Geodesics and Particle Orbits

The dynamics of timelike geodesics is also captured by (2.22). The only difference to null geodesics is that the effective potential following from (2.20) has an additional $1/r$ term.

$$V_{\text{eff}}(r) = -\frac{G_N M}{r} + \frac{J^2}{2r^2} - \frac{J^2 G_N M}{r^3}. \tag{2.27}$$

The potential (2.27) is plotted in Fig. 2.3. Again, one can use mechanics intuition to analyze different possibilities for trajectories of timelike test particles. The main difference in the effective potential for null geodesics plotted above in Fig. 2.2 is the possible presence of a minimum, which means that stable circular orbits are possible. Moreover, while for null geodesics there was a universal shape of the effective potential, for timelike geodesics the shape of the effective potential depends in an essential way on the angular momentum $J$.

In this part, we analyze timelike radial paths and circular orbits; a more detailed analysis of generic orbits is deferred to Exercise 2.12. Again we start with simple special cases.

**> Radial geodesics**

Setting $\sigma = -1,\ J = 0$ in the energy conservation equation (2.20) yields

$$\dot{r}^2 = v_\infty^2 - \frac{r_h}{r} \qquad v_\infty^2 = E^2 - 1 \tag{2.28}$$

which describes radial timelike geodesics. Since for $J = 0$ the GR correction in (2.20) drops out, the motion is identical to the Newtonian case. If $v_\infty^2 \geq 0$, the geodesics can reach $r = \infty$ where $v_\infty$ is the velocity of the particle at infinity. If $v_\infty^2 < 0$ the particle does not reach infinity. The motion is like a projectile radially shot off starting at some $r_0$, with initial velocity (as measured by the particle itself) $v_0^2 = v_\infty^2 - \frac{r_h}{r_0}$. If $v_0$ is positive, the projectile reaches the maximum distance $r_{\text{max}} =$

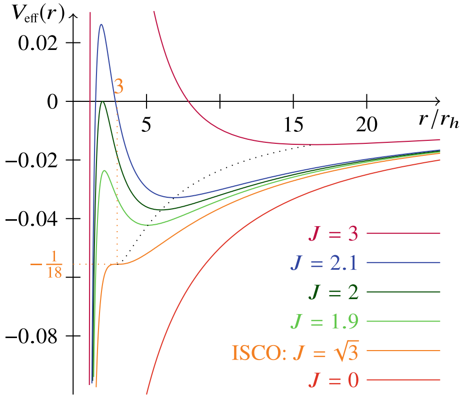


**Fig. 2.3** Effective potential (2.27). We set $2G_N M = 1$ and used the six values $J = 0$ (red), $J = \sqrt{3}$ (orange), $J = 1.8$ (green), $J = 2$ (dark green), $J = 2.1$ (blue), and $J = 3$ (purple). The critical value $J = \sqrt{3}$ leads to the ISCO; see the main text. The dotted black curve shows the locations of the minima of the potential (for different values of $J$) where stable circular orbits arise

$\frac{r_h}{v_\infty^2}$ before radially falling back into the black hole. It smoothly passes through the radius $r = r_h$ at a finite proper time, while the coordinate time $t$ blow up (see Exercise 2.13).

---

Consider now circular orbits around the black hole. While in Newtonian gravity stable circular orbits can exist at any value of the radius, the GR correction implies that there is the smallest value of the radius where circular orbits are stable. As this orbit is of phenomenological significance, we highlight it here.

## > Innermost Stable Circular Orbit (ISCO)

Circular geodesics that are marginally (un)stable obey simultaneously $\dot{r} = \ddot{r} = 0$. In terms of the effective potential (2.27), we are looking for solutions for the radius $r_{\text{ISCO}}$ and angular momentum $J_{\text{ISCO}}$ of $V_{\text{eff}}(r_{\text{ISCO}})' = V_{\text{eff}}(r_{\text{ISCO}})'' = 0$. Subtracting these two quadratic equations

$$r_{\text{ISCO}}^2 - \frac{J_{\text{ISCO}}^2}{G_{\text{N}} M} r_{\text{ISCO}} + 3J_{\text{ISCO}}^2 = 0 = r_{\text{ISCO}}^2 - \frac{3J_{\text{ISCO}}^2}{2G_{\text{N}} M} r_{\text{ISCO}} + 6J_{\text{ISCO}}^2 \tag{2.29}$$

from each other and dividing by $J_{\text{ISCO}}^2$ establishes the ISCO radius

$$r_{\text{ISCO}} = 6G_{\text{N}} M = 3r_h \,. \tag{2.30}$$

Inserting this result into either of the (2.29) and solving for $J_{\text{ISCO}}$ yields the critical angular momentum

$$J_{\text{ISCO}} = \pm\sqrt{3}\, r_h \,. \tag{2.31}$$

The Schwarzschild ISCO is located at twice the photon-sphere radius. Unstable circular orbits are possible for radii between the photon-sphere and the ISCO. Stable circular orbits are possible for all radii greater than the ISCO radius (2.30) or, equivalently, for all angular momenta with absolute values greater than the one of the ISCO angular momentum (2.31). This can be seen explicitly from the shape of the effective potential for various values of the angular momentum in Fig. 2.3.

---

Having discussed the two most relevant special cases, we consider again the generic situation and focus on one particular application, the perihelion shift, which is one of the classic tests of the Schwarzschild solution, and of GR.

## > Generic orbits and perihelion shift

Numerical integration of the energy conservation equation (2.22) with the effective potential (2.27) for arbitrary values of $E$ and $J$ is straightforward, but not particularly illuminating. Studying some aspects of generic geodesics is deferred to Exercise 2.13.

Here, we review a slick derivation of perihelion shifts of nearly circular orbits (to reduce clutter, we set $G_{\rm N} = 1$ in this derivation). The motion on such orbits is approximately a radial harmonic oscillator and an angular harmonic oscillator. When their frequencies coincide there is no perihelion shift, since after each angular orbit of $2\pi$ the radial orbit will be back to its initial state. This is no longer the case when these two frequencies differ. The approximate radius of the nearly circular orbit is given by the larger solution of $V_{\rm eff}(r)' = 0$

$$r_\pm = \frac{J^2}{2M}\Big(1 \pm \sqrt{1-\frac{12M^2}{J^2}}\Big). \tag{2.32}$$

The frequency of the radial harmonic oscillator is given by

$$\omega_r^2 = V_{\rm eff}(r_+)'' = \frac{1}{r_+^4}\big(3J^2 - 2Mr_+ - 4Mr_-\big)\,. \tag{2.33}$$

The frequency of the angular harmonic oscillator is given by

$$\omega_\phi^2 = \dot\phi^2 = \frac{J^2}{r_+^4}\,. \tag{2.34}$$

In Newtonian theory radial and angular frequency are equal to each other, which implies that nearly circular orbits do not have a perihelion shift.[1] Comparing the frequencies (2.33) and (2.34) in the limit of large angular momentum yields

$$\omega_r = \omega_\phi\left(1-\frac{12M^2}{J^2}\right)^{1/4} = \omega_\phi\left(1-\frac{3M^2}{J^2} + \mathcal{O}(M^4/J^4)\right) \tag{2.35}$$

which allows establishing the approximate precession rate

$$\Delta\phi = 2\pi(\omega_\phi - \omega_r) \approx \frac{6\pi M^2}{J^2} \approx \frac{6\pi M}{A(1-e^2)}\,. \tag{2.36}$$

A classic way to express the precession rate is in terms of eccentricity $e$ and aphelion $A$ of the elliptic orbit, using the Newtonian formula $J^2/M = A(1-e^2)$, which we did in the last equality above. Inserting the mass of the Sun, $M \approx 2\cdot 10^{30}$ kg, the aphelion of Mercury, $A \approx 7\cdot 10^{10}$ m, and its eccentricity $e \approx 0.2$ yields approximately $\Delta\phi \approx 0.1$ arcseconds/revolution. Since Mercury has around 415 revolutions/century, we get roughly $\Delta\phi \approx 42$ arcseconds/century (a more precise result is $\Delta\phi \approx 42.97$ arcseconds/century), agreeing with the observed perihelion shift

[1] This statement is true in a two-body system. When other bodies are present perihelion shifts do arise, but they can be treated perturbatively within Newtonian gravity and were accounted for already in the nineteenth century.

$\Delta_{\text{obs}}\phi = (575.310 \pm 0.002)$ arcseconds/century [151] upon subtracting the contributions from Newtonian corrections due to other solar bodies, which gives $\Delta\phi_{\text{Newton}} \approx$ 532 arcseconds/century and thus $\Delta_{\text{obs}}\phi - \Delta\phi_{\text{Newton}} \approx 43.31$ arcseconds/century.

### 2.2.3 Eddington–Finkelstein Coordinates

As mentioned when introducing the tortoise coordinate, it takes a logarithmically long time for a radial null ray to pass through the surface $r = r_h$ from an asymptotic observer's perspective. However, for the null ray itself, it takes no time to pass beyond $r = r_h$. This suggests that one can use the null directions to construct coordinate systems which remove (part of) the coordinate singularity at $r = r_h$. The perhaps simplest example for such coordinates is Eddington–Finkelstein (EF) coordinates.

EF coordinates come in two versions, in- and outgoing, since we have in- and outgoing null coordinates

$$v = t + \int \frac{\mathrm{d}r}{f(r)} \qquad u = t - \int \frac{\mathrm{d}r}{f(r)}\,. \tag{2.37}$$

The Schwarzschild metric in ingoing EF coordinates $v, r, \theta, \phi$ takes the form

$$\mathrm{d}s^2 = -f(r)\,\mathrm{d}v^2 + 2\mathrm{d}r\mathrm{d}v + r^2\,\mathrm{d}\Omega^2 \tag{2.38}$$

where $v \in (-\infty, +\infty),\ r > 0$. Here, we have already extended the range of $v, r$ to also cover the region $r < r_h$. As we see at zeros of $f(r)$, we find a smooth geometry. At $f = 0$ both $r$ and $v$ directions become null, cf. (2.37). Moreover, $\partial_v$ which is a globally defined Killing vector field is spacelike (timelike) in the region $f < 0$ ($f > 0$), whereas the vector $\partial_r$ vector is always null, future-oriented, and normal to $\partial_v$. The $v, r$ coordinate system is called ingoing EF coordinate because $v =$ const. lines at constant angles correspond to ingoing light rays. As we will discuss in the next subsection, this coordinate system is useful for exploring the causal structure of spacetime.

Nevertheless, ingoing EF coordinates are still singular on half of the degenerate hyperboloid discussed around (2.12), so one needs to supplement them with other coordinate patches for global discussions. A complementary patch is provided by outgoing EF coordinates. They are defined similarly, using the outgoing null direction $u$ and $r$ as coordinates. Analogous ideas may be employed to define Gaussian null coordinates (cf. Exercise 2.14).

## 2.3 Maximal Extensions and Causal Diagrams

Our geodesic analysis indicates that there are observers (for instance, freely falling ones) who can pass through $r = r_h$ radius without feeling any singular behavior. This means one should be able to find coordinate systems in which metric components are explicitly smooth around $r = r_h$.

Regardless of which coordinate system is being used, one can investigate the geodesics of test particles and check whether they hit the boundaries of the coordinate patch with finite or infinite affine parameters. If it takes infinitely long to reach the boundary, it is called 'complete' and no extension is possible; however, if a boundary is reached with a finite affine parameter, then an extension must be possible unless the boundary is a singularity (in which case it is called 'incomplete').

In this section, we explore these issues for the Schwarzschild geometry, starting with a more precise formulation of the previous paragraph.

### 2.3.1 Geodesic Completeness and Maximal Analytic Extension

Locally, spacetime is generically specified through its metric, which is often represented in a specific coordinate system. One may then question if this coordinate system covers the whole spacetime or whether it can still be extended. To formulate this question systematically, one may explore spacetime as seen by geodesics. If it happens that there are geodesics that can reach spacetime boundaries and nothing singular happens there, then one may smoothly extend the geodesics by simply extending the range of the geodesics' affine parameter to arbitrary real values. In general four situations may occur for geodesics:

1. they can approach boundaries in infinite proper time, length, or affine parameter; these are called 'asymptotic boundaries' and the geodesics are said to be 'complete';
2. they may hit a singularity (for instance, a curvature singularity) in finite proper time, length, or affine parameter; these are called 'singularities' and the geodesics are said to be 'incomplete';
3. they can reach a coordinate boundary of spacetime in finite proper time, length, or affine parameter, and it is not possible to extend spacetime beyond this boundary; an example of this behavior is AdS which will be discussed later in this chapter; for asymptotically flat spacetimes we can disregard this option;
4. they can reach a coordinate boundary of spacetime in finite proper time, length, or affine parameter, and it is possible to extend spacetime beyond this boundary; examples of such behavior are coordinate singularities, and the corresponding geodesics are said to be 'extendible'; this case is dealt with by changing to more suitable coordinates and extending the range of the geodesics.

A spacetime is called *geodesically complete* if all its geodesics can be extended to arbitrary values of the affine parameter. Geodesically complete spacetimes are non-singular by definition. Otherwise, a spacetime is called *geodesically incomplete*, which by definition means it is singular (for more on this, see Chap. 3).

If all geodesics fall into the first three cases above, then the coordinate system is called *inextendible* and provides the *maximal analytic extension* of the spacetime. If the fourth case arises for at least one geodesic, the coordinate system is called *extendible* and we should switch to a better coordinate system to find the maximal analytic extension or, alternatively, describe spacetime using a collection of different (partly overlapping) coordinate charts. For inextendible spacetimes, the geodesic endpoints are either at asymptotic boundaries or singularities.

After these general considerations, we consider a simple warm-up example that we have already encountered.

**Minkowski space in Rindler coordinates**

Consider flat space in Rindler coordinates

$$\mathrm{d}s^2 = -a^2\rho^2\mathrm{d}\tau^2 + \mathrm{d}\rho^2 + \mathrm{d}y^2 + \mathrm{d}z^2 \tag{2.39}$$

with $\rho \geq 0$, $\tau, y, z \in \mathbb{R}$. This coordinate system is associated with an accelerated observer with uniform acceleration $a$ and appears as a near horizon approximation in (2.10). There is a (coordinate) singularity at $\rho = 0$. It is easy to check that some geodesics reach $\rho = 0$ with finite affine parameter, so the coordinate system above must be extendible. Indeed, we constructed such a coordinate system in (2.12).

We recall here the main step. Introduce new coordinates

$$t = \rho\cosh(a\tau), \qquad x = \rho\sinh(a\tau) \tag{2.40}$$

in terms of which the Rindler metric takes the form of a standard Minkowski metric

$$\mathrm{d}s^2 = -\mathrm{d}t^2 + \mathrm{d}x^2 + \mathrm{d}y^2 + \mathrm{d}z^2. \tag{2.41}$$

In this new coordinate system, we can extend the range of coordinates and allow $t, x \in \mathbb{R}$. Equation (2.40) shows that the Rindler patch $\rho \geq 0$, $\tau \geq 0$ corresponds to $t \geq 0$, $t \geq x$. Therefore, Rindler coordinates cover one-quarter of the Minkowski space. This will be made more precise in Sect. 2.3.4 when discussing Carter–Penrose diagrams. Conversely, Minkowski space provides a geodesic completion of Rindler space.

### 2.3.2 Kruskal Coordinates for Schwarzschild Geometry

As our geodesic analysis indicates, Schwarzschild spacetime (2.1) is not geodesically complete. The ingoing EF coordinates (2.37) already provide one such extension based on ingoing null geodesics. Null geodesics (2.21) can reach the singularity at $r = 0$ with finite affine parameter. The EF coordinates (ingoing or outgoing; see Exercise 2.14) are based on a single null coordinate, $u$ or $v$, but for Kruskal coordinates both of them are used simultaneously. As the first step, we rewrite the Schwarzschild metric as

$$\mathrm{d}s^2 = -f(r)\,\mathrm{d}u\mathrm{d}v + r^2\,\mathrm{d}\Omega^2 \tag{2.42}$$

where $u - v = 2r_*$ and $u + v = 2t$. So far, we have not gained much since (2.42) still is singular at zeros of $f(r)$. To overcome this, we follow [40] and define new null coordinates $U, V$

$$U = -e^{-\kappa u} \qquad\qquad V = e^{\kappa v} \tag{2.43}$$

sloppywith surface gravity $\kappa := \frac{1}{2}\frac{\mathrm{d}f}{\mathrm{d}r}|_{f=0} \neq 0$. For Schwarzschild $\kappa = 1/(2r_h) = 1/(4G_{\mathrm{N}}M)$. In Kruskal coordinates $U, V$, the Schwarzschild metric reads

$$\mathrm{d}s^2 = -\frac{e^{-2\kappa r}}{2\kappa^3 r}\mathrm{d}U\mathrm{d}V + r^2\mathrm{d}\Omega^2 \tag{2.44}$$

with $r = r(UV)$ implicitly defined as

$$UV = -\frac{r - r_h}{r_h}e^{2\kappa r} \qquad\qquad \frac{V}{U} = -e^{2\kappa t}\,. \tag{2.45}$$

As opposed to other coordinate systems we discussed, there is no coordinate obstruction in taking both $U$ and $V$ to range over all real numbers. The only remaining restriction is $UV < 1$ because $UV = 1$ is the locus of the singularity at $r = 0$. In this way, we get an analytic extension of Schwarzschild coordinates $t, r$, as well as ingoing or outgoing EF coordinates $v, r$ or $u, r$.

From (2.45), we learn that the product of the null coordinates vanishes at $r = r_h$, $UV = 0$. Therefore, depending on the signs of $U$ and $V$ the full Schwarzschild black hole spacetime has four quadrants, as depicted in the Kruskal diagram Fig. 2.4.

- **Region I:** $U < 0$, $V > 0$ which covers a region $r > r_h$; this is called 'outside region';
- **Region II:** $U > 0$, $V > 0$ which covers a region $r < r_h$; this is called 'black hole region';
- **Region III:** $U > 0$, $V < 0$ which covers another region $r > r_h$; this is another outside region;
- **Region IV:** $U < 0$, $V < 0$ which covers another region $r < r_h$; this is called 'white hole region'.

One can show that Kruskal coordinates $U, V$ provide the maximal extension of the Schwarzschild geometry, as all geodesics in the coordinate system upon extension of the range of their affine parameters either hit the singularity at $r = 0$ ($UV = 1$) or the asymptotic infinity regions at infinite $U$ or $V$ (or both).

Each of the coordinate systems discussed so far (Schwarzschild, EF, and Kruskal) have their specific features, merits, and drawbacks, some of which we address below.

- Schwarzschild coordinates make manifest the timelike Killing vector $\partial_t$. Moreover, the relation and difference to Newton gravity through the evaluation of geodesics is particularly transparent. The main drawback is the coordinate singularity at $r = r_h$ so that only one of the four regions, typically region **I**, is covered.

- EF coordinate systems make manifest the globally defined Killing vector fields $\partial_v$ or $\partial_u$. They have no coordinate singularity on half of the surface $r = r_h$, and one can use them to analytically extend past $r = r_h$ along one null direction. A technical advantage is that EF coordinates are explicit and often lead to simpler equations as compared to Schwarzschild or Kruskal-type coordinates. The main drawback is that only half of the maximally extended Schwarzschild geometry is covered by a single coordinate patch. In particular, ingoing coordinates $v, r$ cover regions **I**, **II** or **III**, **IV** and outgoing coordinates $u, r$ cover regions **I**, **IV** or **II**, **III** (see Exercise 2.16). Note, however, that taken together all four regions are nearly fully covered by these EF patches. The only open region not covered in any EF patch is around the bifurcation point where all four regions meet.
- Kruskal coordinates provide a maximal extension and allow to cover the whole Schwarzschild manifold with one coordinate patch. However, these coordinates are only defined implicitly and usually make expressions for geodesics, Killing vectors, and other observables more complicated (see Exercise 2.16).

Besides these commonly used coordinate systems, there are infinitely many others, for example, see Exercise 2.17 or Sect. 6.6; see also [152].

### 2.3.3 Structure of Lightcones and Preliminary Notion of Horizon

In- and outgoing EF coordinates are useful for the considerations of local lightcones. Take the Schwarzschild black hole in ingoing EF coordinates (2.38) and focus on the inside region $f(r) < 0$ (i.e. $r < r_h$). In that region, we have the inequality

$$2\mathrm{d}r\mathrm{d}v = \mathrm{d}s^2 + f(r)\,\mathrm{d}v^2 - r^2\mathrm{d}\Omega^2 \leq \mathrm{d}s^2 \tag{2.46}$$

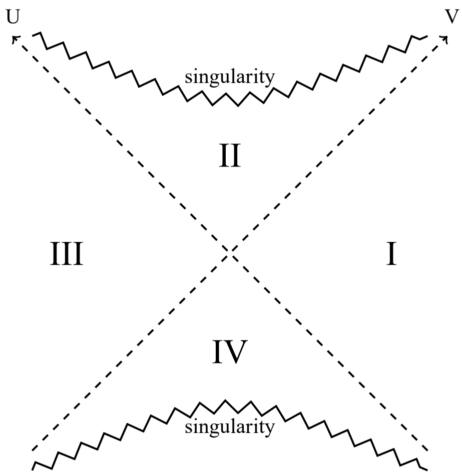


**Fig. 2.4** Kruskal diagram of Schwarzschild black hole. See text for definitions of regions **I–IV**. The boundary between the regions, $r = r_h$ or $UV = 0$, is shown dashed. The singularity, $r = 0$ or $UV = 1$, is shown zigzag. Lines of constant $U$ and $V$ are at 45° in this diagram

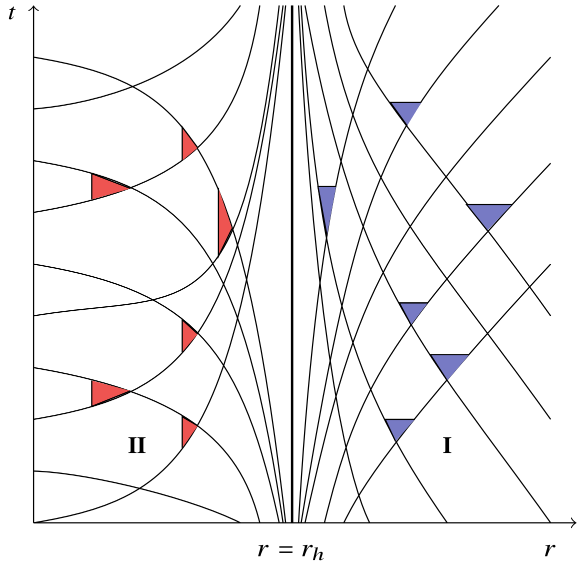


**Fig. 2.5** Future-oriented lightcones inside (region **II**) and outside (region **I**) the horizon for a Schwarzschild black hole. No future-oriented lightcone in region **II** passes to region **I**

which shows that the filled lightcone, $\mathrm{d}s^2 \leq 0$, implies

$$\mathrm{d}r\,\mathrm{d}v \leq 0\,. \tag{2.47}$$

Taking $v$ as the affine parameter along some future-directed causal curve in the interior, we have $\mathrm{d}v > 0$. The inequality (2.47) then implies $\mathrm{d}r \leq 0$ for all such curves. That is, *any causal curve which starts in the region $f < 0$ never passes to the region $f \geq 0$*. In other words, if a physical observer starts in region **II** in the Kruskal diagram (the black hole or inside region, $f < 0$), they will always remain there, and in particular can never escape to region **I** (the outside region, $f > 0$).

The analysis above shows that $f = 0$ is a special place in spacetime: light rays or any other future-directed causal curve in the $f < 0$ region never crosses to the $f > 0$ region. The part of the locus $f = 0$ covered by ingoing EF coordinates is referred to as ‘future horizon’, a notion which we are going to make more precise in the next chapter. As we showed above, the horizon acts like a semi-permeable membrane: signals can pass through it from the outside region to the inside region but not vice versa. This is the defining property of a classical black hole.

The structure of local lightcones (in Schwarzschild coordinates) is depicted in Fig. 2.5.

Similarly, one may use outgoing EF coordinates (see Exercise 2.14). This coordinate system covers regions **IV, I** of the Kruskal diagram. For all future-oriented causal curves $\mathrm{d}u > 0$ in region **IV**, we find $\mathrm{d}r \geq 0$ by arguments analogous to above. That is, *all future-directed causal curves in the $f < 0$ region necessarily pass to the $f > 0$ region*. We have the time-reversed situation as compared to above, so here the locus $f = 0$ is referred to as ‘past horizon’. The white hole region **IV** is a semi-permeable membrane that works in the other direction: all future-directed causal signals necessarily escape from the white hole region to the outside region.

### 2.3.4 Carter–Penrose Causal Diagrams

A disadvantage of spacetime diagrams like the Kruskal diagram, Fig. 2.4 or Fig. 2.5, is their non-compactness. It would be nicer if we could draw some compact diagrams where we can see the most essential features of spacetimes. Three of these features that we would like to capture diagrammatically are

1. *Horizons.* These are null hypersurfaces that separate causally disconnected regions, like regions **I** and **II** in Fig. 2.4.
2. *Singularities.* These are regions that for some reason are excised from spacetime, e.g. because there is a curvature singularity or closed timelike curves (CTCs). An example is the locus $r = 0$ in the Schwarzschild geometry. (For a detailed discussion and classification of singularities, see [153, 154].)
3. *Asymptotic regions.* These are places that are infinitely far away (in either spatial, temporal, or null direction) from observers in the interior. One of our main goals is to map them to a finite distance without losing information about horizons or singularities.

In addition, there can be coordinate boundaries, for instance, $r = 0$ in spherical coordinates.

Carter–Penrose diagrams are designed to make these three features visual and explicit in a compact form. Often, they are just called Penrose diagrams, and for the sake of brevity, we adopt this convention from now on.

The notion of the horizon is the key concept in black hole physics. To build up an intuition for this concept, we explore the Schwarzschild example. A more abstract and concise definition of a horizon and the fact that there could be different kinds of horizons will be discussed in Chap. 3.

Given the importance of null curves in studying the causal structure of spacetime, we note the following theorem: *Angles (including Lorentz-angles) are invariant under conformal rescalings of the metric,*

$$g_{\mu\nu} \to \tilde{g}_{\mu\nu} = \Omega^2(x) g_{\mu\nu} \,. \tag{2.48}$$

The quantity $\Omega$ is called the conformal factor. A consequence of the theorem is that two metrics differing only by a conformal factor have the same set of null geodesics and the same causal structure, including horizons. Go through Exercise 2.20 for the proof of these statements. Another important aspect is that choosing the conformal factor to be singular (zero or infinity) can allow mapping infinite to finite distances, thereby compactifying spacetime without changing its causal structure, which is precisely what we want for Penrose diagrams. This is known as 'conformal compactification'.

An example of a Euclidean conformal compactification is stereographic projection, which provides a map between the Euclidean 2-plane and the sphere. A key step in stereographic projection is that one point has to be added, namely the point at infinity. This is an example of a '1-point-compactification'; see Exercise 2.21. In the Lorentzian pendant what we end up adding typically is not a point, but, e.g. for asymptotically flat spacetimes a whole lightcone at infinity.

Penrose diagrams have the same dimension as the spacetime manifold. Since we are interested in 4-dimensional spacetimes, we have to draw 4-dimensional Penrose diagrams. Fortunately, many black hole solutions are so symmetric that up to two of the dimensions can be dropped. For instance, spherically symmetric black holes like Schwarzschild require only 2-dimensional diagrams to represent the essence of the causal structure of spacetime; each point in the interior of such a diagram then represents a 2-sphere of varying size.

We provide now a rough cooking recipe for constructing Penrose diagrams, followed by several examples[2] :

1. Find the maximal analytic extension of spacetime, as discussed in Sect. 2.3.1.
2. Find all asymptotic regions (in many coordinate systems, this simply means sending the coordinates to $\pm\infty$; in that case introduce new coordinates that map $\mathbb{R}$ to a finite interval, say, $(-\frac{\pi}{2}, \frac{\pi}{2})$, e.g. with the tan-function).
3. Study the behavior of the metric in the asymptotic regions and check whether some suitable conformal factor (2.48) can be pulled out to make the metric finite when the asymptotic boundaries are reached. As discussed, this requires a singular conformal factor.
4. Add the unphysical boundary points. (In the tan-example, we compactify intervals $(-\frac{\pi}{2}, \frac{\pi}{2})$ to $[-\frac{\pi}{2}, \frac{\pi}{2}]$.)
5. Draw a compact diagram that contains all the boundaries and special loci (singularities, horizons, and asymptotic regions).

Due to the conformal transformation (2.48) in the fourth step, the resulting diagram will not faithfully represent lengths, but it will faithfully represent all Lorentz angles and null geodesics, which always correspond to lines of 45°.

### Penrose diagram of flat space

Minkowski space in lightcone/spherical coordinates ($u = t - r$, $v = t + r$)

$$\mathrm{d}s^2 = -\,\mathrm{d}u\,\mathrm{d}v + \frac{(v-u)^2}{4}\,\mathrm{d}^2\Omega \qquad u, v \in \mathbb{R} \quad v \geq u \tag{2.49}$$

is already maximally extended. To bring $u, v$ coordinates to a finite range, we use the tan-function

$$u = \tan U \qquad v = \tan V \qquad U, V \in [-\frac{\pi}{2}, \frac{\pi}{2}] \quad V \geq U \tag{2.50}$$

[2] Each of the items can be, and eventually will be, made more precise and explicit. However, to get started we do not need to handle all eventualities but focus on key aspects instead. A more efficient version of this recipe is to avoid the construction of a maximal analytic extension; instead, construct and compactify EF patches, and in the end, glue them together on overlap regions. For details of this algorithm in a 2-dimensional context, see [155].

in terms of which the metric reads

$$ds^2 = \frac{1}{(2\cos U\cos V)^2}\left[-4dUdV + \sin(V-U)^2 d^2\Omega\right]. \tag{2.51}$$

The metric above is singular at the asymptotic region where either $U$, $V$ or both tend to $\pm\frac{\pi}{2}$. To obtain a regular metric, we go to an unphysical metric that differs from the one above by a conformal factor

$$\tilde{ds}^2 = -4dUdV + \sin(V-U)^2 d^2\Omega. \tag{2.52}$$

This metric is regular in the whole range of coordinates, including the boundary values $\pm\frac{\pi}{2}$. There are five qualitatively different portions of the asymptotic boundary:

1. Future null infinity $\mathfrak{I}^+$, when $V \to \frac{\pi}{2}$ $(v \to \infty)$ while $U$ $(u)$ is arbitrary;
2. Past null infinity $\mathfrak{I}^-$, when $U \to -\frac{\pi}{2}$ $(u \to -\infty)$ while $V$ $(v)$ is arbitrary;
3. Spacelike infinity $\boldsymbol{i^0}$, when $V \to \frac{\pi}{2}$ $(v \to \infty)$ while $U \to -\frac{\pi}{2}$ $(u \to -\infty)$;
4. Future timelike infinity $\boldsymbol{i^+}$, when $U, V \to +\frac{\pi}{2}$ $(u, v \to +\infty)$;
5. Past timelike infinity $\boldsymbol{i^-}$, when $U, V \to -\frac{\pi}{2}$ $(u, v \to -\infty)$.

This information is depicted in the Penrose diagram, Fig. 2.6. For comparison and contrast, the Penrose diagram of 2-dimensional Minkowski space in Rindler coordinates is depicted in Fig. 2.7.

---

Consider now another example of a maximally symmetric spacetime, namely 4-dimensional anti-de Sitter ($AdS_4$) space, which has $SO(3,2)$ isometries. $AdS_4$ is

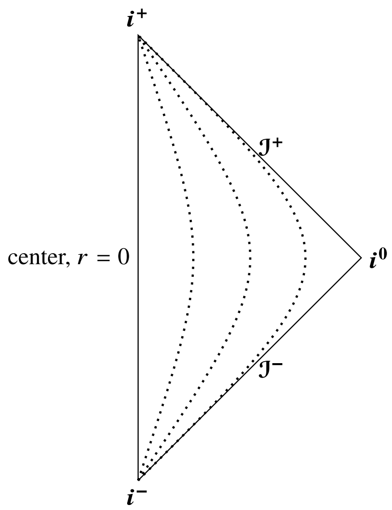


**Fig. 2.6** Penrose diagram of 4-dimensional Minkowski space. The dotted lines are constant $r$ timelike geodesics. Null geodesics are 45° lines. Each point in the interior corresponds to a 2-sphere

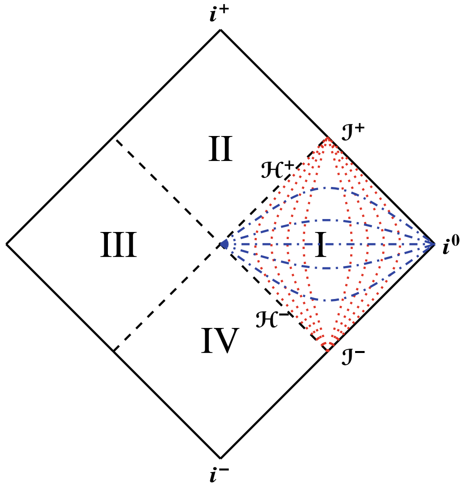


**Fig. 2.7** Penrose diagram of 2-dimensional Minkowski space and the part covered by a Rindler wedge. Rindler coordinates cover region **I**. The Rindler horizon is denoted by dashed lines, labeled by $\mathcal{H}^{\pm}$. The dotted red (dash-dotted blue) curves are constant $\rho$ ($\tau$) lines. Constant $\rho$ curves are constant acceleration paths in Minkowski space

a vacuum solution in the presence of a negative cosmological constant ($\Lambda = -\frac{3}{\ell^2}$, where $\ell$ is the AdS radius)

$$R_{\mu\nu} = -\frac{3}{\ell^2} g_{\mu\nu}\,. \tag{2.53}$$

Solving the Einstein equations (2.53) yields the maximally extended metric in global AdS coordinates

$$ds^2 = -\ell^2(1 + \frac{r^2}{\ell^2})d\tau^2 + \frac{dr^2}{1 + \frac{r^2}{\ell^2}} + r^2 d\Omega^2 \qquad \tau \in \mathbb{R} \qquad r \in \mathbb{R}_0^+\,. \tag{2.54}$$

For AdS, it is customary (though not necessary) to compactify only the spatial directions and keep time non-compact. Also, this hybrid situation of non-compact and compact directions is referred to as a Penrose diagram. We compactify again using the tan-function, $r = \ell \tan\chi,\ \ \chi \in [0, \pi/2]$, yielding

$$ds^2 = \frac{\ell^2}{\cos^2\chi}\left[-d\tau^2 + d\chi^2 + \sin^2\chi\, d\Omega^2\right]. \tag{2.55}$$

The unphysical metric whose spacetime diagram we draw differs from the physical metric above by a conformal factor that is singular at the boundary.

$$ds^2 = -d\tau^2 + d\chi^2 + \sin^2\chi\, d\Omega^2. \tag{2.56}$$

We compactify by allowing $\chi \in [0, \frac{\pi}{2}]$ instead of $\chi \in [0, \frac{\pi}{2})$. Since the metric is spherically symmetric, we suppress again the $S^2$ part.

We see important differences in Minkowski space when considering radial null geodesics $\tau = \pm\chi$, which reach the asymptotic boundary $\chi = \pi/2$ in finite coordinate time $\tau$. In Minkowski space, it takes null geodesics an infinite amount of affine

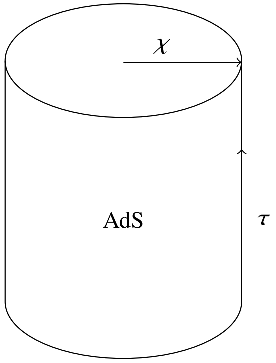


**Fig. 2.8** Penrose diagram of $\mathrm{AdS}_D$. The circle represents a $(D-2)$-dimensional sphere, where $D$ is the spacetime dimension. The $\mathbb{R} \times S^{D-2}$ cylinder is the $\mathrm{AdS}_D$ causal boundary and the coordinate along the cylinder axis is global AdS time $\tau$

parameters to reach any of the asymptotic boundaries. The second crucial difference is that Minkowski space had lightlike boundaries, whereas in AdS the locus $\chi = \frac{\pi}{2}$ is timelike. This information is summarized in the Penrose diagram in Fig. 2.8.

## Penrose diagram of de Sitter space

Maximally symmetric spacetimes of positive curvature and Lorentzian signature are called de Sitter (dS) and have SO(4, 1) isometry. They solve the vacuum Einstein equations with a positive cosmological constant ($\Lambda = \frac{3}{\ell^2}$ where $\ell$ is the AdS radius)

$$R_{\mu\nu} = \frac{3}{\ell^2} g_{\mu\nu} \,. \tag{2.57}$$

The so-called static patch metric of dS

$$\mathrm{d}s^2 = -\ell^2 (1 - \frac{r^2}{\ell^2}) \mathrm{d}t^2 + \frac{\mathrm{d}r^2}{1 - \frac{r^2}{\ell^2}} + r^2 \mathrm{d}\Omega^2 \tag{2.58}$$

resembles the AdS metric (2.54), but with crucial sign differences. This is to be expected, since the only change between AdS and dS is the sign of the cosmological constant.

The coordinate system (2.58) covers a part of global dS space. The coordinate transformation $\tanh t = \frac{\sin \tau}{\cos \chi}$, $r = \ell \frac{\sin \chi}{\cos \tau}$ yields dS in global coordinates

$$\mathrm{d}s^2 = \frac{\ell^2}{\cos^2 \tau} \left[ -\mathrm{d}\tau^2 + \mathrm{d}\chi^2 + \sin^2 \chi \, \mathrm{d}\Omega^2 \right] \tag{2.59}$$

where $\tau \in [-\pi/2, +\pi/2]$, $\chi \in [0, \pi]$. The above metric is conformal to the Einstein static universe $\mathbb{R} \times \mathrm{S}^3$ and is of the desired form for discussing the Penrose diagram. As in the AdS case, the radial null geodesics are $\tau = \pm\chi$ and the geometry is spherically symmetric and one may suppress the $\mathrm{S}^2$ part.

The conformal factor $1/\cos^2 \tau$ blows up at a $\tau = \pm\pi/2$. The crucial difference with the AdS case is that this happens at two constant time slices, which are spacelike

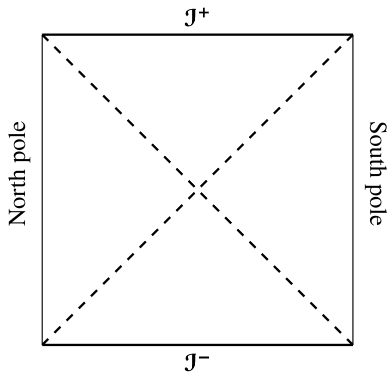


**Fig. 2.9** Penrose diagram of dS. Each point in the interior is a 2-sphere and each constant time slice a 3-sphere. North and South poles are timelike lines. Future and past observer horizons are the dashed lines. Future and past null infinity are spacelike asymptotic boundaries

hypersurfaces. In the case of dS, these hypersurfaces are two $S^3$. That is, while null geodesics can reach $\tau = \pm\pi/2$, time does not advance after that. So, unlike the AdS case, we do not have a causal timelike boundary. This information may be summarized in the Penrose diagram Fig. 2.9. See [156] for more discussions.

---

To summarize, the conformal boundary of dS, flat, and AdS spacetimes are respectively spacelike, null, and timelike.

## Penrose diagram of Schwarzschild black hole

Kruskal coordinates (2.44) cover all of the Schwarzschild geometry. Since the geometry is spherically symmetric, we suppress the spherical part and focus only on the part of metric (2.44) spanned by the null coordinates $U$, $V$. Like in the construction of the Penrose diagram for Minkowski space in Fig. 2.6, we compactify $U$, $V$

$$\tau = \frac{\tan^{-1} U + \tan^{-1} V}{2} \qquad \chi = \frac{\tan^{-1} U - \tan^{-1} V}{2} \tag{2.60}$$

where $\tau \in [-\pi/2, +\pi/2]$ and $\chi \in [-\pi, +\pi]$.

The resulting Penrose diagram depicted in Fig. 2.10 is a compact version of the Kruskal diagram in Fig. 2.4. Here are its key features:

- $\tau = \chi$ line is the future-oriented horizon $\mathcal{H}^+$;
- $\tau = -\chi$ line is the past-oriented horizon $\mathcal{H}^-$;
- $\tau = \pm\pi/2$ corresponds to $r = 0$, the curvature singularity;
- $\tau + \chi = \pm\pi$ line is the future null infinity $\mathcal{I}^+$;
- $\tau - \chi = \pm\pi$ line is the past null infinity $\mathcal{I}^-$;
- $\tau = \pi/2$, $\chi = \pm\pi/2$ points are the future timelike infinity $\boldsymbol{i}^+$;
- $\tau = -\pi/2$, $\chi = \pm\pi/2$ points are the past timelike infinity $\boldsymbol{i}^-$;
- $\chi = \pm\pi$ are spacelike infinity $\boldsymbol{i}^0$.

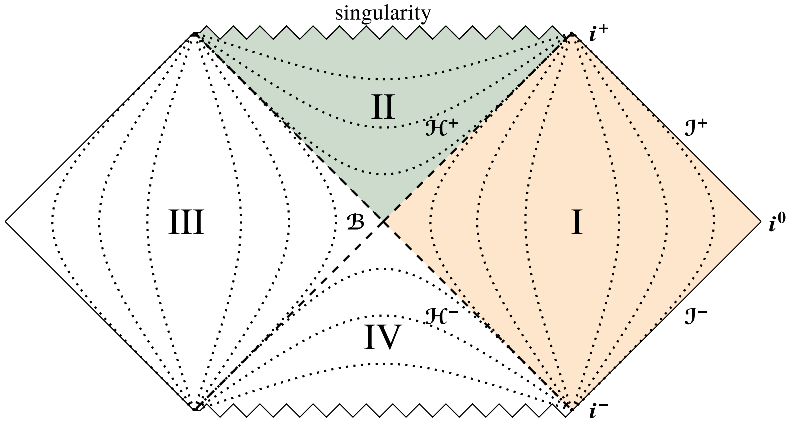


**Fig. 2.10** Penrose diagram of Schwarzschild black hole. It is a compact version of the Kruskal diagram, Fig. 2.4. Regions **I, II** (or regions **III, II**) denote the black hole and regions **III, IV** (or regions **IV, I**) the white hole. The dotted lines depict constant $r$ surfaces which are timelike in regions **I, III** and spacelike in regions **II, IV**

There is the important locus where the future and past horizons meet at $\tau = \chi = 0$, denoted by $\mathcal{B}$ in Fig. 2.10, which is called the *bifurcation point* (or more precisely *bifurcation surface*, as it is indeed a 2-sphere of radius $r = r_h$; see Exercise 2.23). As discussed in detail in Chap. 3, future and past horizons $\mathcal{H}^\pm$ are generated by the flow of the Killing vector $\zeta_H$ (2.132) at $UV = 0$.

We end this discussion with two remarks on nomenclature. To emphasize the fact that the Schwarzschild geometry is static in the exterior and that the black hole is not being formed but has been there from the beginning, it is also called the eternal Schwarzschild black hole. To stress that this geometry has two disconnected asymptotic regions, it is called a two-sided black hole, in contrast to a physical black hole which results from gravitational collapse; see Fig. 2.11.

### 2.3.5 Realistic Black Holes and Wormholes

More realistic black holes generically result from gravitational collapse, briefly discussed in Chap. 1. The geometry before black hole formation is typically a flat (or (A)dS) space slightly deformed by matter. Then it evolves into a geometry that eventually settles to a spacetime with a curvature singularity screened by a horizon. During the collapse, higher multipole moments of the matter distribution are radiated away quickly so that the final state is in general a rotating black hole. To simplify matters and discuss qualitative aspects of gravitational collapse, we consider non-rotating cases where spherical symmetry can be assumed. In this case, the final outcome approaches the Schwarzschild solution. This process is depicted in the Penrose diagram 2.11.

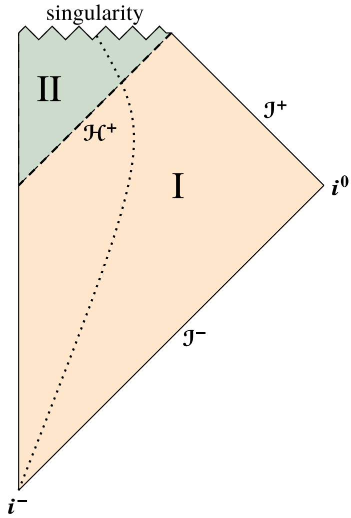


**Fig. 2.11** Penrose diagram of physical black hole that arises as a result of gravitational collapse of matter (see Chap. 4). Matter is confined to the left of the dotted line. As compared to Fig. 2.10, there is no bifurcation sphere, no past horizon, no white hole region, and no second asymptotic region. Figure 2.10 depicts a two-sided, eternal black hole whereas the above shows a one-sided black hole

The Penrose diagram of a collapsed star, Fig. 2.11, is quite different from the Penrose diagram 2.10 of the eternal Schwarzschild black hole: for collapse, it is one-sided, while for the eternal black hole it is two-sided and also features a past horizon, a white hole region, and a past singularity. See Chaps. 3 and 4 for more discussions.

The eternal Schwarzschild black hole inspired the concept of wormholes, a term which was coined in [157]. The inspiration for this is the Flamm diagram, Fig. 2.12, which connects the two outside regions **I, III**. The throat in this diagram is called Einstein–Rosen bridge [158]; see Exercise 2.19. The diagram is slightly misleading since it suggests one can travel through the throat. If that were possible, we would indeed have a wormhole—a spacetime where one can take a shortcut from one spacetime point to another. However, the Schwarzschild wormhole is not traversable within GR. Nevertheless, it inspired the search for traversable wormholes.

Here is a definition of (Lorentzian) wormholes [159, 160]. Given a spacetime with a Minkowski signature containing a compact region $\Omega$, the region $\Omega$ contains a wormhole if the following properties hold: the topology of $\Omega$ is of the form $\Omega \sim \mathbb{R} \times \Sigma$ and $\Sigma$ is spacelike with a boundary of 2-sphere topology, $\partial\Sigma \sim S^2$. The search for traversable stable wormholes has a long history and continues even today [159, 161–163].

## 2.4 Einstein–Maxwell Theory and Reissner–Nordström Black Holes

The Schwarzschild solution in gravity in many ways resembles the Coulomb solution in Maxwell's theory, so it seems natural to combine them. Consider the Einstein–Maxwell theory with Lagrangian

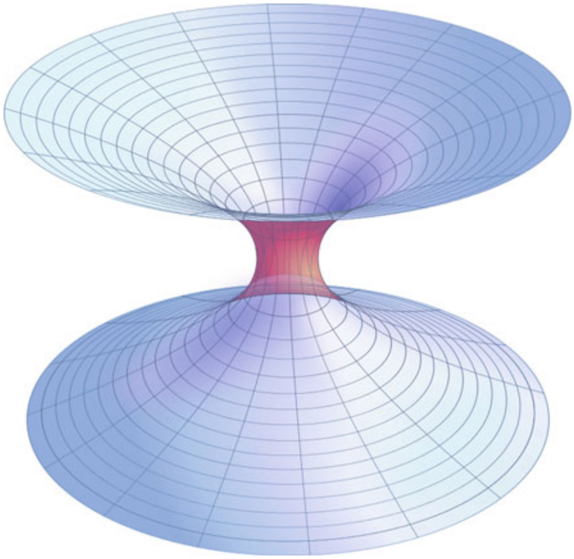

**Fig. 2.12** Constant time slice of Schwarzschild wormhole (compare with the Flamm diagram 2.1). See Exercise 2.19. *Source* wikipedia

$$\mathcal{L}=\frac{1}{16\pi G_{\rm N}}(R-F^2), \qquad F^2=F_{\mu\nu}F^{\mu\nu}, \quad F_{\mu\nu}:=\partial_\mu A_\nu-\partial_\nu A_\mu \tag{2.61}$$

and fields equations

$$R_{\mu\nu}-\frac{1}{2}Rg_{\mu\nu}=8\pi G_{\rm N}T_{\mu\nu}=2\big(F_{\mu\lambda}F_\nu{}^\lambda-\frac{1}{4}g_{\mu\nu}F_{\lambda\rho}F^{\lambda\rho}\big) \tag{2.62a}$$

$$\nabla^\mu F_{\mu\nu}=0 \tag{2.62b}$$

which in four dimensions yields $R=0=T^\mu_\mu$. For simplicity from now on, we set $G_{\rm N}=1$ in this section by choice of units.

The most general spherically symmetric solution to Einstein–Maxwell theory is known as Reissner–Nordström (RN) [46,47]. In the Schwarzschild coordinates, the metric is given by (2.1) with

$$f(r)=1-\frac{2M}{r}+\frac{Q_e^2+Q_m^2}{r^2} \tag{2.63}$$

where $Q_e$ and $Q_m$ are electric and magnetic monopole charges, respectively. The abelian connection in the same coordinates reads

$$A=-\frac{Q_e}{r}\,\mathrm{d}t-Q_m\,\cos\theta\,\mathrm{d}\varphi\,. \tag{2.64}$$

The field configurations (2.1), with (2.63) and (2.64), solve the field equations (2.62). The non-vanishing components of the stress tensor are given by $T^t{}_t=T^r{}_r=-T^\theta{}_\theta=-T^\varphi{}_\varphi=-\frac{Q_e^2+Q_m^2}{8\pi r^4}$.

**Reissner–Nordström metric**

In Schwarzschild coordinates, the RN metric reads

$$\mathrm{d}s^2 = -\Big(1 - \frac{2M}{r} + \frac{Q_e^2 + Q_m^2}{r^2}\Big)\,\mathrm{d}t^2 + \frac{\mathrm{d}r^2}{\Big(1 - \frac{2M}{r} + \frac{Q_e^2+Q_m^2}{r^2}\Big)} + r^2\,\mathrm{d}\Omega^2 \quad (2.65)$$

where $M$ is the mass, $Q_e$ the electric charge, $Q_m$ the magnetic charge, and $\mathrm{d}\Omega^2$ the metric of the round 2-sphere.

Here are the main properties of the RN solution (2.64)–(2.65):

- It is static and spherically symmetric.
- It solves the field equations (2.62).
- It has ADM mass $M$ and electric and magnetic charges $Q_e$, $Q_m$.
- It has up to two horizons at roots of $f(r) = 0$ (2.63),

$$r_\pm = M \pm \sqrt{M^2 - Q_e^2 - Q_m^2}. \quad (2.66)$$

- If the inequality $M \geq \sqrt{Q_e^2 + Q_m^2}$ holds the metric (2.65) describes a black hole, otherwise it describes a naked singularity, which here means that the curvature singularity is not screened by a horizon and asymptotic observers have access to it.
- If this inequality is strict, $M > \sqrt{Q_e^2 + Q_m^2}$, we have generic black holes; in that case, expanding around the outer horizon, $r = r_+ + f'(r_+)\rho^2/4$, the near horizon geometry is Rindler space (2.40) with surface gravity

$$\kappa = \frac{r_+ - r_-}{2r_+^2}\,. \quad (2.67)$$

  The Penrose diagram of generic RN black holes is shown in Fig. 2.13.
- If this inequality is saturated, $M = \sqrt{Q_e^2 + Q_m^2}$ the two horizons coincide, $r_+ = r_-$ and we have extremal black holes where surface gravity $\kappa$ vanishes; in that case, expanding around the extremal horizon $r = M(1+\rho)$ to leading order yields the Robinson–Bertotti metric [164, 165]

$$\mathrm{d}s^2 = M^2\big(-\rho^2\,\mathrm{d}t^2 + \frac{\mathrm{d}\rho^2}{\rho^2} + \mathrm{d}\theta^2 + \sin^2\theta\,\mathrm{d}\varphi^2\big) \quad (2.68)$$

  where for convenience we also rescaled time by $M$. The corresponding manifold is a direct product of $\mathrm{AdS}_2$ and $S^2$. The Penrose diagram of extremal RN black holes is shown in Fig. 2.14.
- If this inequality is violated, $M < \sqrt{Q_e^2 + Q_m^2}$, we have an example of a naked singularity. Its Penrose diagram is shown in Fig. 2.15.

- While the outer horizon at $r_+$ is physical, in the sense that we can probe it experimentally and have good reason to believe in its existence, neither of this is true for the inner horizon at $r_-$; in fact, the inner horizon is a Cauchy horizon and likely to be unstable against small perturbations due to infinite blueshift factors; see Chap. 3 for more discussions.
- In the extremal case, one can construct multi-centered black hole solutions by 'superposing' black hole geometries; see Exercise 2.36.
- Kruskal coordinates do not cover the whole RN manifold. In Fig. 2.16, the patches covered by various coordinate systems are shown. Israel coordinates were defined for Schwarzschild and RN black holes in [166] (see Exercise 2.17). An extension of Israel coordinates covering the whole RN manifold was given by Klösch and Strobl [167]. The metric in these EF-inspired coordinates reads ($Q^2 := Q_e^2 + Q_m^2$)

$$\mathrm{d}s^2 = -2\,\mathrm{d}u\,\mathrm{d}\rho - K(u,\ \rho)\ \mathrm{d}u^2 + r^2(u,\ \rho)\ \mathrm{d}\Omega^2 \tag{2.69}$$

where

$$r(u,\ \rho) := \rho\ \sin(u)\,\alpha(u) + M - \sqrt{M^2 - Q^2}\ \cos(u) \tag{2.70}$$

with $\alpha(u) := \sqrt{M^2 - Q^2}\,(2M^2 - Q^2)/Q^4 + (M^2 - Q^2)\,2M/Q^4\ \cos(u)$ and

$$K(u,\ \rho) := \frac{2\alpha(u)\ \sin(u)\,\partial_u r(u,\ \rho) + 1 - \frac{2M}{r(u,\rho)} + \frac{Q^2}{r^2(u,\rho)}}{\alpha^2(u)\ \sin^2(u)}\,. \tag{2.71}$$

The patches covered by various coordinate systems are shown in Fig. 2.16.

## 2.5 Kerr Solution and Its Basic Analysis

Astrophysical black holes rotate and are thus not described by the Schwarzschild solution since rotation breaks spherical symmetry to ellipsoidal symmetry. Moreover, the addition of angular momentum breaks the time-reversal symmetry $t \to -t$. So, rotating black holes can be stationary if they have a timelike Killing vector. We provide now a slick derivation of the Kerr metric based on this observation, starting with flat spacetime in ellipsoidal coordinates, $x = \sqrt{r^2 + a^2}\ \sin\theta\ \cos\varphi$, $y = \sqrt{r^2 + a^2}\ \sin\theta\ \sin\varphi$, $z = r\ \cos\theta$,

$$\mathrm{d}s^2 = -\,\mathrm{d}t^2 + \frac{\rho^2}{r^2 + a^2}\ \mathrm{d}r^2 + \rho^2\ \mathrm{d}\theta^2 + (r^2 + a^2)\ \sin^2\theta\ \mathrm{d}\varphi^2 \tag{2.72}$$

with $t \in \mathbb{R}$, $r \in \mathbb{R}^+$, $\theta \in [0, \pi)$, $\varphi \sim \varphi + 2\pi$, the definition $\rho^2 := r^2 + a^2\ \cos^2\theta$, and some constant parameter $a$ (if $a = 0$ we have manifest spherical symmetry).

With hindsight, we represent the Minkowski line-element (2.72) in so-called Boyer–Lindquist coordinates, which are actually the same coordinates as above, but reorganized slightly differently.

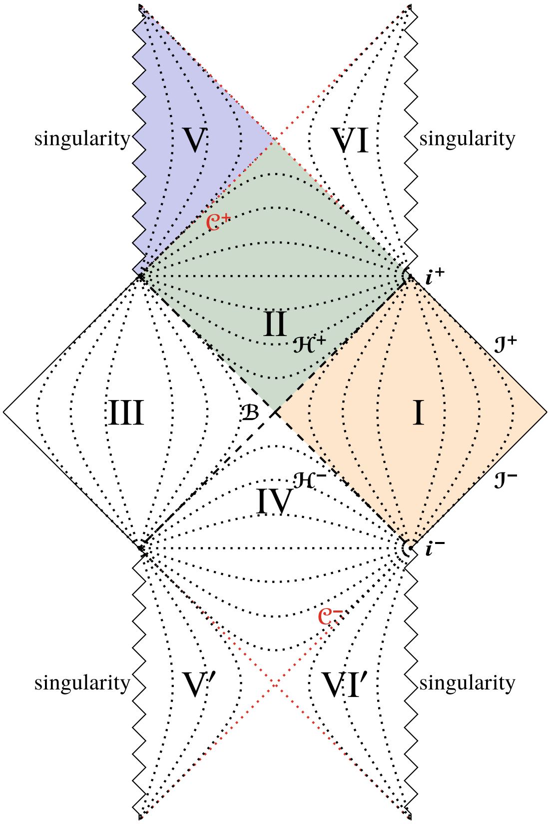


**Fig. 2.13** Penrose diagram of generic (non-extreme) RN black hole. The colored regions can be covered by an ingoing EF patch. The meaning of regions **I–IV** is identical to Fig. 2.10. The regions **V, VI** (and their primed versions) are bounded by parts of the Cauchy horizon and the singularity. The diagram can be extended above and below to an infinite strip, possibly with periodic identifications of primed and unprimed regions with the same numbers. In actual black holes, only regions **I** and **II** exist

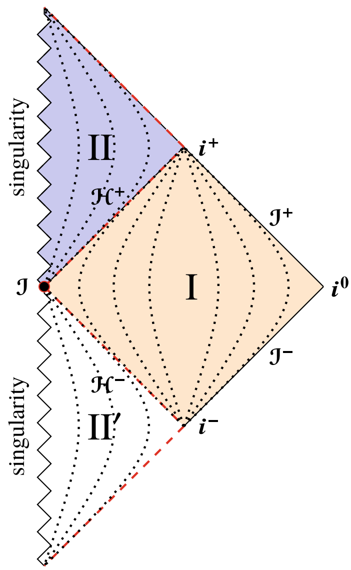


**Fig. 2.14** Penrose diagram of extremal RN black hole. The colored regions can be covered by an ingoing EF patch. The locus denoted by $\mathfrak{J}$ is an internal infinity, corresponding to an infinite Einstein–Rosen bridge. The diagram can be extended above and below to an infinite strip, possibly with periodic identifications of regions **II** and **II**′. Extremal black holes are not expected to exist

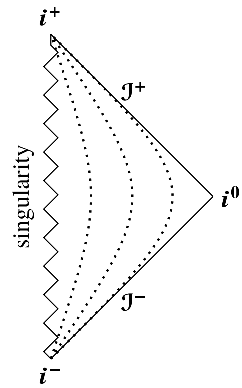


**Fig. 2.15** Penrose diagram of RN naked singularity for $M < \sqrt{Q_e^2 + Q_m^2}$. If cosmic censorship was correct, this solution cannot arise in Nature

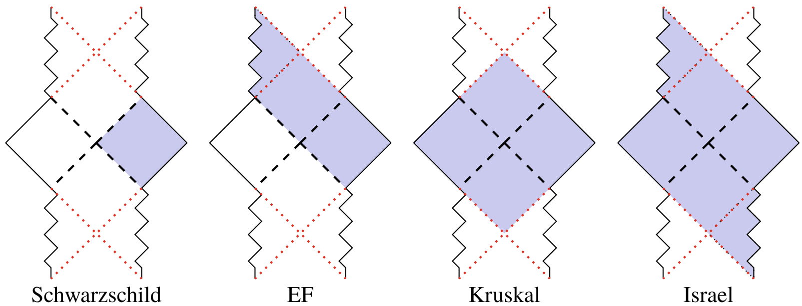


**Fig. 2.16** Regions of RN covered by various coordinate systems. From left to right: Schwarzschild, EF, Kruskal, and Israel coordinates. The whole manifold is covered by Klösch–Strobl coordinates (2.69)

$$\mathrm{d}s^2 = -\frac{\Delta}{\rho^2}\big(\mathrm{d}t - a\sin^2\theta\,\mathrm{d}\varphi\big)^2 + \frac{\rho^2}{\Delta}\,\mathrm{d}r^2 + \rho^2\,\mathrm{d}\theta^2 + \frac{(r^2+a^2)^2}{\rho^2}\sin^2\theta\,\Big(\mathrm{d}\varphi - \frac{a}{r^2+a^2}\,\mathrm{d}t\Big)^2. \tag{2.73}$$

The function $\Delta$ can be read off from (2.72), $\Delta = r^2 + a^2$. The special case $a = 0$ recovers the Minkowski metric in spherical coordinates.

So far, we have just represented Minkowski space in some coordinates that are convenient for our purposes, but we have not introduced any black hole mass. While we do not know yet how to do this for Kerr, we know already how to do it for Schwarzschild. Namely, take the manifestly spherically symmetric line-element (2.73) with $a = 0$ and use for the function $\Delta$ the expression $\Delta\big|_{a=0} = r^2 - 2Mr$.

Thus, we know that the metric in Boyer–Lindquist coordinates (2.73) solves the vacuum Einstein equations $R_{\mu\nu} = 0$ for functions $\Delta$ given by $\Delta = r^2 - 2Mr$ (limit of no rotation, $a = 0$) or $\Delta = r^2 + a^2$ (limit of no mass, $M = 0$). A plausible ansatz for the function $\Delta$ in the presence of rotation *and* mass is $\Delta = r^2 + a^2 + h(r)$.

Demanding that the metric (2.73) has vanishing Ricci scalar establishes $\mathrm{d}^2h/\mathrm{d}r^2 = 0$ so that $h(r) = c - 2Mr$. The vanishing of the Ricci tensor component $R_{\theta\theta} = 0$ implies $c = 0$. It is straightforward to check that for vanishing $c$, all other Ricci tensor components also vanish, meaning that the metric (2.73) with $\Delta = r^2 - 2Mr + a^2$ solves the vacuum Einstein equations for any values of mass $M$ and rotation parameter $a$. This metric is known as the Kerr solution.

Historical note: The derivation and coordinates used by Kerr [25] differ from above and exploited instead algebraic properties of the Weyl tensor. For more detailed discussion on Kerr black hole, see [168, 169].

**Kerr solution in Boyer–Lindquist coordinates**

The Kerr solution is described by the metric ($\theta \in [0, \pi)$, $\varphi \sim \varphi + 2\pi$)

$$\boxed{\begin{aligned} \mathrm{d}s^2 = &-\frac{\Delta}{\rho^2}\left(\mathrm{d}t - a\sin^2\theta\,\mathrm{d}\varphi\right)^2 + \frac{\rho^2}{\Delta}\,\mathrm{d}r^2 + \rho^2\,\mathrm{d}\theta^2 \\ &+ \frac{(r^2+a^2)^2}{\rho^2}\sin^2\theta\left(\mathrm{d}\varphi - \frac{a}{r^2+a^2}\,\mathrm{d}t\right)^2 \end{aligned}} \tag{2.74}$$

with the functions

$$\boxed{\rho^2 := r^2 + a^2\cos^2\theta \qquad\qquad \Delta := r^2 - 2Mr + a^2} \tag{2.75}$$

depending on the mass $M$ and the rotation parameter $a$. For this solution to be a black hole, its mass must be positive and sufficiently big, $M \geq |a|$. If this inequality does not hold, the Kerr solution describes a naked singularity.

### 2.5.1 Basic Properties of Kerr Black Hole

Here are the main properties of the Kerr solution (2.74), (2.75):

- It solves the vacuum Einstein equations $R_{\mu\nu} = 0$.
- It is asymptotically flat and the special case of $M = 0$ is just (a section of) the flat space.
- It is stationary and axisymmetric with $\partial_t$, $\partial_\phi$ as Killing vectors. Note that, due to rotation, $\partial_t$ is not hypersurface orthogonal, i.e. orthogonal to constant $t$ surfaces. Likewise, $\partial_\phi$ is not hypersurface orthogonal.
- Kerr geometry is not static and is hence not time-reversal symmetric. Nonetheless, it is circular as $t \to -t, \phi \to -\phi$ is a $Z_2$ symmetry of the Kerr solution; see Exercise 2.4.
- It has ADM mass and angular momentum

$$M_{\mathrm{ADM}} = M\,, \qquad J_{\mathrm{ADM}} = Ma\,. \tag{2.76}$$

- It has in general two horizons, the outer horizon at $r = r_+$ and the inner horizon at $r = r_-$ with

$$r_\pm = M \pm \sqrt{M^2 - a^2}\,. \tag{2.77}$$

- The Killing vector fields

$$\xi_{\rm H}^{\pm} = \partial_t + \Omega_{\rm H}^{\pm}\,\partial_\varphi\,, \qquad \Omega_{\rm H}^{\pm} = \frac{a}{r_\pm^2 + a^2} \tag{2.78}$$

become null at the respective horizons $r = r_\pm$. The quantity $\Omega_{\rm H}^{\pm}$ is the (outer or inner) horizon angular velocity. This name is justified since in the co-rotating frame, $\phi = \varphi - \Omega_{\rm H}^{\pm} t$, the near horizon geometry is static.
- In this co-rotating frame, one may expand the metric around $r = r_+$. In doing so, the $r, t$-part of the geometry becomes a Rindler space with surface gravity

$$\kappa = \frac{r_+ - r_-}{2r_+(r_+ + r_-)}\,. \tag{2.79}$$

One may work out surface gravity at the inner horizon. The result is the same as (2.79) but with $r_\pm \to r_\mp$. The surface gravity at the inner horizon is negative, meaning that particles are repelled from the inner horizon.
- It has an ergoregion, defined as follows. The vector field $\partial_t$ is timelike asymptotically. As we move to smaller $r$ there is a surface, the *ergosphere*, where its norm vanishes and beyond it becomes spacelike. The ergosphere is a constant-$t$ surface defined by

$$r_{\rm ergo}(\theta) = M + \sqrt{M^2 - a^2\cos^2\theta}\,. \tag{2.80}$$

The ergoregion is the part of the Kerr spacetime between the ergosphere and the outer horizon; see Fig. 2.17. Within the ergoregion both Killing vectors are spacelike. Since $r_+ \leq r_{\rm ergo}(\theta) \leq 2M = r_+ + r_-$, the ergoregion vanishes for the static case $a = 0$, as expected. See Exercise 2.28 for further analysis.
- For later purposes, it is of interest to determine the area of the outer horizon at $r = r_+$,

$$A = 4\pi\left(r^2 + a^2\right)\big|_{r=r_+} = 4\pi r_+(r_+ + r_-) = 8\pi M^2\left(1 + \sqrt{1 - a^2/M^2}\right). \tag{2.81}$$

- There is an extremal version of Kerr with confluent horizons, $r_- \to r_+$, and vanishing surface gravity (2.79).
- It has a ring singularity at $r = 0$ and $\theta = \pi/2$ where the Kretschmann scalar $R^{\alpha\beta\gamma\delta}R_{\alpha\beta\gamma\delta}$ is infinite; see [170] and references therein.
- In principle, one can extend the geometry past $r = 0$, into a region where $r^2 < 0$. However, in this region the Killing vector $\partial_\phi$ becomes timelike, leading to closed timelike curves (CTCs). The ring singularity is the boundary beyond which CTCs develop.

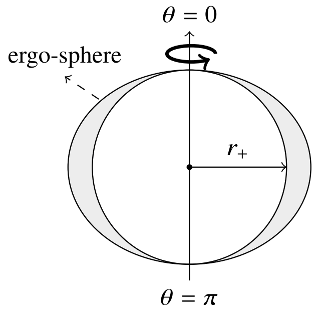


**Fig. 2.17** Ergosphere and ergoregion (shaded) in the $r, \theta$ plane (suppressing the $\phi$ direction)

- As in the RN case, the inner horizon is a Cauchy horizon and the same remarks apply as for this case; in particular, the Cauchy horizon is not expected to exist in astrophysical black holes which are results of gravitational collapse.
- From the properties above, it is clear that the causal structure of Kerr resembles the causal structure of RN. However, it is hard to draw higher-dimensional Penrose diagrams, and for Kerr, we cannot exploit spherical symmetry to reduce the dimension to two. So for Kerr, one either draws 2-dimensional slices through or projections of 4-dimensional Penrose diagrams. Choosing a slice corresponding to polar angle $\theta = \pi/2$ and dropping the $S^1$ generated by angular rotations yields a 2-dimensional diagram of the same form as for RN; see Fig. 2.13 for the generic case, Fig. 2.14 for the extremal case, and Fig. 2.15 for the naked singularity case. However, this diagram does not completely reflect the causal structure of Kerr. An alternative to Penrose diagrams for visualizing the global structure is projection diagrams [171] which are defined in such a way that they are always 2-dimensional. For generic Kerr black holes, they look essentially like the Penrose diagram, Fig. 2.13.

The existence of an ergoregion is one of the main physical differences to Schwarzschild black holes and has profound phenomenological consequences since it is accessible to an outside observer. In that region, no object can remain stationary with respect to an asymptotic observer but rather has to co-rotate with the black hole. Moreover, energy as measured by an asymptotic observer can become negative, which allows extracting (rotational) energy from the black hole, as long as the Kerr parameter $a$ is non-zero. For particles, this energy extraction is known as the Penrose process, while for the scattering of waves whose reflection amplitude is bigger than the ingoing amplitude the phenomenon is called superradiance.

### 2.5.2 Geodesics of Kerr Geometry

Black holes found in the sky are believed to be well-modeled by a Kerr geometry. Thus, null and timelike geodesics of Kerr are of great importance for black hole observations. The timelike geodesics are of particular importance as they essentially determine the path of particles in the accretion disk. Among them, the ISCO is the most important one, especially when it comes to black hole images created by EHT observations [62]. The location of the ISCO is crucial for phenomenology, so we derive it in what follows.

Assume that the 4-velocity $u^\mu$ of the test particle moving on a geodesic is normalized, $g_{\mu\nu}u^\mu u^\nu = \sigma$, with $\sigma = 0$ for null and $\sigma = -1$ for timelike geodesics. As for Schwarzschild, two evident constants of motion are the Noether charges associated with stationarity, $E := -g_{t\mu}u^\mu$, and axisymmetry, $J := -g_{\varphi\mu}u^\mu$. An additional (non-evident) constant of motion, the Carter constant $C$ [172], follows from the Kerr Killing tensor (see Exercise 2.9). In terms of these four constants, the geodesic equation leads to four first order ordinary differential equations,

$$\Delta\,\rho^2\,\dot{t} = \big((r^2+a^2)^2 - a^2\Delta\,\sin^2\theta\big)\,E - 2aMJ\,r \tag{2.82}$$

$$\Delta\,\rho^2\,\dot{\varphi} = 2aME\,r + \big(\rho^2 - 2Mr\big)\,\frac{J}{\sin^2\theta} \tag{2.83}$$

$$\begin{aligned}\rho^4\,\dot{r}^2 &= r^4\,(E^2+\sigma) - 2\sigma Mr^3 + r^2\,\big(a^2(E^2+\sigma) - J^2 - C\big)\\ &\quad + 2Mr\,\big(C + (J-aE)^2\big) - a^2C \end{aligned}\tag{2.84}$$

$$\rho^4\,\dot{\theta}^2 = C + \Big(a^2(E^2+\sigma) - \frac{J^2}{\sin^2\theta}\Big)\,\cos^2\theta\,. \tag{2.85}$$

For simplicity—and also since accretion disks are localized close to the equatorial plane—we focus on vanishing Carter constant, $C = 0$, and solve (2.85) by setting $\theta = \pi/2$ for timelike geodesics, $\sigma = -1$; further analyses of the null geodesics are deferred to Exercise 2.26. In that case, the radial evolution equation (2.84) can be written in terms of an effective potential,

$$\frac{\dot{r}^2}{2} + V_{\text{eff}} = \mathcal{E} \qquad\qquad V_{\text{eff}} = -\frac{M}{r} + \frac{J^2 - 2a^2\mathcal{E}}{2r^2} - \frac{M(J-aE)^2}{r^3} \tag{2.86}$$

that depends on energy $\mathcal{E} = (E^2-1)/2$ when the Kerr parameter is non-zero. The conditions for having a circular orbit, $V_{\text{eff}} = \mathcal{E}$ and $\mathrm{d}V_{\text{eff}}/\,\mathrm{d}r = 0$, together with the marginal stability condition $\mathrm{d}^2V_{\text{eff}}/\,\mathrm{d}r^2 = 0$ lead to three algebraic equations that can be solved for energy $\mathcal{E}$, angular momentum $J$, and ISCO-value of the radial coordinate $r_{\text{ISCO}}$. The latter two equations are solved in terms of $r_{\text{ISCO}}$ by $3(J-aE)^2 = r_{\text{ISCO}}^2$ and $J^2 - a^2E^2 = 2Mr_{\text{ISCO}} - a^2$. The remaining equation $V_{\text{eff}} = \mathcal{E}$ yields a quartic equation for $r_{\text{ISCO}}$ that has a unique positive root

$$\frac{r_{\text{ISCO}}}{M} = 3 + \sqrt{x^2 + 3a^2/M^2} \mp \sqrt{(3-x)\big(3 + x + 2\sqrt{x^2+3a^2/M^2}\big)} \tag{2.87}$$

sloppywhere the upper (lower) sign refers to a test particle co-rotating with the black hole, $a > 0$ (counter-rotating with the black hole, $a < 0$), and $x := 1 + (1 - a^2/M^2)^{1/3}[(1+a/M)^{1/3} + (1-a/M)^{1/3}]$. The static case, $a = 0$, $x = 3$, recovers the Schwarzschild result (2.30), $r_{\text{ISCO}} = 6M = 3r_+$. For extremal co-rotating Kerr black holes, $a = M$ implies $x = 1$ and $r_{\text{ISCO}} = r_+ = M$. This is crucial for phenomenology and means that strongly rotating black holes can have co-rotating accretion disks that extend almost all the way to the horizon, so that accretion disk physics allows to probe near horizon features of black holes. For generic values of $0 < a/M < 1$, the radius of the co-rotating ISCO varies between the horizon and the Schwarzschild ISCO. Extremal counter-rotating orbits yield $r_{\text{ISCO}} = 9r_+ = 9M$ and hence are farther than the Schwarzschild ISCO.

**> Frame-dragging and Lense–Thirring effect in Kerr geometry**

Non-staticity of the Kerr metric leads to frame-dragging and the Lense–Thirring effect; see [173] and refs. therein. Frame-dragging means that observers with vanishing angular momentum, $J = 0$, have non-zero coordinate angular velocity $\omega = \mathrm{d}\varphi/\,\mathrm{d}t = -g_{t\varphi}/g_{\varphi\varphi}$. As (2.82) and (2.82) show, frame-dragging occurs both for timelike and null geodesics; see Exercise 2.27 for more analysis.

The Lense–Thirring effect is the precession of a gyroscope placed in the external field of a rotating body. The Lense–Thirring 4-frequency $\omega^\mu = -\frac{1}{2}\,\epsilon^{\mu\nu\lambda\rho}k_\nu\nabla_\lambda k_\rho$ is given by the twist of the timelike Killing vector $k = \partial_t$. This frequency is non-zero as $k_\mu$ is not orthogonal to constant-$t$ hypersurfaces provided the Kerr parameter is non-zero, $a \neq 0$; see Exercise 2.2.

These effects are not particular to Kerr and apply to generic non-static spacetimes. For Kerr, they are simple enough to be explored analytically.

## 2.6 Black Holes in (A)dS Backgrounds

There are numerous reasons why adding a cosmological constant to Einstein's theory is of physical relevance and significance:

1. From an EFT perspective, the cosmological constant is the only relevant term other than the Ricci scalar. Applying Gell-Mann's 'totalitarian principle' (everything that is not forbidden is compulsory), there is no reason to set the cosmological constant to zero as there is no obvious symmetry forbidding it.
2. From a phenomenological perspective, our present universe and its inflationary phase to a good approximation are described by assuming there is a positive cosmological constant.
3. The best-studied implementation of the holographic principle, the AdS/CFT correspondence, requires a negative cosmological constant.
4. A negative cosmological constant removes some IR divergences and makes the canonical ensemble well-defined for black holes, so even if one is interested in isolated black holes where Minkowski space is a good approximation it is helpful to add a negative cosmological constant to effectively put the black hole in a box.

It is straightforward to generalize the Schwarzschild solution by considering the most general spherically symmetric solution of the vacuum Einstein equations

$$R_{\mu\nu} - \frac{1}{2} R g_{\mu\nu} = -\Lambda g_{\mu\nu} \tag{2.88}$$

in the presence of a cosmological constant $\Lambda$ known as Kottler metric or, equivalently, Schwarzschild-(A)dS.

$$\mathrm{d}s^2 = -K(r)\,\mathrm{d}t^2 + \frac{\mathrm{d}r^2}{K(r)} + r^2\,\mathrm{d}\Omega_k^2 \qquad K(r) = -\frac{\Lambda}{3}r^2 + k - \frac{2M}{r}. \tag{2.89}$$

Here, $k = 0, \pm 1$ is the curvature of the internal space described by $\mathrm{d}\Omega_k^2$ and $M$ is the black hole mass parameter. For $k = 1$, we have a black hole similar to Schwarzschild with $\mathrm{d}\Omega^2 = \mathrm{d}\theta^2 + \sin^2\theta\,\mathrm{d}\varphi^2$ being the line-element of the round 2-sphere. For $k = 0$, we get instead a black-brane type of solution where $\mathrm{d}\Omega^2 = \mathrm{d}x_1^2 + \mathrm{d}x_2^2$ is intrinsically flat, which allows black holes with toroidal horizon topology when compactifying the flat directions, $x_i \sim x_i + 2\pi$. For $k = -1$, the internal space is hyperbolic, $\mathrm{d}\Omega^2 = \mathrm{d}\rho^2 + \sinh^2\rho\,\mathrm{d}\varphi^2$.

Depending on the sign of the cosmological constant, there are various interesting possibilities for black hole solutions. Before discussing them, we point out a common convention, namely to replace the cosmological constant by a curvature length scale $\ell \propto |\Lambda|^{-1/2}$, the dS radius $\Lambda = 3/\ell^2$ or AdS radius $\Lambda = -3/\ell^2$, respectively.

### 2.6.1 Schwarzschild-dS Black Holes

For a positive cosmological constant, we need $k = 1$ to have black holes

$$\mathrm{d}s^2 = -\Big(-\frac{r^2}{\ell^2} + 1 - \frac{2M}{r}\Big)\,\mathrm{d}t^2 + \frac{\mathrm{d}r^2}{-\frac{r^2}{\ell^2} + 1 - \frac{2M}{r}} + r^2\left(\mathrm{d}\theta^2 + \sin^2\theta\,\mathrm{d}\varphi^2\right) \tag{2.90}$$

which then have up to two horizons from the two positive roots of a cubic equation. In the limit of a large dS radius, they are located at

$$r_\Lambda = \ell - M - \frac{3M^2}{2\ell} + \mathcal{O}(1/\ell^2) \qquad r_h = 2M + \frac{8M^3}{\ell^2} + \mathcal{O}(1/\ell^4)\,. \tag{2.91}$$

The locus $r_\Lambda$ is interpreted as a cosmological horizon (for a small cosmological constant $r_\Lambda$ is large), while the locus $r_h$ is interpreted as a black hole horizon (for a small cosmological constant it approaches the Schwarzschild radius).

A finite curvature radius makes the black hole bigger as compared to Schwarzschild, while adding a mass to a cosmological spacetime decreases the size of the cosmological horizon. Thus, there is a maximal value for the mass where both horizons coalesce and the black hole becomes extremal. Extremality arises for

$\ell = 3\sqrt{3}\,M$. Taking the near horizon limit of Schwarzschild-dS (analogously to the Robinson–Bertotti limit) yields the Nariai solution [174,175]

$$ds^2_{\text{Nariai}} = \frac{\ell^2}{3}\left(-\sin^2\chi\ d\tau^2 + d\chi^2 + d\theta^2 + \sin^2\theta\ d\varphi^2\right) \tag{2.92}$$

where $\chi, \theta \in [0,\ \pi]$ and $\varphi \sim \varphi + 2\pi$. This geometry is $dS_2 \times S^2$ with equal radii for $dS_2$ and $S^2$ parts. In other words, for $\ell = 3\sqrt{3}\,M$ the black hole interpolates between the $dS_2 \times S^2$ geometry at the horizon and $dS_4$ at large $r$.

As we saw, the only allowed horizon topology for black holes with $\Lambda \geq 0$ is $S^2$. For $\Lambda < 0$, however, we can have various horizon topologies, i.e. topological black holes [176,177] (see Exercise 2.31). There are other important technical differences; in particular, there is only one horizon and no extremal solution in AdS, unless one adds, e.g. rotation or charge.

### 2.6.2 Schwarzschild-AdS and Topological Black Holes

For negative cosmological constant $k$ can take any value, allowing for different horizon topologies. To see this, let us study static solutions.

1. For $k = +1$ we have a usual AdS–Schwarzschild black hole

$$ds^2 = -\left(\frac{r^2}{\ell^2} + 1 - \frac{2M}{r}\right) dt^2 + \frac{dr^2}{\frac{r^2}{\ell^2} + 1 - \frac{2M}{r}} + r^2\left(d\theta^2 + \sin^2\theta\ d\varphi^2\right) \tag{2.93}$$

with a single spherical horizon. This is so because two of the roots of the cubic equation determining the radius of the horizon are now complex. Defining the dimensionless mass parameter $\tilde{m} = \frac{M}{\ell} + \sqrt{\frac{M^2}{\ell^2} + \frac{1}{27}}$ yields

$$r_h = \ell\,\tilde{m}^{1/3} - \frac{\ell}{3}\,\tilde{m}^{-1/3} = 2M - \frac{8M^3}{\ell^2} + O(M^5/\ell^4)\,. \tag{2.94}$$

We see that the effect of a small negative cosmological constant is to make the horizon shrink to a slightly smaller size. For very small AdS radius, the horizon is located close to the origin, $r_h = (2\ell^2 M)^{1/3} + O(\ell^{4/3}/M^{1/3})$. See Exercise 2.31 for more discussion and Fig. 2.18 for the Penrose diagram.

2. For $k = 0$, we have black holes with toroidal horizon topology described by metrics

$$ds^2 = -\left(\frac{r^2}{\ell^2} - \frac{2M}{r}\right) dt^2 + \frac{dr^2}{\frac{r^2}{\ell^2} - \frac{2M}{r}} + r^2\left(dx_1^2 + dx_2^2\right) \tag{2.95}$$

where $x_{1,2} \sim x_{1,2} + 2\pi$.

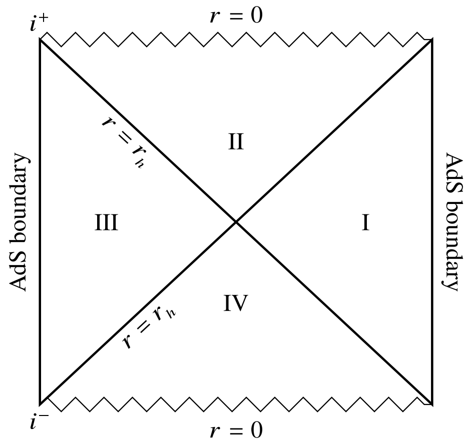


**Fig. 2.18** Penrose diagram of AdS–Schwarzschild black hole. The asymptotic boundary is timelike, exactly as for AdS; see Fig. 2.8. The rest of the diagram is identical to the Schwarzschild Penrose diagram 2.10

3. For $k = -1$ horizon is the hyperbolic space $\mathrm{H}^2$, which is non-compact. One may orbifold $\mathrm{H}^2$ by the discrete subgroup of its isometry group $SO(2, 1)$, $\Gamma_g$, $g > 1$. This orbifolding does not change the local properties of the $\mathrm{H}^2$, in particular its curvature. Moreover, it is freely acting on $\mathrm{H}^2$ and hence leads to a smooth, compact 2-dimensional surface of genus $g$, $\Sigma_g$ [176]. In this case, the black hole metric

$$\mathrm{d}s^2 = -\left(\frac{r^2}{\ell^2} - 1 - \frac{2M}{r}\right) \mathrm{d}t^2 + \frac{\mathrm{d}r^2}{\frac{r^2}{\ell^2} - 1 - \frac{2M}{r}} + r^2\, \mathrm{d}\Omega_g^2 \qquad (2.96)$$

contains the metric $\mathrm{d}\Omega_g^2$ for a genus $g$ surface $\Sigma_g$ of curvature radius one. The metric (2.96) has only one horizon at the real positive root of $\frac{r^2}{\ell^2} - 1 - \frac{2M}{r} = 0$.

Therefore, in the AdS case we can have surfaces of any given genus $g$ as the horizon: $g = 0$ (spherical, for $k = 1$), $g = 1$ (toroidal, for $k = 0$), and $g > 1$ (hyperbolic, for $k = -1$). The metrics (2.95) and (2.96) provide simple counterexamples to the spirit of 'topological censorship', according to which horizons must have spherical topology; since the corresponding theorem assumes asymptotic flatness there is no contradiction, because we need a negative cosmological constant to obtain higher genus horizon topologies.

As for $k = 1$, we also have a Nariai-like solution, $\mathrm{AdS}_2 \times \Sigma_g$. See Exercise 2.32 for more.

The discussion here generalizes to rotating and charged black holes in (A)dS. As we shall discuss an even bigger set of solutions encompassing all of them, we postpone such generalizations to the next section.

## 2.7 Plebanski–Demianski Black Holes

All black holes discussed so far are special cases of a seven-parameter family of black hole solutions found by Plebanski and Demianski [178]. The seven parameters are mass $M$, angular momentum $J = a\,M$, electric and magnetic charges $Q_e$ and $Q_m$, cosmological constant $\Lambda$, NUT charge $l$ and acceleration $\alpha$.[3] For vanishing charges, $Q_e = Q_m = 0$, these are locally vacuum solutions to the Einstein equations (of Petrov type D; see [133, 179] for a definition of this algebraic classification), while switching on charges requires additionally a Maxwell field. The Plebanski–Demianski black hole metric in Boyer–Lindquist coordinates is given by [180]

$$\mathrm{d}s^2 = \frac{1}{\Omega^2}\Big(-\frac{\Delta}{\rho^2}\big(\mathrm{d}t-(a\sin^2\theta-2l\cos\theta)\,\mathrm{d}\varphi\big)^2+\frac{\rho^2}{\Delta}\,\mathrm{d}r^2+\frac{\rho^2}{P}\,\mathrm{d}\theta^2 + \frac{P\,\sin^2\theta}{\rho^2}\big(a\,\mathrm{d}t-(r^2+a^2+l^2)\,\mathrm{d}\varphi\big)^2\Big) \tag{2.97}$$

with the functions

$$P = 1 + ak_1\,\cos\theta + a^2k_2\,\cos^2\theta \tag{2.98}$$

$$\Omega = 1-\alpha\,\big(l+a\cos\theta\big)\,r \qquad\qquad \rho^2 = r^2+\big(l+a\cos\theta\big)^2 \tag{2.99}$$

the Killing norm

$$\Delta = \Big(\big(k+Q_e^2+Q_m^2\big)\big(1+2\alpha l\,r\big)-2Mr+\frac{k}{a^2-l^2}\,r^2\Big)\,\big(1-\alpha(a+l)\,r\big)\,\big(1+\alpha(a-l)\,r\big) - \frac{\Lambda}{3}\,r^2\,\big(r^2+2\alpha l(a^2-l^2)\,r+a^2+3l^2\big) \tag{2.100}$$

and the constants

$$k = \big(a^2-l^2\big)\,\frac{1+\alpha l\,\big(2M-3\alpha\,(Q_e^2+Q_m^2)\big)-\Lambda\,l^2}{1+3\alpha^2l^2(a^2-l^2)} \tag{2.101}$$

$$k_1 = 4\alpha^2 l\big(k+Q_e^2+Q_m^2\big)-2\alpha\,M+4l\,\frac{\Lambda}{3} \tag{2.102}$$

$$k_2 = \alpha^2\,\big(k+Q_e^2+Q_m^2\big)+\frac{\Lambda}{3}\,. \tag{2.103}$$

These solutions are explicitly axisymmetric and stationary. Horizons are located at zeros of the Killing norm (2.100). Since this is a quartic function of the radial coordinate $r$, there are up to four horizons. If the seven parameters are in appropriate ranges,

[3] The cosmological constant $\Lambda$ is a parameter of the theory. As discussed in the (A)dS–Schwarzschild examples, it crucially affects the properties of the solution. We, therefore, include it together with the constants of motion parameters.

the outermost horizon is a black hole horizon. As long as the rotation parameter is not smaller than the NUT charge, $a^2 \geq l^2$, there is the same ring-like singularity as for Kerr at $\rho = 0$.

Some notable special black hole cases not discussed so far are

- **Kerr–Newman (KN).** For $\Lambda = \alpha = l = 0$, we obtain charged rotating black holes [49]. The constants simplify to $k = a^2$, $k_1 = k_2 = 0$, and the functions simplify to $\Omega = P = 1$, $\rho^2 = r^2 + a^2 \cos^2\theta$ and

$$\Delta_{\text{KN}} = r^2 - 2Mr + a^2 + Q_e^2 + Q_m^2 \,. \tag{2.104}$$

  The metric is hence that of a Kerr geometry with $\Delta$ given as above. Thus, there are up to two horizons as long as $M^2 \geq a^2 + Q_e^2 + Q_m^2$, and the causal structure and Penrose diagram of Kerr and KN solutions are similar. If this inequality saturates extremal KN, black holes are obtained. Further special cases of KN discussed before are Kerr ($Q_e = Q_m = 0$), RN ($a = 0$), and Schwarzschild ($Q_e = Q_m = a = 0$).
- **Kerr–Taub–NUT.** For $\Lambda = \alpha = Q_e = Q_m = 0$, we obtain rotating black holes with a NUT charge (where 'NUT' is an eponymous acronym referring to Newman, Unti, and Tamburino) [181,182]. The NUT charge compares to the mass like a magnetic monopole compares to an electric one and hence sometimes is referred to as 'magnetic mass'. Due to the presence of the NUT-charge, the solution is not asymptotically flat, but it is *asymptotically locally flat*; it is asymptotically a Minkowski space up to certain identification by its isometries [108]; see Exercise 2.40 for more comments. In this case, the horizon topologically is still a 2-sphere, but has now conical singularities at the poles $\theta = 0, \pi$. The constants simplify to $k = a^2 - l^2$, $k_1 = k_2 = 0$, and the functions simplify to $\Omega = P = 1$, $\rho^2 = r^2 + (l + a\cos\theta)^2$ and

$$\Delta_{\text{Kerr–Taub–NUT}} = r^2 - 2Mr + a^2 - l^2 \,. \tag{2.105}$$

  Thus, again there are up to two horizons as long as $M^2 \geq a^2 - l^2$. If this inequality saturates, extremal Kerr–Taub–NUT black holes are obtained.
- **Accelerated Kerr.** For $\Lambda = Q_e = Q_m = l = 0$, we obtain accelerated Kerr black holes. The constants simplify to $k = a^2$, $k_1 = -2\alpha M$, $k_2 = \alpha^2 a^2$, and the functions simplify to $\Omega = 1 - \alpha a \cos\theta\, r$, $P = 1 - 2\alpha a\, M \cos\theta + \alpha^2 a^4 \cos^2\theta$, $\rho^2 = r^2 + a^2 \cos^2\theta$ and

$$\Delta_{\text{accelerated Kerr}} = \left(r^2 - 2Mr + a^2\right)\left(1 - \alpha^2 a^2 r^2\right). \tag{2.106}$$

  In addition to the two horizons present for Kerr black holes, there is an acceleration horizon if $\alpha \neq 0$.

## 2.8 Vaidya Metric as Example for Non-stationary Black Holes

All black hole solutions discussed so far are stationary, which means that they provide a fair description of black holes after the formation process (like gravitational collapse) has settled down and before semiclassical effects like Hawking evaporation become relevant. In this section, we discuss a simple class of non-stationary black holes characterized by the so-called Vaidya metric [183].

The simplest Vaidya metric

$$\mathrm{d}s^2 = 2\,\mathrm{d}r\,\mathrm{d}v - \left(1 - \frac{2M(v)}{r}\right)\mathrm{d}v^2 + r^2\,\mathrm{d}\Omega^2 \tag{2.107}$$

describes a dynamical version of the Schwarzschild black hole in the ingoing EF coordinates (2.38). The only difference to the Schwarzschild black hole is that $m(v)$ is a function of advanced time $v$ rather than a constant; all other quantities have their usual meaning ($r$ is the radial coordinate and $\mathrm{d}\Omega^2$ is the line-element of the round 2-sphere). The above geometry is an Einstein vacuum solution only for constant $M$. In general, we have a spherically symmetric source of null dust. This can be seen explicitly by calculating the Ricci tensor associated with the metric (2.107).

$$R_{\mu\lambda}\big|_{r>0} = \frac{2}{r^2}\,\frac{\mathrm{d}M(v)}{\mathrm{d}v}\,\delta^v_\mu\delta^v_\lambda. \tag{2.108}$$

Since $g^{vv} = 0$ the Ricci scalar vanishes, the Ricci tensor (2.107) is therefore proportional to the energy–momentum tensor. We see that only the flux component $T_{vv}$ is non-zero, which means that the metric (2.107) describes matter that is ingoing along the null direction $v$.

A special case is the shock-wave formation of a Schwarzschild black hole with the choice

$$M(v) = \theta(v)\,M\,. \tag{2.109}$$

For negative advanced times, the geometry is locally Minkowski, while for positive advanced times it is locally Schwarzschild. At $v = 0$ there is a delta-like localization of collapsing lightlike matter. The Penrose diagram is shown in Fig. 2.19.

A remarkable aspect of (2.107) with (2.109) is that the geometry solves the vacuum Einstein equations everywhere except at $v = 0$, where it has a delta-like localized energy–momentum tensor as a source. Moreover, the special case (2.109) leads to an energy–momentum tensor

$$T_{\mu\lambda}\big|_{r>0} = \frac{M}{4\pi G_{\mathrm{N}}\,r^2}\,\delta^v_\mu\delta^v_\lambda\,\delta(v) \tag{2.110}$$

that is localized at $v = 0$ with a delta-function. A different way to understand this localized energy–momentum tensor is by patching together two vacuum solutions at a null hypersurface; see Exercise 2.41 for more detail.

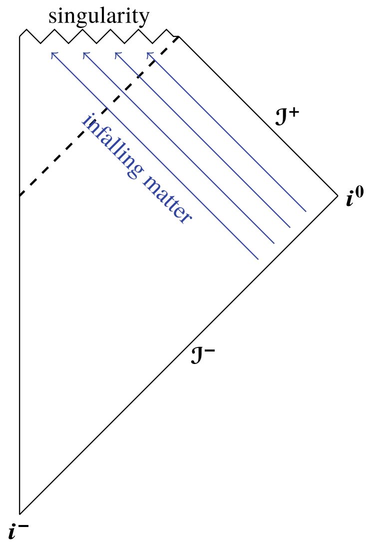


**Fig. 2.19** Penrose diagram of Vaidya black hole, analogous to Fig. 2.11

A straightforward generalization of the metric (2.107) is to consider arbitrary radial and (advanced) time-dependence in the $vv$-component:

$$\mathrm{d}s^2 = 2\,\mathrm{d}r\,\mathrm{d}v - \big(1 - f(v, r)\big)\,\mathrm{d}v^2 + r^2\,\mathrm{d}\Omega^2. \tag{2.111}$$

For $f = 2m(v)/r$, the Vaidya metric above is recovered. The Einstein tensor associated with (2.111) has now additional entries besides the flux component $G^r{}_v$:

$$G^\mu{}_\lambda = \frac{\dot f}{r}\,\delta^\mu_r\delta^v_\lambda - \frac{f'}{r}\,\delta^\mu_\lambda - \frac{f}{r^2}\left(\delta^\mu_v\delta^v_\lambda + \delta^\mu_r\delta^r_\lambda\right) - \frac{f''}{2}\left(\delta^\mu_\theta\delta^\theta_\lambda + \delta^\mu_\varphi\delta^\varphi_\lambda\right). \tag{2.112}$$

Here, prime means derivatives with respect to $r$ and dot derivatives with respect to $v$. For $f(v, r) = 2M(v)/r + Q(v)^2/r^2$ (2.112), we obtain the so-called Vaidya–Bonnor solution, which describes time-dependent charged black holes; see Exercise 6.22 for more discussions.

## Further Reading

Classification and cataloging of solutions, in particular black hole solutions, to GR with various matter contents and analysis of these solutions is still an ongoing program. For some books on (black hole) solutions, we refer to [133, 180, 184, 185] and for particle motion and geodesic/probe analysis to [186]. For a historical/autobiographic review on Kerr geometry and Kerr–Schild coordinates, see [187].

## Exercises

**2.1 Schwarzschild Killing vectors.**

Verify that (2.4) are indeed Killing vectors solving the Killing equation (2.3) and check that they satisfy the algebra $\{\xi_i, \xi_j\}_{\text{L.B.}} = f_{ij}{}^k \xi_k$, where L.B. stands for the Lie bracket and $f_{ij}{}^k$ are structure constants of $so(3)$.

**2.2 Hypersurface orthogonality.**

Consider a hypersurface defined through $\Phi(x^\mu) = 0$ and let $\mathbf{n}_\mu$ denote the 1-form field normal to it $\mathbf{n}_\mu = N\partial_\mu\Phi$, where $N$ is a normalization factor.

(1) Show that $\mathbf{n}$ satisfies the Frobenius theorem,

$$\mathbf{n}_{[\mu}\nabla_\nu\mathbf{n}_{\alpha]} = 0. \tag{2.113}$$

(2) One can always choose the coordinate system such that $\Phi(x)$ is one of the coordinates. Call this coordinate system $y^\mu$ where $y^1 = \Phi(x)$ while the other $y^\mu$ span the hypersurface. Consider the vector field $\mathbf{Y} := \partial_y$. Show that in general $\mathbf{Y}$ and $\hat{\mathbf{n}}^\mu := g^{\mu\nu}\mathbf{n}_\nu$ are not parallel, i.e.

$$(g_{\mu\nu} - \mathbf{n}_\mu\mathbf{n}_\nu)\mathbf{Y}^\nu \neq 0. \tag{2.114}$$

(3) Find the condition for $\mathbf{Y}$ to be normal to the $\Phi = 0$ hypersurface, i.e. to be *hypersurface orthogonal*.

**2.3 More on stationarity and staticity**

It is well-known that one can use flows of a given vector field $V$ to locally define the normal coordinate $v$ such that $V = \partial_v$.

(1) Show that in normal coordinates $\partial_v g_{\alpha\beta} = 0$ if $V$ is a Killing vector and therefore the most general form of a *stationary* metric with $\partial_t$ as a Killing vector is

$$\mathrm{d}s^2 = -g_{tt}\mathrm{d}t^2 + 2g_{ti}\mathrm{d}t\mathrm{d}x^i + g_{ij}\mathrm{d}x^i\mathrm{d}x^j, \qquad i, j = 1, 2, 3, \tag{2.115}$$

where $g_{tt}, g_{ti}, g_{ij}$ are $t$-independent functions.

(2) Show that $g_{\alpha v} = 0, \alpha \neq v$ means $\partial_v$ is orthogonal to $v = \text{const.}$ surfaces. In this case, the Killing vector $v$ is called *hypersurface orthogonal*.

(3) One can further restrict (2.115) to *static* metrics. Show the most general form of the metric may be written as

$$\mathrm{d}s^2 = -g_{tt}\mathrm{d}t^2 + g_{ij}\mathrm{d}x^i\mathrm{d}x^j, \qquad i, j = 1, 2, 3, \tag{2.116}$$

where $g_{tt}, g_{ij}$ are $t$-independent functions.

(4) The above form for static spacetimes (2.116), while quite general, depends on the choice of coordinate $t$. There is, however, a coordinate independent definition of staticity: *Stationary geometries in which their timelike Killing vector field is hypersurface orthogonal are static*. Show that this definition and the one based on the reflection symmetry of the timelike coordinate $t$ are equivalent.

**2.4 More on circular spacetimes.**

A subclass of stationary spacetimes are those which are also axisymmetric, i.e. besides $\xi_t := \partial_t$ they have another Killing vector $\xi_\phi := \partial_\phi$ which is along the $2\pi$ periodic coordinate $\phi$.

(1) Starting from (2.116) restrict it so that it gives the most general form of an stationary-axisymmetric metric in $t, r, \theta, \phi$ coordinate system.

(2) A subclass of stationary-axisymmetric metrics are those which are invariant under simultaneous inversion of $t, \phi$, $(t, \phi) \to (-t, -\phi)$. These spacetimes are called *circular* spacetimes [188]. Write down the most general form of metrics for circular spacetimes.

(3) The above definition based on double inversion symmetry, while quite general, depends on the choice of coordinates $t, \phi$. One can, however, provide a more 'covariant' definition of circularity. Show that for all circular spacetimes [133]

$$\xi_t^{[\mu}\xi_\phi^{\nu}\nabla^\alpha\xi_t^{\beta]} = 0, \qquad \xi_t^{[\mu}\xi_\phi^{\nu}\nabla^\alpha\xi_\phi^{\beta]} = 0. \tag{2.117}$$

(4) Show that all Plebanski–Demianski black holes are circular.

(5) Show that in Einstein–Maxwell theory, a necessary condition to obtain non-circular solution is

$$J^{[\mu}\xi_t^{\nu}\xi_\phi^{\lambda]} \neq 0, \tag{2.118}$$

where $J$ is the charge current sourcing the Maxwell field. Show that in the adapted coordinates, $\xi_t = \partial_t, \xi_\phi = \partial_\phi$; this means $J^r$ or $J^\theta$ components should be non-zero.

**2.5 Curvature invariants of Schwarzschild geometry.**

To argue that $r = 2G_{\rm N}m$ is not a curvature singularity besides the Kretschmann invariant (2.8), one should explore higher curvature invariants, scalars made from higher powers of Riemann curvature and its derivatives. In four dimensions, these are scalars constructed by various powers of Riemann curvature $R_{\alpha\beta\mu\nu}$, inverse metric $g^{\mu\nu}$, and the Levi–Civitá tensor $\epsilon^{\alpha\beta\mu\nu}$.

(1) Compute the Gauss–Bonnet invariant, $\epsilon^{\alpha\beta\mu\nu}\epsilon^{\lambda\rho\sigma\gamma}R_{\alpha\beta\lambda\rho}R_{\mu\nu\sigma\gamma}$.

(2) Show that any invariant which involves $\epsilon^{\alpha\beta\mu\nu}$, like $\epsilon^{\alpha\beta\mu\nu}R_{\alpha\beta\rho\gamma}R_{\mu\nu}{}^{\rho\gamma}$ is zero.

(3) Schwarzschild is Ricci-flat and hence all information in its Riemann curvature is in the Weyl tensor. Compute the Weyl tensor for the Schwarzschild geometry.

(4) Show that for a Schwarzschild black hole, all curvature invariants made from higher powers of Riemann (or Weyl) tensors are not independent of the Kretschmann invariant. Use the symmetries and number of independent non-vanishing components of Riemann. Show that all curvature invariants are smooth at $r = 2G_{\rm N}m$ while blowing up at $r = 0$.

**2.6 More on ADM mass and angular momentum.**

For asymptotic flat stationary spacetimes, one may use the expansion $g_{\mu\nu} = \eta_{\mu\nu} + h_{\mu\nu}$, where $h_{\mu\nu}$ is small asymptotically.

(1) Show that the linearized Einstein equation takes the form

$$\Box h_{\mu\nu} + \partial_\mu \partial_\nu h - \partial_\alpha \partial_\mu h^\alpha{}_\nu - \partial_\alpha \partial_\nu h^\alpha{}_\mu = 16\pi G_\text{N}(T_{\mu\nu} - \frac{1}{2}\eta_{\mu\nu} T) \tag{2.119}$$

where $\Box$ is the flat space d'Alembertian, $h = \eta^{\mu\nu} h_{\mu\nu}$, $T = \eta^{\mu\nu} T_{\mu\nu}$ and $h^\mu{}_\nu = \eta^{\mu\alpha} h_{\alpha\nu}$.

(2) Show that for stationary cases where $h_{\mu\nu}$ have no time-dependence, the $tt$ component of the above equation yields the ADM energy

$$E := \int_{\substack{\text{const. } t\\ \text{slice}}} T_{tt} = \frac{1}{8\pi G_\text{N}} \oint_{S^2_\infty} \mathrm{d}\Sigma_j\ \partial_j h_{tt} = \frac{1}{16\pi G_\text{N}} \oint_{S^2_\infty} \mathrm{d}\Sigma_j\ (\partial_i h_{ji} - \partial_j h_{ii}), \tag{2.120}$$

where in the last equation $i$ index denotes asymptotic spatial Cartesian coordinates and $\mathrm{d}\Sigma_j$ is the element of the area of the $S^2$ at infinity.

(3) Similarly, one may define the ADM angular momentum

$$J_{ij} := \int_{\substack{\text{const. } t\\ \text{slice}}} (T^t{}_i x_j - T^t{}_j x_i) = \frac{1}{16\pi G_\text{N}} \oint_{S^2_\infty} \mathrm{d}\Sigma_k\, [(\partial_k h^t{}_i - \partial_i h^t{}_k) x_j - (i \leftrightarrow j)]. \tag{2.121}$$

(4) Show that the above in polar coordinates reproduce ADM mass and angular momentum (2.14).

**2.7 More on geodesic reparameterization invariance.**

(1) Starting from the action (2.15) and that the Lagrangian is independent of $\lambda$, show that $g_{\mu\nu}\dot{x}^\mu \dot{x}^\nu =$ const. on the particle trajectory.

(2) Work out the Euler–Lagrange equations of the action (2.15) and show that it reproduces the geodesic equation (1.1).

(3) Consider the action

$$I = \int_\gamma \mathrm{d}\lambda\ g_{\mu\nu}\dot{x}^\mu \dot{x}^\nu \tag{2.122}$$

and show that it yields the same EOM as the action (2.15).

(4) The action (2.122) is not invariant under general path reparameterizations $\lambda \to f(\lambda)$. Viewing reparameterization invariance as a gauge freedom, the action (2.122) may be viewed as a gauge-fixed form of (2.15). Find this gauge fixing.

(5) While not invariant under general reparameterizations, (2.122) is scaled just by a coefficient under a restricted set of such reparameterizations, $\lambda \to a\lambda + b$, the *affine* parameter. Verify that the geodesic equation (1.1), although not invariant under general path reparameterizations, is invariant under affine transformations.

**2.8 Conserved quantities on geodesics.**

(1) Metrics with isometries yield conserved quantities. Let $\xi$ be the Killing vector field associated with a given isometry, $\mathcal{L}_\xi g_{\mu\nu} = 0$. Show that

$$P_\xi = \xi_\mu \dot{x}^\mu = \text{const.} \tag{2.123}$$

along the geodesic. This is a consequence of Noether's theorem which associates the conserved charge $P_\xi$ to a symmetry $\xi$.

(2) One may view the particle motion as Hamiltonian dynamics on a phase space. To this end, one may choose the path parameter $\lambda$ to be the Hamiltonian time. There is a natural Poisson bracket defined on the phase space,

$$\{x^\mu, p^\nu\}_{\text{P.B.}} = \delta^{\mu\nu}, \qquad p^\mu \equiv \frac{\mathrm{d}x^\mu}{\mathrm{d}\lambda}. \tag{2.124}$$

Using the above show that for any two Killing vector fields $\xi_1, \xi_2$,

$$\{P_{\xi_1}, P_{\xi_2}\}_{\text{P.B.}} = P_{\{\xi_1,\xi_2\}_{\text{L.B.}}}. \tag{2.125}$$

That is, momenta associated with the Killing vectors satisfy the same algebra as the Killing vectors.

**2.9 Killing tensors.**

As a generalization of Killing vectors, one can define a rank $k$ Killing tensor $K^{\mu_1\mu_2\cdots\mu_k}$ as a symmetric tensor obeying the Killing tensor equation

$$\nabla^{(\mu_1}K^{\mu_2\mu_3\cdots\mu_{k+1})} = 0 \tag{2.126}$$

where $(\cdots)$ stands for symmetrization.

(1) With this definition, one can readily see that any metric with Levi–Civitá connection is indeed a second rank Killing tensor.

(2) Let $\xi_i^\mu$ be Killing vectors; show that any symmetric product of them,

$$K^{\mu_1\mu_2\cdots\mu_n} := \mathcal{K}_{(i_1 i_2\cdots i_n)}\xi_{i_1}^{\mu_1}\cdots\xi_{i_n}^{\mu_n} \tag{2.127}$$

where $\mathcal{K}_{(i_1 i_2\cdots i_n)}$ are some constants, is a Killing tensor. Killing tensors which may be written in terms of lower rank Killing tensors are called reducible.

(3) Show that the rank $k$ Casimirs of the algebra of Killing vectors form a rank $k$ Killing tensor.

(4) Consider two Killing tensors $K_{(1)}$ and $K_{(2)}$ of rank $n, m$. Their *Schouten–Nijenhuis bracket* [189,190] is defined as

$$\begin{aligned}{}_{\text{SN}}^{\mu_1\mu_2\cdots\mu_{m+n-1}} &:= n\mathcal{K}_{(1)}^{\alpha(\mu_1\mu_2\cdots\mu_{n-1}}\nabla_\alpha\mathcal{K}_{(2)}^{\mu_n\mu_{n+1}\cdots\mu_{m+n-1})} \\ &\quad - m\mathcal{K}_{(2)}^{\alpha(\mu_1\mu_2\cdots\mu_{m-1}}\nabla_\alpha\mathcal{K}_{(1)}^{\mu_m\mu_{m+1}\cdots\mu_{m+n-1})}.\end{aligned} \tag{2.128}$$

Show the above bracket yields another Killing tensor from two given Killing tensors. Show also that metric (as a second rank Killing tensor) commutes with all Killing tensors.

(5) Show that for geodesic paths $x^\mu(\tau)$,

$$P_K := K_{\mu_1\mu_2\cdots\mu_k}\dot{x}^{\mu_1}\dot{x}^{\mu_2}\cdots\dot{x}^{\mu_k} \tag{2.129}$$

is a conserved quantity on a geodesic. In particular, $g_{\mu\nu}\dot{x}^\mu\dot{x}^\nu = \text{const.}$ for any geodesic.

(6) The Carter constant $C$ [172] for the Kerr metric is related to a Killing two-tensor, $C = C_{\mu\nu}\dot{x}^\mu\dot{x}^\nu$. Find $C_{\mu\nu}$ for Kerr and KN geometries. What is $C_{\mu\nu}$ for the Schwarzschild case?

**2.10 More on comparison of fiducial and free-fall observers.**

We discussed in Sect. 2.1.5 how to compare the frequencies two *fido*s measure. One may repeat the same analysis for two free-fall observers and a free-fall and a *fido* at the same radius.

(1) Consider two radially free-fall observers. Their paths are given by (2.28). Assume both of them start at rest in the asymptotic region, $v_\infty = 0$. Therefore, for both $\dot{r}^2 = r_h/r, \dot{t} = (1 - r_h/r)^{-1}$.

(1-1) Show that their boost factor at a given radius $r$ is locally given by

$$\gamma(r) := 1/\sqrt{1 - \left(\frac{\mathrm{d}r}{\mathrm{d}t}\right)^2} = \left(1 - \frac{r_h}{r} + \frac{2r_h^2}{r^2} - \frac{r_h^3}{r^3}\right)^{-1/2}.$$

(1-2) Suppose that the observer at infinity is sending in a signal of frequency $\omega_\infty$. Show that the frequencies of two such free-fall observers at radii $r_A, r_B$ measure are related as $\gamma(r_A)^{-1}\omega_A = \gamma(r_B)^{-1}\omega_B = \omega_\infty$.

(1-3) Show that the velocity as measured by the asymptotic observer and hence the boost factor is maximized at $r = r_{\text{ISCO}} = 3r_h$, while the boost factor is equal to one at $r = \infty$ and $r = r_h$.

(1-4) Compare this with the case of two *fido*s at different radii.

(2) Complete the above analysis by comparing frequencies measured by a *fido* and a free-fall observer (as described above) at the same radius $r$. Analyze this for $r = r_h$ case.

**2.11 Near horizon geodesics.**

(1) Study geodesics of the near horizon metric (2.10).

(2) Show that the geodesics of the Schwarzschild geometry in the near horizon region match with the geodesics found in (1) of this exercise.

(3) Study null geodesics at $\rho = \rho_0$ of the near horizon metric. How much coordinate time does it take to send and receive a light signal between two antipodal points on the $S^2$?

(4) Repeat the above exercise for the Kerr geometry given in (2.74).

**2.12 Cross-section of Schwarzschild black holes.**

(1) Using (2.26), compute the light deflection angle as a function of the impact parameter for orbits in the $r > 3G_{\text{N}}M$ region.

(2) Compute the differential and total cross-section of a black hole for light rays. Since the gravity force is long-range, one would expect the total cross-section to be infinite, as in the Rutherford scattering.

(3) GR deviations from Newtonian gravity may be quantified through the difference between this cross-section and the Rutherford cross-section. Compare this regularized total cross-section with the area of the photon-sphere.

(4) Repeat the above three parts for timelike geodesics.

(5) Bonus level: Repeat the above for Kerr black hole.

**2.13 More on timelike geodesics in Schwarzschild geometry.**

(1) Redo the analysis of radial timelike geodesics in the asymptotic observer's frame. How much time does it take for a particle starting at $r_0 > 2G_{\mathrm{N}}M$ to pass $r = 2G_{\mathrm{N}}M$?

(2) Analyze the trajectories of a free massive particle, i.e. write the counterpart of (2.26) for timelike geodesics and explore its solutions.

**2.14 Outgoing Eddington–Finkelstein and Gaussian null coordinate systems.**

(1) The outgoing EF coordinate system uses $r, u$ given in (2.37). Show that in this coordinate system the metric is

$$\mathrm{d}s^2 = -f(r)\,\mathrm{d}u^2 - 2\mathrm{d}r\mathrm{d}u + r^2\mathrm{d}\Omega^2\,. \tag{2.130}$$

Here, $u \in (-\infty, +\infty)$, $r > 0$, and $\partial_u$ is a globally defined Killing vector field which becomes null at $f = 0$, and is spacelike (timelike) in $f < 0$ ($f > 0$) regions. The vector $\partial_r$ is past-oriented null and $\partial_r \cdot \partial_u = -1$.

(2) One can use any (globally defined) vector field $N$ to define a coordinate system. Such coordinate systems, if the vector is timelike, spacelike, or null, are respectively called Gaussian timelike, spacelike, or null coordinate systems. We first discuss the Gaussian null case:

– Define the coordinate $r$ such that $N = \partial_r$.
– Define the coordinate $v$ such that $\partial_v \cdot \partial_r = 1$.
– One may then define two other spacelike coordinates $x^a$.

Show that the metric in Gaussian null coordinate takes the form

$$\mathrm{d}s^2 = g_{vv}\mathrm{d}v^2 + 2\mathrm{d}r\mathrm{d}v + 2g_a\mathrm{d}v\mathrm{d}x^a + g_{ab}\mathrm{d}x^a\mathrm{d}x^b. \tag{2.131}$$

Depending on the symmetries and the specific solution under consideration, metric coefficients $g_{vv}, g_a, g_{ab}$ can have specific general features.

(3) Verify that the ingoing and outgoing EF coordinate systems are indeed in Gaussian null form.

(4) Repeat the above procedure for a (timelike) Gaussian coordinate system based on the timelike vector field $T$.

**2.15 Geodesic completeness of flat space.**

Show that flat space in Minkowski coordinates is geodesically complete by studying possible extensions of null, timelike, and spacelike geodesics.

**2.16 More on EF and Kruskal coordinates.**

(1) Convince yourself that the original Schwarzschild $t, r$ coordinates, with $r > r_h$, cover only quadrant **I**, the ingoing EF coordinates quadrants **I, II** or **III, IV** and outgoing EF coordinates quadrants **I, IV** or **II, III**, where the quadrants refer to the Kruskal diagram 2.4.

(2) Show that in Kruskal coordinates, the Killing vector field which is of unit norm at infinity and is timelike in the region $UV < 0$ is of the form

$$\zeta_H = \frac{1}{\kappa}(V\partial_V - U\partial_U)\,. \tag{2.132}$$

What is the norm of this vector at the horizon $UV = 0$?

**2.17 Schwarzschild and Reissner–Nordström geometries in various coordinates.**

(1) *Isotropic coordinates.* Find the coordinate transformation which bring the Schwarzschild geometry to the spatially isotropic form

$$\mathrm{d}s^2 = -G(\rho)\mathrm{d}t^2 + F(\rho)\mathrm{d}x_i\mathrm{d}x_i \qquad \rho^2 := x_i x_i \tag{2.133}$$

where $x_i$ are Cartesian coordinates on the spatial sections.

– What are the functions $F, G$?

– Which of the four quadrants of the Kruskal diagram 2.4 do the isotropic coordinates cover?

– Write the RN metric in isotropic coordinates. Specifically, write the metric for the extremal case and verify that in this case $F = G^{-1}$.

(2) *Israel coordinates* [44]. Consider the metric

$$\mathrm{d}s^2 = 2\mathrm{d}u\mathrm{d}z + (\frac{z^2}{2Mr})\mathrm{d}u^2 + r^2\mathrm{d}\Omega^2 \tag{2.134}$$

where $r = 2M + uz/(4M)$ and $u, z \in \mathbb{R}$.

– Show this is a vacuum Einstein solution.

– Show that in the region $uz > 0$, the metric is converted to the Schwarzschild solution upon $t = r - 2M\ln(\frac{u}{2z})$.

– Explore radial timelike geodesics of (2.134).

– Where is horizon $r = 2M$ in this coordinate system?

– Which part of the maximally extended Schwarzschild geometry is covered in this coordinate system?

– One may also write the RN metric in Israel coordinates, where the $\frac{z^2}{2Mr}$ is replaced by $(\frac{z}{r_+ r})^2\,((r_+ - r_-)r - r_+ r_-)$ and $r_\pm$ are the inner and outer horizon radii. Show that $r = r_+ + \frac{uz(r_+ - r_-)}{2r_+^2}$. Find $t = t(r, u, z)$ which brings this metric to the usual RN coordinate system.

**2.18 Couch–Torrence inversion symmetry of extremal Reissner–Nordström.** Consider the extremal RN metric,

$$\mathrm{d}s^2 = -f^2(r)\mathrm{d}t^2 + \frac{\mathrm{d}r^2}{f^2(r)} + r^2\mathrm{d}\Omega^2, \qquad f(r) = 1 - \frac{Q}{r}. \tag{2.135}$$

(1) Rewrite the metric in coordinate $R = \frac{Q}{r-Q}$.

(2) Show that upon inversion of $R$, $R \to 1/R$, the metric goes to itself up to the conformal factor $R^2$.

(3) Show that a similar inversion symmetry does not work for extremal KN black holes.

The above observation that the extremal RN metric is conformally invariant under a radial inversion was first made by Couch and Torrence [191]; see [192] for more recent follow-ups and references.

**2.19 Einstein–Rosen bridge.**

Consider the constant time slice of Schwarzschild solution in the isotropic coordinates,

$$\mathrm{d}s^2 = \left(1 + \frac{M}{2\rho}\right)^4 \left(\mathrm{d}\rho^2 + \rho^2\mathrm{d}\Omega^2\right). \tag{2.136}$$

(1) Show (2.136) has two asymptotically flat regions $\rho \to 0$ and $\rho \to \infty$.

(2) Show that these two asymptotically flat regions are related by a 'throat' at $\rho = M/2$. Constant $t$ surfaces in the isotropic coordinates are Einstein–Rosen bridges.

**2.20 Null geodesics of two conformally related metrics.**

Consider two metrics $\tilde{g}_{\mu\nu}$, $g_{\mu\nu}$ related by a Weyl scaling

$$\tilde{g}_{\mu\nu} = \Omega^2(x)g_{\mu\nu} \tag{2.137}$$

where we assume the conformal factor $\Omega$ to be a smooth positive function over the spacetime.

(1) Show that the Christoffel symbols of the two spacetimes are related as

$$\tilde{\Gamma}^{\alpha}{}_{\mu\nu} = \Gamma^{\alpha}{}_{\mu\nu} + \Omega^{-1}(\delta^{\alpha}{}_{\mu}\partial_\nu\Omega + \delta^{\alpha}{}_{\nu}\partial_\mu\Omega - g_{\mu\nu}\partial^{\alpha}\Omega). \tag{2.138}$$

(2) Consider a lightlike path whose velocity is given by the null vector field $u^\mu$. Show that whenever $g_{\mu\nu}u^\mu u^\nu = 0$ also $\tilde{g}_{\mu\nu}u^\mu u^\nu = 0$.

(3) Recall that $\frac{\mathrm{d}\Omega}{\mathrm{d}\lambda} = u^\mu\partial_\mu\Omega$, where $\lambda$ is the affine parameter along the path. Then show that the null geodesic equation for $\tilde{g}$ and $g$ are related by a change of path parameter. Find this path reparametrization as a function of $\Omega$.

**2.21 Stereographic coordinates.**

Consider the Euclidean plane in two dimensions in polar coordinates, $\mathrm{d}s^2 = \mathrm{d}r^2 + r^2\,\mathrm{d}\varphi^2$ with $\varphi \sim \varphi + 2\pi$ and $r \in \mathbb{R}_0^+$. Introduce the new coordinate $\theta$ defined by $r = \cot\frac{\theta}{2}$ and check the range of this coordinate, as well as what happens when you take $r \to \infty$. Which Euclidean manifold do you obtain when adding the point $r = \infty$?

**2.22 Penrose diagram for AdS$_2$.**

$AdS_2$ in global coordinates is given by

$$\mathrm{d}s^2 = \frac{L^2}{\cos^2\theta}\left(-d\tau^2 + d\theta^2\right) \tag{2.139}$$

where $-\pi/2 \leq \theta \leq \pi/2$. Draw the Penrose diagram of $AdS_2$ and show that it is a vertical strip with two disconnected boundaries at $\theta = \pm\pi/2$. This is in contrast with the cylinder depicted in Fig. 2.8 for higher-dimensional AdS spaces.

**2.23 Getting acquainted with $\tau$, $\chi$ coordinates of Schwarzschild metric** (2.60).

(1) Recalling (2.43), show that both of the interesting $\tau = \pm\chi$ lines correspond to $r = r_h$ in the original Schwarzschild coordinate system. For this reason, $\mathcal{H}^\pm$ are called *bifurcation horizon* and their intersection is the bifurcation surface $\mathcal{B}$ (cf. Fig. 2.6).

(2) Show that on the whole Penrose diagram, the flow of the coordinate $\tau$ is always along upward vertical lines.

(3) Analyze the flow of Schwarzschild time $t$ in regions **I**, **II**, **III** and **IV**. Note that $\partial_t$ is a timelike Killing vector only in regions **I**, **III**, while in regions **II**, **IV** this Killing vector is spacelike. Can we use $t$ as the physical time in regions **I**, **III**?

(4) Draw a constant $t$ and a constant $\tau$ slice on the Penrose diagram. Are these Cauchy surfaces? Note the time orientation of these surfaces.

(5) Draw constant $r$ and constant $\chi$ curves in various regions of the Penrose diagram. When do these coincide?

(6) Convince yourself that $\tau + \sigma_1\chi = \sigma_2\pi$, where $\sigma_1, \sigma_2 = \pm 1$, indeed correspond to future and past null infinities, respectively for $\sigma_1\sigma_2 = +1$ and $\sigma_1\sigma_2 = -1$.

**2.24 More examples of Penrose diagrams.**

(1) Consider a plane-wave geometry

$$\mathrm{d}s^2 = -2\mathrm{d}u\mathrm{d}v - H(u,\, r,\, \phi)\mathrm{d}v^2 + \mathrm{d}r^2 + r^2\mathrm{d}\phi^2, \quad u, v \in \mathbb{R},\; r \in [0,\infty),\; \phi \in [0, 2\pi] \tag{2.140}$$

with the simple choice $H(u,\, r,\, \phi) = \mu^2 r^2$. Draw a Penrose diagram of this geometry. See [193] for hints and discussions.

(2) Draw the Penrose diagram corresponding to a 'one-sided AdS–Schwarzschild' black hole, i.e. the geometry associated with a spherically symmetric gravitational collapse in AdS.

(3) Repeat (2) for the spherically symmetric gravitational collapse on the dS geometry.

(4) Draw the Penrose diagram of the collapsing charged and/or rotating matter.

**2.25 Geodesics and particle paths in Reissner–Nordström geometry.**

(1) Explore null and timelike geodesics in the RN black hole. In particular, derive the radius of the photon-sphere and the ISCO.

(2) Study the motion of a particle of mass $m$ and charge $q$ around a RN black hole of mass $M$ and charge $Q$. Note that in this case due to the presence of Coulomb force, the particle does not move on a geodesic. Explore the innermost circular orbit. Can the radius of this circular orbit (for a range of $q/m$) be smaller than the ISCO radius of part (1) of this exercise?

**2.26 Null geodesics and photon-sphere of Kerr geometry.**

(1) Work out null geodesics, radial, and in general those with non-zero impact parameters for the Kerr geometry. Discuss cases with $C = 0$ and $C \neq 0$, where $C$ is the Carter constant of motion discussed in Sect. 2.5.2.

(2) Discuss what is the shape of the photon-sphere in Kerr geometry. How does the photon-sphere depend on the Kerr parameter $a/M$? Analyze the extremal regime $a/M \to 1$.

**2.27 Zero angular momentum observer of Kerr geometry.**

Consider an observer with zero angular momentum $J$ and define its angular velocity (as measured by the asymptotic observer) as $\Omega := \mathrm{d}\phi/\mathrm{d}t$.

(1) Compute $\Omega$ as a function of $r, \theta$.

(2) Show that $\frac{\Omega}{Ma} > 0$.

(3) At which radii does $\Omega(r, \theta)$ become $\theta$-independent?

(4) Show that $\Omega(r \to \infty) = 0$ and $\Omega(r = r_+) = \Omega_{\mathrm{H}}^+$ given in (2.78).

(5) What is the maximum value of $\Omega(r, \theta)$ and at which $r, \theta$ does it happen?

(6) One may conversely explore how far one can co-rotate with a black hole of a given mass and angular momentum. That is, consider an observer (not necessarily a free-fall observer) with angular velocity $\Omega_{\mathrm{H}}^+$. How far can one go out and still remain on a timelike or null trajectory in the region $r > r_+$?

**2.28 More on the ergoregion.**

(1) While $\partial_t$ and $\partial_\phi$ are both spacelike in the ergoregion, find their linear combinations which are timelike. That is, what are the allowed values of $\alpha$ in the linear combination $\xi = \partial_t + \alpha \partial_\phi$ that make $\xi$ a timelike Killing vector in the ergoregion?

(2) Compute the area of the ergosphere and compare it to the area of the outer horizon. For which value of the Kerr parameter $a/M$ is the area of the ergosphere maximized?

**2.29 Gyromagnetic factor of Kerr–Newman black holes**

According to the theory of Dirac spinors, a charged fermion of charge $q$ and mass $m$ that is described by the Dirac equation has a magnetic dipole moment $\boldsymbol{\mu}$,

$$\boldsymbol{\mu} = \frac{q}{2m}\, g\, \boldsymbol{S} \tag{2.141}$$

where $\boldsymbol{S}$ is its spin vector and $g$ is the gyromagnetic ratio. Dirac's theory predicts $g = 2$ for any Dirac particle at the classical level.

Brandon Carter observed in [172] that the KN black hole also has $g = 2$. To see this, consider a KN black hole of mass $M$ and electric charge $Q$ and rotation parameter $a$.

(1) What is the magnetic dipole moment $\mu_{\text{KN}}$ associated with the geometry as viewed by the asymptotic static observer?

(2) Compute $\mu_{\text{KN}}/J_{\text{KN}}$ where $J_{\text{KN}}$ is the angular momentum of the black hole. Show that in analogy to (2.141) the black hole has $g = 2$, as a usual Dirac particle.

(3) In a similar way, one can show that the KN solution has quadrupole or higher poles. Compute the magnetic quadrupole for the KN geometry. Note that Dirac particles do not have such quadrupole.

**2.30 Distributional energy–momentum tensor for Schwarzschild black holes.**

Show that Schwarzschild black holes have a distributional energy–momentum tensor localized at the center of the black hole, $T^{\mu}{}_{\nu} = -M/G_{\text{N}}\, \delta^{(3)}(x)\, \delta^{\mu}_{t_*}\delta^{t_*}_{\nu}$ where $t_* = t - 2M\ln(2M - r)$ and $t, r$ are the Schwarzschild time and radial coordinates. Bonus level: generalize this to other black holes, like RN or Kerr.

**2.31 More on AdS–Schwarzschild solutions.**

As discussed, on an AdS background we can have all possible horizon topologies, $\text{S}^2$, $\text{T}^2$, and a general handle body of genus $g > 1$. These black holes besides their horizon topology have different physical properties explored in this exercise.

(1) Show that for $k = +1, 0, -1$, the isometry of the black hole solution (2.89) besides the time translation respectively involves $SO(3)$, $ISO(2)$, $SO(2,1)$.

(2) Compute surface gravity of black holes in (2.89) for various $k$.

(3) For the AdS case ($\Lambda < 0$), explore the dependence of surface gravity on $k$ for a given mass parameter $M$.

(4) Is there a (black hole) solution that interpolates between $\text{AdS}_4$ in the asymptotic region and the Nariai-like solution (2.142) in the interior?

**2.32 The Nariai-like $\text{AdS}_2 \times \Sigma^2_g$ solution.**

Show that the metric

$$\mathrm{d}s^2 = \frac{\ell^2}{3}\left(-\sinh^2\rho\ \mathrm{d}\tau^2 + \mathrm{d}\rho^2 + \mathrm{d}\chi^2 + \sinh^2\chi\ \mathrm{d}\varphi^2\right) \tag{2.142}$$

solves (2.88), which is an $\text{AdS}_2 \times \text{H}^2$ solution with equal radii for $\text{AdS}_2$ and $\text{H}^2$ parts.

**2.33 Observer dependence of ergoregion for Kerr–AdS black holes.**

Show that Kerr–AdS black holes have no ergoregion, in the sense that there are asymptotic observers who see a Killing vector that is timelike from the asymptotic boundary all the way to the black hole horizon. Explain why no such observers exist for asymptotically flat Kerr black holes.

**2.34 ISCO for (A)dS black holes.**

(1) Explore the ISCO for dS–Schwarzschild black holes of mass $M$. Compare the ISCO radius to that of Schwarzschild black holes.

(2) Explore the ISCO for AdS–Schwarzschild black holes of mass $M$ and with horizon curvature $k$. Does the ISCO radius depend on the horizon topology? Compare again with Schwarzschild.

**2.35 Penrose diagram of cosmological backgrounds.**

Consider the Friedmann–Lemaître–Robertson–Walker (FLRW) metric in the comoving frame,

$$\mathrm{d}s^2 = -\,\mathrm{d}t^2 + a^2(t)(\mathrm{d}\boldsymbol{x} \cdot \mathrm{d}\boldsymbol{x}) \tag{2.143}$$

where $a(t)$ is the scale factor. Let $a(t) = t^{1+\alpha}$. Study the causal structure of this geometry and draw its Penrose diagram for $\alpha > 0$ and $\alpha < 0$.

**2.36 Majumdar–Papapetrou multi-centered black hole solution.**

The first multi-centered black hole solution was constructed independently by Majumdar and Papapetrou in 1947 [194, 195]. In this exercise, we review their construction.

(1) Consider an extremal RN solution of mass and electric charge $M = Q$ (we are working in $G_\mathrm{N} = 1$ units). Study the radial trajectory of particles with charge $q$ and mass $m$. Show that for $m > q$ the particle falls into the black hole, while for $m < q$ it is repelled, and for $m = q$ there is no force. That is, for $m = q$ one can place the test particle in any arbitrary point with respect to the extremal black hole.

(2) The no force condition discussed above still holds if we consider backreaction of the test particle. That is, we can have a static solution consisting of two extremal mass/charge centers of, e.g. charges $Q_1$, $Q_2$. To see this, start with the following ansatz:

$$\begin{aligned} \mathrm{d}s^2 &= -\frac{1}{U^2(\boldsymbol{x})}\mathrm{d}t^2 + U^2(\boldsymbol{x})\; \mathrm{d}\boldsymbol{x} \cdot \mathrm{d}\boldsymbol{x} \\ A(\boldsymbol{x}) &= \frac{1}{U(\boldsymbol{x})}\; \mathrm{d}t\,. \end{aligned} \tag{2.144}$$

– Show that the ansatz (2.144) solves the field equations if

$$\nabla^2 U(\boldsymbol{x}) = 0 \tag{2.145}$$

where $\nabla^2$ is the (flat) Laplacian in three dimensions.

– The most general solution is hence

$$U(\boldsymbol{x}) = 1 + \sum_n \frac{Q_n}{|\boldsymbol{x} - \boldsymbol{x}_n|}$$

describing a multi-centered solution with charges $Q_n$ sitting at $\boldsymbol{x}_n$.

(3) Show that for single-centered solution the above reduces to an extremal RN solution, written in isotropic coordinates (cf. Exercise 2.17).

(4) Study isometries, asymptotics, and the causal structure of a generic multi-centered solution. See [196] for more discussion and analysis.

(5) Explore the circular orbits and ISCO for a multi-centered black hole.

**2.37 Multi-centered stationary black holes—Israel–Wilson solutions.**

Motivated by the Majumdar–Papapetrou multi-centered solution, a stationary generalization was constructed in [197], which we review in this exercise.

(1) Starting with the ansatz

$$ds^2 = -\frac{1}{U^2(\boldsymbol{x})}(dt + \boldsymbol{\omega} \cdot d\boldsymbol{x})^2 + U^2(\boldsymbol{x})\, d\boldsymbol{x} \cdot d\boldsymbol{x} \tag{2.146}$$

show that the above solves the field equations of Einstein–Maxwell theory if

$$\nabla^2 U(\boldsymbol{x}) = 0 \qquad \nabla \times \boldsymbol{\omega} = i\left[U\nabla\bar{U} - \bar{U}\nabla U\right] \tag{2.147}$$

where $\nabla^2$ is (flat) Laplacian in three dimensions and $U$ is in general a *complex* solution, and the field strength is given by

$$F_{ti} = \partial_i \Phi, \qquad F^{ij} = |U|^2\, \epsilon^{ijk}\partial_k \chi \tag{2.148}$$

where $U^{-1} = \Phi + i\chi$. The most general solution is again

$$U(\boldsymbol{x}) = 1 + \sum_n \frac{Q_n}{|\boldsymbol{x} - \boldsymbol{x}_n|} \qquad Q_n = M_n + iN_n. \tag{2.149}$$

Show that for real solutions, the case $N_n = 0$ reduces to the Majumdar–Papapetrou solution discussed in Exercise 2.36.

(2) Show for the single-centered case that the solution above reduces to an extremal charged-NUT solution.

(3) Study the asymptotic behavior of the solution and discuss what are its NUT charges. For further discussion, see [196].

(4) Explore whether we can have such multi-centered solutions for extremal Kerr geometries. Can we 'sum up' extremal Kerr metrics, just like extremal RN or extremal charged-NUT solutions? Why/Why not?

**2.38 Near horizon extremal Kerr geometry.**

In this exercise, we explore the near horizon limit for extremal Kerr black holes, $a = M$ in (2.74).

(1) Perform the coordinate transformation

$$r = a + \epsilon\rho, \qquad t = \tau/\epsilon, \qquad \varphi = \phi + \frac{t}{2a} \tag{2.150}$$

where $\epsilon$ is a parameter.

(2) Take the limit $\epsilon \to 0$ while keeping $\rho, \tau, \varphi$ fixed and show that the extremal Kerr geometry reduces to [198, 199]

$$\mathrm{d}s^2 = a^2\Gamma(\theta)\Big( - r^2\mathrm{d}t^2 + \frac{\mathrm{d}r^2}{r^2} + \mathrm{d}\theta^2 + \gamma(\theta)^2(\mathrm{d}\varphi + r\,\mathrm{d}t)^2\Big) \tag{2.151}$$

where

$$\Gamma = 1 + \cos^2\theta\,, \qquad \gamma(\theta) = \frac{2\sin\theta}{1+\cos^2\theta}\,. \tag{2.152}$$

(3) Show that the above is a solution to the Einstein vacuum equations.

(4) Explore isometries of this solution and show that it has four Killing vectors

$$\xi_- = \partial_t \qquad \xi_0 = t\partial_t - r\partial_r \qquad \xi_+ = \frac{1}{2}(t^2 + \frac{1}{r^2})\partial_t - tr\partial_r - \frac{1}{r}\partial_\varphi \qquad \xi_\phi = \partial_\varphi \tag{2.153}$$

which span $SL(2,\mathbb{R}) \times U(1)$. (It was shown that this is the unique vacuum Einstein solution with these isometries [200].)

**2.39 Kerr–Schild coordinates. [201]**

Kerr–Schild coordinates allow decomposing a metric

$$g_{\mu\nu} = \eta_{\mu\nu} + H\,k_\mu k_\nu \tag{2.154}$$

into the Minkowski metric $\eta$, a scalar function $H$, and a vector $k^\mu = \eta^{\mu\nu}k_\nu$ that is null vector with respect to $\eta$. Of course, not every metric can be written in the Kerr–Schild form.

(1) Show that $k_\mu$ is also null with respect to $g_{\mu\nu}$.

(2) Show that Schwarzschild and Kerr can be brought to the Kerr–Schild form.

(3) Write the RN solution in Kerr–Schild form and determine the Maxwell gauge field in Kerr–Schild coordinates.

(4) Starting with the Kerr–Schild metric (2.154), show that the Einstein(–Maxwell) equations imply geodecity of $k_\mu$. What is the equation for $H$?

(5) Can the AdS or dS geometries be written in the Kerr–Schild form (2.154)?

(6) Generalize the Kerr–Schild form (2.154) by replacing $\eta$ with another background $\bar{g}_{\mu\nu}$ and $k_\mu$ to be a null vector field with respect to $\bar{g}_{\mu\nu}$. Can (A)dS–Schwarzschild be written in this generalized Kerr–Schild form with $\bar{g}$ being the (A)dS metric?

(7) Show that all metrics in the Plebanski–Demianski family are of the generalized Kerr–Schild form.

**2.40 More on asymptotically locally flat vacuum solutions.**

Consider the Kerr–Taub–NUT family of solutions, i.e. $\Lambda = \alpha = Q_e = Q_m = 0$ solution in the Plebanski–Demianski family (2.97).

(1) Explore the asymptotic behavior of the geometries, i.e. large $r$ behavior in the metric (2.97). Show that the NUT charge $l$ appears explicitly in the asymptotic metric.

(2) Explore the isometries of this asymptotic metric and show that locally it is like a Minkowski space $M_4$. Show that globally it is an orbifold of Minkowski space, $M_4/\Gamma_l$, where $\Gamma_l$ is a certain element in the Poincarè isometry group specified by the NUT charge parameter $l$.

(3) Find $\Gamma_l$ and use the above picture to give a geometric meaning to the NUT charge.

(4) Extend the ADM charge analysis such that it captures the NUT-type charges.

(5) Explore the near horizon region of the Kerr–Taub–NUT geometry. What is the geometry and metric of the constant $t$ surface at $r = r_h$? What is the topology of the horizon?

(6) Bonus level: Repeat the exercise for the Kerr–AdS–Taub–NUT case.

**2.41 Collapsing null dust-shell and Vaidya solutions.**

The Vaidya metric with step-function mass function (2.109) is a solution to Einstein equations with null dust-shell energy–momentum tensor (2.110). The same solution may be viewed as two vacuum solutions corresponding to the two sides (in and out) of the null shell. Construct this solution using Israel junction conditions [108,202]. That is, match a Minkowski space at $v < 0$ to a Schwarzschild space of mass $m$ at $v > 0$ and show that the tension of the shell at $v = 0$ is given by (2.110).

**2.42 McVittie solutions.**

One may ask what is the geometry associated with a star, assumed to be a spherically symmetric body of mass in a cosmological FLRW (2.143) background. Such a solution was first written by McVittite in 1933 [203] with metric

$$\mathrm{d}s^2 = -G(\rho,t)\mathrm{d}t^2 + F(\rho,t)\left[\mathrm{d}\rho^2 + \rho^2\mathrm{d}\Omega^2\right] \tag{2.155}$$

with

$$F(\rho,t) = \frac{\mu_0^2}{\mu(t)^2}\left(1+\frac{\mu(t)}{2\rho}\right)^4, \qquad G(\rho,t) = \left(\frac{1-\frac{\mu(t)}{2\rho}}{1+\frac{\mu(t)}{2\rho}}\right)^2 \tag{2.156}$$

where $\mu(t)$ is a function of $t$ and $\mu_0$ is $\mu(t)$ at some initial time $t_0$.

(1) Show that for $\mu(t) = \text{const.}$, the McVittie geometry reduces to Schwarzschild in isotropic coordinates, *cf.* (2.133) in Exercise 2.17.

(2) Find the energy–momentum tensor $T^{\mu}{}_{\nu}$ which makes (2.155) a solution to Einstein equations. If we write in the form of a perfect fluid, $T^{\mu}{}_{\nu} = \mathrm{diag}(-\rho(t), P(t), P(t), P(t))$, find $\rho(t)$, $P(t)$ in terms of $\mu(t)$. What is the equation of state of the perfect fluid?

(3) Compute the ADM mass of (2.155) and show it is $\mu(t)/G_{\mathrm{N}}$ which is time-dependent. Explore the time-dependence of the mass.

(4) What is the causal and horizon structure of the McVittie solution? See [204] for further discussions.

# Formal Definitions and Classic Theorems

# 3

**Abstract**

In this chapter, we make more precise the basic notions associated with black holes, starting in Sect. 3.1 with the mathematical definition of black holes and various definitions of horizons. We discuss their physical significance. In Sect. 3.2, we summarize classic theorems and conjectures, namely singularity theorems, focusing theorem, area theorem, uniqueness theorems, topology theorems, and the cosmic censorship conjecture. In Sect. 3.3, we focus on the area theorem, also known as the second law.

## 3.1 Mathematical Definitions of Black Holes and Horizons

In the previous chapter, we discussed solutions to the Einstein equations that had a null hypersurface dividing the spacetime into two causally disconnected regions. This null hypersurface was called ‘horizon’, but we were not precise about its definition. In this section, we review different notions of horizons, some of which are defined locally and others globally. We also provide the precise definition of a classical black hole. Each of the definitions while useful in physically interesting cases has its own limitations which we are going to point out.

### 3.1.1 Killing Horizon and Surface Gravity

We start with a simple, local, and covariant horizon definition, whose main drawback is that it does not apply to generic time-dependent black holes, but rather requires stationarity.

A null surface $\mathcal{N}$ is a codimension-1 hypersurface whose normal $l$ is null, $l^2 = 0$. For concreteness, assume the hypersurface defined by $r = r_0 = \text{const.}$, where $r$ is some adapted ‘radial’ coordinate. Then the normal vector is given by $l^\mu = f(x^\nu)g^{\mu r}$ with some non-vanishing normalization function $f(x^\nu)$, and $l^2 = 0$ implies $g^{rr} = 0$.



D. Grumiller and M. M. Sheikh-Jabbari, *Black Hole Physics*, Graduate Texts in Physics,
https://doi.org/10.1007/978-3-031-10343-8_3

If the null vector $l$ is a Killing vector $\xi$ for some choice of the function $f(x^\nu)$, then the null surface $\mathcal{N}$ is called a Killing horizon.

The normal vector $l$ to a null hypersurface is also tangent to it, implying that $l^\mu = \mathrm{d}x^\mu/\mathrm{d}\lambda$ generates a null geodesic $x^\mu(\lambda)$ parameterized by $\lambda$. The non-affinity of the geodesic $l^\mu \nabla_\mu l^\nu|_{\mathcal{N}} = l^\nu \; \mathrm{d}\ln f/\mathrm{d}\lambda$ depends on the normalization function $f$. For constant $f$, the null geodesic is affinely parametrized. For Killing horizons, the non-affinity of the null geodesic has a physical interpretation as surface gravity.

**Surface gravity**

The surface gravity $\kappa$ of a Killing horizon with normal Killing vector $\xi$ is defined as non-affinity parameter of the null geodesic

$$\xi^\mu \nabla_\mu \xi^\nu \big|_{\mathcal{N}} =: \kappa \xi^\nu \tag{3.1}$$

where $|\xi|^2_{\mathcal{N}} = 0$. A straightforward calculation (see Exercise 3.1) yields

$$\boxed{\kappa^2 = -\frac{1}{2}(\nabla_\mu \xi_\nu)^2\big|_{\mathcal{N}}\,.} \tag{3.2}$$

Surface gravity depends on the normalization of the Killing vector $\xi$. Rescaling $\xi \to \alpha\xi$ with some constant $\alpha$ also rescales surface gravity correspondingly, $\kappa \to \alpha\kappa$. Therefore, surface gravity is uniquely defined only if the normalization of the Killing vector $\xi$ is fixed. In many black hole applications, this is done by assuming a preferred normalization of $\xi$ in the asymptotic region. For example, in the Kerr family of black holes, one assumes $\lim_{r\to\infty} \xi \cdot \partial_t = -1$ so that $\xi = \partial_t + \Omega_{\mathrm{H}}\,\partial_\varphi$.

Once the normalization is fixed, surface gravity turns out to be a specific constant that characterizes key properties of stationary black holes. This theorem is known as the zeroth law of black hole mechanics.

**Zeroth law of black hole mechanics**

Surface gravity $\kappa$ is a constant over a Killing horizon with Killing vector $\xi$.

A necessary condition for this theorem to hold is $\xi^\mu \partial_\mu \kappa = 0$ on the Killing horizon. A partial proof is left as an exercise, see Exercise 3.1. A full proof will be provided in Sect. 5.5.1.

The definition of a Killing horizon is covariant and local in contrast to other horizon definitions we shall encounter below. However, it is not necessarily an observer-independent notion and does not necessarily describe a black hole spacetime. The prime non-black hole example is a Rindler observer of constant acceleration $a$ in a flat spacetime, which perceives a Rindler horizon with surface gravity $\kappa = a$ (see Exercise 3.7).

Nevertheless, Killing horizons are a useful notion for black holes, but require stationarity, while generic black hole spacetimes do not necessarily feature any Killing vector. Thus, the discussion in this section cannot be applied to non-stationary black holes.

A special case arises when surface gravity vanishes for a stationary black hole.

> **Extremal black holes**

A Killing horizon with vanishing surface gravity, $\kappa = 0$, is called degenerate. A black hole with a degenerate Killing horizon is called extremal.

Examples include extremal RN ($M^2 = Q_e^2 + Q_m^2$) and extremal Kerr ($M^2 = a^2$). As we also see from these examples, for extremal black holes, the mass parameter $M$ is specified in terms of parameters of the solution, which are related to other conserved charges of the system.

---

In many stationary black hole applications with $\kappa \neq 0$, the Killing horizon bifurcates. That is, the horizon has two branches that intersect on a codimension-2 spacelike surface called bifurcation surface $\mathcal{B}$, see Fig. 3.1. For some black holes, like Kerr or KN, the bifurcation surface is a compact orientable surface of spherical topology. As discussed in Sect. 2.7 on AdS backgrounds, the bifurcation surface can have a generic topology.

To see how the Killing horizon bifurcates, locally parametrize the Killing vector generating the horizon as $\xi = \partial_\sigma$. Next, consider a congruence of null geodesics parametrized by $s = s(\sigma)$ such that their velocity is along $\xi$, i.e.

$$\xi^\mu = f(s)\frac{\mathrm{d}x^\mu}{\mathrm{d}s} \qquad\qquad f(s) = \frac{\mathrm{d}s}{\mathrm{d}\sigma}\,. \tag{3.3}$$

The definition (3.1) implies $\kappa = \partial_\sigma \ln|f|$. Constancy of $\kappa$ along orbits of $\xi^\mu$ for $\kappa \neq 0$ yields

$$f = \kappa s \qquad\qquad s = \pm e^{\kappa\sigma}\,. \tag{3.4}$$

There is a positive and a negative branch for orbits of $\xi^\mu$, $s \in (-\infty, 0)$ and $s \in (0, \infty)$. Each of the two branches in turn has an outgoing and an ingoing branch, corresponding to the two possible null directions, so in total, there are four separate lines on a bifurcate Killing horizon, which join at the bifurcation surface $\mathcal{B}$. The horizon generating Killing vector field vanishes at the bifurcation surface, $\xi^\mu|_{\mathcal{B}} = 0$. Bifurcate Killing horizons split the spacetime into four regions ('wedges'), see Fig. 3.1. The simplest example with a bifurcate Killing horizon is 2-dimensional Rindler spacetime, see (2.39). There, the four wedges correspond to $x > |t|$ (right wedge), $x < -|t|$ (left wedge), $t > |x|$ (upper wedge) and $t < -|x|$ (lower wedge), where $t, x$ are standard Minkowski coordinates (2.41).

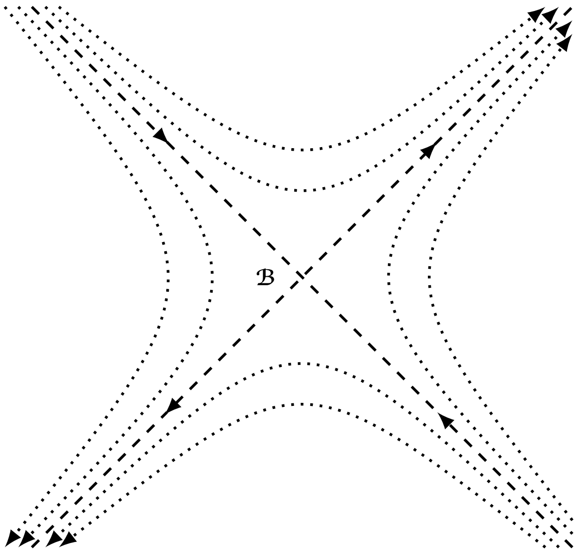


**Fig. 3.1** Dotted lines show orbits of $\xi^\mu$, dashed lines show the bifurcate Killing horizon with bifurcation surface $\mathcal{B}$, and arrows denote the Killing flow

### 3.1.2 Event Horizon and Mathematical Black Hole Definition

Our second definition, the event horizon, is covariant and global. It is used to define the term 'black hole' mathematically. Its main drawback is that one needs to be able to define and know the infinite future of spacetime, which makes this notion rather limited for practical applications such as astrophysics or numerical GR. Additional drawbacks are discussed at the end of this subsection.

In order to define an event horizon, we need a couple of other definitions, starting with the causal past of a point $p$. It is denoted by $J^-(p)$ and comprises the set of all events in spacetime that can be reached from $p$ by a causal curve, i.e. either a timelike or a null geodesic (see, e.g. the left plot in Fig. 3.2). The timelike past of a point $p$ is defined similarly, replacing 'causal' with 'timelike' in the definition above, and is denoted by $I^-(p)$. The same definition extends to arbitrary sets $\Sigma$ of points, $J^-(\Sigma)$. The boundary of the causal past of some set $\Sigma$ is denoted by an overdot, $\dot{J}^-(\Sigma)$. In Fig. 3.2, we show two examples in 2-dimensional Minkowski space.

The second notion we need is future null infinity, denoted by $\mathscr{I}^+$. We have encountered it already in the construction of Penrose diagrams. For a precise definition, we refer to [132]. Whenever a Penrose diagram exists, $\mathscr{I}^+$ is defined as the set of all points at the conformal boundary of the Penrose diagram that do have a non-vanishing timelike past in the spacetime manifold. In asymptotically flat spacetimes, $\mathscr{I}^+$ is itself a null curve, while in AdS, it is timelike, and in dS, it is spacelike; see Fig. 3.3.

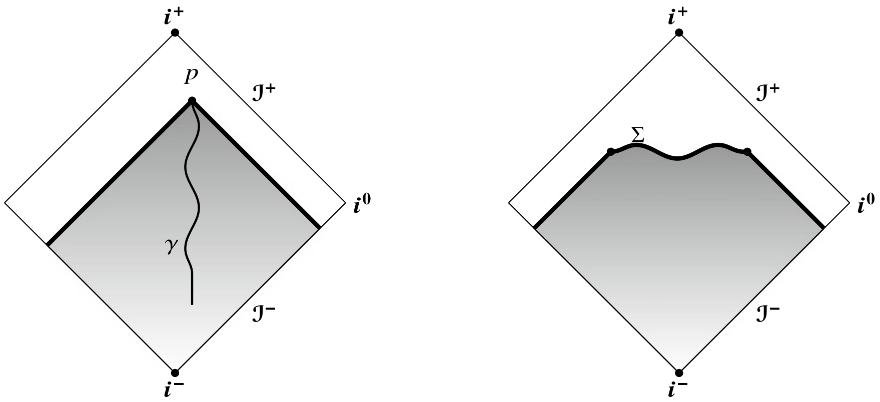


**Fig. 3.2** Left plot: shaded area is $I^-(p)$ (with boundaries: $J^-(p)$); $\gamma$ is a generic causal curve with future endpoint $p$. Right plot: shaded region is $I^-(\Sigma)$ (with boundaries: $J^-(\Sigma)$)

### Future event horizon

Given a spacetime manifold $\mathcal{M}$ with future null infinity $\mathscr{I}^+$, the future event horizon $\mathcal{H}^+$ is defined as

$$\mathcal{H}^+ := \dot{J}^-(\mathscr{I}^+) \cap \mathcal{M} \tag{3.5}$$

In words: the future event horizon is the intersection of the boundary of the causal past of future null infinity with the spacetime manifold.

Often the qualifier 'future' is omitted and one just talks about the event horizon, meaning the future event horizon.

The mathematical definition of a black hole is very similar and shows that the event horizon is the boundary of the black hole region.

### Mathematical black hole

Given a spacetime manifold $\mathcal{M}$ with future null infinity $\mathscr{I}^+$, the black hole region $\mathcal{BH}$ is defined as

$$\mathcal{BH} := \mathcal{M} - J^-(\mathscr{I}^+) \tag{3.6}$$

In words: the black hole region is the complement of the causal past of future null infinity within the spacetime manifold.

For example, Schwarzschild-AdS, Schwarzschild, and Schwarzschild-dS black holes are displayed in Fig. 3.3. The black hole region is shaded in red and the future event horizon is visible as red lines, while $\mathscr{I}^+$ is visible as blue lines.

If one is interested in white holes and past event horizons, one can introduce them by exchanging future with past and $\mathscr{I}^+$ with $\mathscr{I}^-$ in the definitions of black holes and future event horizon.

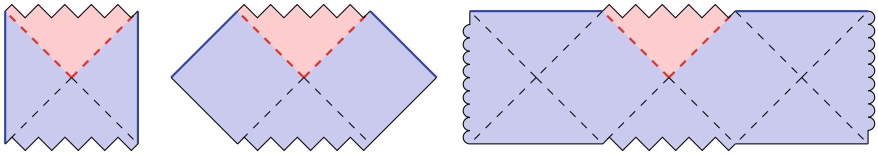

**Fig. 3.3** Black hole (shaded red), event horizon (red lines), $\mathscr{I}^+$ (blue lines), and timelike past of $\mathscr{I}^+$ (shaded blue); from left to right: Schwarzschild-AdS, Schwarzschild, and Schwarzschild-dS (to be continued or identified at wavy lines)

We conclude this subsection by listing problematic issues of the black hole definition in terms of an event horizon. The most prominent one we mentioned already: this definition is useless for astrophysics and cumbersome for numerical GR since it requires the knowledge of the infinite future. Relatedly, its teleological nature means there is no physical experiment that can reliably detect an event horizon. For example, in the Vaidya black hole, cf. Sect. 2.8, an observer can be trapped behind an event horizon even though the spacetime is Minkowski space in some open patch; in Fig. 2.19, this applies to observers to the left of the infalling matter—some of them will be outside the event horizon, some of them inside, and some of them on it, but all of them observe precisely the same local physics.

Additionally, the definition does not apply to spacetimes that do not allow for conformal completion, such as Lifshitz, Schrödinger or warped black holes, see [205]. Even within the class of spacetimes that allow conformal completions, there is a number of technical issues, such as the possibility of several inequivalent conformal completions, poor differentiability of $\mathscr{I}^+$, etc., see [138] for more on these mathematical aspects and suggested improvements.

Last but not least, once quantum effects are taken into account none of the definitions in this section or in textbooks like [138] are expected to be applicable. We shall come back to this problematic issue of not knowing precisely what a black hole is, quantum mechanically, in the final chapters of this book.

In Sect. 3.2.5, we will discuss classic theorems that are built around the notion of the event horizon.

### 3.1.3 Apparent Horizons and Trapped Surfaces

The shortcomings of Killing and event horizons led to the development of additional notions of horizons that apply to non-stationary spacetimes and do not require knowledge of the infinite future. Among the most prominent such definitions are apparent horizons.

In order to define them, we need to introduce the notion of trapped surfaces, which are closed codimension-2 surfaces with negative expansions. Apparent horizons are then marginally trapped surfaces. Let us unpack this statement.

The induced metric on the trapped surface

$$q_{\mu\nu} = g_{\mu\nu} + l_\mu n_\nu + n_\mu l_\nu \tag{3.7}$$

is constructed from the spacetime metric $g_{\mu\nu}$ and the two null normals $l, n$, ($l^2 = n^2 = 0$) normalized conveniently, $l^\mu n_\mu = -1$. By convention, we assign $l$ to be outward pointing and $n$ to be inward pointing, whenever this distinction makes sense. Given these data, the expansions are defined as

$$\theta^+ := q_{\mu\nu}\nabla^\mu l^\nu \qquad\qquad \theta^- := q_{\mu\nu}\nabla^\mu n^\nu. \tag{3.8}$$

Depending on the signs of the expansions, we have now the following possibilities:

1. **Normal surface.** $\theta^+ > 0, \theta^- < 0$
2. **Trapped surface.** $\theta^\pm < 0$
3. **Anti-trapped surface.** $\theta^\pm > 0$
4. **Marginally trapped surface.** $\theta^+ = 0, \theta^- < 0$
5. **Marginally anti-trapped surface.** $\theta^+ > 0, \theta^- = 0$
6. **Extremal surface.** $\theta^\pm = 0$

The apparent horizon is defined to be the outermost marginally trapped surface.[1]

Advantages of this definition are the applicability to numerical GR, the (quasi-) locality of the definition, and the generality, i.e. no restriction to stationarity is necessary like for Killing horizons.

A key distinction to the previous horizon definitions (and to the one in the next subsection) is that the codimension-1 hypersurface generated by the time-evolution of an apparent horizon can have any signature, whereas Killing, event, and Cauchy horizons are always null hypersurfaces. This property can allow describing the growth and decay of a black hole in terms of a growing/shrinking apparent horizon. See Fig. 3.4 for a typical example, from which the teleological nature of the event horizon is evident: it exists even in vacuum and before any physical black hole formation has happened; by contrast, the apparent horizon keeps growing as more and more matter falls into the black hole and asymptotically approaches the event horizon after the formation process has settled down.

The main disadvantage of apparent horizons is that they are slicing-dependent; indeed, even for a spacetime as simple as Schwarzschild, it is possible to slice it in such a way that no apparent horizon exists [207].[2] Thus, the absence of apparent horizons is not proof of the absence of black hole formation. Despite this, apparent horizons remain a key diagnostic tool in numerical GR to study black hole formation [113].

---

[1] This is the definition most commonly used in numerical GR and seems to be the most practical one; there are alternative definitions of apparent horizons that require asymptotic flatness and additional conditions, see, e.g. [206]. The qualifier 'outermost' is required to make sure that there is no larger marginally trapped surface. We should also note that the term apparent horizon is also commonly used in the context of cosmology where it usually refers to a particle horizon, see Exercise 3.15.

[2] For spherically symmetric spacetimes this problem is absent as long as the slicing respects spherical symmetry [208]. Typically, as long as one is not actively looking for trouble, apparent horizons are convenient tools in applications.

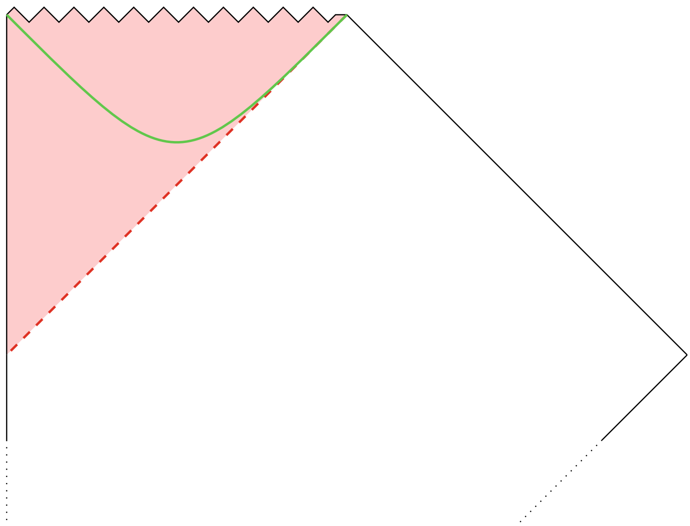

**Fig. 3.4** Apparent horizon (green) and event horizon (red) in Vaidya-like black hole

### 3.1.4 Cauchy Horizons and Predictability

The horizon definitions above are intended in a positive way, i.e. to define interesting properties (such as the existence of black holes) in spacetime. By contrast, Cauchy horizons defined in this subsection may indicate problematic aspects of spacetime.

Again we need a couple of definitions.

- Achronal sets are defined to be subsets of the spacetime manifold that have no pair of points $p, q$ such that $q \in I^+(p)$, i.e. no pair of points can be connected by a timelike curve, but they can be connected by spacelike or null curves. Typical achronal sets are constant time slices of a spacetime. The Killing or event horizon of a Schwarzschild black hole or asymptotic (future or past) asymptotic infinity in flat spacetime are other examples of achronal sets.
- Future/past inextendible curves are curves without future/past endpoint.
- The future domain of dependence $D^+(S)$ of a closed achronal set $S$ is given by the set of all points $p$ in spacetime such that every past inextendible causal curve through $p$ intersects $S$. The past domain of dependence $D^-(S)$ is defined analogously, replacing future $\leftrightarrow$ past. The physical significance of $D^-(S)$ is that it defines the part of spacetime that can causally affect the data on $S$. Similarly, solutions to standard (hyperbolic) field equations in the $D^+(S)$ region are uniquely determined by initial data on $S$. The domain of dependence $D(S)$ is the union of future and past domain of dependences. See Fig. 3.5.

We define now the Cauchy horizon of a closed achronal set $S$, $C(S)$:

$$C(S) := \left(\overline{D^+(S)} - I^-[D^+(S)]\right) \cup \left(\overline{D^-(S)} - I^+[D^-(S)]\right) \tag{3.9}$$

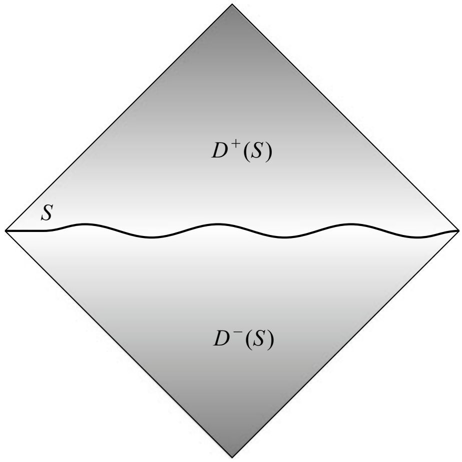


**Fig. 3.5** Future and past domains of dependence for an achronal surface $S$

In plain English, the Cauchy horizon $C(S)$ is the boundary of the domain of dependence of $S$.

Relatedly, a Cauchy surface is a (non-empty) closed achronal set $\Sigma$ in some (connected) spacetime manifold if and only if $C(\Sigma) = \varnothing$. That is, a Cauchy surface is a constant time slice (which may have null segments) without a Cauchy horizon. Spacetimes with a Cauchy surface $\Sigma$ are called globally hyperbolic. Cauchy surfaces are physically important as they serve as surfaces one can put initial data on and deterministically evolve them using Einstein or other field equations. Given the importance of Cauchy surfaces for physics, generic achronal sets are also called partial Cauchy surfaces. In this terminology, a Cauchy surface is a partial Cauchy surface on $\mathcal{M}$ such that $\mathcal{M} = \mathfrak{D}^+(\Sigma) \cup \mathfrak{D}^-(\Sigma)$, see Figs. 3.6 and 3.11 for examples of Cauchy surfaces. See Exercise 3.17 for an alternative definition of (partial) Cauchy surface and horizon.

A Cauchy horizon for a given achronal set $S$, $C(S)$, provides a boundary for predictability and deterministic classical evolution from $S$. As such, it is not a property of spacetime itself, but of the set, which may simply be too small to provide enough data to predict all events in spacetime. In globally hyperbolic spacetimes, a Cauchy horizon can always be avoided by suitably extending the set $S$ to the whole spacetime. However, this need not be possible in generic spacetimes, because even after an infinite extension of $S$, there could be a Cauchy horizon. Whenever this happens, Cauchy horizons are properties of spacetimes, easily spotted in Penrose diagrams. The presence of a spacetime Cauchy horizon means that spacetime is not globally hyperbolic. An undesirable aspect of a spacetime Cauchy horizon is the loss of predictability: physics in regions beyond the Cauchy horizon is not uniquely determined from initial data on $S$.

In Fig. 3.6, we revisit the Schwarzschild Penrose diagram, where we have drawn two Cauchy surfaces $\Sigma_1$, $\Sigma_3$ and the partial Cauchy surface $\Sigma_2$. For an observer remaining in region I for all practical purposes, $\Sigma_2$ is like a Cauchy surface since the domain of dependence of $\Sigma_2$ is precisely the full region I, so all events therein can

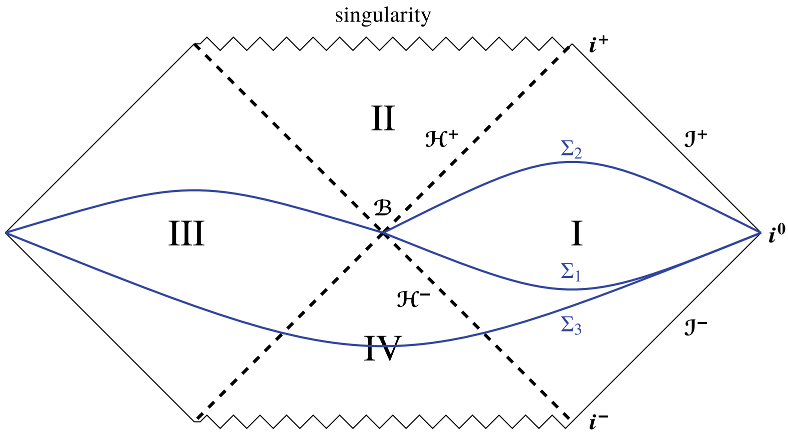


**Fig. 3.6** (Partial) Cauchy surfaces for Schwarzschild

be predicted/retrodicted using the initial data on $\Sigma_2$. Schwarzschild does not have a Cauchy horizon and hence is globally hyperbolic.

In Fig. 3.7, we revisit the RN Penrose diagram. The red lines highlight the future and past Cauchy horizons $\mathcal{C}^{\pm}$. Three typical partial Cauchy surfaces $\Sigma_1$, $\Sigma_2$, $\Sigma_3$ are also depicted. Since neither of them can be extended further, the Cauchy horizon is a property of the RN spacetime, rather than a property of the partial Cauchy surfaces. With initial data on these surfaces in principle, one can predict (or retrodict) everything that happens in regions I, II, III, and IV. The RN black hole is not globally hyperbolic.

Cauchy horizons are arguably artifacts[3] of some approximation and hence should not be taken as seriously as event horizons (or apparent horizons), which are more stable features of spacetimes. The usual argument is to switch on some perturbations on geometric background with spacetime Cauchy horizon, and to observe that near the Cauchy horizon, the perturbation gets infinitely enhanced due to blue shifts [209]; see Sect. 3.2.7 for more discussion. (The precise nature of that singularity remains a research topic; see, e.g. [210].) Thus, this line of argument suggests that Cauchy horizons are converted into singularities when (arbitrarily small) interactions are taken into account.

### 3.1.5 Other Horizon Definitions

We collect, in this final subsection, additional prominent horizon notions, namely stretched, isolated, and dynamical horizons.

[3] Important exceptions are asymptotically AdS spacetimes. In this case, the failure of global hyperbolicity is irrelevant if one considers radial evolution instead of temporal evolution. Instead of initial data, one thus provides boundary data, which can be interpreted holographically; see Chap. 8.

**Fig. 3.7** RN black hole with Cauchy horizon (red lines)

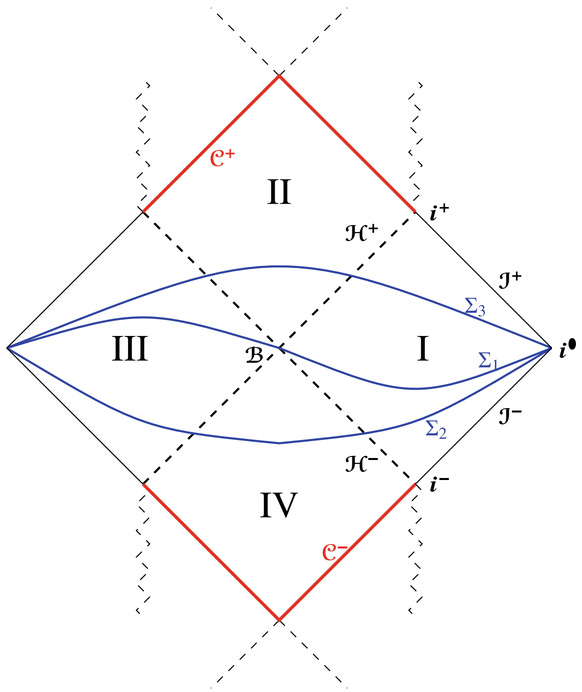


**Fig. 3.8** Stretched horizon $\mathcal{S}$ for an eternal Schwarzschild black hole

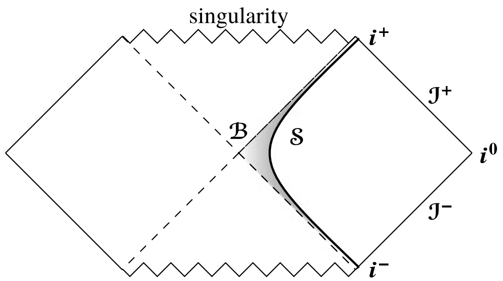


**Stretched horizon.** A stretched horizon is an inextendible timelike codimension-1 surface located outside the event horizon. Typically, it involves a stretching parameter such that the stretched horizon coincides with the event horizon in the limit of that parameter going to zero. It can be a useful notion when studying quantum physics close to the horizon. The key physical idea is that there should be a UV cutoff on the infinite redshift factors. The inverse of this cutoff is essentially the spatial distance between stretched and event horizon. In Fig. 3.8, we display the stretched horizon for an eternal Schwarzschild black hole.

**Isolated horizon.** An isolated horizon is a codimension-1 null hypersurface that generalizes the notion of a Killing horizon and, like apparent horizons, is marginally trapped. However, no Killing vector is necessary to define isolated horizons. The physical key assumption is that there is no matter flux across the null hypersurface, so the black hole is in equilibrium, even though its surroundings may be dynamical.

Thus, isolated horizons describe only those parts of a horizon of time-dependent black holes where no essential dynamics happens. The black hole must neither grow nor shrink to be well-approximated by an isolated horizon. See [206,211] and Exercise 3.14 for more on the definition of isolated horizons.

**Dynamical horizon.** While isolated horizons are an improvement over Killing horizons in terms of generality, over event horizons in terms of quasi-locality, and over apparent horizons, in terms of slicing independence, they fail to be applicable to some of the most interesting aspects of black hole physics like black hole formation. Dynamical horizons repair this deficiency since they allow for matter fluxes while keeping the positive aspects of isolated horizons. Dynamical horizons are space-like marginally trapped codimension-1 hypersurfaces. See [206,211] for more on dynamical horizons and further horizon concepts not covered in this book.

A Penrose diagram displaying various horizon notions for a Vaidya black hole is shown in Fig. 3.9. Before $v_0$ spacetime is locally Minkowski, but due to its teleological nature, there is already part of Minkowski spacetime hidden behind the event (red dashed) or stretched (red dotted $r = 2M + \epsilon$) horizon. For comparison, the line $r = 2M$, which at late times coincides with the event horizon, is shown as a gray dotted curve. Between $v_0$ and $v_1$ matter, indicated by the blue arrows, falls into the black hole. The dynamical horizon (thick green line) grows between $v_0$ and $v_1$ until it reaches the isolated horizon (blue thick line). Since no matter is assumed to fall into the black hole at later times, the isolated horizon here coincides with part of the event horizon. After $v_1$, spacetime is locally Schwarzschild. The physical black hole region is shaded in gray. The red shaded region depicts the part of the spacetime that would be considered as part of the black hole according to the mathematical definition, but that is not part of the physical black hole; the light red shaded region shows the part of spacetime behind the stretched horizon that is not also behind the event horizon. The line $r = 0$ on the left looks like a boundary of the Penrose diagram, but is really just the center; recall that, at each point, one should imagine a 2-sphere of varying size, and this size shrinks to zero at $r = 0$. The upper left part of the Penrose diagram was stretched to the left as compared to Fig. 2.19 only for better visibility of the dynamical horizon.

## 3.2 Classic Conjectures and Theorems

The precise definitions in the previous section allow us to prove numerous theorems and formulate sharp conjectures regarding uniqueness, singularities, and certain convexity properties. It is not the purpose of this book to fully do justice to these theorems; the interested reader is instead referred to the extensive literature and classic textbooks, e.g. [132,138].

We shall discuss in some detail one of the technical tools that features prominently in several theorems, namely the Raychaudhuri equation. We do this partly to highlight generic structures of how the proofs of such theorems work, and partly because this equation has several applications besides being a tool to prove theorems, in other areas of gravitational physics, in particular in cosmology.

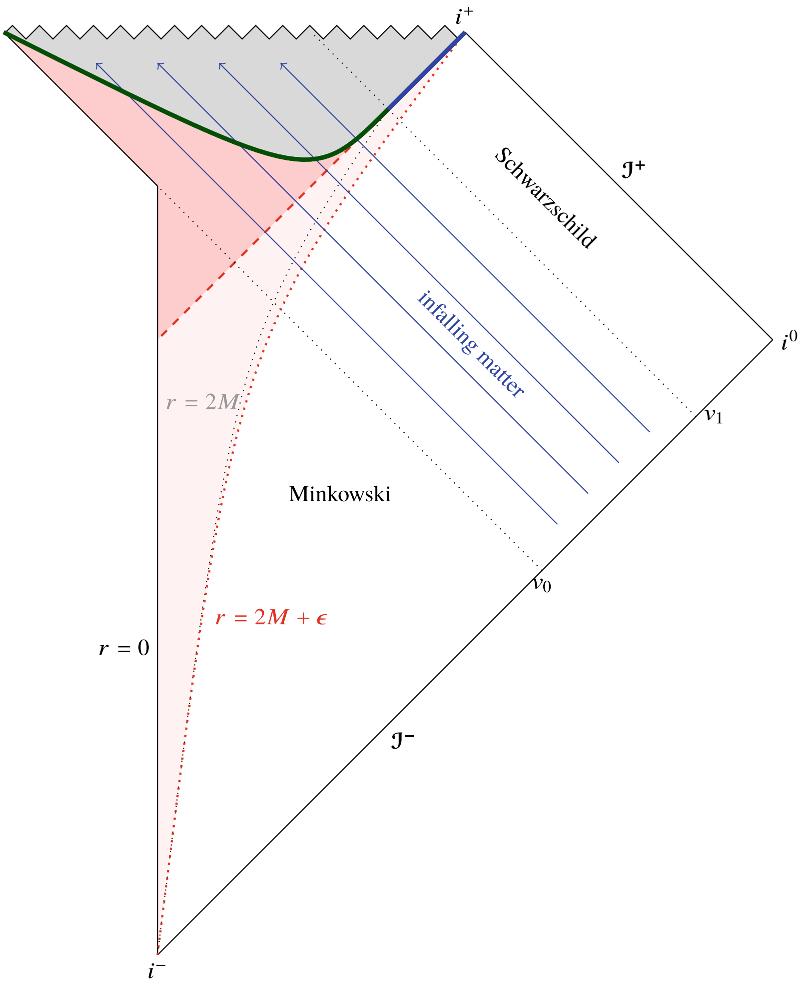


**Fig. 3.9** Vaidya black hole with matter fluxes between $v = v_0$ and $v = v_1 > v_0$. Dynamical (green) and isolated (blue) horizons bound the physical black hole. Event (red dashed) and stretched (red dotted) horizons bound the mathematical black hole. The part of spacetime $v > v_1$ is described by the Schwarzschild metric and $v < v_0$ by the Minkowski metric

### 3.2.1 Raychaudhuri Equation

Congruence is a set of curves such that exactly one curve goes through each point in spacetime, i.e. the curves do not intersect. A geodesic congruence is a congruence where each curve in the set is a geodesic. For now, we are interested in timelike geodesic congruences. One can think of this congruence as the paths of a family of massive test particles propagating in some background spacetime.

Consider a geodesic congruence in a spacetime of generic dimension $D$ and denote the tangent vector field to the congruence by $t^\mu$, normalize it, $t^2 = -1$, and define the velocity tensor field $B_{\mu\nu} := \nabla_\nu t_\mu$. Due to normalization and geodecity, $t_\nu \nabla_\mu t^\nu = t^\mu \nabla_\mu t^\nu = 0$. That is, the velocity tensor projects to zero when contracted with the tangent vector, $B_{\mu\nu} t^\nu = B_{\mu\nu} t^\mu = 0$. The tensor $\Pi_{\mu\nu} = g_{\mu\nu} + t_\mu t_\nu$ has the same property, $\Pi_{\mu\nu} t^\nu = \Pi_{\mu\nu} t^\mu = 0$, but additionally is a projector mathematically, since it is idempotent, $\Pi^\mu{}_\nu \Pi^\nu{}_\lambda = \Pi^\mu{}_\lambda$. Using this projector, we decompose the velocity tensor into its algebraically irreducible components: a trace part (expansion $\Theta := B^\mu{}_\mu$), a symmetric traceless part (shear $\sigma_{\mu\nu} := B_{(\mu\nu)} - \frac{1}{D-1}\,\Theta\,\Pi_{\mu\nu}$) and an antisymmetric part (twist $\omega_{\mu\nu} := B_{[\mu\nu]}$),[4] so that

$$B_{\mu\nu} = \sigma_{\mu\nu} + \omega_{\mu\nu} + \frac{1}{D-1}\,\Theta\,\Pi_{\mu\nu}\,. \tag{3.10}$$

Raychaudhuri's equation is a statement about acceleration, in particular about the rate of change of the expansion $\Theta$. Taking the trace of the identity $t^\lambda \nabla_\lambda B_{\mu\nu} = \nabla_\nu (t^\lambda \nabla_\lambda t_\mu) - (\nabla_\nu t^\lambda)(\nabla_\lambda t_\mu) + t^\lambda [\nabla_\lambda,\, \nabla_\nu] t_\mu = -B^\lambda{}_\nu B_{\mu\lambda} - R^\alpha{}_{\mu\lambda\nu} t^\lambda t_\alpha$ yields

$$t^\lambda \nabla_\lambda B^\mu{}_\mu = -B^{\mu\nu} B_{\nu\mu} - R_{\mu\nu} t^\mu t^\nu \tag{3.11}$$

which is almost the final result. Defining $\mathrm{d}/\,\mathrm{d}\tau := t^\mu \nabla_\mu$ and expanding the quadratic term in $B$ in terms of its irreducible components (3.10) establishes Raychaudhuri's equation.

**Raychaudhuri equation**

$$\boxed{\frac{\mathrm{d}\Theta}{\mathrm{d}\tau} = -\frac{1}{D-1}\,\Theta^2 - \sigma_{\mu\nu}\sigma^{\mu\nu} + \omega_{\mu\nu}\omega^{\mu\nu} - R_{\mu\nu} t^\mu t^\nu} \tag{3.12}$$

This is a pure geometric equation and is true for any geodesic congruence. A key aspect of the right-hand side of Raychaudhuri's equation is that the first and second terms are non-positive, and the third term vanishes for twist-free congruences. The sign of the last term can be positive or negative. In particular, if the spacetime solves the Einstein equations and the energy–momentum tensor satisfies the Strong Energy Condition (SEC, see below), the last term is non-positive.

### 3.2.2 Classical Energy Conditions

The right-hand side of Raychaudhuri's equation (3.12) contains the term $R_{\mu\nu} t^\mu t^\nu$, which is not manifestly positive. Various proofs assume certain 'curvature conditions' requiring non-negativity of this term or other suitable combinations of Ricci tensor

[4] Note that in our conventions the symmetric and antisymmetric parts of a tensor are defined as $B_{(\mu\nu)} := \frac{1}{2}(B_{\mu\nu} + B_{\nu\mu})$ and $B_{[\mu\nu]} := \frac{1}{2}(B_{\mu\nu} - B_{\nu\mu})$.

along causal vector fields. The main task of such curvature conditions is to guarantee suitable convexity conditions, e.g. see [132,212]. Such curvature conditions on-shell may be mapped onto energy conditions. For example, if we take the trace-reversed Einstein equations and contract them twice with a timelike vector field $t^\mu$,

$$R_{\mu\nu}t^\mu t^\nu = 8\pi G_{\rm N}\left(T_{\mu\nu}t^\mu t^\nu + \tfrac{1}{2}T\right) \tag{3.13}$$

then the convexity condition required in Raychaudhuri's equation, $R_{\mu\nu}t^\mu t^\nu \geq 0$, is implied by the SEC,

$$\text{SEC}: \qquad T_{\mu\nu}t^\mu t^\nu + \frac{1}{2}T \geq 0, \qquad \forall \text{ timelike } t^\mu. \tag{3.14}$$

Since the SEC is violated already by some physically relevant cases, e.g. the inflationary phase of our universe or its current accelerated expansion phase today, it is not physically reasonable to assume that all physical matter should satisfy such a condition. Therefore, a zoo of seemingly reasonable alternative energy conditions was invented.[5] The most universal of these classical energy conditions is the so-called null energy condition (NEC),

$$\text{NEC}: \qquad T_{\mu\nu}k^\mu k^\nu \geq 0 \qquad \forall k^\mu k_\mu = 0 \tag{3.15}$$

Several classical theorems about focusing, singularities, and area growth of black holes can be sharpened by assuming NEC instead of one of its stronger cousins. While reasonable for classical matter, NEC fails semiclassically. In such cases, and even fully quantum mechanically, an averaged version of NEC holds, the so-called averaged null energy condition (ANEC).

$$\int \mathrm{d}x^\lambda \, \langle T_{\mu\nu}\rangle \, k_\lambda k^\mu k^\nu \geq 0 \qquad \forall k^\mu k_\mu = 0 \tag{3.16}$$

Here $\langle\,\rangle$ denotes the expectation value, and the integral extends over the null direction generated by $k^\mu$ from past to future null infinity. ANEC was proved in [215,216]. We shall come back to quantum versions of NEC, QNEC, in Sect. 8.2.

[5] Within Einstein GR, the SEC and NEC are equivalent to a simple curvature condition. There are, however, two other energy conditions usually discussed. The Weak Energy Condition (WEC) which states $T_{\mu\nu}t^\mu t^\nu \geq 0$ for any timelike $t^\mu$ and Dominant Energy Condition (DEC) which stipulates for any future-oriented causal vector field $C^\mu$, $-T^\mu{}_\nu C^\nu$ is future-oriented causal vector field. The DEC is, e.g. used in the proof of cosmic no-hair theorem by Wald [213] and WEC is used to argue for the nonexistence of superluminal propagation or in the analysis of traversable wormholes. See [214] for more discussions on the energy conditions.

### 3.2.3 Singularity Theorems

Before addressing singularity theorems, we should define what is meant by 'singularity'. There is a biodiversity of singularities, including singularities in curvature invariants, in deficit angles (orbifold singularity), in the causal structure, in the topological structure, and in tidal forces, e.g. see [153,217]. The classical general relativistic perspective is to remove all singularities from spacetime, thereby defining a spacetime to be singular if it has some boundaries that can be reached with finite proper time or finite affine parameter. In other words, we can verify that spacetime is singular by sending test particles in all possible directions and checking whether or not they reach the end of maximally extended spacetime in finite proper time. If they do, then we say spacetime is geodesically incomplete, which is used as a synonym for spacetime being singular.

The overall strategy of proving singularity theorems is as follows. Assume some convexity conditions (like an energy condition) and some trapping conditions (like the negativity of expansion), then use tools like Raychaudhuri's equation to deduce the existence of a singularity. Physically, the conclusion of these theorems is that black holes contain singularities, which is just a way of the classical theory telling us that it should not be applied to the center of a black hole. So one can replace 'singularity' with 'breakdown of the classical approximation'.

**> Focusing theorem**

We show a simple theorem that implements and illustrates the strategy outlined above. Let $t^\mu$ be the tangent vector field in a timelike twist-free geodesic congruence and assume $R_{\mu\nu}t^\mu t^\nu \geq 0$. If the expansion $\Theta$ associated with this congruence takes the negative value $\Theta_0$ at any point of a geodesic, then the expansion diverges to $-\infty$ along that geodesic within a proper time $\tau \leq (D-1)/|\Theta_0|$.

The proof of this theorem uses Raychaudhuri's equation (3.12), which together with the assumptions stated in the theorem yields the differential inequality $\mathrm{d}\Theta/\mathrm{d}\tau \leq -\Theta^2/(D-1)$. Integrating this inequality establishes

$$\Theta^{-1}(\tau) \geq \Theta^{-1}(\tau_0) + (\tau - \tau_0)/(D-1) \tag{3.17}$$

Without loss of generality, we fix $\tau_0 = 0$ to be the time when $\Theta = \Theta_0 < 0$, and hence see that the left-hand side must have a zero at some finite time $\tau \leq (D-1)/|\Theta_0|$. This implies that $1/\Theta$ goes to zero from below so that $\Theta \to -\infty$. This is what we wanted to prove.

---

Note that the theorem above only shows a singularity in the congruence and not a singularity in spacetime. However, similar assumptions and proof techniques are used in the actual singularity theorems. We state now a classic singularity theorem by Hawking and Penrose [45].

> **Singularity theorem**

Assuming the following four conditions, spacetime contains at least one incomplete timelike or null geodesic, and hence by definition has a singularity. 1. $R_{\mu\nu}k^\mu k^\nu \geq 0$ for all null and timelike $k^\mu$, 2. No CTCs exist, 3. Spacetime is generic, in the sense that there is at least one point on each timelike geodesic where, for any given causal vector $k^\mu$, $R_{\mu\nu\lambda\sigma}k^\mu k^\nu \neq 0$, 4. At least one of the following three properties holds: I. spacetime is a closed universe, II. spacetime possesses a trapped surface, and III. there is a point where the expansion of all future (or past) directed null geodesics emanating from this point becomes negative along each of these geodesics.

For applications to black hole physics property II. holds, so if the first three assumptions also hold then black hole spacetimes are necessarily singular.

The status and zoology of singularity theorems is summarized in [138,218].

### 3.2.4 Asymptotic Flatness

It is useful to have a notion for spacetimes that approximate Minkowski spacetime at large distances, namely asymptotic flatness. There are different classes of possibilities for defining this notion:

1. one could demand a certain fall-off behavior of the metric components, e.g. in some adapted coordinate system (e.g. Minkowski/Cartesian coordinates);
2. one could demand certain fall-off behavior of the Riemann-tensor components;
3. one could require an asymptotic (conformal) boundary identical to that of Minkowski spacetime, i.e. with $\mathfrak{I}^+$, $\mathfrak{I}^-$ and $i^0$, and possibly also with $i^\pm$.

These notions are not completely independent from each other and given some extra assumptions either of them can imply the other two, see e.g. [219] and Exercise 3.21.

The first one is the most straightforward to define: we can simply demand that there exists a coordinate system $x^\mu$ such that the metric is given by

$$g_{\mu\nu} = \eta_{\mu\nu} + o(1) \qquad r = \sqrt{\sum_i x_i^2} \to \infty\,. \tag{3.18}$$

More suitable coordinate systems, like Bondi–Sachs coordinates, are used in practice; see e.g. [220]. According to this definition, any asymptotically flat metric can be split into a fixed asymptotic background $\bar{g}_{\mu\nu}$ and subleading terms $\delta g_{\mu\nu}$,

$$g_{\mu\nu} = \bar{g}_{\mu\nu} + \delta g_{\mu\nu}, \tag{3.19}$$

where $\bar{g}_{\mu\nu}$ is a fixed metric of vanishing curvature, a metric for flat space. A disadvantage of this definition can be its coordinate-dependence or rather, the necessity to

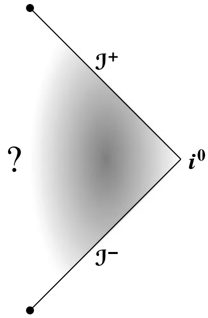


**Fig. 3.10** Asymptotic structure of asymptotically flat spacetimes. The question mark indicates that the interior of the Penrose diagram could be continued in infinitely many different ways, including all the asymptotically flat black hole solutions discussed in Chap. 2

perform a diffeomorphism to bring the metric into the form (3.18) or, more generally, into the form (3.19). Moreover, this definition is local, so it is blind to global aspects. An advantage of this definition is that it allows introducing the notion of asymptotic Killing vectors $\xi$,

$$\mathcal{L}_\xi g_{\mu\nu} = \mathcal{O}(\delta g_{\mu\nu}) \tag{3.20}$$

where $g_{\mu\nu}$ is any metric subject to the fall-off conditions (3.19) and $\delta g_{\mu\nu}$ are allowed fluctuations therein. The asymptotic Killing vectors are approximate isometries of the metric up to order $\delta g_{\mu\nu}$. This notion of asymptotic Killing vectors is of relevance far beyond asymptotically flat applications, and we shall come back to it in later chapters. (See also Exercises 3.21 and 3.22.)

The second possibility is slightly less coordinate dependent, but still local. Again, we take a limit of some radial coordinate $r \to \infty$ and investigate the components of the Riemann tensor in the Cartan formulation (see Appendix C). For asymptotic flat spacetimes

$$R_{abcd} = o(1) \qquad r \to \infty \tag{3.21}$$

where $R_{abcd}$ is defined in (C.14). In many applications, one can further specify the precise fall-off behavior by parametrizing $R_{abcd} \sim \mathcal{O}(r^{-\lambda})$ with some positive $\lambda$ (which can differ for different components). For asymptotically flat geometries in the Plebanski–Demianski family, using the radial coordinate defined in (2.97), it turns out $\lambda \geq 3$.

The third option is coordinate independent and global. Thus, it can be the most useful one for proving certain theorems. Indeed, when assuming asymptotic flatness in theorems in the next sections, we always mean this global notion. The key aspect is that the spacetime must allow a conformal compactification, i.e. the drawing of a Penrose diagram, and the asymptotic boundary must look like in Fig. 3.10. So in short, any spacetime that has a conformal compactification leading to the same form of $\mathscr{I}^+$, $\mathscr{I}^-$, and $i^0$ as Minkowski space is called asymptotically flat. This definition of asymptotic flatness includes most of the black hole solutions discussed in Chap. 2, most notably the family of Kerr black holes. However, there is a lot of fine print in this definition (not spelled out here) regarding smoothness properties of the compactified metric; see for instance [2,221].

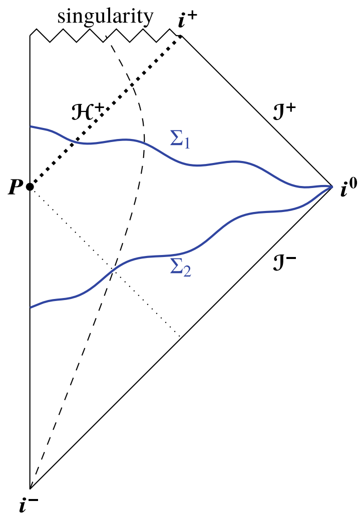


**Fig. 3.11** Event horizon for collapsing matter has a past endpoint $\boldsymbol{P}$; dotted line: continuation of the null geodesic which reaches $\boldsymbol{i}^+$; dashed line: typical matter trajectory during collapse; $\Sigma_i$: Cauchy surfaces

### 3.2.5 Horizon Theorems

We collect here three classic theorems that relate to event horizons, postponing a discussion of black hole uniqueness, cosmic censorship, and the area theorem to the following sections.

The first one concerns the question of whether or not event horizons can end in the past and/or the future. When considering dynamically generated black holes through the collapse of matter, the event horizon indeed has a past endpoint; see Fig. 3.11. However, it cannot have a future endpoint, as guaranteed by Penrose's theorem [41]:

**Horizon theorem I.** Future event horizons cannot have future endpoints.

See Exercise 3.23 for a hint on the proof and some important byproducts of the theorem. A similar theorem holds, where the instances of the word 'future' are replaced by 'past'.

The second theorem is by Hawking [222] and relates event horizons to other horizon notions, showing that under certain conditions this global horizon definition reduces to a local one.

**Horizon theorem II.** In stationary asymptotically flat spacetimes, an event horizon is necessarily a Killing and an apparent horizon.

The converse is not necessarily true, i.e. a Killing horizon need not be an event horizon, with Rindler space as the simplest counterexample. For a proof of this theorem within Einstein–Maxwell theory, see [132].

The third and final theorem is concerned with the topology of constant time sections of the event horizon. Since all Kerr black holes in asymptotically flat space have spherical horizon topology, it is fair to ask whether this is accidental or a generic feature of black holes. The answer is provided by the next theorem.

**Topology theorem.** In stationary asymptotically flat 4-dimensional spacetimes, each connected component of the compact cross-section of the event horizon with some achronal slice is topologically a 2-sphere.

In particular, toroidal or higher genus topologies of isolated black holes are prohibited by this theorem. For proofs with varying sets of assumptions, see e.g. [223–225].

There are two simple ways to evade the topology theorem: the first one we encountered already in Sect. 2.6, where the assumption of asymptotic flatness was replaced by asymptotic AdS behavior. The second possibility is to consider more than four spacetime dimensions. Indeed, in five spacetime dimensions, black rings exist [226] with horizon topology $S^1 \times S^2$; see Sect. 7.4, and [227] for the zoology of these higher-dimensional black objects.

### 3.2.6 Uniqueness Theorems

Historically, the first uniqueness theorem is due to Birkhoff (1923) [228][6] which states that any spherically symmetric vacuum solution to Einstein gravity is static and hence given by the Schwarzschild solution. The converse does not hold in general (staticity does not necessarily imply spherical symmetry), but it does so for black holes.

**Uniqueness of Schwarzschild solution**, Israel (1967) [230]. Let $(\mathcal{M}, g)$ be a static, asymptotically flat, vacuum black hole spacetime solution that is regular on, and outside an event horizon, then $(\mathcal{M}, g)$ is isometric to the Schwarzschild solution. This theorem establishes that static vacuum multi-black hole solutions do not exist [231].

**Uniqueness of Kerr solution**, Carter (1971) [232] and Robinson (1975) [233]. If $(\mathcal{M}, g)$ is a stationary, axisymmetric, asymptotically flat vacuum spacetime suitably regular on, and outside, a connected event horizon, then $(\mathcal{M}, g)$ is a member of the 2-parameter non-extremal Kerr family of solutions [25]. The parameters are mass $M$ and angular momentum parameter $a$, with $M > |a|$. The Carter–Robinson theorems, therefore, generalize the previous considerations by relaxing staticity to stationarity and spherical symmetry to axisymmetry and establish the uniqueness of Kerr black holes as the only asymptotically flat stationary and axisymmetric vacuum spacetimes that are non-singular on and outside an event horizon.

**Rigidity theorem**, Hawking (1972) [223]. This theorem strengthens the Carter–Robinson results by proving that for black holes stationarity implies axisymmetry. We note that the rigidity theorem implies **Horizon theorem II.** of the previous section, that the event horizon of a stationary black hole solution is also a Killing horizon.

**Uniqueness of RN solution.** In 1968, Israel [234] extended the Birkhoff theorem to Einstein–Maxwell theory and proved the uniqueness of RN black hole as the only static, asymptotic flat electrovac solution which is regular outside its horizon. Israel's theorem established that spherical symmetry follows from the other assumptions. We note that the multi-black hole Majumdar–Papapetrou solutions, see Exercise 2.36, does not respect the regularity condition and hence is not at odds with this theorem.

[6] We note that a similar theorem was presented by J.T. Jebsen [229] two years earlier.

**Uniqueness of KN solution**, Mazur (1982) [235] and Bunting (1983) [236]. Carter, Robinson, and Hawking's rigidity theorems for Einstein vacuum solutions have been extended to Einstein–Maxwell theory. A stationary, asymptotically flat analytic solution of the Einstein–Maxwell equations that is suitably regular on, and outside an event horizon is axisymmetric and necessarily falls into the non-extremal KN family.

The original uniqueness theorems were proven for non-degenerate horizon cases, non-extremal Kerr or KN black holes. These proofs have, however, been extended to the extremal case, e.g. see [200,237,238].

**No-hair statements.** There has been a continued effort in extending and generalizing uniqueness theorems for stationary black hole solutions for Einstein gravity with different matter fields, asymptotic behavior, and in diverse dimensions. The no-hair theorem/conjecture of Wheeler states that a black hole solution is described by just a few numbers. In the case of asymptotically flat solutions to Einstein–Maxwell theory in four dimensions, these few numbers are mass $m$, angular momentum parameter $a$, electric, or magnetic charges. See [239] and references therein for a more detailed discussion on the stationary black holes and their (non)uniqueness.

### 3.2.7 Cosmic Censorship Conjecture

Singularity theorems show that there are always singularities hidden behind black hole horizons. Cosmic censorship conjecture (CCC) conjectures that the converse is true as well: singularities are always hidden by horizons. Singularities that violate cosmic censorship are often referred to as 'naked'.

The original motivation for the CCC was the somewhat misguided belief that singularities lead to a loss of predictability or lack of determinism and that Nature should have a mechanism built-in, such as cosmic censorship, to forbid this. The current perspective on singularities is quite different: if they were accessible to a distant observer they would provide excellent probes for testing QG, so what breaks down is not predictability but rather the classical approximation. However, it appears to be true that most singularities are screened by black hole or observer horizons, including the Big Bang singularity.

While there are counterexamples to the strictest formulation of CCC already in relatively simple systems, like spherically symmetric Einstein-massless-Klein–Gordon theory [240,241], these examples do not represent generic situations. It is possible to generate naked singularities from fine-tuned initial data, but in the whole set of possible initial data, they represent a set of measure zero in known examples. Thus, refined versions of CCC could hold.

The statements above are known as 'weak CCC'. There is also a strong CCC (which is logically independent of the weak CCC, as neither implies the other), which states that Cauchy horizons should not form through Cauchy evolution. The physical motivation here is that, in realistic situations, we may not expect a loss of predictability, and hence no Cauchy horizon. However, again there are counterexamples for some formulations of strong CCC [210], so both weak and strong CCC keep evolving with our understanding of classical and quantum gravity.

## 3.3 Optical Focusing Equation and Area Theorem (2nd Law)

The discussion that led to Raychaudhuri's equation (3.12) can be generalized to null geodesic congruences. The expansion $\theta = \nabla_\mu k^\mu$ (with null tangent vector $k^\mu = (\mathrm{d}/\,\mathrm{d}\lambda)^\mu$ and affine parameter $\lambda$) obeys [242]

$$\frac{\mathrm{d}\theta}{\mathrm{d}\lambda} = -\frac{\theta^2}{D-2} - \sigma^{\mu\nu}\sigma_{\mu\nu} - R_{\mu\nu}k^\mu k^\nu \tag{3.22}$$

where $\sigma^{\mu\nu}$ is again the shear. The expansion can be interpreted geometrically as the logarithmic derivative of an area element $A$ spanned by infinitesimally neighboring null geodesics,

$$\theta = \lim_{A\to 0} \frac{\mathrm{d}\ln A}{\mathrm{d}\lambda} \tag{3.23}$$

The classic focusing theorem states

$$\frac{\mathrm{d}\theta}{\mathrm{d}\lambda} \leq 0 \tag{3.24}$$

provided the null curvature condition holds, $R_{\mu\nu}k^\mu k^\nu \geq 0$, except at caustics (i.e. loci where $\theta \to -\infty$). The null curvature condition holds provided the classical Einstein equations are obeyed and matter obeys the NEC (3.15).

An interesting consequence of the focusing theorem is Hawking's area theorem, also known as the second law of black hole mechanics [77]. See [243] for a proof under rather generic assumptions.

**> Second law of black hole mechanics**

The area of sections of future event horizons in spacetimes satisfying the NEC is non-decreasing toward the future, provided the horizon is geodesically complete or spacetime has a globally hyperbolic conformal completion.

To highlight the similarity to the second law of thermodynamics, the area law is often schematically written as

$$\boxed{\delta A \geq 0} \tag{3.25}$$

suggesting the interpretation of area being proportional to entropy.

The idea in Hawking's original proof is to show that all ways of changing the area yield increasing it. Geometrically, there are two sources of area change: 1. null generators could be added to (or subtracted from) the horizon, and 2. existing null generators could expand or contract. Regarding the former, subtracting generators would contradict Penrose's theorem as the generators of the future event horizon have no future endpoint, and hence option 1. can only result in an area increase. The second option can be studied locally for each area element. We exploit (3.23), rewritten as $\mathrm{d}A/\,\mathrm{d}\lambda = A\theta$. Then it is sufficient to show that, given suitable regularity assumptions, the expansion is non-negative on the horizon, $\theta \geq 0$. The latter part may be proven by contradiction: assuming $\theta < 0$ leads either to a singularity (which is assumed to be absent as part of the input in the theorem) or to a caustic (which would lead to timelike-connected points on the horizon, another impossibility). Thus, horizon generators cannot contract, which proves the second law.[7]

## Further Reading

Classic textbooks and reviews include the Hawking–Ellis book on the large-scale structure of spacetime [132], the textbook by Wald [109], lecture notes by Townsend [244] and by Reall [245].

Singularity theorems specifically are covered in [246,247], uniqueness theorems in [239], rigidity theorems in [248,249] and references therein, and attempts to construct black holes with scalar hair in [250,251]. No-hair theorems are summarized in [252] and its observational tests in [253,254].

The CCC is discussed in gravitational collapse at linerized level [255–258] and non-linearly in [259].

## Exercises

**3.1 More on non-affinity and surface gravity.**

(1) How does changing the normalization of the vector field $l$ which is normal to a null surface $\mathcal{N}$ at $r = 0$, i.e. $\xi^\mu = N l^\mu$, affect the non-affinity parameter $\kappa_{_{(l)}}$ defined as

$$l^\mu \nabla_\mu l_\nu = \kappa_{_{(l)}} l_\nu. \tag{3.26}$$

(2) Show that there is always a normalization $N$ for which $\xi^\mu$ becomes the velocity vector for an affinely parametrized null geodesic at $r = 0$.

(3) Noting that $\xi^\mu$ is a Killing vector, show that (3.1) implies either $\kappa = 0$ or $\xi^2|_\mathcal{N} = 0$.

(4) Show that (3.1) may also be written as

$$-\frac{1}{2}\nabla_\mu \xi^2\big|_\mathcal{N} = \kappa \xi_\mu \tag{3.27}$$

(5) Starting from (3.1), using the Killing equation and that $\xi_{[\alpha}\nabla_\mu \xi_{\nu]}|_\mathcal{N} = 0$, prove (3.2).

[7] We thank Roberto Emparan for suggestions that improved this paragraph.

(6) Prove that for a Killing horizon surface gravity $\xi \cdot \nabla\kappa|_{\mathcal{N}} = 0$, i.e. $\kappa$ is a constant on orbits of $\xi$.

For the proof, one needs to use the Killing equation $\nabla_\mu \xi_\nu + \nabla_\nu \xi_\mu = 0$ and (3.28).

(7) Show that $R_{\mu\nu}\xi^\mu\xi^\nu|_{\mathcal{N}} = -2\kappa^2$.

(8) Show that $\mathrm{d}\xi = 2\kappa\boldsymbol{\epsilon}$, where $\boldsymbol{\epsilon}$ is the 2-form binormal to the bifurcation surface $\mathcal{B}$ and is normalized as $\boldsymbol{\epsilon}_{\mu\nu}\boldsymbol{\epsilon}^{\mu\nu} = -2$.

**3.2 Some useful Killing vector identities.**

(1) Show that for any Killing vector field $\xi_\mu$,

$$\nabla_\mu \nabla_\nu \xi_\alpha = -R_{\beta\mu\nu\alpha}\xi^\beta. \tag{3.28}$$

(2) If we have a hypersurface orthogonal (cf. Exercise 2.2) Killing vector field $\xi_\mu$

$$\xi_\mu R_{\mu[\alpha}\xi_{\beta]} = 0, \qquad \xi_\mu R_{\mu[\alpha}\nabla_\beta \xi_{\gamma]} = 0. \tag{3.29}$$

**3.3 More on Killing horizon.**

(1) Are all black hole geometries with a Killing horizon necessarily stationary?

(2) Congruences of null geodesics containing generators of a Killing horizon have vanishing shear, twist, and expansion at the horizon. To show this, we take the following steps:

(2-1) Show the generators of a Killing horizon are hypersurface orthogonal and hence have vanishing twist $\omega$ at the horizon.

(2-2) Consider a Killing horizon generated by the Killing vector $\xi$. The affinely parametrized tangent to the generators of horizon $v^\mu$ can be written as $v^\mu = f\xi^\mu + hu^\mu$ where $h$ is a function such that $h = 0$ at the horizon, $f$ is an arbitrary function and $u^\mu$ is a vector field. The latter two are smooth at the horizon. Compute $\nabla_\mu v_\nu$ and show it vanishes at the horizon.

**3.4 Killing horizon versus ergosphere.**

Consider a Kerr black hole in the usual Boyer–Lindquist coordinates. As discussed in Sect. 2.5.1, ergosphere is the hypersurface at which the Killing vector field $\partial_t$ becomes null (while it is spacelike/timelike inside/outside the ergoregion). Does this mean that the ergosphere is a Killing horizon? If not, why is precisely the ergosphere not a Killing horizon?

**3.5 An alternative way to compute surface gravity.**

Suppose that horizon is specified by $\Phi(r) = 0$ and let $n_\mu$ be the unit 1-form along $\mathrm{d}\Phi$.

(1) Show that $n^\nu$ is spacelike in the region outside the outer horizon and becomes null on the horizon.

(2) Using this, one can decompose the metric as

$$g_{\mu\nu} = h_{\mu\nu} + n_\mu n_\nu, \qquad h_{\mu\nu}n^\nu = 0. \tag{3.30}$$

One can then compute extrinsic curvature of the constant $r$ surfaces, $K_{\mu\nu} = \nabla_\mu n_\nu$. Show that,

$$(\mathrm{d}\xi)_{\alpha\beta} = n_{[\alpha} K_{\beta]\mu} \xi^\mu \quad \text{computed at the horizon,} \tag{3.31}$$

where $\xi_\mu$ is the horizon generating Killing vector field. From the above, one can then read surface gravity $\kappa$ using the 1-form $n$.

(3) Use this method to compute surface gravity for a Kerr black hole, both for the outer and the inner horizons.

**3.6 Causal structure on a null hypersurface.**

(1) Show that any two points $P$, $Q$ on any null hypersurface cannot be timelike separated.

(2) Show that there is always a dimension one curve on a null surface over which the points are null separated.

(3) Consider two vector fields $\xi$ and $X$. Let $\xi$ be null on the null surface $\mathcal{N}$ and $X$ spacelike over $\mathcal{N}$. Show that $\xi + X$ is necessarily a spacelike vector field.

Note that the above statements are true for any null hypersurface, in particular, for event horizons.

**3.7 Killing horizons in flat space.**

(1) Consider 4-dimensional Minkowski space parametrized as

$$\mathrm{d}s^2 = -2\,\mathrm{d}u\,\mathrm{d}v + \mathrm{d}y^2 + \mathrm{d}z^2. \tag{3.32}$$

Show that constant $u$ or $v$ hypersurfaces are null surfaces that may be viewed as Killing horizons of vanishing surface gravity.

(2) In flat space, we can have null surfaces with non-vanishing surface gravity. For this, consider a Rindler spacetime (2.39), flat space as seen by an accelerated observer. Show that $\partial_\tau$ generates a Killing horizon whose surface gravity is $a$.

(3) Show that $\rho = 0$ in the Rindler space is indeed a bifurcate horizon. Here the bifurcation surface is the $yz$ plane which is noncompact and has a planar topology.

**3.8 Surface gravity for generic stationary metrics.**

(1) Consider a generic static, spherically symmetric geometry:

$$\mathrm{d}s^2 = g_{tt}(r)\,\mathrm{d}t^2 + g_{rr}(r)\,\mathrm{d}r^2 + r^2\,\mathrm{d}\Omega_2^2. \tag{3.33}$$

This geometry may be a solution to the Einstein equations with some matter content.

(1-1) Show that $\xi = \partial_t$ produces a Killing horizon at roots of $1/g_{rr}$, $r = r_h$.

(1-2) Show that surface gravity $\kappa$ is

$$\kappa = \frac{1}{2} \frac{\partial_r g_{tt}}{\sqrt{-g_{rr} g_{tt}}}\Big|_{r=r_h}. \tag{3.34}$$

(1-3) What are the conditions on $g_{tt}$, $g_{rr}$ if we want the metric (or its Euclidean sector) to be smooth at $r = r_h$?

(2) Repeat the above for a generic stationary, axisymmetric geometry. Start with writing the counterpart of (3.33) for the stationary case.

**3.9 Surface gravity for inner horizon.**

Black holes like Kerr or KN typically have an outer (event) horizon and an inner (Cauchy) horizon. For the family of Plebanski–Demianski black holes, these two are Killing horizons.

(1) Compute the surface gravity for the inner and outer Killing horizons of KN black holes, respectively $\kappa_+, \kappa_-$.

(2) Show that $\kappa_- \leq 0$ and $\kappa_+ \geq 0$ for the Plebanski–Demianski family.

(3) Show that $|\kappa_-| \geq \kappa_+$ for generic Plebanski–Demianski black holes, where the equality happens for the extremal case.

(4) Check whether the above can be a generic feature of any stationary black hole.

**3.10 More on trapped surfaces.**

(1) Show that from our definitions (3.8) it follows that $\theta^+ \geq \theta^-$.

(2) Consider a spherically symmetric situation, and let $r$ be the radial coordinate. Consider a sphere of radius $R$. Show that the sphere is a trapped surface if $R$ decreases along any future null direction. So all null rays emanating from the sphere move toward its center.

(3) When is a trapped surface also a null surface?

(4) Consider an FLRW cosmology (2.143) which has an accelerated expansion, i.e. $\alpha > 0$ in the notation of Exercise 2.35. Show that the cosmological horizon is an anti-trapped surface.

**3.11 On apparent, Killing and event horizons.**

(1) Show trace of extrinsic curvature for any Killing horizon is zero.

(2) Show the bifurcation surface of a Killing horizon is an extremal surface.

(3) Prove that for a stationary asymptotically flat spacetime an apparent horizon is also a Killing and an event horizon.

(4) Show that the apparent horizon resides inside the event horizon, as depicted in Fig. 3.4. That is, argue that inside an apparent horizon, there is always a black hole, contrary to an event horizon.

Hint: Consider a collapsing spherically symmetric thin shell of matter in a vacuum. The exterior of the shell is a portion of the Schwarzschild spacetime and the interior of the hollow shell is exactly flat Minkowski space.

**3.12 Another definition for event horizon.**

Show the following definition for event horizon is equivalent to the one given in Sect. 3.1.2. Consider any event $P$ and let us define the past (future) particle horizon $\mathcal{H}_p(P)$ ($\mathcal{H}_f(P)$) as the boundary of $I^-(P)$ ($I^+(P)$) in Fig. 3.2. Choose the point $P$ such that $\mathcal{H}_p(P)$ ($\mathcal{H}_f(P)$) includes $\mathscr{I}^-$ ($\mathscr{I}^+$). Then, the event horizon of manifold

$\mathcal{M}$ is

$$\mathcal{H}_{p/f}(\mathcal{M}) = \bigcup_{\forall P} \mathcal{H}_{p/f}(P).$$

**3.13 More on stretched horizons.**

Consider a Schwarzschild black hole of mass $M$ and suppose that the asymptotic observer has a UV cutoff $\Lambda$ on the frequency of waves she can detect. Recalling the redshift factor and supposing that a *fido* sitting at a constant $r$ close to the horizon can measure frequencies as high as Planck mass $M_{\rm Pl}$, where would this observer place the stretched horizon?

**3.14 Isolated horizons.**

Let $\mathcal{S}$ denote a trapped surface, as defined in the previous exercise and let $T_{\mu\nu}$ be the energy–momentum tensor on the spacetime. Isolated horizon ($IH$) is then a codimension-1 null hyper surface of $\mathbb{R} \times \mathcal{S}$ topology such that the momentum flow of causal matter is always inward on $IH$, i.e.

$$P^2|_{IH} \leq 0, \quad \text{where} \quad P^i_\mu := T_{\mu\nu}\ell^\nu_i, \tag{3.35}$$

and $\mathcal{L}_{\ell_i} C|_{IH} = 0$ where $\ell_i, i = 1, 2$ denote the two usual canonically normalized null vectors $\ell, n$ and $C$ is the connection 1-form on $IH$.

Using the Raychaudhuri equation and Einstein field equations, analyze the implications of having an isolated horizon for the shear and the twist of the null vector fields $\ell^\mu_i$.

**3.15 Particle and apparent event horizons in cosmology.**

Consider an FLRW spacetime (2.143). Let $t = 0$ denote the big bang time. For an observer at comoving time $t_0$, show that

(1) cosmological (event) horizon is at comoving radius $r_e = \int_{t_0}^{\infty} \mathrm{d}t/a(t)$, where $a(t)$ is the scale factor;

(2) cosmological particle horizon is at $r_p = \int_0^{t_0} \mathrm{d}t/a(t)$.

Study $r_e, r_p$ for positive and negative values of the $\alpha$ parameter in Exercise 2.35.

**3.16 Domain of dependence of a half spaces.**

(1) Consider a $(1+1)$-dimensional flat spacetime parametrized by $t, x$. What is the domain of dependence for $x > 0$ region? Show that this is the Rindler wedge.

(2) Consider an $\mathrm{AdS}_2$ space with metric $\mathrm{d}s^2 = \ell^2(-z^2\mathrm{d}t^2 + \frac{\mathrm{d}z^2}{z^2})$, with $z \in [-\infty, +\infty]$. What is the domain of dependence for the $z \geq 0$ region?

**3.17 An alternative definition for Cauchy surface and horizon.**

In Sect. 3.1.4, we defined the Cauchy horizon of a manifold $\mathcal{M}$ starting from a Cauchy horizon for an achronal set $S$ and then defined a Cauchy surface. Here we outline a definition that first defines a Cauchy surface while leaving out some details as exercises.

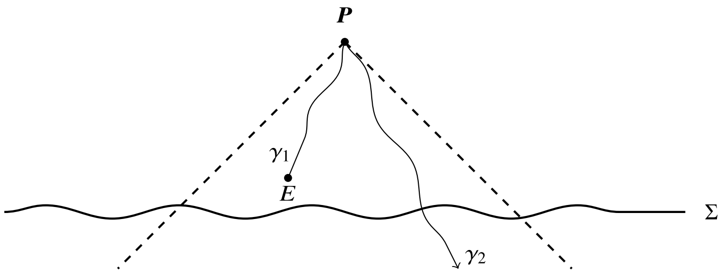


**Fig. 3.12** Partial Cauchy surface $\Sigma$ and the past lightcone of a point $P$. $\gamma_1$ has a past endpoint $E$ and is hence past extendible and $\gamma_2$ is a past inextendible curve through $P$

To this end, let us start with the following definitions:
A *(partial) Cauchy surface* is a codimension-1 hypersurface that no causal curve intersects it more than once. Thus, a vector field normal to a partial Cauchy surface is never spacelike.

(1) Show that a partial Cauchy surface is achronal, i.e. it is a spacelike or null surface. Argue that no two points on a partial Cauchy surface are timelike separated.
A *past (future) inextendible causal curve*, as the name suggests, is a causal curve which do not have a past (future) endpoints in a given manifold with metric $g$ on it, $(\mathcal{M}, g)$, see Fig. 3.12.
*Future domain of dependence* of a partial Cauchy surface $\Sigma$, $D^+(\Sigma)$ is

$$D^+(\Sigma) = \left\{ \begin{array}{c} \forall P \in \mathcal{M} \text{ such that every past-directed inextendible} \\ \text{causal curve through point } P \text{ intersects } \Sigma \end{array} \right\} \tag{3.36}$$

A manifold $\mathcal{M}$ is *globally hyperbolic* if there exists a surface $\Sigma$ such that $\mathcal{M} = D^+(\Sigma) \cup D^-(\Sigma)$.

(2) Show that if such $\Sigma$ exists, it constitutes a Cauchy surface for $\mathcal{M}$. Show that this definition for a Cauchy surface matches the one given in Sect. 3.1.4.
*Cauchy horizon:* If a spacetime is not globally hyperbolic then $D^+(\Sigma)$ $(D^-(\Sigma))$ has future (past) boundary in $\mathcal{M}$. Null boundaries of $D^+(\Sigma)$ $(\mathcal{D}^-(\Sigma))$ are called future (past) Cauchy horizon.

(3) Show the above definition of the Cauchy horizon that matches the one given in the main text.

**3.18 More on Cauchy horizons.**

(1) Consider a negative mass Schwarzschild geometry and draw its future and past Cauchy horizons.

(2) Consider the causal diagram of a process of collapse which yields a naked singularity. Show that it does not have a past Cauchy horizon. Draw its future Cauchy horizon.

(3) Consider AdS space in Poincaré coordinates. Show that the Poincaré horizon is a degenerate Killing horizon, nonetheless, it is not an event horizon. Note that AdS space is not globally hyperbolic and does not have a Cauchy horizon.

(4) Show that for extremal black holes which have degenerate horizons, the event, Killing, and Cauchy horizons coincide.

(5) The above fact about extremal black holes means the region inside the horizon of an extremal black hole is dynamically decoupled from the region outside. To establish this, show that it takes infinite physical time, as measured by the near horizon observer, to pass through the horizon.

**3.19 On global hyperbolicity of some usual spacetimes.**

(1) Show that Minkowski space is globally hyperbolic. Draw some typical Cauchy surfaces $\Sigma$ on its Penrose diagram.

(2) Show that the Schwarzschild spacetime is also globally hyperbolic. Draw some typical Cauchy surfaces $\Sigma$ on its Penrose diagram.

Do we need to go maximally extended Kruskal coordinates to see that the geometry is globally hyperbolic, or just, e.g. the original Schwarzschild or EF coordinate system (covering regions I, II in its Penrose diagram) is enough?

(3) Is the spacetime associated with a spherical symmetric collapse globally hyperbolic? If yes, draw some typical Cauchy surfaces $\Sigma$ on its Penrose diagram.

(4) Is a naked singularity (like a negative mass Schwarzschild geometry) globally hyperbolic? Does it admit a Cauchy surface?

(5) Show that AdS space is not globally hyperbolic. Therefore, to have a well-defined (deterministic) evolution on AdS space, we need to solve an initial+boundary value problem.

(6) Is dS spacetime globally hyperbolic?

**3.20 Raychaudhuri equation versus geodesic deviation equation**

A standard method to encode and measure Riemann curvature is through the geodesic deviation equation. Consider two close-by timelike geodesics in an affinely parametrized congruence of geodesics and let $\tau$ be the affine parameter. The geodesic deviation equation is governing the separation between the two geodesics change in time from $\tau$ to $\tau + \Delta\tau$.

Compare this geodesic deviation equation and (3.11) or the Raychaudhuri equation.

**3.21 More on asymptotic flat geometries.**

We gave two different notions of asymptotic flatness, one based on asymptotic fall-off of metric and the other on that of Riemann curvature. The purpose of this exercise is to explore how these two are related to each other.

To this end, let's consider (3.19) and let $\bar{e}^a_\mu$ be the 'asymptotic orthonormal frame' (cf. Appendix C) such that $\bar{g}_{\mu\nu} = \eta_{ab}\bar{e}^a_\mu \bar{e}^b_\nu$ and define

$$\delta g_{ab} := \bar{e}^\mu_a \bar{e}^\nu_b \, \delta g_{\mu\nu} = \mathcal{O}(r^{-\beta}), \tag{3.37}$$

where $\bar{e}^\mu_a \bar{e}^a_\nu = \delta^\mu_\nu$ and $r$ is the asymptotic radial coordinate defined in (3.18). In the above, $\beta$s can take different positive values for different components of metric.

(1) Let us suppose that we start with a metric with given fall-off exponents $\beta$s. Compute what are the Riemann fall-off exponents $\lambda$s, cf. (3.21).

(2) Work out $\beta$s and $\lambda$s for the asymptotically locally flat Plebanski–Deminaski family of black holes discussed in Sect. 2.7.

(3) Work out $\beta$s and $\lambda$s for GW on a flat space.

(4) Consider the KN metric which is stationary and axisymmetric. Being asymptotically flat, it has asymptotic Poincaré symmetry. Explore the asymptotic behavior of the metric under the other eight symmetry generators (Killing vectors) in the Poincaré algebra. That is, compute $\mathcal{L}_\xi g_{\mu\nu}$ at leading order in large $r$, where $\xi$ are the asymptotic Poincaré generators.

(5) Repeat the previous exercise replacing KN with GW.

**3.22 Asymptotically AdS geometries.**

One may extend the definition of asymptotic flatness to other asymptotic behavior. For that, we may just take $\bar{g}_{\mu\nu}$ to be our fixed and chosen asymptotic metric (instead of Minkowski) and $r$ is a typical radial coordinate which is taken to be larger than any other physical length/scale in the problem. Or equivalently, one may compare Riemann curvature $R_{\mu\nu\alpha\beta}[g]$ of the spacetime with metric $g$ with Riemann curvature of a given asymptotic metric $\bar{g}$ and then one can compute Riemann curvature in in an orthonormal frame $R_{abcd}[\bar{g}]$, cf. (C.14), such that

$$R_{abcd}[g] - R_{abcd}[\bar{g}] \sim \mathcal{O}(r^{-\lambda}), \quad \lambda \geq 0. \tag{3.38}$$

In particular, one may have asymptotic AdS spaces, for which $R_{\mu\nu\alpha\beta}[\bar{g}] = -\frac{1}{L^2}(\bar{g}_{\mu\alpha}\bar{g}_{\nu\beta} - \bar{g}_{\mu\beta}\bar{g}_{\nu\alpha})$, where $L$ is the AdS radius.

(1) Explore asymptotic Killing vectors of asymptotic $AdS_4$ spaces and show that they include so(3, 2) asymptotic isometry.

(2) Compute $\lambda$s for the Kerr-AdS black hole.

(3) Bonus level: Repeat part (2) of this exercise for asymptotically AdS Plebanski–Demianski black holes.

**3.23 Proof of Penrose theorem and its byproducts.**

(1) Prove Penrose's theorem that future (past) event horizons cannot have future (past) endpoints. Use *reductio ad absurdum* for the proof: assume that such an endpoint exists and then show it is in contradiction with the definition of an event horizon.

(2) As a byproduct of the above theorem, show that future endpoint of a future horizon in asymptotic flat spacetimes can intersect asymptotic infinity only at $\boldsymbol{i}^+$ and not at any other point on $\mathscr{I}^+$.

(3) Show that null geodesics can only cross into future event horizons; they can't leave it.

**3.24 More on energy conditions.**

(1) Show that among the classical local (non-averaged) energy conditions NEC is the weakest, i.e. DEC, WEC, and SEC all imply NEC.

(2) Show that DEC implies WEC.

(3) Work out what ANEC, NEC, WEC, SEC, and DEC imply for a perfect fluid with energy-momentum tensor (4.28).

See [214] for more discussions on energy conditions and their implications.

**3.25 A consequence of dominant energy condition.**

Let $(\mathcal{M}_3, g)$ be a constant time slice on an asymptotically flat Riemannian 3-manifold. Assume $\mathcal{M}_3$ to be a totally geodesic submanifold. Show that the condition of $\mathcal{M}_3$ to have a non-negative scalar curvature is equivalent to the spacetime obeying the DEC.

**3.26 More on black hole horizon topology.**

Suppose we have a black hole with a bifurcate Killing horizon $\mathcal{B}$. For a black hole, by definition $\mathcal{B}$ is a 2d surface of finite volume.

(1) Argue using the definition of a bifurcate Killing horizon that $\mathcal{B}$ cannot be a non-orientable surface.

(2) Should $\mathcal{B}$ be a connected surface or can have disconnected pieces?

(3) Suppose that $\mathcal{B}$ is a connected orientable 2d surface. These are classified by their Euler character $\chi = 2 - 2g - b$, where $b$ is the number of punctures (boundaries). In the family of AdS black holes, we discussed topological black holes which have arbitrary $g$ but with $b = 0$. Can $\mathcal{B}$ have a non-zero $b$? See [260] for further discussions.

**3.27 Penrose mass inequality**

The Penrose mass inequality was proposed in a seminar in 1971 which was cited in [222] and mentioned in [53]. It gives a lower bound for the total (ADM) mass of asymptotically flat spacetimes in terms of the area of suitable surfaces that represent black holes. Its validity is supported by the CCC and its proof (or disproof) is an important problem in relation to gravitational collapse [261]. It asserts that for a black hole of mass $M$ and area $A$ in natural units $c, \hbar, G_\mathrm{N}$ equal to 1

$$M \geq \sqrt{\frac{A}{16\pi}}. \tag{3.39}$$

(1) Check that the above inequality hold for all black holes in the Plebanski–Demianski family.

(2) In the family of KN black holes, explore when the equality is saturated.

(3) In the KN family, when is the ratio $M/\sqrt{A}$ maximized?

To present the proof of the above inequality, it should be made precise. A precise version of this inequality, called Riemann–Penrose inequality, has been proven in [262]. See also [261, 263] for more updates.

**3.28 Optical Raychaudhuri equation.**

(1) Derive the Raychaudhuri equation for null geodesic congruences (3.22). Note the difference in the coefficient of expansion squared term in null (3.22) and timelike (3.12).

(2) The optical Raychaudhuri equation (3.22) is derived assuming that the null congruence is affinely parametrized. Repeat the analysis assuming that our null geodesics have a non-affinity parameter $\kappa$ (3.26). Show this leads to an extra $\kappa\theta$ term in the right-hand side of (3.22).

# Probing Black Holes, Their Formation and Stability

# 4

**Abstract**

This chapter is devoted to observational signatures and the detection of black holes. We start with some general remarks in Sect. 4.1. Black holes can be probed by light or other fields scattered off them leading to gravitational lensing, black hole shadows, and associated images, as discussed in Sect. 4.2. Superradiance, the Penrose process, and black hole mining are investigated in Sect. 4.3. GW from black hole mergers can be (and have been) detected from far away, as outlined in Sect. 4.4. Aspects of black hole accretion disks are mentioned in Sect. 4.5. The formation process of black holes in shock-wave collisions is summarized in Sect. 4.6. Some physical processes, like the ringdown phase after a black hole merger, are adequately described by perturbation theory, using, e.g. quasi-normal modes (QNMs), developed in Sect. 4.7. A similar analysis allows addressing the linear stability of black holes. Non-perturbative aspects, such as critical collapse and non-linear stability of black holes, are addressed in Sect. 4.8.

## 4.1 General Remarks on Black Hole Observations

Like in any empirical science, it is necessary to confront our theoretical knowledge about black holes with observations. However, it is non-trivial to observe celestial bodies that by their very definition do not emit light. Thus, naturally black hole observations are more indirect than observations of luminous stars or galaxies. We list here a number of ways in which black holes can be observed and refer to the remainder of this chapter for elaborations on some of these methods. We start with well-established methods and toward the end of the list move to future possibilities for observations and more speculative avenues to detect black holes. In the end of the chapter, we have provided a list of references for further reading.

- **Indirect evidence.** GR predicts the possibility of black hole solutions as rather generic endpoints of gravitational collapse and Chandrasekhar's considerations



D. Grumiller and M. M. Sheikh-Jabbari, *Black Hole Physics*, Graduate Texts in Physics,
https://doi.org/10.1007/978-3-031-10343-8_4

which were briefly reviewed in Chap. 1, show that gravitational collapse is inevitable for stars similar to but slightly heavier than our Sun. In this sense, every test of GR indirectly supports the existence of black holes.

- **Accretion disks.** Black holes can be detected more easily if there is luminous matter surrounding them, e.g. in the form of accretion disks in X-ray binaries, e.g. see [112,264,265]. Observations of accretion disks and their spectra together with numerical simulations of such disks allow reliably extracting the mass of the invisible center inside the accretion disk. If the mass is significantly higher than the Chandrasekhar/TOV limit, the most plausible (and sometimes the only plausible) explanation of the invisible object is that it is a black hole. Accretion disks are often accompanied by relativistic jets emanating from the poles, but it is less clear how to deduce the black hole's nature just from the observation of jets. Another relevant observational feature is quasi-periodic oscillation. The first black hole observation, Cygnus X-1, was made in the 1970s, though the conclusion that it was indeed a black hole was consolidated not before the 1990s, see [266].
- **Motion of nearby stars.** For the supermassive black hole near the center of our Galaxy, Sagittarius A*, there is a neat way of observing it: there is a handful of visible stars that move on Keplerian orbits around some invisible center. These stars have been tracked since 1995, so the orbits are very accurate [267–271]. Indeed, the 2021 physics Nobel prize was in part given to such precise observations. From these orbits, one can deduce the mass of the invisible object, which is about $4.3 \times 10^6 M_\odot$ with a size smaller than 0.002 lightyears, which is still larger than the Schwarzschild radius but not by much. The only plausible explanation for this invisible object is that it is a black hole. Similar supermassive black holes have been observed in the center of numerous other galaxies and could be (is widely believed to be) a generic feature of them.
- **Gravitational waves.** Black holes emit GW when two of them coalesce in a merger. Such a black hole merger was indeed the basis of the historic discovery of GW by LIGO in 2015 [23] and afterward. While GW in general provides only small signals, the amount of power radiated in black hole mergers is humongous and exceeds the combined power of all light sources in the observable universe (for the first black hole merger, GW150914, the peak power was $3.6 \times 10^{49}$ Watt) [272]. The shape of the signal during the 'inspiral-merger-ringdown' process and until the two merging black holes (or two compact objects) settle into a black hole, carries invaluable information about the merger process and the resulting black hole [273–278].
- **Shadows.** The EHT has produced the first image of a black hole in 2019 [26,279]. The basic idea is that in order to observe an invisible object (the black hole) in front of the background universe, we need to shine some light on it. This light may come from the accretion disk or, other luminous matter behind the black hole in our line of sight yielding the black hole shadow. The behavior of null geodesics near black hole horizons produces a characteristic shadow, that is nicely captured by that image. The black hole in question, M87, is a supermassive black hole in a nearby galaxy.

One should, however, note that black hole shadows are observer dependent and then in principle depend on the angle between the direction toward the black hole and the line of sight of the observer. Moreover, they depend on the distance to the black holes and also on whether this distance is constant or vary in time. See Exercise 4.2 for more discussions.

- **Photon-sphere.** Not too far outside the horizon there are up to two photon-spheres, where light travels on circular orbits. The photon-spheres in principle are observable [280], and even though they have not been observed at the time of writing this book, one may expect their observation in the near future (see [281] and references therein).
- **Memory effects.** Yakov Zel'dovich and Alexander Polnarev discovered an IR (long distance, low energy) effect of GWs, now known as the memory effect [282], see also [283]. Namely, a GW passing through an array of detectors in general leaves behind a persistent change in the mutual distance between any pairs of detectors. This displacement memory effect could be measured in the near future (at the time of writing this book), e.g. by LIGO. In the past few years, several new types of memory effects were uncovered, as well as their relations to asymptotic symmetries and QFT soft theorems; for lecture notes on this IR triangle, see [284]. In particular, a memory effect produced at the black hole horizon by a transient gravitational shock-wave was discussed in [285].
- **Gravitational lensing.** In principle, it could be possible to detect black holes through microlensing. The black hole itself acts as a lens for light rays that pass nearby. So far microlensing has not been used successfully as a way to detect black holes, but it allows to place bounds on PBHs (see the next item) [286].
- **Primordial black holes.** All items above concern mostly black holes with masses above a couple of solar masses. However, as briefly reviewed in Chap. 1, black holes in principle may exist in any mass range, all the way down to the Planck mass. A particular class of black holes of potential phenomenological interest is PBHs, created shortly after the Big Bang (if they exist). PBHs may constitute a part of the observed dark matter. In addition to some of the detection methods above, a new possibility is to observe the Hawking radiation of PBHs, see, e.g. [287] for a discussion of detection methods and how to extract experimental bounds. The bounds on the allowed mass range of PBHs are tightening rapidly with more data becoming available; see, e.g. [75] for a recent update, which quote $10^{16}$–$10^{17}$g, $10^{20}$–$10^{24}$g, and 10–$10^2$ $M_\odot$. The last possibility is contentious but of special interest in view of the recent detection of black hole mergers by LIGO/Virgo.
- **Axion clouds.** Axions are among the prime dark matter candidates. They have not been detected yet, so this item is at the same level as the previous one. However, if they exist, they may provide an interesting link between the heaviest compact objects in our universe, black holes, and (presumably) the lightest ones, axions. Namely, in some models, axions are so light that their Compton wavelength is of the order of the Schwarzschild radius of stellar black holes. Whenever that happens, axion clouds can form around black holes, converting them into gigantic 'atoms' with characteristic GW patterns that would allow both the indirect

detection of axions and provide a novel way to detect single black holes (without companion and not being involved in a black hole merger); see [288].

Despite this impressive list of observational evidence or observation prospect for black holes, we state the caveat that all of them rely on the assumption that GR is the correct theory of gravity at the relevant distance scales (e.g. a few kilometers for stellar sized black holes). Typically, alternative explanations that avoid black holes are far more contrived than just assuming that GR and its predictions of black holes are correct.

## 4.2 Black Hole Photon-Sphere, Shadows, and Images

We have seen in Sect. 2.2.1 that Schwarzschild black holes have a photon-sphere at $r^\circ = 3r_h/2 = 3M$, which is the (unstable) orbit where lightlike particles travel on circles around the black hole. It lies at half the radial distance of the ISCO. As we saw in Sect. 2.5 for Kerr black holes, the situation is more intricate. The location of the ISCO depends on whether the orbit is co-rotating or counter-rotating with the black hole, and in addition to the horizon radius, it depends on the Kerr parameter $a$. Moreover, Kerr black holes have two photon-spheres, both lying in the equatorial plane, at radial distance

$$r^\circ_\pm = 2M\left[1 + \cos\left(\frac{2}{3}\,\arccos\frac{\pm|a|}{M}\right)\right]. \tag{4.1}$$

For slowly rotating black holes, both photon-spheres are close to the Schwarzschild photon-sphere, $r^\circ_\pm = 3M \pm 2a/\sqrt{3} + \mathcal{O}(a^2/M)$. For extremal Kerr black holes, the inner photon-sphere approaches the horizon, while the outer one is two Schwarzschild radii away from the center, $r^\circ_- = M$, $r^\circ_+ = 4M$.

There are three interesting aspects of the photon-sphere:

- By definition you can see the back of your own head if you were able to hover on the equatorial plane of the photon-sphere and look into a direction tangential to their intersection.
- There is an interesting centrifugal-force reversal for Schwarzschild black holes at the photon-sphere: outside the photon-sphere observers feel the usual outward centrifugal force, while inverse the centrifugal force pulls the observer inwards toward the black hole horizon; on the photon-sphere no centrifugal force is felt, regardless of the speed of the orbit.
- The black hole photon-sphere in principle leaves an imprint in images of black holes and their shadows, though at the time of writing this book the photon-sphere has not been observed yet; for further discussions see e.g. [281] and references therein.

## 4.3 Penrose Process, Super-Radiance, and Black Hole Mining

Classical black holes are known for having surfaces of no return and that things cannot escape from them to the outside. There is, however, a surprising physical effect for rotating black holes that allows, at least in principle, to 'mine' black holes as abundant sources of energy. This effect is called superradiance when referring to wave scattering and as Penrose process when referring to particle scattering.

To get quickly to the key point, let us focus first on particle scattering, i.e. the Penrose process. The key observation is that there exists an ergoregion outside the horizon where the Killing vector that asymptotically generates time translations, $k = \partial_t$, becomes spacelike. This implies that in the ergoregion there can be particle states of negative energy as measured by an asymptotic observer. So in principle, it is possible to throw some unstable object (with energy $E^i$ as measured by an asymptotic observer) into the ergoregion that splits into two subsystems, one of which has negative energy $E_1^f = -p^\mu k_\mu < 0$, where $p^\mu$ is the 4-momentum of the subsystem, while the other one has positive energy, $E_2^f > 0$. If the negative energy subsystem falls into the black hole, the positive energy subsystem is allowed to escape to infinity by conservation laws; more details are deferred to Exercise 4.3. Then, the outgoing energy $E_2^f = E^i - E_1^f > E^i$ is bigger than the ingoing one. The black hole has 'gained' negative energy and some of its energy (mass) has been carried away from the hole.

To address the superradiance, the wave-scattering version of the Penrose process, we need to deal with black hole perturbations. We are not going to do this in full generality, but restrict ourselves for the time being to scalar perturbations $\phi(x^\alpha)$ on Schwarzschild black hole background, in order to understand the techniques involved. These perturbations satisfy the Klein–Gordon equation

$$\partial_\mu\big(\sqrt{-g}\,g^{\mu\nu}\partial_\nu\big)\,\phi(x^\alpha) = 0 \tag{4.2}$$

which for the Schwarzschild metric (2.1), (2.2) allow a convenient decomposition in terms of spherical harmonics and plane waves

$$\phi(t,\,r,\,\theta,\,\varphi) = \sum_{l=0}^{\infty}\sum_{m=-l}^{l}\frac{\psi_l(r,\,\omega)}{r}\,Y_{lm}(\theta,\,\varphi)\,e^{-i\omega t}\,. \tag{4.3}$$

Using this decomposition together with the tortoise coordinate $r_* = r + r_h\,\ln\big(\frac{r}{r_h} - 1\big)$ reduces the Klein–Gordon equation (4.2) to the Regge–Wheeler equation

$$\Big(\frac{\mathrm{d}^2}{\mathrm{d}r_*^2} + \omega^2 - V_l(r)\Big)\,\psi_l(r_*,\,\omega) = 0 \tag{4.4}$$

with the effective potential

$$V_l(r) = \Big(1 - \frac{r_h}{r}\Big)\Big(\frac{l(l+1)}{r^2} + \frac{r_h}{r^3}\Big)\,, \qquad r_h = 2G_{\mathrm{N}}M \tag{4.5}$$

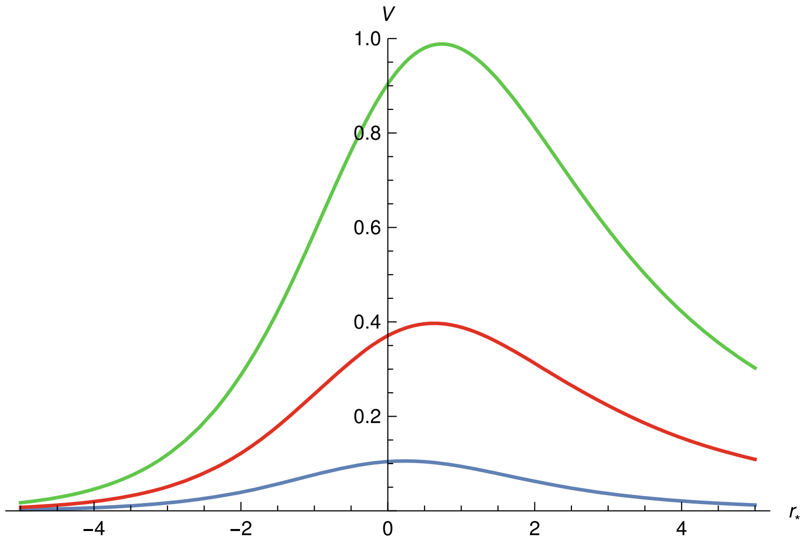


**Fig. 4.1** Effective potential (4.5) for $l = 0, 1, 2$ and unit Schwarzschild radius. The height of the maximum increases with $l$ since there is more centrifugal barrier

Thus, we have a standard (quantum-)mechanical problem of potential scattering on potentials depicted in Fig. 4.1.

On the horizon ($r_* \to -\infty$) we must impose infalling boundary conditions, while at infinity ingoing as well as outgoing (reflected) modes can exist.

$$\lim_{r_* \to -\infty} \hat{\psi}_l = e^{-i\omega r_*} \qquad \lim_{r_* \to \infty} \hat{\psi}_l = \big(A_R(\omega) e^{i\omega r_*} + e^{-i\omega r_*}\big) \frac{1}{A_T(\omega)} \tag{4.6}$$

The functions $A_R(\omega)$ and $A_T(\omega)$ are reflection and transmission amplitudes, respectively. A linearly independent set of modes is the complex conjugate of (4.4). Since the Wronskian of two linearly independent solutions of the Regge–Wheeler equation (4.4) is constant, evaluation at $r_* = \pm\infty$ yields a quadratic relation between transmission and reflection amplitudes (which should look familiar from quantum mechanics),

$$|A_R|^2 + |A_T|^2 = 1\,. \tag{4.7}$$

The squares of the amplitudes are reflection and transmission probabilities, and their sum adds up to one.

Now consider Kerr black holes, where instead of the Regge–Wheeler equations perturbations solve the Teukolsky equation [289]. We do not discuss this equation in detail in the main text but merely highlight the key technical aspect (see Appendix D for details of the Teukolsky equation). The ansatz for the modes (4.6) still works, except that in the near horizon limit there is a shift $\omega \to \omega - m\,\Omega$, where $m$ is the magnetic quantum number in the spherical harmonics decomposition and $\Omega = a/(r_+^2 + a^2)$ is the Kerr horizon velocity (also the tortoise coordinate derivative changes to $\mathrm{d}/\mathrm{d}r_* = \Delta/(r^2+a^2)\,\mathrm{d}/\mathrm{d}r$. The constancy of the Wronskian now leads to a condition slightly different from (4.7), namely

$$|A_R|^2 + \left(1 - \frac{m\Omega}{\omega}\right)|A_T|^2 = 1\,. \tag{4.8}$$

If the inequality

$$m\Omega > \omega \tag{4.9}$$

holds, plugging this inequality into relation (4.8),

$$|A_R|^2 - 1 = \left(\frac{m\Omega}{\omega} - 1\right)|A_T|^2 > 0 \tag{4.10}$$

shows that $|A_R| > 1$ in this case. Thus, the reflected amplitude is bigger than the incoming one! This is superradiant scattering and allows extracting energy from a Kerr black hole, similar to the Penrose process discussed at the beginning of this section.

Superradiance only occurs when (4.9) holds which means for modes with positive spin $m$. So modes that extract energy from the black hole, necessarily also take away angular momentum and slow down the Kerr black hole, see Exercise 4.4 for more analysis. Note also that the superradiance effect is similar to stimulated emission in atomic physics and in analogy one may expect a spontaneous emission effect. Such spontaneous superradiance can be shown to occur once quantum effects for the field perturbations are taken into account. So, the existence of an ergoregion yields a quantum mechanical instability.

Of course, when this process is repeated often, eventually backreactions need to be taken into account. Energy extraction slows down the black hole, so the energy extracted is basically rotational energy. Both from the particle picture and the wave picture it is clear that there is a natural endpoint of black hole mining: when the ergoregion ceases to exist or, equivalently, when $\Omega \to 0$, neither the Penrose process nor superradiance are possible anymore and this type of energy extraction ends. Given that for most astrophysical black holes the spin is a sizable fraction of the mass, not small $a/M$ ratio, black holes could provide an enormous amount of energy through mining processes a la Penrose or superradiant scattering.

## 4.4 Gravitational Waves and Black Hole Mergers

Consider the vacuum Einstein equations in $D$ spacetime dimensions and some solution thereof, $\bar{g}_{\mu\nu}$, referred to as 'background metric', such that $\bar{R}_{\mu\nu} = 0$. All barred quantities are constructed from this background metric. Perturbations around any such background are given by metrics $g_{\mu\nu} = \bar{g}_{\mu\nu} + h_{\mu\nu}$. Linearizing in the perturbation $h_{\mu\nu}$ means that classically they have to obey the linearized Einstein equations

$$\bar{\nabla}^\lambda\bar{\nabla}_\mu h_{\lambda\nu} + \bar{\nabla}^\lambda\bar{\nabla}_\nu h_{\lambda\mu} - \bar{\nabla}_\mu\bar{\nabla}_\nu h^\lambda{}_\lambda - \bar{\nabla}^2 h_{\mu\nu} + \bar{g}_{\mu\nu}\bar{\nabla}^2 h = 0 \tag{4.11}$$

where $h = \bar{g}^{\mu\nu} h_{\mu\nu}$. The linearized equations (4.11) can also be derived from expanding Einstein–Hilbert action for $g_{\mu\nu} = \bar{g}_{\mu\nu} + h_{\mu\nu}$ to second order in perturbation which leads to the quadratic action,

$$16\pi G_{\mathrm{N}}\, \delta^{(2)} I_{\mathrm{EH}} = \frac{1}{2} \int \mathrm{d}^D x \sqrt{-\bar{g}}\, h^{\mu\nu}\, \bar{\Box}_{\mu\nu}{}^{\lambda\rho} h_{\lambda\rho} \tag{4.12}$$

with the wave operator

$$\bar{\Box}_{\mu\nu}{}^{\lambda\rho} = \delta_\nu^\rho \bar{\nabla}^\lambda \bar{\nabla}_\mu + \delta_\mu^\rho \bar{\nabla}^\lambda \bar{\nabla}_\nu - \bar{g}^{\lambda\rho} \bar{\nabla}_\mu \bar{\nabla}_\nu - \delta_\mu^\rho \delta_\nu^\lambda \bar{\nabla}^2 + \bar{g}_{\mu\nu} \bar{g}^{\lambda\rho} \bar{\nabla}^2 \tag{4.13}$$

In many applications it is useful to decompose the perturbations into transverse-traceless tensor part $h^{\mathrm{TT}}_{\mu\nu}$, vector (or gauge) part $\xi_\nu$ and trace part $h$.

$$h_{\mu\nu} = h^{\mathrm{TT}}_{\mu\nu} + \bar{\nabla}_\mu \xi_\nu + \bar{\nabla}_\nu \xi_\mu + \frac{1}{D}\, \bar{g}_{\mu\nu}\, h \qquad \bar{\nabla}^\mu h^{\mathrm{TT}}_{\mu\nu} = 0 = \bar{g}^{\mu\nu} h^{\mathrm{TT}}_{\mu\nu} \tag{4.14}$$

Infinitesimal diffeomorphisms of the background metric induce gauge redundancies, i.e. $h_{\mu\nu}$ is defined up to gauge transformations $\mathcal{L}_\xi \bar{g}_{\mu\nu} = \bar{\nabla}_\mu \xi_\nu + \bar{\nabla}_\nu \xi_\mu$. A covariant family of gauge fixing conditions (with parameter $\alpha \in \mathbb{R}$) is given by

$$\bar{\nabla}_\mu h^\mu{}_\nu = \alpha \partial_\nu h^\mu{}_\mu \tag{4.15}$$

For $\alpha = \frac{1}{2}$, this is known as 'harmonic gauge' or 'de Donder gauge', which may also be represented in a more background independent way $\nabla^2 x^\mu = 0$ where $x^\mu$ are the coordinates, or $\partial_\nu(\sqrt{-\det g}\; g^{\mu\nu}) = 0$. In this gauge, it is particularly easy to count the number of graviton polarizations: the gauge choice (4.15) fixes $D$ of the $D(D+1)/2$ components of $h_{\mu\nu}$ and permits residual gauge transformations generated by vector fields obeying $\bar{\nabla}^2 \xi_\mu = 0$, thereby eliminating another $D$ components of $h_{\mu\nu}$. Thus, Einstein gravity in $D \geq 3$ spacetime dimensions has $D(D-3)/2$ independent graviton polarizations.

### > Gravitational waves in 4-dimensional Minkowski space

On a Minkowski background, the wave equation (4.11) in de Donder gauge simplifies to a tensorial version of Maxwell's equations in Lorenz gauge

$$\boxed{\partial^2 h_{\mu\nu} = 0} \tag{4.16}$$

which is solved, using the superposition principle, in terms of plane waves

$$h_{\mu\nu} = \epsilon_{\mu\nu}(k)\, e^{i k_\mu x^\mu} \tag{4.17}$$

with null momentum, $k^2 = 0$, and a polarization tensor $\epsilon_{\mu\nu} = \epsilon_{\nu\mu}$ compatible with de Donder gauge, $k_\mu \epsilon^\mu{}_\nu = \frac{1}{2}\, k_\nu \epsilon^\mu{}_\mu$. The four residual gauge transformations,

$\partial^2\xi_\mu = 0$, can be used to set to zero the mixed components, $\epsilon_{0i} = 0$, as well as the trace, $\epsilon^\mu{}_\mu = 0$, of the polarization tensor. For a GW traveling in $z$-direction, $k^\mu = \omega\,(1,\ 0,\ 0,\ 1)$, these gauge fixing conditions imply

$$\epsilon_{\mu\nu} = \begin{pmatrix} 0 & 0 & 0 & 0 \\ 0 & \epsilon_+ & \epsilon_\times & 0 \\ 0 & \epsilon_\times & -\epsilon_+ & 0 \\ 0 & 0 & 0 & 0 \end{pmatrix} =: \epsilon_+\epsilon^+_{\mu\nu} + \epsilon_\times\epsilon^\times_{\mu\nu}\,. \tag{4.18}$$

The two helicity states $\epsilon^+_{\mu\nu}$ and $\epsilon^\times_{\mu\nu}$ are often referred to as 'plus-polarization' and 'cross-polarization', respectively.

---

With a single test particle, it is impossible to detect GW, so let us assume there are two massive test-particles, one at the origin and the second at some finite distance $L_0$ along the $x$-axis. For concreteness, consider a plus-polarized planar GW along the $z$-direction, $h_{\mu\nu} = \epsilon^+_{\mu\nu}\, f(t-z)$ with $f(t-z) \ll 1$, so that the perturbed metric reads

$$\mathrm{d}s^2 = -\,\mathrm{d}t^2 + \big(1 + f(t-z)\big)\,\mathrm{d}x^2 + \big(1 - f(t-z)\big)\,\mathrm{d}y^2 + \mathrm{d}z^2\,. \tag{4.19}$$

If both test particles where at rest originally, $u^\mu_{1,2} = (1,\ 0,\ 0,\ 0)$, the geodesic equation to linearized order reads $\mathrm{d}u^\mu/\,\mathrm{d}\tau = -\delta\Gamma^\mu{}_{00}$. Since $\delta\Gamma^\mu{}_{00}$ vanishes, the particles remain at rest and the coordinate distance between them does not change. However, their proper distance

$$L(t) = \int_0^{L_0} \mathrm{d}x\,\sqrt{1+f(t)} \qquad \Rightarrow \qquad \frac{\Delta L_0}{L_0} = \frac{L(t)-L_0}{L_0} \approx \frac{1}{2}\,f(t) \tag{4.20}$$

changes in a time-dependent way. For periodic functions $f$, the proper distance oscillates periodically around its mean value $L_0$, which is a measurable effect.

Like light waves, GW needs a source. In the former case, typical sources are accelerated charges, producing dipole (and higher multipole) radiation. In the latter case, typical sources are accelerated masses, producing quadrupole (and higher multipole) radiation. To take into account sources, it is useful to define the trace-reversed fluctuations $\tilde{h}_{\mu\nu} := h_{\mu\nu} - \frac{1}{2}\,\eta_{\mu\nu}\,h^\lambda{}_\lambda$ in terms of which de Donder gauge reads $\partial_\mu\tilde{h}^\mu{}_\nu = 0$ and the linearized Einstein equations on the flat background simplify to

$$\partial^2\tilde{h}_{\mu\nu} = -16\pi G_{\mathrm{N}}\,T_{\mu\nu}\,. \tag{4.21}$$

In terms of the retarded Green function the general solution to the inhomogeneous wave equation (4.21) yields

$$\tilde{h}_{\mu\nu}(t,\mathbf{x}) = 4G_{\mathrm{N}}\int \mathrm{d}^3x'\,\frac{T_{\mu\nu}(t-|\mathbf{x}-\mathbf{x}'|,\,\mathbf{x}')}{|\mathbf{x}-\mathbf{x}'|} \tag{4.22}$$

Taylor-expanding around the origin, $\mathbf{x}' = 0$, the first term reads $\tilde{h}^{\mu\nu}(t, \mathbf{x}) = \frac{4G_{\rm N}}{r} \int T^{\mu\nu} + \cdots$ where the quantities

$$M := \int T^{00} = \int \mathrm{d}^3x'\, T^{00}(t - |\mathbf{x} - \mathbf{x}'|, \mathbf{x}') \tag{4.23}$$

$$P^i := \int T^{0i} = \int \mathrm{d}^3x'\, T^{0i}(t - |\mathbf{x} - \mathbf{x}'|, \mathbf{x}') \tag{4.24}$$

are mass and 3-momentum of the source. Using twice partial integration identities like $\int \mathrm{d}^3x'\, T^{\mu i} = -\int \mathrm{d}^3x' x'^i \partial_j T^{\mu j}$ and the conservation equation $\partial_\mu T^{\mu\nu} = 0$, establishes the emission formula

$$\tilde{h}^{ij}(t, \mathbf{x}) = \frac{2G_{\rm N}}{r} \frac{\mathrm{d}^2 Q^{ij}(t)}{\mathrm{d}t^2}\Big|_{t \to t - |\mathbf{x} - \mathbf{x}'|} \tag{4.25}$$

in terms of the (second time-derivative of the) quadrupole moment of the source, $Q^{ij}(t) := \int \mathrm{d}^3x'\, x'^i x'^j\, T^{00}(t, \mathbf{x}')$. Introducing the tracefree quadrupole moment,

$$q_{ij} := Q_{ij} - \tfrac{1}{3}\,\delta_{ij}\delta^{kl} Q_{kl} = \int \mathrm{d}^3x' \left( x'^i x'^j - \frac{1}{3}\delta_{ij}(x')^2 \right) T^{00}(t, \mathbf{x}') \tag{4.26}$$

allows to write the average power radiated away by GW (also called 'gravitational luminosity') succinctly as

$$\boxed{P^{\rm GW} = \frac{G_{\rm N}}{5} \langle \dddot{q}_{ij} \dddot{q}^{ij} \rangle\,.} \tag{4.27}$$

A conceptual key point in deriving (4.27) is to define the gravitational stress tensor. While in general one cannot covariantly define gravitational energy–momentum tensor (see, e.g. [290,291] and references therein), in our case, where we are dealing with the linearized theory, it is straightforward to do so. One may simply treat (4.12) as an action for perturbations $h_{\mu\nu}$ and compute the corresponding energy–momentum tensor in the standard canonical way. Doing so, the flux component of it is obtained as $T^{GW}_{tz} = \frac{1}{16\pi G_{\rm N}} \langle \dot{\epsilon}_+^2 + \dot{\epsilon}_\times^2 \rangle$ from its plus- and cross-polarization amplitudes, cf. (4.18). Here the average is over several wavelengths. The electromagnetic analog of (4.27) is the formula for the average power emitted by an oscillating dipole, $P^{\rm EM} \sim \langle \ddot{p}_i \ddot{p}^i \rangle$, with dipole moment $p_i$. Since there is no dipole GW, up to a numerical factor, the formula (4.27) thus can be guessed purely on dimensional grounds and by analogy to electromagnetism. To make this analogy more manifest, sometimes gravitoelectromagnetism is invoked, where the Weyl tensor is decomposed into electric and magnetic parts, $E_{\mu\nu} = C_{\mu\lambda\nu\rho} u^\lambda u^\rho$, $B_{\mu\nu} = \frac{1}{2}\,\epsilon_{\mu\lambda}{}^{\sigma\tau} C_{\nu\rho\sigma\tau} u^\lambda u^\rho$, with respect to some observer with 4-velocity $u^\mu$; see for instance [133,292] and references therein.

Binary systems (e.g. consisting of black holes or neutron stars) emit GW over an extended time period. The gravitational luminosity formula (4.27) permits us to estimate the power radiated by such systems. For instance, a system with characteristic mass $M$ and period $T$ has a power given by $P \sim (M/T)^{10/3}$ and therefore a period decrease given by $\mathrm{d}T/\mathrm{d}t \sim -(M/T)^{5/3}$; see Exercise 4.11 for more analysis. Long before the direct detection of GW, the period decrease of the Hulse–Taylor pulsar provided striking indirect evidence for their existence [293].

While precise templates for GW-forms are an ongoing research field, e.g. see [273,278] and its citations, it is easy to provide an upper bound on the GW emission from a black hole merger, using energy conservation and the second law of black hole mechanics, cf. discussions in Sect. 5.5. For two Schwarzschild black holes of equal mass, this upper bound is about 29% of the total mass of original black holes. Even if the actual gravitational radiation is only a small fraction of that number, the energy radiated away in form of GW can easily be of the order of solar masses! Thus, there can be a substantial amount of power in such mergers, larger than typical local events in our universe. Indeed, it was a merger of two black holes that led to the first detection of GW [294].

While the most straightforward explanation of the first GW event is that we have witnessed the merger of two Kerr black holes, it is conceivable that something different from Kerr black holes could mimic that event. Future GW measurements may allow constraining the tidal Love numbers[1] of the sources and thus allow discriminating between Kerr black holes and their speculative alternatives.

## 4.5 Accretion Disk Physics

Accretion disks around black holes are one of the key players in black hole detection through X-ray spectra [264,299]. The physics involved is quite intricate and involves viscous magnetohydrodynamics, which can be studied numerically, e.g. see [300] and references therein. To get the first glimpse into accretion disk physics, we consider an unrealistic toy model, namely a perfect fluid [264,265,301]. Since perfect fluids in GR are useful also in several other contexts, such as cosmology or holography, we provide some details, despite the inapplicability to accretion disk phenomenology.

To the lowest order in a derivative expansion, the fluid data available are the velocity $u^\mu$, normalized without loss of generality to $u^\mu u_\mu = -1$, the energy density $\rho$ and the pressure $p$. The perfect fluid stress tensor

$$T_{\mu\nu}^{\text{perf}} = \rho u_\mu u_\nu + P\,\Pi_{\mu\nu} \qquad \Pi_{\mu\nu} := u_\mu u_\nu + g_{\mu\nu} \tag{4.28}$$

[1] Tidal Love numbers measure the tidal deformability of a self-gravitating object [295] and are zero for usual black holes, as crystallized in no-hair theorems. We will not go into details, but just mention here that there are two types of Love numbers, parity even ('electric') and parity-odd ('magnetic'). For Schwarzschild black holes, all Love numbers vanish, so these black holes cannot be tidally deformed. Rotating black holes have non-vanishing Love numbers in general, but they are still pretty stiff, i.e. cannot easily be deformed; see, e.g. [296]. For more discussions on Love numbers, e.g. see [297,298] and references therein.

for consistency must obey $\nabla_\mu T^{\mu\nu} = 0$. Contracting this conservation equation with the velocity $u_\nu$ yields the general relativistic analog of the continuity equation, while contraction with the projection operator $\Pi_{\nu\lambda}$ yields the analog of the Euler equations

$$\text{Continuity:} \qquad \nabla_\mu \big(u^\mu \rho\big) + p\nabla_\mu u^\mu = 0, \tag{4.29}$$

$$\text{Euler:} \qquad \big(\rho + p\big)\, u^\mu \nabla_\mu u^\nu + \Pi^{\nu\mu} \nabla_\mu p = 0 \tag{4.30}$$

The label 'projection operator' is due to the properties $u^\mu \Pi_{\mu\nu} = 0$ and $\Pi^\mu_\nu \Pi^\nu_\lambda = \Pi^\mu_\lambda$. The equations above are not uniquely solvable, as in $D$ dimensions for a given metric there are $D+2$ variables $\rho,\, p;\, u^\mu$ but $D+1$ equations $\nabla_\mu T^{\mu\nu} = 0$, $u^\mu u_\mu = -1$. One extra equation is usually supplemented by an equation of state relating energy density $\rho$ and pressure $p$, for instance, some barotropic equation of state expression pressure as some given function of energy density, $p = p(\rho)$. The simplest ones describe dust, $p = 0$, radiation, $p = \rho/3$, and the vacuum (cosmological constant), $p = -\rho$ and stiff matter $p = \rho$.

The perfect fluid is not a realistic model of an accretion disk, as one cannot omit the effects of viscosity. For the latter, one needs to go higher order in the derivative expansion of the stress–energy tensor, and effects from magnetic fields. The latter is usually taken into account using magnetohydrodynamics, often neglecting general relativistic corrections, see [302] for a review. The additional data available are field strength $F_{\mu\nu}$, current $j_\mu$, shear viscosity $\eta$ and bulk viscosity $\zeta$. The equations to be solved are the covariant conservation equation and the Maxwell equations,

$$\nabla_\mu T^{\mu\nu} = 0 \qquad \epsilon^{\mu\nu\lambda\tau}\partial_\nu F_{\lambda\tau} = 0 \qquad \nabla_\mu F^{\mu\nu} = 4\pi j^\nu \tag{4.31}$$

with the derivative expansions

$$T_{\mu\nu} = T^{\text{perf}}_{\mu\nu} + T^{\text{Max}}_{\mu\nu} - 2\eta\left(\Pi^\lambda_\mu \Pi^\tau_\nu \nabla_{(\lambda} u_{\tau)} - \tfrac{1}{3}\,\Pi_{\mu\nu}\nabla_\lambda u^\lambda\right) + \zeta\, g_{\mu\nu}\nabla_\lambda u^\lambda + \cdots \tag{4.32}$$

$$j_\mu = \rho_0 u_\mu + \sigma F_{\mu\nu} u^\nu + \cdots \tag{4.33}$$

where $T^{\text{Max}}_{\mu\nu} = \frac{1}{8\pi G_{\text{N}}}\big(F_{\mu\lambda}F^\lambda{}_\nu - \frac{1}{4}\, g_{\mu\nu} F_{\lambda\rho}F^{\lambda\rho}\big)$ is the stress tensor of the Maxwell field, $\rho_0$ the rest-frame charge density and $\sigma$ the conductivity coefficient.

## Blandford–Znajek mechanism

We end this section by discussing another Kerr black hole mining process, the Blandford–Znajek effect [303]. This effect is the basic engine for relativistic jets from active galaxies and gamma or X-ray bursts. Consider a Kerr black hole which is threaded by magnetic field lines supported by external currents flowing in an equatorial disk. Such magnetic fields are ubiquitously produced when the black hole accretes ordinary matter. If the magnetic field strength is large enough, it yields an efficient electron–positron pair production which can then form a force-free plasma of accelerated charges. Energy and angular momentum is then transferred outward through electromagnetic radiation. In this way, the gravitational energy of the infalling matter into the black hole as well as the energy and spin from the black hole itself can be extracted electromagnetically. One may show that in real physical situations, accreted charges do not significantly contribute to the geometry of a rotating hole. See [303,304] and also Exercise 4.13 for more detailed analysis.

## 4.6 Black Hole Formation in Shock-Wave Collisions

In principle, it is possible to generate black holes from the collision of localized packages of energy fluxes (traveling at or close to, the speed of light). While no black holes are known to be generated in this fashion, such formation processes still have applications, e.g. within the context of the AdS/CFT correspondence where this process is dual to the formation of a finite temperature non-Abelian plasma. In this section, we develop the basics of black hole formation through shock-waves.

As warm-up, let us consider electrodynamics with a $\delta$-source $j^+ = \delta(x^-)\,\rho^{(+)}(x^i)$, where we use lightcone coordinates for the 2-dimensional plane through which the electromagnetic shock-wave travels, $\eta_{+-} = 1, \eta_{\pm\pm} = 0, \eta_{ij} = \delta_{ij}$, where $x^i$ denote the transverse coordinates. The Maxwell connection $A = \theta(x^-)\,\partial_i \lambda^{(+)}(x^j)\,\mathrm{d}x^i$ solves Maxwell's equations with this source, provided $\partial_i \partial_i \lambda^{(+)} = -\rho^{(+)}$. The only non-vanishing field strength components are $F_{-i} = \delta(x^-)\,\partial_i \lambda^{(+)}$. Apart from a delta-localization at $x^- = 0$ the field strength vanishes, as it should since the connection is a locally pure gauge for positive and negative values of $x^-$. We can superimpose a second solution where we replace above everywhere $+$ with $-$. This configuration describes the collision of two electromagnetic shock-waves localized at $x^- = 0$ and $x^+ = 0$. No particles are produced in this collision as a consequence of the linearity of Maxwell's theory.

Consider as the next step Yang–Mills theory with the same kind of source. We can still use the same technique and logic as for Maxwell's theory, except on and within the forward lightcone. Thus, as long as either $x^+$ or $x^-$ is negative the solution of the Yang–Mills equations sourced by $j^\pm = \delta(x^\mp)\,\rho^{(\pm)}(x^i)$ are given by Yang–Mills gauge connections $A = (\theta(x^-)\theta(-x^+)\,\alpha_i^{(+)} + \theta(-x^-)\theta(x^+)\,\alpha_i^{(-)})\,\mathrm{d}x^i$, where the $\alpha_i^{(\pm)}$ are pure gauge and obey $\partial_i \alpha_i^{(\pm)} = \rho^{(\pm)}$. (In the Abelian case we had $\alpha_i^{(\pm)} = \partial_i \lambda^{(\pm)}$.) The key difference to Maxwell's theory is that Yang–Mills theory is non-linear and therefore the superposition principle cannot be applied. In particular, in the forward lightcone, the connection is no longer a pure gauge but satisfies the vacuum Yang–Mills equations. This means that we have particle production in the collision of two non-Abelian shock-waves, see Sect. 3 of [305].

**Aichelburg–Sexl black hole.** Einstein gravity is also a non-linear theory and as in non-Abelian Yang–Mills theory, one may expect particle production in the forward lightcone of two colliding gravitational shock-waves. This is indeed what happens. The first step is to analyze a single shock-wave. This was done in seminal work by Aichelburg and Sexl [306], who considered an ultrarelativistic boost of the

Schwarzschild metric in the limit of vanishing mass, keeping fixed the energy. Their result

$$ds^2 = -2\,dx^+\,dx^- + \delta_{ij}\;dx^i\,dx^j + H(x^i)\,\delta(x^-)\;dx^{-\,2} \tag{4.34}$$

describes a single gravitational shock-wave traveling along retarded time $x^- = 0$ with some profile $H$ that depends only on the transverse coordinates $x^i$. For Schwarzschild $H \propto \ln\rho$, where $\rho = \sqrt{x^i x^j\,\delta_{ij}}$, while for Schwarzschild–Tangherlini in $D > 4$ dimensions $H \propto \rho^{4-D}$. In all cases, the profile function solves Poisson's equation $\nabla^2 H \propto \delta^{(D-2)}(x^i)$ in the transverse dimensions.

Describing the collision of two gravitational shock-waves is possible in the coordinates (4.34), but not necessarily convenient. The technical reason is that the metric (4.34) contains delta-distributions, which leads to jumps in geodesics and their tangents. This can be remedied by introducing Rosen coordinates

$$\bar{x}^- = x^-,\;\; \bar{x}^+ = x^+ + H\,\theta(x^-) + x^-\theta(x^-)(\nabla H)^2/4,\;\; \bar{x}^i = x^i + x^-/2\,\nabla_i H\,\theta(x^-)$$

in terms of which geodesics and tangents are continuous across the shock at $x^- = 0$. In these new coordinates, the metric that describes the collision of gravitational shock-waves, is continuous and piecewise differentiable, see Exercise 4.14 for more analysis. The Rosen coordinates allow one to *superpose* two shock-waves moving along $z$ direction toward each other at an impact parameter $b$. One can then analyze the collision of such shock-waves each with total energy $\mu$. Such a collision can yield an apparent horizon and a marginally trapped surface for sufficiently small $b$. The maximum $b$ which leads to a trapped surface is $b_{\text{max}} \approx 3.219 G_{\text{N}}\mu$ and the total cross-section for black hole production is bigger than $\pi b^2_{\text{max}} \approx 32.55(G_{\text{N}}\mu)^2$; see [307] for detailed analysis.

## 4.7 Black Hole Perturbations and Linear Stability

In QFT slang, stationary black holes are solitons. Solitons can be excited harmonically and the small excitations may be treated in linear order and perturbatively. It is fair to ask if the same can happen for black holes and how black holes react once such excitations/perturbations are turned on and whether they remain stable. Black holes interact gravitationally with surrounding matter and quantum fields, such as accretion disks, companion stars, axion clouds, etc. and these interactions can be viewed as excitation on black holes. In many situations, a perturbative description is adequate, where we can assume a split into a black hole background and perturbations around it, similar to our discussion of GW in Sect. 4.4.

Such a perturbative treatment has numerous applications in a black hole context, including radiation generated by objects falling into a black hole, late-time behavior of the gravitational field after black hole formation, scattering and absorption of fields/particles on black holes, perturbative GW generation and checking perturbative stability of black holes. Here, we focus on three somewhat related topics: QNMs, black hole stability, and GW emission from black hole binaries.

### 4.7.1 Quasi-normal Modes

QNMs are a generalization of normal modes to cases where the modes can decay. Typically, this arises because the system is open. Thus, as opposed to usual harmonic oscillations there is exponential decay, which is accommodated by allowing the frequencies to have an imaginary part. For black holes, QNMs arise since at the black hole horizon all perturbations are purely ingoing. The QNMs are imprinted in GW emission or other fields probing (or scattered off) the black hole and are characteristic of a black hole of given mass and angular momentum. Describing perturbed (or 'ringing') black holes through QNMs is a good approximation as long as the perturbation is sufficiently small. In practice, QNMs provide an adequate description of the ringdown phase after a black hole merger. Historically, QNMs were a milestone in numerical relativity, see, e.g. [308, 309] for reviews.

For simplicity, we focus on scalar QNMs of Schwarzschild black holes, see [310] for the original work on the topic. Since scalar perturbations of the latter are described by the Regge–Wheeler equation (4.4), we exploit the latter to introduce QNMs. The potential $V_l(r)$ (4.5) tends to zero at both of its ends (see Fig. 4.1) and it has no normalizable bound states; hence, there are no normal modes associated with scalar perturbations of Schwarzschild black holes. A QNM is defined to be a perturbation which is *purely infalling at the horizon and purely outgoing at infinity.* For the scalar perturbations which are solution to the Regge–Wheeler equation, these are modes with complex frequency $\omega_{\text{QNM}}$ obeying the boundary conditions

$$\lim_{r_*\to-\infty} \psi(r_*,\, \omega_{\text{QNM}}) \sim e^{-i\omega_{\text{QNM}} r_*} \qquad \lim_{r_*\to\infty} \psi(r_*,\, \omega_{\text{QNM}}) \sim e^{i\omega_{\text{QNM}} r_*}\,. \tag{4.35}$$

The first one just means that the mode is purely infalling on the horizon, cf. (4.6), while the second one means that the mode is purely outgoing at infinity. Moreover, in order for the QNMs to be well-defined in both limits (4.35), the frequency should have a negative imaginary part,

$$\omega_{\text{QNM}} = \omega_R - i\,\omega_I \qquad \omega_I > 0\,. \tag{4.36}$$

The QNM frequencies depend only on the mass $M$ of the Schwarzschild black hole and can be calculated numerically. The lowest-lying QNM (for $l = 2$) is given by

$$M\,\omega_{\text{QNM}}(2, 0) \approx 0.37367 - i\,0.08896\,. \tag{4.37}$$

For a three solar mass Schwarzschild black hole, these numbers translate into a real part corresponding to a frequency of about 4 kHz and a decay time of about 1.8 milliseconds. This means the relevant time scale for QNM decay in stellar mass black holes is milliseconds, and the relevant frequency range kHz. In the limit of large imaginary part, there is an efficient method complexifying the radial coordinate and calculating monodromies to determine an exact expression for the QNMs [311], yielding

$$\lim_{n\to\infty} M\,\omega_{\text{QNM}} = \frac{\ln 3}{8\pi} - \frac{i}{4}\left(n + \frac{1}{2}\right) + \mathcal{O}(1/\sqrt{n})\,. \tag{4.38}$$

This result, while interesting, is of little use for phenomenology, which cares mostly about a few lowest-lying QNMs, since the other ones are damped away too quickly.

Generalizations of QNMs to Kerr and other black holes are conceptually straightforward, see [312] for original analytical work on the topic. By analogy to (4.37), (4.38) the QNM spectrum depends only on the black hole parameters and on some pure numbers that are calculable either numerically or, in certain limits, analytically. In an astrophysical context, QNMs are characteristic features of a black hole with a given mass and angular momentum.

### 4.7.2 Late-Time Tails and Linearized Stability

Linearized stability of black holes would mean that sufficiently small, but otherwise generic, perturbations of black holes decay sufficiently fast as a function of time, and in particular do not make the black hole disappear. Technically, linearized stability means boundedness of the perturbations. There are some heuristics gained from the fact that the imaginary part of all QNMs is negative, so that they all decay exponentially rather than growing in time, see the discussion above. However, QNMs alone are misleading, since they suggest exponential fall-off at late times, which is incorrect. Instead, late-time tails decay only monomially in time [313]. For Schwarzschild, the result is (see Exercise 4.17)

$$\lim_{t\to\infty} \psi \sim t^{-2l-3} \tag{4.39}$$

where $l$ is again the angular momentum number in (4.4). This can be derived from an analysis of the Green function

$$\Big(\frac{\mathrm{d}^2}{\mathrm{d}r_*^2} + \omega^2 - V_l(r)\Big)\, G(r_*,\, r,\omega) = \delta(r_* - r) \tag{4.40}$$

subject to suitable boundary conditions, see Exercise 4.17. The time-evolution of $\psi$ for $t > 0$ with some initial data is given by

$$\psi(r_*,\, t) = \int \mathrm{d}r\, G(r_*,\, r,\, t)\, \partial_t \psi(r,\, 0) + \int \mathrm{d}r\, \partial_t G(r_*,\, r,\, t)\, \psi(r,\, 0)\,. \tag{4.41}$$

Thus, knowing the late-time tail of the Green function (4.40) is sufficient to determine the late-time tail of the perturbation $\psi$. A general proof of the boundedness of the wave equation on Schwarzschild backgrounds was given by Kay and Wald [314]. For a more general discussion that includes also linearized stability of Kerr black holes; see [315].

### 4.7.3 Perturbative Aspects of Black Hole Binaries

Finally, consider GW emission from black hole binary systems. There are two phases where perturbative methods can be useful: the initial, inspiraling phase and the final, ringdown phase after the two black holes have merged.

In the latter, one can model the system as a single perturbed black hole and exploit the lowest-lying QNMs to determine GW emission, see, e.g. [276] and references therein. Since the QNM spectrum depends only on the mass and spin of the final black hole (see Sect. 4.7.1 above), observational data from GW emission in the ringdown phase can be used to put bounds on mass and spin of the final black hole state after a merger.

In the inspiralling phase, as long as the black holes are sufficiently far away from each other, one can essentially consider one black hole as a perturbation of the other. To be more specific, one can use multipole expansions, post-Newtonian expansions (in inverse powers of the vacuum speed of light), post-Minkowskian expansions (in inverse powers of Newton's constant), far-zone expansions (in inverse powers of the distance from the center of mass) and in practice combinations thereof are used, see the extensive review [316] and references therein. As an example, we quote a result for energy loss due to GW emission to second post-Newtonian order for a nearly circular orbit [317].

$$
\begin{aligned}
-\frac{\mathrm{d}E}{\mathrm{d}t} = \frac{32\eta^2}{5}\frac{m^5}{r^5}\Bigg[1 - \frac{m}{r}\left(\tfrac{5}{4}\,\eta + \tfrac{2927}{336}\right) \\
+\frac{m^{3/2}}{r^{3/2}}\left(4\pi - \tfrac{1}{12}\sum_{i=1,2}\hat{L}\cdot\chi_i\left(75\eta + 73\frac{m_i^2}{m^2}\right)\right) \\
+\frac{m^2}{r^2}\left(\tfrac{380}{9}\,\eta + \tfrac{293383}{9072} - \tfrac{1}{48}\,\eta\left(223\,\chi_1\cdot\chi_2 - 649\,(\hat{L}\cdot\chi_1)(\hat{L}\cdot\chi_2)\right)\right)\Bigg]
\end{aligned}
\tag{4.42}
$$

Here $m = m_1 + m_2$ is the total mass, $\eta = m_1 m_2/m^2$ is the reduced mass in units of the total mass, $r$ is the orbital separation, $\chi_{1,2}$ are the black hole spins in units of the individual masses $m_{1,2}$, $\hat{L}$ is a unit vector pointing in the direction of the orbital angular momentum, and the dot denotes the Euclidean inner product between the various 3-vectors. The lowest order term is just the Newtonian quadrupole and the $m/r$ term its first post-Newtonian correction. The $m^{3/2}/r^{3/2}$ terms contain a contribution from tails (the $4\pi$-term) and from spin-orbit coupling (the remainder). The second line contains second post-Newtonian corrections as well as spin-spin corrections.

In order to provide accurate templates for experiments, it is necessary to go beyond the second post-Newtonian approximation. At third order, regularization is necessary to cure the infinite self-field of point particles, which can lead to ambiguities, see [318] for a discussion and resolution. An alternative to deal with the UV divergences is the application of EFT methods [319].

## 4.8 Gravitational Collapse and Non-linear Stability

The perturbative analysis in the previous section led to a wealth of applications and physical effects. However, some phenomena cannot be seen using perturbation theory, including the very existence of a black hole, which is not just a small perturbation of a trivial vacuum solution, but rather like a solitonic solution in QFT. Especially the classic black hole creation through gravitational collapse, which involves non-perturbative and non-linear physics, has a strong physical motivation—after all, this is how stellar-mass black holes are generated—and exhibits interesting phenomena, both from a physical and a mathematical perspective [52, 320]. We discuss now one of these phenomena, the critical collapse [110].

### 4.8.1 Critical Collapse and Choptuik Exponent

Consider some generic 1-parameter family of initial data, with normalized family parameter $p \in [0,\ 1]$, such that near $p = 0$ a black hole never forms and near $p = 1$ a black hole always forms. By continuity there must be some critical value of the family parameter, $p = p_*$, where a black hole barely forms, separating the initial data family into members where no black hole forms, $0 \leq p < p_*$ and members where always a black hole forms, $1 \geq p > p_*$. Near the critical point, Choptuik discovered through his numerical studies a critical phenomenon reminiscent of phase transitions in statistical mechanics: Just above the threshold of black hole formation the mass of the final black hole obeys

$$M = M_0\,(p - p_*)^\gamma \qquad\qquad 0 < p - p_* \ll 1 \tag{4.43}$$

where $M_0$ is some non-universal mass scale and $\gamma$ is a universal critical exponent—a pure number that does not depend on which 1-parameter family of initial data is chosen. This critical exponent is, therefore, a property of the particular theory but does not depend on details of initial data.

For the spherically symmetric collapse of a massless scalar field in 4-dimensional Einstein gravity, the final state above $p_*$ is a Schwarzschild black hole and the Choptuik critical exponent is approximately $\gamma \approx 0.37$. See Exercise 4.18 for some aspects of this dynamical system. In this particular example, Choptuik observed another phenomenon besides the critical scaling exponent, namely discrete self-similarity of the critical solution with an echoing period $\Delta \sim 3.44$ [110]. For a continuous version of self-similarity; see Exercise 4.19.[2]

If the initial data are infinitely fine-tuned to $p = p_*$, the final state is not a black hole but rather a naked singularity, which disproved an earlier version of cosmic censorship, see e.g. [322]. This critical solution is an attractor of codimension-1 in

[2] The features of universality, critical tuning of parameters, power-law scaling of observables, critical exponents, and self-similarity also appear in the theory of critical phenomena and phase transitions, see [321].

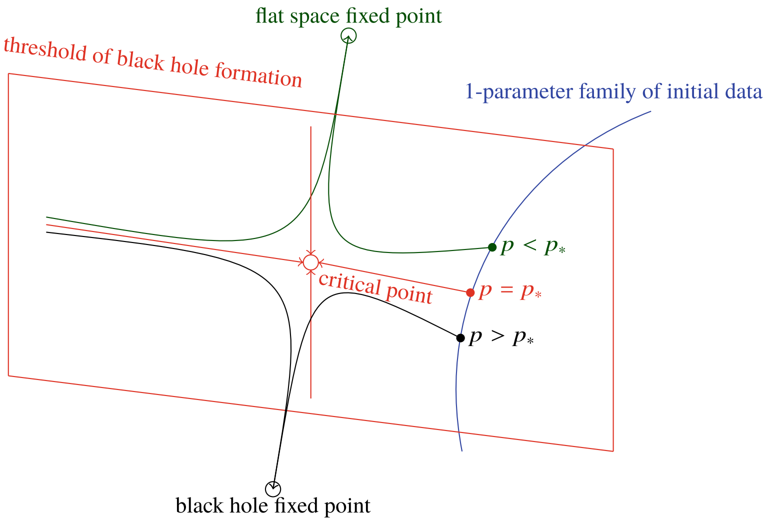


**Fig. 4.2** Critical solution as codimension-1 attractor. Trajectories with $p < p_*$ end up in the flat space basin (green), whereas trajectories with $p > p_*$ end up in the black hole basin (black). The smaller $|p - p_*|$ the longer the trajectory approaches the critical solution $p = p_*$ (red)

the space of initial data. This means that for any set of initial data the evolution will be such that initially, one flows toward the critical solution, but eventually, a single unstable mode kicks in and the final solution moves away from the critical point, either toward a final state describing the dispersion of waves on a non-black hole background (for any $p < p_*$ in any family of initial data) or toward a final state describing a black hole (for any $p > p_*$ in any family of initial data). See Fig. 4.2 for an illustration.

There are numerous generalizations of Choptuik's original study to less symmetric configurations, higher and lower dimensions, different asymptotic behavior, etc. See [323] for a review.

### 4.8.2 On Non-linear Stability of Black Hole Solutions

We already discussed in the previous section that simple black hole solutions like Schwarzschild or Kerr are stable against linear perturbations. Given the highly non-linear nature of Einstein's equations, extending this result to a generic non-linear local perturbation is quite a non-trivial statement. Non-linear stability addresses the question of what happens to perturbations of initial data for arbitrary times, taking into account the full non-linearity of Einstein's equations.

Even for arguably the simplest of all spacetimes, Minkowski, it is quite non-trivial to prove its non-linear stability [55]. Therefore, it is perhaps not surprising that the non-linear stability of the simplest of all black hole spacetimes, Schwarzschild, was only proven more than a century after Schwarzschild found his solution [56]. The proof of non-linear stability of generic Kerr black holes is still missing, though recent work was able to prove it in the case of slow rotation [324]. Rather than providing details of these proofs, we highlight here only their key aspects. Assuming generic vacuum initial data sets that are sufficiently close to, say, the Schwarzschild black hole the main theorem of [56] states that the maximal Cauchy development of these initial data has the following three properties: 1. it evolves into a spacetime with $\mathfrak{I}^+$ that has a black hole event horizon, 2. it remains globally close to the Schwarzschild black hole in the exterior region and 3. it asymptotes back to a Schwarzschild black hole at late times. These three properties together define what is meant by 'non-linear stability'. One of the challenges to a general proof is to avoid assuming any symmetry on the initial data (for more symmetric initial data several simpler proofs of non-linear stability had been found already in the past millennium; e.g. see [325] as a historically important first papers on the topic).

## Further Reading

In this chapter, we touched upon possible observational signatures of black holes but did not elaborate on them. This is a fast-evolving and active research area. For further reading, besides the references given in the main text, we refer the readers to either original papers or recent review articles. For example, one may look at the 'Black hole roadmap' [140] and references therein; for gravitational radiation from post-Newtonian sources with applications to inspiralling compact binaries see [316] and follow-ups.

For superradiance and possible observation of black holes through it; see [326] and the follow-up papers.

For accretion disks and their theory and its testing via observations; see [301] and references therein and [327]. For the Blandford–Znajek mechanism; see and a critical analysis of the process see [304,328–331].

There is a lot of effort going into the analysis of the three phases, inspiral, merger, and ringdown in black hole binary systems. One can learn from black hole merger gravitational-wave ringdowns and in particular, whether that is a probe of the event horizon (and why it is really not); see [332].

As discussed, reconstructing black hole shadows is a way to study black holes. The two main questions in this arena are, (1) Can we use black holes shadows to distinguish a black hole from other compact objects which are not black holes? or Does the black hole shadow probe the event horizon geometry? (2) How much one can learn from the shadow regarding the black hole (e.g. its horizon radius and angular momentum)? See e.g. [333,334] and references therein or their citations for more discussions.

For geodesic stability and QMNs see [335] and for QMNs for AdS black holes; see [336–339].

For a very good set of lecture notes on the (in)stability of black hole solutions; see [315] and references therein.

For gravitational collapse and spacetime singularities; see [241,278,340–343].

## Exercises

**4.1 Photon-sphere radii for Kerr black hole.**

Explore null geodesics of the Kerr geometry and derive the photon-sphere radii (4.1).

**4.2 Can different black holes cast the same shadow?**

One can ask if there is a shadow-degeneracy among family of black hole solutions. In this exercise, we formulate this question for a class of static-spherically symmetric asymptotically flat black hole geometries with metric,

$$\mathrm{d}s^2 = -V(R)A(R)\,\mathrm{d}t^2 + \frac{\mathrm{d}R^2}{V(R)B(R)} + R^2\,\mathrm{d}\Omega^2, \qquad V(R) = 1 - \frac{2m}{R}, \quad (4.44)$$

and $A(R)$, $B(R) \to 1$ at large $R$.

(1) Study null geodesic in the equatorial plane $\theta = \pi/2$ and parametrize the impact parameter of these paths by $b$. Write down the geodesic equation as

$$g_{RR}\dot{R}^2 + \mathcal{U}(R) = 0, \qquad \mathcal{U} := g^{tt}(\frac{1}{b} - \mathcal{H})(\frac{1}{b} + \mathcal{H}) \quad (4.45)$$

where dot denotes derivative with respect to the affine parameter. Read $\mathcal{H}$ and the effective potential $\mathcal{U}$ in terms of metric functions.

(2) Show that light rings happen at radius $R_{\mathrm{LR}}$ where

$$\frac{\mathrm{d}\mathcal{H}}{\mathrm{d}R}\Big|_{R_{\mathrm{LR}}} = 0, \qquad b_{\mathrm{LR}} = \frac{1}{\mathcal{H}(R_{\mathrm{LR}})}. \quad (4.46)$$

(3) Black hole shadows are observer dependent. Suppose that we have an observer at $R_{\mathrm{obs}} \gg R_{\mathrm{LR}}$ and suppose that black hole is at angle $\beta$ from the line of sight. Show that the The connection between the impact parameter $b$ of a generic light ray and the observation angle $\beta$ are related as

$$b = \frac{\sin\beta}{\mathcal{H}(R_{\mathrm{obs}})}. \quad (4.47)$$

(4) Consider black holes of ADM mass $M$ in the class of metrics (4.44). (Note that in general $M \neq m$.) Show different black holes of the same mass cast the same shadow as seen by the observer at $R_{\mathrm{obs}}$ if the observer angle $\beta$ is the same form them. Show that for two shadow-degenerate black holes with functions $A^{(1)}(R)$, $A^{(2)}(R)$,

$$\left(\frac{b^{(1)}_{\mathrm{LR}}}{b^{(2)}_{\mathrm{LR}}}\right)^2 = \frac{A^{(2)}(R_{\mathrm{obs}})}{A^{(1)}(R_{\mathrm{obs}})}. \quad (4.48)$$

See [334] for a detailed analysis on shadow-degeneracy for more generic black hole geometries.

**4.3 More on Penrose process for Kerr black hole.**

Consider a Kerr black hole of mass $M$ and angular momentum $J = Ma$, and a particle of momentum $p_\mu$ (as measured by an asymptotic observer). Let $k = \partial_t$ be the timelike Killing vector along the asymptotic time direction and $\xi_{\rm H} = \partial_t + \Omega\partial_\phi$ be the future-oriented vector field which becomes null at the horizon. Consider the particle to decay into two particles in the ergoregion with momenta $p^1_\mu$, $p^2_\mu$. Choose $E_1 = p_1 \cdot k < 0$.

(1) Show the condition for a particle of momentum $p^1_\mu$ to fall into the black hole is $-p_1 \cdot \xi_{\rm H} \geq 0$.

(2) Considering the conservation laws, show that the other particle which has positive energy in principle can come out of the ergoregion and fly off to infinity.

(3) Show the condition obtained in (1) of this exercise means the extraction of energy should necessarily be accompanied by extraction of angular momentum from the black hole. What are the maximum energy and angular momentum a particle can carry out in a Penrose process described above?

(4) If the Penrose process can continue for a long time, and at each step $\delta M$, $\delta J$ can be taken from the black hole, when does the Penrose process stops?

(5) How much energy and angular momentum (which percentage of the original $M$, $J$) can in principle be extracted from the black hole via this process?

**4.4 More on superradiance for Kerr black hole.**

(1) Show that (4.9), which is the condition for having superradiance, can occur for physical modes. Compare this condition with the condition obtained in (1) of the previous exercise.

(2) Consider a scalar field theory with energy–momentum tensor

$$T_{\mu\nu} = \partial_\mu \Phi \partial_\nu \Phi - \frac{1}{2}(\partial\Phi)^2 g_{\mu\nu},$$

and a mode $\Phi = \Phi_0 \cos(\omega t - m\phi)$ which takes part in the superradiance. Show the power lost across the horizon by this mode is

$$P = \frac{1}{2}\Phi_0^2 \omega(\omega - m\Omega) A_{\rm H}$$

where $A_{\rm H}$ is the horizon area.

(3) In a similar way, compute the angular momentum lost across the horizon.

(4) What are the maximum energy and angular momentum one can extract from a black hole via the superradiance process?

(5) Starting from a Kerr black hole, can we reach an extremal black hole or a static Schwarzschild black hole at the end of the superradiance process?

**4.5 Uniformized Regge–Wheeler equation.**

Show that the Regge–Wheeler equation (4.4) with the potential (4.5) can be uniformized to depend only on two dimensionless parameters, $l$ and $\tilde{M} = M\omega$, by introducing dimensionless radii $z_* = \omega r_*$ and $z = \omega r$. In particular, this shows that mass $M$ and frequency $\omega$ enter only through their product $\tilde{M}$. Finally, show an alternative uniformization where you keep the spectral parameter, $\sigma = M\omega$, but rescale all radii in geometrized units, $r_* = 2My_*$ and $r_2My$, to eliminate the mass.

**4.6 Leading large radius terms in Regge–Wheeler equation.**
Show that at large radii the (uniformized, see the previous exercise) Regge–Wheeler equation turns into a simple potential problem with superpotential

$$W_l(z) = -\frac{l+1}{z}$$

and potential $V_l = W_l^2 - W_l'$. Show that the partner potential $\hat{V}_l = W_l^2 + W_l'$ is related to $V_l$ by a spectral shift $l \to l+1$. Use this fact together with the ladder operator $a_l = \partial_z + W_l$ to derive a recursion formula for the wave function $\psi_l$ in terms of $\psi_{l-1}$. Compare your result with direct integration of this second order differential equation. Note: this is a simple application of supersymmetric quantum mechanics, see e.g. [344].

**4.7 High frequency limit of Regge–Wheeler equation.**
Show that in the high frequency limit $\omega M \to \infty$ the Regge–Wheeler equation (4.4) with the potential (4.5) turns into a confluent hypergeometric differential equation. Solve it and use Stirling's formula for the Gamma-function to derive that in this limit the reflection coefficient defined in (4.6) is given by

$$|A_R|^2 \approx e^{-8\pi\omega M} .$$

Hint: It is useful to keep the Schwarzschild radial coordinate $r$, uniformize to $y$ defined in Exercise 4.5 and to rescale $\psi_l = \phi_l/\sqrt{1-1/y}$ before addressing any limits.

**4.8 Linearized Einstein equations.**
Derive the linearized Einstein equations (4.11) as well as the quadratic action (4.12).
Hint: use $\delta R_{\mu\nu} = \bar{\nabla}_\lambda \delta\Gamma^\lambda{}_{\mu\nu} - \bar{\nabla}_\nu \delta\Gamma^\lambda{}_{\mu\lambda}$ and $\delta\Gamma^\lambda{}_{\mu\nu} = \frac{1}{2}\,\bar{g}^{\lambda\rho}\,(\bar{\nabla}_\mu h_{\nu\rho} + \bar{\nabla}_\nu h_{\mu\rho} - \bar{\nabla}_\rho h_{\mu\nu})$.

**4.9 Gravitational wave equation.**
Derive the wave equation $\bar{\nabla}^2 h_{\mu\nu} = 0$ from the linearized Einstein equations (4.11) in de Donder gauge (4.15) with $\alpha = \frac{1}{2}$ for any background metric with $\bar{R}^\lambda{}_{\rho\mu\nu} = 0$. Hint: use $[\bar{\nabla}_\mu, \bar{\nabla}_\nu]h_{\lambda\rho} = 0$ up to terms linear in the background Riemann tensor.

**4.10 Quadrupole emission formula.**
Derive the quadrupole emission formula (4.25) by suitably manipulating the integral $\int \mathrm{d}^3x' T^{ij}(t - |\mathbf{x} - \mathbf{x}'|,\ \mathbf{x}')$ as described in the main text.

**4.11 Gravitational wave luminosity.**

Derive the average power radiated away by GW (4.27) using the hints in the main text after that formula.

**4.12 Period decrease in binary systems.**

Starting from the GW luminosity formula (4.27) derive the estimate for the power $P \sim (M/T)^{10/3}$ for a binary system of mass $M$ and initial period $T$.
Hint: use Kepler's third law $R^3 \propto T^2 M$ to eliminate lengths from the quadrupole moment

$$Q_{xx} = MR^2 \cos^2(t/T),\ \ Q_{xy} = MR^2 \cos(t/T) \sin(t/T),\ \ Q_{yy} = MR^2 \sin^2(t/T).$$

**4.13 More on Blandford–Znajek effect.**

Here we provide a simplified derivation of the Blandford–Znajek mechanism, more details may be found in [328,345]. Consider a stationary-axisymmetric electromagnetic field on the Kerr background parametrized in the Boyer–Lindquist coordinates, $t, x^i, x^i = \{r, \theta, \phi\}$. Denote electric and magnetic fields by $E_i = -F_{ti}$, $B^i = \frac{1}{2}\epsilon^{ijk} F_{jk}$. For this system $E_\phi = 0$. Define polar flux of the magnetic flux tube,

$$\Phi = \int B^i \mathrm{d}s_i. \tag{4.49}$$

(1) Show that the angular velocity of electromagnetic field, $\Omega_e$

$$\Omega_e := \frac{E_r}{\sqrt{\gamma} B^\theta} = -\frac{E_\theta}{\sqrt{\gamma} B^r}, \tag{4.50}$$

is a constant along the magnetic field lines. In the above, $\gamma$ is the determinant of the constant $t$ slice of the metric. Show also that the second equality in (4.50) follows from the first equality. Using this constancy of $\Omega_e$, argue that $\Omega_e$ is a function of magnetic flux $\Phi$.

(2) Show that the 'azimuthal magnetic field' $B_{\mathrm{T}}$,

$$B_{\mathrm{T}} := N g_{\phi\phi} B^\phi, \tag{4.51}$$

where $N$ is the lapse function and $g_{\phi\phi}$ is the corresponding metric component in the Boyer–Lindquist coordinates, is also a constant along the field lines. Therefore, $B_{\mathrm{T}}$ is also a function of $\Phi$.

(3) Show electric charge, energy and angular momentum cannot flow across the wall of the magnetic flux tube.

(4) Show energy flux $\mathcal{E}$ and angular momentum flux $\mathcal{J}$ of electromagnetic field satisfy the following equations,

$$\frac{\mathrm{d}\mathcal{E}}{\mathrm{d}\Phi} = -B_{\mathrm{T}}\Omega_e, \qquad \frac{\mathrm{d}\mathcal{J}}{\mathrm{d}\Phi} = -B_{\mathrm{T}}. \tag{4.52}$$

(5) Next, let us impose the Blandford-Znajek 'horizon boundary conditions' which imply that at the horizon,

$$B_{\mathrm{T}} = -f(\theta)(\Omega_h - \Omega_e)\partial_\theta \Phi, \tag{4.53}$$

where $\Omega_h$ is horizon angular velocity and $f(\theta)$, $\partial_\theta \Phi$ are two positive functions. Argue that in the force-free electrodynamics limit the above is a sensible choice.

(6) Argue that if $\Omega_h > \Omega_e$, then $B_{\mathrm{T}} < 0$ and hence there is a positive torque and energy flux. That is, the accretion disk is electromagnetically transferring energy outside the plasma tube (the accretion disk).

(7) Argue that, as in the superradiance/Penrose process, the ergoregion (and not the horizon) plays an important role. To this end, consider electron–positron pair production from the vacuum due to the presence of a (strong) magnetic field which can happen in the ergoregion.

**4.14 *pp*-wave, plane waves, Brinkmann and Rosen coordinate systems.**
(1) Plane-fronted GW with parallel rays, *pp*-waves, are spacetimes which support a covariantly constant null Killing vector field $v^\mu$, $\nabla_\mu v_\nu = 0$, $v_\mu v^\mu = 0$. Show that the most general form of a *pp*-wave metric is

$$\mathrm{d}s^2 = -2\,\mathrm{d}x^+\,\mathrm{d}x^- - F\ \mathrm{d}x^{-2} + 2\omega_i\ \mathrm{d}x^-\,\mathrm{d}x^i + g_{ij}\ \mathrm{d}x^i\,\mathrm{d}x^j, \qquad i,j = 1,\cdots,D-2 \tag{4.54}$$

where $F, \omega_i, g_{ij}$ are functions of $x^-, x^i$ and the null Killing vector $v = \frac{\partial}{\partial x^+}$.

(2) Plane-waves, are a special class of *pp*-waves where the null Killing vector field is *globally defined* and have planar symmetry. Show that the most general form of a plane wave metric is of the form

$$\mathrm{d}s^2 = -2\,\mathrm{d}x^+\,\mathrm{d}x^- - F(x^-)x_i x^i\,\mathrm{d}x^{-2} + \delta_{ij}\,\mathrm{d}x^i\,\mathrm{d}x^j, \qquad i,j = 1,\cdots,D-2. \tag{4.55}$$

A specific class of plane wave with $F(x^-) = const.$ is called a homogeneous plane wave.

(3) The above coordinate system for a plane wave is called *Brinkmann coordinate* system. Find the coordinate transformation upon which it can be brought to the *Rosen coordinates*:

$$\mathrm{d}s^2 = -2\,\mathrm{d}X^+\,\mathrm{d}X^- - \mathcal{G}_{ij}(X^-)\,\mathrm{d}x^i\,\mathrm{d}x^j, \qquad i,j = 1,\cdots,D-2. \tag{4.56}$$

(4) Show that plane waves cannot be black holes, i.e. cannot have event horizons. See [346] for more discussions.

(5) Draw the Penrose diagram of a generic homogeneous plane wave. See Sect. II. of [193] for more discussions.

(6) The plane wave (4.34) is written in the Brinkmann coordinate system. Apply the coordinate transformation given in the text and bring it to the Rosen coordinate system which takes the form,

**4.15 Penrose limit and plane waves.**

Penrose in [347] proved that near a null geodesic, every Lorentzian spacetime looks like a plane wave. To see this, consider an observer boosted up to the speed of light and at the same time zoom onto a region infinitesimally close to the (lightlike) geodesic the observer is moving on. Then, in the limit, the observer would see a plane wave. Follow the steps out listed below to recover Penrose's proof.

(1) Let $u$ be a coordinate affinely parameterizing a null geodesic. Show that one can always find a coordinate system such that metric takes the form

$$\mathrm{d}s^2 = R^2\left[-2\,\mathrm{d}u\,\mathrm{d}\tilde{v} + \mathrm{d}\tilde{v}^2 + 2\tilde{\omega}_i\ \mathrm{d}\tilde{v}\,\mathrm{d}\tilde{x}^i + \tilde{g}_{ij}\ \mathrm{d}\tilde{x}^i\,\mathrm{d}\tilde{x}^j\right], \tag{4.57}$$

where $\tilde{\omega}_i$, $\tilde{g}_{ij}$ are functions of $u$, $\tilde{v}$, $\tilde{x}^i$.

(2) Zoom onto the null geodesic by taking $R \to \infty$ while keeping the following fixed,

$$v = R^2\tilde{v}, \quad x^i = R\tilde{x}^i, \tag{4.58}$$

Show in the limit the metric takes the form of a plane wave in the Rosen coordinates (see the previous exercise).

**4.16 QNMs and Kammerton A.**

'Kammerton A' is a musical convention referring to a sound signal with a frequency 440 Hz. Calculate the mass of a Schwarzschild black hole (in units of $M_\odot$) whose lowest-lying QNM rings with Kammerton A. What is the damping time of this mode (in milliseconds)?

**4.17 Late-time tails of Schwarzschild perturbations.**

Consider the Green function (4.40) with the homogeneous contribution fixed by requiring suitable boundary conditions. To simplify matters assume non-vanishing angular momentum number $l > 0$ and show that at large $r_*$ the potential is well-approximated by

$$V_l(r_* \to \infty) \approx \frac{l(l+1)}{r_*^2} + \frac{2Ml(l+1)}{r_*^3}\ln\frac{r_*}{2M} = \frac{l(l+1)}{r_*^2} + \delta V_l$$

hence producing a branch cut in the Green function. Then use a Born-type of approximation ($\psi_0$ is the solution of the equation below for $\delta V_l = 0$)

$$\left(\frac{\mathrm{d}^2}{\mathrm{d}r_*^2} + \omega^2 - \frac{l(l+1)}{r_*^2}\right)\psi = \delta V_l\,\psi_0$$

linearizing in $\delta V_l$ to derive the result

$$G(r_*,\ r,\ t) \propto \frac{\theta(t)}{t^{2l+3}}$$

with a time-independent proportionality factor. This result, together with (4.41), proves (4.39). For hints and details; see [348].

**4.18 On Choptuik critical collapse.**
Consider the Einstein massless Klein–Gordon model in $D > 3$ spacetime dimensions and impose spherical symmetry on the scalar field $\Phi = \Phi(t, r)$ and the metric

$$\mathrm{d}s^2 = -\alpha^2(t, r)\,\mathrm{d}t^2 + a^2(t, r)\,\mathrm{d}r^2 + r^2\,\mathrm{d}\Omega^2_{S^{D-2}}\,.$$

Simplify the coupled Einstein and Klein–Gordon equations to three independent partial differential equations for the functions $\alpha$, $a$, and $\Phi$. Verify in particular, how the dimension $D$ enters these equations and consider how this may affect numerical studies of these partial differential equations.

**4.19 Continuous self-similarity.**
As in the previous exercise, consider the Einstein massless Klein–Gordon model in $D > 3$ spacetime dimensions. In addition to spherical symmetry, impose continuous self-similarity, i.e. the existence of a conformal Killing vector field $\xi$

$$(\mathcal{L}_\xi g)_{\mu\nu} = 2g_{\mu\nu}\,.$$

Using continuous self-similarity, simplify the three independent partial differential equations obtained in the previous exercise to ordinary differential equations and solve them.

**4.20 Non-linear stability versus cosmic censorship conjecture and uniqueness theorems.**
As stated non-linear stability problem is concerned with how a given solution to Einstein GR reacts to a generic perturbation after a long time the perturbation is turned on and whether the final solution is still close to the original solution.

(1) Convince yourself that a necessary condition for non-linear stability is that the perturbation should not lead to the formation of an apparent (event) horizon.

(2) Convince yourself that CCC (both strong and weak versions), cf. Sect. 3.2.7, are necessary conditions for the non-linear stability of the spacetime.

(3) With the same token, convince yourself that topology and uniqueness theorems, cf. Sects. 3.2.5 and 3.2.6, are necessary conditions for the non-linear stability of the corresponding black hole solutions.

Note that these are necessary conditions and in general one may need other conditions, e.g. asymptotic boundary conditions, to make them sufficient too.

# Black Hole Charges and Thermodynamics

# 5

**Abstract**

In this chapter, we start with an overview of systematic methods to compute gravitational charges in Sect. 5.1 and present the Komar charges in Sect. 5.2. We then introduce the solution phase space method as a precise and handy formulation to define conserved charges for black holes in Sect. 5.3. While this method can be used for asymptotically stationary black holes, it is most conveniently used for stationary black holes with a Killing horizon. For the latter family, we provide a concise derivation of the entropy as Noether charge in Sect. 5.4 and of the four laws of black hole thermodynamics in Sect. 5.5.

## 5.1 Introduction to Systematic Methods for Charge Computation

In Chap. 2 we gave the ADM prescription for computing the mass and angular momentum of asymptotic flat solutions. In this section, we give a brief historical overview of the definitions of charges in GR and expand on them and their applications in later sections (and the appendices).

In classical mechanics, mass and angular momentum are usually viewed as (conserved) charges associated with some symmetries via the seminal theorems by Emmy Noether. Defining conserved charges in a covariant way has been a challenge within GR or other generally covariant theories in which the spacetime metric is a dynamical object and there is no preferred time direction. The question we will be dealing with in this section is to define a covariant symmetry-based definition of conserved charges for a given solution, including black hole solutions.

Black hole solutions generically come with a set of isometries generated by Killing vectors, and/or with specific ‘asymptotic isometries’ generated by asymptotic Killing vectors like in (3.20). In words, asymptotic Killing vectors are vector fields that keep the metric invariant up to a given/prescribed asymptotic form. These exact or asymptotic isometries can be used to define conserved charges through appropriate extensions and generalizations of Noether’s theorems.



D. Grumiller and M. M. Sheikh-Jabbari, *Black Hole Physics*, Graduate Texts in Physics,
https://doi.org/10.1007/978-3-031-10343-8_5

Arthur Komar [349] presented the first covariant conserved charge formula, based on isometries. Komar's work was shortly followed by the ADM papers [148, 150, 350] that define charges associated with asymptotic Poincaré isometries on constant time slices of asymptotic flat spacetimes. Compared to Komar's formula, the ADM analysis has the advantage that only asymptotic isometries are used, which are not necessarily Killing vectors; also, it leads to the quite handy formulas (2.14). On the other hand, it has the drawback that it is only applicable to asymptotic flat spacetimes, and to compute the ADM charges one needs to know the asymptotic behavior of the solution.

The question of black hole charges is closely related to the notion of the gravitational energy-momentum pseudo-tensor. This notion is of significance because in physical processes we typically have a localized gravitational object (like a black hole) interacting with GW that can travel to infinity while carrying energy-momentum. There are several different proposals for defining energy-momentum flow and stress tensor for a given spacetime and separating the contribution of localized objects and waves which fly off to infinity. Conceptually, this is a consequence of a key difference between linearized gravity and Maxwell's theory: while photons are not charged, gravitons are 'charged' under their own gauge symmetry, i.e. they carry energy and thus interact with themselves already classically.

The first systematic approach to defining charges was based on the ADM $3 + 1$ decomposition. This was followed by the Regge–Teitelboim Hamiltonian method [351]. The connection between the two was made more manifest and formulated through the Brown–York quasi-local energy and stress tensor [352, 353], which reproduces the ADM mass and angular momentum in asymptotic flat spacetimes. Each of these methods has its own advantages and shortcomings. For instance, they may not be covariant enough or crucially depend on the form of the Einstein–Hilbert action or on the asymptotic behavior of fields. These shortcomings have been discussed and to some extent addressed in several subsequent works. For example, the ADM or Brown–York formulation has been extended to asymptotic AdS geometries [354–358] (see [359] for a nice overview) and asymptotic flat solutions to higher derivative theories of gravity [360]. Here we focus on more covariant notions of conserved charges which we find more convenient and useful for treatments of black holes. The discussion on Hamiltonian approaches will be deferred to the Appendix F.

In this chapter, we first discuss the Komar charges and then briefly discuss the Iyer–Wald formulation and its extension to the solution phase space method. A more detailed treatment may be found in the Appendix G.

## 5.2 Komar Charges

According to Noether's theorem a global continuous symmetry yields a conserved current $J^\mu$, $\nabla_\mu J^\mu = 0$. One can integrate the component of this current along the normal vector of a constant time slice $\Sigma_t$ and define the charge

$$Q_t := \int_{\Sigma_t} J^t \,. \tag{5.1}$$

This charge is conserved, i.e. $Q_{t_1} = Q_{t_2}, \forall t_1, t_2$, provided that

$$\oint_{\partial\Sigma_{t_1}} \mathrm{d}\Sigma_i \; J^i = \oint_{\partial\Sigma_{t_2}} \mathrm{d}\Sigma_i \; J^i \tag{5.2}$$

where $\partial\Sigma_t$ is the boundary of our constant time slice and $\mathrm{d}\Sigma_i$ is its area element. The charge is conserved if there is no flux passing through the boundary of spacetime, matching with physical intuition.

In generally covariant theories, diffeomorphism invariance of the matter part of the action yields conservation of the energy-momentum tensor, $\nabla_\mu T^{\mu\nu} = 0$. Being a symmetric tensor one cannot define a conserved charge as above. However, if we have a Killing vector $\xi^\mu$ one may define the current $J^\mu_\xi = T^{\mu\nu}\xi_\nu$. Conservation of this current follows directly from the Killing equation and conservation of the energy-momentum tensor. One can hence use this current to define conserved charges for any given Killing vector field.

The above defines a conserved charge associated with a matter distribution. One can attribute a closely related (but not exactly identical) conserved charge to a geometry/spacetime using Einstein's equations. Let us define the "Komar conserved current" $\mathcal{K}^\mu_\xi$,

$$\mathcal{K}^\mu_\xi := c_\xi (T^{\mu\nu} - \frac{1}{2} T g^{\mu\nu})\xi_\nu \,, \tag{5.3}$$

whose conservation immediately follows from Einstein's equations, which yields $R = -8\pi G_{\mathrm{N}} T$, and $\xi^\mu \partial_\mu R = 0$ for any Killing vector field $\xi$. Here $c_\xi$ is an arbitrary constant introduced for later convenience. Einstein's equations convert the Komar conserved current

$$\mathcal{K}^\mu_\xi = \frac{c_\xi}{8\pi G_{\mathrm{N}}} R^{\mu\nu}\xi_\nu, \tag{5.4}$$

into a purely geometric quantity. Therefore, one can define the Komar charge,

$$Q_\xi := \int_{\Sigma_t} \mathcal{K}^0_\xi = \frac{c_\xi}{16\pi G_{\mathrm{N}}} \oint_{\partial\Sigma_t} \mathrm{d}\xi \tag{5.5}$$

where in the second equality we used the Killing vector identity (3.28), yielding

$$R_{\mu\nu}\xi^\nu = -\nabla^\nu\nabla_\mu\xi_\nu, \qquad \xi^\mu\partial_\mu R = 0\,. \tag{5.6}$$

The second equality (5.5) is written in the form language: $\xi$ is a 1-form and $\mathrm{d}\xi$ is a 2-form, $(\mathrm{d}\xi)_{\mu\nu} = \nabla_\mu\xi_\nu - \nabla_\nu\xi_\mu$, which is integrated over a compact-spacelike codimension-2 surface $\partial\Sigma_t$. By definition we take,

$$c_\xi = \begin{cases} -1 & \xi \;\; \text{timelike} \\ \frac{1}{2} & \xi \;\; \text{spacelike} \end{cases} \tag{5.7}$$

to reproduce the ADM charges for asymptotic flat spacetimes (see Exercise 5.2).

We close this part with some remarks about the Komar formula (5.5):

1. It is a geometric quantity and one may hence associate its value to a spacetime. If we have a localized object like a black hole, it then computes charges associated with the black hole. (However, compare with Exercise 2.30, which associates a distributional energy-momentum tensor to black holes.)
2. It is a surface integral, i.e. codimension-2 integral. By contrast, the Noether charge (5.1) or the first equality in (5.5) is a volume integral, i.e. codimension-1 integral. To arrive at the surface integral we used field equations. In this respect, the situation is similar to the Gauss law in electrodynamics. Noether's theorem is a result of any global continuous symmetry. However, as in gravity and electrodynamics, it can happen that this global symmetry is the global part of a gauge symmetry. In such cases, the Noether volume integrals can always be related to a surface integral. The slogan is: global symmetries lead to codimension-1 charges, gauge symmetries to codimension-2 (surface) charges.
3. The Komar formula (5.5) yields a conserved charge for any Killing vector field $\xi$, being spacelike, timelike or null. We have discussed the first two. The latter arises e.g. for Killing horizon or for asymptotic flat spacetimes near $\mathfrak{I}$. The null case needs a separate analysis, which we return to in the coming sections.
4. While for vacuum solutions $R_{\mu\nu} = 0$ seemingly the Komar current (5.4) vanishes, the final expression in (5.5) is non-zero for Schwarzschild or Kerr black holes. This apparent discrepancy is related to the distributional stress tensor of these black holes, see Exercises 2.30 and 5.1.

## 5.3 Solution Phase Space Method

The ADM charges, while very handy and practically useful, only work for asymptotic flat spaces. Also, their computation requires knowing the solution all the way to the asymptotic region. Moreover, both ADM and Komar charges, as presented and discussed above, only work for Einstein gravity. The ADM and Komar formulas were extended to asymptotic (A)dS spacetimes within Einstein gravity [357, 358, 361] and beyond Einstein gravity [360, 362]. Nonetheless, a simple universal formula that works for every asymptotic behavior and every theory does not seem to exist in these settings. One can overcome these shortcomings of ADM and Komar formulas with the *solution phase space method* (SPSM), which we discuss here. For some references see [363–368].

The SPSM is based on the covariant phase space formalism reviewed in Appendix G. It starts with a set of solutions to the field equations of a generic diffeomorphism- and gauge invariant theory. These solutions come with a number of parameters $p_\alpha$, like $m, a, q$ in a KN solution. We denote these solutions by $\Phi(x; p_\alpha)$, where the fields are collectively denoted by $\Phi(x)$. We distinguish between solution parameters and theory parameters. The former are typically constants of motion, while the latter comprise Newton's constant, the cosmological constant, and mass or interaction parameters in a field theory.

In diffeomorphism- and gauge invariant theories, given a solution $\Phi(x; p_\alpha)$, we can generate a whole class of solutions by applying diffeomorphisms and/or gauge transformations. This class of solutions typically comes with some number of arbitrary parameter functions, $F_a(x)$. The solutions within a class may be physically equivalent to the original solution, as they are just obtained by diffeomorphisms or gauge transformations from the original solution. However, some of these would-be diffeomorphisms or gauge transformations can change the physical state. To distinguish which of these diffeomorphisms/gauge transformations are pure gauge, referred to as "proper", and which are not, referred to as "non-proper", one checks whether there is a non-trivial surface charge associated with them (see Appendix G for more details). Hereafter, we only consider the non-proper diffeomorphism- and gauge transformations and include them in our parameter functions $F_a(x)$.

The non-proper gauge transformations may be understood as follows. Let us for definiteness restrict to vacuum Einstein theory in four dimensions. It is known that its field equations form a Cauchy problem [2,369–371]. Therefore, the most general solution is completely specified by a set of Cauchy data which are typically given by the value of the metric and its first time derivative along the constant time slice, the Cauchy surface. These Cauchy data in 4-dimensional theory are hence specified by $6 + 6$ functions over the 3-dimensional constant time slice. Out of these $2 + 2$ carry the information of the gravitons propagating into spacetime but $4 + 4$ are free. Four of these may be specified through our choice of coordinates, but four that are functions over the codimension-1 Cauchy surface remain. The information about these latter is parametrized in our *solution space* $\mathcal{S}$, i.e. , the set of solutions $\Phi(x; p_\alpha; F_a(x))$. In other words, the non-proper gauge transformations are carrying the information of the (initial) Cauchy data.

Under a non-proper diffeomorphism- and gauge transformations generated by $\chi(x)$, $F_a \to F_a + \delta_\chi F_a$ and under a parametric variation $p_\alpha \to p_\alpha + \delta p_\alpha$. One can then move in the solution space $\mathcal{S}$ by these non-proper gauge transformations and by parametric variations:

$$\begin{aligned} \delta_\chi \Phi &:= \Phi(x; p_\alpha; F_a(x) + \delta_\chi F_a) - \Phi(x; p_\alpha; F_a(x)) \\ \hat{\delta}_p \Phi &:= \Phi(x; p_\alpha + \delta p_\alpha; F_a(x)) - \Phi(x; p_\alpha; F_a(x)). \end{aligned} \tag{5.8}$$

The $\chi$-transformations here are generic and may also be field-dependent. The solution may also have some discrete parameters that do not appear in our analysis here, as we are only considering continuous transformations.

In the generally covariant theories we are studying, $\chi_a$ includes field perturbations generated by infinitesimal diffeomorphisms $\epsilon_m$. If we have other internal gauge symmetries, like in Einstein–Maxwell or Einstein–Yang–Mills theories, it will also include gauge transformations $\lambda_n$, i.e. $\chi_a \in \{\epsilon_m, \lambda_n\}$. Therefore, in general,

$$\delta_\chi \Phi := \mathcal{L}_\epsilon \Phi(x; p_\alpha; F_a(x)) + \delta_\lambda \Phi(x; p_\alpha; F_a(x)) \tag{5.9}$$

where the first term denotes the Lie derivative of the fields under the diffeomorphisms $\delta x^\mu = -\epsilon^\mu(x)$ and the second is their gauge transformations.

Importantly, $\delta_\chi \Phi$, $\hat{\delta}_p \Phi$ both satisfy linearized field equations. One should note, however, that there are variations around a given configuration in the solution space $\delta\Phi$ that satisfy linearized field equations but are not among our (non-proper) gauge or parametric variations. As an example, we mention the Schwarzschild solution with a GW perturbation on it.

### 5.3.1 Solution Space Is a Phase Space

As discussed, the tangent space of the solution space manifold $\mathcal{S}$ has different subspaces, e.g., those spanned by non-proper diffeomorphism- and gauge transformations $\delta_\chi \Phi$ or those with parametric variations $\hat{\delta}\Phi$. By construction and the fact that we are only considering non-proper gauge transformations, if we suppress the parametric variations, $\mathcal{S}$ defines a phase space (see discussions in the Appendix G). Let us denote the associated symplectic form by $\Omega(\delta_1\Phi, \delta_2\Phi, \Phi)$.

Next, let us focus on the parametric variations. The set of solutions $\Phi(x^\mu; p_\alpha)$ with tangent space restricted to $\hat{\delta}\Phi$ constitute a sub-manifold $\mathcal{S}_p$ of $\mathcal{S}$. One may then show that the same symplectic 2-form $\Omega$ is well-defined on $\mathcal{S}_p$. That is, $\hat{\Omega}$ defined as

$$\hat{\Omega} := \Omega(\hat{\delta}_1\Phi, \hat{\delta}_2\Phi, \Phi) = \int_\Sigma \boldsymbol{\omega}(\hat{\delta}_1\Phi, \hat{\delta}_2\Phi, \Phi) \tag{5.10}$$

where

$$\boldsymbol{\omega}(\hat{\delta}_1\Phi, \hat{\delta}_2\Phi, \Phi) = \hat{\delta}_1\boldsymbol{\Theta}(\hat{\delta}_2\Phi, \Phi) - \hat{\delta}_2\boldsymbol{\Theta}(\hat{\delta}_1\Phi, \Phi)\,, \tag{5.11}$$

constitutes a well-defined symplectic 2-form on $\mathcal{S}_p$, i.e. , $(\mathcal{S}_p; \hat{\Omega})$ forms a phase space. This is the section of the full solution phase space over which we are limited to move only along parametric variations.

### 5.3.2 Exact Symmetries and the Associated Charges

Among the transformations $\chi_a$, there is an important subsector of *exact symmetries* $\eta_i$, which is the main focus in this section. These are the set of diffeomorphism- and gauge transformations that do not move us in the solution space, i.e. $\delta_{\eta_i}\Phi = 0$. Such $\eta$s are in general field-dependent, $\eta_i = \eta_i[\Phi]$. Therefore, the set of parametric variations $\hat{\delta}\Phi$ and those associated with non-proper gauge transformations $\delta_\chi\Phi$ only overlap at $\delta\Phi = 0$ cases, i.e. on the set of exact symmetries.

Exact symmetries include spacetime isometries generated by Killing vectors. In the presence of gauge fields, the exact symmetries are not limited to the Killing vectors; there could be a subset of the internal gauge transformations that does not change a given solution. For example, the Maxwell gauge field corresponding to a set of static charges, in the static gauge, is invariant under the global part of the $U(1)$ gauge transformations. Moreover, in presence of gauge fields, spacetime isometries may not necessarily keep the gauge field intact; they may transform the gauge field up to an internal gauge transformation and hence do not physically change the solution. In this sense, the notion of invariance under exact symmetries should be extended to invariance up to internal gauge transformations. This latter has interesting consequences, as we shall discuss below.

As discussed in the Appendix G, one may in general define charge variations for both $\chi_a$ and parametric variations (5.8). If finite and integrable, these charge variations may be integrated to give surface charges, which are functions over the solution phase space $\mathcal{S}$. There is a one-to-one relation between symmetry generators $\chi_a$ and the associated charges $Q_{\chi_a}$. In this section, we discuss charges associated with parametric variations and exact symmetries, using the same machinery of the covariant phase space formalism.

Let us restrict ourselves to $\mathcal{S}_p$ part of the solution phase space. In this sector, besides the parametric variations $\hat{\delta}\Phi$, we can also consider exact symmetries which do not move us on the phase space. We define the charge variation associated with an exact symmetry $\eta$ as

$$\hat{\not{\delta}} Q_\eta = \oint_{\partial\Sigma} \boldsymbol{k}_\eta(\hat{\delta}\Phi, \Phi)\,. \tag{5.12}$$

See Appendix G for conventions. Note that in general $\hat{\delta}\eta \neq 0$; i.e. we may have *parameter dependent* transformations.

In order for the charge variation $\hat{\not{\delta}} Q_\eta$ to be well-defined over $\mathcal{S}_p$ it should be integrable over the parameter space. As discussed, an exact symmetry $\eta$ can involve a Killing vector $\xi$ and a gauge transformation $\lambda$, then the above leads to the integrability condition for parametric variations,

$$\oint_{\partial\Sigma} \Big(\xi \cdot \boldsymbol{\omega}(\hat{\delta}_1\Phi, \hat{\delta}_2\Phi, \Phi) + \boldsymbol{k}_{\hat{\delta}_1\eta}(\hat{\delta}_2\Phi, \Phi) - \boldsymbol{k}_{\hat{\delta}_2\eta}(\hat{\delta}_1\Phi, \Phi)\Big) \approx 0\,. \tag{5.13}$$

If integrable, this means that there exists a charge $Q_\eta$ such that $\hat{\delta} Q_\eta = \hat{\not{\delta}} Q_\eta$. The above integrability condition may constrain normalization of symmetry generators $\eta$. We note that (5.13) is linear in the (parametric) field variations and hence if $\eta_1$ and $\eta_2$ are two generators with integrable conserved charges, then $c_1\eta_1 + c_2\eta_2$ (for any $c_1, c_2$ which are constant on spacetime and on the solution space), would be also integrable.

If for any exact symmetry $\eta$, $\hat{\not{\delta}} Q_\eta = 0$ over the whole solution phase space $\mathcal{S}_p$, we have proper transformations among parametric variations $\hat{\delta}\Phi$. The existence of such trivial parametric variations means that some of our solution parameters $p_\alpha$ are artifacts and unphysical. One may rewrite the solutions by removing them through redefinitions of other parameters or through proper diffeomorphism- and gauge transformations. In the end, the number of continuous physical parameters and the number of independent exact symmetries should match.

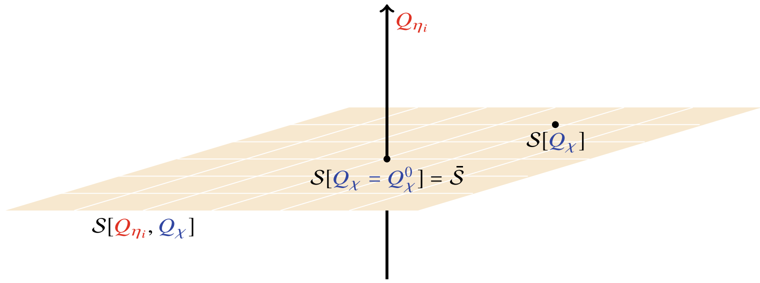


**Fig. 5.1** Schematic depiction of the phase space of a solution family $\mathcal{S}[Q_{\eta_i}, Q_\xi]$. The vertical axis exhibits different solutions specified by different values of exact symmetry charges $Q_{\eta_i}$ (e.g. mass and angular momentum), i.e. , it labels points in $\mathcal{S}_p$. The horizontal plane is constructed by the action of non-proper diffeomorphisms $\chi_a$. Each point shows a geometry in the phase space identified by charges $Q_{\chi_a}$. Moving on the horizontal plane does not change the exact charges $Q_{\eta_i}$

If integrable, $\hat{\delta} Q_\eta$ can be integrated over $\mathcal{S}_p$ to obtain $Q_\eta[\Phi(p_\alpha)]$. To do so, however, we need to choose an appropriate reference point $Q_\eta[\bar{\Phi}]$:

$$Q_\eta[\Phi(p_\alpha)] = \int_{\bar{p}}^{p} \hat{\delta} Q_\eta + Q_\eta[\bar{\Phi}]\,, \tag{5.14}$$

where the integration is performed over arbitrary integral curves that connect a reference field configuration $\bar{\Phi}$ to the $\Phi$ on the solution phase space $\mathcal{S}_p$. Integrability then implies that the charge is independent of the integration path.

Finally, dealing with the exact symmetries for which $\delta_\eta \Phi = 0$, brings the interesting result that the boundary $\mathbf{Y}$ term (which is an ambiguity or a freedom in the definition of $\boldsymbol{\omega}$, cf. (G.8)) would not contribute to the exact symmetry charges we are discussing here. Thus for the computation of conserved Noether charges one may only focus on the Lee–Wald symplectic structure density $\boldsymbol{\omega}_{\text{LW}}$. Therefore, in what follows, to simplify the notation, we will only consider the Lee–Wald symplectic structure density and simplify the notation by dropping the LW index.

Before discussing an example, we summarize our discussions so far about the solution phase space $\mathcal{S}$ in the Fig. 5.1.

### > Charges associated with Kerr-AdS black hole

As an example we discuss the Kerr-AdS black hole, which is a solution to the Einstein–Hilbert theory with negative cosmological constant. The bulk Lagrangian density for this theory

$$\mathcal{L} = \frac{1}{16\pi G_{\text{N}}}\Big(R + \frac{6}{\ell^2}\Big) \tag{5.15}$$

has the metric as only dynamical field. The metric of the Kerr-AdS black hole in coordinates that are non-rotating at infinity, is given as [372]

$$\mathrm{d}s^2 = -\Delta_\theta\left(\frac{1+\frac{r^2}{\ell^2}}{\Xi} - \Delta_\theta f\right)\mathrm{d}t^2 + \frac{\rho^2}{\Delta_r}\mathrm{d}r^2 + \frac{\rho^2}{\Delta_\theta}\mathrm{d}\theta^2 - 2\Delta_\theta f a \sin^2\theta\,\mathrm{d}t\mathrm{d}\varphi$$
$$+\left(\frac{r^2+a^2}{\Xi} + f a^2\sin^2\theta\right)\sin^2\theta\,\mathrm{d}\varphi^2\,, \tag{5.16}$$

where

$$\rho^2 = r^2 + a^2\cos^2\theta\,, \qquad \Delta_r = (r^2+a^2)(1+\frac{r^2}{\ell^2}) - 2Gmr\,,$$
$$\Delta_\theta = 1 - \frac{a^2}{\ell^2}\cos^2\theta\,, \qquad f = \frac{2Gmr}{\rho^2}\,, \qquad \Xi = 1 - \frac{a^2}{\ell^2}\,. \tag{5.17}$$

The solution is specified by two parameters $m$ and $a$; $G, \ell$ are parameters of the theory. One may readily check that (5.16) asymptotes to $\mathrm{AdS}_4$.

To employ our formulation, we start with parametric variations for this solution, which explicitly are

$$\hat{\delta} g_{\mu\nu} = \frac{\partial g_{\mu\nu}}{\partial m}\delta m + \frac{\partial g_{\mu\nu}}{\partial a}\delta a\,. \tag{5.18}$$

In the absence of gauge fields, our exact symmetries are identical to the Killing vectors $\xi$. The metric has two obvious Killing vectors $\partial_t, \partial_\varphi$ and of course, any linear combination of these two with arbitrary $m, a$-dependent coefficients is also a Killing vector. Nonetheless, as we will see, not any combination of these Killing vectors leads to integrable charges.

**Mass.** One can calculate $\hat{\delta} Q_{\partial_t}$ using $\boldsymbol{k}^{\mathrm{E}}_\xi$ from (G.29), and choosing $\partial\Sigma$ to be *any* 2-dimensional, spacelike, smooth and closed surface which surrounds the black hole. For simplicity, one can choose $\partial\Sigma$ to be constant $t, r$ surfaces, with arbitrary $t, r \neq 0$. Using (5.18) as variations in (G.29), the result is

$$\hat{\delta} Q_{\partial_t} = \frac{1}{\Xi^2}\delta m + \frac{4ma}{\Xi^3\ell^2}\delta a\,. \tag{5.19}$$

One may then verify that $\hat{\delta} Q_{\partial_t}$ is integrable over the solution phase space, by a direct check of (5.13). Explicitly, the Killing vector $N\partial_t$ with normalization $N = 1$ leads to an integrable charge. Alternatively, one may observe that $(\hat{\delta}_1\hat{\delta}_2 - \hat{\delta}_2\hat{\delta}_1)Q_{\partial_t} = 0$, and hence $\hat{\delta} Q_{\partial_t}$ (5.19) is variation of a function on the parameters $m, a$. That function is explicitly $\frac{m}{\Xi^2}$ + const., where the const. should be a constant over solution phase space, i.e. it should be independent of parameters of the solution. However, it could be a function of the parameters of the theory, like $\ell$ or $G_{\mathrm{N}}$. We fix this constant by choosing the pure $\text{AdS}_4$ spacetime ($m = a = 0$ case) as the reference point with $Q_{\partial_t}[\bar{\Phi}] = 0$, we find the mass of Kerr-AdS black holes

$$M := Q_{\partial_t} = \frac{m}{\Xi^2} \tag{5.20}$$

is given by the mass parameter $m$, but rescaled with the factor $\Xi$ defined in (5.17).

**Angular momentum.** A similar calculation for the Killing vector $\partial_\varphi$, on any surface of constant $t$, $r$ surrounding the black hole, (considering the standard additional minus sign) leads to

$$-\hat{\delta} Q_{\partial_\varphi} = \frac{a}{\Xi^2}\delta m + \frac{m(1+3\frac{a^2}{l^2})}{\Xi^3}\delta a\,, \tag{5.21}$$

which is also integrable over the parameters. The reference point $Q_{\partial_\varphi}[\bar{\Phi}]$ can be chosen to vanish on the solutions with $a = 0$. Hence, the angular momentum for the Kerr-AdS black hole is

$$J := -Q_{\partial_\varphi} = \frac{ma}{\Xi^2}\,. \tag{5.22}$$

This method to compute charges works quite well for asymptotic AdS cases. Using other methods (e.g. see [359] for a review) to compute similar charges may lead to infinite values that need regularization. By contrast, our conserved charges are not only finite but also completely specified by an appropriate choice of the reference point. We stress two other features of our method. (1) It unambiguously works for any spacetime (black hole or not) that has Killing vectors, regardless of its asymptotic behavior. (2) Charges may be computed by integrating over a constant $t$, $r$ surface for any $r$. The result will be $r$-independent by the virtue that exact symmetry charges are symplectic (see Appendix G).

## > Extremal KN near horizon geometry

To show how our method works for geometries that are not necessarily black holes but still have some Killing vectors, and also to show an example with $U(1)$ gauge symmetry, we choose the near horizon extremal KN geometry as our second example. This geometry is a solution to the Einstein–Maxwell theory (2.61) and is specified through

$$\mathrm{d}s^2 = \Gamma(\theta)\Big(-r^2\mathrm{d}t^2 + \frac{\mathrm{d}r^2}{r^2} + \mathrm{d}\theta^2 + \gamma(\theta)(\mathrm{d}\varphi + kr\,\mathrm{d}t)^2\Big)\,, \tag{5.23}$$

$$A = f(\theta)(\mathrm{d}\varphi + kr\,\mathrm{d}t) - er\,\mathrm{d}t\,, \tag{5.24}$$

where

$$\Gamma(\theta) = q^2 + a^2(1+\cos^2\theta)\,, \quad \gamma(\theta) = \left(\frac{q^2+2a^2\sin\theta}{q^2+a^2(1+\cos^2\theta)}\right)^2\,, \quad k = \frac{2a\sqrt{q^2+a^2}}{q^2+2a^2}\,,$$
$$f(\theta) = \frac{-\sqrt{q^2+a^2}\,qa\sin^2\theta}{q^2+a^2(1+\cos^2\theta)}\,, \qquad e = \frac{q^3}{q^2+2a^2}\,. \tag{5.25}$$

This solution has two parameters, $a$ and $q$ and has $SL(2,\mathbb{R}) \times U(1)_\varphi$ isometry with the Killing vectors

$$\xi_- = \partial_t\,, \quad \xi_0 = t\partial_t - r\partial_r\,, \quad \xi_+ = \frac{1}{2}(t^2 + \frac{1}{r^2})\partial_t - tr\partial_r - \frac{k}{r}\partial_\varphi\,, \qquad \xi_\phi = \partial_\varphi. \tag{5.26}$$

Not all four isometries preserve the gauge field. Three of them, $\xi_-$, $\xi_0$, and $\partial_\varphi$, are exact symmetries, $\mathcal{L}_{\xi_-}A = \mathcal{L}_{\xi_0}A = \mathcal{L}_{\xi_\phi}A = 0$, while $\xi_+$ is not: under $\xi_+$ the solution goes to itself up to an internal $U(1)$ transformation, $\delta_{\xi_+}A = \frac{e}{r^2}\mathrm{d}r \neq 0$. Thus, if we combine the fourth isometry $\xi_+$ with an appropriate $U(1)$ transformation,

$$\eta_+ = \{\xi_+, \frac{e}{r} + \text{const.}\} \tag{5.27}$$

we have a fourth exact symmetry. The constant above can be a function of parameters $q$ and $a$. Its choice should respect the integrability of $\delta Q_{\eta_+}$. A consistent choice, as will become apparent below, is to set it to zero.

This solution has conserved charges associated with its five exact symmetries, four generated by $\xi_-$, $\xi_0$, $\xi_\phi$, $\eta_+$ and one for the global part of the $U(1)$ gauge symmetry. For the Einstein–Maxwell theory, the $\boldsymbol{k}_\epsilon$ for generic $\epsilon = \{\xi, \lambda\}$ is given in (G.28) and the parametric variations for this solution are

$$\hat{\delta} g_{\mu\nu} = \frac{\partial g_{\mu\nu}}{\partial a}\delta a + \frac{\partial g_{\mu\nu}}{\partial q}\delta q\,, \qquad \hat{\delta} A_\mu = \frac{\partial A_\mu}{\partial a}\delta a + \frac{\partial A_\mu}{\partial q}\delta q\,. \tag{5.28}$$

**Angular momentum.** Choosing $\eta = \{\partial_\varphi, 0\}$ as generator of angular momentum, one can insert the parametric variations into $\boldsymbol{k}_\eta$. The charge variation (5.12) may then be computed, for simplicity we choose $\partial\Sigma$ to be surfaces of constant $t$, $r$, yielding

$$-\hat{\delta} Q_{\partial_\varphi} = \frac{q^2+2a^2}{G_{\mathrm{N}}\sqrt{q^2+a^2}}\delta a + \frac{qa}{G_{\mathrm{N}}\sqrt{q^2+a^2}}\delta q\,. \tag{5.29}$$

As is explicitly seen $\hat{\delta} Q_{\partial_\varphi}$ is integrable over the parameters/solution phase space. With a natural choice of $Q_{\partial_\varphi}[\bar{\Phi}] = 0$ for $a = 0$, as the reference point, angular momentum for this solution is found to be

$$J = \frac{\sqrt{a^2+q^2}}{G_{\mathrm{N}}}a\,. \tag{5.30}$$

This result is in agreement with the known angular momentum for the extremal KN black hole.

***$SL(2,\mathbb{R})$* charges.** For $\eta_- = \{\xi_-, 0\}$, $\eta_0 = \{\xi_0, 0\}$ and $\eta_+ = \{\xi_+, \frac{e}{r}\}$, a similar analysis yields

$$\hat{\delta} Q_{\eta_-} = \hat{\delta} Q_{\eta_0} = \hat{\delta} Q_{\eta_+} = 0\,. \tag{5.31}$$

Hence, by the choice of reference $Q_{\eta_{0,\pm}}[\bar{\Phi}] = 0$ for an arbitrary member $\bar{\Phi}$ of these solutions, one arrives at

$$Q_{\eta_-} = Q_{\eta_0} = Q_{\eta_+} = 0. \tag{5.32}$$

This result is the expected consequence of invariance under the non-Abelian $SL(2,\mathbb{R})$ exact symmetry group.

**Electric charge.** Choosing $\eta = \{0, 1\}$ as generator of the electric charge $Q$, the $\delta Q_\eta$ as integration of $\boldsymbol{k}_\eta$ given in (G.28) would reduce simply to the standard result of the Gauss law

$$\delta Q := \delta Q_\eta = \frac{-1}{16\pi G_{\mathrm{N}}} \oint_{\partial\Sigma} \epsilon_{\mu\nu\mu_1\mu_2}\, \delta(\sqrt{-g}\delta F^{\mu\nu})\, \mathrm{d}x^{\mu_1} \wedge \mathrm{d}x^{\mu_2}\,, \tag{5.33}$$

For the specific solution (5.24) and for the parametric variations (5.28), we find $\hat{\delta} Q = \frac{\delta q}{G_{\mathrm{N}}}$. So, by integration over parameters, the electric charge of this geometry is obtained to be $Q = \frac{q}{G_{\mathrm{N}}}$.

We end this example with some remarks:

1. The asymptotics of this geometry is neither flat nor AdS. Nonetheless, our formulation works for solutions with these more general asymptotics.
2. According to the SPSM, the conserved charges of exact symmetries are independent of the chosen smooth and closed surface $\partial\Sigma$. This example exhibits that a similar feature extends to the case in presence of matter fields.
3. It is worth mentioning that the ADM formalism [148,150,350] or its asymptotic AdS extensions [360,362] cannot be used to derive angular momentum of this near horizon geometry. Also, using the Komar integral [349] leads to incorrect angular momentum. This example shows one of the advantages of our proposed method over these well-known methods.

## 5.4 Entropy as a Conserved Charge

If the black hole horizon is a bifurcate Killing horizon, a Cauchy surface $\Sigma$ may be chosen to have a boundary on the bifurcation surface $\mathcal{B}$. For asymptotically flat spacetimes the other boundary is spatial infinity $\boldsymbol{i^0}$, i.e. $\partial\Sigma = \mathcal{B} \cup \boldsymbol{i^0}$, see e.g. , $\Sigma_2$ in Fig. 3.6.

It is then natural to define the surface charges associated with a black hole solution phase space, both for exact and non-exact symmetries. We will show below that one may associate a conserved charge with the exact symmetry of a Killing horizon. This conserved charge may be attributed to the black hole entropy. In the following two subsections, we apply the Noether–Wald method and covariant phase space formalism to derive the black hole entropy as a conserved charge.

### 5.4.1 Entropy as a Noether Charge

Let us consider a general covariant gravitational theory with some dynamical fields collectively denoted by $\Phi$. The Lagrangian $\mathcal{L}$ is a scalar density on the $d$-dimensional spacetime manifold spanned by $x^\mu$ and in general

$$\mathcal{L} = \mathcal{L}_G(R_{\mu\nu\alpha\beta}; g_{\mu\nu}) + \mathcal{L}_{\text{matter}}, \tag{5.34}$$

where the gravitational part $\mathcal{L}_G$ is the sector involving functions of Riemann curvature and its derivative, and $\mathcal{L}_{\text{matter}}$ is the rest of the Lagrangian. For the analysis below it is more convenient to use the language of forms. Let us denote the Hodge dual of the Lagrangian as $d$-form $\mathbf{L}$. The Noether current associated with a smooth vector $\xi^\mu$, the $(d-1)$-form $\mathbf{J}_\xi$, is defined as

$$\mathbf{J}_\xi := \mathbf{\Theta}(\delta_\xi \Phi) - \xi \cdot \mathbf{L}\,. \tag{5.35}$$

The $\mathbf{\Theta}$ term is the standard surface $(d-1)$-form which is read from variation of the Lagrangian $\delta \mathbf{L} = \mathbf{E}\delta\Phi + \mathrm{d}\mathbf{\Theta}(\delta\Phi)$ where d is the exterior derivative on the spacetime, and $\mathbf{E}$ denotes the EOM. Using the identity $\mathrm{d}(\xi \cdot \mathbf{L}) = \delta_\xi \mathbf{L}$ we arrive at the celebrated Noether theorem:

$$\mathrm{d}\mathbf{J}_\xi = \mathbf{E}\delta_\xi\Phi \quad \Rightarrow \quad \mathrm{d}\mathbf{J}_\xi \approx 0 \tag{5.36}$$

where $\approx$ means equivalence on-shell. By the Poincaré lemma, $\mathbf{J}$ is an exact form on-shell, i.e. $\mathbf{J} \approx \mathrm{d}\mathbf{Q}$. The Noether charge density $\mathbf{Q}$ is a $(d-2)$-form that is locally built out of $\Phi$ and $\xi$.

So far we reviewed the standard Noether charge construction. Vivek Iyer and Robert Wald made the following proposition for computing the black hole entropy [373]. The Noether–Wald charge is the $(d-2)$-form

$$\mathbf{Q}_\xi = \mathbf{X}^{\mu\nu}(\Phi)\nabla_{[\mu}\xi_{\nu]} + \mathbf{W}_\mu(\Phi)\xi^\mu + \mathbf{Y}(\Phi, \delta_\xi\Phi) + \mathrm{d}\mathbf{Z}(\Phi, \xi) \tag{5.37}$$

where $\mathbf{X}^{\mu\nu}$, $\mathbf{W}_\mu$, $\mathbf{Y}$ and $\mathbf{Z}$ are covariant quantities that are locally constructed from fields and their derivatives, $\mathbf{Y}$ is linear in $\delta_\xi\Phi$, and $\mathbf{Z}$ is linear in $\xi$. This decomposition of $\mathbf{Q}$ is not unique in the sense that there are many different ways for writing $\mathbf{Q}$ in the form (5.37), i.e. $\mathbf{W}_\mu$, $\mathbf{X}^{\mu\nu}$, $\mathbf{Y}$ and $\mathbf{Z}$ are not uniquely determined by $\mathbf{Q}$. Let us choose $\mathbf{X}^{\mu\nu}$ to be

$$(\mathbf{X}^{\mu\nu})_{\mu_3\ldots\mu_d} = -\frac{\delta\mathcal{L}}{\delta R_{\alpha\beta\mu\nu}}\boldsymbol{\epsilon}_{\alpha\beta\mu_3\ldots\mu_d}\,, \tag{5.38}$$

where $\boldsymbol{\epsilon}$ and $R_{\alpha\beta\mu\nu}$ are, respectively, volume form and Riemann tensor.

The Wald entropy is then defined as [374]

$$\boxed{S_{\text{BH}}^{\text{W}} := 2\pi \int_{\mathcal{B}} \mathbf{X}^{\mu\nu}\boldsymbol{\epsilon}_{\mu\nu}} \tag{5.39}$$

in which $\boldsymbol{\epsilon}_{\mu\nu}$ is the binormal tensor to the $(d-2)$- bifurcation surface $\mathcal{B}$, normalized as $\boldsymbol{\epsilon}_{\mu\nu}\boldsymbol{\epsilon}^{\mu\nu} = -2$. The Noether charge (5.37) is equal to the Wald entropy (5.39) if the $\mathbf{W}_\mu$-, $\mathbf{Y}$- and $\mathbf{Z}$-ambiguities vanish, and recalling the identity

$$(\mathrm{d}\xi_{\text{H}})_{\mu\nu} = 2\kappa\boldsymbol{\epsilon}_{\mu\nu}\,, \tag{5.40}$$

relating the horizon generating Killing vector $\xi_{\text{H}}$ with surface gravity $\kappa$.

We now argue that these ambiguities do not contribute to the Noether charge for $\xi_{\text{H}}$ [373]:

- $\mathbf{Y}$ does not contribute because $\mathbf{Y}$ is linear in $\delta_{\xi_{\text{H}}}\Phi$, and since $\xi_{\text{H}}$ is a Killing vector, $\delta_{\xi_{\text{H}}}\Phi = 0$.
- $\mathrm{d}\mathbf{Z}$ does not contribute because its integral over bifurcation surface $\mathcal{B}$ vanishes.
- $\mathbf{W}_\mu\xi^\mu$ does not contribute as long as $W$ remains finite at $\mathcal{B}$ because $\xi_{\text{H}}$ vanishes at the bifurcation surface $\mathcal{B}$.

## Wald entropy as Noether charge

Dropping these ambiguities, we have shown the conserved Noether–Wald charge associated with the horizon Killing vector is equal to

$$Q_{\zeta_{\text{H}}} = \int_{\mathcal{B}} \mathbf{Q}_{\zeta_{\text{H}}} = S_{\text{BH}}^{\text{W}}, \qquad \zeta_{\text{H}} := \frac{2\pi}{\kappa}\xi_{\text{H}}. \tag{5.41}$$

That is, *entropy is the Noether charge associated with Killing vector* $\zeta_{\text{H}}$. We crucially note that this normalization for $\zeta_{\text{H}}$ was a choice made and does not come from first principles. Note also that as the above derivation apparently shows (cf. (5.38)), the entropy does not depend on the "matter part" of the Lagrangian and only receives contributions from the "gravitational parts".

As an example let us consider the $d$-dimensional case where the gravity part of the action is given by Einstein–Hilbert, yielding

$$(\mathbf{X}^{\mu\nu})_{\mu_3\ldots\mu_d} = -\frac{\sqrt{-g}}{16\pi G_{\text{N}}}\frac{\delta R}{\delta R_{\alpha\beta\mu\nu}}\boldsymbol{\epsilon}_{\alpha\beta\mu_3\ldots\mu_d} = -\frac{\sqrt{-g}}{8\pi G_{\text{N}}}\boldsymbol{\epsilon}^{\mu\nu}{}_{\mu_3\ldots\mu_d}. \tag{5.42}$$

Plugging this into (5.39) we find

$$\boxed{S^{\mathrm{W}}_{\mathrm{BH}} = \frac{A_{\mathrm{H}}}{4G_{\mathrm{N}}}\,.} \tag{5.43}$$

This is the famous area law for BH entropy, which after reintroducing constants like Planck and Boltzman constants $\hbar$, $k_{\mathrm{B}}$ (see Exercise 5.5) yields

$$S_{\mathrm{BH}} = \frac{A_{\mathrm{H}} k_{\mathrm{B}} c^3}{4\hbar G_{\mathrm{N}}}\,. \tag{5.44}$$

### 5.4.2 Entropy and Solution Phase Space Method

As discussed, besides the Noether method, one may use the SPSM to compute charge variations and if integrable, the charges. One may use this method to compute the entropy as well. We define the entropy variation as

$$\hat{\delta} S := \oint_{\mathcal{B}} \boldsymbol{k}_{\zeta_{\mathrm{H}}}(\hat{\delta}\Phi, \Phi) = \frac{2\pi}{\kappa} \oint_{\mathcal{B}} \boldsymbol{k}_{\xi_{\mathrm{H}}}(\hat{\delta}\Phi, \Phi)\,, \tag{5.45}$$

where $\boldsymbol{k}_{\zeta_{\mathrm{H}}}(\hat{\delta}\Phi, \Phi)$ is defined in Appendix G and in the second equality above we have used its linearity in $\zeta_{\mathrm{H}}$. As the above equation shows, integrability of the charge over the solution phase space crucially depends on the normalization factor for $\zeta_{\mathrm{H}}$, as in (5.41).

That $\hat{\delta} S$ defined above is integrable should be checked and verified for each and every case. If integrable, one may prove that this entropy and the Wald entropy (5.39) are indeed equivalent, provided that the arguments for the vanishing of **W**, **Y**, **Z** go through.[1]

We recall that the covariant phase space method has also its own ambiguities [373], which arise when we use the Poincaré lemma on the spacetime or on the phase space. (Reference [376] calls these freedoms rather than ambiguities and fixes them by suitable physical requirements.) See the discussion in Appendix G. These freedoms do not appear in the entropy, again because $\xi_{\mathrm{H}}$ is a Killing vector vanishing at the bifurcation surface $\mathcal{B}$ and because $\delta_{\xi_{\mathrm{H}}}\Phi = 0$.

Finally, we remark that the entropy is a symplectic charge, i.e. , it could be computed by integration over any compact spacelike codimension-2 surface. In particular, the integration surface need not be the bifurcation surface $\mathcal{B}$ [377]. This may be proven along the same lines as in the previous section.

[1] While this is generically the case, there are examples within scalar-tensor theories (explicitly Horndeski theories) where the **W** ambiguity does not vanish. For these cases, the Wald formula should be handled with special care [375].

### 5.4.3 Entropy in Cases Involving Gauge Fields

In the analysis of the previous part, we assumed that $\zeta_{\rm H}$ is an exact symmetry. In the presence of gauge fields, it is typically not an exact symmetry and one may hence need to extend the Iyer–Wald formulation. For the discussion on the need for such an extension see [364–366,368], and for a clear-cut analysis see [377].

To this end, we construct an exact symmetry based on the Killing vector $\zeta_{\rm H}$. That is, we accompany $\zeta_{\rm H}$ with an appropriate gauge transformation $\lambda^a_{\zeta_{\rm H}}$ and construct $\eta_{\rm H} = (\zeta_{\rm H}, \lambda^a_{\zeta_{\rm H}})$ such that it is an exact symmetry. An example of this was shown in the extremal KN near horizon geometry in Sect. 5.3.2. To find $\lambda^a_{\zeta_{\rm H}}$ we note that $\zeta_{\rm H}$ is a symmetry of the solution, and hence

$$\mathcal{L}_{\zeta_{\rm H}} F^a = 0\,, \tag{5.46}$$

where $F^a = \mathrm{d}A^a$ is the gauge field strength. Using the Cartan's identity $\mathcal{L}_\xi X = \xi\cdot \mathrm{d}X - \mathrm{d}(\xi\cdot X)$, we learn

$$\mathrm{d}(\zeta_{\rm H}\cdot \mathrm{d}A^a) = 0 \qquad \overset{\text{locally}}{\Longrightarrow} \qquad \zeta_{\rm H}\cdot \mathrm{d}A^a = \mathrm{d}\mathcal{X}^a_{\rm H} \tag{5.47}$$

where $\mathcal{X}^a_{\rm H}$ is a scalar function. Then, using once again the Cartan identity, $\mathcal{L}_{\zeta_{\rm H}} A^a - \mathrm{d}(\zeta_{\rm H}\cdot A^a) = \mathrm{d}\mathcal{X}^a_{\rm H}$, we find

$$\mathcal{L}_{\zeta_{\rm H}} A^a = \mathrm{d}(\zeta_{\rm H}\cdot A^a + \mathcal{X}^a_{\rm H}) := \mathrm{d}\lambda^a_{\zeta_{\rm H}}\,. \tag{5.48}$$

That is, $\zeta_{\rm H}$ is an isometry generator *up to a gauge transformation*. As a result,

$$\eta_{\rm H} = \left\{\zeta_{\rm H}, -\lambda^a_{\zeta_{\rm H}} + \text{const.}\right\} \tag{5.49}$$

would be generator of an exact symmetry, with a constant over the spacetime that may depend on solution parameters and can be determined by the integrability condition over the solution phase space $\mathcal{S}_p$.

Although we have examples of solutions for which $\lambda^a_{\zeta_{\rm H}}$ is not zero (cf. the near horizon extremal KN geometry discussed in the previous section), the known black hole solutions are typically written in a gauge where $\zeta_{\rm H}$ is an exact symmetry, $\delta_{\zeta_{\rm H}} A^a = 0$, i.e. $\lambda^a_{\zeta_{\rm H}} = 0$. So, let us focus on these cases. One may then check that the *integrability condition* (5.13) fixes the constant part as

$$\eta_{\rm H} = \left\{\zeta_{\rm H}, -\frac{2\pi}{\kappa}\Phi^a_{\rm H}\right\}, \tag{5.50}$$

where $\Phi^a_{\rm H} = \zeta_{\rm H}\cdot A^a|_{\text{horizon}}$ are the horizon electric potentials. The details are left to the Exercise 5.8.

**Summary**

For non-extremal black holes with a Killing horizon as solutions to covariant gravitational theories, the entropy $S$ can be defined as the conserved charge associated with $\eta_{\rm H}$ (5.50) calculated on any smooth and closed $(d-2)$-dim surface surrounding the black hole.

If integrable, the definition (5.45) with $\eta_{\rm H}$ from (5.50) reproduces the same results as the Iyer–Wald entropy in cases without gauge field. We close this part with some further comments:

1. Entropy is defined as the conserved charge $Q_{\eta_{\rm H}}$ using SPSM, instead of the Noether–Wald charge.
2. The surface of integration need not be the bifurcation surface, as $\eta_{\rm H}$ is an exact symmetry. Since we are using SPSM, we need not rely on the vanishing of $\eta_{\rm H}$ over the horizon to kill the **W** ambiguity of the Noether–Wald charge.
3. One may check that if we do not include the gauge transformation part in our symmetry generator $\eta_{\rm H}$, the entropy will be typically non-integrable over $\mathcal{S}_p$.

To illustrate the above formulas in practice, we present the computation of the entropy for the two examples we discussed in the previous section.

**Entropy for Kerr-AdS**

The Killing vector generating the horizon of the Kerr-AdS black hole (5.16) is

$$\xi_{\rm H} = \partial_t + \Omega_{\rm H}\partial_\varphi, \qquad \Omega_{\rm H} = \frac{a(1+\frac{r_{\rm H}^2}{\ell^2})}{r_{\rm H}^2+a^2} \tag{5.51}$$

and $r_{\rm H}$ is the radius of its event horizon and a solution to $\Delta_r = 0$ (5.17), explicitly

$$(r_{\rm H}^2+a^2)(r_{\rm H}^2+\ell^2) - 2G_{\rm N}m\ell^2 r_{\rm H} = 0. \tag{5.52}$$

A direct examination of (5.13), noting that $\Omega_{\rm H}$ is parameter dependent and hence $\hat{\delta}\xi_{\rm H} \neq 0$, reveals that the charge associated with $\xi_{\rm H}$ is *not* integrable over the sector of the phase space with parametric variations. Nonetheless, one may check the charge is integrable for $\zeta_{\rm H} := \frac{2\pi}{\kappa}\xi_{\rm H}$, where

$$\kappa = \frac{r_{\rm H}(1+\frac{a^2}{\ell^2}+3\frac{r_{\rm H}^2}{\ell^2}-\frac{a^2}{r_{\rm H}^2})}{2(r_{\rm H}^2+a^2)} \tag{5.53}$$

is surface gravity. The details are left as an exercise to the reader and more remarks may be found in Appendix B of [377]. One can integrate $\hat{\delta}Q_{\zeta_{\rm H}}$ to obtain the corresponding charge, the entropy. We emphasize that $\hat{\delta}Q_{\zeta_{\rm H}}$ may be defined over any codimension-2, compact spacelike surface $\partial\Sigma$ that surrounds the black hole and not necessarily the bifurcation horizon; this surface can be even inside the horizon. The result, independently of the choice of such $\partial\Sigma$, is

$$\hat{\delta} Q_{\zeta_{\mathrm{H}}} = \frac{\partial \left(\frac{\pi(\mathrm{r}_{\mathrm{H}}^2 + a^2)}{G_{\mathrm{N}}\,\Xi}\right)}{\partial m}\delta m + \frac{\partial \left(\frac{\pi(\mathrm{r}_{\mathrm{H}}^2 + a^2)}{G_{\mathrm{N}}\,\Xi}\right)}{\partial a}\delta a\,. \tag{5.54}$$

By choosing the pure AdS$_4$ spacetime as the reference point with $Q_{\zeta_{\mathrm{H}}}[\bar{\Phi}] = 0$, (5.54) results in the entropy for Kerr-AdS black hole

$$S = Q_{\zeta_{\mathrm{H}}} = \frac{\pi(\mathrm{r}_{\mathrm{H}}^2 + a^2)}{G_{\mathrm{N}}\,\Xi}\,, \tag{5.55}$$

in agreement with the results of [378,379]. We end this example with some comments:

1. The above discussions stress the role of the normalization of $\xi_{\mathrm{H}}$ by $2\pi/\kappa$ and the integrability of its charge. Integrability is generally highly sensitive to the appropriate choice of vector fields. For example, had we chosen the metric in Boyer–Lindquist coordinates (which can be found, e.g. in [379]), the time would be something different than $t$ in (5.16). Let us denote it by $\tau$. One may then check that $\partial_\tau$ does *not* yield an integrable conserved charge. As a result, our SPSM formulation can be used for investigating appropriate Killing vector fields associated with mass or other conserved integrable charges.
2. Entropy has been found as a Hamiltonian generator, instead of Noether–Wald charge of $\zeta_{\mathrm{H}}$. Notice that they are different by the last term in (G.13). That extra term vanishes on the bifurcation of the horizon because $\zeta_{\mathrm{H}}$ vanishes there. This is a key point in allowing us to define entropy on *any* surface $\partial\Sigma$ and free us from defining it on the bifurcation surface only as is prescribed in Wald's entropy [374].
3. For the extremal case, where $\kappa = 0$, there is no properly normalized Killing vector field $\zeta_{\mathrm{H}}$. For this case, however, there are infinitely many such Killing vectors in the *near horizon region* [367]. We will consider this in our next example.

---

**> Entropy for near horizon extremal KN geometry.**

While not a black hole and not having an event horizon, the near horizon extremal KN geometry (5.23) has null Killing vectors that vanish at codimension-2 compact surfaces, see Fig. 5.2. These geometries have Killing horizons that are in fact bifurcate Killing horizons [367,380]. One may hence apply our formulation for the calculation of its entropy.

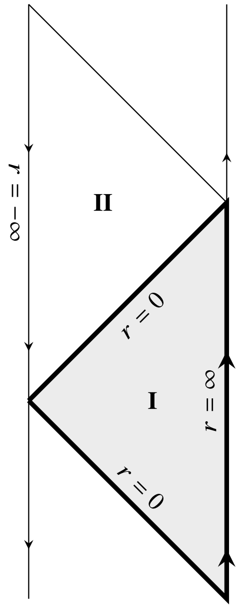


**Fig. 5.2** Penrose diagram for near horizon extremal KN black hole, suppressing the angular directions [380]. The positive and negative $r$ values of the coordinates used in (5.23) respectively cover regions **I** and **II**. Arrows on the boundaries show the flow of time $t$, which is reversed between regions **I** and **II**

As discussed in [367], any surface of constant time and radius, dubbed as $\mathcal{H}$, is the bifurcation point of a Killing horizon. To see this, recall that this geometry has $SL(2,\mathbb{R}) \times U(1)_\varphi$ isometry (5.26). The $SL(2,\mathbb{R})$ part has three non-commuting Killing vectors and any arbitrary linear combination of them is also a Killing vector. In particular, consider

$$\xi_{\mathcal{H}}(t_{\mathcal{H}}, r_{\mathcal{H}}) = -\frac{t_{\mathcal{H}}^2 r_{\mathcal{H}}^2 - 1}{2r_{\mathcal{H}}}\xi_- + t_{\mathcal{H}} r_{\mathcal{H}} \xi_0 - r_{\mathcal{H}}\xi_+ - k\partial_\varphi \,. \tag{5.56}$$

where $t_{\mathcal{H}}$ and $r_{\mathcal{H}}$ are two arbitrary parameters. One may check that this vector vanishes at $t = t_{\mathcal{H}}, r = r_{\mathcal{H}}$. Therefore, every $\xi_{\mathcal{H}}(t_{\mathcal{H}}, r_{\mathcal{H}})$ generates a bifurcation horizon at $t = t_{\mathcal{H}}, r = r_{\mathcal{H}}$. Let's denote such constant $t, r$ surfaces by $\mathcal{H}$. One may then use (3.1) or (3.2) to compute surface gravity associated with $\xi_{\mathcal{H}}(t_{\mathcal{H}}, r_{\mathcal{H}})$ at $\mathcal{H}$. This yields $\kappa = 1$ and is independent of $t_{\mathcal{H}}, r_{\mathcal{H}}$ [380]. So, the normalized horizon Killing vectors would be

$$\zeta_{\mathcal{H}} = \frac{1}{2\pi}\xi_{\mathcal{H}}(t_{\mathcal{H}}, r_{\mathcal{H}}).$$

Although $\zeta_{\mathcal{H}}$ are Killing vectors, they are not exact symmetries because $\delta_{\zeta_{\mathcal{H}}} A = \frac{-2\pi e r_{\mathcal{H}}}{r^2}\mathrm{d}r \neq 0$. Instead, $\{\zeta_{\mathcal{H}}, \frac{-2\pi e r_{\mathcal{H}}}{r} + \text{const.}\}$ are exact symmetries. The constant by the integrability condition can be fixed to $2\pi e$ [377], i.e.

$$\eta_{\mathcal{H}} = \left\{\zeta_{\mathcal{H}}, 2\pi e\Big(\frac{r - r_{\mathcal{H}}}{r}\Big)\right\}. \tag{5.57}$$

Similarly to $\zeta_{\mathcal{H}}$, the exact symmetry generator $\eta_{\mathcal{H}}$ also vanishes at the bifurcation surface $\mathcal{H}$ at $t = t_{\mathcal{H}}, r = r_{\mathcal{H}}$. Inserting $\eta_{\mathcal{H}}$ and the parametric variations in (5.45), we obtain

$$\hat{\delta} Q_{\eta_{\mathcal{H}}} = \frac{4\pi a}{G_{\text{N}}}\delta a + \frac{2\pi q}{G_{\text{N}}}\delta q \,. \tag{5.58}$$

Integrating over the solution phase space, the entropy is found as

$$S := Q_{\eta_{\mathcal{H}}} = \frac{\pi(2a^2 + q^2)}{G_{\text{N}}} \,. \tag{5.59}$$

As expected, this result is independent of $t_{\mathcal{H}}$, $r_{\mathcal{H}}$ and the bifurcation surface $\mathcal{H}$ chosen.

## 5.5 Four Laws of Black Hole Thermodynamics

In their famous paper, James Bardeen, Brandon Carter, and Stephen Hawking [77], laid out the idea that black holes and their dynamics regardless of the details, follow four laws that closely resemble the laws of thermodynamics. These laws are results of the classical dynamics governed by generally covariant field equations and some assumptions on the black hole solution, like having a Killing horizon and stationarity. These four laws of black hole mechanics turned out to be not just resembling, but exactly the laws of thermodynamics in the presence of black holes and horizons [381], after Hawking's discovery of semiclassical black hole radiation [78,79]. Here, we discuss the laws of black hole thermodynamics.

The general picture for black hole thermodynamics is that stationary black holes behave like thermodynamical systems at equilibrium specified by a temperature and some other chemical potentials. Moreover, the horizon is where this thermodynamic system is located. The precise derivations and proofs of the laws of black hole thermodynamics, besides stationarity, usually use the existence of Killing horizons. Nonetheless, the thermodynamic description of black holes and the general picture is believed to be true in more general setups where the system is not strictly stationary and we allow an adiabatic flow of energy and charges into the black hole, as we have in usual thermodynamical systems.

### 5.5.1 Zeroth Law

The zeroth law states that the black hole temperature is a constant over the horizon and is proportional to surface gravity,

$$\boxed{\text{Zeroth Law:} \qquad T_{\text{H}} = \frac{\kappa}{2\pi} = \text{const.}} \tag{5.60}$$

We will discuss this in detail in the next chapter where we show that indeed $T_{\rm H}$ is the temperature of the Hawking radiation, black body radiation emitted from the horizon of the black hole, as measured by the observer sitting in the asymptotic region of spacetime.

**> Constancy of surface gravity over the Killing horizon**

To show that surface gravity is constant on the horizon, it is sufficient to prove $v^\mu\partial_\mu\kappa = 0$ at the horizon for any vector $v$ tangent to the horizon. If we denote the null Killing vector field generating the horizon by $\xi^\mu_{\rm H}$ and the $D-2$ linearly independent spacelike vectors spanning the horizon by $e^\mu_a$, $a = 1, 2, \ldots, D-2$ such that $\xi_{\rm H}\cdot e_a = 0$, then $\xi^\mu_{\rm H}\partial_\mu\kappa = e^\mu_a\partial_\mu\kappa = 0$ at the horizon. The relation $\xi^\mu_{\rm H}\partial_\mu\kappa = 0$ directly follows from the definition of $\kappa$ as surface gravity; see Exercise 3.1.

To show $e^\mu_a\partial_\mu\kappa = 0$ one should provide some further information. This extra piece of information may be provided if we have a bifurcate Killing horizon and recall that $\xi_{\rm H}$ vanishes at the codimension-2 bifurcation surface $\mathcal{B}$, cf. Chap. 3. (In our conventions here $\mathcal{B}$ is spanned by $e^\mu_a$.) The proof is left as an exercise to the reader, see Exercise 5.7. For physically interesting problems like gravitational collapse, we do not have a bifurcate horizon and we need other arguments to provide this further information.

Within Einstein gravity and using Einstein equations, the DEC, cf. Sect. 3.2.2, can provide this extra piece of information. To see how this works, we recall that for the Killing horizon,

$$R_{\mu\nu}\xi^\mu_{\rm H}\xi^\nu_{\rm H} = 0 = T_{\mu\nu}\xi^\mu_{\rm H}\xi^\nu_{\rm H} \qquad \text{at the horizon,} \tag{5.61}$$

where in the second equality we have used the Einstein field equations. DEC implies that $P_\mu := T_{\mu\nu}\xi^\nu_{\rm H}$ is a causal (timelike or null) vector at the horizon. Therefore, $P^\mu =$ is parallel to $\xi^\mu_{\rm H}$ at the horizon (see part (3) of Exercise 3.6) and hence $R_{\mu\nu}\xi^\nu_{\rm H}$ is a vector along $\xi_{{\rm H}\,\mu}$, i.e.

$$\xi_{{\rm H}\,[\mu}R_{\nu]\alpha}\xi^\alpha_{\rm H} = \xi_{{\rm H}\,[\mu}\partial_{\nu]}\kappa = 0 \qquad \text{at the horizon.} \tag{5.62}$$

The above means that $\partial_\mu\kappa$ is parallel to $\xi_{{\rm H}\,\mu}$ at the horizon and that $v^\mu\partial_\mu\kappa = 0$ at the horizon for any vector $v$ tangent to the horizon.

---

Besides the temperature, if we have conserved charges other than the energy in the system, like angular momentum and electric charge, there are associated chemical potentials. The constancy of these chemical potentials over the horizon is also a part of the first law. The horizon angular velocity $\Omega_{\rm H}$ is a constant because for a Killing horizon, $\xi_{\rm H}$ is hypersurface orthogonal at the horizon. This physically means that all points on the horizon of stationary black holes are rotating at the same speed. Note that $\Omega_{\rm H}$ is by definition the angular velocity measured in the *asymptotically static* coordinate system.

The chemical potential associated with the electric charge, the horizon electric potential $\Phi_{\rm H}$, is defined as

$$\Phi_{\rm H} := \xi_{\rm H} \cdot A_{\rm H}, \tag{5.63}$$

where $A_{\rm H}$ is the 1-form electric field for the black hole solution computed at the horizon. The constancy of $\Phi_{\rm H}$ follows from the fact that $\xi_{\rm H}$ is an isometry of the metric as well as a symmetry of the gauge field, see Exercise 5.8. It means that the horizon of a stationary black hole is an equipotential surface.

### 5.5.2 First Law and Its Derivation

While at equilibrium, thermodynamical systems allow for variations/perturbations that respect energy conservation, i.e. satisfy the first law of thermodynamics. The first law is typically written as $\not{\delta} Q = \delta U - \sum_n \mu_n \delta q_n$ where $\not{\delta} Q$ denotes the heat transfer, $U$ is the internal energy, $\mu_n$ are the chemical potentials and $q_n$ are other conserved charges the system may have. These variations/perturbations, as discussed in Sect. 5.3, may be parametric variations or perturbations satisfying field equations linearized over the stationary black hole background. As familiar from standard thermodynamics, the heat perturbation is denoted by $\not{\delta} Q$, since $Q$ is not an integrable charge over the phase space (of the statistical mechanical system). It may be written in terms of the entropy $S$, through the Clausius relation $\not{\delta} Q := T\delta S$.

Black holes as thermodynamical systems satisfy a similar first law, which readily follows from our earlier preparations of Sect. 5.1. A black hole behaves like a heat reservoir at a given temperature and chemical potentials. The other charges and the energy then include the black hole plus anything else that is outside the horizon of the black hole. The variations and perturbations are associated with changes in the charges with fixed chemical potentials, which may be due to interactions of the black hole with its environment, e.g. , things that fall into the black hole or may be emitted by it.

There are two versions of the first law of black hole mechanics, one which was originally discussed by Bardeen, Carter and Hawking in [77] and the more general one which was first derived by Iyer and Wald in [373,374]. Both of these versions require black holes to have a Killing horizon. In the Bardeen–Carter–Hawking derivation the perturbations appearing in the first law are the parametric variations (cf. Sect. 5.3) whereas the Iyer–Wald derivation is more general and besides parametric variations involves any perturbation which satisfies linearized EOM. Here we discuss this more general first law which is a consequence of diffeomorphism invariance of the field theory governing black hole and its environment.

Given our SPSM discussion in Sect. 5.3 the first law is a direct consequence of the equation which relates horizon generating Killing vector $\xi_{\rm H}$ to the other Killing vectors of the system, e.g. for Kerr or Kerr-(A)dS black hole,

$$\xi_{\rm H} = \partial_t + \Omega_{\rm H} \partial_\phi,$$

with the normalization that $t$ is denoting the time coordinate for the asymptotic observer, who is assumed to be static (non-rotating) to define $\Omega_{\rm H}$. As discussed, entropy is an integrable charge of $\xi_{\rm H}$ properly normalized by the inverse of the temperature $2\pi/\kappa$:

$$\zeta_{\rm H} = \frac{2\pi}{\kappa}\left(\partial_t + \Omega_{\rm H}\partial_\phi\right) , \tag{5.64}$$

For the cases where we have gauge fields, as discussed in Sect. 5.4.2, we need to consider

$$\eta_{\rm H} = \left\{\zeta_{\rm H}, -\frac{2\pi}{\kappa}\Phi^a_{\rm H}\right\} , \tag{5.65}$$

as the exact symmetry generating the horizon.

## Derivation of the first law

Here we follow the derivation given in [377]. Assume that a stationary non-extremal black hole is given as a solution to a covariant gravitational theory in $d$-dimensional spacetime with generic fields collectively called $\Phi$. Let the horizon be generated by the exact symmetry $\eta_{\rm H}$, e.g. as in (5.65), we have $\delta_{\eta_{\rm H}}\Phi = 0$. The Lee–Wald symplectic current density

$$\boldsymbol{\omega}(\delta\Phi, \delta_{\eta_{\rm H}}\Phi, \Phi) = \delta\boldsymbol{2}(\delta_{\eta_{\rm H}}\Phi, \Phi) - \delta_{\eta_{\rm H}}\boldsymbol{2}(\delta\Phi, \Phi) , \tag{5.66}$$

which is linear in $\delta_{\eta_{\rm H}}\Phi$, vanishes. Integrating $\boldsymbol{\omega}$ over an arbitrary $(d-1)$-dimensional spacelike surface $\Sigma$ with two closed and smooth boundaries $\partial_1\Sigma$ and $\partial_2\Sigma$ surrounding the black hole, and noting (G.9), we obtain

$$\int_\Sigma \boldsymbol{\omega}(\delta\Phi, \delta_{\eta_{\rm H}}\Phi, \Phi) = \int_\Sigma \mathrm{d}\boldsymbol{k}_{\eta_{\rm H}}(\delta\Phi, \Phi) \tag{5.67}$$

$$= \oint_{\partial_2\Sigma} \boldsymbol{k}_{\eta_{\rm H}}(\delta\Phi, \Phi) - \oint_{\partial_1\Sigma} \boldsymbol{k}_{\eta_{\rm H}}(\delta\Phi, \Phi) . \tag{5.68}$$

Since $\delta_{\eta_{\rm H}}\Phi = 0$,

$$\oint_{\partial_1\Sigma} \boldsymbol{k}_{\eta_{\rm H}}(\delta\Phi, \Phi) = \oint_{\partial_2\Sigma} \boldsymbol{k}_{\eta_{\rm H}}(\delta\Phi, \Phi) , \tag{5.69}$$

one may drop the index 1 or 2 on $\partial_i\Sigma$. As in (5.45) we define the entropy perturbation as

$$\delta S := \oint_{\partial\Sigma} \boldsymbol{k}_{\eta_{\rm H}}(\delta\Phi, \Phi) . \tag{5.70}$$

The generator $\eta_{\rm H} = \{\zeta_{\rm H}, -\frac{2\pi}{\kappa}\Phi_{\rm H}\}$ can be decomposed as

$$\eta_{\rm H} = \left\{\frac{2\pi}{\kappa}\partial_t, 0\right\} + \left\{\frac{2\pi\Omega_{\rm H}}{\kappa}\partial_\phi, 0\right\} + \left\{0, -\frac{2\pi}{\kappa}\Phi_{\rm H}\right\} . \tag{5.71}$$

Since $\boldsymbol{k}$ is linear in the generators, the entropy variation reads

$$\delta S = \frac{2\pi}{\kappa}\oint_{\partial\Sigma} \boldsymbol{k}_{\partial_t}(\delta\Phi, \Phi) + \frac{2\pi\,\Omega_{\mathrm{H}}}{\kappa}\oint_{\partial\Sigma} \boldsymbol{k}_{\partial_\phi}(\delta\Phi, \Phi) - \frac{2\pi}{\kappa}\Phi_{\mathrm{H}}\oint_{\partial\Sigma} \boldsymbol{k}_{\{0,1\}}(\delta\Phi, \Phi)\,. \tag{5.72}$$

Recalling our definitions for mass, angular momenta and electric charge, cf. Sect. 5.3, and using (5.60) yields the first law of black hole thermodynamics.

$$\boxed{\text{First Law:} \qquad \delta M = T_{\mathrm{H}}\delta S + \Omega_{\mathrm{H}}\delta J + \Phi_{\mathrm{H}}\delta Q} \tag{5.73}$$

We close our derivation with some comments and remarks:

- The above derivation works for any stationary and axisymmetric black hole with a Killing horizon, as a solution to a generic gravity theory with generic matter content in any dimension, even if we do not know the explicit form of the solution. It only uses the diffeomorphism invariance of the theory.
- The charge variations above may correspond to any perturbation on the background black hole solution. In particular, for the parametric variations, it yields the Bardeen–Carter–Hawking form of the first law [77], which in our notations is,
$$\hat{\delta} M = T_{\mathrm{H}}\hat{\delta} S + \Omega_{\mathrm{H}}\hat{\delta} J + \Phi_{\mathrm{H}}\hat{\delta} Q. \tag{5.74}$$
- In our derivation, unlike the one in [373], we need not take the $\partial_1\Sigma$, $\partial_2\Sigma$ to be the bifurcation surface of the horizon or $\boldsymbol{i^0}$ at infinity. As emphasized in Sect. 5.3, the charges associated with exact symmetries are symplectic and may be defined by integration over any codimension-2 spacelike compact surface $\partial\Sigma$. Therefore, as long as we have the Killing horizon and the appropriately normalized $\eta_{\mathrm{H}}$, we can derive the first law.
- While the existence of a Killing horizon and $\eta_{\mathrm{H}}$ is an essential part of our derivation, the integrations need not be done at the horizon. This surface can be a bit inside or a bit outside the horizon. Also, our derivation makes it evident that the charge perturbations and in particular the energy perturbation in the first law can have any sign. Explicitly, the same first law should hold when a black hole acts as a sink, accreting matter into it, or when it acts as a source when due to quantum effects it Hawking-radiates (see the next chapter), or when two black holes coalesce and merge.
- While our derivation is more general than the one of Iyer–Wald [373] in the sense mentioned above, it is a bit stricter, as we require $\partial_t$, $\partial_\phi$ to be Killing (exact) symmetries of the background, i.e. we have assumed stationarity and axisymmetry. One may, however, repeat the same steps as above and only assume having $\partial_t$, $\partial_\phi$ as *asymptotic symmetries*, plus having a Killing horizon. In this case, we will then need to limit our integration surfaces $\partial_1\Sigma$, $\partial_2\Sigma$ to be the bifurcation surface and $\boldsymbol{i^0}$ for asymptotically flat cases (or the constant time surface at the boundary of AdS, for asymptotic AdS spaces).

- In our derivation, while we used existence of a bifurcate Killing horizon, we did not require it be the outer (event) horizon. All the analysis above in principle also holds for inner horizons and there exists an inner horizon first law. Despite negative surface gravity on inner horizons, such thermodynamic-like relations exist also in the form of zeroth and first law of inner horizon black hole mechanics. See Exercise 5.10 for more details as well as [382] and refs. therein.

---

### First law for KN black hole

The KN black hole is a solution to Einstein–Maxwell theory described by ($\theta \in [0, \pi)$, $\varphi \sim \varphi + 2\pi$)

$$
\begin{aligned}
\mathrm{d}s^2 &= -\frac{\Delta}{\rho^2}\big(\mathrm{d}t - a\sin^2\theta\,\mathrm{d}\varphi\big)^2 + \frac{\rho^2}{\Delta}\,\mathrm{d}r^2 + \rho^2\,\mathrm{d}\theta^2 \\
&+ \frac{(r^2+a^2)^2}{\rho^2}\sin^2\theta\big(\mathrm{d}\varphi - \frac{a}{r^2+a^2}\,\mathrm{d}t\big)^2 \\
A &= \frac{qr}{\rho^2}(\mathrm{d}t - a\; sin^2\theta \mathrm{d}\varphi)
\end{aligned}
\tag{5.75}
$$

where

$$
\rho^2 := r^2 + a^2\cos^2\theta \qquad\qquad \Delta := r^2 - 2mr + a^2 + q^2. \tag{5.76}
$$

This solution has three parameters $m, a, q$ and is the unique asymptotically flat solution to Einstein–Maxwell theory with a given mass, angular momentum, and electric charge. This solution is stationary and axisymmetric with Killing vectors $\partial_t, \partial_\varphi$. The horizons radii $r_{\mathrm{H}}$ are given by roots of $\Delta$, $r_{\mathrm{H}}^2 - 2mr_{\mathrm{H}} + a^2 + q^2 = 0$. Here we take the outer horizon for which

$$
r_{\mathrm{H}} = m + \sqrt{m^2 - q^2 - a^2}. \tag{5.77}
$$

The surface gravity, horizon angular velocity and electric potentials are

$$
\kappa = \frac{r_{\mathrm{H}}^2 - q^2 - a^2}{2(r_{\mathrm{H}}^2 + a^2)r_{\mathrm{H}}}, \qquad \Omega_{\mathrm{H}} = \frac{a}{a^2 + r_{\mathrm{H}}^2}, \qquad \Phi_{\mathrm{H}} = \xi_{\mathrm{H}} \cdot A\Big|_{r=r_{\mathrm{H}}} = \frac{qr_{\mathrm{H}}}{r_{\mathrm{H}}^2 + a^2}, \tag{5.78}
$$

where $\xi_{\mathrm{H}} = \partial_t - \Omega_{\mathrm{H}}\partial_\varphi$ is the Killing vector generating the horizon.

One may use the ADM method or our SPSM to read the mass $m$, angular momentum $J$, entropy $S$ and electric charge $Q$:

$$
M = \frac{m}{G_{\mathrm{N}}}, \qquad J = \frac{ma}{G_{\mathrm{N}}}, \qquad Q = \frac{q}{G_{\mathrm{N}}}, \qquad S = \frac{\pi(r_{\mathrm{H}}^2 + a^2)}{G_{\mathrm{N}}} \tag{5.79}
$$

To verify the first law for parametric variations, we note that

$$\delta M = \frac{\delta m}{G_{\rm N}}\,, \quad \delta J = \frac{\delta m a + m\delta a}{G_{\rm N}}\,, \quad \delta Q = \frac{\delta q}{G_{\rm N}}\,, \quad \delta S = \frac{2\pi(r_{\rm H}\delta r_{\rm H} + a\delta a)}{G_{\rm N}}\,. \tag{5.80}$$

It is then immediate to observe that $\frac{\kappa}{2\pi}\delta S = \delta M - \Omega_{\rm H}\delta J - \Phi_{\rm H}\delta Q$.

**Smarr relations**

The first law involves a relation between charge variations and the chemical potentials and as discussed above can be proved under very general conditions for any black hole solution to a generic diffeomorphism invariant gravity theory. In this sense, the first law is universally true. On the other hand, we discussed some different methods to compute the charges. One may then ask if a relation similar to the first law but with charges rather than charge variations, can still hold in general. As was first done by Larry Smarr [383], given (5.78), (5.79), one can easily observe that for the KN black hole there is such a simple relation,

$$M = 2T_{\rm H}S_{\rm BH} + 2\Omega_{\rm H}J + \Phi_{\rm H}Q\,. \tag{5.81}$$

The factors of two in the above for the $Q = 0$ case may be obtained using a scaling argument attributed to Gary Gibbons: One may integrate the first law, noting that the horizon area and $J = ma$ are scaling as mass squared [244]. Similar relations exist for other black holes (see Exercise 5.11). However, they cannot be computed by integrating the first law. The reason is that the chemical potentials are in general functions of all the charges. The Smarr type relations are not universal, unlike the first law; their form depends on the theory as well as the asymptotic behavior of the solution, see e.g. Exercise 5.11.

### 5.5.3 Second Law and Its Generalizations

In ordinary thermodynamics, the second law stipulates that entropy variation of a closed system in any physical process should always be non-negative as we move forward in time. In presence of a black hole horizon, things can fall into the black hole and become inaccessible to the outside observer. Therefore, the entropy variation as seen by the outside observer can become negative, violating the ordinary second law.

One may argue that thermodynamical systems in presence of black holes are in fact open systems and need not respect the second law. However, as usual in thermodynamical systems, one would expect to be able to close the system by adding the sink or source to the system and viewing the sink or source as a part of the thermodynamical system. This viewpoint was adopted by Bekenstein [76,384]. He saved the second law of thermodynamics from violations by postulating the generalized second law [385]: the sum of ordinary entropy of systems outside black hole $S_{\text{out}}$ and the total black hole entropy $S_{\text{BH}}$ should not decrease,

$$\boxed{\text{Generalized Second Law:} \qquad \delta(S_{\text{BH}} + S) \geq 0} \tag{5.82}$$

As the first example, let us consider a gas of photons at a given temperature $T$ and energy $\delta E$ which falls into a Schwarzschild black hole of mass $M$. The latter, as discussed is a system at the Hawking temperature $1/T_{\text{H}} = 8\pi G_{\text{N}} M$ and the entropy $S^0_{\text{BH}} = 4\pi G_{\text{N}} M^2$. The entropy of the initial system is hence $S_{\text{BH}} + 4\delta E/(3T)$. When the gas of photons falls into the black hole, assuming $\delta E \ll M$, the black hole settles down into a new black hole of mass $M + \delta E$, and hence its entropy is $4\pi G_{\text{N}}(M + \delta E)^2 \simeq S^0_{\text{BH}} + \delta E/T_{\text{H}}$, as expected from the first law discussed in the previous section. The generalized second law is then satisfied if $\delta E/T_{\text{H}} \geq 4\delta E/(3T)$ or $T_{\text{H}} \leq 3T/4$. Recall that the wavelength $\lambda$ of a photon that can be absorbed into the black hole should obey $\lambda \leq 4r_{\text{H}}$. This implies the inequality $k_{\text{B}} T = 2\pi/\lambda \geq \pi/(2r_{\text{H}})$ for the temperature of the photons. Since $T_{\text{H}} = 1/(4\pi r_{\text{H}})$ for a Schwarzschild black hole, then $T_{\text{H}} \leq T/(2\pi^2)$. Therefore, the generalized second law is satisfied. Similarly, one may verify the second law for other types of black holes and for other kinds of matter falling into the black hole.

If this other system is another black hole, then the statement of the second law for Einstein gravity simply reduces to Hawking's area theorem (cf. discussions in Sect. 3.3).

Our discussions so far were mainly classical, where the black holes act as a "sink", for matter accreting into the black hole or for black hole mergers. Quantum mechanically, as we will see in the next chapter, black holes can also behave as "sources" from which things can leak out. It turns out that our discussions here and the laws of black hole thermodynamics, in particular the second law, extend to the semiclassical level, as long as there exists a background independent diffeomorphism invariant gravity description. This is significant because, as we shall see, during the process of Hawking radiation the area theorem does not hold due to a failure of the energy condition assumed by the theorem. We shall discuss this in the next chapter, especially Sects. 6.5 and 6.6. More formal proofs of the second law and more discussions once quantum effects are also taken into account may be found in [386–388].

### 5.5.4 Third Law and Extremal Black Holes

The third law of thermodynamics has been formulated in a variety of ways and is perhaps not as clean and clear as the other laws. The third law is to describe the behavior of thermodynamics systems at and close to absolute zero temperature, where quantum physics is believed to be essential. A classic(al) statement of the third law is Walter Nernst's unattainability principle with two possible statements: (1) isothermal reversible processes become isentropic in the limit of zero temperature;

(2) the temperature of a system cannot be reduced to zero in a finite number of operations. Planck has a stronger version which also takes quantum effects into account: As $T \to 0$, the entropy of any system tends to zero. This essentially means that the vacuum state is unique, which is not true for all quantum systems, including black holes.

Namely, In the case of black holes, where the temperature is given by surface gravity, the zero-temperature limit corresponds to extremal black holes. Planck's version of the third law does not hold, because extremal black holes do have non-vanishing entropy that depends on their charges. However, Nernst's statement still holds [389]: It is impossible by any physical process, no matter how idealized, to reduce surface gravity to zero in a finite sequence of operations.

$$\boxed{\text{Third Law:} \qquad \kappa \to 0 \text{ impossible}} \tag{5.83}$$

A precise statement of the black hole third law due to Werner Israel is: No continuous process in which the energy-momentum tensor of the accreted matter remains bounded and satisfies the WEC in a neighborhood of the apparent horizon can reduce the surface gravity of a black hole to zero within a finite advanced time for a network of observers encircling the horizon. See [389] for more discussions and the proof. This implies that one cannot form an extremal black hole through a gravitational collapse process. It also implies that a non-extreme black hole cannot reduce to an extremal black hole through the Penrose process. If true at the quantum level, this also implies that one cannot reach an extremal black hole through the Hawking radiation process. In the next chapter, we provide further discussions on the latter point.

## Further Reading

Besides the references provided in the main text and also in Appendices F and G, we refer the reader to original papers on developing further gauge symmetries and covariant phase space formalism [390–394] or lecture notes and theses [395–397]. For the computation of charges and laws of black hole thermodynamics see [352, 387, 388, 390, 398–402]. The converse of deriving thermodynamics from Einstein gravity, i.e. to derive the Einstein equations by assuming some thermodynamical relations, was pioneered by Ted Jacobson [403], see also [404] for more recent developments.

## Exercises

**5.1 Triviality of Komar charges for vacuum solutions?**

A quick (but incorrect) argument evaluates the Komar charges of vacuum solutions to zero: take the expression (5.4) and use the vacuum Einstein equations $R_{\mu\nu} = 0$ to deduce $\mathcal{K}^{\mu}_{\xi} = 0$. Why is this argument incorrect for black holes but correct for Minkowski space?

**5.2 On Komar charges.**

(1) Using (3.28) prove (5.6).

(2) Use the Komar formula for Kerr geometry and compute the conserved charges associated with its two Killing vectors $\xi = \partial_t, \partial_\phi$, respectively mass, and angular momentum. Show that $c_\xi$ given in (5.7) indeed reproduces the same conventions for the ADM mass and angular momentum for Kerr black hole.

(3) Use the Komar formula to compute mass and angular momentum for AdS-Kerr and dS-Kerr solutions.

**5.3 More on generic variations (5.8).**

(1) Show that variations $\delta_\chi \Phi$, $\hat{\delta}_p \Phi$ (5.8) both satisfy linearized field equations. Explore which other solutions to linearized EOM could be there that are not among these two variations.

(2) Show that any two successive parametric and gauge variations always commute,

$$\hat{\delta}_p \delta_\chi \Phi(x; p_\alpha; F_a(x)) = \delta_\chi \hat{\delta}_p \Phi(x; p_\alpha; F_a(x)) \tag{5.84}$$

while two successive parametric transformations or two successive diffeomorphism- and gauge transformations need not commute.

(3) Show that the above implies

$$(\delta_\chi \hat{\delta}_p - \hat{\delta}_p \delta_\chi) Q_{\eta_i}[\Phi] = 0 \qquad \forall \chi, p_\alpha. \tag{5.85}$$

That is, any exact symmetry charge $Q_{\eta_i}$, and any charge associated with non-proper diffeomorphism- and gauge transformations $Q_{\chi_a}$ commute with each other.

**5.4 W-ambiguity of the Noether charge.** Show that shifting the Lagrangian by a total derivative, $\mathbf{L} \to \mathbf{L} + \mathrm{d}\mathbf{W}$, yields a $\mathbf{W}$-ambiguity term in the Noether current (5.35) and the corresponding charge.

**5.5 More on Bekenstein–Hawking entropy.**

(1) In the Bekenstein–Hawking entropy (5.43) reintroduce factors of $\hbar$, $c$ and Boltzmann constant $k_{\mathrm{B}}$ such that $S^{\mathrm{W}}_{\mathrm{BH}}$ is indeed dimensionless, as the entropy should be. Verify similar factors in the Hawking temperature (5.60).

(2) Compute the Hawking temperature and the entropy of a Schwarzschild black hole of mass $M = 10^5 M_\odot$. Compare this with the entropy of thermal gas of photons with the same energy filling a sphere of Schwarzschild radius of the black hole. When can the entropy of the black hole and the photon system become equal (at which energy or temperature for photons)?

**5.6 On the equivalence of Wald entropy and the SPSM entropy.**

Going through the formulation and definition of $\mathbf{k}_{\zeta_{\mathrm{H}}}$, prove that the Wald entropy (5.39) and the SPSM entropy (5.45), assuming the integrability of the latter and upon an appropriate choice of the reference value, are indeed yielding the same result.

**5.7 On constancy of surface gravity on bifurcate Killing horizon.**

Suppose that we have a bifurcate Killing horizon generated by $\xi_{\mathrm{H}}$ and a bifurcation surface $\mathcal{B}$ spanned by $e_a^\mu$ $a = 1, 2, \ldots, D-2$, over which $\xi_{\mathrm{H}}$ vanishes. Show that the surface gravity $\kappa$ is a constant over the bifurcate horizon.

**5.8 On constancy of horizon electric potential.**

(1) Starting from $\mathcal{L}_{\xi_{\mathrm{H}}} A = 0$, where $A$ is the gauge field 1-form, show that $\Phi_{\mathrm{H}}$ (5.63) is a constant over the horizon.

(2) Note that $\xi_{\mathrm{H}}$ being a symmetry implies $\mathcal{L}_{\xi_{\mathrm{H}}} F = 0$, where $F = \mathrm{d}A$ is the gauge field strength. Show that this yields a weaker condition that $\Phi_{\mathrm{H}}$ is constant up to $\mathcal{L}_{\xi_{\mathrm{H}}} \lambda$ where the scalar function $\lambda$ is a possible gauge transformation.

(3) Work out (5.50).

**5.9 Four Laws of near horizon extremal KN geometry dynamics.**

As discussed in Sect. 5.1, the definitions of charges and entropy are not limited to black holes, and our analysis may be repeated for more a general class of near horizon extremal geometries. It is hence expected that these may also follow the four laws. This is indeed the case, see [367,405] for more details. In particular, one may prove the first law. Starting from $\eta_{\mathrm{H}}$ given in (5.57) prove the first law among parametric variations of the charges of near horizon-extremal KN geometry discussed in this chapter.

**5.10 Inner horizon zeroth and first laws.**

The zeroth law and constancy of surface gravity over the horizon, cf. Sect. 5.5.1, is implied by the existence of a Killing horizon. Our derivations of the first law, cf. Sect. 5.5.2, relies on diffeomorphism invariance of the theory and existence of a Killing horizon. In typical black holes like KN, besides the outer (event) horizon, the inner horizon is also a Killing horizon. One, hence, expects zeroth and first laws of black hole thermodynamics should also hold for the inner horizon too. This exercise explores these issues.

(1) Compute the surface gravity associated with inner horizons in the KN family, using general formula (3.1) for the Killing vector generating the inner horizon.
Hint: You should find negative surface gravity, which is a sign of thermal instability of the inner horizon and may be viewed as an argument for the CCC.

(2) Show that entropy (the Noether charge associated with the Killing vector generating the inner horizon) equals the area of the inner horizon over $4G_{\mathrm{N}}$.

(3) Work through the derivations in Sect. 5.5.2 and work out the inner horizon first law for the KN black holes.

**5.11 More on the Smarr relation.**

(1) Explore the Smarr relation for Kerr-AdS solution whose charges was discussed in Sect. 5.1, see also [378,379,406].

(2) Explore the Smarr relation for Plebenaski–Demianski solutions of Sect. 2.7.

**5.12 On products of entropies of the inner and outer horizons.**

(1) Consider a KN black hole. Find the product of areas of inner and outer horizons. Show that this product only depends on the charge and angular momentum and is independent of the mass.

(2) Repeat the above for the most general seven parameter family of Plebenaski–Demianski solutions, cf. Sect. 2.7.

(3) In stationary black holes, the coordinates are typically chosen such that the horizons are sitting at zeros of $g^{rr}$ component of metric. For asymptotic flat cases, $g^{rr} = 0$ is typically, a polynomial equation of the form $1 - \frac{2m}{r} + \sum_{n\geq 2} \frac{q_n}{r^n} = 0$, where $q_n$ are combinations of other conserved charges of the system, besides the mass. The fact that the first subleading term at large $r$ is given by $2m$ follows from the ADM mass formula. Using this fact to argue for general "area-product" relations for black holes.

**5.13 No force condition for extremal black holes.**

Consider an extremal RN black hole of charge $Q$. When can a particle of charge $q$ and mass $m$ fall into the black hole? Show that if $m = q$ the black hole does not exert any force on the particle.

**5.14 Thermodynamic volume and extended black hole first law?**

In the usual first law of thermodynamics, we have a work term, a $-P\mathrm{d}V$ term, where $P$ is the pressure and $V$ is the volume. In the case of black holes our analysis and derivations did not yield such a term, as "volume of a back hole" is not a usually well-defined Noether-type conserved charge. Nonetheless, one may consider black holes on AdS or dS backgrounds, where there is a non-zero cosmological constant $\Lambda$ in the background, and treat $\Lambda$ as a pressure.

(1) Consider Kerr AdS black hole (5.16). Show that it satisfies the standard first law,

$$\mathrm{d}S = \frac{2\pi}{\kappa}(\mathrm{d}M - \Omega_{\mathrm{H}}\mathrm{d}J). \tag{5.86}$$

(2) Let $P = \alpha\Lambda$ for some constant $\alpha$ be the pressure. Add a term $P\mathrm{d}V$ term to the above first law and treat $\Lambda$ or $\ell$ as a parameter that can vary. Find the thermodynamic volume $V$ such that this "generalized" first law is satisfied.

(3) Extend the above to charged black holes on dS or AdS backgrounds.

For the notion of thermodynamical volume of black holes and black hole enthalpy see [407–409]. The above treatment while seemingly working, is ad hoc, see [410, 411] for a more symmetry-based treatment.

**5.15 Spherical symmetry for $SU(2)$ gauge field**

To see the subtle interrelation between diffeomorphism- and gauge transformations consider spherically symmetric $SU(2)$ gauge fields $A_\mu$,

$$\mathcal{L}_{\xi_m} A_\mu = \partial_\mu \Lambda_m - i[A_\mu,\ \Lambda_m] \tag{5.87}$$

where $\xi_m$ $(m = 1, 2, 3)$ are the three Killing vectors associated with spherical symmetry (see (2.4)), and $\Lambda_m$ are $SU(2)$-valued scalar fields that generate gauge transformations. Show that the Witten ansatz [412]

$$A = \begin{pmatrix} 0 \\ 0 \\ a_0 \end{pmatrix} \mathrm{d}t + \begin{pmatrix} 0 \\ 0 \\ a_1 \end{pmatrix} \mathrm{d}r + \begin{pmatrix} \Phi_1 \\ \Phi_2 \\ 0 \end{pmatrix} \mathrm{d}\theta + \begin{pmatrix} \Phi_2 \\ -\Phi_1 \\ -i\cot\theta \end{pmatrix} \sin\theta \ \mathrm{d}\varphi \tag{5.88}$$

is compatible with spherical symmetry (5.87) for arbitrary (real) scalar fields $\Phi_i = \Phi_i(t, r)$ and calculate the parameters $\Lambda_m$ in (5.87). In (5.88) the column-vectors refer to the three $SU(2)$ generators $T^i$ with commutation relations $[T^i, T^i] = \epsilon^{ijk}T^k$, so that, e.g. $\Lambda_m = \Lambda_m^i T^i$. Show particularly $\Lambda_1 = 0$ and $\Lambda_2 + i\Lambda_3 = T^3\, e^{i\varphi}/\sin\theta$.

# 6 Semiclassical Aspects of Black Holes

**Abstract**

In this chapter, we study the semiclassical aspects of black holes, in which the black hole is viewed as a classical background while other fields or particles are treated quantum mechanically. We first discuss the variational principle for gravity theories in Sect. 6.1. Then, in Sect. 6.2, we briefly review QFT on curved backgrounds, which leads to the Unruh effect (Sect. 6.3) and, when applied to black hole backgrounds, to the Hawking effect (Sect. 6.4). We then review Bekenstein's arguments for black hole entropy and entropy bounds in Sect. 6.5. In Sect. 6.6, we discuss tunneling, in Sect. 6.7 black hole evaporation, and in Sect. 6.8 the membrane paradigm. We close this chapter with preliminary remarks in Sect. 6.9 on the information puzzle and apparent loss of unitarity in the semiclassical analysis.

## 6.1 Variational Principle

So far our analysis was classical. While we also introduced Lagrangians or actions, their role was merely a handy tool to provide EOM. For a quantum or semiclassical treatment, however, actions play a more fundamental role, for instance, in the path integral. Semiclassically, the theory is expanded around the saddle point of the action. To the lowest order, the effective action is then given by the on-shell action.

The fact that the first variation of the action is required to vanish implies more than the classical field equations, since boundary and corner terms must also vanish. Let us neglect corner terms and suppose that we start with an action $I$ functionally depending on some fields that we collectively denote by $\Phi$

$$I[\Phi] = \int_{\mathcal{M}} \mathrm{d}^D x \, \sqrt{-g} \, \mathcal{L}(\Phi, \, \partial\Phi) \, . \tag{6.1}$$

Variation of the action yields

$$\delta I[\Phi] = \int_{\mathcal{M}} E(\Phi, \, \partial\Phi) \, \delta\Phi + \int_{\partial\mathcal{M}} \Theta(\Phi, \, \partial\Phi; \, \delta\Phi) \, . \tag{6.2}$$



D. Grumiller and M. M. Sheikh-Jabbari, *Black Hole Physics*, Graduate Texts in Physics,
https://doi.org/10.1007/978-3-031-10343-8_6

The volume term $E$ on the right-hand side vanishes on-shell by definition. The boundary term $\Theta$ should vanish for all variations $\delta\Phi$ allowed by the boundary conditions. If this is not the case, then either boundary terms must be added to the action or the boundary conditions must be refined. Note that (6.2) is an integrated version of (G.3) and the latter is written in the language of forms.

Before specializing the discussion on the Einstein–Hilbert action, we encourage the reader to consider Exercise 6.1 as a warm-up.

### 6.1.1 Gibbons–Hawking–York Boundary Term

For a gravity theory, often a Dirichlet boundary value problem is desired where the metric is fixed at the boundary $\partial\mathcal{M}$, while its normal derivative is free to fluctuate

$$\delta g_{\mu\nu}\big|_{\partial\mathcal{M}} = 0 \qquad\qquad n^\alpha\nabla_\alpha\delta g_{\mu\nu}\big|_{\partial\mathcal{M}} \neq 0\,. \tag{6.3}$$

We have used here a split of the full metric $g$ into boundary metric $h$ (also known as 'first fundamental form') and normal vector $n$

$$g_{\mu\nu} = h_{\mu\nu} + n_\mu n_\nu \qquad\qquad n^\mu n_\mu = 1 \tag{6.4}$$

assuming that the boundary has a spacelike normal vector, as it does in most applications. We show now that the Einstein–Hilbert action is incompatible with such a boundary value problem.

The first variation of the Einstein–Hilbert action leads to the Einstein equations in the bulk plus total derivative terms, e.g. see [8]

$$\delta I_{\text{EH}} \approx \frac{1}{16\pi G_{\text{N}}}\int_{\mathcal{M}} \mathrm{d}^D x\sqrt{-g}\,\nabla^\mu\big(\nabla^\nu\delta g_{\mu\nu} - g^{\alpha\beta}\nabla_\mu\delta g_{\alpha\beta}\big)\,. \tag{6.5}$$

Using Stokes' theorem, the total derivative terms in (6.5) are converted into boundary terms

$$\delta I_{\text{EH}} \approx \frac{1}{16\pi G_{\text{N}}}\int_{\partial\mathcal{M}} \mathrm{d}^{D-1} x\sqrt{-h}\,n^\mu\big(\nabla^\nu\delta g_{\mu\nu} - g^{\alpha\beta}\nabla_\mu\delta g_{\alpha\beta}\big)\,. \tag{6.6}$$

To proceed, we need to introduce the extrinsic curvature tensor (also known as the second fundamental form)

$$K_{\mu\nu} := h_\mu^\alpha h_\nu^\beta\,\nabla_\alpha n_\beta = \frac{1}{2}\left(\mathcal{L}_n h\right)_{\mu\nu} \tag{6.7}$$

which like the boundary metric $h_{\mu\nu}$ projects to zero when contracted with the normal vector $n^\mu$. The trace of extrinsic curvature is defined as $K := K_\mu^\mu = \nabla_\mu n^\mu$. Using

$$\begin{aligned}
n^\mu\nabla^\nu\,\delta g_{\mu\nu} &= n^\mu(h^{\nu\alpha} + n^\nu n^\alpha)\nabla_\alpha\,\delta g_{\mu\nu}\,,\\
n^\mu h^{\nu\alpha}\nabla_\alpha\,\delta g_{\mu\nu} &= n^\mu h^{\nu\alpha}\nabla_\alpha[(h_\mu^\gamma + n_\mu n^\gamma)(h_\nu^\beta + n_\nu n^\beta)\,\delta g_{\beta\gamma}]\\
&= -K^{\mu\nu}\,\delta g_{\mu\beta} + K n^\mu n^\nu\delta g_{\mu\nu} + \text{ total boundary derivative,}
\end{aligned} \tag{6.8}$$

the result (6.6) can be reformulated as[1]

$$\delta I_{\text{EH}} \approx -\frac{1}{16\pi G_{\text{N}}} \int_{\partial\mathcal{M}} \text{d}^{D-1}x\sqrt{-h}\,\big(h^{\mu\nu}n^\alpha\nabla_\alpha\delta g_{\mu\nu} + (K^{\mu\nu} - Kn^\mu n^\nu)\,\delta g_{\mu\nu}\big)\,. \tag{6.9}$$

The first term in (6.9) generically is non-zero for the Dirichlet boundary value problem (6.3). Thus, the Einstein–Hilbert action is inconsistent with (6.3).

To resolve this issue, we add suitable boundary terms to the bulk action since they do not affect the bulk EOM, but may convert the result for the variation (6.6) or (6.9) into something compatible with the boundary value problem (6.3). Specifically, we need a boundary term that preserves diffeomorphisms along the boundary and that is capable of canceling the normal derivative of the fluctuations of the metric in (6.6). Such boundary terms should involve scalars constructed from the extrinsic curvature $K$ or Riemann curvature $\mathcal{R}$ of the boundary $\mathcal{M}$. We keep only the first few terms in a derivative expansion of the boundary action

$$I_{\partial\mathcal{M}} = \frac{1}{16\pi G_{\text{N}}} \int_{\partial\mathcal{M}} \text{d}^{D-1}x\sqrt{-h}\,\big(b_0 + b_1 K + b_2\mathcal{R} + \ldots\big) \tag{6.10}$$

where the ellipsis refers to higher derivative terms (such as $K^{\mu\nu}K_{\mu\nu}$ or $K\mathcal{R}$) and $\mathcal{R}$ is the boundary Ricci scalar (constructed from the boundary metric $h_{\mu\nu}$ and the boundary covariant derivative $\mathcal{D}_\mu := h^\nu_\mu\nabla_\nu$). Terms intrinsic to the boundary (like the boundary cosmological constant $b_0$ or the boundary Einstein–Hilbert term $b_2\mathcal{R}$) will not help us to get a well-defined Dirichlet boundary value problem, since they cannot produce normal derivatives $n^\mu\nabla_\mu$. Thus, we set $b_0 = b_2 = 0$, focus on the term $b_1 K$ and vary it. Using the definition $K = \nabla_\mu n^\mu$ as well as $\delta n_\mu = \frac{1}{2}\, n_\mu n^\alpha n^\beta\,\delta g_{\alpha\beta}$ yields (see Appendix A for more details)

$$\delta K = \frac{1}{2}\, h^{\mu\nu}n^\alpha\nabla_\alpha\delta g_{\mu\nu} - \frac{1}{2}\, Kn^\mu n^\nu\,\delta g_{\mu\nu} + \text{total boundary derivative} \tag{6.11}$$

Comparing with the variation (6.9), we deduce that we should choose $b_1 = 1$ to get consistency with the Dirichlet conditions (6.3).

### > Einstein–Hilbert action with Gibbons–Hawking–York boundary term

The full action for Einstein gravity (at this stage of our discussion) compatible with a Dirichlet boundary value problem (6.3) consists of the bulk action $I_{\text{EH}}$ plus a boundary action $I_{\text{GHY}}$, known as Gibbons–Hawking–York boundary term.

[1] We assume here that the boundary $\partial\mathcal{M}$ has no boundary; if this assumption is relaxed the total derivative term is converted into a corner contribution $1/(16\pi G_{\text{N}})\int_{\partial^2\mathcal{M}}\text{d}^{D-2}x\sqrt{|\sigma|}\,n^\mu_\sigma n^\nu\,\delta g_{\mu\nu}$, where $n^\mu_\sigma$ is the outward pointing unit normal of the corner and $|\sigma|$ is the determinant of the induced metric at the corner.

$$\boxed{I = I_{\mathrm{EH}} + I_{\mathrm{GHY}} = \frac{1}{16\pi G_{\mathrm{N}}} \int_{\mathcal{M}} \mathrm{d}^D x \sqrt{-g} \big(R - 2\Lambda\big) + \frac{1}{8\pi G_{\mathrm{N}}} \int_{\partial\mathcal{M}} \mathrm{d}^{D-1} x \sqrt{-h}\, K} \tag{6.12}$$

### 6.1.2 Brown–York Stress Tensor

The first variation of the action (6.12) (assuming a smooth boundary) is given by

$$\begin{aligned} \delta I = &-\frac{1}{16\pi G_{\mathrm{N}}} \int_{\mathcal{M}} \mathrm{d}^D x \sqrt{-g}\, \big(R^{\mu\nu} - \frac{1}{2}\, g^{\mu\nu} R + \Lambda g^{\mu\nu}\big)\, \delta g_{\mu\nu} \\ &- \frac{1}{16\pi G_{\mathrm{N}}} \int_{\partial\mathcal{M}} \mathrm{d}^{D-1} x \sqrt{-h}\, \big(K^{\mu\nu} - h^{\mu\nu} K\big)\, \delta g_{\mu\nu} \end{aligned} \tag{6.13}$$

The tensor multiplying the variation $\delta g_{\mu\nu}$ at the boundary (up to a factor) is known as Brown–York stress tensor

$$T^{\mu\nu}_{\mathrm{BY}} := \frac{1}{8\pi G_{\mathrm{N}}} \big(K^{\mu\nu} - h^{\mu\nu} K\big)\,. \tag{6.14}$$

It is important to realize that further boundary terms can be added to the action (6.12) without spoiling the Dirichlet boundary value problem (6.3), for instance, by choosing $b_0 \neq 0$ or $b_2 \neq 0$ in (6.10). As we shall see explicitly in later chapters, these terms are actually necessary for many applications. The reason for this is that even though we have a well-defined Dirichlet boundary value problem, we still may not have a well-defined variational principle, in the sense that there could be allowed variations of the metric that do not lead to a vanishing first variation (6.13) on some solutions of the EOM, just like in the mechanics example of Exercise 6.1. Also, the Brown–York stress tensor is not finite in general, and again this problem can be resolved by adding suitable boundary terms, known as ‘holographic counterterms’ in the context of gravity on an AdS background and in AdS/CFT, see Chap. 8.

## 6.2 Quantization on Black Hole Backgrounds

For many applications, it is sufficient to study QFT on a fixed gravitational background, without taking into account the backreactions upon the geometry. The most prominent examples are provided by black hole backgrounds (to study the Hawking effect) and dS backgrounds (to study primordial fluctuations in inflationary models).

The key aspect is that the gravitational background induces specific external conditions imposed on the quantum fields, which can lead to particle creation. Conceptually, what is happening is similar to the Schwinger effect, where electron–positron pairs are generated in an external electric field.

There are several different ways to quantize black hole backgrounds and extract the physical observables necessary to deduce the Hawking effect, e.g. using Bogoliubov transformations or exploiting anomalies or path integral methods. Readers unfamiliar with QFT on curved backgrounds should consult Appendix E before proceeding.

A key insight is that, a change of basis can convert a vacuum state to an excited state, and such changes of bases appear naturally in time-dependent backgrounds and in spacetimes with horizons. Technically, a key step in any approach to quantum fields on black hole backgrounds is to make sure that matter fields are infalling and that the expectation value of the stress tensor is finite on the future event horizon.

In the next section, we discuss the Unruh effect, which captures some generic aspects of (non-extremal) black holes, and then turn to the Hawking effect.[2]

## 6.3 Unruh Effect

Consider a uniformly accelerated observer in Minkowski space with constant acceleration $a$. Such an observer will see a Rindler horizon. As discussed in several examples in Chap. 2, near the horizon of non-extremal black holes, we find a Rindler space, and therefore, this scenario captures some universal features of black holes, which we will discuss at the end of the next section when we have all relevant results available.

For simplicity (and with no loss of anything essential), consider two spacetime dimensions and suppose that the only quantum field that has local excitations is a massless scalar field obeying the Klein–Gordon equation $\Box\phi = 0$. Using rapidity/boost coordinates

$$t = \frac{1}{a}\, e^{a\xi}\, \sinh(a\tau) \qquad\qquad x = \frac{1}{a}\, e^{a\xi}\, \cosh(a\tau) \tag{6.15}$$

converts the Minkowski metric $-\,\mathrm{d}t^2 + \mathrm{d}x^2$ into the Rindler metric in conformal coordinates

$$\mathrm{d}s^2 = e^{2a\xi}\,\big(-\,\mathrm{d}\tau^2 + \mathrm{d}\xi^2\big), \qquad \tau, \xi \in \mathbb{R}. \tag{6.16}$$

Note that, only the Rindler wedge $x > |t|$ is covered by the Rindler metric (6.16), see Fig. 6.1. At $x = \pm t$ (or, equivalently, $\tau \to \pm\infty$), there is an acceleration (Rindler) horizon, which is a non-extremal Killing horizon with surface gravity (cf. Exercise 3.7)

$$\kappa = a\,. \tag{6.17}$$

[2] Similar effects appear in early universe cosmology, black hole analog systems, and, e.g. Bose–Einstein condensates, where also quasi-particles are generated through non-trivial Bogoliubov transformations. The keyword in these contexts is ‘two-mode squeezed state’, see [413].

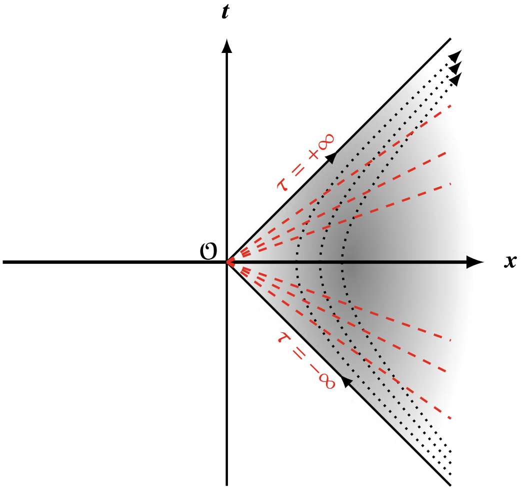


**Fig. 6.1** $2d$ Rindler wedge (shaded area). Dotted lines are constant $\xi$, which are trajectories of uniformly accelerated observers. Red dashed lines are constant $\tau$. The origin $O$ corresponds to $\xi = -\infty$. The Rindler observer formulates physics only in the shaded region. Her in- and out-states, which appear in the S-matrix elements she measures, are, respectively, defined at past and future Rindler horizons $\tau = -\infty$ and $\tau = +\infty$

### 6.3.1 Unruh Vacuum State

The Klein–Gordon equation on the Rindler background

$$\big( - \partial_\tau^2 + \partial_\xi^2 \big)\phi = 0 \tag{6.18}$$

has normalized plane wave solutions

$$\psi_k^\pm = \frac{1}{\sqrt{2\pi\omega}}\, e^{\mp i\omega\tau + ik\xi} \qquad \omega = |k| \tag{6.19}$$

that are positive frequency for the upper sign in the Rindler wedge $x > |t|$, where 'positive frequency' is defined with respect to the proper-time Killing vector $\partial_\tau$. In the left Rindler wedge, $x < |t|$, the flow of this Killing vector field is in the other direction, so in that wedge, $\psi_k^-$ corresponds to positive frequency modes. The sets of modes (6.19) together with their complex conjugates provide a normalized complete basis for solutions to the wave equation (here we have a continuous version of the normalization condition (E.4) of Appendix E).

$$\text{Rindler basis:} \qquad \phi = \int \mathrm{d}k \left( a_k^+ \psi_k^+ + a_k^- \psi_k^- + a_k^{+\dagger} \psi_k^{+*} + a_k^{-\dagger} \psi_k^{-*} \right) \tag{6.20}$$

Alternatively, we could use plane waves $\eta_k$ in Minkowski space as modes, which also provide a complete basis,

$$\text{Minkowski basis:} \qquad \phi = \int \mathrm{d}k \left( b_k^+ \chi_k^+ + b_k^- \chi_k^- + b_k^{+\dagger} \chi_k^{+*} + b_k^{-\dagger} \chi_k^{-*} \right). \tag{6.21}$$

The corresponding vacua are defined as

$$a_k^{\pm}|0_R\rangle = 0 \qquad b_k^{\pm}|0_M\rangle = 0 \tag{6.22}$$

where the subscripts 'R' and 'M' stand for 'Rindler' and 'Minkowski', respectively.

### 6.3.2 Unruh Temperature, Bogoliubov Transformations

To see whether these vacua differ, we need the Bogoliubov coefficients transforming between Rindler and Minkowski modes and check whether positive frequency modes in Rindler space map to positive frequency modes in Minkowski space, or if there is a mixing between positive and negative frequency modes. As shown in Exercise 6.5, the result is

$$a_k^{\pm} = \frac{1}{\sqrt{2\sinh\frac{\pi\omega}{\kappa}}}\left(e^{\frac{\pi\omega}{2\kappa}}b_k^{\pm} + e^{-\frac{\pi\omega}{2\kappa}}b_{-k}^{\mp\dagger}\right) \tag{6.23}$$

where $\kappa$ is surface gravity (6.17) of the Rindler horizon. The modes $\chi_k^{\pm}$ in (6.21) are also obtained as part of Exercise 6.5.

Importantly, we see a mixing between annihilation and creation operators in the Bogoliubov transformation (6.23), just like in Appendix E. This implies that the Rindler number operators in the right Rindler wedge

$$N_k^R = a_k^{+\dagger}a_k^{+} \tag{6.24}$$

do not annihilate the Minkowski vacuum.

$$\langle 0_M|N_k^R|0_M\rangle = \frac{e^{-\pi\omega/\kappa}}{2\sinh\frac{\pi\omega}{\kappa}}\langle 0_M|b_{-k}^{-}b_{-k}^{-\dagger}|0_M\rangle \simeq \frac{1}{e^{2\pi\omega/\kappa}-1} \tag{6.25}$$

In the last equality, we have renormalized the 1-particle state, $\langle 0_M|b_{-k}^{-}b_{-k}^{-\dagger}|0_M\rangle \simeq 1$. The final result (6.25) shows not only that a Rindler observer sees particle excitations, but also additionally proves that these excitations have a thermal spectrum with the Unruh temperature [81].

$$\boxed{T_U = \frac{\kappa}{2\pi}} \tag{6.26}$$

### 6.3.3 Unruh Temperature, Euclidean Field Theory Analysis

There is a shortcut to derive the Unruh temperature (6.26). Namely, continuing analytically to Euclidean signature, $\tau_{\mathrm{E}} := i\tau$, converts the Rindler metric (6.16) into the flat Euclidean metric in polar coordinates (see Exercise 6.6). Requiring smoothness of this space and absence of conical deficit angle implies that the Euclidean time should have the periodicity

$$\tau_{\mathrm{E}} \sim \tau_{\mathrm{E}} + \beta \qquad\qquad \beta = T_U^{-1}\,. \tag{6.27}$$

QFT Green functions inherit this periodicity property, which is known as Kubo–Martin–Schwinger condition [414,415] and a defining property of thermal states in a QFT, where the periodicity in Euclidean time is the inverse temperature. We shall come back to the Euclidean (path integral) formulation in later sections of this chapter; for the time being, this is merely a convenient shortcut for reading off the Hawking–Unruh temperature.

### 6.3.4 Discussion

To avoid conceptual confusion, here are some clarifying comments regarding the crucial result (6.26). The EEP (extended to the semiclassical level) implies that a stationary Minkowski observer and a Rindler observer should provide the same physical description for local processes they both have causal access to. In particular, both should agree on the fact that a Rindler detector (some particle detector carried along by the Rindler observer) clicks and measures Rindler quanta with the thermal spectrum (6.25). The interpretation of these events, however, differs between the two observers: the Rindler observer sees a thermal bath, but the Minkowski observer sees a detector into which constantly energy is put by accelerating it, which leads to the emission of particles whenever there is a click in the detector. The energy contained in the Rindler quanta is provided by acceleration.

As a nice brain teaser, one may ask 'Since the EP tells us that accelerating is the same as being at rest in a gravitational field should observers standing on Earth not observe Rindler quanta?', which has essentially the same answer as the related question 'Does an electron at rest on Earth radiate?', namely 'no'. The Unruh effect applies also to detectors that accelerate only for a finite time, where there is no eternal (event) horizon and the spectrum deviates slightly from a thermal one. Finally, it is not easy to detect the Unruh effect since even a modest Unruh temperature of one nanokelvin would require accelerations of the order of $10^{11}$ m/s$^2$.

While the Unruh effect applies to accelerated observers and requires only special relativity, the universality of the Rindler approximation of non-extremal Killing horizons together with the EEP suggests that a similar effect should take place in black hole backgrounds. This is indeed the case, as we review in the next section.

As depicted in Fig. 6.1, a Rindler observer has only access to the $x > 0$ region of any constant $t$-slice in Minkowski space. This, among other things, means that the Rindler observer has only access to half of the Fock space of a field theory on Minkowski space. Despite this fact, Rindler and Minkowski field theories yield the same physical correlation functions for operators defined in the Rindler wedge. This can be understood and explained by quantum information notions, in particular, entanglement, between the $x > 0$ and $x < 0$ regions as seen by the Rindler observer.

In essence, the Unruh temperature accounts for the half of Fock space the Rindler observer does not have access to. These aspects will be discussed further in Chap. 8.

## 6.4 Hawking Effect

In the previous section, we saw that the presence of an acceleration horizon leads to non-trivial Bogoliubov coefficients in the transformation between the natural base of modes for an accelerated observer and a Minkowski observer. Alternatively, we saw that regularity of the Euclidean continuation of Rindler spacetime yields the Kubo–Martin–Schwinger condition of a thermal state at the Unruh temperature. Assuming that the EEP works at the semiclassical level, both statements and corresponding results should also extend to black hole horizons.

Interestingly, so far there appears to be no comprehensive science-history book on the discovery of Hawking radiation. We provide now a brief summary thereof. As often with great discoveries, it was in the air already sometime before Hawking's seminal paper. In particular, Zel'dovich, Starobinsky [416], and others were working on radiation from rotating black holes in the early 1970s, and for sure this inspired Hawking after his 1973 visit to Moscow. However, the conclusion by Zel'dovich and Starobinsky at that time was that Schwarzschild black holes do not radiate (which seemed fair, given that they are static; this conclusion was also suggested by the classical Penrose process, which needs an ergo-region to function). Independently, Page (at that time a graduate student) in discussions with Feynman also discovered radiation from rotating black holes, but once they realized that Zel'dovich and Starobinsky had already discovered this radiation they dropped the subject. Ironically, part of Hawking's motivation for his breakthrough was to prove Bekenstein [76] wrong,[3] i.e., to show that (Schwarzschild) black holes cannot have an entropy since this would imply that they must radiate, which seemed impossible. While it is moot to speculate about alternative histories, it does seem likely that the Hawking effect would have been discovered even without Hawking's key contributions in the mid-1970s [79,417], for instance by Unruh [81].

### 6.4.1 Heuristics of Hawking Effect from Vacuum Fluctuations

QFT, the union of quantum mechanics and special relativity, allows pair creation from the vacuum. In the plain Minkowski vacuum, the characteristic time-scale associated with such a pair creation for virtual (anti-)particles of mass $m$ is estimated using Heisenberg's uncertainty principle and yields $t \sim 1/m$. Of course, in the Minkowski vacuum, such particle pairs always remain virtual and real pair production is barred by energy conservation. If we have a non-trivial background with a new vacuum and that background can provide the energy for creating real pairs, then the picture

[3] See for instance the section on the first law in [77], which concludes erroneously that the black hole temperature must vanish.

changes. There is generically another scale in the game in the presence of such backgrounds. For instance, a sufficiently strong background external electric field $E \gtrsim m_e$ can yield the production of real electron–positron pairs of mass $m_e$ through the famous Schwinger effect [418].

Stationary black holes may be viewed as backgrounds that can provide the energy source for similar pair production and the vacuum state associated with the observer at the black hole horizon can be different from that of the observer in asymptotic infinity. The asymptotic observer associates a characteristic scale, namely surface gravity $\kappa$ to the horizon. So, on general QFT grounds, one can expect pair production with a rate associated with that scale. A heuristic picture of the Hawking effect, which will be made more precise in later in Sect. 6.6, is thus as follows: virtual particle-anti-particle pairs are created outside and inside the black hole. Occasionally, particles behind the horizon may tunnel out and escape to infinity, leaving inside the black hole a particle with negative energy as measured by an asymptotic observer. Alternatively, particle pairs outside the horizon may split so that one particle escapes to infinity with positive energy, while the partner with negative energy is captured by the black hole. Either way, the black hole gains negative energy, i.e. it loses energy to Hawking radiation. From this heuristic picture, it is clear that Hawking radiation is entangled with the black hole interior, which will be important for later chapters. What remains unclear at this stage is that Hawking radiation has a thermal spectrum. A slick way to derive its temperature is Euclidean continuation.

### 6.4.2 Hawking Temperature from Euclidean Continuation

Consider some black hole horizon that is also a non-extremal Killing horizon with surface gravity $\kappa$ (this includes most of the black holes we discussed in Sect. 2, in particular, Kerr black holes) and expand it near the horizon which we put at $\rho = 0$, see Exercise 6.7

$$\mathrm{d}s^2 = -\kappa^2\rho^2\,\mathrm{d}t^2 + \mathrm{d}\rho^2 + \dots \tag{6.28}$$

where the ellipsis refers to additional (angular) dimensions, rotation terms, and higher order terms in $\rho$, none of which are relevant for the regularity argument. Analytically continuing to Euclidean time, $t_\mathrm{E} := it$, yields again the Euclidean plane in polar coordinates, provided we identify periodically $t_\mathrm{E} \sim t_\mathrm{E} + 2\pi/\kappa$.[4]

**Hawking temperature**

By the same argument as in the Unruh case, we, therefore, arrive at the Hawking temperature.

$$\boxed{T_\mathrm{H} = \frac{\kappa}{2\pi}} \tag{6.29}$$

[4] Reading off the temperature from the Euclidean continuation of the near horizon metric was first used in the PhD thesis of Malcolm Perry [419], see also [420]. We thank Mahdi Godazgar and Malcolm Perry for the comment.

This is the temperature associated with Hawking radiation as seen by the asymptotic flat static observer, see Exercise 6.8 for more. The above formula is identical to the zeroth law (5.60) and to the Unruh temperature (6.26). The formula engraved on Hawking's tombstone (without subscripts) is the special case of (6.29) for the Schwarzschild black hole (where $\kappa = 1/(4M)$), which with all conversion factors restored is

$$T_{\mathrm{H}} = \frac{\hbar c^3}{8\pi G_{\mathrm{N}} k_{\mathrm{B}} M} \,. \tag{6.30}$$

While usually these conversion factors just unnecessarily clutter equations, in this particular case, their presence is gratifying in the sense that $\hbar$ shows we deal with a semiclassical effect, $c$ shows we have particle creation, $G_{\mathrm{N}}$ shows that gravity is at work and Boltzmann's constant $k_{\mathrm{B}}$ shows that we have a thermodynamical quantity. Plugging in numbers for stellar black holes yields temperatures in the nanokelvin regime, which is orders of magnitude smaller than the average temperature of the cosmic microwave background. Thus, the Hawking effect will not be observable for stellar-mass black holes until the universe has cooled down about 9 additional orders of magnitude, which will not happen in anyone's lifetime. For rotating and/or supermassive black holes, the temperature is even smaller, so the only chance to observe the Hawking effect is to spot rather light black holes (e.g. PBHs) or to consider analog condensed matter systems. Hawking radiation carried by massless particles (gravitons and photons) has a characteristic wavelength $\lambda \sim 1/T_{\mathrm{H}}$, which is of the order of the size of the black hole.

### 6.4.3 Hawking Radiation from Ray-Tracing

The derivation of Hawking radiation using Bogoliubov coefficients is also analogous to the derivation of the Unruh effect in Sect. 6.3.2. The main observation is that the vacuum for an observer at past null infinity differs from the vacuum for an observer at future null infinity if we insist that modes are purely infalling at the future horizon. A consequence of the same type of calculation as in the previous section is that, the asymptotic observer near future null infinity sees outgoing Hawking quanta with a thermal spectrum at the Hawking temperature (6.29). This temperature may then be associated with the black hole, as we usually do in any thermal system emitting blackbody radiation.

Here we follow Hawking's original derivation using the ray-tracing method [417], which implements the ideas above. Consider a physical black hole, generated, e.g. by the collapse of a mass shell, like in Fig. 6.2, and assume spherical symmetry for simplicity, i.e. the final state is a Schwarzschild black hole.

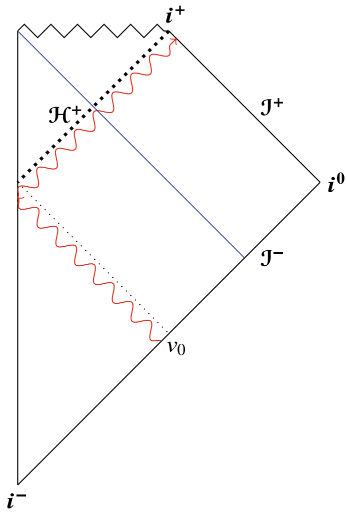


**Fig. 6.2** Collapsing shell (thin blue line) forming a black hole and 'last ray' (wiggly red line) escaping the black hole just before the advanced time $v = v_0$

Initial data can be provided at Cauchy surfaces approaching either $\mathfrak{I}^-$ or approaching $\mathcal{H}^+ \cup \mathfrak{I}^+$. Considering a scalar field obeying the Klein–Gordon equation

$$\nabla^2 \phi = 0 \tag{6.31}$$

on the black hole background, we have two natural mode expansions, one adapted to $\mathfrak{I}^-$

$$\phi_{\mathfrak{I}^-} = \int \mathrm{d}\omega \left(a_\omega \psi_\omega + a^\dagger_\omega \psi^*_\omega\right) \tag{6.32}$$

and one adapted to $\mathcal{H}^+ \cup \mathfrak{I}^+$

$$\phi_{\mathfrak{I}^+} = \int \mathrm{d}\omega \left(b_\omega \chi_\omega + b^\dagger_\omega \chi^*_\omega\right) . \tag{6.33}$$

For what follows, we can neglect the angular dependence, i.e. we focus on the $s$-wave sector.

Inside the shell, we use standard light-cone coordinates, advanced time $v = t + r$ and retarded time $u = t - r$. Outside the shell, we use their Regge–Wheeler analogs, $v = t + r_*$ and $u = t - r_*$ as well as Kruskal coordinates $U, V$ defined in (2.43). For a Schwarzschild black hole of mass $M$, we have $r_* = r + 2M \ln |r/(2M) - 1|$. The respective positive frequency modes then simplify to

$$\psi_\omega \propto e^{-i\omega v} \qquad \chi_\omega \propto e^{-i\omega u} \tag{6.34}$$

and are related by some Bogoliubov transformation (E.11). The remaining task is to determine the coefficients $\beta_{\omega\tilde{\omega}}$. If they are non-zero, then we do have particle creation, as discussed in Appendix E. Following Hawking, we determine these coefficients using the ray-tracing method. Further technical aspects of this derivation are addressed in the exercises of Appendix E.

Because the retarded time $u$ tends to infinity as the horizon is approached there is a pile-up of modes in the near horizon region, so the geometric optics approximation is very good. This means we can effectively treat the modes as rays. So any ray emanating from $\mathfrak{I}^-$ gets reflected at the origin and bounces off to $\mathfrak{I}^+$, as long as it was emitted before the advanced time $v_0$ (see Fig. 6.2). The last ray $v = v_0$ barely escapes the black hole. We focus now on rays emitted just before that, $v = v_0 - \epsilon$ with small $\epsilon$. These rays get reflected at the origin and will arrive at a Kruskal (!) retarded time $U = -\epsilon$ (the last ray arrives exactly at $U = 0$). By virtue of the relation (2.43), we obtain

$$u = -\frac{1}{\kappa}\,\ln\epsilon \tag{6.35}$$

showing that indeed the geometric optics approximation is good as long as $0 < \epsilon \ll 1$ since the modes

$$\chi_\omega \propto e^{\frac{i\omega}{\kappa}\,\ln\epsilon} \tag{6.36}$$

oscillate rapidly. Tracing back all these modes to $\mathfrak{I}^-$ and setting $v_0$ to zero, without loss of generality, yields

$$\psi_\omega(v) = \theta(-v)\,e^{\frac{i\omega}{\kappa}\,\ln(-v)}\,. \tag{6.37}$$

While (6.37) was only derived for small values of $v$, we simply assume this is the correct form for all values of $v$, since the precise form of the very early modes should not affect the final result.

The remainder is now a technical exercise, starting with a Fourier transformation of (6.37).

$$\tilde\psi_\omega(\tilde\omega) = \int_{-\infty}^{\infty} \mathrm{d}v\,e^{i\tilde\omega v}\,\psi_\omega(v) = \int_0^{\infty} \mathrm{d}v\,e^{i\tilde\omega v + \frac{i\omega}{\kappa}\,\ln(-v)} \tag{6.38}$$

A useful property of $\tilde\psi_k$ is its behavior under energy reflection

$$\tilde\psi_\omega(-\tilde\omega) = -e^{-\frac{\pi\omega}{\kappa}}\,\tilde\psi_\omega(\tilde\omega) \qquad \tilde\omega > 0\,. \tag{6.39}$$

This implies in particular, that positive frequency modes at $\mathfrak{I}^+$ match onto a mixture of positive and negative frequency modes at $\mathfrak{I}^-$ (and vice versa). These (inverse) Bogoliubov coefficients are given by

$$\beta_{\omega\tilde\omega} = \tilde\psi_\omega(-\tilde\omega) = -e^{-\frac{\pi\omega}{\kappa}}\,\tilde\psi_\omega(\tilde\omega) = -e^{-\frac{\pi\omega}{\kappa}}\,\alpha_{\omega\tilde\omega} \tag{6.40}$$

where the last equality uses the $\alpha$-set of Bogoliubov coefficients (E.11). As shown in Appendix E, the final conclusion is that the particle number operator at $\mathfrak{I}^+$ evaluated in the vacuum state associated with $\mathfrak{I}^-$,

$$\langle N_\omega\rangle = \frac{1}{e^{2\pi\omega/\kappa} - 1} \tag{6.41}$$

has the same Planck spectrum as the Rindler number operator evaluated in the Minkowski vacuum (6.25). From the result (6.41), Hawking was able to conclude that black holes emit thermal radiation with the Hawking temperature (6.29).

Below we present another efficient way to derive the Hawking effect, namely from anomalies [421].

### 6.4.4 Hawking Radiation from Anomalies

One way to define anomalies is by observing that a symmetry of the action can fail to preserve the path integral measure. As a consequence, 1-loop effects destroy the classical symmetry, i.e., the symmetry is anomalous. Since anomalies are 1-loop effects there are efficient tools to deal with them, see the textbook [422].

Consider for simplicity black holes that are effectively in two dimensions (like Schwarzschild–Tangherlini), with a metric $\mathrm{d}s^2 = -2e^{2\Omega}\,\mathrm{d}x^+\,\mathrm{d}x^-$, where $x^\pm = (\mathrm{d}t \pm \mathrm{d}z)/\sqrt{2}$. The key assumption is to postulate that the expectation value of the stress-energy tensor is covariantly conserved

$$\nabla_\mu \langle T^{\mu\nu}\rangle = 0\,. \tag{6.42}$$

In the present case, this expands to $\partial_+\langle T_{--}\rangle + \partial_-\langle T_{+-}\rangle - 2(\partial_-\Omega)\langle T_{+-}\rangle = 0$ and a similar equation with $\pm$ indices interchanged. This means that knowing the trace-component of the stress tensor, $\langle T_{+-}\rangle$, it is possible to determine the flux components of the stress tensor, $\langle T_{\pm\pm}\rangle$, up to important integration constants.

While for conformally coupled matter, the trace of the energy–momentum tensor vanishes classically, this no longer is true when 1-loop effects are taken into account. This is the famous trace anomaly [423], which relates the expectation value of the trace of the stress-energy tensor to the Ricci scalar of the background geometry, with a numerical coefficient that depends on the precise matter content. For a single scalar field minimally coupled in two dimensions, the result is [424] $\langle T_{+-}\rangle = \partial_z^2\Omega/(24\pi)$, where on static backgrounds $\partial_z = \sqrt{2}\partial_+ = -\sqrt{2}\partial_-$. Integrating the conservation equation (6.42) then establishes the flux component

$$\langle T_{--}\rangle = \frac{1}{24\pi}\left(\partial_z^2\Omega - (\partial_z\Omega)^2\right) + T_- \tag{6.43}$$

with the integration constant $T_-$, and similarly for $\langle T_{++}\rangle$. The last step is to fix the integration constant, which is done by choosing the appropriate vacuum.

The three best-known choices are the Unruh vacuum, the Hartle–Hawking vacuum, and the Boulware vacuum. The latter demands the absence of fluxes at infinity, leading to $T_\pm = 0$, but the price is that the stress tensor then diverges at the horizon due to infinite blueshift factors. The Hartle–Hawking vacuum is of relevance for a black hole in equilibrium with a thermal bath at the Hawking temperature: for each Hawking quantum that is emitted a corresponding quantum is absorbed by the black hole from the heat bath. For black hole evaporation, the most relevant choice is the

Unruh vacuum, where $T_-$ is fixed such that the stress tensor remains finite at the future event horizon

$$T_- = \frac{\left(\partial_z \Omega|_{\text{h}}\right)^2}{96\pi} = \frac{\kappa^2}{24\pi} = \frac{\pi}{6}\, T_{\text{H}}^2\,. \tag{6.44}$$

In the last equality, we related the flux to a temperature using the 2-dimensional version of the Stefan–Boltzmann law. (This uses as input the knowledge that the Hawking flux is associated with Hawking quanta with a thermal spectrum; this input can be taken from the Euclidean calculation above, which is complementary in the sense that it allows deducing that black holes are thermal states, but is not explicit about the Hawking radiation). For asymptotically flat black holes, the asymptotic flux is just given by $T_-$, which, therefore, is the Hawking flux. The last equality in (6.44) allows to express the temperature in terms of surface gravity, thereby recovering Hawking's formula (6.29).

An alternative derivation of Hawking radiation that uses gravitational anomalies is provided in [425].

### 6.4.5 Greybody Factors

Through a variety of methods we have seen that black holes, in the approximation that we used, behave like black bodies with Planck spectrum

$$\langle N_\omega \rangle = \frac{1}{e^{\omega/T_{\text{H}}} - 1} \tag{6.45}$$

at the Hawking temperature (6.29). The physics of black hole evaporation is slightly more complicated, however, since the Hawking radiation gets scattered on the black hole geometry and, moreover, can backreact on the geometry. For instance, scalar modes emitted from a Schwarzschild black hole have to pass through the potential in Fig. 4.1. Thus, generally the black hole decay rate

$$\Gamma = \sigma(\omega)\, \langle N_\omega \rangle \frac{\mathrm{d}^4 k}{(2\pi)^4} \tag{6.46}$$

features an additional greybody factor $\sigma(\omega)$. The word 'greybody' is a reminder that we do not have perfect black body radiation as a consequence of backscattering and backreaction. To leading order, the greybody factor $\sigma(\omega)$ equals the classical absorption cross section. This means that the perturbative methods developed in Chap. 4 can be applied to calculate greybody factors, see e.g. [426], which uses the WKB approach to derive QNMs and greybody factors.

Greybody factors are not merely an annoyance, spoiling the pristine black body radiation, but can give important clues about quantum aspects of black holes, see e.g. [427] and references therein.

### 6.4.6 Discussion

From the derivations above, it should be clear that we needed practically no dynamical information to derive the Hawking effect; the key input in all derivations was the presence of a (stationary) horizon with non-zero surface gravity and the need to map the vacuum state of an observer at the horizon to the one at asymptotic infinity. Whether we deal with an eternal black hole or the one arising as a result of gravitational collapse and also whether additional matter degrees of freedom are present is irrelevant for the conclusion that (almost) stationary black holes are thermal states with the Hawking temperature (6.29).

As shown above, the appearance of Hawking radiation can be understood in a number of different ways. For readers with a QFT background, perhaps the most intuitive explanation is that the presence of a black hole horizon provides external conditions for the quantum fluctuations, so in the same way that external electric fields lead to particle production via the Schwinger effect or accelerated detectors produce Rindler quanta and click via the Unruh effect, black holes can do the same via the Hawking effect. A related interpretation in terms of tunneling of virtual particles through the horizon will be reviewed in Sect. 6.6 below.

## 6.5 Black Hole Entropy and Alternative Derivations

Thermal states do not only have a temperature; there is usually also an entropy associated with them. As discussed in Chap. 5, especially Sect. 5.5, black holes are not different in this regard. The fact that black holes must have an entropy was found by Bekenstein, before the discovery of the Hawking effect and triggered by discussions with Wheeler. In a famous gedankenexperiment, Wheeler mixes hot and cold tea, thereby committing the crime of increasing the entropy of the universe. He remarked in conversations with his student Bekenstein that he could 'conceal from all the world the evidence of my crime' [428] by dropping the teacup into a black hole. Bekenstein's response a few months later was 'You don't destroy entropy when you drop those teacups into the black hole. The black hole already has entropy and you only increase it!'. Bekenstein saved the second law of thermodynamics from violations by postulating the generalized second law [385] (see Sect. 5.5)

$$\delta(S_{\rm BH} + S) \geq 0. \tag{6.47}$$

where $S_{\rm BH}$ is the black hole (or BH) entropy and $S$ the entropy of the rest of the universe. In Sect. 5.5, we argued that for stationary black holes with bifurcate Killing horizon in Einstein gravity theory

$$S_{\rm BH} = \frac{A_h}{4} \tag{6.48}$$

where $A_h$ is the horizon area.

However, Bekenstein did not have the Hawking effect at his disposal, so let us recall some of the arguments that led him to an entropy formula similar to (6.48). First of all, the black hole uniqueness theorems tell us that the final black hole state is characterized just by a few numbers, but the collapse process is far more intricate and involves matter/radiation with a large amount of entropy. The only way to avoid a contradiction with the second law of thermodynamics is to attribute entropy to black holes. This argument does not explain the functional form of entropy, only that it should be non-zero and plausibly be bigger if the mass of the black hole increases (since the entropy associated with the formation process will be bigger if the mass of the final black hole state is bigger). Second, if we want to associate entropy with black holes, this entropy should obey the second law of thermodynamics if the entropy of the rest of the universe can be neglected. Thus, we are looking for a quantity that scales with some positive power of mass and is monotonically increasing as a function of time in any physical process. Luckily for Bekenstein, the second law of black hole mechanics was around when he confronted this issue, so he deduced that a natural candidate for the black hole entropy is the area of the event horizon, with some unknown numerical prefactor [76]. Bekenstein guessed the prefactor incorrectly; as explained above, the correct prefactor $\frac{1}{4}$ in (6.48) is obtained easily equipped with Hawking's results. Hawking's calculation also eliminates one of the main objections against Bekenstein's proposal that black holes have an entropy: if black holes had an entropy they must also have a temperature and radiate, and everyone knew (before 1974) that black holes could not radiate. So, after Bekenstein's and Hawking's results and discussions, it was established by 1975 that (stationary) black holes which are classical solutions to Einstein gravity, at the semiclassical level behave like thermodynamic systems: they have entropy and emit black body (Hawking) radiation at the Hawking temperature (6.29).

In Sect. 5.5, we discussed that black hole entropy can be derived as a conserved charge for black holes with a Killing horizon. This derivation, while interesting and significant, does not reflect the semiclassical nature of the entropy and also relies on the choice of $2\pi/\kappa$ as the normalization of the horizon generating Killing vector field. In what follows, we present an alternative path integral derivation of the entropy due to Gibbons and Hawking.

### 6.5.1 Euclidean Effective Action and Gibbons–Hawking Derivation

There are numerous derivations of the entropy law (6.48). One of them, due to Gibbons and Hawking [429], uses the classical approximation to the Euclidean path integral to derive the partition function, which in turn yields free energy and entropy. We review here this derivation for non-rotating black holes and explain how to generalize to rotating black holes afterward.

Starting point is the analytic continuation of time, $t \to t_{\mathrm{E}} = it$. The Euclidean path integral then leads to the partition function

$$Z(T) = \sum_{\bar{g}} \int_{\mathrm{bc}} \mathcal{D}\delta g \mathcal{D}\phi \; e^{-\Gamma[\bar{g},\, \delta g,\, \phi;\, T]} \tag{6.49}$$

where we split the Euclidean metric into some classical background $\bar{g}$ and fluctuations $\delta g$. The matter fields are summarily denoted by $\phi$ and can include scalars, fermions, gauge fields, and more exotic matter fields; to reduce clutter, we will omit matter fields; the subscript 'bc' indicates that the path integral is performed only over a set of field configurations compatible with certain regularity and boundary conditions; the (instanton-like) sum is over all classical backgrounds $\bar{g}$ compatible with these conditions; the measure under the path integral subsumes gauge-fixing and ghost contributions; the quantity $\Gamma$ is the Euclidean action; the dependence on the parameter $T$ is a reminder that we impose as part of the boundary conditions that all our field configurations are compatible with a temperature fixed to the value of $T$, in particular they are compatible with the Kubo–Martin–Schwinger condition and periodicity in Euclidean time $t_{\mathrm{E}} \sim t_{\mathrm{E}} + \beta$ with $\beta = T^{-1}$; finally, the semi-colon denotes that the action is a functional of the quantities to the left of the semi-colon and a function of temperature.

In the semiclassical approximation, the action can be expanded around the classical background

$$\Gamma[\bar{g},\, \delta g;\, T] = \Gamma_{\mathrm{EOM}}[\bar{g};\, T] + \frac{\mathrm{d}\Gamma[\bar{g},\, \delta g;\, T]}{\mathrm{d}\delta g}\,\delta g + \frac{1}{2}\,\frac{\mathrm{d}^2\Gamma[\bar{g},\, \delta g;\, T]}{\mathrm{d}\delta g^2}\,\delta g^2 + \dots \tag{6.50}$$

where the ellipsis denotes cubic and higher orders in the fluctuations $\delta g$. The first term on the right-hand side of (6.50), $\Gamma_{\mathrm{EOM}}[\bar{g};\, T]$, is the Euclidean on-shell action, the second term vanishes since we require the action to have a well-defined variational principle and the third term contains quadratic fluctuations that physically capture information about specific heat of the system.

The semiclassical partition function as a function of temperature to leading and next-to-leading order is given by

$$Z(T) \simeq e^{-\Gamma_{\mathrm{EOM}}[\bar{g}_d;\, T]} \times \int_{\mathrm{bc}} \mathcal{D}\delta g \mathcal{D}\phi \, e^{-\frac{1}{2}\,\frac{\mathrm{d}^2\Gamma[\bar{g}_d,\, \delta g;\, T]}{\mathrm{d}\delta g^2}\,\delta g^2}\,. \tag{6.51}$$

We have made two approximations in (6.51): we have dropped all cubic and higher terms in fluctuations $\delta g$, thus neglecting 2- and higher-loop corrections and we have truncated the sum over all classical saddles to a single contribution from the dominant saddle $\bar{g}_d$, thus neglecting instanton corrections.

The classical approximation is particularly simple and shows that the on-shell action is minus the log of the partition function

$$\Gamma_{\mathrm{EOM}}[\bar{g}_d;\, T] \simeq -\ln Z(T) \tag{6.52}$$

which means that temperature times on-shell action is the classical free energy

$$F(T) = -T\ \ln Z(T) \simeq T\Gamma_{\text{EOM}}[\bar{g}_d;\ T]\,. \tag{6.53}$$

Since free energy is a thermodynamic potential, all other thermodynamic variables can be derived from it. In particular, entropy is given by

$$S(T) = \big(1 - \beta\partial_\beta\big)\ln Z(\beta) = -\frac{\mathrm{d}F(T)}{\mathrm{d}T}\,. \tag{6.54}$$

Semiclassically, free energy receives a multiplicative correction that can be calculated case-by-case since the path integral (6.51) is Gaussian. The generic form of the semiclassical partition function is then

$$Z(T) = e^{-\Gamma_{\text{EOM}}[\bar{g}_d;\ T]} \times Z_1(T) \quad \Rightarrow \quad F(T) = T\Gamma_{\text{EOM}}[\bar{g}_d;\ T] + T\ \ln Z_1(T) \tag{6.55}$$

To see what the first semiclassical correction does to entropy consider for illustration an on-shell action of the form $\Gamma \propto -T^\gamma$ and 1-loop corrections of the form $Z_1 \propto T^{\alpha\gamma}$ with some real numbers $\gamma, \alpha$. Classically, entropy scales like $T^\gamma$. The 1-loop correction to free energy is then given by $\alpha\, T\ \ln T^\gamma$, so taking its $T$-derivative produces a term logarithmically in the classical entropy with a prefactor $\alpha$, as well as an order unity term that competes with corrections we have neglected. This conclusion is rather generic, so denoting the classical approximation for entropy by $S_c$ the 1-loop corrected result is

$$S = S_c + \alpha\ \ln S_c + \mathcal{O}(1) \tag{6.56}$$

with some numerical coefficient $\alpha$ that depends on the matter content, the dimension, and the thermodynamical ensemble, but it does not depend on the specific UV completion. Since semiclassically $S_c \gg 1$ for macroscopic black holes one can, therefore, use not only the BH entropy (6.48) as a test for QG, but also the calculation of the coefficient $\alpha$ (while $\ln S_c$ is much smaller than $S_c$ it is still a large number as compared to the genuinely quantum corrections of $\mathcal{O}(1)$). See Chap. 9 for more discussions. A nice summary of these logarithmic corrections for various black holes is contained in [430].

A technical difficulty that we mentioned already in earlier sections is that the Einstein gravity bulk action is insufficient for the semiclassical approximation, since it neither leads to a finite on-shell action in general, nor to a well-defined variational principle. Therefore, one needs to make sure that the action $\Gamma$ used in the path integral (6.47) contains suitable boundary terms that remedy these deficiencies.

We consider now the Schwarzschild black hole. The actions used by Gibbons and Hawking consists of the Einstein–Hilbert bulk action (which trivially vanishes on-shell on vacuum solutions to the Einstein equations), the Gibbons–Hawking–York boundary term and a counterterm that Gibbons and Hawking argued to be the

Gibbons–Hawking–York boundary term for the vacuum state.[5] Thus, the on-shell action evaluated for the Schwarzschild black hole $\bar{g}_S$

$$\Gamma_{\text{EOM}}[\bar{g}_S;\ T] = \frac{1}{8\pi G_{\text{N}}} \int_0^\beta \mathrm{d}t_{\text{E}} \int_{S^2} \mathrm{d}^2x\sqrt{-\gamma}\,\big(K - K_0\big) \tag{6.57}$$

contains not only extrinsic curvature, but also subtracts a reference extrinsic curvature $K_0$ so that $\Gamma_{\text{EOM}} = 0$ when evaluated for Minkowski space. In the integral on the right-hand side (6.57), we have indicated that we are going to use Schwarzschild coordinates (2.1). In these coordinates, it is easy to show for an $r = \text{const.}$ hypersurface that the normalized normal vector is given by $n^\mu = \sqrt{1-2M/r}\,\delta_r^\mu$ and hence $K = K_0 + \partial_r n^r$ and $K_0 = 2/r$ so that the action (6.57) evaluates to

$$\Gamma_{\text{EOM}}[\bar{g}_S;\ T] = \frac{1}{8\pi G_{\text{N}}}\,4\pi\beta \lim_{r\to\infty} r^2\partial_r n^r = \beta\,\frac{M}{2G_{\text{N}}} \tag{6.58}$$

leading to the free energy $F = T\Gamma_{\text{EOM}}[\bar{g}_S;\ T] = \frac{M}{2G_{\text{N}}} = \frac{1}{4\pi G_{\text{N}} T}$ and the BH entropy $S = -\partial F/\partial T = (4\pi T^2 G_{\text{N}})^{-1} = 4\pi M^2/G_{\text{N}} = \frac{A_h}{4G_{\text{N}}}$.

We conclude this topic by adding angular momentum and charge(s) to the black hole; conceptually little changes, other than the partition function now depending on more parameters, $Z = Z(T,\ \Omega,\ \Phi,\ \dots)$, where $\Omega$, $\Phi$ are angular rotation and electrostatic potential of the black hole and the ellipsis denotes further possible parameters. We leave this extension as an exercise for the reader, Exercise 6.21.

### 6.5.2 Entropy Bounds

Bekenstein argued that the entropy of any physical system obeys a bound, based on the gedankenexperiments inspired by Wheeler's questions about black holes and entropy. The original Bekenstein bound states that the entropy $S$ of any physical system with energy $E$ confined to a size of radius $R$ obeys the inequality

$$S \le 2\pi E\, R\,. \tag{6.59}$$

To be a bit more precise, the radius is given by $R = \sqrt{\frac{A}{4\pi}}$, where $A$ is the area of the smallest sphere encircling the physical system. Since gravitational stability requires $2M \le R$ the Bekenstein bound (6.59) can be rephrased as

$$S \le \frac{A}{4} \tag{6.60}$$

[5] This method of 'background subtraction' works here but is not very satisfying conceptually; we shall see in later sections that, at least for black holes in AdS, there is a more satisfying approach known as holographic renormalization.

thus making the connection to black hole entropy more obvious. While there are various gedankenexperiments and calculations supporting the Bekenstein bound, it is easy to find counterexamples. For instance, during gravitational collapse, the size of the collapsing star (just before hitting the singularity) can become arbitrarily small, so that the area in (6.60) gets arbitrarily small while entropy remains what it was initially. Such a system thus violates the Bekenstein bound (6.60).

Apart from various counterexamples, there are fundamental criticisms of the Bekenstein bound (6.59): it is not covariant with respect to diffeomorphisms, since it requires specifying some area in some coordinates; it suffers from the so-called species problem, i.e. one can increase the entropy arbitrarily without changing the energy by adding copies of the same type of particle (e.g. by increasing the number of neutrino families from three to some large number $N$); it can be violated simply by throwing in negative energy states (e.g. some system dominated by Casimir energy). The latter two problems were overcome by Horacio Casini [431], who reformulated the Bekenstein bound in terms of the information-theoretic notion of relative entropy. This reformulation converts the Bekenstein bound (6.59) to a theorem in QFT, namely non-negativity of relative entropy, and does not suffer from the species problem. However, the Casini version of the Bekenstein bound no longer has anything obvious to do with black holes or gravity; it is a true statement about relative entropy in any unitary QFT.

The remaining deficiency of the Bekenstein bound is overcome by the covariant entropy bound conjectured by Raphael Bousso [432], proven in [433], which brings back gravity into the game. The Bousso bound

$$\Delta S \leq \frac{\Delta A}{4} \tag{6.61}$$

formally looks similar to the Bekenstein bound (6.60), but there are important differences. In particular, both sides of the Bousso bound (6.61) are covariant. The left-hand side, $\Delta S$, denotes the entropy on a light-sheet, which is a null hypersurface whose cross-sectional area is monotonically increasing in the direction emanating from the initial area $A_i$. The right-hand side gives the difference between initial area $A_i$ and final area $A_f$, $\Delta A = A_i - A_f$, on the light sheet.

## 6.6 Parikh–Wilczek Tunneling

Hawking's analysis for particle production by black holes bypasses the complications of gravitational collapse and black hole formation but misses to describe the Hawking effect as a local process. Maulik Parikh and Frank Wilczek (PW) provided a novel method for computing the Hawking radiation spectrum addressing this shortcoming [434–436].

The PW method is more local and makes it apparent that the Hawking radiation is due to virtual pair creation close to the horizon, as anticipated originally by Hawking. The produced particles are virtual since they have imaginary momentum. One of the particles can then tunnel outside while the other remains inside the black hole. The vacuum state is chosen such that the particles outside the horizon have positive energy and those inside have negative. The energy of a particle changes sign as it crosses the horizon, so this process can materialize with zero total energy. The particles remaining inside the horizon hence reduce the energy of the black hole by the same amount that the particle tunneled outside the horizon carries off as radiation. Once the particle has tunneled outside, it can get converted into a real particle with real momentum, which eventually can be measured by some detector far away from the black hole.

### 6.6.1 Painlevé Coordinates

To illustrate how the tunneling idea works, we focus on Schwarzschild black holes. During the pair production and tunneling process, the geometry is not fixed and static. However, for large black holes, one may assume stationarity to a good approximation. It is customary, in this context, to employ Painlevé coordinates [32],

$$\mathrm{d}s^2 = -\Big(1 - \frac{2M}{r}\Big)\mathrm{d}t^2 + 2\sqrt{\frac{2M}{r}}\,\mathrm{d}t\,\mathrm{d}r + \mathrm{d}r^2 + r^2\mathrm{d}\Omega^2 \,. \tag{6.62}$$

This coordinate system is smooth at the future event horizon $r = 2M$ and has the additional feature that $t =$ const. slices are 3-dimensional Euclidean space in spherical coordinates. The price to pay is that the metric (6.62) is stationary but not static.

Radial null geodesics in (6.62) are determined by

$$\dot{r} := \frac{\mathrm{d}r}{\mathrm{d}t} = \pm 1 - \sqrt{\frac{2M}{r}} \,. \tag{6.63}$$

With the assumption that $t$ increases toward the future, the upper (lower) sign in (6.63) corresponds to outgoing (infalling) geodesics. Near the horizon, $r = 2M + \rho$, $\rho \ll 2M$ the above to leading order in $\rho$ become, $\mathrm{d}\rho/\mathrm{d}t = \kappa\rho$ (outgoing) and $\mathrm{d}\rho/\mathrm{d}t = -2 + \kappa\rho$ (infalling), where $\kappa = 1/(4M)$ is the surface gravity. As we see the Painlevé time coordinate clearly differentiates between the infalling and outgoing null rays, respectively, $\rho \sim -2t$ and $\kappa t \sim \ln \rho$. Therefore, for an outgoing trajectory passing through the horizon Painlevé time $t$ picks up an imaginary $2\pi/\kappa$ factor. This observation is at the heart of the PW tunneling method.

The other crucial ingredient that goes beyond Hawking's original derivation is to include the back-reaction of a massless particle of energy $E$. The full analysis may be found in [437] and the result is as follows. Consider a system of fixed *total mass* $M$, which may consist of a black hole and the massless shell of particles of energy $E$. When the particle shell is emitted, the black hole mass becomes $M - E$, and hence the particle(s) will travel on geodesics of the back-reacted metric

$$\mathrm{d}s^2 = -\left(1 - \frac{2(M-E)}{r}\right)\mathrm{d}t^2 + 2\sqrt{\frac{2(M-E)}{r}}\,\mathrm{d}t\,\mathrm{d}r + \mathrm{d}r^2 + r^2\mathrm{d}\Omega^2 \,, \tag{6.64}$$

yielding the change $M \to M - E$ in (6.63).

### 6.6.2 Painlevé–Parikh–Wilczek Vacuum

The Killing vector $\partial_t$ is timelike outside the horizon ($r > 2M$) and one may use it to define the Hamiltonian. We then have negative and positive frequency states with respect to this Hamiltonian. The details of quantizing waves in this coordinate system near the horizon are the same as in previous sections, but the vacuum state differs slightly. The vacuum is chosen such that it is annihilated by negative frequency modes with respect to $\partial_t$; such a state looks non-singular and essentially empty to a free-fall observer passing through the horizon. This vacuum differs from the standard Unruh vacuum or Hartle–Hawking vacuum near the horizon, which is defined to annihilate negative frequency modes with respect to the EF coordinate $v$ (or the Kruskal coordinate $V$).

In the PW picture, Hawking radiation is pair creation *just inside* the horizon with one partner tunneling outside the horizon where it will have a positive frequency mode, while the negative frequency mode remains inside. Alternatively, pair creation may happen *just outside* the horizon with the negative energy particle falling into the black hole and the one outside escapes to infinity. Both tunneling processes contribute to the Hawking radiation and their *amplitudes* must be summed and then squared to get the tunneling probability rate.

To compute the probability of the tunneling process, one may use a complete field theory analysis or a quantum mechanics approximation for a spherical shell of particles using the WKB approximation. The latter is justified due to the large blueshift factor between the local *fido* sitting near the horizon compared to the observer in the distance who sees radiation of the typical wavelength of the size of the black hole. Therefore, the *fido* sees essentially a point particle.

**Particle tunneling-out channel.** Assuming that the created particles are free and only feel the effects of the background, the tunneling amplitude for the spherical shell of particles is given by the imaginary part of the action for an $s$-wave outgoing positive energy particle that crosses the horizon outwards from $r_{\text{in}}$ to $r_{\text{out}}$,

$$\operatorname{Im} I = \operatorname{Im} \int_{r_{\text{in}}}^{r_{\text{out}}} p_r \, \mathrm{d}r = \operatorname{Im} \int_{r_{\text{in}}}^{r_{\text{out}}} \int_0^{p_r} \mathrm{d}p_r' \, \mathrm{d}r \ . \tag{6.65}$$

This is the volume of the phase space of a free particle that tunnels through the horizon. It can be evaluated without entering into the details of the solution, recalling $\dot{r} = \frac{\mathrm{d}H}{\mathrm{d}p_r}|_r$ , where $H$ is the Hamiltonian. Changing the integration from momentum to energy and switching the order of integrations yields

$$\operatorname{Im} I = \operatorname{Im} \int_M^{M-E} \int_{r_{\text{in}}}^{r_{\text{out}}} \frac{\mathrm{d}r}{\dot{r}} \, \mathrm{d}H = \operatorname{Im} \int_0^{+E} (-\mathrm{d}E') \int_{r_{\text{in}}}^{r_{\text{out}}} \frac{\mathrm{d}r}{1 - \sqrt{\frac{2(M-E')}{r}}} \,, \tag{6.66}$$

where we have used the back-reacted geodesic (6.63), and $H = M - E'$. The $r$ integral can be performed noting that there is a simple pole at $r_p = 2(M - E' + i\epsilon)$, where we used $E' \to E' - i\epsilon$ for which the positive energy solutions decay in time (the lower half complex $E'$ plane). We hence obtain

$$\mathrm{Im}\ I = 4\pi E\,(M - \frac{E}{2}) = \frac{\pi E}{\kappa}(1 - 2\kappa E)\ , \tag{6.67}$$

provided $r_{\rm in} > r_{\rm out}$. In the second equality, we inserted the result for surface gravity, $\kappa = (4M)^{-1}$.

**Anti-particle tunneling-in channel.** This calculation is analogous to above, with the changes $E \to -E$ in (6.64) and $\sqrt{\frac{2M}{r}} \to -\sqrt{\frac{2M}{r}}$. Thus, an infalling negative energy particle has as imaginary part of the action

$$\mathrm{Im}\ I = \mathrm{Im} \int_0^{-E} \mathrm{d}E' \int_{r_{\rm out}}^{r_{\rm in}} \frac{\mathrm{d}r}{-1 + \sqrt{\frac{2(M+E)}{r}}} = +4\pi E(M - \frac{E}{2})\ , \tag{6.68}$$

where the $E'$ integral has been performed over the $E' + i\epsilon$ contour.

**Tunneling rate.** Both the particle or anti-particle tunneling channels contribute to the rate for the Hawking process and one should add their amplitudes and the square to obtain the semiclassical tunneling rate.

$$\Gamma \sim e^{-2\,\mathrm{Im}\ I} = e^{-8\pi E(M - \frac{E}{2})} = e^{+\Delta S_{\rm BH}} \tag{6.69}$$

where $\Delta S_{\rm BH}$ is the change in the BH entropy. For the case of Schwarzschild black hole, reintroducing constants of nature, it is given by

$$\Delta S_{\rm BH} = \frac{4\pi G_{\rm N}}{\hbar c}\left((M - E/c^2)^2 - M^2\right)\ . \tag{6.70}$$

The above rate of emission for a particle of energy $E$ may also be written as

$$\Gamma(E) = e^{-\beta E + \frac{E^2}{2(M_{\rm Pl}c^2)^2}} \qquad \beta := \frac{1}{k_{\rm B} T_{\rm H}} = \frac{\hbar c}{8\pi G_{\rm N} M} \tag{6.71}$$

which is the Boltzmann factor for a particle with energy $E$ at inverse temperature $\beta$, plus an $E^2$-correction. The temperature in (6.71) recovers Hawking's result (6.30). Thus, in addition to confirming Hawking's derivation, the PW tunneling leads to an extra contribution, negligible at large mass, accounting for some back-reactions.

Standard arguments then yield the Planck spectral flux

$$\rho(\omega) = \frac{\mathrm{d}\omega}{2\pi} \frac{|\,T(\omega)|^2}{e^{+\beta\omega - \omega^2/M_{\rm Pl}^2} - 1}\ , \tag{6.72}$$

that includes a correction term quadratic in the frequency $\omega$ from back-reactions. The quantity $|\,T(\omega)|^2$ is the frequency-dependent transmission coefficient for the outgoing particle to reach future infinity without backscattering. As discussed in previous sections, $T(\omega)$ may be computed from a more complete treatment of the modes, whose semiclassical behavior near the turning point we have discussed here.

### 6.6.3 Discussion of Parikh–Wilczek Tunneling

We close this section with some comments on PW tunneling.

- Hawking radiation may be viewed as a tunneling process over a potential barrier. The shape of the potential and where the barrier is (in spacetime) depends on the emitted object, due to back-reaction effects and the energy, charge, and angular momentum conservations.
- The location of the maximum of the potential is somewhere between the horizon of the original black hole (before the emission) and the horizon of the black hole after the emission of the shell.
- The final result $e^{\Delta S_{\text{BH}}}$ suggests that the Painlevé coordinate system does not play a crucial role. However, the choice of the vacuum state is important and carries physical meaning.
- The tunneling method can be extended and applied to other cases, like emission of neutral or charged particles and particles of various spin from RN, KN, and AdS–Schwarzschild, see Exercises 6.12–6.16 for various examples. In all these cases, the final result for the tunneling rate is governed by the change in the entropy of the black hole during the process, up to conservation laws.
- While the emission spectrum (6.71) is not exactly thermal, the process may be viewed as adiabatic, as long as $E \ll M$ and the first law of thermodynamics and the other conservation laws always hold on the tunneling trajectory. The arguments in Sect. 5.5.3 apply here and the generalized second law, once the entropy of emitted particles is also taken into account, is respected. As for the third law, see Exercises 6.13 and 6.14.
- The emission probability is the exponential of the change in the entropy of the final and initial black holes

$$\Gamma = |\text{amplitude}|^2 \times (\text{phase space factor}) \sim \frac{e^{S_{\text{final}}}}{e^{S_{\text{initial}}}} = e^{\Delta S} \,, \tag{6.73}$$

  can be viewed as the ratio of the number of final and initial states in the ensemble of black hole microstates. This is suggestive of the existence of an underlying statistical mechanical system (black hole microstates).

## 6.7 Black Hole Evaporation

As discussed, black holes behave like a thermal system at a given temperature and radiate off their mass, angular momentum, and other charges through an almost perfect black body radiation. Let us consider the case of a Schwarzschild black hole, which radiates off its energy according to Stephan–Boltzmann's law

$$\frac{\mathrm{d}E}{\mathrm{d}t} = \sigma A T_{\text{H}}^4 \,, \qquad \sigma := \frac{\pi^2 k_{\text{B}}^4}{60\hbar^3 c^2} \tag{6.74}$$

where $A$ is the black hole horizon area. Since

$$\delta E = -\delta M c^2\,, \qquad A = 16\pi (G_{\rm N} M/c^2)^2\,, \qquad k_{\rm B} T_{\rm H} = \frac{\hbar c^3}{8\pi G_{\rm N} M} \tag{6.75}$$

we have

$$\frac{{\rm d}M}{{\rm d}t} = -\frac{\lambda}{M^2}\,, \qquad \lambda = \frac{\hbar c^6}{2^{10}\cdot 3\cdot 5\pi G_{\rm N}^2}\,. \tag{6.76}$$

So it seems that there is nothing to stop a black hole to shed off all its mass and *evaporate*. We note that out-of- thermality corrections to the Hawking radiation, like those in the tunneling method, as long as energy conservation is satisfied, does not bar a black hole from total evaporation. Integrating the above, we find the lifetime of the black hole

$$\tau = \frac{\hbar c^6\, M^3}{5120\pi G_{\rm N}} \simeq 2.1\times 10^{67}\left(\frac{M}{M_\odot}\right)^3 \text{yrs}\,. \tag{6.77}$$

The above equations show that a Schwarzschild black hole becomes hotter as it radiates off its mass, so the corrections to the thermal distribution and the back-reaction effects become more relevant as we approach the last stages of black hole evaporation. One may explore if such corrections can become so important that can stop the total evaporation and lead to the so-called black hole remnants (see Exercise 6.18). Moreover, a similar black hole evaporation process will also take place for rotating and/or charged black holes, where besides mass they radiate off angular momentum and/or charge (see Exercise 6.17). If long-lived, such neutral black holes can play the role of dark matter (see Exercise 6.19).

See seminal paper series by Don Page [438–442] and their followups for more detailed analysis of charged and/or rotating black holes in various physical setups.

## 6.8 Membrane Paradigm

The EEP implies that any *fido* who always remains outside the horizon should be able to give a complete local account of physics, at least classically, through the information available to her without ever knowing what is inside the horizon. In other words, for this class of observers, one may excise the geometry at the horizon provided that we replace the excised region with a 'membrane' at the boundary of the excised region, the horizon.

According to the 'membrane paradigm' [443], a black hole horizon to an observer who always stays outside the horizon, appears to behave exactly like a dynamical fluid membrane described by physical properties like tension, resistivity, shear, and bulk viscosity. It is described by local but Carrollian hydrodynamics governed by a dissipative Navier–Stokes-like equation, Joule's heat equation, and Ohm's law.[6] See [444,445] for more on Carrollian field theories and how they appear at black hole horizons. These equations, classically, are reminiscent of the bulk theory and its field equations. Semiclassically, via a Euclidean path integral analysis, the membrane free energy accounts for the BH entropy and provides a direct derivation of the Hawking radiation where the imaginary part of the action for the classically forbidden process yields a 'corrected Boltzmann factor' for emission at the Hawking temperature. The membrane paradigm may be viewed as giving a bit more dynamical context to the black hole thermodynamics as well as a framework to perform 'light-cone quantization' of the black hole horizon theory.

The main difference between a horizon membrane and a real membrane such as a soap bubble is that there is no real membrane there from the free-fall observer viewpoint and that the former is acausal, recall that an (event) horizon is a null surface and a causal boundary of *fido*s. Nonetheless, since the membrane picture provides a useful insight into the problem of horizon dynamics and hopefully a handle on its quantization, we will briefly discuss it here. A more detailed and complete account may be found in [434,443,446].

### 6.8.1 Membrane Action and Dynamics, Classical Analysis

The key point we start with is that horizon is the boundary of all causal curves from the outside observer's viewpoint and that a *fido* on one side of the horizon should be able to describe physics exclusively and uniquely through the information available her. While these facts are precise and true at the classical level, one may extend them, as we do in the following, to also hold at semiclassical and quantum levels.

For practical purposes, a regulated version of the horizon, the stretched horizon, is used as the boundary. We take the stretched horizon to be a timelike $(2+1)$-dimensional surface which is at distance $\epsilon$ from the null horizon. We denote the out-pointing spacelike unit normal vector to the stretched horizon by $n^\nu$, $n^2 = 1$ and take our *fidos* to follow worldlines with velocity $u^\mu$, $u^2 = -1$, $n \cdot u = 0$. In the $\epsilon \to 0$ limit, both $n^\mu$ and $u^\mu$ become null vector tangent and/or normal to horizon $\mathcal{H}$; $\epsilon n^\mu = l^\mu = \epsilon u^\mu$, $l^2 = 0$. Upon choosing appropriate boundary terms for the gravity and matter actions, Einstein equations projected at the boundary yield the basic membrane equations which describe its physical properties. The details of the analysis may be found in the Appendix H and here we quote the final result.

Conservation of energy of the membrane (see Appendix H) takes the form of the heat transfer equation for a 2-dimensional fluid

$$T\left(\frac{\mathrm{d}\Delta S}{\mathrm{d}\tau} - \frac{1}{\kappa}\frac{\mathrm{d}^2\Delta S}{\mathrm{d}\tau^2}\right) = \left(\zeta\theta^2 + 2\eta\sigma_{ab}\sigma^{ab} + T_{\mu\nu}n^\mu u^\nu\right)\Delta A\ , \tag{6.78}$$

[6] Carrollian theories arise as zero speed of light limit, $c \to 0$, of relativistic theories. This is in contrast with the Galilean limit, $c \to \infty$.

where $u^\mu \partial_\mu := \mathrm{d}/\mathrm{d}\tau$, $\theta$ is the expansion of the null congruence $l$ and $\sigma$ is its shear (see Sects. 3.2.1 and 3.3), $T_{\mu\nu}$ is the energy–momentum tensor of the matter fields on the membrane and the temperature $T$ and the entropy $S$ are given by

$$S = C\frac{k_{\mathrm{B}}}{\hbar G_{\mathrm{N}}}A\ , \qquad T = \frac{\hbar}{8\pi k_{\mathrm{B}} C}\kappa\ , \tag{6.79}$$

where $C$ is some proportionality constant which is not classically determined. Quantum mechanically, e.g. using Euclidean on-shell action, its value is fixed to be 4.

### 6.8.2 Membrane Action, Semiclassical Analysis

As discussed, the dissipative behavior in the membrane description at the classical level arises as a result of the regularity requirement at the (stretched) horizon, once we cut out the high-frequency (UV) modes residing between the horizon and the stretched horizon. One may then ask if a similar picture (states cutout) can work at the quantum level. If such a membrane quantum description exists, the black hole entropy may then be associated with the logarithm of the number of these UV modes. Here we discuss similar 'semiclassical' and a more quantum version of the regularity conditions within the membrane paradigm.

#### 6.8.2.1 Membrane Free Energy and Black Hole Entropy

The semiclassical regularity condition is provided by the absence of a conical singularity at the stretched horizon in Euclidean geometry. That is, the imaginary time, $\tau = it$, in the near horizon geometry for a stationary black hole is periodic, $\tau \sim \tau + \beta$, $\beta = \frac{2\pi}{\kappa}$ where $\kappa$ is surface gravity [22,429]. This Euclidean geometry is smoothly capping off at the horizon like a cigar and does not cover the black hole 'interior'. In this Euclidean framework, one may consider the Euclidean path integral (partition function) which is a suitable tool for reading off thermodynamical quantities. The partition function is the path integral over all Euclidean field configurations collectively denoted by $\Psi$ with $\beta$ periodicity (for fermions, we may need to impose anti-periodic boundary conditions, see e.g. [447]) and with given boundary field values $\varphi$. In the presence of rotation and electric charges we need to also fix the value of the 'chemical potentials' associated with these charges, respectively, horizon angular velocity $\Omega_{\mathrm{H}}$ and $\Phi_{\mathrm{H}}$. That is, we integrate over metrics with a given horizon angular velocity and electric field configurations with a given horizon electric potential. We also need to fix similar boundary conditions in the asymptotic region, which we typically choose it to be a static frame with vanishing electric potential. In a stationary phase approximation, the partition function is

$$\mathcal{Z} = \int \mathcal{D}\Psi \exp\left(-S_{\mathrm{bulk}}[\Psi] - S_{\mathrm{b'dry}}[\varphi]\right) \approx \exp\left(-S_{\mathrm{bulk}}[\Psi_{\mathrm{cl}}] - S_{\mathrm{b'dry}}[\varphi_{\mathrm{cl}}]\right) . \tag{6.80}$$

Here we have set $\hbar = 1$, $G_{\mathrm{N}} = 1$ and $S_{\mathrm{bulk}}$, $S_{\mathrm{b'dry}}$ denote the bulk and boundary Euclidean actions. The boundary action includes both the action at the asymptotic boundary as well as the (membrane) action at the boundary, as we discussed earlier in this section.

The explicit computation of the on-shell action is straightforward and depending on the boundary conditions in the asymptotic region may need regularizations, similar to the analysis performed in Sect. 6.1. Here we focus on asymptotic flat stationary solutions to the Einstein–Maxwell theory we discussed earlier, i.e. the KN black holes [22,448]. The details of the calculation are left as an exercise to the reader (see Exercise 6.21). Here we only present the results. The bulk action, in this case, yields $-\frac{1}{2}\beta Q\Phi_{\rm H}$. The horizon boundary term gives $S_{\rm BH} = \frac{A}{4}$ where $A$ is the horizon area. The asymptotic boundary term yields $\frac{1}{2}\beta M - \beta\Omega_{\rm H} J$. Putting these together and recalling that $-\ln \mathcal{Z} = \beta F$, where $F$ is the Helmholtz free energy, then,

$$F = \frac{1}{2}M - \Omega_{\rm H} J - \frac{1}{2}\Phi_{\rm H} Q - T_{\rm H} S_{\rm BH} = 0, \qquad \beta = 1/T_{\rm H}, \tag{6.81}$$

where we used Smarr relation (5.81).

The 'total free energy' is the sum of the membrane free energy and the sum of bulk and asymptotic free energies. Its vanishing is due to a precise cancelation between the two. The basic idea of the membrane paradigm is that from the outside observer's viewpoint the black hole is replaced by a membrane. The membrane's free energy coincides with the black hole free energy. Its value is given by the on-shell Gibbons–Hawking term which is $\frac{\kappa\beta A}{8\pi G_{\rm N}} = \frac{A}{4G_{\rm N}}$. This is due to the fact that, for a stationary horizon, extrinsic curvature $K = \kappa$. That is, the membrane partition function is simply $e^{-S_{\rm BH}}$. We stress that this fixes the numeric coefficient $C$ in (6.79) to 4. Vanishing of the 'total free energy' makes manifest conservation of energy and other charges: the energy and charges of anything falling through the horizon, dissipating into the membrane, are provided by the stuff in the outside region.

#### 6.8.2.2 Black Hole Emission in the Membrane Picture

The results of the previous section on black hole entropy and membrane free energy can be readily combined with the analysis of Sect. 6.6 to give the emission rate of a black hole. This is due to the fact that, as discussed, in the tunneling picture during the tunneling, the first law of black hole dynamics is satisfied which is guaranteed by the on-shell condition used in deriving the semiclassical partition function (6.80). Therefore, the emission rate from a membrane which is the tunneling rate through the membrane is given by the ratio of the black hole (membrane) free energies after and before the emission.

The tunneling analysis of Sect. 6.6 was performed by computing the on-shell action for a particle pair production at the stretched horizon; it was a quantum particle analysis on a classical background. One may upgrade the same analysis by promoting the particle theory to a field theory, e.g. a scalar theory (minimally) coupled to the background with appropriate boundary terms. The computation of the imaginary part of the Euclidean path integral for this theory in the stationary phase approximation, as expected, yields the same result as the tunneling method for particles, see [434] for more details.

**Concluding remarks for the section**

As discussed, classical regularity at the stretched horizon for the outside observers implies that one can excise the inside region and replace it with a membrane that has its own stress tensor and charge density. These are subject to continuity equations (like the Navier–Stokes and Joule's heat equations and Ohm's law). These physical properties and the membrane are, in fact, to represent the high-frequency (UV) modes residing between the horizon and the stretched horizon, which are excised.

We discussed that similar regularity requirements at the semiclassical level can be imposed through the periodicity of fields in the Euclidean Wick-rotated geometry, and also through fixing other chemical potentials like horizon angular velocity and Coulomb potential. This semiclassical regularity yields that the membrane partition function is $e^{-S_{\rm BH}}$ which suggests that the logarithm of the number of 'quantum degrees of freedom' associated with the membrane, the black hole entropy, is $S_{\rm BH}$.

One may ask if this semiclassical regularity condition can be a result of a more quantum regularity condition. Such a 'quantum regularity' may arise from integrating out (tracing over) the part of the density matrix associated with the UV modes, yielding an entangled density matrix on the cutout (excised) Hilbert space. The 'classical-quantum correspondence principle' then implies that the quantum entanglement entropy should be equal to the thermodynamics entropy [449,450]. We shall discuss this picture further in Chap. 9.

We close this section by noting that the analysis presented here is mainly based on the 'old membrane paradigm', which does not emphasize the Carrollian nature of the physics at null surfaces (horizons). The 'new membrane paradigm', which is emerging at the time of writing this book and is still in progress, builds upon Carrollian physics. See, e.g. [444,445,451–453] for some papers in this direction.

## 6.9 Information Puzzle and Apparent Loss of Unitarity

As discussed in earlier chapters, black holes can classically form with usual GR dynamics and quite generic matter content. Once semiclassical effects are also considered, black holes generically Hawking-evaporate their mass and charges into thermal radiation. In the analysis of Sect. 6.6, we showed that considering local backreactions due to conservation of energy and other charges within the semiclassical treatment yields a slight deviation from complete Boltzmann thermal distribution. Nonetheless, this out-of-thermality remains very small until the very last stages of the black hole evolution when the black hole becomes very small and hot. But there is nothing to stop the black hole from evaporating completely, yielding a final state consisting essentially of thermal radiation. The corresponding Penrose diagram is shown in Fig. 6.3.

Black hole evaporation has sparked a decades-long discussion about information loss that is still not over yet. There are different layers and viewpoints to this discussion, and therefore, various proposals for addressing it. One viewpoint is that

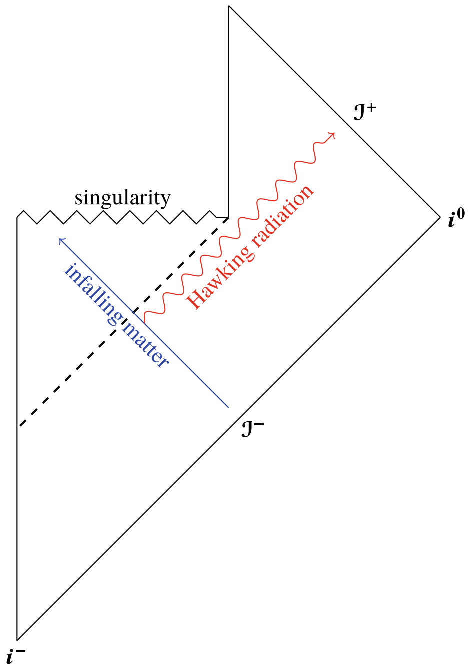


**Fig. 6.3** Penrose diagram of evaporating black hole in semiclassical approximation

since black hole evaporation arises in a semiclassical analysis, the resolution of the issue should also be sought at the same level. Another viewpoint is that, black hole evaporation is inherently a quantum effect and its resolution is only possible in a fully-fledged QG setting. A third viewpoint is that black hole evaporation is a deeply quantum phenomenon and its resolution needs quantum information notions like entanglement (between the black hole and Hawking radiation and within the Hawking radiation itself) and its formulation need not necessarily involve QG, which is presumably best formulated through quantum informatic notions. In this latter viewpoint, the information loss issue is viewed as a window to QG. In this part, we discuss the first, semiclassical, viewpoint, and the QG and quantum information viewpoints will be left to Sect. 9.2 and Chap. 10.

**Information loss as seen by the outside observer.** An outside observer witnesses information loss in the following sense [80]: while the initial state forming the black hole might be pure (e.g. , lots of laser lights shining toward a common center), the final state after the black hole has evaporated completely is thermal, and hence appears to be a mixed state. The transition from a pure state to a mixed state is only possible if the evolution operator is non-unitary. That is, information loss means non-unitarity in the evolution of black holes.

In this description, we are in a similar situation as when shining a laser on a cold piece of coal (or burning a book), which also leads to information loss for nearly all practical purposes. The apparent conversion of a pure initial state to a mixed final state is the core of the information loss problem for the outside observer. In the case of a piece of coal, there is universal agreement that information is not lost in principle; it is only very hard to retrieve. If one places an array of ultra-sensible detectors around the piece of coal and collects patiently all photons emitted, one should be able to eventually find correlations between these photons that show small deviations from a mixed thermal state and in principle allow to reconstruct the initial state.

In the case of a black hole, there is an agreement (with a few notable exceptions[7]) that information can be retrieved in principle in essentially the same way as for the piece of coal [82]. Thus, black holes are thermal states, by which we mean they are pure states that are exponentially close to mixed states. As long as we probe black holes only with simple experiments, they will be indistinguishable from a mixed state and we have information loss for nearly all practical purposes, but no information loss in principle. So in the end, there is no clash with quantum mechanics or unitarity—black holes behave precisely like any other quantum system. This conclusion/assumption was called 'central dogma' in [455], which collects evidence in its favor.

**Black hole complementarity.** We discussed how an outside observer describes the information loss issue. One may ask how a free-fall observer describes and formulates the information loss. Within classical GR, the EEP may be used to translate observations of outside and free-fall observers to each other. Recalling the discussions of earlier sections in this chapter, it is quite natural to expect EEP to be extended to the semiclassical regime too. In fact, the Unruh effect (cf. Sect. 6.3) is a manifestation of this expectation. A more detailed and careful analysis of this expectation was formulated as "black hole complementarity" by 't Hooft [456] and Susskind [83]: The outside observer, who does not see the inside horizon region, already has access to all the possible physical observables, just like the free-fall observer. That is, what these observers see is equivalent, but 'complementary' to each other. To be precise, black hole complementarity, besides the EEP, may be formulated through three extra postulates [91]:

I. The process of formation and evaporation of a black hole, as viewed by an outside (distant) observer, can be completely described by a unitary local QFT the S-matrix of which describes the evolution from infalling matter to outgoing Hawking-like radiation.
II. Outside the stretched horizon of a massive black hole, physics can be described as a good approximation by a set of semiclassical field equations.
III. To an outside observer, a black hole appears to be a quantum system with discrete energy levels. The entropy of the black hole in a microcanonical ensemble description is the logarithm of the dimension of the Hilbert subspace of states describing the black hole, the black hole microstates.

[7] The main counter-argument about the resolution in the main text is inspired by Unruh's 'analog black holes' [454], which may be interpreted to indicate that black holes are open quantum systems and hence non-unitarity is not a problem but rather an expected feature of black holes. While this still is a logical possibility, the scenario mentioned in the main text seems more plausible to most researchers.

**No cloning theorem.** In unitary quantum systems, the no-cloning theorem states that two identical copies of a generic quantum state cannot be accessed by a single observer. An immediate issue that arises is the apparent violation of the no-cloning theorem in black holes. Suppose we have some quantum state falling into the black hole together with the infalling observer. If the black hole is large enough, the EP allows to dismiss gravity effects (beyond Newtonian ones) at the scale of the horizon and gives the infalling observer enough time to perform some state tomography experiments to deduce the infalling quantum state. So far so good. However, according to the central dogma above also the outside observer needs to be able to measure (at least in principle) the infalling quantum state; this observer can interpret the information about this state to be stored at/outside the black hole horizon. This now seems to contradict the no-cloning theorem: we need two identical copies of the infalling quantum state, one that passes the horizon and one that remains on/outside the horizon.

The resolution of the no-cloning paradox is immediate and by fiat in black hole complementarity as it states that there is no observer anywhere in spacetime who has simultaneous access to both copies of the quantum state. Even if true, it is not obvious that the no-cloning paradox can be avoided, since one can set up gedanken-experiments with observers falling into black holes, surviving long enough inside so that they can exit the black hole again and then communicate with the outside observer so that they both have access to the quantum copies of the infalling quantum state. It requires precise calculations to show that these apparent paradoxes can be avoided, see [457].

**Firewalls.** The status of black hole complementarity was challenged by the firewall paradox [91], whose main argument was that the following three statements cannot be simultaneously true: 1. Hawking radiation is in a pure state, 2. effective QFT can be applied slightly inside/outside the horizon, and 3. the EP holds (in particular, for large black holes there is no 'drama' at the event horizon). Giving up the last assumption leads to firewalls, i.e. , some (UV-)drama at the horizon. A succinct way of phrasing the essence of the firewall paradox in terms of entanglement properties appeared already in earlier work by Samir Mathur [458], which we are going to discuss in Sect. 9.2.

In conclusion, despite more than four decades of dispute, the community has not reached a final verdict on information loss in evaporating black holes, though it is fair to say that most of us believe information is not lost. A recent summary of the status of black hole evaporation, (avoidance of) information loss, and (the absence of) firewalls is [455].

## Further Reading

Some textbooks containing a semiclassical discussion of black holes and the Hawking effect include the one by Mukhanov and Winitzki [459], by Carroll [5], by Frolov and Novikov [134] by Susskind and Lindesay [135], and the lectures notes by Townsend [244]. A (semi-)classic textbook is Birrell and Davies [460].

## Exercises

**6.1 Variational principle and holographic renormalization in mechanics.**

Consider the Hamiltonian $H(q,\ p) = p^2/2 + 1/q^2$ with the bulk action $I[q,\ p] = \int_0^{t_c} \big( - q\,\dot{p} - H(q,p)\big)\,\mathrm{d}t$ in the limit of infinite $t_c$ with the boundary conditions $\lim_{t_c\to\infty}\delta p \neq 0$, $\lim_{t_c\to\infty} q \to +\infty$ and $\lim_{t_c\to\infty}\delta q =$ finite.

(1) Show that one needs to add a 'Gibbons–Hawking–York' boundary term $qp$ to have a Dirichlet boundary value problem where $\delta p$ is unconstrained at the boundary.

(2) Show that such an action has no well-defined variational principle and is infinite on-shell.

(3) Finally, show that subtracting the 'holographic counterterm' $S(q,t)$ as boundary contribution to the action solves both of these problems, where $S(q,t)$ is Hamilton's principal function.

**6.2 Boundary conditions can change the physical spectrum.**

The simplest example where the title of this exercise is true is the quantum mechanics of a free particle on the half-line $x \geq 0$. To see this, consider the time-independent Schrödinger equation $-\psi''(x) = E\,\psi(x)$ and look for bound state solutions, i.e. normalizable wave-functions $\psi(x)$ with $E < 0$. For Dirichlet or Neumann boundary conditions you should find no such bound states, confirming naive classical intuition. However, for Robin boundary conditions $\psi(0) + \alpha\,\psi'(0) = 0$ (with some positive, finite $\alpha$) show that there is exactly one bound state with energy $E = -1/\alpha^2$. Discuss also the limiting cases $\alpha \to 0$ (Dirichlet) and $\alpha \to \infty$ (Neumann).

**6.3 Boundary term for null boundaries.**

The Gibbons–Hawking–York boundary term (6.12) is constructed to work for a spacelike or timelike boundary surface. For null boundary surfaces, like asymptotic null infinite of flat space or black hole horizons, it should be reconsidered. Explore this problem. See [461,462] for useful references on this question.

**6.4 Boundary term for beyond Einstein theories.**

The Gibbons–Hawking–York boundary term (6.12) is constructed to work for the Einstein–Hilbert action.

(1) Construct the appropriate boundary term for $f(R)$ gravity theory, $\mathcal{L} = \sqrt{-g}\, f(R)$ where $R$ is the Ricci scalar. Work out Brown–York quasi-local energy-momentum tensor for this case.

(2) Construct the appropriate boundary term for $D$-dimensional Lovelock theory [463]. Work out the Brown–York quasi-local energy-momentum tensor for this case.

See [8,464–468] for useful references on these questions.

**6.5 Bogoliubov transformation between Rindler and Minkowski modes.**

Take the Rindler modes $\psi_k^\pm$ defined in (6.19) and their complex conjugates to build properly normalized modes $\chi_k^\pm$ defined in Minkowski space,

$$\chi_k^\pm = \frac{1}{\sqrt{2\sinh\frac{\pi\omega}{\kappa}}}\left(e^{\frac{\pi\omega}{2\kappa}}\psi_k^\pm + e^{-\frac{\pi\omega}{2\kappa}}\psi_{-k}^{\mp *}\right). \tag{6.82}$$

Having derived this result, prove the correctness of the Bogoliubov transformation (6.23) stated in the main text.

**6.6 Euclidean Rindler space.**

Take the Rindler metric (6.16) and continue analytically to Euclidean time, $\tau_\mathrm{E} = i\tau$.

(1) Show that this Euclidean manifold is smooth only if Euclidean time is identified periodically with period $2\pi/a$. To this end, use the 'polar coordinate' $\rho = e^{a\xi}/a$.

(2) Show that the Rindler Hamiltonian $i\partial_\tau$ corresponds to the generator of boosts in the $2d$ Minkowski space spanned by $\xi, t$.

(3) Argue that the temperature as seen by accelerated observers at different constant $\xi_0$ values (dotted lines in Fig. 6.1) is $T_{\xi_0} = \frac{ae^{a\xi_0}}{2\pi}$.

(4) The result in (3) above shows that the Unruh temperature is not invariant under translation in $\xi$ or in $\rho = e^{a\xi}$. Show that the Unruh vacuum state is not invariant under such translation either. Work out how the Unruh vacuum and the corresponding Bogoliubov transformations change under this translation.

**6.7 Surface gravity for generic stationary black holes.**

Consider a black hole geometry of the form

$$\mathrm{d}s^2 = -N(r,\theta)\mathrm{d}t^2 + \frac{\mathrm{d}r^2}{F(r,\theta)} + R^2(r,\theta)\left[\mathrm{d}\theta^2 + \Gamma(r,\theta)(\mathrm{d}\phi + \Omega(r,\theta)\mathrm{d}t)^2\right], \tag{6.83}$$

where $N(r,\theta)$, $F(r,\theta)$ have simple roots at constant $r = r_\mathrm{H}$ and other functions $R, \Gamma, \Omega$ are smooth and non-zero functions at $r_\mathrm{H}$.

(1) Expand the metric around $r = r_\mathrm{H}$ and bring the metric to a generic form (6.28).

(2) What are the conditions on $N$, $F$ functions for having a constant ($\theta$ independent) $\kappa$?

(3) Write the explicit form of $\kappa$ in terms of the first derivatives of metric functions with respect to $r$ at $r_\mathrm{H}$.

(4) What are functions $N, F, R, \Omega, \Gamma$ for a Kerr geometry? Read $\kappa$ from the generic formula obtained in item (3) and compare it with the expression for surface gravity of the Kerr metric.

(5) Bonus level: Repeat the above for the Plebanski–Demianski family of geometries discussed in Sect. 2.7.

**6.8 Hawking radiation as viewed by different observers.**

Consider a Kerr black hole of usual parameters $m, a$.

(1) Argue that the Hawking formula $T_{\mathrm{H}} = \kappa/(2\pi)$ is the temperature of Hawking radiation as measured by the asymptotic static observer.

(2) What is the temperature a rotating observer at infinity associates with the Hawking temperature?

(3) What is the temperature of Hawking radiation as measured by an observer rotating with angular velocity $\Omega$ (with respect to the asymptotic flat observer) and sitting at a constant radial coordinate $r$.

(4) What is the temperature as seen by a freely falling observer as she passes at radial coordinate $r$?

**6.9 Specific heat of black holes.**

Calculate the specific heat of a Schwarzschild black hole and discuss thermodynamical consequences.

**6.10 Boulware vacuum.**

Assume that the integration constant $T_-$ that determines the asymptotic flux vanishes and show that the stress tensor flux components in Kruskal coordinates diverge on the horizon.

**6.11 Background subtraction for Euclidean Schwarzschild.**

All three problems mentioned in Sect. 6.5.1 arise already for Schwarzschild black holes in GR. This exercise is concerned with the first problem, the finiteness of the Euclidean on-shell action. After convincing yourself that the bulk action trivially vanishes, show that taking into account the Gibbons–Hawking–York boundary term, the action diverges in the limit where the boundary approaches the asymptotic boundary. Provide an ad-hoc solution to this problem, known as 'background subtraction', by subtracting the Euclidean action of a reference state, namely globally flat space. (Alternative solutions, such as holographic renormalization, will be addressed in later chapters.)

**6.12 Parikh–Wilczek method for neutral particle emission off an RN black hole.**

(1) Starting with the RN solution, show that in the Painlevé time it takes the form

$$\mathrm{d}s^2 = -\left(1 - \frac{2M}{r} + \frac{Q^2}{r^2}\right)\mathrm{d}t^2 + 2\sqrt{\frac{2M}{r} - \frac{Q^2}{r^2}}\,\mathrm{d}t\,\mathrm{d}r + \mathrm{d}r^2 + r^2\mathrm{d}\Omega^2 \,, \quad (6.84)$$

(2) Show that the EOM for an outgoing massless particle (a null geodesic) is

$$\dot{r} := \frac{\mathrm{d}r}{\mathrm{d}t} = +1 - \sqrt{\frac{2M}{r} - \frac{Q^2}{r^2}} \,. \quad (6.85)$$

The ‘back-reacted’ path with $M \to M - E$ when self-gravitation is included [469].

(3) Show that the imaginary part of the action for a positive energy outgoing particle is

$$\operatorname{Im} I = \operatorname{Im} \int_0^{+E} (-\mathrm{d}E') \int_{r_{\text{in}}}^{r_{\text{out}}} \frac{\mathrm{d}r}{1 - \sqrt{\frac{2(M-E')}{r} - \frac{Q^2}{r^2}}} , \tag{6.86}$$

which, as discussed in the main text, should be evaluated by deforming the contour integral $E' \to E' - i\epsilon$ prescription.

(4) Show that the above integral has a simple pole at $r_p = M - E' + i\epsilon + \sqrt{(M - E' + i\epsilon)^2 - Q^2}$ with residue $\sqrt{(M - E')^2 - Q^2}/r_p^2$, and therefore

$$\operatorname{Im} I = \frac{1}{2} \int_0^{+E} \frac{(-\mathrm{d}E')}{T_{\mathrm{H}}(M - E')} = \frac{1}{2} \int_M^{M-E} \mathrm{d}S_{\mathrm{BH}}(X) , \tag{6.87}$$

where

$$T_{\mathrm{H}}(X) := \frac{1}{2\pi} \frac{\sqrt{X^2 - Q^2}}{(X + \sqrt{X^2 - Q^2})^2} , \tag{6.88}$$

is the Hawking temperature of a black hole of mass $X$ and charge $Q$, and in the second equality in (6.87), we have used the first law, which, for cases involving vanishing charge variation, becomes $\mathrm{d}X = T_{\mathrm{H}}(X)\, \mathrm{d}S_{\mathrm{BH}}(X)$, with $S_{\mathrm{BH}}(X)$ being the BH entropy of an RN black hole of mass $X$ and charge $Q$.

Equation (6.87) makes it apparent that, during the tunneling, we allow variation in the temperature, along with the change in the energy, but such that the first law holds. This is, in fact, the essence of the Parikh–Wilczek tunneling method, recalling that the first law is nothing but conservation of the energy.

(5) Finally, compute the tunneling probability for the neutral particles of energy $E$ and show it is

$$\Gamma(E) \sim e^{-2 \operatorname{Im} I} e^{+\Delta S_{\mathrm{BH}}} \tag{6.89}$$

where

$$\Delta S_{\mathrm{BH}} = S_{\mathrm{BH}}(M - E, Q) - S_{\mathrm{BH}}(M, Q), \qquad S_{\mathrm{BH}}(M, Q) = \pi (M + \sqrt{M^2 - Q^2})^2. \tag{6.90}$$

(6) To see the appearance of a Boltzmann factor and deviations from it, study $E \lesssim M, Q$ expansion in $\Delta S_{\mathrm{BH}}$,

$$\Delta S_{\mathrm{BH}} = -\frac{\partial S_{\mathrm{BH}}}{\partial M} E + \frac{1}{2} \frac{\partial^2 S_{\mathrm{BH}}}{\partial^2 M} E^2 + \mathcal{O}(E^3) = -\beta E + \gamma E^2 + \mathcal{O}(E^3), \tag{6.91}$$

where

$$\beta = \frac{2S_{\rm BH}}{\sqrt{M^2 - Q^2}}, \qquad \gamma = \frac{\beta^2}{4S_{\rm BH}^2}\left(4S_{\rm BH} - \sqrt{4S_{\rm BH}^2 - \beta^2 Q^2}\right). \tag{6.92}$$

The above expansion is only valid in the regime $S_{\rm BH} \gtrsim \beta Q/2$, where $\gamma$ is strictly positive.

(7) Argue that the $\sqrt{M^2 - Q^2}$ in the transition rate is a manifestation of the third law of black hole thermodynamics, see Exercise 6.14 for further analysis in the extremal $M = Q$ limit.

**6.13 More on Parikh–Wilczek Tunneling method for charged particles.**

Charged black holes emit predominantly charged particles of the same sign. These particles, despite the Coulomb repulsion, still feel a potential barrier and need to tunnel. Considering charged emissions brings about two new features: (1) The particles are now moving on a curve that is not a (null) geodesic due to the presence of the Lorentz force; (2) The Painlevé–Parikh–Wilczek vacuum state should be chosen such that it breaks charge conjugation invariance (as well as the time-reversal). In this exercise, we take the reader through the respective analysis.

Recall that the horizon of a charged black hole is an equipotential surface, a conducting sphere of radius $r_{\rm H}$ and charge $Q$. The electric field energy can be lowered by emitting a shell of charge $q$.

(1) Show, using the method of images, the effective potential for the system when the charge $q$ is at radius $r$ is

$$V(r) \;=\; q\left(\frac{Q-q}{r} - \frac{q r_{\rm H}}{r^2 - r_{\rm H}^2}\right), \tag{6.93}$$

where we consider configurations of image charge which leave the potential on the sphere constant and the field at infinity fixed. The second term, which is attractive, dominates over the first term in the near horizon limit producing an electric potential barrier. In the gravitational problem, the situation is just the reverse. With back-reaction neglected, there is nothing but the gravitational barrier which is overcome by the fact that the horizon is a constant-temperature surface and 'almost thermal' fluctuations provide the possibility of the emission.

The above potential analysis can be useful in extending the neutral emission analysis to charged cases, e.g. we first note that the first term in (6.93) at the horizon is $q\Phi_{\rm H}(Q-q)$.

(2) Work out the equation for the path of a particle of charge $q$ in metric (6.84).

(3) By an appropriate choice of the vacuum state, work out the tunneling amplitude and show

$$\Gamma(E, q) \sim e^{-2\,{\rm Im}\, S} e^{+\Delta S_{\rm BH}} \qquad \Delta S_{\rm BH} = S_{\rm BH}(M-E, Q-q) - S_{\rm BH}(M, Q). \tag{6.94}$$

with $S_{\rm BH}(M, Q) = \pi(M + \sqrt{M^2 - Q^2})^2$, as the probability of emission of shells of energy $E$ and charge $q$, which we assume $q \geq 0$. The above makes it manifest the energy and charge conservations and that the first law is always holding along the way while the tunneling happens.

(4) Compare the tunneling rate of a black hole of mass $M$ and charge $Q$ to complete radiation when it radiates off its entire mass and charge to the case where it radiates down to an extremal black hole of charge $q < Q$. Note that this latter is in principle a function of $q$, for which $q$ is the rate maximized.

See [470] for more details.

**6.14 Tunneling from and to extremality?**

In the previous exercise, we established how the charge and mass of a black hole can be reduced through tunneling.

(1) Consider the neutral emission rate (6.89). What is the tunneling rate of an extremal black hole? What is the tunneling rate of charged particles (6.94) from an extremal black hole? Draw $\Gamma(E, q)$, for which $E, q$ (6.94) is maximized.

(2) Given (6.94), explore the tunneling rate from a generic non-extremal black hole to an extremal one.

(3) Show that $S_{\rm BH}(M - E, Q - q) > S_{\rm BH}(M, Q)$. As $0 \leq E \leq M$, argue that the tunneling can proceed until $M - E \geq Q - q$. That is, the extremality bound can never be crossed. On the other hand, as $0 \leq q \leq Q$, show that

$$\frac{2qQ - q^2}{2(M + \sqrt{M^2 - Q^2})} < E \leq M - Q + q, \qquad 0 \leq q \leq Q. \tag{6.95}$$

Therefore, for neutral emission ($q = 0$), $0 < E \leq M - Q$ while for the case where all the charge is radiated off ($q = Q$), $\frac{Q^2}{2(M+\sqrt{M^2-Q^2})} < E \leq M$. In particular, we note that if the black hole is initially extremal $M = Q$, $\frac{2qQ-q^2}{4Q} < E \leq q$.

(4) Study near extremal behavior of (6.94), i.e. when $M - Q = \Delta << Q$. Discuss the $E/\Delta \lesssim 1$ case. Is the spectrum nearly thermal?

**6.15 Parikh–Wilczek tunneling method for other black holes.**

(1) Work through the Parikh–Wilczek method for asymptotic AdS black holes, e.g. for AdS-Schwarzschild. You may consult with [471].

(2) Work out the Parikh–Wilczek tunneling method for stationary KN black holes. You may consult with [472,473].

**6.16 Parikh–Wilczek method and emission of particles of various spins.**

Explore how the tunneling method works for vector (spin one) and Dirac (spin 1/2) particles; see [470] for hints and comments.

**6.17 Life-time of a rotating black hole.**

Consider a Kerr black hole of mass $M$ and angular momentum $J = Ma$. Use the fact that a rotating black hole is a thermal system at a given temperature and (rotation/spin) chemical potential, as governed by the first law, and compute its lifetime. Compare this with the lifetime of a Schwarzschild black hole of the same mass.

**6.18 Parikh–Wilczek correction to the black hole lifetime.**
Starting from (6.69) for a Schwarzchild black hole, compute the black hole lifetime and compare it with (6.77).

**6.19 Lower mass bound for primordial black holes.**
Suppose that the early universe provides us with a mechanism to produce all sorts of black holes in a wide range of mass $M$ and angular momentum $J = Ma$. Find the parameter space $(M, a)$ of such PBHs which have a lifetime more than the age of the universe, about 13.8 billion years.

Bonus level: Note that, in the real world, we have the cosmic microwave background radiation at a given temperature $T_{\rm CMB}$ and a black hole can Hawking-radiate if its temperature is more than the cosmic microwave background temperature. Refine the above analysis considering the thermal history of the universe and its temperature as a function of cosmic time. The PBHs if light and long-lived enough can act like dark matter candidates.

**6.20 Membrane partition function when things fall into the black hole.**
As discussed, membrane partition function for stationary black holes is nothing but $e^{-S_{\rm BH}}$. For non-stationary cases, one would expect this to give the change in the entropy of the black hole as things fall into it. Using the fact that, for non-stationary black holes, the extrinsic curvature also includes a term for the expansion of the horizon, $K = \kappa + \theta$, calculate the entropy of the system as matter falls into the membrane in a nonequilibrium process. For this computation, assume 'instantaneous thermalization' i.e. instantaneous growth of the horizon and hence its entropy.

**6.21 Gibbons–Hawking method for stationary charged black holes.**
In Sect. 6.5.1, we discussed the derivation of free energy and entropy for static black holes using the Euclidean path integral method. Extend this analysis to the black holes of the KN family with angular momentum and charge(s). To this end, work out the bulk and horizon and asymptotic boundary on-shell actions for the KN solution and carefully study near horizon and asymptotic values of the bulk Lagrangian as well as the boundary Gibbons–Hawking and Maxwell contributions given in (H.3). The Ricci scalar in the bulk and boundary Maxwell terms vanish and give no contribution. The relevant bulk and boundary terms are hence the Maxwell and Gibbons–Hawking–York terms.

This extension should lead to the partition function that now depends on more parameters, $Z = Z(T, \Omega, \Phi, \dots)$, where $\Omega, \Phi$ are angular rotation and electrostatic potential of the black hole and the ellipsis denotes further possible parameters. A technical issue is that mixed terms in the metric $\mathrm{d}t\,\mathrm{d}\varphi$ produce unwanted factors of $i$ after Euclidean continuation. The simplest remedy is to multiply also the angular momentum by compensating factors of $i$.

**6.22 Membrane paradigm and non-stationary black holes.**

Recall that according to the membrane paradigm, there is a membrane that encodes all the physics inside the (stretched) horizon, and that the stretched horizon is a regulated version of the causal boundary of the outside observers. This membrane picture can be extended to the non-stationary black holes, e.g. those in the sky which accrete matter. In these cases, the horizon is typically a timelike surface and one need not consider the stretched horizon to 'regularize' the problem. In this sense, the membrane paradigm should work for these even more naturally.

Consider a charged Vaidya black hole

$$\mathrm{d}s^2 = -\left(1 - \frac{2M(u)}{r} + \frac{Q^2(u)}{r^2}\right)\mathrm{d}u^2 - 2\,\mathrm{d}u\,\mathrm{d}r + r^2\left(\mathrm{d}\theta^2 + \sin^2\theta\mathrm{d}\phi^2\right)\,, \tag{6.96}$$

where $M(u)$, $Q(u)$ are, respectively, the Bondi mass and electric charge measured at future null infinity. The above is a solution to Einstein–Maxwell-matter theory with

$$T_{uu} = \frac{1}{8\pi r^2}\left[\left(1 - \frac{2M(u)}{r} + \frac{Q^2(u)}{r^2}\right)\frac{Q^2(u)}{r^2} + \frac{1}{r}\frac{\partial Q^2(u)}{\partial u} - 2\frac{\partial M(u)}{\partial u}\right]\,. \tag{6.97}$$

$M(u)$, $Q(u)$ are arbitrary functions of $u$.

Consider the special case

$$M(u) = (au + b)\Theta(u_0 - u)\,, \quad Q(u) = \eta M(u)\,, \tag{6.98}$$

where $a < 0$ and $|\eta| \le 1$, with $|\eta| = 1$ at extremality.

(1) Read the membrane stress tensor and electric current.

(2) Work out the Navier–Stokes, Joule's heat transfer, and the electric current continuity for the membrane fluid.

(3) Compute the Euclidean path integral (partition function) for the membrane.

(4) Compute the emission rate and study its time ($u$) dependence.

More details may be found in [434].

**6.23 A pure state cannot unitarily evolve to a mixed state.**

Let $U(t_1, t_2)$ be the evolution operator from time $t_1$ to $t_2$. Suppose that at $t_1$, a system is in a pure state, i.e. its density matrix $\rho(t_1)$ has an eigenvalue one and the rest of its eigenvalues are zero. Show that the density matrix at $t_2$, $\rho(t_2)$, obtained by a unitary evolution $U(t_1, t_2)^\dagger = U(t_1, t_2)^{-1}$, is necessarily a pure state.

Conversely, show that if $\rho(t_2)$ is a mixed state can only be obtained from a pure state through a non-unitary evolution operator $U(t_1, t_2)$.

# 7 Gravity and Black Holes in Diverse Dimensions

**Abstract**

Gravity in dimensions other than four is often used as a playground to explore theoretical issues and (quantum) aspects of black holes. In Sect. 7.1, we provide the rationale for studying black holes in lower dimensions. Sections 7.2 and 7.3 are devoted, respectively, to gravity in three and two spacetime dimensions. Black holes in higher dimensions provide a setup to explore how classical theorems like topology and uniqueness theorems work, and we study them in Sect. 7.4. Higher-dimensional gravity theories are closely related to string theory and allow for black rings, strings, and branes, which we construct and explore in Sect. 7.5. In Sect. 7.6 we briefly discuss black holes in a large number of dimensions.

## 7.1 Why Gravity in Lower Dimensions?

Our macroscopic world has three spatial and one time dimensions, while UV completions of GR, such as string theory, may require additional dimensions. So why study lower-dimensional gravity?

The answer is foremost technical simplicity while maintaining conceptual complexity. For instance, various puzzles associated with semiclassical or quantum aspects of black holes (microstates and entropy, evaporation and unitarity, entanglement, smoothness of interior region, holographic aspects, etc.) arise independently of the dimension. If they can be solved in a technically more manageable framework, such as in lower-dimensional gravity, we may learn valuable lessons regarding semiclassical or quantum aspects of black holes that are independent of the dimension.[1]

How low can we go? If we want to keep the defining property of a black hole, a horizon, then we need at least one spatial and one time dimension. Thus, the lowest possible dimension for black hole toy models is two. If additionally, we

[1] Some additional motivation for studying gravity in two dimensions stems from the conjecture that at small distances gravity is effectively 2-dimensional, see [474] and refs. therein.



D. Grumiller and M. M. Sheikh-Jabbari, *Black Hole Physics*, Graduate Texts in Physics,
https://doi.org/10.1007/978-3-031-10343-8_7

want our underlying gravity theory to be GR then two dimensions are too low since the Einstein tensor vanishes kinematically for any 2-dimensional metric. Thus, the lowest possible dimension for black hole toy models based on GR is three. We start with the latter case. Nonetheless, if we go beyond Einstein gravity, e.g. by adding a scalar and possibly other fields, gravity in two dimensions can become dynamically non-trivial. We discuss this case afterward.

## 7.2 Gravity in Three Dimensions

The 3-dimensional Einstein–Hilbert action

$$I_{\mathrm{EH}}[g_{\mu\nu}] = \frac{1}{16\pi G} \int \mathrm{d}^3x \sqrt{-g}\,\big(R - 2\Lambda\big) \tag{7.1}$$

leads to a theory that has no local physical degree of freedom, so a first impulse may be to dismiss the theory as trivial. This local triviality extends to geometry: the Einstein equations determine the Ricci-tensor in terms of the metric, and since the Weyl-tensor vanishes in three dimensions also the Riemann-tensor is determined in terms of the metric. In fact, all solutions to the Einstein equations

$$R_{\mu\nu} - \frac{1}{2}\, g_{\mu\nu} R + \Lambda g_{\mu\nu} = 0 \tag{7.2}$$

are locally flat or (A)dS$_3$, depending on the sign of the cosmological constant $\Lambda$.

Another line of thought comes to the opposite conclusion, namely that the theory is so complicated that it does not even exist: The Newton constant $G_{\mathrm{N}}$ has a dimension of length, so like in higher spacetime dimensions 3-dimensional Einstein gravity is power counting non-renormalizable.

Both considerations are too naive. Let us start dispelling the triviality argument. While it is true that locally the theory is trivial, solutions can have non-trivial global properties, such as black hole event horizons, and physical charges like mass or angular momentum. Moreover, the physical phase space (or its quantum mechanical Hilbert space version) can be non-trivial, despite the absence of local physical excitations.

The non-existence result is harder to dismiss completely—we do not know for which values of the coupling constants (if any) Einstein gravity exists as a fully-fledged quantum theory—but it is at least possible to dismiss the naive argument above. The main point is that the Riemann tensor (even off-shell) is determined by the Ricci-tensor, which in turn is (on-shell) determined by the metric so that any possible counterterm or divergence can be absorbed by field redefinitions and renormalization of the cosmological constant.

So rather than using naive arguments in one way or another let us focus on actual calculations in the remainder of this section. For further reading on $3d$ gravity, one may consult [475].

### 7.2.1 BTZ Black Holes and Bañados Geometries

We focus on Einstein gravity with negative cosmological constant, $\Lambda = -1/\ell^2$, where $\ell$ is the AdS$_3$ radius. In 1992 it came as a surprise that this theory allows for black hole solutions.

**BTZ solution [476,477]**

Maximo Bañados, Claudio Teitelboim [Bunster] and Jorge Zanelli (BTZ) showed that the metric ($\varphi \sim \varphi + 2\pi$)

$$\mathrm{d}s^2_{\mathrm{BTZ}} = -\frac{(r^2 - r_+^2)(r^2 - r_-^2)}{\ell^2 r^2}\,\mathrm{d}t^2 + \frac{\ell^2 r^2\,\mathrm{d}r^2}{(r^2 - r_+^2)(r^2 - r_-^2)} + r^2\Big(\mathrm{d}\varphi - \frac{r_+ r_-}{\ell r^2}\,\mathrm{d}t\Big)^2 \tag{7.3}$$

solves the Einstein equations (7.2) with $\Lambda = -1/\ell^2$. For $r_+ \geq r_- \geq 0$ the locus $r = r_+$ ($r = r_-$) is the outer (inner) horizon of a rotating black hole. Together with Henneaux they constructed the solutions above as quotients of AdS$_3$ that avoid singularities (such as CTCs) in the whole spacetime region $r \geq r_+$.

Here are the main physical properties of BTZ black holes (7.3):

- locally AdS$_3$: $R_{\mu\nu} = -\frac{2}{\ell^2}\,g_{\mu\nu}$
- up to two Killing horizons: event horizon at $r = r_+$ and inner horizon at $r = r_-$
- rotation: black hole horizon rotates with angular rotation parameter $\Omega_{\mathrm{BTZ}} = \frac{r_-}{\ell r_+}$
- mass and angular momentum: using methods discussed in Sect. 5.1,

$$M_{\mathrm{BTZ}} = \frac{r_+^2 + r_-^2}{8\ell^2 G_{\mathrm{N}}}, \qquad J_{\mathrm{BTZ}} = \frac{r_+ r_-}{4\ell G_{\mathrm{N}}} \tag{7.4}$$

- temperature and entropy of the BTZ event horizon are given by

$$T_{\mathrm{BTZ}} = \frac{r_+^2 - r_-^2}{2\pi r_+ \ell^2}\,, \qquad S_{\mathrm{BTZ}} = \frac{\pi r_+}{2G_{\mathrm{N}}} \tag{7.5}$$

- With the above one may readily verify the first law and Smarr relations

$$T_{\mathrm{BTZ}}\delta S_{\mathrm{BTZ}} = \delta M_{\mathrm{BTZ}} - \Omega_{\mathrm{BTZ}}\delta J_{\mathrm{BTZ}}\,, \qquad \frac{1}{2}T_{\mathrm{BTZ}}S_{\mathrm{BTZ}} = M_{\mathrm{BTZ}} - \Omega_{\mathrm{BTZ}}J_{\mathrm{BTZ}} \tag{7.6}$$

- extremal BTZ: confluent horizons, $r_- \to r_+$, have vanishing surface gravity and equal mass and angular momentum, $\ell^2 M_{\mathrm{BTZ}}^2 = J_{\mathrm{BTZ}}^2$.

Analytic continuation to imaginary values of $r_+$ leads to new solutions that are not black holes. Choosing $r_+ = i\ell\,\nu$ with $\nu \in (0, 1)$ and $r_- = 0$ leads to geometries without horizons, but with conical singularities at the origin $r = 0$. The conical deficit angle is given by $1-\nu$. Conical deficits describe particles in $AdS_3$, so the physical interpretation of these geometries is that they are not quite vacuum geometries but rather have a particle located at the origin. Inserting $r_+ = i\ell$ and $r_- = 0$ into the metric (7.3) yields global $AdS_3$.

All the geometries above are special cases of the class of Bañados geometries [478], which are solutions to the Einstein equations (7.2) with $\Lambda = -1/\ell^2$ labelled by two arbitrary functions $\mathcal{L}_\pm(x^\pm)$.

$$\begin{aligned} \mathrm{d}s^2 = \mathrm{d}\rho^2 - \left(e^{2\rho/\ell} + e^{-2\rho/\ell}\mathcal{L}^+(x^+)\mathcal{L}^-(x^-)\right)\mathrm{d}x^+\,\mathrm{d}x^- \\ + \mathcal{L}^+(x^+)\left(\mathrm{d}x^+\right)^2 + \mathcal{L}^-(x^-)\left(\mathrm{d}x^-\right)^2, \qquad x^\pm = t \pm \ell\varphi \end{aligned} \tag{7.7}$$

For constant $\mathcal{L}_\pm$ the BTZ solutions (7.3) are recovered with $\mathcal{L}_+ + \mathcal{L}_- = (r_+^2 + r_-^2)/(2\ell^2)$ and $\mathcal{L}_+ - \mathcal{L}_- = r_+ r_-/\ell^2$ upon redefining the radial coordinate suitably [479]. The Bañados geometries (7.7) have two globally defined Killing vectors, generically one timelike and one spacelike. There are black holes in the family of these geometries for which one of these Killing vectors becomes null at the horizon [480].

### 7.2.2 Chern–Simons Formulation

Reformulating gravity as a gauge theory brings several technical and conceptual advantages since gauge theories are typically simpler than gravity theories. Three-dimensional gravity has a gauge theoretic formulation of Chern–Simons (CS) type.

**> Chern–Simons formulation of $AdS_3$ Einstein gravity [481,482]**

Ana Achúcarro and Paul Townsend showed in 1986 that $AdS_3$ Einstein gravity can be reformulated as CS gauge theory with action

$$I_{\mathrm{CS}}[A^\pm] = \frac{k}{4\pi}\int\langle A^+\wedge\mathrm{d}A^+ + \tfrac{2}{3}\,A^+\wedge A^+\wedge A^+\rangle - \frac{k}{4\pi}\int\langle A^-\wedge\mathrm{d}A^- + \tfrac{2}{3}\,A^-\wedge A^-\wedge A^-\rangle \tag{7.8}$$

with CS level given by

$$k = \frac{\ell}{4G_{\mathrm{N}}} \tag{7.9}$$

and $sl(2,\,\mathbb{R})$ connections $A^\pm = A^{a\,\pm}L_a$ with $a = 0, \pm1$. In the standard basis where the $sl(2)$ generators obey the commutation relations $[L_a,\,L_b] = (a-b)\,L_{a+b}$ the (non-degenerate) bilinear form is defined by its non-zero entries $\langle L_1\,L_{-1}\rangle = -1$ and $\langle L_0\,L_0\rangle = \frac{1}{2}$. The relation between the connection 1-forms $A^{a\,\pm}$ and the Cartan variables reads $A^{a\,\pm} = \frac{1}{2}\,\epsilon^{abc}\omega_{bc} \pm \frac{1}{\ell}\,e^a$. The field equations imply gauge-flatness, $F^\pm = \mathrm{d}A^\pm + A^\pm\wedge A^\pm = 0$, which in Cartan variables translates to the conditions of vanishing torsion and constant curvature.

The metric is recovered from the relations

$$g_{\mu\nu} = \frac{\ell^2}{2} \langle (A^+_\mu - A^-_\mu)(A^+_\nu - A^-_\nu) \rangle \,. \tag{7.10}$$

As an example let us recover in the CS formulation the solutions corresponding to the Bañados geometries (7.7). Quite generally, a convenient ansatz for the connection that separates the radial dependence from the dependence of boundary coordinates is given by

$$A^\pm = b_\pm^{-1}(\rho) \Big( \mathrm{d} + a^\pm(x^+,\, x^-) \Big)\, b_\pm(\rho) \,. \tag{7.11}$$

Picking the group elements $b_\pm = e^{\pm\rho/\ell\, L_0}$ and choosing the boundary connections in so-called highest weight gauge

$$a^\pm = \pm\big(L_{\pm 1} - \mathcal{L}_\pm(x^\pm)\, L_{\mp 1}\big)\, \frac{\mathrm{d}x^\pm}{\ell} \tag{7.12}$$

recovers the Bañados geometries (7.7) using the expression for the metric (7.10) together with the Baker–Campbell–Hausdorff formula $e^{\rho/\ell L_0} L_{\pm 1} e^{-\rho/\ell L_0} = e^{\mp\rho/\ell} L_{\pm 1}$.

### 7.2.3 Canonical Boundary Charges

Applying the general results on canonical boundary charges summarized in Sect. 5.1 to the CS theory (7.8) is straightforward. For concreteness we assume that the CS theory is defined on a cylinder, since this captures most cases of interest, including $AdS_3$ gravity.

**> Canonical boundary charges in CS theories**

The CS theory (7.8) has two towers of canonical boundary charges

$$\boxed{\delta Q[\varepsilon^+,\, \varepsilon^-] = \frac{k}{2\pi} \oint \langle \varepsilon^+\, \delta A^+ \rangle - \frac{k}{2\pi} \oint \langle \varepsilon^-\, \delta A^- \rangle \,.} \tag{7.13}$$

The integral is performed over the boundary $S^1$ of the cylinder on which the CS theory is defined. The parameters $\varepsilon^\pm$ comprise all boundary condition preserving transformations,

$$\delta_{\varepsilon^\pm} A^\pm = \mathrm{d}\varepsilon^\pm + [A^\pm,\, \varepsilon^\pm] = \mathcal{O}(\delta A^\pm) \tag{7.14}$$

where $\delta A$ are gauge connection fluctuations allowed by the boundary conditions.

Whether or not the canonical boundary charges (7.13) are finite, non-trivial, integrable and/or conserved depends on the precise boundary conditions. The class of choices (7.11) with $\delta b_\pm = 0$ defining $\hat{\varepsilon}^\pm = b_\pm \varepsilon^\pm b_\pm^{-1}$ always lead to finite charges since the radial dependence drops out from the general expression (7.13),

$$\delta Q[\hat{\varepsilon}^+,\, \hat{\varepsilon}^-] = \frac{k}{2\pi} \oint \langle \hat{\varepsilon}^+ \, \delta a^+ \rangle - \frac{k}{2\pi} \oint \langle \hat{\varepsilon}^- \, \delta a^- \rangle \tag{7.15}$$

which now only contains the boundary connections $a^\pm$. This is a considerable simplification and reduces the amount of guesswork one has to make when trying to invent novel boundary conditions. Gauge transformations acting on the boundary connections simplify to

$$\delta_{\hat{\epsilon}^\pm} a^\pm = \mathrm{d}\hat{\epsilon}^\pm + [a^\pm,\, \epsilon^\pm]\,. \tag{7.16}$$

Varying within the phase space of Bañados geometries is achieved imposing Brown–Henneaux boundary conditions [483]. The configuration (7.11)–(7.12) is their CS equivalent and implies

$$\delta a^\pm = \mp \delta \mathcal{L}_\pm(x^\pm)\, L_{\mp 1}\, \frac{\mathrm{d}x^\pm}{\ell} \tag{7.17}$$

for the allowed variations of the gauge connection. We study now the associated canonical boundary charges (7.15). The boundary conditions are preserved by

$$\hat{\varepsilon}^\pm = \lambda^\pm(x^\pm)\, L_{\pm 1} - \ell \lambda^\pm(x^\pm)'\, L_0 + \left(\tfrac{\ell^2}{2} \lambda^\pm(x^\pm)'' - \mathcal{L}_\pm(x^\pm)\lambda^\pm(x^\pm)\right) L_{\mp 1}\,. \tag{7.18}$$

This means there are two free functions, $\lambda^\pm(x^\pm)$, parametrizing all allowed asymptotic symmetries and hence two towers of associated canonical boundary charges.

Plugging (7.17) and (7.18) into the variation of the charges (7.15) and integrating them in field space yields

$$Q[\lambda^+,\, \lambda^-] = \frac{k}{2\pi} \oint \lambda^+ \mathcal{L}_+ \, \mathrm{d}\varphi - \frac{k}{2\pi} \oint \lambda^- \mathcal{L}_- \, \mathrm{d}\varphi\,. \tag{7.19}$$

Under boundary condition preserving transformations (7.16), (7.18) the state-dependent functions transform with infinitesimal Schwarzian derivatives,

$$\pm \frac{1}{\ell}\, \delta_{\lambda^\pm} \mathcal{L}_\pm = \mathcal{L}_\pm' \lambda^\pm + 2\mathcal{L}_\pm\, \lambda^{\pm\prime} - \frac{\ell^2}{2}\, \lambda^{\pm\prime\prime\prime}\,. \tag{7.20}$$

## > Conformal symmetries and Brown–Henneaux central charge

The general discussion of canonical boundary charges in Sect. 5.1 applied to the present case yields the asymptotic symmetry algebra

$$\{Q^\pm[\lambda_1^\pm],\, Q^\pm[\lambda_2^\pm]\} = Q^\pm[\lambda_1^{\pm\prime}\lambda_2^\pm - \lambda_2^{\pm\prime}\lambda_1^\pm] - \frac{k}{4\pi} \oint \lambda_1^{\pm\prime\prime\prime}\lambda_2 \, \mathrm{d}\varphi \tag{7.21}$$

This result implies that the physical phase space of Einstein gravity with Brown–Henneaux boundary conditions is given by two copies of the Virasoro algebra, which is the conformal algebra in two dimensions. This statement is most explicit when introducing Fourier modes, $L_n^\pm := Q[i e^{inx^\pm}]$,

$$i\{L_n^\pm,\, L_m^\pm\} = (n-m)\, L_{n+m}^\pm + \frac{k}{2}\, n^3\, \delta_{n+m,\,0} = (n-m)\, L_{n+m}^\pm + \frac{c_{\mathrm{BH}}}{12}\, n^3\, \delta_{n+m,\,0}\,. \tag{7.22}$$

The Brown–Henneaux central charges can be read off from (7.22):

$$\boxed{c_{\mathrm{BH}}^\pm = 6k = \frac{3\ell}{2G_{\mathrm{N}}}} \tag{7.23}$$

The results above provide a precursor of the $\mathrm{AdS}_3/\mathrm{CFT}_2$ correspondence discussed in the next Chap. 8.

### 7.2.4 Alternative Boundary Conditions to Brown–Henneaux

The Brown–Henneaux boundary conditions (7.11)–(7.12) appear naturally in $\mathrm{AdS}_3$ Einstein gravity but are not the only possibility. Indeed, Geoffrey Compère, Wei Song, and Andrew Strominger provided alternative boundary conditions that do not lead to two copies of the Virasoro algebra as asymptotic symmetries, but instead, a single Virasoro algebra plus a $u(1)$ current algebra [484]. Several other alternative boundary conditions were proposed since then, in some cases with up to four towers of canonical boundary charges [485,486].

The loosest set of boundary conditions, in the sense of providing the largest number (namely six) of independent towers of canonical boundary charges, was provided in [487]. In CS formulation using the ansatz (7.11) these boundary conditions are defined by the choices

$$a^\pm = \sum_{n=-1}^{1} \big(\mu_n^\pm(t,\,\varphi)\ \mathrm{d}t + \mathcal{L}_n^\pm(t,\,\varphi)\ \mathrm{d}\varphi\big)\, L_n \tag{7.24}$$

and, for instance, $b = \exp(L_{-1})\exp(\rho/\ell\, L_0)$, where it is assumed that all chemical potentials are arbitrary but fixed, $\delta\mu_n^\pm = 0$, while the remaining functions characterize the physical state and are allowed to vary, $\delta\mathcal{L}_n^\pm \neq 0$. The asymptotic symmetries induced by the choice (7.24) are two $sl(2,\,\mathbb{R})$ current algebras.

All other boundary conditions are either special cases of (7.24) (e.g. fixing some of the functions $\mathcal{L}_n^\pm$ to be zero or constant) or deformations where the chemical potentials are assumed to be state-dependent. See for example [488,489] for a Korteweg–de Vries-type of deformation of Brown–Henneaux boundary conditions.

Which of these boundary conditions one should impose depends, as usual, on the precise physical questions one is asking.

### 7.2.5 Beyond AdS$_3$ Einstein Gravity

While AdS$_3$ Einstein gravity has many nice features, there are good motivations to go beyond. We mention now some of them:

- **Vanishing or positive cosmological constant.**

Setting the cosmological constant to zero in (7.1) allows for a discussion along the lines above. In fact, many statements and formulas can be recovered from this discussion by taking the limit of infinite AdS-radius, $\ell \to \infty$. We just provide two examples. Taking the limit $\ell \to \infty$ with fixed $\hat{r}_+ = r_+/\ell$ of the BTZ black hole (7.3) yields flat space solutions that are regular on and outside the remaining horizon $r = r_-$.

$$\mathrm{d}s^2_{\text{FSC}} = \hat{r}_+^2\big(1 - \frac{r_-^2}{r^2}\big)\,\mathrm{d}t^2 - \frac{\mathrm{d}r^2}{\hat{r}_+^2\big(1-\frac{r_-^2}{r^2}\big)} + r^2\left(\mathrm{d}\varphi - \frac{\hat{r}_+ r_-}{r^2}\,\mathrm{d}t\right)^2 \tag{7.25}$$

These solutions are known as "flat space cosmologies" since they describe cosmological solutions that are locally flat [490] (note that $r$ is now the time coordinate). Much like BTZ black holes, these solutions are orbifolds (of flat space). For the second example we take the asymptotic Virasoro symmetry generators $L_n^\pm$ from (7.22) and linearly combine them as $L_n = L_n^+ - L_{-n}^-$, $M_n = (L_n^+ + L_{-n}^-)/\ell$ before taking the limit $\ell \to \infty$. This is an example of an İnönü–Wigner contraction and yields the so-called BMS$_3$ algebra [491] (named after Bondi, van der Burgh, Matzner and Sachs [115,116]) with central charge $c_{\text{M}} = 3/G_{\text{N}}$ [492].

$$i\{L_n,\, L_m\} = (n-m)\,L_{n+m} \qquad\qquad i\{M_n,\, M_m\} = 0 \tag{7.26a}$$

$$i\{L_n,\, M_m\} = (n-m)\,M_{n+m} + \frac{c_{\text{M}}}{12}\,n^3\,\delta_{n+m,\,0} \tag{7.26b}$$

For positive cosmological constant, solutions are locally dS$_3$, which could provide a useful toy model for cosmology. See [493] for some discussions of dS$_3$ Einstein gravity.

- **Conformal gravity.**

Gravity models with more symmetries than diffeomorphisms are sometimes considered as toy models or candidates for UV completions, since it can be possible to gauge away, for instance, curvature singularities. Conformal gravity in particular is a gravity model that is invariant under local Weyl rescalings of the metric

$$g_{\mu\nu}(x^\lambda) \to \tilde{g}_{\mu\nu}(x^\lambda) = e^{2\Omega(x^\lambda)}\,g_{\mu\nu}(x^\lambda) \tag{7.27}$$

with some Weyl factor $\Omega(x^\lambda)$. In three dimensions the three-derivative action

$$I_{\text{CG}}[g_{\mu\nu}] = \frac{k}{4\pi}\int \mathrm{d}^3x\,\epsilon^{\lambda\mu\nu}\Gamma^\rho{}_{\lambda\sigma}\left(\partial_\mu\Gamma^\sigma{}_{\rho\nu} + \tfrac{2}{3}\,\Gamma^\sigma{}_{\mu\tau}\Gamma^\tau{}_{\nu\rho}\right) \tag{7.28}$$

is both diffeomorphism- and Weyl-invariant, as can be checked easily from the Weyl-transformation formula for the Christoffel connection, $\tilde{\Gamma}^{\lambda}{}_{\mu\nu} = \Gamma^{\lambda}{}_{\mu\nu} + \delta^{\lambda}_{\mu}\partial_\nu\Omega + \delta^{\lambda}_{\nu}\partial_\mu\Omega - g_{\mu\nu}g^{\lambda\sigma}\partial_\sigma\Omega$. The EOM descending from the action (7.28)

$$C_{\mu\nu} := \varepsilon_{\mu}{}^{\alpha\beta}\nabla_\alpha\big(R_{\beta\nu} - \tfrac{1}{4}\,g_{\beta\nu}R\big) = 0 \tag{7.29}$$

imply the vanishing of the Cotton tensor $C_{\mu\nu}$ and hence local conformal flatness. Despite of the fact that the conformal gravity action (7.28) and the EOM (7.29) contain three derivatives of the metric there is no local physical degree of freedom due to the additional Weyl symmetry (7.27).

Various ways of imposing (generalizations of) Brown–Henneaux boundary conditions, as well as earlier literature on conformal gravity, are summarized in [494].

- **Topologically massive gravity.**

Stanley Deser, Roman Jackiw and Stephen Templeton discovered a 3-dimensional gravity theory that propagates (massive) gravitons [495,496]. Its action is the sum of the Einstein–Hilbert action (7.1) and the conformal gravity action (7.28). It may seem curious that the addition of two actions, none of which propagates any physical degrees of freedom, leads to a physical degree of freedom. There is a simple explanation: adding both actions means the theory is no longer Weyl invariant, but still contains three derivatives. The EOM

$$R_{\mu\nu} - \tfrac{1}{2}\,g_{\mu\nu}R + \Lambda g_{\mu\nu} + \frac{1}{\mu}\,C_{\mu\nu} = 0 \qquad\qquad \frac{1}{\mu} := 8kG_{\rm N} \tag{7.30}$$

allow for all solutions of Einstein gravity, but contain additional solutions that are not locally (A)dS or locally flat, such as warped, Schrödinger or Lifshitz solutions, see for instance [497,498]. Linearizing around some maximally symmetric background yields graviton fluctuations whose mass is given by $\mu$.

There are numerous other possibilities for gravitons to acquire mass through higher derivative interactions, see for instance [499].

- **Higher spin gravity.**

The reformulation of Einstein gravity as CS theory allows a natural generalization to higher rank gauge groups, for instance generalizing $sl(2)$ to $sl(N)$. Such theories have an interpretation as higher spin theories [500,501] and can provide useful toy models for Vasiliev higher spin gravity [502,503].

## 7.3 Gravity in Two Dimensions

Since any 2-dimensional metric trivially obeys the Einstein equations, $R_{\mu\nu} = \frac{1}{2}\,g_{\mu\nu}R$, they convey no useful information. Thus, Einstein gravity ceases to make sense in two dimensions. The next-simplest theory is a scalar-tensor theory, also known as dilaton gravity (or sometimes "quintessence"), whose field content comprises the dilaton $X$ and the metric $g_{\mu\nu}$. Two-dimensional dilaton gravity arises in numerous ways: from higher curvature/torsion theories, from symmetry reductions of higher-dimensional gravity theories, in non-critical string theory, and as toy models for various aspects of classical and quantum black holes.

There are many formal similarities between 2-dimensional dilaton gravity and 3-dimensional Einstein gravity: both theories are locally trivial but globally non-trivial, have no local physical degree of freedom, and allow for a convenient reformulation as a gauge theory. The main difference between these theories is that Einstein gravity has only one essential free parameter, the cosmological constant, while dilaton gravity has two free functions characterizing its classical properties.

We start with the historically first dilaton gravity model, the Jackiw–Teitelboim (JT) model, before addressing generic dilaton gravity models, their gauge theoretic formulation, and how to obtain all classical solutions, locally and globally.

### 7.3.1 Jackiw–Teitelboim Model

The JT action [504,505]

$$I_{\mathrm{JT}}[X,\ g_{\mu\nu}] = \frac{1}{16\pi G}\int \mathrm{d}^2x\sqrt{-g}\,X\big(R-2\lambda\big) \tag{7.31}$$

leads to constant curvature solutions, $R = 2\lambda$, as can be seen by varying with respect to the dilaton $X$. For negative $\lambda$ solutions are locally $AdS_2$ and have $sl(2,\ \mathbb{R})$ isometries. Comparing with the situation in 3-dimensional Einstein gravity it is suggestive that there could be a gauge theoretic formulation of the JT model based on an $sl(2,\ \mathbb{R})$ connection.

This is indeed the case: the non-abelian BF-action (see e.g. [506] for a review of topological QFTs, including BF-theories)

$$I_{\mathrm{BF}}[\mathcal{X},\ A] = \frac{k}{2\pi}\int \langle \mathcal{X}\left(\mathrm{d}A + A\wedge A\right)\rangle \tag{7.32}$$

reproduces the JT model [507] by choosing the coadjoint scalar $\mathcal{X} = \mathcal{X}^a L_a$ and the connection $A = A^a_\mu L_a\,\mathrm{d}x^\mu$ to be $sl(2)$-valued, $[L_a,\ L_b] = (a-b)\,L_{a+b},\ \ a, b = 0, \pm 1$. The field equations establish gauge-flatness, which translates into the geometric conditions of vanishing torsion and constant (negative) curvature.

### 7.3.2 Generic Dilaton Gravity

Above we were terse since in the following we are considering generic dilaton gravity theories, their gauge theoretic formulation, and classical solutions; the JT model then arises as one particular choice in theory space.

**Table 7.1** Selected dilaton gravity models, their kinetic potentials $U(X)$ and potentials $V(X)$

| Model | $U(X)$ | $V(X)$ |
|---|---|---|
| 1. Schwarzschild (1916) | $\frac{1}{2X}$ | $1$ |
| 2. JT (1984) | $0$ | $X$ |
| 3. Witten (1991) | $\frac{1}{X}$ | $X$ |
| 4. CGHS (1992) | $0$ | $1$ |
| 5. (A)dS$_2$ ground state (1994) | $\frac{a}{X}$ | $X$ |
| 6. Rindler ground state (1996) | $\frac{a}{X}$ | $X^a$ |
| 7. Black Hole attractor (2003) | $0$ | $X^{-1}$ |
| 8. Tangherlini$_D$ (1963) | $\frac{D-3}{(D-2)X}$ | $X^{(D-4)/(D-2)}$ |
| 9. All above: $ab$-family (1997) | $\frac{a}{X}$ | $X^{a+b}$ |
| 10. Liouville gravity (1981) | $a$ | $e^{\alpha X}$ |
| 11. RN (1916) | $\frac{1}{2X}$ | $1 - \frac{Q^2}{X}$ |
| 12. Kottler (1918) | $\frac{1}{2X}$ | $1 + \Lambda X$ |
| 13. Katanaev–Volovich (1986) | $\alpha$ | $X^2 + \Lambda$ |
| 14. BTZ/Achucarro-Ortiz (1993) | $0$ | $\Lambda X - \frac{Q^2}{X} + \frac{J}{X^3}$ |
| 15. KK reduced CS (2003) | $0$ | $\frac{1}{2}X(X^2 - c)$ |
| 16. KK red. conf. flat (2006) | $\frac{1}{2}\tanh(X/2)$ | $\sinh X$ |
| 17. 2D type 0A string Black Hole (2003) | $\frac{1}{X}$ | $X - \frac{q^2}{4\pi}$ |

## > Second order action for generic 2-dimensional dilaton gravity

Generic dilaton gravity is described by the (power-counting renormalizable) action

$$I_{\text{GDG}}[X,\ g_{\mu\nu}] = \frac{1}{16\pi G}\int \mathrm{d}^2x\sqrt{-g}\left(XR - U(X)(\partial X)^2 - 2\lambda\, V(X)\right) + I_m \tag{7.33}$$

depending on two arbitrary functions, the kinetic function $U(X)$ and the potential $V(X)$ (made dimensionless by pulling out a factor $2\lambda$, so that e.g. $V_{\text{JT}} = X$). A third possible function multiplying the Ricci scalar can be redefined to be the dilaton $X$. We have also allowed for the possibility of some matter contribution $I_m$. A list of specific models is contained in Table 7.1.

The EOM ($T_{\mu\nu} = \frac{2}{\sqrt{-g}}\frac{\delta I_m}{\delta g^{\mu\nu}}$ and $\hat{T} = \frac{2}{\sqrt{-g}}\frac{\delta I_m}{\delta X}$)

$$R + U'(\partial X)^2 + 2U\nabla^2 X - 2\lambda V' = -8\pi G\,\hat{T} \tag{7.34a}$$

$$\nabla_\mu\nabla_\nu X - g_{\mu\nu}\,\nabla^2 X + U(\partial_\mu X)(\partial_\nu X) - \tfrac{1}{2}\,g_{\mu\nu}U(\partial X)^2 - \lambda g_{\mu\nu}V = 8\pi G\,T_{\mu\nu} \tag{7.34b}$$

in the absence of matter allow for two classes of solutions: constant and linear dilaton vacua. We discuss here the former and postpone a discussion of the latter until after the gauge theoretic formulation.

Constant dilaton vacua have $X = X_0 = \text{const}$. The second (7.34) yields the condition $V(X_0) = 0$, while the first one shows that curvature is constant for such solutions, $R = 2\lambda V'(X_0)$. Thus, constant dilaton vacua exist only if $V(X_0) = 0$ has solutions; they yield metrics that are either locally flat or (A)dS$_2$.

### 7.3.3 Gauge Theoretic Formulation

As discussed above, the JT model can be reformulated as a BF-type of gauge theory. What about generic dilaton gravity models? They allow a reformulation as non-linear gauge theories [508,509] known as Poisson-sigma model [510]. Given a set of target space coordinates $X^I$, connection 1-forms $A_I$ and a Poisson tensor $P^{IJ}(X^K) = -P^{JI}(X^K)$ obeying the non-linear Jacobi identities

$$P^{IL}\partial_L P^{JK} + P^{JL}\partial_L P^{KI} + P^{KL}\partial_L P^{IJ} = 0 \tag{7.35}$$

a Poisson-sigma model is described by the 2-dimensional bulk action

$$I_{\text{PSM}}[X^I,\ A_I] = \frac{k}{2\pi}\int\Big(X^I\,\mathrm{d}A_I + \tfrac{1}{2}\,P^{IJ}(X^K)\,A_I\wedge A_J\Big) \tag{7.36}$$

that is invariant under gauge transformations

$$\delta_\varepsilon X^I + P^{IJ}\,\varepsilon_J = 0 \qquad\qquad \delta_\varepsilon A_I = \mathrm{d}\varepsilon_I + \big(\partial_I P^{JK}\big)\,A_J\,\varepsilon_K \tag{7.37}$$

which are abelian for constant $P^{IJ}$, of Yang–Mills type for $P^{IJ}$ linear in the target space coordinates and non-linear otherwise. The EOM derived from the action (7.36) are first order in derivatives

$$\mathrm{d}X^I + P^{IJ}\,A_J = 0 \qquad\qquad \mathrm{d}A_I + \tfrac{1}{2}\,\big(\partial_I P^{JK}\big)\,A_J\wedge A_K = 0 \tag{7.38}$$

and allow for a simple class of solutions where all target space coordinates are constant, $X^I = \bar{X}^I = \text{const.}$,

$$P^{IJ}(\bar{X}^k) = 0 \qquad\qquad \mathrm{d}A_I + f_I{}^{JK}\,A_J\wedge A_K = 0 \tag{7.39}$$

where $f_I{}^{JK} = \frac{1}{2}\big(\partial_I P^{JK}\big)$ are constants. Generic solutions have non-constant target space coordinates.

Dilaton gravity emerges by choosing the coupling constant $k = 1/(4G)$, target space coordinates $X^I = (X,\ X^a)$, connections $A_I = (\omega,\ e_a)$, and Poisson tensor

$$P^{Xa} = \epsilon^a{}_b X^b \qquad\qquad P^{ab} = \epsilon^{ab}\,\big(\lambda\,V(X) + \tfrac{1}{2}\,X^a X_a U(X)\big) \tag{7.40}$$

where $\epsilon^{ab}$ is the Levi–Civitá symbol and Latin indices are raised and lowered with the Minkowski metric $\eta_{ab}$. The interpretation of the fields is as follows: $X$ is the dilaton field, $X^a$ are auxiliary scalar fields, $\omega = \frac{1}{2}\epsilon^{ab}\omega_{ab}$ is the dualized spin-connection, $e_a$ is the zweibein 1-form and $U(X)$, $V(X)$ are precisely the same potentials as in the second order action (7.33).

Under dilaton-dependent Weyl transformations $g_{\mu\nu} \to g_{\mu\nu}e^{2\Omega(X)}$ the first order fields transform as

$$X^a \to X^a e^{-\Omega} \qquad e_a \to e_a e^{\Omega} \qquad \omega \to \omega + X^a e_a \Omega' \tag{7.41}$$

and the model is mapped to a new one with transformed potentials

$$U \to U + 2\Omega' \qquad V \to V e^{-2\Omega}\,. \tag{7.42}$$

The functions (which will be useful below)

$$Q(X) := \int^X \mathrm{d}y\, U(y) \qquad w(X) := 2\lambda \int^X \mathrm{d}y\, V(y) e^{Q(y)} \tag{7.43}$$

have simple transformation behavior,

$$Q \to Q + 2\Omega, \qquad w \to w\,. \tag{7.44}$$

### 7.3.4 All Classical Solutions, Locally and Globally

We derive now all classical solutions for all dilaton gravity models (7.33) using the first order formulation (7.36)–(7.40) in lightcone gauge for the flat metric, $\eta_{+-} = 1$, $\epsilon^{\pm}{}_{\pm} = \pm 1$. Let us start with the simple class of solutions (7.39), known in dilaton gravity as "constant dilaton vacua". The auxiliary fields have to vanish, $X^{\pm} = 0$, while the dilaton field must be constant, $X = \bar{X} = \text{const.}$, and solve $V(\bar{X}) = 0$. The right (7.39) then imply torsionlessness and constant curvature, so that all constant dilaton vacua are locally maximally symmetric. Depending on the sign of curvature

$$R = 2\lambda V'(\bar{X}) = \text{const.} \tag{7.45}$$

these solutions are locally either (A)dS$_2$ or Minkowski$_2$.

We address now the more interesting generic solutions. A convenient trick is to exploit dilaton-dependent Weyl rescalings (7.41)–(7.42) to map the model to a new one with vanishing kinetic potential, $U(X) = 0$, then solve this model and in the end perform the inverse Weyl transformation to obtain the solutions of the original model. The EOM (7.38) with (7.40) for vanishing $U(X)$ read

$$\mathrm{d}X - X^- e^+ + X^+ e^- = 0 \qquad \mathrm{d}X^{\pm} \mp X^{\pm}\omega \mp e^{\pm}\lambda V = 0 \tag{7.46}$$

$$\mathrm{d}\omega + e^+ \wedge e^- \lambda V' = 0 \qquad \mathrm{d}e^{\pm} \mp \omega \wedge e^{\pm} = 0 \tag{7.47}$$

Since we are interested in solutions where $X^{\pm}$ do not vanish everywhere let us assume $X^{+} \neq 0$ in a given patch and define a new 1-form $Z := e^{+}/X^{+}$. Then the left (7.46) implies $e^{-} = X^{-}Z - \mathrm{d}X/X^{+}$, while the right (7.46) with upper sign yields the connection $\omega = \mathrm{d}X^{+}/X^{+} - \lambda V\, Z$. The right (7.47) with upper sign establishes that $Z$ is closed, $\mathrm{d}Z = 0$, which locally means it is exact, $Z = \mathrm{d}u$. Two of the remaining three equations are redundant with the rest, so we need to solve only one additional equation. Taking the linear combination of $X^{-}$ times the upper sign right (7.46) plus $X^{+}$ times its lower sign version and using the left (7.46) yields $\lambda V\ \mathrm{d}X - \mathrm{d}(X^{+}X^{-}) = 0$, which integrates to

$$\tfrac{1}{2}\, w(X) - X^{+}X^{-} = M \tag{7.48}$$

where $M$ is an integration constant essentially corresponding to the mass of a given solution and $w$ is defined in (7.43). The metric in the unphysical conformal frame is then given by

$$\mathrm{d}s^2\big|_{U=0} = 2e^{+} \otimes e^{-} = \big(w(X) - 2M\big)\ \mathrm{d}u^2 - 2\,\mathrm{d}u\ \mathrm{d}X \tag{7.49}$$

where we used $u$ and $X$ as coordinates.

**General solution to generic dilaton gravity models**

Transforming back to the original conformal frame establishes the general solution of all dilaton gravity models in an EF patch

$$\boxed{\mathrm{d}s^2 = e^{Q(X)}\,\big(w(X) - 2M\big)\ \mathrm{d}u^2 - 2\,\mathrm{d}u\,\mathrm{d}r} \tag{7.50}$$

expressed in terms of the functions defined in (7.43). The solution for the dilaton in these coordinates is given by integrating $e^{Q(X)}\ \mathrm{d}X = \mathrm{d}r$.

Here are the main physical properties of the solutions (7.50):

- local curvature non-trivial: $R = 2e^{-Q(X)}\frac{\mathrm{d}}{\mathrm{d}X}\left(e^{Q(X)}\lambda V(X) + U(X)(M - \tfrac{1}{2}\, w(X))\right)$
- generalized Birkhoff theorem: all solutions have the Killing vector $\partial_u$
- conserved mass: all solutions depend on the integration constant $M$
- Killing horizons: for every solution of $w(X_h) - 2M = 0$ there is a Killing horizon
- temperature: surface gravity for each horizon yields $T_h = \frac{w'(X_h)}{4\pi}$

Our initial assumption $X^{+} \neq 0$ is true in the whole EF patch, but not globally. If $X^{+} = 0$ and $X^{-} \neq 0$ the same calculation can be repeated, yielding a mirror flipped EF patch (exchanging in- and out-going null directions). Except for bifurcation points, where $X^{\pm} = 0$, the whole manifold can be covered by these EF patches. For more details on the global structure see the review article [424], the series of papers by Thomas Klösch and Thomas Strobl [155,511,512] and references therein. A generalization of the action (7.33) to generic models that are not power-counting renormalizable (but otherwise soluble by essentially the same methods) can be found in [513].

## 7.4 Why Gravity in Higher Dimensions?

Historically, gravity in higher (than four) dimensions was motivated by Einstein himself in the 1920s, in his grand project of geometrization of all the other forces/interactions. In particular, within the Kaluza–Klein (KK) theory [514–516] one may get 4-dimensional Einstein–Maxwell-dilaton theory from a KK reduction of the 5-dimensional Einstein gravity over a circle. The program of geometrization was then naturally incorporated within string and M theory [517–519] where 10- and 11-dimensional supergravities appear as low energy effective theory, see Appendix I for a brief discussion. Consequently, a large class of high-dimensional (super)gravity theories with various matter contents in dimensions lower than 10 appear through the compactification procedure, a generalization of the usual KK reduction.

Besides the connections and motivations from QG candidates like string theory, higher-dimensional gravity theories may be viewed as an arena to examine various theorems about classical black hole solutions, like topology and uniqueness theorems as well as semiclassical thermodynamical aspects in particular notions like BH entropy and the area law. In this part, we briefly discuss some of the results with this latter motivation, while also mentioning some basic features of various supergravity theories in diverse dimensions. For more detailed discussions on the latter the reader may consult the books on the topic, e.g. [520–522]. Finally, even when mainly interested in GR, considering (a large number of) dimensions $D$ can be beneficial for pragmatic reasons since $1/D$ provides a small parameter that can be exploited for perturbation theory. We address such applications in the last section of this chapter.

The simplest gravity theory in generic dimension $D$ is given by the Einstein–Hilbert term with possibly a cosmological constant term and a matter Lagrangian $\mathcal{L}_{\text{mat}}$,

$$I_{\text{EH}} = \frac{1}{16\pi G_{\text{N}}} \int \mathrm{d}^D x \sqrt{-g}\,\big(R - 2\Lambda + \mathcal{L}_{\text{mat}}\big) \tag{7.51}$$

and the field equations

$$R_{\mu\nu} - \frac{1}{2} R g_{\mu\nu} + \Lambda g_{\mu\nu} = 8\pi G_{\text{N}}\, T_{\mu\nu}, \tag{7.52}$$

where $G_{\text{N}}$ is the $D$-dimensional Newton constant which in natural units (setting $\hbar$, $c$ equal to one) $16\pi G_{\text{N}} = (2\pi)^{D-3}\ell_{\text{Pl}}^{D-2}$ and $T_{\mu\nu}$ is the energy-momentum tensor of the matter part. The matter Lagrangian $\mathcal{L}_{\text{mat}}$ typically involves some dilaton fields and various form fields. In the next sections we discuss some simple cases for $\mathcal{L}_{\text{mat}}$ and solutions to the field equations.

## 7.5 Higher-Dimensional Black Hole/Ring/Brane Solutions

As in the $D = 4$ case, a great deal of effort has been devoted to constructing, analyzing and classifying solutions to (7.52), see e.g. [227]. To start, we discuss vacuum solutions with and without cosmological constant and then consider solutions with simple matter fields.

### 7.5.1 Tangherlini Solution

The simplest higher-dimensional solution we discuss is the Tangherlini solution [48], satisfying $R_{\mu\nu} = 0$. This is a spherically symmetric and hence static solution and a direct generalization of the Schwarzschild geometry to $D$ dimensions:

$$\mathrm{d}s^2 = -F(r)\,\mathrm{d}t^2 + \frac{\mathrm{d}r^2}{F(r)} + r^2\,\mathrm{d}\Omega_{D-2}^2, \qquad F(r) = 1 - \left(\frac{r_h}{r}\right)^{D-3}, \tag{7.53}$$

where $\mathrm{d}\Omega_{D-2}^2$ is the metric on the round $S^{D-2}$. Like the Schwarzschild solution, (7.53) has an event horizon at $r = r_h$ and a curvature singularity at $r = 0$.

The higher-dimensional RN solution describes a static, spherically symmetric charged black hole. The metric was also written by Tangherlini [48] and has the same form as (7.53) but with

$$F(r) = 1 - \frac{2\mu}{r^{D-3}} + \frac{q^2}{r^{2(D-3)}}, \tag{7.54}$$

and the 1-form Maxwell field $A = \frac{Q}{(D-3)r^{D-3}}dt$. This solution carries electric charge $Q = \sqrt{(D-2)(D-3)/2}\,q$ and its ADM mass is $M = \frac{(D-2)\Omega_{D-2}}{8\pi G_\mathrm{N}}\mu$, where $\Omega_{D-2}$ is the volume of the $(D-2)$-dimensional unit sphere.

### 7.5.2 Myers–Perry Black Holes

After this warm-up example, we explore higher-dimensional counterparts of the rotating Kerr geometry, which were constructed by Rob Myers and Malcolm Perry [523], for an instructive review see [524]. To present the Myers–Perry (MP) black hole, we start with a suitable coordinate system on a $(D-2)$-dimensional sphere:

$$\mathrm{d}s^2 = \sum_{n=1}^{K} \mathrm{d}\mu_n^2 + \mu_n^2\,\mathrm{d}\phi_n^2, \qquad \sum_{n=1}^{K} \mu_n^2 = 1, \qquad K = \frac{D-1}{2}, \quad D \text{ odd} \tag{7.55a}$$

$$\mathrm{d}s^2 = \mathrm{d}\mu_0^2 + \sum_{n=1}^{K} \mathrm{d}\mu_n^2 + \mu_n^2\,\mathrm{d}\phi_n^2, \quad \mu_0^2 + \sum_{n=1}^{K} \mu_n^2 = 1, \; K = \frac{D-2}{2} \quad D \text{ even} \tag{7.55b}$$

where $\phi_n \in [0, 2\pi]$. The difference between the odd and even dimensions appears as a result of the fact that the isometry group of $S^{D-2}$ is $SO(D-1)$ and its rank, is $(D-1)/2$ for odd $D$ and $(D-2)/2$ for even $D$; the number of independent $U(1)$ Killing vectors (i.e. the number of $\phi_n$ coordinates in (7.55)) is equal to this rank. This is the same number as the independent spins (angular momenta) one may turn on in a $D$-dimensional spacetime.

The metric of MP black holes in even dimensions ($D \geq 4$) is given by

$$\begin{aligned} \mathrm{d}s^2 = &-\mathrm{d}t^2 + \frac{\mu r}{\Pi F}\left(\mathrm{d}t + \sum_{n=1}^{K} a_n \mu_n^2 \, \mathrm{d}\phi_n\right)^2 + \frac{\Pi F}{\Pi - \mu r}\,\mathrm{d}r^2 \\ &+ \sum_{n=1}^{K} (r^2 + a_n^2)(\mathrm{d}\mu_n^2 + \mu_n^2 \, \mathrm{d}\phi_n^2) + r^2 \, \mathrm{d}\mu_0^2 \end{aligned} \tag{7.56}$$

where

$$F = 1 - \sum_{n=1}^{K} \frac{a_n^2 \mu_n^2}{r^2 + a_n^2}, \qquad \Pi = \prod_{n=1}^{K} (r^2 + a_n^2)\,. \tag{7.57}$$

The above for $D = 4$, $K = 1$ reduces to the usual Kerr solution.

For odd dimensions ($D \geq 5$), the metric takes the form

$$\mathrm{d}s^2 = -\mathrm{d}t^2 + \frac{\mu r^2}{\Pi F}\left(\mathrm{d}t + \sum_{n=1}^{K} a_n \mu_n^2 \, \mathrm{d}\phi_n\right)^2 + \frac{\Pi F}{\Pi - \mu r^2}\,\mathrm{d}r^2 + \sum_{n=1}^{K} (r^2 + a_n^2)(\mathrm{d}\mu_n^2 + \mu_n^2 \, \mathrm{d}\phi_n^2), \tag{7.58}$$

with the same $F$, $\Pi$ given above.

The above are solutions to the vacuum Einstein equations, $R_{\mu\nu} = 0$. They are asymptotically flat ($r \to \infty$). One may read off their mass and angular momenta using the standard ADM asymptotic expansion:

$$M = \frac{(D-2)\Omega_{D-2}}{16\pi G_{\mathrm{N}}}\mu, \qquad J_n = \frac{\Omega_{D-2}}{8\pi G_{\mathrm{N}}}\mu a_n = \frac{2}{D-2} M a_n \tag{7.59}$$

where $\Omega_{D-2}$ is the area of the $(D-2)$-unit sphere. For $a_n = 0$ we recover the Tangherlini solution (7.53) and for $\mu = 0$ the metric reduces to a $D$-dimensional flat space in a rotating coordinate system. The MP solutions are stationary. The isometry group of the solution for general $a_n$ is $R_t \times U(1)^K$ and for the special case where all rotation parameters $a_n$ are equal it can enhance to $R_t \times U(K)$.

### > Horizon structure and topology

The horizons are sitting at constant $r$ at zeros of $g^{rr}$. That is, $\Pi - \mu r = 0$ for even $D$ and $\Pi - \mu r^2 = 0$ for odd $D$. These equations are polynomials of degree $2K$ and thus have $2K$ solutions. These solutions are not necessarily real and positive, so the number of horizons is typically less than $2K$. For odd $D$, the equation becomes a polynomial of degree $K$ for $R = r^2$. In this case, the existence of positive roots requires $\mu \geq \sum_n \prod_{m \neq n} a_m^2$. Moreover, when only one of the $a_n$ is zero we have a special case with vanishing horizon ($r = 0$). This case corresponds to the extremal vanishing horizon cases analyzed in [525,526].

In general, the existence and number of horizons depend on the parameters $\mu, a_n$. It is possible that the horizon equation has double roots. In this case, we have extremal MP black holes. One can show that the horizons which arise at the zeros of $g^{rr} = 0$ are all Killing horizons, see Exercise 7.18. Moreover, similarly to the 4$d$ Kerr case, one can show that the outermost horizon, if it exists, is an event horizon and the innermost one is a Cauchy horizon. One can readily observe that the horizon topology for all MP black holes without non-extremal vanishing horizon is $S^{D-2}$.

**Singularity structure**

While some of the metric coefficients blow-up at particular values of $r$, not all of these are spacetime singularities. For example, for generic $a_n$ values, the horizon geometry is smooth. Nonetheless, for the special case of $a_K = 0$ (and all the other $a_n \neq 0$) in odd dimensions, the horizon geometry (at $r = 0$) becomes singular [525]. One can show that [524] for even $D$ and generic $a_n$, $r = 0$ is a curvature singularity on a $(D-3)$-sphere. For odd $D$ and for generic, non-equal, nonzero $a_n$, one can extend the geometry to negative $r^2$ values and the curvature singularity appears at $r^2 = -a_s^2$, where $a_s = min(|a_n|)$. For special cases when $a_K = 0$ or when more than one spin parameter has the value $\pm a_s$, the singular surface is not the entire $(D-1)$-surface at $r^2 = -a_s^2$ [524].

With this information, one can study the maximal analytic extension of the MP black holes and draw the Penrose diagram. For generic cases, the Penrose diagram (in which the $(D-2)$-dimensional angular part is suppressed) takes the same form as the 4$d$ Kerr black hole.

As discussed in the opening of this subsection, the extension of the RN solution to higher dimensions is almost trivial. Nonetheless, it appears that writing down analytic solutions for higher-dimensional counterparts of KN, i.e. charged MP black holes, is quite non-trivial and has not been achieved to date.

### 7.5.3 Five-Dimensional Black Ring Solution

As discussed in Chap. 3, in 4$d$ we have the uniqueness and topology theorems stating that the Kerr geometry is the only asymptotic flat vacuum solution. The arguments of these theorems does not go through in generic higher-dimensional asymptotic flat solutions. In particular, here we focus on the 5$d$ example, where besides the 5$d$ MP black hole with $S^3$ horizon topology, there are black ring solutions with $S^2 \times S^1$ horizon topology. The $5d$ black ring in general comes with three parameters, a mass parameter and two spin (rotation) parameters. It is instructive to start with rewriting flat $5d$ Minkowski geometry in the ring coordinate system [226,227]

$$\mathrm{d}s^2 = -\,\mathrm{d}t^2 + \frac{R^2}{(x-y)^2}\left[(y^2-1)\,\mathrm{d}\psi^2 + \frac{\mathrm{d}y^2}{y^2-1} + (1-x^2)\,\mathrm{d}\phi^2 + \frac{\mathrm{d}x^2}{1-x^2}\right], \tag{7.60}$$

where $\psi, \phi \in [0, 2\pi]$, $x \in [-1, 1]$ and $y \in (-\infty, -1]$. Here $R$ is a free parameter setting the radius of the ring in $\psi$ direction. The ring coordinate system threads the spatial sector with topologically $S^2 \times S^1$ slices. To see this, consider the constant $y = y_0 < -1$ slices and rename $x = \cos\theta, \theta \in [0, \pi]$. The $(x-y)^{-2}$ prefactor never blows up or vanishes at this slice and the metric is (up to a conformal factor) that of $S^2 \times S^1$. When we approach $y = -1, x = 1$ region the metric takes the form of an $\mathbb{R}^4$ while around $y = -1, x = -1$ it is conformal to $\mathbb{R}^4$. So, away from the asymptotic $y = -1$ region the metric (7.60) is well suited for describing a ring geometry.

In this coordinate system the double spinning black ring (Pomeransky–Sen'kov) [527] solution takes the form:

$$\begin{aligned}\mathrm{d}s^2 = &-\frac{F(x,y)}{H(y,x)}\,\mathrm{d}\psi^2 - 2\frac{J(x,y)}{H(y,x)}\,\mathrm{d}\psi\,\mathrm{d}\phi + \frac{F(y,x)}{H(y,x)}\,\mathrm{d}\phi^2 \\ &+ \frac{2k^2 H(x,y)}{(x-y)^2(1-\nu)^2}\Big(\frac{\mathrm{d}x^2}{G(x)} - \frac{\mathrm{d}y^2}{G(y)}\Big) - \frac{H(y,x)}{H(x,y)}(\mathrm{d}t + \Omega(x,y))^2\end{aligned} \tag{7.61}$$

where

$$\begin{aligned}G(x) &= (1-x^2)(1+\lambda x+\nu x^2) \qquad (7.62)\\ H(x,y) &= 1+\lambda^2-\nu^2+2\lambda\nu(1-x^2)y+2\lambda x(1-\nu^2y^2)+\nu(1-\lambda^2-\nu^2)x^2y^2\\ J(x,y) &= \frac{2\lambda\nu^{1/2}k^2(1-x^2)(1-y^2)}{(x-y)(1-\nu)^2}\\ &\quad\big[1+\lambda^2\nu^2+2\lambda\nu(x+y)-\nu(1-\lambda^2-\nu^2)xy\big]\\ \Omega(x,y) &= -\frac{2k\lambda((1+\nu)^2-\lambda^2)^{1/2}}{H(y,x)}\Big[\nu^{1/2}y(1-x^2)\,\mathrm{d}\phi\\ &\quad+\frac{1+y}{1-\lambda+\nu}\big(1+\lambda-\nu+\nu(1-\lambda-\nu)yx^2+2\nu x(1-y)\big)\,\mathrm{d}\psi\Big]\\ F(x,y) &= \frac{2k^2}{(x-y)^2(1-\nu)^2}\Big[G(y)\Big(2\lambda^2+\lambda((1-\nu)^2+\lambda^2)x+(1+\nu)((1-\nu)^2\\ &\quad-\lambda^2)x^2+\lambda(1-\lambda^2-3\nu^2+2\nu^3)x^3+\nu(1-\nu)(1-\lambda^2-\nu^2)x^4\Big)\\ &\quad+(1-y^2)G(x)\big((1+\nu)((1-\nu)^2-\lambda^2)+\lambda(1-\lambda^2+2\nu-3\nu^2)y\big)\Big].\end{aligned}$$

In (7.61) $\psi$ parametrizes the ring direction (cf. discussions below) and $k > 0$ is a dimensionful parameter associated with the radius of the ring. The dimensionless parameters $\nu$, $\lambda$ specify the two rotation parameters ranging in

$$0 \leq \nu < 1 , \qquad 2\sqrt{\nu} \leq \lambda < \nu + 1 . \tag{7.63}$$

The parameter $\nu$ controls the rotation along the $\phi$ direction, such that $\nu = 0$ reduces to the singly rotating ring of Roberto Emparan and Harvey Reall [226]. The asymptotic region of the solution is specified by $y \to -1, x \to 1$ limit where we find a flat $5d$ Minskowski space, there one can read the ADM mass and angular momenta:

$$M = \frac{3\pi k^2 \lambda}{G_{\text{N}}(1+\nu-\lambda)} \tag{7.64a}$$

$$J_\psi = \frac{2\pi k^3 \lambda \sqrt{(1+\nu)^2 - \lambda^2}\left(\nu^2 + (\lambda - 6)\nu + \lambda + 1\right)}{G_{\text{N}}(1-\nu)^2(1+\nu-\lambda)^2} \tag{7.64b}$$

$$J_\phi = \frac{4\pi k^3 \lambda \sqrt{\nu}\sqrt{(1+\nu)^2 - \lambda^2}}{G_{\text{N}}(1-\nu)^2(1+\nu-\lambda)} \tag{7.64c}$$

The horizon is the solution to $G(y) = 0$, $1 + \lambda y_h + \nu y_h^2 = 0$. Recalling (7.63) the above equation has two negative, real roots. The bigger root corresponds to the outer horizon,

$$y_h = \frac{-\lambda + \sqrt{\lambda^2 - 4\nu}}{2\nu}, \tag{7.65}$$

which is a Killing and event horizon (see Exercise 7.19). The ring becomes extremal if the two roots coincide, which happens if $\nu^2 = 4\lambda$. Therefore, a single spinning ring cannot become extremal.

### ⊳ Single-spin, Emparan–Reall ring and its horizon topology

To grasp physics of ring solution, in particular its specific feature, the horizon topology, it is instructive to consider the simpler case of Emparan–Reall single-spin ring [226]. To this end consider the simpler case of a single spin ring with $\nu = 0$. In this case the metric simplifies and we get

$$\begin{aligned} \mathrm{d}s^2 = -\frac{H(y)}{H(x)}(\mathrm{d}t - C\frac{1+y}{H(y)}\,\mathrm{d}\psi)^2 - \frac{2k^2 G(y) H(x)}{(x-y)^2 H(y)}\,\mathrm{d}\psi^2 + \frac{2k^2 G(x)}{(x-y)^2}\,\mathrm{d}\phi^2 \\ + \frac{2k^2 H(x)}{(x-y)^2}\left(\frac{\mathrm{d}x^2}{G(x)} - \frac{\mathrm{d}y^2}{G(y)}\right), \end{aligned} \tag{7.66}$$

where $0 \leq \lambda < 1$,

$$C = 2k\lambda(1+\lambda)\sqrt{\frac{1+\lambda}{1-\lambda}}, \qquad H(x) = 1 + 2\lambda x + \lambda^2, \qquad G(y) = (1+\lambda y)(1-y^2).$$

Mass and angular momenta for this solution are

$$M = \frac{3\pi k^2\lambda}{G_{\rm N}(1-\lambda)}, \qquad J_\phi = 0, \qquad J_\psi = \frac{2\pi k^3\lambda}{G_{\rm N}}\left(\frac{1+\lambda}{1-\lambda}\right)^{3/2}.$$

As we see $J_\phi = 0$ and we are dealing with a single-spin geometry. $\lambda = 0$ recovers the $5d$ flat space.

The horizon is at the root of $G(y)$, $y_h = -1/\lambda$, where the metric takes the form

$$\mathrm{d}s_{\rm H}^2 = \frac{4k^2(1+\lambda)^2}{H(x)}(\mathrm{d}\psi - \varpi\,\mathrm{d}t)^2 + \frac{2k^2\lambda^2 G(x)}{(1+\lambda x)^2}\,\mathrm{d}\phi^2 + \frac{2k^2\lambda^2 H(x)}{(1+\lambda x)^2 G(x)}\mathrm{d}x^2\,, \tag{7.67}$$

where $\varpi = \frac{1}{2k}\sqrt{\frac{1-\lambda}{1+\lambda}}$ is the horizon angular velocity. To explore the topology of the above $3d$ space, it is useful to make the coordinate transformation $x = \cos\theta$, where $\theta \in [0, \pi]$. We first note that the $(x, \phi)$-part has the topology of an $S^2$. This is due to the fact that around $g_{\phi\phi} = 0$ which happens at $\theta = 0, \pi$, the metric takes the form $\frac{2k^2\lambda^2}{1+\lambda}(\mathrm{d}\theta^2 + \theta^2\mathrm{d}\phi^2)$ for $\theta \sim 0$ and $\frac{2k^2\lambda^2}{1-\lambda}(\mathrm{d}\theta^2 + (\pi-\theta)^2\mathrm{d}\phi^2)$ for $\theta \sim \pi$. Therefore, there is no deficit angle in this part. On the other hand the coefficient of the $\mathrm{d}\psi^2$ term does not vanish as we move in the $\theta$-direction; it increases from $(2k)^2$ at $\theta = 0$ to $(2k(1+\lambda)/(1-\lambda))^2$ at $\theta = \pi$. Note also that the $\sqrt{\det g_{\rm H}} = 4k^3\lambda^2(1+\lambda)/(1+\lambda x)^2$ for the horizon metric (7.67) and it does not vanish and is finite for any $x$. Therefore, the $\psi$-direction is the ring direction and the horizon topology is $S^2 \times S^1$ and the horizon area is $32\pi^2 k^3\lambda^2/(1-\lambda)$.

The ring is supported by the angular momentum $J_\psi$ along the ring direction. It is notable that $J_\psi/M^{3/2} \geq \sqrt{G_{\rm N}/\pi}$ and is limited from below, whereas a similar combination for the single-spin MP black hole is limited from above (cf. Exercise 7.17). This shows how (single-spin) rings and holes cover two different regions in the parameter space of asymptotically flat $5d$ Einstein vacuum solutions.

One may explore many different physical properties of the black rings, such as their singularity structure, ergoregions, superradiance, and (in)stability and thermodynamics (see Exercise 7.21). Moreover, similar black ring solutions, with or without electric and dipole charges have been constructed in higher dimensions. For these matters, we refer the reader to the very good review on the topic [227].

### 7.5.4 Asymptotic AdS Vacuum Black Hole Solutions

One may find black hole solutions to (7.52) for $\Lambda = -\frac{(D-1)(D-2)}{2\ell^2}$ and $T_{\mu\nu} = 0$. Among these black holes, we briefly study solutions that are asymptotic to an AdS$_D$ $(D > 3)$ spacetime of radius $\ell$. The first example in this class is AdS-Schwarzschild black hole which is static and spherically symmetric with $R_t \times SO(D-1)$ isometry:

$$\mathrm{d}s^2 = -f(r)\,\mathrm{d}t^2 + \frac{\mathrm{d}r^2}{f(r)} + r^2\,\mathrm{d}\Omega_{D-2}^2\,, \qquad f(r) = 1 + \frac{r^2}{\ell^2} - \left(\frac{r_0}{r}\right)^{D-3}\,. \tag{7.68}$$

As we see in the $r \gg r_0$ limit this reduces to $\mathrm{AdS}_D$ space in global coordinates and in the flat space limit $r, r_0 \gg \ell$ we recover (7.53). The solution has a horizon at $f(r = r_h) = 0$. This is a Killing horizon generated by $\xi_t = \partial_t$ Killing vector and horizon is a round $S^{D-2}$. The mass of this black hole is given by [528]

$$M = \frac{(D-2)\Omega_{D-2}}{16\pi G_{\mathrm{N}}} r_0^{D-3}\,. \tag{7.69}$$

This black hole has a curvature singularity, as in the Tangherlini solution, at $r = 0$. While the small $r$ region, $r/\ell \sim$ finite, looks like the Tangherlini black hole, in the large $r$ region it is different and hence the causal structure of this black hole has some crucial differences to Schwarzschild.

As we see in the Penrose diagram for the AdS-Schwarzschild black hole Fig. 2.18, the left and right boundary regions are causally disconnected and the direction of time flow on the two sides is the opposite.

As in the $D$-dimensional asymptotic flat space case, we can add $[(D-1)/2]$ angular momenta to the above static solution and construct stationary MP-AdS black holes, which are again vacuum AdS solutions. The horizon of these black holes has a topology of $S^{D-2}$. While in principle there is no objection to having an AdS-black ring solution, an explicit analytic metric for such a geometry has not been written down.

As we discussed in Sect. 2.6.2 asymptotic $\mathrm{AdS}_4$ black holes do not respect the topology theorem; the horizon is a smooth, compact 2-dimensional surface, which in general can be specified by the Euler character of the horizon. Similar features extend to the higher-dimensional AdS black holes. The metric for simplest topological black holes is given by

$$\mathrm{d}s^2 = -f(r)\,\mathrm{d}t^2 + \frac{\mathrm{d}r^2}{f(r)} + r^2\,\mathrm{d}\Sigma_k^2\,, \qquad f(r) = k + \frac{r^2}{\ell^2} - \left(\frac{r_0}{r}\right)^{D-3}\,, \tag{7.70}$$

where $k = +1, 0, -1$ and the horizon $\Sigma_k$ is a $(D-2)$-dimensional maximally symmetric surface with a Ricci tensor: $R^i{}_j = k\delta^i{}_j$. Therefore, $k = 1$ corresponds to spherical topology, $k = 0$ to toroidal topology and $k = -1$ to the negatively curved hyperbolic space $\mathrm{H}^{D-2}$. For the latter case, to make the horizon compact we should mod out $\mathrm{H}^{D-2}$ by finite subgroups of its isometry group $SO(D-2, 1)$.

### 7.5.5 Black Branes

Black holes are geometries whose horizon has compact constant time slices. However, in general, such slices may be non-compact. In particular, one may have a planar horizon, in which case the geometry is called black brane. In $D$-dimensional spacetime, the horizon can be a $(p+1)$-dimensional null surface. Such black branes generically source a $(p+1)$-form field $A_{p+1}$ (minimally) coupled to $D$-dimensional Einstein gravity and usually also involve a dilaton field,

$$S = \frac{1}{16\pi G_{\rm N}} \int \mathrm{d}^D x \sqrt{-g} \left( R - \frac{1}{2}(\partial\phi)^2 - \frac{1}{2(p+2)!} e^{-\alpha(p)\phi} F_{p+2}^2 \right) , \tag{7.71}$$

where

$$F_{p+2} = dA_{p+1}, \qquad \alpha^2(p) = \frac{2(p+1)^2}{D-2} - 2(p-1) \,. \tag{7.72}$$

These are the typical supergravity actions in arbitrary dimensions.

One may then verify that [529–531]

$$\mathrm{d}s^2 = f_-(r)^{\frac{q}{D-2}} \Big( - \frac{f_+(r)}{f_-(r)} \mathrm{d}t^2 + \mathrm{d}x_i \, \mathrm{d}x_i \Big)$$
$$+ f_-(r)^{\frac{\alpha^2}{2q}} \Big( \frac{\mathrm{d}r^2}{f_+(r) f_-(r)} + r^2 \, \mathrm{d}\Omega_{q+1}^2 \Big) \tag{7.73a}$$

$$A_{p+1} = \left( \frac{\sqrt{r_+ r_-}}{r} \right)^q \mathrm{d}t \wedge \mathrm{d}x_1 \cdots \wedge \mathrm{d}x_p \tag{7.73b}$$

$$e^{-2\phi} = f_-(r)^\alpha \tag{7.73c}$$

where $i = 1, \ldots, p$ denote directions along the brane, $q = D - p - 3$, and

$$f_\pm(r) = 1 - \Big( \frac{r_\pm}{r} \Big)^q \,. \tag{7.74}$$

This black $p$-brane solution has an event horizon at $r = r_+$ with horizon topology $R^p \times S^{q+1}$. The solution has a curvature singularity at $r = r_-$. In the extremal case $r_- = r_+$ the two horizons coincide. There are also solitonic brane solutions to the same theory (7.71), which carry magnetic charge of the $(p+1)$-form. These are $(D-p-4)$-branes with $(p+2)$-form magnetic flux through the transverse $S^{p+2}$.

The next black brane solution we discuss is the black $p$-brane on an AdS$_{p+2}$ background. As mentioned in Sect. 2.6.2, on AdS$_{p+2}$ we can have black holes of various topologies including $T^p$. This latter may be viewed as a black $p$-brane solution, corresponding to $k = 0$ case in (7.70). These solutions are asymptotic to AdS space in Poincaré patch, where the horizon is parallel to the Poincaré horizon. The AdS-black brane solution is conveniently written as $(i = 1, \ldots, p)$

$$\mathrm{d}s^2 = \frac{\ell^2}{z^2} \left[ -f(z)\, \mathrm{d}t^2 + \frac{\mathrm{d}z^2}{f(z)} + \mathrm{d}x_i \, \mathrm{d}x_i \right] , \qquad f(z) = 1 - (\frac{z}{z_h})^{p+1} , \tag{7.75}$$

which solves the AdS-Einstein vacuum EOM.

## 7.6 Black Holes in Large Number of Dimensions

If one keeps the spacetime dimension $D$ arbitrary in GR, one can generate a small parameter $1/D$ by taking the limit $D \gg 1$. Small parameters typically allow perturbative treatments. So the large $D$ limit of GR could be an efficient tool for calculations.

In the large $D$ limit, the number of graviton polarizations $D(D-3)/2$ grows like $D^2/2$, reminiscent of the growth of gluon polarizations in the large $N$ limit of $SU(N)$ Yang–Mills. Additionally, the Newton potential gets diluted exponentially, $\Phi \sim r^{3-D}$, meaning that the gravitational field is strongly localized at its source and Coulomb-like tails become less relevant. It is this second aspect, more than the first one, that turned out to be fruitful for simplifications, see [532,533] for additional motivations and references.

Unsurprisingly, black holes are a key player in many large $D$ considerations. To get a bit of large $D$ intuition, consider Schwarzschild–Tangherlini black holes (7.53). For fixed $D$ they are characterized by a single scale, the horizon length $r_h$. However, if we allow $1/D$ to be a (small) parameter, then other scales are generated, like $r_h/D$. This smaller scale is clearly separated from the horizon scale, $r_h/D \ll r_h$. The physical role of the smaller scale is that it characterizes the slope of the Newton potential near the horizon, $\frac{\partial\Phi}{\Phi}|_{r_h} \sim D/r_h$. Moreover, it allows to define a "near zone", $r - r_h \leq \mathcal{O}(r_h/D)$, where the Newton potential is order unity, and a "far zone", $r > r_h$, where the Newton potential effectively vanishes and geometry practically becomes Minkowski space. Thus, most of the interesting physics is localized in a small region around the horizon, which permits an effective membrane description of large $D$ black holes (compare with the membrane paradigm in Sect. 6.8).

The mechanism of localizing (steep) gradients near the horizon is unfortunate for numerics—black hole formation in numerical GR becomes increasingly challenging as the dimension grows—but a godsend for analytic discussions. For a summary of results see the review [533], including a discussion of QNMs, an effective membrane theory, a simple derivation of the Gregory–Laflamme instability (see also Exercise 7.24), black hole mergers, and holographic applications.

## Further Reading

For lower-dimensional black holes there are classic textbooks [475,534,535], but especially the older ones are somewhat outdated as there were considerable developments in lower-dimensional gravity after the 1990s. More up-to-date info is contained in various reviews.

For 2-dimensional dilaton gravity see [424,536–538]; for 3-dimensional Einstein gravity see [478,539,540].

For higher-dimensional black holes, there is a paper collection by Gary Horowitz [227,541].

## Exercises

**7.1 Witten black hole** [542]

Consider 2-dimensional dilaton gravity with potentials $U(X) = 1/X$, $V(X) = X$ and construct all solutions to the classical EOM, locally and globally.

**7.2 Reissner–Nordström as Poisson-sigma model.**

Take Einstein–Maxwell theory in four dimensions, spherically reduce to dilaton-Maxwell in two dimensions and find a gauge theoretic reformulation as Poisson-sigma model with 4-dimensional target space and Poisson tensor of rank 2.

**7.3 Ricci in three dimensions.**

Show that for any 3-dimensional metric $g_{\mu\nu}$,

$$R_{\mu\nu\alpha\beta} = -\epsilon_{\mu\nu\rho}\epsilon_{\alpha\beta\lambda}G^{\rho\lambda}$$

where $\epsilon$ is the totally antisymmetric tensor, $R_{\mu\nu\alpha\beta}$ is the Riemann curvature, and $G^{\rho\lambda}$ is the Einstein tensor.

**7.4 BTZ black holes are quotients of $\mathbf{AdS_3}$.**

Show that non-rotating BTZ black holes, (7.3) with $r_- = 0$, are quotients obtained via identifications of $AdS_3$ by $e^{2\pi\xi}$ with the Killing vector $\xi = \frac{r_+}{\ell}\big(x\partial_u + u\partial_x\big)$ where $u, x$ refer to embedding coordinates,

$$\mathrm{d}s_4^2 = -\,\mathrm{d}u^2 - \mathrm{d}v^2 + \mathrm{d}x^2 + \mathrm{d}y^2, \qquad -u^2 - v^2 + x^2 + y^2 = -\ell^2.$$

**7.5 Penrose diagram of rotating BTZ.**

Construct 2-dimensional slices (assuming constant angle) through Penrose diagrams of rotating BTZ black holes, and discuss also the special cases of non-rotating and extremal BTZ.

**7.6 More on Bañados geometries and BTZ black holes.**

(1) Do rotating BTZ black holes have an ergo-region? Are you sure?

(2) Prove that all Bañados geometries (7.7) solve the Einstein equations (7.2) with negative cosmological constant, $\Lambda = -1/\ell^2$.

(3) Show that in general Bañados geometries have at least two globally defined Killing vectors.

(4) Explore the existence of black holes, with event and Killing horizons, in Bañados family of solutions and compute surface gravity, horizon angular velocity, and horizon area for them. What is the shape of the horizon as seen by the asymptotic observer using the $t, \rho, \phi$ coordinate system? These questions have been explored in [479,480].

(5) Analyze null geodesics around a Bañados geometry and show these black holes do not have shadows.

**7.7 Equivalence to Chern–Simons formulation.**
Verify that the CS connections (7.11), (7.12) lead to the Bañados geometries (7.7) by using the relation (7.10) between metric and CS connections.

**7.8 Flat space Chern–Simons connection.**
Provide the CS formulation for flat space Einstein gravity and find boundary conditions for the connection that permits all flat space cosmologies (7.25).

**7.9 Weyl invariance of Cotton tensor.**
Check invariance of the Cotton tensor (7.29) under local Weyl rescalings (7.27).

**7.10 Topologically massive gravitons in $AdS_3$.**
Linearize the TMG EOM (7.30) around global $AdS_3$ and show that there is a physical degree of freedom corresponding to a massive graviton excitation.

**7.11 Most general $2d$ dilaton gravity solution space.**
The most general 2d dilaton gravity model is given by the action (7.33), with $U(X)(\partial X)^2 + 2\lambda V(X)$ replaced by $\mathcal{V}\big(X,\, (\partial X)^2\big)$. Find all classical solutions of this theory.

**7.12 Gauge transformations vs. diffeomorphisms.**
Show that gauge transformations in the gauge theoretic formulation of 3- and 2-dimensional gravity generate on-shell diffeomorphisms, provided the gauge parameter $\lambda_I$ is chosen as

$$\lambda_I = A_{I\mu}\,\xi^\mu$$

where $A_{I\mu}$ is the gauge-connection and $\xi^\mu$ the vector field that generates the diffeomorphism.

**7.13 Spherical reduction.**
Take Einstein gravity in $D > 2$ dimensions and assume spherical symmetry by considering adapted metrics

$$\mathrm{d}s^2 = g_{\alpha\beta}\;\mathrm{d}x^\alpha\,\mathrm{d}x^\beta + \frac{1}{\lambda}\,X^{2/(D-1)}\;\mathrm{d}^2\Omega_{S^{D-1}}$$

where $\lambda = \text{const.}$, $\alpha, \beta = 0, 1$ and $\mathrm{d}^2\Omega_{S^{D-2}}$ is the metric of the round $(D-2)$-sphere. Insert the ansatz above into the $D$-dimensional Einstein–Hilbert action (disregarding boundary terms) and show that after integrating out the angular part you get a $2d$ dilaton gravity action (7.33) with potentials

$$U(X) = -\frac{D-2}{D-2}\,\frac{1}{X} \qquad\qquad V(X) \propto X^{(D-4)/(D-2)}\,.$$

**7.14 Chaos in Jackiw–Teitelboim gravity and holographic Lyapunov exponent.**

Holographically calculate the Lyapunov exponent using the JT model as follows. Consider an $AdS_2$ black hole of mass $M$ and temperature $T$, mimicking a thermal state on the field theory side. Add an infalling massless particle of energy $\delta M \ll M$, mimicking a small perturbation on the field theory side. Consider additionally some outgoing signal near the horizon, both in the unperturbed geometry and in the backreacted one. Show that the time-delay $\delta T$ generated by this backreaction is given by

$$\delta T \propto e^{\lambda_L \delta t}$$

where $\delta t$ is the expected waiting time (without backreaction). Calculate the holographic Lyapunov exponent $\lambda_L$ and show that it saturates the chaos bound

$$\lambda_L = 2\pi T\,.$$

**7.15 Higher-dimensional Birkhoff theorem.**

(1) Show any asymptotically flat spherically symmetric vacuum solution is necessarily static and is of the form (7.53).

(2) One may extend the above to the higher-dimensional RN black hole: Show any spherically symmetric, asymptotically flat solution to Einstein–Maxwell theory in $D$ dimensions ($D > 4$) is necessarily static and is of the form (7.54). Work out the expressions for the ADM mass and charge given for this solution.

**7.16 Shadow of a Tangherlini black hole.**

Studying the null geodesics around a higher-dimensional Schwarzschild (Tangherlini) black hole, compute the radius of the shadow of this black hole and compare it with the 4-dimensional case.

**7.17 Single-spin MP black hole.**

To obtain a better understanding of MP black holes, it is instructive to consider a single-spin case in $D$ dimensions. This case may be viewed as a higher dimensional extension of Kerr geometry.

(1) Write down the metric (7.56) when only one of the rotation parameters $a_n$ is non-zero, $a_1 = a, a_n = 0\ n > 1$.

(2) Repeat the same for the odd dimensional case (7.58).

(3) Show that for the $D = 5$ case, the extremality bound yields $J/M^{3/2} \leq 4\sqrt{2G_N}/(3\sqrt{3\pi})$.

(4) Explore the first law in these cases. Work out Smarr relation and discuss how the Gibbons' scaling argument cf. discussions in the end of Sect. 5.5.2, can be extended to $D$ dimensional case.

**7.18 Killing horizons of MP black hole.**

(1) Analyzing the geometry of MP black holes near the horizons, compute horizon angular velocities at each horizon, $\Omega_n^{(h)}$, where $n = 1, \ldots, K$ and $h$ enumerates which horizon we are focusing on.

(2) As a direct generalization of the $4d$ Kerr geometry, one can construct the Killing vector

$$\zeta^{(h)} = \partial_t + \sum_n \Omega_n^{(h)} \partial_{\phi_n}. \tag{7.76}$$

Show that $\zeta^{(h)}$ becomes null at horizon $h$.

(3) Compute the surface gravity at each horizon $\kappa^{(h)}$ using the usual formula $(\kappa^{(h)})^2 = 1/4(\nabla_\mu \zeta_\nu)^2$.

**7.19 Near horizon limit of MP black holes.**

(1) Show the geometry arising in the near horizon of a generic MP black hole may be brought to Rindler space$\oplus H$, where $H$ is the $(D-2)$-dimensional bifurcation horizon surface. Show $H$ has $S^{D-2}$ topology.

(2) Repeat the near horizon analysis for the extremal MP black holes and show that the Rindler part is replaced with a geometry conformal to $\mathrm{AdS}_2$, the geometry is $\mathrm{AdS}_2 \ltimes_w H$), where $\ltimes_w$ stands for a warped-fibred product, with $\mathrm{SL}(2,\mathbb{R}) \times \mathrm{U}(1)^K$ isometry.

**7.20 Ergoregions and causal structure of MP black holes.**

(1) As in the $4d$ Kerr, the infinite redshift surface, where $g_{tt} = 0$ is different than the horizon in generic MP black holes. Explore the ergoregion, the space between the infinite redshift surface, and the horizons for the MP black holes.

(2) In the MP black holes one can in principle extend the radial coordinate $r$ to regions where one develops CTCs. We usually excise the geometry in those regions to avoid CTC. Analyze the CTC in MP black holes.

**7.21 Horizon angular velocity and Smarr relation for the black rings.**

(1) Show that the horizon angular velocities of the doubly spinning ring (7.61) is given by

$$\Omega_\psi = \frac{1}{2k}\sqrt{\frac{1+\nu-\lambda}{1+\nu+\lambda}}, \qquad \Omega_\phi = \frac{\lambda(1+\nu) - (1-\nu)\sqrt{\lambda^2 - 4\nu}}{2k\lambda\sqrt{\nu}}\Omega_\psi \tag{7.77}$$

(2) Show that

$$\zeta_H = \partial_t + \Omega_\psi \partial\psi + \Omega_\phi \partial_\phi \tag{7.78}$$

becomes null at the horizon of the ring, i.e. at $y = y_h$ (7.65). Using this work out the surface gravity at the horizon:

$$\kappa \equiv 2\pi T_H = \frac{(y_h^{-1} - y_h)(1-\nu)\sqrt{\lambda^2 - 4\nu}}{4k\lambda(1+\nu+\lambda)} \tag{7.79}$$

(3) Show that the horizon area $A_{\rm H}$ for the ring is

$$A_{\rm H} \equiv 4G_{\rm N} S_{\text{Black Ring}} = \frac{32\pi^2 k^3 \lambda(1+\nu+\lambda)}{(y_h^{-1} - y_h)(1-\nu)^2} \tag{7.80}$$

(4) Show that the ADM mass and angular momenta satisfy the Smarr relation

$$\frac{2}{3}M = T_{\rm H} S_{\text{Black Ring}} + \Omega_\psi J_\psi + \Omega_\phi J_\phi \tag{7.81}$$

**7.22 More analysis on AdS-Schwarzschild.**

(1) Compute the surface gravity $\kappa$ for the AdS-Schwazrzschild solution (7.70) and show that it satisfies the first law $\kappa\, \mathrm{d}A_{\rm H} = 8\pi G_{\rm N}\, \mathrm{d}M$, where $A_{\rm H}$ is the horizon area and $M$ is the black hole mass (7.69). What is the Smarr relation for this black hole?

(2) Study null and timelike radial geodesics of AdS-Schwazrzschild and compute how much coordinate time $t$ it takes for a free particle to travel from $r_i > r_h$ to infinity and to the horizon.

**7.23 More on black $p$-branes.**

(1) Investigate Penrose diagram and causal structure of the extremal and non-extremal $p$-brane solutions in $D$-dimensional gravity theories. In particular show that the causal structure of extremal "electric branes" ($p < (D-4)/2$) self-dual ($p = (D-4)/2$) and "magnetic branes" ($p > (D-4)/2$) are in general different. See [543] for $p = 2, 5$; $D = 11$ and generic $p$ in $D = 10$ theories.

(2) Compute surface gravity, ADM mass, and $(p+1)$-form charge of the black $p$-brane solution (7.73) and verify the Smarr formula and first law of black hole mechanics for the brane.

**7.24 Gregory–Laflamme instability** [544,545]**.**

Black $p$-branes which have non-spherical horizons are prone to an instability. For example, let us consider a black string in five dimensions which is an uplift 4-dimensional Schwarzschild solution to five dimensions over a circle of radius $R$. The horizon topology of this solution is hence $\mathrm{S}^2 \times \mathrm{S}^1$. The same 5$d$ theory has a solution which is an array of $N$ 4$d$ Schwarzschild black holes with uniform spacing $2\pi R/N$ over the fifth circle. One may choose the black string and the array to have equal total mass (or equivalently, equal mass per unit length over the circle).

(1) Compute entropy of the string and the array and show that $S_{\rm array}/S_{\rm string} \sim (R/r_{\rm H})^{1/2}$ where $r_{\rm H}$ is the Schwarzschild radius of the 4$d$ black holes in the array.

(2) Argue that for $R \gtrsim r_{\rm H}$ the string is unstable and more stable configuration is the array.

(3) Does the above analysis also work in the decompactified $R \to \infty$ limit?

(4) Repeat the above analysis for charged branes/strings. Are extremal $\mathrm{D}_p$-branes also suffering from Gregory–Laflamme instability?

**7.25 Near horizon of D3-brane solution.**

(1) Consider an extremal 3-brane solution to a 10-dimensional theory, i.e. the solution (7.73) with $r_+ = r_-$ for $p = 3$, $D = 10$. Take the near horizon limit and show that we get an $\mathrm{AdS}_5 \times \mathrm{S}^5$ geometry. This was the starting point of the celebrated Maldacena's AdS/CFT duality, see Chap. 8 for more detailed discussion.

(2) One may start with a near-extremal 3-brane solution, with $r_+ - r_- = \ell^5/z_h^4$, $\ell^2/z_h \ll r_+$. Show that in this case we obtain the AdS-black brane solution (7.75) for $p = 3$. Compute the surface gravity and the energy/mass for the AdS-black-brane solution.

**7.26 AdS-Soliton solution.**

Since Einstein equations are invariant under Wick rotations, one of the usual solution generating techniques in GR is to make double Wick rotations.

(1) Show from (7.75) one can obtain the so-called AdS-soliton metric [528]

$$
\begin{aligned}
\mathrm{d}s^2 &= \frac{\ell^2}{z^2}\left[-\,\mathrm{d}t^2 + \frac{\mathrm{d}z^2}{f(z)} + f(z)\,\mathrm{d}y^2 + \mathrm{d}x_i\,\mathrm{d}x_i\right], \\
f(z) &= 1 - (\frac{z}{z_h})^{p+1}, \; i = 1, \ldots, p-1 ,
\end{aligned}
\tag{7.82}
$$

where we have put the "emblackening" factor in front of a spatial coordinate, rather than time. Verify directly that this is indeed a Einstein AdS-vacuum solution.

(2) Unlike the AdS-black-brane solution (7.75) $z = z_h$ region is singular. To remove the singularity one may compactify $y$ on a circle of radius $R$. Compute $R$ such that the geometry has no deficit angle and is free of conical singularity.

(3) Compute the energy associated with this geometry and compare it with the AdS-black-brane one. Despite the fact that this energy is negative, this solution has been shown to be stable [528], as it has the lowest possible energy given the boundary conditions (with $R^{1+(p-1)} \times S^1$ boundary).

**7.27 Large $D$ GR and 2$d$ dilaton gravity.**

Derive an effective action for spherically symmetric GR in infinite dimensions and show that this limit recovers the 2-dimensional Witten black hole. (You can use Table 7.1 and compare your results with [546].)

# 8 Aspects of Holography

**Abstract**

In this chapter, we explore some aspects of holographic correspondences, in particular the AdS/CFT duality. While we assume familiarity with all preceding chapters, the sections herein are self-contained. Therefore, readers familiar with more basic material can read them independently from the earlier parts of the book. Section 8.1 introduces basics of holography. Section 8.2 is devoted to the holographic formulation of quantum information-theoretic concepts in field theories, including entanglement entropy and mutual information. These concepts have proven useful for understanding puzzles regarding black holes. In Sect. 8.3, we discuss black holes in AdS space and their holographic description in terms of thermal field theories. Section 8.4 discusses the notion of asymptotic symmetries and reviews the seminal Brown–Henneaux analysis. The notion of asymptotic symmetries may be extended to boundary symmetries which are essential to the soft hair proposal, introduced and discussed in Sect. 8.5. Extremal black holes, while of less observational relevance, are often used as a testing ground for black hole microstate counting. In this regard, we discuss the attractor mechanism in Sect. 8.6 and briefly review the Kerr/CFT correspondence in Sect. 8.7. In Sect. 8.8, we briefly mention other aspects of holography and their applications to strongly coupled/correlated systems.

## 8.1 Basics of Holography

The holographic principle postulates that QG in $D+1$ dimensions is equivalent to some QFT in $D$ dimensions [85,86]. A concrete realization within string theory is Juan Maldacena's AdS/CFT correspondence [88] that relates type IIB string theory compactified on $\mathrm{AdS}_5 \times S^5$ to $\mathcal{N}=4$ super-Yang–Mills theory in four dimensions. An important special case is the supergravity approximation, in which AdS/CFT relates classical Einstein gravity (or rather, its supersymmetric version) to strongly coupled $\mathcal{N}=4$ super-Yang–Mills in the limit of a large number of 'colors'.



D. Grumiller and M. M. Sheikh-Jabbari, *Black Hole Physics*, Graduate Texts in Physics,
https://doi.org/10.1007/978-3-031-10343-8_8

The AdS/CFT correspondence can be used in either direction, meaning that we can exploit semiclassical gravity calculations to learn about strongly coupled CFTs or weakly coupled CFT calculations to learn about QG. Examples of the former are applications to heavy-ion collisions or condensed matter physics, examples of the latter so far arise mostly in lower dimensions, particularly in $AdS_3/CFT_2$. Typically, if a calculation is easy on one side of the correspondence it becomes hard on the other side, like other strong/weak dualities in physics. See the textbook [547].

Besides Maldacena's strong/weak AdS/CFT correspondence there is also the weak/weak type of duality found by Igor Klebanov and Alexander Polyakov [548], and independently by Ergin Sezgin and Per Sundell [549] relating Mikhail Vasiliev's higher spin theory on $AdS_4$ to the 3-dimensional $O(N)$ vector model. Proposals for holography beyond AdS/CFT exist as well but are less established.

As holography in general and AdS/CFT, in particular, is an ongoing research endeavor we focus here specifically on the aspects of relevance for black hole physics, from which the holographic principle emerged. For applications of AdS/CFT see [547] and references therein.

Even with this pre-selection of topics, it is impossible to comprehensively cover holography in a single chapter. Therefore, we provide a summary and outlook at its end as a guide to further literature.

### 8.1.1 AdS/CFT, the Precise Statement

An important class of observables in any QFT is correlation functions of gauge invariant observables, for which Steve Gubser, Igor Klebanov and Alexander Polyakov [89] and independently Edward Witten [90] found the following dictionary

$$\boxed{\Big\langle \exp\Big(\int j(x)\,\mathcal{O}(x)\Big)\Big\rangle_{\text{CFT}} = Z_{\text{gravity}}\Big[\phi(x,z)|_{z\to 0} = j(x)\Big]}\,. \tag{8.1}$$

The left-hand side is evaluated in the CFT. Here $\mathcal{O}(x)$ is some gauge invariant operator whose source is given by $j(x)$. The expression on the left-hand side is nothing but the generating functional of correlation functions, yielding arbitrary $n$-point functions by taking $n$ functional derivatives with respect to the sources and then setting them to zero. The right-hand side is evaluated in QG; in the supergravity approximation, this reduces to an evaluation in classical gravity. In that limit the quantity $Z_{\text{gravity}}$ is the classical partition function evaluated with boundary conditions for the field $\phi$ given by the function $j(x)$ (which coincides with the source on the CFT side), where the limit $z \to 0$ denotes approaching the asymptotically AdS boundary (while $x$ are the boundary coordinates). The field $\phi$ must be the one corresponding to the gauge invariant operator $\mathcal{O}$.

To see heuristically why $AdS_{d+1}$ is so intimately related to $CFT_d$ let us consider a geometrization of renormalization group flow in a generic QFT, where in addition to the Minkowski coordinates $x^\mu$ we introduce energy $E$ as additional coordinate. The most general metric compatible with $d$-dimensional Poincaré symmetries is given by $\mathrm{d}s^2 = f_1(E)\,\mathrm{d}E^2 + f_2(E)\,\eta_{\mu\nu}\,\mathrm{d}x^\mu\,\mathrm{d}x^\nu$. If we assume that the QFT has scale symmetry, $x^\mu \to \lambda x^\mu$, $E \to \lambda^{-1}E$, then the most general line-element compatible with $d$-dimensional Poincaré symmetries and scale symmetry is given by

$$\mathrm{d}s^2 = \ell^2\left(\frac{\mathrm{d}E^2}{E^2} + E^2\,\eta_{\mu\nu}\,\mathrm{d}x^\mu\,\mathrm{d}x^\nu\right) \tag{8.2}$$

where we introduced some arbitrary but fixed length scale $\ell$ to have correct units. Remarkably, the metric (8.2) describes Poincaré patch AdS$_{d+1}$ with AdS radius $\ell$ and asymptotic boundary at $E \to \infty$. The isometries of AdS$_{d+1}$, $SO(d,2)$, match with the conformal symmetry of a CFT$_d$. Besides the matching of symmetries, another aspect evident from (8.2) is the UV/IR connection in AdS/CFT [550]: the deep IR on the gravity side ($E \to \infty$) is mapped to the deep UV on the CFT side, and vice versa.

### 8.1.2 Gravity in Anti-De Sitter Space

To see the features outlined above explicitly, let us start by generalizing (8.2) to locally asymptotically AdS spacetimes

$$\mathrm{d}s^2\big|_{\text{LaAdS}} = \frac{\ell^2}{E^2}\,\mathrm{d}E^2 + \left(\ell^2E^2\,\gamma^{(0)}_{\mu\nu} + \gamma^{(2)}_{\mu\nu} + \cdots\right)\mathrm{d}x^\mu\,\mathrm{d}x^\nu \tag{8.3}$$

where $\ell$ is the AdS radius, $\mu, \nu = 0, 1, \ldots, D-1$, assuming $D \geq 3$, and the ellipsis refers to terms that vanish when $E \to \infty$ is approached. We may further restrict $\gamma^{(0)}_{\mu\nu} = \eta_{\mu\nu}$, as it is the case for Poincaré-patch or global AdS. The quantity $\gamma^{(2)}_{\mu\nu}$ may depend arbitrarily on $x^\mu$, which are often referred to as 'boundary coordinates'.

Gaussian normal coordinates, $\rho = \ell\,\ln(\ell E)$, are a bit simpler and yield the so-called Fefferman–Graham expansion,

$$\boxed{\mathrm{d}s^2\big|_{\text{LaAdS}} = \mathrm{d}\rho^2 + \left(e^{2\rho/\ell}\,\gamma^{(0)}_{\mu\nu} + \gamma^{(2)}_{\mu\nu} + \cdots\right)\mathrm{d}x^\mu\,\mathrm{d}x^\nu\,.} \tag{8.4}$$

where the ellipsis denotes terms that vanish as $\rho$ tends to infinity. To regularize intermediate results, we introduce an arbitrarily large, but finite, cutoff $\rho = \rho_c$ where the boundary is placed. A technical advantage of Gaussian normal coordinates (8.4) is that the normal vector of this boundary has only non-vanishing component $n_\rho = n^\rho = 1$, yielding simple expressions for the extrinsic curvature tensor

$$K_{\mu\nu} = \nabla_\mu n_\nu = -\Gamma^\rho{}_{\mu\nu} = \frac{1}{\ell}\,e^{2\rho_c/\ell}\,\gamma^{(0)}_{\mu\nu} + \cdots \qquad K_{\rho\mu} = 0 = K_{\rho\rho}\,. \tag{8.5}$$

Below we are going to use these expressions.

The usual locally asymptotically AdS boundary conditions require

$$\delta\gamma^{(0)}_{\mu\nu} = 0 \qquad \delta\gamma^{(2)}_{\mu\nu} = \text{arbitrary}\,. \tag{8.6}$$

The fixed metric $\gamma^{(0)}_{\mu\nu}$ is often called 'boundary metric'. We call any metric consistent with the expansion (8.4) and the boundary conditions (8.6) 'locally asymptotically AdS' or just 'asymptotically AdS'.

There are numerous generalizations of (8.4), (8.6): we could change the coordinates; we could switch on mixed terms $\mathrm{d}\rho\,\mathrm{d}x^\mu$; we could consider non-flat boundary metrics; we could relax or alter the conditions (8.6) by allowing fluctuations of the boundary metric; we could consider terms that are subleading as compared to $\gamma^{(0)}$ but more dominant than $\gamma^{(2)}$; there could be subleading terms polynomial in $\rho$, etc. As always, boundary conditions are a choice, and the precise choice is dictated by the physical questions one would like to address. The boundary conditions above are often useful enough, so we restrict them.

### 8.1.3 Holographic Renormalization

Holographic counterterms are boundary contributions to the action that do not change the boundary value problem, but that do render the variational principle well-defined. Examples of candidates for such terms are the boundary cosmological constant and the boundary Ricci scalar appearing in (6.10). We focus here on asymptotically AdS boundary conditions.

Let us reconsider the on-shell action, the Brown–York stress tensor and the variational principle for asymptotically AdS spacetimes, starting from the action (6.12) and using the results (8.4)–(8.5). The bulk Ricci scalar is constant, $R = 2D/(D-2)\Lambda = -D(D-1)/\ell^2$. The bulk volume form is determined from $\sqrt{-g} = e^{\rho/\ell(D-1)}\sqrt{-\gamma^{(0)}}\,\big(1+\mathcal{O}(e^{-2\rho/\ell})\big)$. The boundary volume form is given by the same expression, but evaluated at the cutoff surface $\rho=\rho_c$, $\sqrt{-h} = e^{\rho_c/\ell(D-1)}\sqrt{-\gamma^{(0)}}\,\big(1+\mathcal{O}(e^{-2\rho_c/\ell})\big)$. Finally, the trace of extrinsic curvature (8.5) evaluates to $K=(D-1)/\ell\,\big(1+\mathcal{O}(e^{-2\rho_c/\ell})\big)$. Plugging these results into the Einstein–Hilbert action with Gibbons–Hawking–York boundary term yields

$$I = \Big(-\frac{D-1}{8\pi G\,\ell^2}\int\limits_{\rho_0}^{\rho_c}\mathrm{d}\rho\, e^{\rho/\ell(D-1)} + \frac{D-1}{8\pi G\,\ell}\,e^{\rho_c/\ell(D-1)}\Big)\int \mathrm{d}^{D-1}x\,\sqrt{-\gamma^{(0)}} + \cdots \tag{8.7}$$

which in the large $\rho_c$ limit evaluates to something infinite

$$I\big|_{\rho_c\gg 1} = e^{\rho_c/\ell(D-1)}\,\frac{D-2}{8\pi G\,\ell}\int \mathrm{d}^{D-1}x\,\sqrt{-\gamma^{(0)}}\,\big(1+\cdots\big)\,. \tag{8.8}$$

Similarly, the Brown–York stress tensor (6.14) is infinite as the cutoff tends to infinity,

$$T^{\mathrm{BY}}_{\mu\nu} = \frac{1}{8\pi G}\big(K_{\mu\nu}-h_{\mu\nu}K\big) = e^{2\rho_c/\ell}\,\frac{2-D}{8\pi G\,\ell}\,\gamma^{(0)}_{\mu\nu} + \mathcal{O}(1)\,. \tag{8.9}$$

Worst of all, the variational principle is not well-defined for some variations that preserve our boundary conditions (8.6). Indeed, evaluating the variation (6.13) on-shell and setting to zero $\delta\gamma^{(0)}_{\mu\nu}$ yields

$$\delta I\big|_{\text{EOM}} = e^{(D-3)\rho_c/\ell}\,\frac{D-2}{16\pi G\,\ell}\int \mathrm{d}^{D-1}x\,\sqrt{-\gamma^{(0)}}\,\gamma^{\mu\nu}_{(0)}\,\delta\gamma^{(2)}_{\mu\nu} + \cdots \neq 0\,. \tag{8.10}$$

Thus, we recover the same problems that we encountered in the simple mechanics model in Exercise 6.1.

It is suggestive that the resolution could also be the same: simply add suitable boundary terms that do not violate our Dirichlet boundary value problem. Adding such boundary terms is known as 'holographic renormalization' (holographic, since we are adding boundary terms, and renormalization, since we convert infinite quantities like on-shell action and Brown–York stress tensor into finite ones). The full action is given by

$$\Gamma[g_{\mu\nu}] = I_{\text{EH}}[g_{\mu\nu}] + I_{\text{GHY}}[\gamma_{\mu\nu},\ K_{\mu\nu}] + I_c[\gamma_{\mu\nu}] \tag{8.11}$$

where the holographic counterterm is of the form ($\mathcal{R}$ is the boundary Ricci scalar)

$$I_c[g_{\mu\nu}] = \int_{\partial\mathcal{M}} \mathrm{d}^{D-1}x\,\sqrt{-h}\,\big(c_0 + c_2\,\mathcal{R} + \cdots\big). \tag{8.12}$$

We have again adhered to the principle to write down all possible terms compatible with the symmetries (boundary diffeomorphisms and boundary Lorentz invariance) and displayed explicitly the first two terms in a derivative expansion; depending on the dimension one might need more than these two terms. The coefficients $c_0$, $c_2$, etc. are fixed such that all the problems encountered above go away. We could also determine them by solving a Hamilton–Jacobi equation (as in Exercise 6.1), but it is often more efficient to simply start with an ansatz like (8.12) and determine the coefficients by direct calculation. If the matter is present, the holographic counterterms can additionally depend on the matter fields. See [357,551–553] for explicit expressions of the holographically renormalized Brown–York stress tensor in various dimensions.

For the sake of concreteness we consider 3-dimensional vacuum Einstein gravity with flat boundary metric, $\gamma^{(0)}_{\mu\nu} = \eta_{\mu\nu}$, as particular case. It turns out that only $c_0$ is needed in the holographic counterterm (8.12). Choosing $c_0 = -1/(8\pi G_{\text{N}}\ell)$ solves all the aforementioned problems so that the holographically renormalized action

$$\Gamma_{\text{AdS}_3}[g_{\mu\nu}] = \frac{1}{16\pi G_{\text{N}}}\int \mathrm{d}^3x\sqrt{-g}\left(R + \frac{2}{\ell^2}\right) + \frac{1}{8\pi G_{\text{N}}}\int \mathrm{d}^2x\sqrt{-h}\left(K - \frac{1}{\ell}\right) \tag{8.13}$$

is finite on-shell, has a well-defined variation principle, and yields the holographically renormalized Brown–York stress tensor

$$T^{\text{BY-ren}}_{\mu\nu} = \frac{1}{8\pi G_{\text{N}}}\left(K_{\mu\nu} - h_{\mu\nu}K + h_{\mu\nu}\,\frac{1}{\ell}\right) = -\frac{1}{8\pi G_{\text{N}}\,\ell}\,\gamma^{(2)}_{\mu\nu} \tag{8.14}$$

which is finite, conserved, and traceless.

### 8.1.4 Holographic Correlation Functions

A particular example of the holographic dictionary (8.1) is the calculation of $n$-point correlation functions of the stress tensor

$$\langle T_{\mu_1\nu_1}(x_1^\lambda)\dots T_{\mu_n\nu_n}(x_n^\lambda)\rangle_{\text{CFT}}^{\text{connected}} = \frac{\delta\Gamma\big[g_{\mu\nu}(\rho,\, x^\lambda)\big|_{\rho\to\infty} = \gamma_{\mu\nu}^{(0)}\big]}{\delta\gamma_{(0)}^{\mu_1\nu_1}(x_1^\lambda)\dots\delta\gamma_{(0)}^{\mu_n\nu_n}(x_n^\lambda)} \tag{8.15}$$

on the gravity side. Since every CFT has the stress tensor as part of its operators, we focus here on such correlation functions. For other types of correlation functions and further checks of AdS/CFT see, e.g. [554,555].

The 1-point function yields the (holographically renormalized) Brown–York stress tensor discussed above. The 2-point functions can be found in [556] and the 3-point functions were calculated in [557]. They match with corresponding CFT results, thereby providing evidence for the correctness of AdS/CFT. Calculating arbitrary $n$-point functions by repeatedly varying the action is cumbersome. In $\text{AdS}_3/\text{CFT}_2$ the proof of the dictionary (8.15) works recursively [558], by proving the Belavin–Polyakov–Zamolodchiov identity [559]

$$\langle T_{zz}(z_1)T_{zz}(z_2)\dots T_{zz}(z_n)\rangle_{\text{CFT}}^{\text{connected}} = \sum_{i=2}^{n}\left(\frac{2}{z_{1i}^2}+\frac{1}{z_{1i}}\partial_{z_i}\right)\langle T_{zz}(z_2)\dots T_{zz}(z_n)\rangle \tag{8.16}$$

through complete induction, where we used conformal coordinates $g_{zz} = g_{\bar z\bar z} = 0$, $g_{z\bar z} = 1$, the definition $z_{nm} := z_n - z_m$ and displayed only the holomorphic sector (the anti-holomorphic one is analogous). Starting point of this proof is the gravitational 2-point function

$$\langle T_{zz}(z_1)T_{zz}(z_2)\rangle_{\text{CFT}}^{\text{connected}} = \frac{3\ell}{4G_{\text{N}}\, z_{12}^4} \tag{8.17}$$

which coincides with the 2-point function of the (holomorphic component of the) stress tensor in a $\text{CFT}_2$ with central charge $c = 3\ell/(2G_{\text{N}})$ [483]. The first step in the recursion relation then yields the 3-point function

$$\langle T_{zz}(z_1)T_{zz}(z_2)T_{zz}(z_3)\rangle_{\text{CFT}}^{\text{connected}} = \frac{3\ell}{2G_{\text{N}}\, z_{12}^2 z_{23}^2 z_{13}^2} \tag{8.18}$$

which coincides again with the corresponding $\text{CFT}_2$ result. Further iterations yield all higher $n$-point functions coinciding with corresponding $\text{CFT}_2$ results, see [558] for a proof in the CS formulation and for explicit results for correlation functions up to $n = 5$.

## 8.2 Holography and Quantum Information

Feynman's slogan 'everything is particle' has dominated a lot of the early attempts to address quantum aspects of gravity, including the Hawking effect and black hole evaporation. Eventually, the community realized that it is useful to apply in addition Wheeler's slogan 'everything is information'. Indeed, after the turn of the millennium, numerous concepts and techniques from quantum information have entered the analyses of black holes, particularly in a holographic context.

An early milestone in these developments was the Ryu–Takayanagi (RT) formula for holographic entanglement entropy [560]. Entanglement is a key concept in quantum mechanics and entanglement entropy is a particular entanglement measure (see [561] for an overview of entanglement measures and [562] for a review of entanglement entropy). For a bipartite quantum system with a direct product Hilbert space $\mathcal{H} = \mathcal{H}_A \otimes \mathcal{H}_B$, we can define the reduced density matrix

$$\rho_A = \mathrm{Tr}_B\, \rho \tag{8.19}$$

where $\rho$ is the density matrix of some general state (normalized such that $\mathrm{Tr}\rho = 1$) and $\mathrm{Tr}_B$ indicates that we trace out all degrees of freedom associated with the Hilbert space $\mathcal{H}_B$. Entanglement entropy is defined as the von Neumann entropy of the reduced density matrix.

$$S_A = -\mathrm{Tr}\big(\rho_A \ln \rho_A\big). \tag{8.20}$$

If there is a matrix representation of the reduced density matrix $\rho_A$ with eigenvalues $\lambda_i$ then entanglement entropy is given as a sum/integral $S_A = -\sum_i \lambda_i \ln \lambda_i$. This means that eigenvalues that are either 1 or 0 do not contribute to entanglement entropy. Entanglement entropy inherits several key properties from von Neumann entropy, including unitarity $S_A(U^\dagger \rho U) = S_A(\rho)$, semi-positivity $S_A \geq 0$, boundedness $S_A \leq \ln D_A$ (with $D_A$ being the dimension of $\mathcal{H}_A$) and concavity $S_A(\sum_i \mu_i \rho_i) \geq \sum_i \rho_i S_A(\rho_i)$ (for all sets of non-negative $\mu_i$ normalized so that $\sum_i \mu_i = 1$). Moreover, whenever $\rho$ is a pure state we have the identity $\rho_A = \rho_B$. From the definition (and from Exercise 8.6) it is evident that entanglement entropy counts the number of entangled bits between the subsystems $A$ and $B$.

Since holography tells us that every observable on the CFT side should have a corresponding observable on the gravity side there must be some gravitational way to calculate entanglement entropy. The RT proposal

$$S_A = \frac{\text{area}}{4G_{\mathrm{N}}} \tag{8.21}$$

resembles the BH formula for thermal entropy (5.43), but the meaning of 'area' is different. Here it is the area of an extremal surface attached to the asymptotic AdS boundary whose boundary is homologous to the boundary of the entangling region in the CFT, see Fig. 8.1. The original proposal was improved by Veronica Hubeny, Mukund Rangamani and Tadashi Takayanagi [563] so that it works also for arbitrary time-dependent spacetimes. Conceptually, their generalization is similar to Bousso's

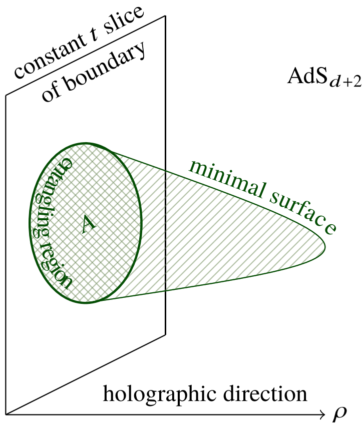


**Fig. 8.1** RT surface is a $d$-dimensional minimal surface attached to some entangling region $A$ on a constant time slice of the conformal boundary of asymptotically AdS$_{d+2}$ with holographic direction $\rho$

covariant generalization (6.61) of the Bekenstein bound and also involves light sheets (with vanishing expansion). Besides its conceptual richness, the RT formula (8.21) provides a useful tool to calculate entanglement entropy in holographic QFTs, which on the field theory side is notoriously hard.

Even without calculating it, the simple fact that entanglement entropy is given in terms of extremal/minimal surfaces allows showing in a simple picture a property called strong subadditivity [564] that otherwise requires a more elaborate proof [565].

$$S_{A\cup B} + S_{B\cup C} \geq S_{A\cup B\cup C} + S_B \qquad S_{A\cup B} + S_{B\cup C} \geq S_A + S_C. \tag{8.22}$$

The left-hand sides contain the sum of entanglement entropies obtained when taking the union of the entangling regions $A$ and $B$, and $B$ and $C$. The right-hand side of the first inequality contains the sum of entanglement entropy of region $B$ and of the union of all three regions. The right-hand side of the second inequality contains the sum of entanglement entropy of regions $A$ and $C$. Strong subadditivity is the statement that the left-hand sides are not smaller than the right-hand sides. The graphic proof is contained in Fig. 8.2 (for simplicity the graphic shows a situation where the field theory is 2-dimensional so that equal time-slices are 1-dimensional and minimal surfaces are geodesics, but the same proof works in any higher dimension).

The proof works as follows (we discuss it only for the first line in the figure, as the second line is analogous). In the first graphic, the green and red curves symbolize holographic entanglement entropy of $S_{A\cup B}$ and $S_{B\cup C}$, respectively. The graph after the equality is a trivial identity where only the color of the curves has changed for illustration. The interpretation is now that the red curve starts and ends at the endpoints of region $B$, while the green curve starts at the outermost endpoint of $A$ and ends at the outermost endpoint of $C$. The last figure plots holographic entanglement entropy for region $B$ (red curve) and the union of regions $A$, $B$, and $C$ (green curve). The inequality sign comes about because the curves in the middle figure by definition are longer than the geodesics in the right figure. This concludes the holographic proof of strong subadditivity.

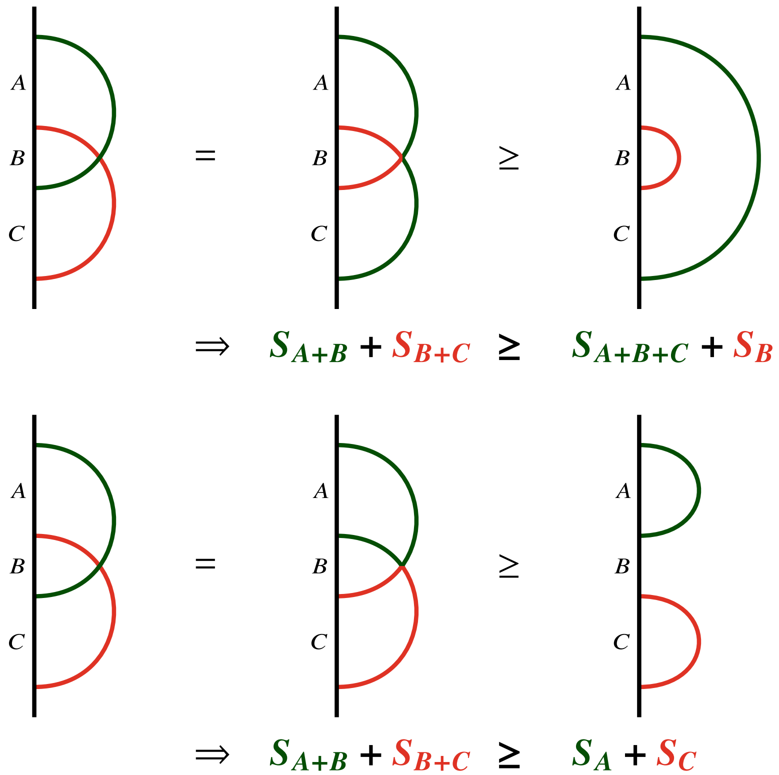


**Fig. 8.2** Graphic proofs of strong subadditivity inequalities using holographic entanglement entropy

To give the simplest example for holographic entanglement entropy: in $AdS_3/CFT_2$ a simply connected entangling region is just a spatial interval of size $L$ bounded by two points, and the extremal surface is a geodesic connecting these two points. The length of this geodesic yields entanglement entropy according to the RT formula (8.21). For a planar $CFT_2$ at zero temperature this prescription yields (see Exercise 8.7)

$$S_A = \frac{\ell}{2G_{\mathrm{N}}} \ln \frac{L}{a} = \frac{c}{3} \ln \frac{L}{a} \,. \tag{8.23}$$

Here we used the Brown–Henneaux result for the central charge $c = \frac{3\ell}{2G_{\mathrm{N}}}$; moreover, we had to introduce a cutoff $a$ to evaluate the length of the geodesic, since the asymptotic AdS behavior trivially renders their lengths infinite unless a cutoff surface is introduced. This divergence has a physical origin on the CFT side as well: there is a UV divergence in entanglement entropy since there are infinitely many pairs that can be entangled if we zoom into smaller and smaller distances; in lattice models, the typical cutoff scale is the lattice spacing. The calculation on the CFT side uses the replica method, which replaces $\rho_A \ln \rho_A$ by $\rho_A^n$ with some integer $n$, the trace of which can be calculated. The final result is analytically continued to real $n$, and finally the limit $n \to 1^+$ is taken; see [566] for a review of the calculation of entanglement entropy on the CFT side.

Staying in three dimensions, we can introduce 'velocity' and 'acceleration' of entanglement entropy, both of which have nice interpretations. Let us start with the former. Consider entanglement entropy for a Poincaré invariant state (e.g. the vacuum) for an entangling region of length $L$. Then define the velocity-like expression

$$c(L) := 3L\,\frac{\mathrm{d}S_A(L)}{\mathrm{d}L}\,. \tag{8.24}$$

This is precisely the Casini–Huerta $c$-function [567].[1] For $L \to 0$ the function $c(L \to 0) \to \frac{3\ell}{2G_{\mathrm{N}}}$ coincides with the UV central charge, and for $L \to \infty$ it coincides with the IR central charge $c(L \to \infty) \to c_{\mathrm{IR}} \leq \frac{3\ell}{2G_{\mathrm{N}}}$. In between it is a monotonically decreasing positive function.

The 'acceleration' of entanglement entropy can be defined in a more Lorentz covariant way by considering null deformations of one of the endpoints of the entangling region and then taking second derivatives with respect to the deformation parameter.

$$\frac{\mathrm{d}^2 S_A(\lambda)}{\mathrm{d}\lambda^2}\Big|_{\lambda=0} + \frac{6}{c}\left(\frac{\mathrm{d}S_A(\lambda)}{\mathrm{d}\lambda}\Big|_{\lambda=0}\right)^2 \tag{8.25}$$

The reason for the second term is the transformation behavior of entanglement entropy under diffeomorphisms,

$$\delta_\varepsilon S_A = \varepsilon S_A' - \frac{c}{12}\,\varepsilon'\,. \tag{8.26}$$

The combination appearing in (8.25) transforms with an infinitesimal Schwarzian derivative. See Exercise 8.9 and [569,570] for more details on this expression.

Inspired by the quantum focusing conjecture [571] the combination (8.25) was shown to appear in a local quantum inequality, the quantum null energy condition (QNEC).[2]

$$2\pi\,\langle T_{kk}\rangle \geq \frac{\mathrm{d}^2 S_A(\lambda)}{\mathrm{d}\lambda^2}\Big|_{\lambda=0} + \frac{6}{c}\left(\frac{\mathrm{d}S_A(\lambda)}{\mathrm{d}\lambda}\Big|_{\lambda=0}\right)^2. \tag{8.27}$$

Here $\langle T_{kk}\rangle$ is the expectation value of the double projection of the $\mathrm{CFT}_2$ stress tensor into the same null direction $k$ as used in the null deformations of the entangling region on the right-hand side of (8.27). QNEC is the only known energy condition that is local for the stress tensor and valid when quantum effects are taken into

[1] The proof that this is a $c$-function is instructive and short, so the reader is strongly encouraged to consult Sect. 3 of [568] to verify it. The only input is Lorentz invariance, unitarity, and the use of strong subadditivity.

[2] In higher dimensions the second term on the right-hand side is absent, but the first term looks essentially the same, up to a geometric factor coming from the induced metric at the boundary of the entangling region. For details see [572].

account. Its violation is argued to imply a violation of unitarity. Proofs of QNEC under increasingly relaxed assumptions are contained in these references [572–575].

We conclude this section by the cautionary remark that the RT formula (8.21) requires the validity of the large $N$ limit. At finite values of $N$, there are semiclassical corrections from bulk entanglement [576]. A quantum proposal for holographic entanglement entropy beyond the 1-loop approximation involves the concept of quantum extremal surfaces [577].

## 8.3 AdS Black Holes and Holography

As in the flat space case, black holes on an AdS background can be a result of gravitational collapse (one-sided black holes) or may be eternal (two-sided black holes), as depicted in Fig. 8.3. For both of these cases, it takes finite coordinate time for the outgoing null rays outside black hole to reach the AdS (causal) boundary. In either of the cases, we may have large or small AdS black holes. For large black holes, whose horizon radius is comparable to the AdS radius, the Hawking radiation from a black hole in the AdS background can reach thermal equilibrium. That is, a large AdS black hole is like a black hole in a box with fixed temperature at the boundary. A small black hole, whose horizon radius is much smaller than the AdS radius, essentially behave like a black hole in a flat background, as expected intuitively.

In this section, we study some aspects of AdS black holes in view of the Ad/CFT duality.

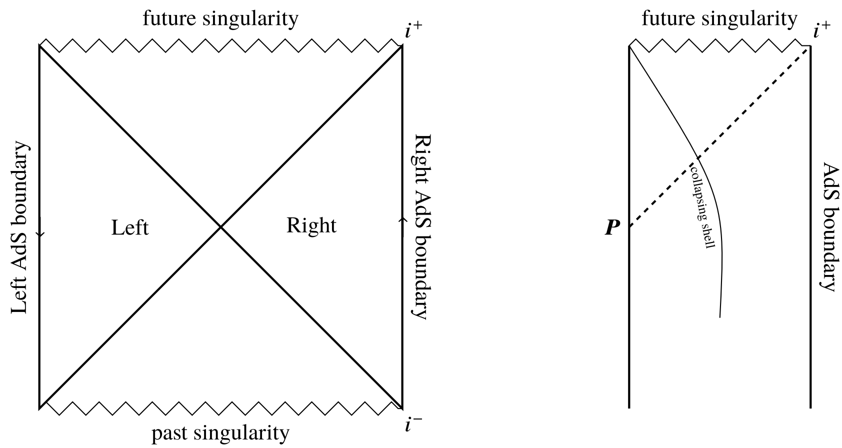


**Fig. 8.3** Penrose diagrams for two-sided eternal AdS black hole (left) and the one-sided case (right). One-sided case is a result of gravitational collapse and has neither a past curvature singularity nor a bifurcate horizon. The eternal AdS has two causally disconnected boundaries and the arrows on each boundary show the flow of Killing time

### 8.3.1 Black Holes as Thermal States

In Chap. 5 we summarized the classical indications that black holes were thermal states, which was then supported by semiclassical calculations in Chap. 6. In particular, we saw schematically how Gibbons and Hawking derived the free energy from the on-shell action, but a delicate issue that we were slightly vague about is the determination of the boundary terms, which are crucial for obtaining the correct (finite) free energy. Fortunately, we just discussed in the previous section how this issue is resolved in an asymptotically AdS context. Thus, we specify now the Gibbons–Hawking derivation to black holes in AdS.

For simplicity, we consider here BTZ black holes introduced in the 3-dimensional gravity discussion in Chap. 7, but we stress that the essence of the calculation does not change in higher dimensions (for the 2-dimensional case see Exercise 8.11).

In general, our task is to evaluate the holographically renormalized action (8.13) on-shell for all classical saddle points compatible with our specified values for inverse temperature $\beta$ and the angular velocity $\Omega$ (which plays the role of a chemical potential $\mu$). However, currently, we are interested in a specific saddle point, namely the BTZ black hole (7.3). We shall come back to competing saddle points in the next subsection when discussing the Hawking–Page phase transition.

Inserting (7.3) into (8.13) and using the definitions $\Omega = r_-/(\ell r_+)$, $\beta = 1/T_{\text{BTZ}}$ with (7.5) yields the holographically renormalized on-shell action

$$\Gamma_{\text{BTZ}}[\beta,\ \Omega] = -\frac{\pi^2\ell^2}{2G_{\text{N}}\beta(1-\Omega^2\ell^2)}\,. \tag{8.28}$$

This implies that the BTZ free energy is given by

$$F_{\text{BTZ}}[T,\ \Omega] = -\frac{\pi^2\ell^2T^2}{2G_{\text{N}}(1-\Omega^2\ell^2)}\,. \tag{8.29}$$

The free energy is negative and its magnitude grows quadratically with the temperature. From this result, one may expect that at high temperatures the dominant saddle point will be the black hole. Moreover, differentiating the free energy with respect to its variables $T$ and $\Omega$ yields all desired thermodynamical quantities. For instance, the expression

$$S_{\text{BTZ}} = -\frac{\partial F_{\text{BTZ}}[T,\ \Omega]}{\partial T} = -\frac{\pi^2\ell^2T}{G_{\text{N}}(1-\Omega^2\ell^2)} = \frac{2\pi r_+}{4G_{\text{N}}} \tag{8.30}$$

recovers the BH result (5.43).

AdS/CFT gives a new twist to this story.

$$Z_{\text{CFT}}[\beta,\ \mu] = \langle 1\rangle_{\text{CFT}} = Z_{\text{gravity}}[\beta,\ \mu] \approx \sum e^{-\Gamma_{\text{EOM}}[\beta,\,\mu]}. \tag{8.31}$$

The first equality is just the definition of the CFT partition function. The quantities $\beta$ and $\mu$, respectively, denote inverse temperature and possible additional chemical potentials. The second equality is the restriction of the master formula (8.1) to 0-point functions. Finally, the last expression is obtained after imposing the supergravity approximation, where instead of superstring theory the holographically renormalized (super)gravity on-shell action is used. The sum extends over all classical saddle points consistent with the choices of inverse temperature and chemical potentials.

This means that in the supergravity approximation black holes in AdS are dual to thermal states in a (large-$N$, strongly coupled) CFT.

### 8.3.2 Hawking–Page Phase Transition

Let us come back to saddle points that could compete with the black hole saddle. We know for sure that at least one such saddle exists, namely thermal AdS. By this, we mean global (Euclidean) AdS, with periodic identifications such that the boundary conditions are met that fix the temperature and the angular velocity.

Sticking with our 3-dimensional example, we insert the global $\text{AdS}_3$ metric into the holographically renormalized on-shell action (8.13), yielding

$$\Gamma_{\text{AdS}}[\beta,\ \Omega] = -\frac{\beta}{8G_{\text{N}}\,\ell^2}\,. \tag{8.32}$$

This implies that the free energy of thermal $\text{AdS}_3$ is a negative constant.

$$F_{\text{AdS}}[\beta,\ \Omega] = -\frac{1}{8G_{\text{N}}\,\ell^2}. \tag{8.33}$$

Comparing the free energies (8.33) and (8.29) we conclude that for small temperatures the dominant saddle is thermal $\text{AdS}_3$, while for large temperatures the dominant saddle is BTZ. The transition from one regime to the other is known as Hawking–Page phase transition.

The discussion above generalizes to arbitrary dimensions, so the Hawking–Page phase transition works universally for any spacetime dimension $D > 2$. See [578] for the original paper. Specifically, on the one hand, one has the thermal gas of massless particles on AdS at temperature $T$ which is conveniently described by a 'thermal AdS' space, a Euclidean AdS space with periodic time coordinate, with period $2\pi/T$. On the other hand, one can have large AdS black holes at a given temperature. There is a first-order phase transition (as our 3d analysis shows) between the thermal AdS and AdS black hole, and thermal AdS at the critical temperature $T_c = \frac{D+2}{2\pi\ell}$, such that for $T > T_c$ system prefers AdS black hole phase and for $T < T_c$ the thermal AdS.

**> Dual field theory interpretation of the Hawking–Page phase transition**

The low-temperature phase is dominated by a state of very low entropy (the field theory dual to thermal AdS), while the high-temperature phase is dominated by a highly entropic state (the field theory dual to a black hole in AdS). In a seminal paper [579], the field theory side of the story was interpreted as confinement/deconfinement phase transition: at low temperatures, the 'gluons' are confined and thus the entropy is relatively low since the state has to be color-neutral; at high temperature the gluons are deconfined, so the entropy scales like $N^2$, where $N$ is the (large) number of colors. According to the AdS/CFT dictionary $N^2$ corresponds to $1/G_{\rm N}$, which gives the correct BH scaling (8.30).

We close this section with a remark on the dual field theory description of gravitational collapse on an AdS background. The collapse, at least for large AdS black holes may be viewed as a thermalization process on the dual field theory side. See Sect. 8.8 for more references and comments.

### 8.3.3 Eternal Black Holes

As mentioned earlier and depicted in Fig. 8.3, we can have one-sided or two-sided (eternal) black holes. The eternal AdS black hole has two causally disconnected boundaries and the proposal is that the AdS black hole is dual to two copies of the CFT that are in a thermally entangled state, the thermofield double state [580]. This 'doubling' feature is very familiar in the context of thermal field theories and goes under the name of the thermofield double formalism [581]. Our discussions here are mainly based on [580]; further discussions may be found in [131].

**> Thermofield double formalism, quick review**

In a thermal field theory with Hamiltonian $\mathbf{H}$ and at inverse temperature $\beta$, a generic $n$-point function is computed as

$$C_n := \mathrm{Tr}\left(\boldsymbol{\rho}_\beta\, \mathcal{O}_1 \cdots \mathcal{O}_n\right), \qquad \boldsymbol{\rho}_\beta := \frac{1}{Z(\beta)} e^{-\beta \mathbf{H}} \tag{8.34}$$

where $Z(\beta) = \mathrm{Tr} e^{-\beta\mathbf{H}}$ is the partition function and the trace is over the Hilbert space $\mathcal{H}$ of the theory. The above may be written as the expectation value over a thermofield double state $|\mathrm{TFD}\rangle$,

$$C_n := \langle \mathrm{TFD}|\mathcal{O}_1 \cdots \mathcal{O}_n|\mathrm{TFD}\rangle = \mathrm{Tr}_{\mathcal{H}_D}\left(\boldsymbol{\rho}_{\rm TFD}\, \mathcal{O}_1 \cdots \mathcal{O}_n\right), \tag{8.35}$$

where $|\mathrm{TFD}\rangle$ is a specific state in the doubled Hilbert space $\mathcal{H}_{\rm D} = \mathcal{H}_{\rm L} \otimes \mathcal{H}_{\rm R}$, with $\mathcal{H}_{\rm L} = \mathcal{H}_{\rm R} = \mathcal{H}$; the operators $\mathcal{O}_i$ are defined on $\mathcal{H}_{\rm L}$. Equation (8.35) implies

$$\boldsymbol{\rho}_{\rm TFD} = |\mathrm{TFD}\rangle\langle\mathrm{TFD}|, \qquad \mathrm{Tr}_{\rm R}\, \boldsymbol{\rho}_{\rm TFD} = \boldsymbol{\rho}_\beta. \tag{8.36}$$

Therefore, the thermally mixed density matrix on $\mathcal{H}_{\rm L}$, $\boldsymbol{\rho}_\beta$, is 'purified' in the doubled Hilbert space $\mathcal{H}_{\rm D}$. One can define a Hamiltonian $\mathbf{H}_{\rm D}$ over the doubled Hilbert space $\mathcal{H}_{\rm D}$. A convenient choice is

$$\mathbf{H}_{\text{tot}} = \mathbf{H} \otimes \mathbf{1} - \mathbf{1} \otimes \mathbf{H} \,. \tag{8.37}$$

The choice of the $\mathbf{H}_{\text{tot}}$, and in particular the minus sign there, is appropriate in the AdS/CFT setting recalling that the arrows of time on the left and right boundaries are in opposite directions, cf. Fig. 8.3. See Exercises 8.13, 8.12, and 8.14 for a quick derivation and more analysis on the thermofield double formalism.

---

To derive the proposal that the state in the CFT$_d$ dual to the eternal AdS$_{d+1}$ black hole is the thermofield double state $|\text{TFD}\rangle$ [580], we should use the statement of the AdS/CFT (8.1) in the form

$$Z_{\text{CFT}}(\Sigma) = Z_{\text{gravity}}[\partial M = \Sigma] \,, \tag{8.38}$$

where $\Sigma = [0,\ \beta/2] \times S^{d-1}$, as depicted in Exercise 8.12, and $Z_{\text{gravity}}[\partial M = \Sigma]$ is the path integral for the Euclidean gravity over half of the Euclidean black hole, in which Euclidean time is restricted to the interval $[0, \beta/2]$. That is, $M$ is a half disk times $S^{d-1}$. The Euclidean region $M$ may be completed into a Lorentzian spacetime as depicted in Fig. 8.4. This setup allows preparing a thermofield double state for the Lorentzian part.

The thermofield double permits computing *two-sided correlators*, i.e. correlators of operators inserted both in the left and right boundaries, e.g., $\langle \text{TFD}|\mathcal{O}_1^{\text{L}}\mathcal{O}_2^{\text{R}}|\text{TFD}\rangle$. Unlike the correlators of operators only in left or right boundaries, the two-sided correlators do not have a simple thermal interpretation. The two-sided correlators are non-zero because of the non-zero entanglement in the thermofield double state. In the gravity picture, such mixed two-point functions in the leading $1/N$ order are associated with spacelike geodesics stretched between the two insertion points at the left and right boundaries. Such geodesics can probe behind the horizon. In an interesting work, Maldacena and Susskind [582] made the ER=EPR proposal:

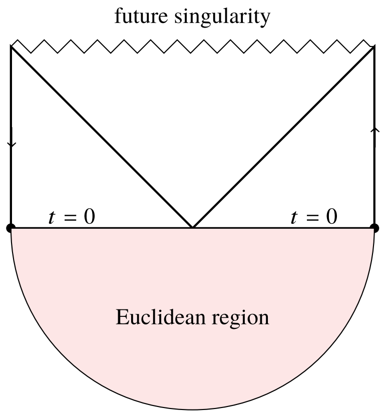


**Fig. 8.4** Euclidean half-AdS, the half-disk (red region) completed by the Lorentzian two-sided AdS black hole in $t > 0$. The Euclidean part prepares a thermofield double state for the Lorentizan

the gravity dual of the two-sided Einstein–Podolsky–Rosen-type correlators is the Einstein–Rosen bridge which connects the left and right parts of the eternal AdS black hole Penrose diagram 8.3. In suggestive words, the Einstein–Rosen bridges are equivalent to entanglement.

## 8.4 Asymptotic Symmetries

Killing vectors generate isometries of a given metric, in the sense that the Lie variation along a Killing vector vanishes when acting on the metric (see Sect. 2.2). Killing vectors lead to conserved charges, defined by Komar integrals (see Sect. 5.1). The main purpose of this subsection is to generalize the notion of Killing vectors to asymptotic Killing vectors where not the metric, but only its asymptotic structure, is preserved. Therefore, when acting with a Lie derivative along an asymptotic Killing vector on a metric that obeys some specified set of boundary conditions, the result is not necessarily zero but rather the metric can vary up to terms allowed by these boundary conditions. While there are always finitely many Killing vectors (as long as the dimension is finite), there can be infinitely many asymptotic Killing vectors, which means that the asymptotic symmetry algebras can be considerably richer than the isometry algebras.

**Asymptotic Killing vectors**

The defining equation for asymptotic Killing vectors

$$\mathcal{L}_\xi g_{\mu\nu} = \mathcal{O}\big(\delta g_{\mu\nu}\big) \tag{8.39}$$

has on the left-hand side the Lie derivative along the asymptotic Killing vector $\xi$ of a metric $g$ compatible with some given set of boundary conditions, and on the right-hand side some metric fluctuation/variation allowed by these boundary conditions.

Once the asymptotic Killing vectors are determined it is also of interest to check their Lie brackets, which yield the asymptotic symmetry algebra.

In many practical applications, one introduces a (partial) gauge fixing and then requires additionally that the fluctuations $\delta g$ also preserve the gauge (or diffeomorphism) conditions, for instance, fixing the Gaussian normal coordinates.

**Example: asymptotic symmetries and asymptotic flatness in two dimensions**

Take the 2-dimensional class of metrics defined near the asymptotic boundary at $r \to \infty$ by

$$g_{\mu\nu}\,\mathrm{d}x^\mu\,\mathrm{d}x^\nu = \sum_{n=-1}^{\infty} g_n(u) r^{-n}\,\mathrm{d}u^2 - 2\,\mathrm{d}u\,\mathrm{d}r \tag{8.40}$$

where all coefficients $g_n$ are allowed to vary so that the allowed metric variations are given by

$$\delta g_{uu} = \mathcal{O}(r) + \mathcal{O}(1) + \mathcal{O}(1/r) + \cdots \qquad \delta g_{ur} = \delta g_{rr} = 0\,. \tag{8.41}$$

The allowed fluctuations (8.41) preserve EF gauge to all orders in the radial coordinate $r$ (a condition which could be relaxed without changing the physics) and lead to asymptotically flat metrics, in the sense that the Ricci scalar tends to zero as $r$ tends to infinity (at least like $1/r^3$). Let us now construct the associated asymptotic Killing vectors. The $rr$-component of (8.39) yields

$$\xi^\mu\partial_\mu g_{rr} + 2g_{r\mu}\partial_r\xi^\mu = -2\partial_r\xi^u = 0 \tag{8.42}$$

from which we conclude that the $u$-component of $\xi$ is $r$-independent. The $ru$-component of (8.39) is more complicated,

$$\xi^\mu\partial_\mu g_{ru} + g_{r\mu}\partial_u\xi^\mu + g_{u\mu}\partial_r\xi^\mu = -\partial_u\xi^u - \partial_r\xi^r + g_{uu}\partial_r\xi^u = 0 \tag{8.43}$$

and together with the previous condition (8.42) allows to deduce the following results for the asymptotic Killing vectors,

$$\xi = \epsilon(u)\,\partial_u + \big(-\epsilon'(u)\,r + \eta(u)\big)\,\partial_r \tag{8.44}$$

where prime denotes derivative with respect to $u$. The $uu$-component of (8.39) does not lead to any new constraint on the asymptotic Killing vectors,

$$\xi^\mu\partial_\mu g_{uu} + 2g_{u\mu}\partial_u\xi^\mu = \mathcal{O}(r) + \mathcal{O}(1) + \mathcal{O}(1/r) + \cdots\,. \tag{8.45}$$

Since the asymptotic Killing vectors (8.44) of the metric (8.40) are parametrized by two arbitrary functions, $\epsilon(u)$ and $\eta(u)$, we have infinitely many asymptotic Killing vectors for this example. The Lie-bracket algebra generated by the asymptotic Killing vectors

$$\big[\xi(\epsilon_1,\eta_1),\,\xi(\epsilon_2,\eta_2)\big]_{\text{Lie}} = \xi\big(\epsilon_1\epsilon_2' - \epsilon_2\epsilon_1',\,(\epsilon_1\eta_2 - \epsilon_2\eta_1)'\big) \tag{8.46}$$

generates the asymptotic symmetries for our example.

Asymptotic Killing vectors generate asymptotic symmetries that can lead to interesting symmetry algebras. We would like to know how these symmetries act on the phase space. The canonical realization of the asymptotic symmetries is through the Poisson/Dirac/Peierls brackets of the boundary (surface) charges $Q[\epsilon]$ introduced in Chap. 5 and discussed in more detail in Appendix G.

**> Canonical realization of asymptotic symmetries**

Given a set of boundary charges $Q[\epsilon]$, where $\epsilon$ generates all boundary condition preserving transformations, which in a gravity context means all asymptotic Killing vectors, the canonical realization of the asymptotic symmetries is given by their Poisson/Dirac/Peierls brackets

$$\{Q[\epsilon_1],\ Q[\epsilon_2]\} = Q[\epsilon_1 \circ \epsilon_2] + Z[\epsilon_1,\ \epsilon_2]\,. \tag{8.47}$$

The right-hand side of (8.47) contains the same structure functions as the Lie-bracket algebra of asymptotic Killing vectors and can additionally contain a central extension $Z[\epsilon_1,\ \epsilon_2]$. The left-hand side of (8.47) can be evaluated conveniently using

$$\delta_{\epsilon_1} Q[\epsilon_2] = \{Q[\epsilon_1],\ Q[\epsilon_2]\}\,. \tag{8.48}$$

Following canonical quantization, we replace Poisson brackets by commutators,

$$i\{\ ,\ \} \to [\ ,\ ]\,. \tag{8.49}$$

We have already discussed an important example, namely the Brown–Henneaux analysis of asymptotically $AdS_3$ solutions, in Sect. 7.2.3. The main conclusion of that analysis was that the canonical realization of the asymptotically $AdS_3$ symmetries leads to two copies of the Virasoro algebra (7.22), which is equivalent to the symmetries governing a $CFT_2$. Since this was, at least in retrospect, an important precursor of AdS/CFT one can exploit similar analyses to conjecture novel holographic correspondences beyond AdS/CFT, by analyzing first the asymptotic Killing vectors, the asymptotic symmetries they generate, and the canonical realization of these symmetries. Another example is Kerr/CFT which we review in Sect. 8.7.

If one finds some QFT in one lower dimension that is defined by the same set of symmetries, one has a candidate for a field theory dual to this gravity theory. This strategy may allow addressing the question of how general holography is and whether/how it works beyond AdS/CFT. Moreover, this approach may be useful in studying and identifying the black hole microstate problem, as discussed in Sect. 8.5.

## 8.5 Soft Hair and Near Horizon Symmetries

The analysis of asymptotic symmetries can be extended to cases where we have a boundary, a physical or hypothetical one. An example of such cases is to view the horizon of a black hole as a boundary for the observers outside the black hole. We discuss here generic properties of non-extremal horizons, assumed to be in equilibrium with a thermal bath. The physical properties of the thermal bath are modeled by the way we impose boundary conditions. Our working definition of a non-extremal horizon is that the line element can be brought into a Rindler-like form,

$$\mathrm{d}s^2 = -\kappa^2\,\rho^2\,\mathrm{d}t^2 + \mathrm{d}\rho^2 + \Omega_{ab}\,\mathrm{d}x^a\,\mathrm{d}x^b + \cdots \tag{8.50}$$

where $\kappa$ is surface gravity (with $\kappa \neq 0$ to guarantee non-extremality), $t$ is time, and $\rho$ is some radial coordinate that vanishes at the horizon. We assume that the horizon is free from singularities and the metric permits a Taylor expansion in $\rho$ in the near horizon region, specifically the 'horizon metric' $\Omega_{ab}$ (where $a = 1, 2, \ldots (D-2)$), is smooth with a non-vanishing determinant, $\Omega = \det \Omega_{ab} \neq 0$. The ellipsis denotes higher-order terms or rotation/boost terms. Consistency with our smoothness assumptions determines the near horizon behavior of the metric, which in a co-rotating frame is given by

$$g_{tt} = -\kappa^2\rho^2 + \mathcal{O}(\rho^3) \qquad\qquad g_{\rho\rho} = 1 + \mathcal{O}(\rho) \tag{8.51}$$

$$g_{t\rho} = \mathcal{O}(\rho^2) \qquad\qquad g_{\rho a} = f_{\rho a}\,\rho + \mathcal{O}(\rho^2) \tag{8.52}$$

$$g_{ta} = f_{ta}\,\rho^2 + \mathcal{O}(\rho^3) \qquad\qquad g_{ab} = \Omega_{ab} + \mathcal{O}(\rho)\,. \tag{8.53}$$

All coefficients above, $\kappa$, $f_{ta}$, $f_{\rho a}$, $\Omega_{ab}$ can depend on time $t$ and the transverse coordinates $x^a$, but not on the radius $\rho$.

Applying the definition of asymptotic Killing vectors $\xi$ defined in (8.39) to the class of metrics above yields

$$\xi^t = \frac{\epsilon}{\kappa} + \mathcal{O}(\rho) \qquad\qquad \xi^\rho = \mathcal{O}(\rho^2) \qquad\qquad \xi^a = \epsilon^a + \mathcal{O}(\rho^2) \tag{8.54}$$

where $\epsilon^a$ depends on $x^a$ and $\epsilon$ depends additionally on $t$ subject to the condition $\partial_t\epsilon + \epsilon^a\partial_a\kappa = \delta\kappa$. The state-dependent functions

$$\mathcal{P} = \frac{\sqrt{\Omega}}{8\pi G_{\mathrm{N}}} \qquad\qquad \mathcal{J}_a = \frac{\sqrt{\Omega}}{16\pi\kappa G_{\mathrm{N}}}\Big(\partial_t f_{\rho a} - 2 f_{ta}\Big) \tag{8.55}$$

transform as

$$\delta\mathcal{P} = \epsilon^a\partial_a\mathcal{P} + \mathcal{P}\partial_a\epsilon^a \tag{8.56a}$$

$$\delta\mathcal{J}_a = \mathcal{P}\partial_a\epsilon + \epsilon^c\partial_c\mathcal{J}_a + \mathcal{J}_c\partial_a\epsilon^c + \mathcal{J}_a\partial_c\epsilon^c\,. \tag{8.56b}$$

The near horizon symmetries are spanned by generators that can be calculated using the methods reviewed in Appendix G. Their variations

$$\delta Q[\epsilon,\,\epsilon^a] = \int \mathrm{d}^{D-2}x\,\big[\epsilon\,\delta\mathcal{P} + \epsilon^a\,\delta\mathcal{J}_a\big] \tag{8.57}$$

are non-trivial and finite.

If the boundary conditions are chosen such that $\epsilon$ and $\epsilon^a$ are state-independent, i.e. $\delta\epsilon = 0 = \delta\epsilon^a$ as in [583], then the charges (8.57) are easily integrated and the canonical realization of the near horizon symmetries is determined by the transformation behavior (8.55) by virtue of (8.48). In this case, $\mathcal{P}, \mathcal{J}_a$, which are respectively charges associates with symmetry generators $\epsilon, \epsilon^a$, are also referred to as 'supertranslations' (since they commute with each other) and 'superrotations' (since they generate diffeomorphisms of the $D-2$ dimensional constant $t$ slice at the horizon).

The parameters $\epsilon^a$ are vectors, while their corresponding charges are 1-form densities of weight one. It is natural to swap their role, so that the charges are 1-forms and their corresponding parameters become densities of weight one. These near horizon boundary conditions are obtained by a change of slicing (see Appendix G),

$$\epsilon^a = \frac{1}{\sqrt{\Omega}}\epsilon^a_{\mathrm{H}} \qquad \epsilon = \epsilon_{\mathrm{H}} - \epsilon^a_{\mathrm{H}}\mathcal{J}^{\mathrm{H}}_a \mathcal{P}^{-1} \tag{8.58}$$

with the 1-form $\mathcal{J}^{\mathrm{H}}_a := \mathcal{J}_a/\sqrt{\Omega}$. The change of slicing amounts to taking the new symmetry generators $\epsilon_{\mathrm{H}}, \epsilon^a_{\mathrm{H}}$ to be state-independent, $\delta\epsilon_{\mathrm{H}} = 0 = \delta\epsilon^a_{\mathrm{H}}$, which renders the previous symmetry generators state-dependent, $\delta\epsilon \neq 0$, $\delta\epsilon^a \neq 0$. In this new slicing, the charges are again integrable and the charge variation (8.57) integrates to

$$Q_{\mathrm{H}}[\epsilon_{\mathrm{H}}, \epsilon^a_{\mathrm{H}}] = \int \mathrm{d}^{D-2}x \left[\epsilon_{\mathrm{H}}\mathcal{P} + \epsilon^a_{\mathrm{H}}\mathcal{J}^{\mathrm{H}}_a\right]. \tag{8.59}$$

The near horizon symmetry transformations (8.56) together with (8.48) yield the Poisson bracket algebra

$$\left\{\mathcal{J}^{\mathrm{H}}_a(x)\,,\,\mathcal{P}(y)\right\} = \frac{1}{8\pi G_{\mathrm{N}}}\frac{\partial}{\partial x^a}\delta(x-y) \tag{8.60a}$$

$$\{\mathcal{P}(x)\,,\,\mathcal{P}(y)\} = 0 \tag{8.60b}$$

$$\left\{\mathcal{J}^{\mathrm{H}}_a(x)\,,\,\mathcal{J}^{\mathrm{H}}_b(y)\right\} = \frac{1}{8\pi G_{\mathrm{N}}\,\mathcal{P}(x)}F_{ba}(x)\,\delta(x-y) \tag{8.60c}$$

where $F_{ab} := \partial_a\mathcal{J}^{\mathrm{H}}_b - \partial_b\mathcal{J}^{\mathrm{H}}_a$.

In three dimensions $F_{ab}$ vanishes and the boundary conditions reduce to those in [584,585], while (8.60) reduces to two copies of $\hat{u}(1)$ current algebras or, equivalently, an infinite tower of Heisenberg algebras. More generally, in any dimension whenever $F_{ab} = 0$ the 1-form $\mathcal{J}^{\mathrm{H}}_a$ is locally exact, $\mathcal{J}^{\mathrm{H}}_a =: \partial_a Q$. Then, the only non-vanishing Poisson bracket (8.60), upon quantization (8.49) yields the Heisenberg algebra,

$$[Q(x),\,\mathcal{P}(y)] = \frac{i}{8\pi G_{\mathrm{N}}}\,\delta(x-y) \tag{8.61}$$

in which the factor $1/(4G_{\mathrm{N}})$ plays the role of Planck's constant $h$.

Both near horizon boundary conditions discussed above allow 'soft hair' excitations in the sense of [114] (see also Sect. 9.5.2). Algebraically, this statement is derived by observing that the Hamiltonian $H$, essentially given by the zero modes of the supertranslations, $\mathcal{P}_0 := \int \mathrm{d}^{D-2}x\,\mathcal{P}$, commutes with all other generators. This means that any near horizon descendant of any state has the same energy as the original state, which implies that all such excitations are soft, i.e. zero energy excitations. In terms of this zero mode, the BH entropy is given by [583,584]

$$S = 2\pi \mathcal{P}_0 \,. \tag{8.62}$$

Inserting the precise numerical factors into the near horizon Hamiltonian $H := Q_{\mathrm{H}}[\epsilon_{\mathrm{H}} = \kappa,\ \epsilon^a_{\mathrm{H}} = 0]$ yields the near horizon first law,

$$\mathrm{d}H = T\ \mathrm{d}S \qquad\qquad T := \frac{\kappa}{2\pi} \,. \tag{8.63}$$

## 8.6 Extremal Black Holes and Attractor Mechanism

Extremal black holes are a specific class of black holes where the inner and outer horizons coalesce. These black holes have vanishing surface gravity and do not have a bifurcate horizon. As we have seen in various examples so far, in the near horizon of extremal black holes we find an $\mathrm{AdS}_2$ space rather than the usual Rindler space. This has been proven for a large class of generic extreme black holes [586]. Moreover, there are uniqueness theorems for the so-called near-horizon extreme geometries in vacuum Einstein theory and Einstein–Maxwell theory in four and five dimensions [586–589]. Here, we give a sketch of the argument.

### 8.6.1 Symmetry Enhancement

Stationary black holes have a Killing vector that becomes null at the horizon. It is convenient to adopt the Gaussian Null Coordinates [248], where the Killing vector $\partial_v$ becomes null at the horizon, chosen to be the locus $r = 0$. In such a coordinate system, the metric

$$\mathrm{d}s^2 = r^2 F(r,x)\mathrm{d}v^2 + 2\mathrm{d}v\mathrm{d}r + 2rh_a(r,x)\mathrm{d}v\mathrm{d}x^a + \Omega_{ab}(r,x)\mathrm{d}x^a\mathrm{d}x^b, \tag{8.64}$$

depends on coordinates $x^a, a = 1, 2, \ldots, D-2$ that span the directions along the compact surface at spatial cross-section of the horizon whose metric is denoted by $\Omega_{ab}$. The functions $F(r,x), h_a(r,x), \Omega_{ab}(r,x)$ are smooth and (by assumption) admit a Taylor expansion around $r = 0$. We also assume that the horizon is non-singular and $\det \Omega_{ab} \neq 0$ at $r = 0$. Black hole extremality is manifest because the $\mathrm{d}v^2$-term starts with a factor of $r^2$. The near-horizon limit

$$r \to r\epsilon, \qquad v \to v/\epsilon, \qquad \epsilon \to 0 \tag{8.65}$$

yields the near-horizon metric

$$\mathrm{d}s^2 = r^2 F(x)\mathrm{d}v^2 + 2\mathrm{d}v\mathrm{d}r + 2rh_a(x)\mathrm{d}v\mathrm{d}x^a + \Omega_{ab}(x)\mathrm{d}x^a\mathrm{d}x^b \,, \tag{8.66}$$

where $F(x) = F(0, x), \cdots$. Besides the $\partial_v$ Killing vector, the metric above also enjoys a scaling symmetry generated by the Killing $r\partial_r - v\partial_v$. This symmetry has appeared as a result of taking the near-horizon limit.

So far, the argument was quite general and only used having an extremal Killing horizon. The next step is to impose the EOM to restrict the form of the remaining functions of $x$. While this depends on the details of the theory and its matter content, working through various examples one finds that generally, the solution enjoys having another Killing vector which together with the two discussed above, yields $O(2, 1)$ or $ISO(1, 1)$ isometries. That is, the geometry, in general, is a warped product of a maximally symmetric 2d space and the compact spatial codimension-2 space. Moreover, this 2d part is $\mathrm{AdS}_2$ if the matter fields satisfy the SEC [586], which encompasses most physical theories of interest. In this case, in a coordinate system that makes the $\mathrm{AdS}_2$ isometries manifest, the metric

$$\mathrm{d}s^2 = W(y)\left(-\rho^2\mathrm{d}\tau^2 + \frac{\mathrm{d}\rho^2}{\rho^2}\right) + \Gamma_{ab}(y)(\mathrm{d}y^a - k^a\rho\mathrm{d}\tau)(\mathrm{d}y^b - k^b\rho\mathrm{d}\tau) \quad (8.67)$$

depends on a constant vector $k^a$ on the $(D-2)$-dimensional compact surface spanned by $y^a$. The functions $W(y)$, $\Gamma_{ab}(y)$ are yet to be fixed through the EOM and depend on the matter content of the theory. For vacuum solutions, it has been shown that in $D = 4, 5$ dimensions there is a unique solution with $SL(2, \mathbb{R}) \times U(1)^{D-3}$ isometry [200,586,588] and that these solutions are coming from the near horizon limit of extremal Kerr ($D = 4$ case) and extremal MP or extremal double rotating ring (in $D = 5$ case). One can show that $SL(2, \mathbb{R})$ invariance implies axisymmetry ($U(1)$ or $U(1)^2$ isometry for $D = 4, 5$ cases) for the smooth Einstein vacuum solutions [590,591]. Similar uniqueness theorems have been proven for solutions of Einstein–Maxwell theory in four and five dimensions. Classification and uniqueness of near-horizon-extremal-geometries in more general theories and higher dimensions is still an open problem, see [587,590,592] for more reading on this topic. As in the black hole case, one may question the (in)stability of the near-horizon-extremal geometries. In general there seems to be a linearly growing mode among perturbations of these geometries [593]; see [594–598] for further studies and analysis.

### 8.6.2 Attractor Mechanism

In gravity theories which generically appear through compactifications of string theory or supergravity to lower dimensions, there are moduli, scalar fields which have no potential and enjoy a shift symmetry. In these theories, there are also some Maxwell fields. The Maxwell term in the action is generically accompanied by an exponential factor of these scalar fields. If we denote the scalars (usually also called dilatons) of the theory by $\Phi_a$, the action is such that the theory is invariant under $\Phi_a \to \Phi_a + \Phi_a^0$ together with appropriate scaling of the gauge fields, for arbitrary constant $\Phi_a^0$. Therefore, starting with any solution shifting the dilatons by an arbitrary constant produces another solution. If this solution is a black hole, then this means that the black hole is not uniquely specified by its mass, charges, and angular momenta and there is an infinite family of them which only differ by a constant shift in their value of the dilaton. The attractor mechanism is the realization that for extremal black holes, while the values of dilatons in the asymptotic region can be different, their values at the horizon only depend on the ADM charges of the black hole. Among other things, the attractor mechanism tells us that the constant value of the dilaton does not appear in the black hole entropy and in general in its laws of thermodynamics [599–601].

Here we sketch the argument for how the attractor mechanism arises in the simplest near-horizon geometry of static extremal solutions to Einstein–Maxwell-Dilaton theory.

$$S = \frac{1}{16\pi G_{\mathrm{N}}}\int \mathrm{d}^4x\sqrt{-g}\left[R - (\partial\Phi)^2 - \frac{1}{2}e^{-2\alpha_1\Phi}(F^1)^2 - \frac{1}{2}e^{-2\alpha_2\Phi}(F^2)^2\right]. \tag{8.68}$$

Here $F^i = \mathrm{d}A^i$ denote the two Maxwell fields we have in our theory. The above action is invariant under the shift $\Phi \to \Phi + \Phi_0$ if we also rescale the gauge field, $A^i_\mu \to e^{\alpha_i\Phi}A^i_\mu$. The main point of the argument relies on the $SL(2,\mathbb{R})$ invariance of the corresponding near horizon geometry. The most general spherically symmetric $SL(2,\mathbb{R})$-invariant $4d$ metric is $\mathrm{AdS}_2\times\mathrm{S}^2$,

$$\mathrm{d}s^2 = R_1^2\left(-r^2\mathrm{d}t^2 + \frac{\mathrm{d}r^2}{r^2}\right) + R_2^2\left(\mathrm{d}\theta^2 + \sin^2\theta\,\mathrm{d}\phi^2\right). \tag{8.69}$$

The same symmetries completely fix the spacetime dependence of the two gauge fields

$$A^i = q_i r\,\mathrm{d}t + p_i\cos\theta\,\mathrm{d}\phi \tag{8.70}$$

and there remain four constants to be determined. Finally, the dilaton field is fixed to be a constant, $\Phi = \Phi_c$, because there is no other scalar function invariant under $SL(2,\mathbb{R})\times SO(3)$ isometries.

The attractor mechanism then tells us that $\Phi_c$ is determined as a function of the electric and magnetic charges $q_i$, $p_i$. To see this, one may work through the EOM of the theory (8.68). However, since the solution ansatz we are considering is a product of maximally symmetric spacetimes (here $\mathrm{AdS}_2$ and $\mathrm{S}^2$), one can show that the EOM may be obtained from the reduced action one finds by plugging the solution ansatz into the action [602,603]. The reduced Lagrangian is

$$L = \frac{R_1^2R_2^2}{16\pi G}\left[\left(-\frac{2}{R_1^2} + \frac{2}{R_2^2}\right) + \sum_{i=1,2} e^{-2\alpha_i\Phi_c}\left(\frac{q_i^2}{R_1^4} - \frac{p_i^2}{R_2^4}\right)\right]. \tag{8.71}$$

One can work out the equations for the three variables $R_1$, $R_2$, $\Phi_c$ in terms of the charges. We leave this as an exercise to the reader. The main point in (8.71) is that there is a non-trivial potential for the constant value of the dilaton $\Phi_c$ and one cannot shift $\Phi_c$ if the $\alpha_i$ are different from each other.

The appearance of this potential for $\Phi_c$ is at the heart of the attractor mechanism. As discussed above, it is based on the $SL(2,\mathbb{R})$-invariance of the near-horizon-extremal geometries that fixes the $(t, r)$-dependence of the fields. This behavior is hence not expected to happen in generic black holes. Here we presented the simplest possible case. However, the attractor mechanism arises from the enhancement of isometries in the near horizon extremal geometries—for generic extremal black holes, black branes, and black rings—and has been extensively discussed in the literature. The attractor behavior has been at the root of the entropy function proposed by Ashoke Sen as a way to account for microstates of extremal black holes. For further readings, we refer the reader to [599,603–606] and their citations for more followups.

## 8.7 Kerr/CFT and Related Topics

The appearance of $AdS_2$ factors in the near-horizon-extremal geometries has prompted the hope that one may use the ideas of AdS/CFT to account for extremal black hole microstates and then use extremal cases as a base to tackle the same problem for generic black holes. Nonetheless, it has not been so straightforward to formulate this idea, in part because of the peculiar feature of $AdS_2$, that it has two disconnected boundaries and the space is simply too small to allow for fluctuations or perturbations which are normalized at both boundaries [607]; $AdS_2/CFT_1$ is not just a simple example of AdS/CFT in higher dimensions. One idea to deal with this is the quantum entropy function mentioned in the previous subsection, which is attempting to formulate a dual of $AdS_2$ gravity as a quantum mechanics system. Another idea is the Kerr/CFT correspondence [199], which we briefly discuss here.

**Statement of Kerr/CFT [199]**

QG in the region very near the horizon of an extreme Kerr black hole is dual to a chiral 2d CFT at central charge $c_L = 12J$, where $J$ is the angular momentum of the extreme Kerr background.

The backbone of the argument leading to the Kerr/CFT proposal is the realization of a single copy of the Virasoro algebra (7.22) as the asymptotic symmetry group of near-horizon extremal Kerr (NHEK) geometry, much in the same way as the $AdS_3$ and Brown–Henneaux example [534] discussed in the previous chapter. The difference is that here we have only a single copy of Virasoro, and hence a chiral CFT appears as the dual field theory. In what follows we show how this single copy of Virasoro is realized.

Let us start with the NHEK geometry

$$\mathrm{d}s^2 = \frac{G_{\mathrm{N}} J \Omega^2(\theta)}{2}\left[-r^2\mathrm{d}t^2 + \frac{\mathrm{d}r^2}{r^2} + \mathrm{d}\theta^2 + \Lambda^2(\theta)(\mathrm{d}\phi - r\,\mathrm{d}t)^2\right] \tag{8.72}$$

where $J$ is the angular momentum of the associated extremal Kerr and

$$\Omega^2 = 1 + \cos^2\theta \,, \qquad \Lambda = \frac{2\sin\theta}{1+\cos^2\theta} \,. \tag{8.73}$$

The above geometry has an $SL(2,\mathbb{R}) \times U(1)_\phi$ isometry algebra with the Killing vectors given in (5.26) but with $k = 1$.

Notably, $J$ in (8.72) appears only as an overall factor. In the NHEK geometry, we have used a coordinate system where the $\mathrm{AdS}_2$-part is in the Poincaré patch with horizon at $r = 0$. This horizon may be removed by an extension to global $\mathrm{AdS}_2$ [199]. The geometry does not have an event horizon, but it has infinitely many Killing horizons. One may compute the surface gravity for these Killing horizons and verify that they all have the same surface gravity $\kappa = 1$ [380] (cf. discussions around (5.56) in Sect. 5.4.3). One should note that surface gravity for the NHEK geometry does not vanish, unlike the surface gravity of the extreme Kerr black hole itself. The fact that all Killing horizons have the same surface gravity is a manifestation of the $SL(2,\mathbb{R})$-invariance of the background. This surface gravity may then be attributed to the Frolov–Thorne temperature $T = 1/(2\pi)$, as discussed in [199].

**Asymptotic symmetry group**

We start with a NHEK background $\bar{g}$ given by (8.72) and allow fluctuations $g_{\mu\nu} = \bar{g}_{\mu\nu} + h_{\mu\nu}$. The asymptotic conditions [199][3]

$$h_{tt} \sim \mathcal{O}(r^2) \qquad h_{t\phi} \sim \mathcal{O}(1) \qquad h_{\phi\phi} \sim \mathcal{O}(1) \tag{8.74}$$

$$h_{t\theta} \sim h_{r\phi} \sim h_{\theta\theta} \sim \mathcal{O}(\frac{1}{r}) \qquad h_{r\theta} \sim h_{tr} \sim \mathcal{O}(\frac{1}{r^2}) \qquad h_{rr} \sim \mathcal{O}(\frac{1}{r^3}) \tag{8.75}$$

are preserved by diffeomorphisms, $\mathcal{L}_\chi g_{\mu\nu} = \mathcal{O}(h_{\mu\nu})$, generated by the vector field

$$\chi[\epsilon(\phi)] = \epsilon(\phi)\partial_\phi - r\epsilon'(\phi)\partial_r + \cdots \,, \tag{8.76}$$

where $\epsilon(\phi)$ is an arbitrary smooth (periodic) function and the ellipsis denotes subleading terms. Note the resemblance of (8.76) to (8.44). While $\chi[\epsilon(\phi)]$ commutes with $\xi_1, \xi_2$ it does not commute with $\xi_0, \xi_4$. Nonetheless, the perturbed geometry still has $SL(2,\mathbb{R}) \times U(1)$ symmetry, as Killing isometries are covariant notions and do not change under diffeomorphisms [608].

Introducing Fourier modes $\chi_n := \chi[ie^{in\phi}]$, the asymptotic symmetry algebra

$$[\chi_n, \chi_m]_{\mathrm{Lie}} = (n-m)\chi_{n+m} \tag{8.77}$$

[3] Note that (8.72) only covers a region very close to the horizon of the original extreme Kerr geometry. Even the 'asymptotic' $r \to \infty$ region is close to the horizon of original Kerr black hole.

is the Witt algebra.

Following the methods of chapter (5), the canonical realization of the asymptotic symmetries (8.77) yields charges $L_n$ whose Poisson bracket algebra has a non-zero central extension

$$i\{L_n, L_m\} = (n-m)\, L_{n+m} + \frac{c}{12}\, n^3 \delta_{n+m,\,0} \qquad c = 12J\,. \tag{8.78}$$

Thus, a single copy of the Virasoro algebra (7.22) is obtained in Kerr/CFT.

The appearance of the Virasoro algebra prompted the Kerr/CFT proposal, in which this algebra is associated with a chiral $CFT_2$. The precise meaning of this chiral $CFT_2$ and its dynamical content is yet to be specified and does not follow from the asymptotic symmetry group analysis, see [609] for a discussion on this. A relevant class of $CFT_2$ has so-called Cardy growth of states where only the central charge of the Virasoro algebra and not other details of the CFT enter in the determination of the asymptotic density of states. See Sect. 9.4, which discusses Cardy growth and the Cardy formula. Assuming that this chiral CFT is at the temperature $T = 1/(2\pi)$ (see the discussions above on surface gravity of the NHEK geometry), one may use the Cardy formula to correctly reproduce the entropy of the NHEK (and hence the associated extremal Kerr black hole).

$$\boxed{S = 2\pi J}\,. \tag{8.79}$$

The Kerr/CFT correspondence has been extended to virtually any extremal black hole/ring, see [610] for a review.

## 8.8 Summary and Outlook

In this chapter we mainly focused on the gravity side of AdS/CFT, addressing also some quantum information aspects of holography. In the first half, we collected the backbone of AdS/CFT, the Gubser–Klebanov–Polyakov–Witten prescription (8.1) of calculating correlation functions, the Fefferman–Graham expansion (8.4) of the metric, holographic renormalization, the RT-proposal for holographic entanglement entropy (8.21), the description of thermal states as black holes (with possible phase transitions), and the concept of asymptotic symmetries. In the second half, we selected three specific holography-inspired topics that particularly relate to black holes, namely soft hair and near horizon symmetries, extremal black holes and the attractor mechanism, and Kerr/CFT.

However, as anticipated at the start of the chapter, this field is still evolving and there are numerous relevant topics that we omitted. We briefly address them here.

Scalar fields play an important role, both in the original AdS/CFT correspondence and in phenomenological applications. Many aspects of scalar fields in AdS can be understood by solving the Klein–Gordon equation on an $AdS_D$ background

$$\left(\nabla^2 - m^2\right)\phi = 0. \tag{8.80}$$

Interestingly, unitarity implies a lower bound on the square of the scalar mass that is negative,

$$m^2\ell^2 \geq -\frac{(D-1)^2}{4} \tag{8.81}$$

known as the Breitenlohner–Freedman bound [611]. This bound emerges from demanding reality of the conformal weight $\Delta_+$ of the dual operator in the CFT

$$\Delta_\pm = \frac{D-1}{2} \pm \frac{1}{2}\sqrt{(D-1)^2 + 4m^2\ell^2}\,. \tag{8.82}$$

For more details on scalar fields in an AdS/CFT context see, e.g. Appendix K of [612] or [547].

There are several holographic relations between black holes and observables in CFTs that we did not mention yet; while some of them will be addressed in the next chapter, here we highlight just one additional example, namely the identification of black hole QNM frequencies (see the discussion in Sect. 4.7.1) with the location of poles in the retarded Green function in a CFT [338].

Numerous applications to holography emerged in the twenty-first century, starting with applications to quark-gluon plasma physics. The black hole formation on the gravity side corresponds to thermalization on the field theory side, and numerous observables were calculated holographically in this context. An emblematic example is the calculation of the ratio of shear viscosity $\eta$ over entropy density $s$ at infinite coupling in the large-$N$ limit [613,614],

$$\frac{\eta}{s} = \frac{1}{4\pi} \approx 0.080\,. \tag{8.83}$$

The experimentally measured value of this ratio at RHIC is surprisingly close to the result (8.83) [615]. Operationally, the harder part of the calculation is the shear viscosity, since entropy density follows from the BH law (5.43). It is calculated through the Kubo formula [414]

$$\eta = \lim_{\omega\to 0}\frac{1}{2\omega}\int \mathrm{d}^4x\, e^{i\omega t}\langle[T_{xy}(x^\mu),\ T_{xy}(0)]\rangle \tag{8.84}$$

where $x^\mu = (t, x, y, z)$ refers to standard Minkowski coordinates. Thus, the calculation of shear viscosity reduces to the calculation of 2-point functions of (mixed spatial) components of the energy-momentum tensor. Holography allows to exploit the dictionary (8.15) to calculate these correlation functions on the gravity side in a simple way, yielding (8.83).

Condensed matter systems can also feature strong coupling/correlation phenomena, including cold atoms [616,617], high-temperature superconductors [618,619], Lifshitz fixed points [620], and strange metals [621]. Since the literature on holographic applications of black hole physics to QCD as well as to condensed matter systems is vast, we confine ourselves to some pointers to textbooks, review articles, and further literature listed below.

## Further Reading

The literature on holography can be overwhelming since the seminal work [88] has acquired over 17 thousand citations at the time of writing this chapter. Therefore, we provide here only a few pointers to selected textbooks and review articles.

For general aspects of AdS/CFT see, e.g. [553,554,622–625]. For a more recent analysis on the thermofield double, how horizons appear in the dual CFT, and how one can probe the geometry behind the horizon using the dual CFT, see [626,627].

Textbooks and reviews focused on quantum information aspects of holography include [131,628–631].

For applications to QCD and/or condensed matter applications of holography see, e.g. [547,632–636].

## Exercises

**8.1 Domain walls and holographic renormalization group flow.**
Consider an $\mathrm{AdS}_3$ domain wall metric

$$\mathrm{d}s^2 = \mathrm{d}\rho^2 + e^{2A(\rho)}\big(-\,\mathrm{d}t^2 + \mathrm{d}x^2\big)$$

that models a renormalization group flow from the UV ($\rho \to \infty$) to the IR ($\rho \to -\infty$), in the sense that this geometry can be dual to the ground state of a $\mathrm{QFT}_2$. Show that this metric has the expected Killing vectors of a $\mathrm{QFT}_2$ and deduce conditions on the function $A(\rho)$ such that the domain wall really can describe a renormalization group flow between $\mathrm{CFT}_2$ fixed points in the UV and IR. In particular, the central charges at the respective fixed points must obey $c_{\mathrm{UV}} \geq c_{\mathrm{IR}}$.

**8.2 Generalized Fefferman–Graham expansion.**
Consider metrics of the form

$$\mathrm{d}s^2 = \mathrm{d}\rho^2 + \big(e^{2\rho/\ell}\eta_{\mu\nu} + e^{\rho}\,\gamma^{(1)}_{\mu\nu} + \gamma^{(2)}_{\mu\nu} + \cdots\big)\,\mathrm{d}x^\mu\,\mathrm{d}x^\nu$$

and calculate the asymptotic expansions for extrinsic curvature $K_{\mu\nu}$ and its trace.

**8.3 Holographic renormalization in $\mathrm{AdS}_5$.**
Renormalize holographically $\mathrm{AdS}_5$ Einstein gravity such that the on-shell action and Brown–York stress tensor are finite and the variational principle is well-defined.

**8.4 Holographic 2-point correlator of stress tensor.**
Calculate in $\mathrm{AdS}_5$ Einstein gravity the 2-point correlator of the boundary stress tensor.

**8.5 Holographic renormalization in 2d dilaton gravity**

Show that the bulk action of generic 2d dilaton gravity (7.33) without matter requires two types of boundary terms

$$I_{\text{GHY}} = \frac{1}{8\pi G_{\text{N}}}\int \mathrm{d}x\sqrt{|\gamma|}\,XK \qquad\qquad I_{\text{ct}} = \int \mathrm{d}x\sqrt{|\gamma|}\,f(X)$$

and calculate $f(X)$ depending on the bulk potentials $U(X)$ and $V(X)$. Use the following assumptions:

- The boundary is a dilaton isosurface at $X \to \infty$.
- The function $w(X)$ defined in (7.43) tends to $\infty$.
- The state space consists of solutions (7.50) with arbitrary $M$.

**8.6 Entanglement entropy of 2-qubit systems.**

Calculate entanglement entropy for the direct product state $|\psi_1\rangle = |0\rangle_A \otimes |0\rangle_B$ and the Bell state $|\psi_2\rangle = \frac{1}{\sqrt{2}}\big(|0\rangle_A \otimes |0\rangle_B + |1\rangle_A \otimes |1\rangle_B\big)$.

**8.7 Holographic entanglement entropy of CFT$_2$.**

(1) The geometry dual to the CFT$_2$ vacuum on the plane is Poincaré patch AdS$_2$,

$$\mathrm{d}s^2 = \frac{\ell^2}{z^2}\big(-\mathrm{d}t^2 + \mathrm{d}x^2 + \mathrm{d}z^2\big)\,. \tag{8.85}$$

Apply the RT prescription (8.21) to calculate entanglement entropy of the CFT$_2$ vacuum for an entangling region of size $L$ (e.g. by placing the endpoints of the interval symmetrically at $z_{1,2} = 0$ and $x_{1,2} = \pm\frac{L}{2}$). Convince yourself that the length of the geodesic connecting these points is infinite and, when regulated, coincides with the result (8.23).

(2) Repeat the above analysis for computing entanglement entropy of a given interval in a $2d$ CFT state with generic Virasoro excitation. Holographically, this is dual to the Bañados geometries (7.7).

**8.8 Lorentz geometry in Casini–Huerta proof.**

This exercise focuses on a simple detail of the Casini–Huerta proof. Consider four events in 2-dimensional Minkowski space labeled by $A_i$, $i = 1, 2, 3, 4$, such that the distances $A = A_1A_2$, $B = A_1A_3$, $C = A_2A_4$, and $D = A_3A_4$ are all spacelike and the line $A_1A_3$ intersects with the line $A_2A_4$. Proof the identity $AD = BC$.

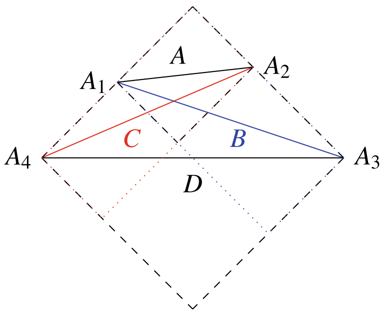


**8.9 QNEC and Schwarzian.**

Show that the QNEC combination $Q = S'' + \frac{6}{c}(S')^2$ defined in (8.25) transforms with a Schwarzian derivative under diffeomorphisms, $\delta_\varepsilon Q = \varepsilon Q' + 2\varepsilon' Q - \frac{c}{12}\,\varepsilon'''$.

**8.10 QNEC with paper and pencil.**

Consider stationary spherically symmetric geometries in three dimensions and calculate the QNEC combination $Q = S'' + \frac{6}{c}(S')^2$ defined in (8.25). In doing so, verify the following statements.

(1) The geodesic Lagrangian $L$ yields two Noether charges given by $Q_1 = \dot{z}\partial L/\partial\dot{z} + \dot{t}\partial L/\partial\dot{t} - L$ and $Q_2 = \partial L/\partial/\dot{t}$, where $t$ is some time coordinate, $z$ some holographic radial coordinate and dot denotes derivatives with respect to the geodesic parameter, which we take to be the third coordinate, $x$.

(2) The deformation parameter $\lambda$ can be calculated by the integrals

$$\lambda = 2\int_0^{\lambda/2} \mathrm{d}t = 2\int_{z_*}^{0} \mathrm{d}z\,\frac{\dot{t}}{\dot{z}}$$

where $z_*$ is the value of the holographic coordinate at the turning point of the geodesic in the bulk.

(3) The deformed spatial length of the entangling interval, $\ell \to \ell + \lambda$, can be calculated by similar integrals

$$\ell + \lambda = 2\int_0^{(\ell+\Lambda)/2} \mathrm{d}x = 2\int_{z_*}^{0} \mathrm{d}z\,\frac{1}{\dot{z}}\,.$$

(4) Using the results above, show that the geodesic length $A$ is calculable but infinite. Therefore, introduce a cutoff at some $z = z_0$ to regularize the geodesic length. Show that the result for the regularized length is of the form

$$A_{\text{reg}} = 2\int_{z_*}^{z_0} \mathrm{d}z\, f(z, z_*, Q_2/Q_1)\,.$$

(5) Define a renormalized length

$$A_{\text{ren}} = 2 \int_{z_*}^{z_0} \mathrm{d}z \left( f(z, z_*, Q_2/Q_1) - \frac{\mathrm{d}A_c(z)}{\mathrm{d}z} \right) - 2A_c(z)$$

with a suitable counterterm $A_c(z)$ and show that the result can be expanded as

$$A_{\text{ren}} = A_0(\ell) + \lambda A_1(\ell) + \frac{\lambda^2}{2} A_2(\ell) + O(\lambda^3)\,.$$

(6) Finally, show that the QNEC combination is given by

$$Q = \frac{c}{6} \left( A_2(\ell) + A_1^2(\ell) \right)$$

.

**8.11 Hawking–Page phase transitions in $2d$ dilaton gravity**

Use the results of Exercise 8.5 to show that the free energy for black hole solutions in generic 2d dilaton gravity is given by $F = M/(8\pi G_{\text{N}}) - TS$, with the Hawking temperature $T = w'(X_h)/(4\pi)$ and the Wald entropy $S = X_h/(4G_{\text{N}})$, where $X_h$ is the value of the dilaton at the horizon, i.e. the outermost solution of the algebraic equation $w(X_h) = 2M$. Assuming the ground state free energy is some non-positive constant, discuss under which conditions on the function $w(X)$ Hawking–Page-like phase transitions arise. (Note: you must assume $w(X \to \infty) \to \infty$ for applying Exercise 8.5, and you must also assume $w(X_h), w'(X_h), w''(X_h) > 0$ in order to have, respectively, positive mass, positive temperature and positive specific heat; for simplicity, you may work with strictly monotonic functions $w(X)$, and as a first try just with monomials, $w(X) \sim X^n$, with some real $n$.)

**8.12 A quick derivation of thermofield double state.**

Consider a $d$-dimensional Euclidean thermal CFT on $S^1_\beta \times S^{d-1}$. One can divide the $S^1_\beta$ into two intervals of length $\beta/2$. Let $\Sigma$ may be the geometry which has two boundaries as depicted below.

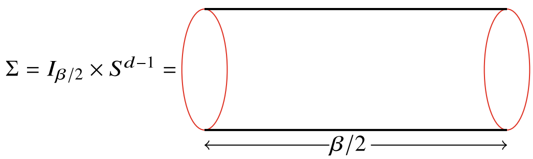


Show that the Euclidean path integral of the CFT over $\Sigma$ yields the thermofield double state (8.86). In this path integral the left and right states in $|\text{TFD}\rangle$ are coming from the contribution of the left and right boundaries of $\Sigma$ to the path integral.

**8.13 More on Thermofield double formalism.**

(1) Show that for a Hamiltonian $\mathbf{H}$ with eigenvalues $E_n$ and energy eigenstates $|n\rangle$, $\mathbf{H}|n\rangle = E_n|n\rangle$,

$$|\text{TFD}\rangle = \frac{1}{\sqrt{Z(\beta)}} \sum_n e^{-\beta E_n/2}\, |n\rangle_{\text{L}} \otimes |n\rangle_{\text{R}} \tag{8.86}$$

(2) Show $\boldsymbol{\rho}_{\text{TFD}} = |\text{TFD}\rangle\langle\text{TFD}|$ and that $Tr_{\text{R}}\boldsymbol{\rho}_{\text{TFD}} = \boldsymbol{\rho}_\beta$ defined in (8.34).

(3) Show that thermofield double state $|\text{TDF}\rangle$ is a stationary state under time evolution defined by the total Hamiltonian $\mathbf{H}_{\text{tot}}$ (8.37). That is, show

$$|\text{TFD}(t)\rangle := e^{i\mathbf{H}_{\text{tot}}t}|\text{TFD}\rangle = |\text{TFD}\rangle. \tag{8.87}$$

**8.14 Entropy of thermofield double state.**

Starting from $\boldsymbol{\rho}_{\text{TFD}}$ (8.36) compute the von Neumann entropy of this density matrix when work on the double Hilbert space $\mathcal{H}_D$. Work the von Neumann (entanglement) entropy of this state after tracing over the left Hilbert space. Show that the latter is indeed the thermal entropy associated with the field theory at inverse temperature $\beta$.

**8.15 Asymptotic symmetries in AdS$_3$.**

Consider a class of 3-dimensional metrics obeying the Brown–Henneaux boundary conditions,

$$\mathrm{d}s^2 = \mathrm{d}\rho^2 + \left(e^{2\rho/\ell}\,\eta_{\alpha\beta} + \gamma^{(2)}_{\alpha\beta} + \mathcal{O}(e^{-2\rho/\ell})\right)\,\mathrm{d}x^\alpha\,\mathrm{d}x^\beta,$$

where $\ell$ is a constant (the AdS-radius), $\eta_{\alpha\beta}$ is the 2-dimensional Minkowski metric (which is kept fixed) and $\gamma^{(2)}_{\alpha\beta}$ is arbitrary (so $\delta\gamma^{(2)}_{\alpha\beta} \neq 0$). Determine all asymptotic Killing vectors and their Lie-brackets.

**8.16 Infinitesimal Schwarzian derivative of boundary stress tensor.**

Verify the transformation behavior (7.20) using the results of the previous exercise.

**8.17 More on near-horizon limits of extremal black holes.**

(1) Show that the metric (8.67) has an $SL(2,\mathbb{R})$ isometry.

(2) Work out the near horizon limit of extremal Kerr and extremal MP black holes and show that they can indeed be written in the form (8.67).

(3) As in the case of ordinary black holes, near-horizon extremal geometries also obey their own law of (thermo)dynamics. While extremal black holes have zero temperature one can show that there is still a notion of the zeroth law: $k^a$ are constants. Similarly one may work through the other laws of black hole mechanics. Work out these laws. See [367,380,637] for more detailed discussion on this.

**8.18 Softness of near horizon excitations of BTZ black holes**

Given the near horizon Hamiltonian $H = \kappa\left(J_0^+ + J_0^-\right)$, where surface gravity $\kappa$ is some positive constant, and the near horizon symmetry algebra

$$[J_n^\pm,\ J_m^\pm] = \tfrac{1}{2}\, n\, \delta_{n+m,\,0}, \qquad [J_n^+,\ J_m^-] = 0,$$

prove algebraically that any descendant $\prod_{\{n_i^\pm > 0\}} J^+_{-n_i^+} J^-_{-n_i^-} |\psi\rangle$ of any state $|\psi\rangle$ has the same energy as that state.

# Quantum Aspects of Black Holes

# 9

**Abstract**

Having discussed classical and semiclassical aspects of black holes, in this chapter we study quantum aspects of black holes. In Sect. 9.1 we discuss some general aspects of black holes in QG. In Sect. 9.2 we discuss black hole complementarity and firewalls. In Sect. 9.3 we focus on black holes in string theory. In Sect. 9.4 we review microstate countings for certain supersymmetric black holes, in particular, we discuss the celebrated Cardy formula, which is the cornerstone of these analyses. In Sect. 9.5 we discuss two proposals for identification (and not just counting) of black hole microstates, the fuzzball and fluffball proposals. We end this chapter with a discussion on the information puzzle within AdS/CFT in Sect. 9.6.

## 9.1 Black Holes and Quantum Gravity

While as of today there is no conclusive observational evidence for the need to correct Einstein gravity, there are some theoretical issues that need to be addressed. For example, the theory allows for solutions with CTCs [638,639] or with singularities, like typical black hole solutions. Moreover, as discussed in earlier chapters, semiclassical treatments lead to the thermodynamic picture for black holes, the Hawking radiation, and eventually total evaporation of black holes, yielding the information puzzle. There is a widely held view that these issues should be remedied in a theory of QG.

The development of QG is however hampered by the smallness of the gravitational interaction and the related lack of experimental data. As opposed to the development of quantum mechanics, which was initially driven by phenomenological input from atomic spectra, there is no "hydrogen atom of QG" yet. However, black holes come close to playing this role.

In the following, we summarize the main reasons why black holes could be crucial in the (theory-driven) development of QG. We order them by relevance, meaning that



D. Grumiller and M. M. Sheikh-Jabbari, *Black Hole Physics*, Graduate Texts in Physics,
https://doi.org/10.1007/978-3-031-10343-8_9

the points near the top are the most compelling ones and the points near the bottom require further research.

- **BH entropy.** Arguably, our least trivial clue so far is the black hole entropy law in the limit of large horizon area $\gg G_{\rm N}$,

$$S_{\rm BH} = \frac{\text{area}}{4G_{\rm N}} + N \ \ln \text{area} + O(1) \tag{9.1}$$

  where $N$ is some real number encoding 1-loop corrections to the BH law. The formula (9.1) serves as a template for experimental data, in the sense that any putative theory of QG failing to reproduce (9.1) would be eyed with great suspicion. While this still leaves room for ambiguities about the precise UV completion of Einstein gravity, one can at least eliminate speculative approaches to QG that violate the BH law (9.1). The reason for our trust in the result (9.1) is that its derivation involves rather established laws of physics, such as quantization of matter fields on some slowly varying background geometry (see Chap. 6). Moreover, the result (9.1) only involves data that are accessible (semi-)classically, like the area of the black hole horizon and the number and type of matter fields (which enter into the number $N$).
- **High energy scattering.** Neglecting gravity, our current "theory of everything" (the universal framework for physical models) is QFT. Within QFT, if we want to resolve small distances in some scattering experiment, we need to go to high energies. However, unlike Yang–Mills gauge theory interactions, gravity cannot be screened, so if we go to sufficiently high energies we can no longer neglect gravity since eventually, black holes will form as a result of high energy scattering [307,640,641]. Once black holes start forming, the existence of a horizon prevents us from resolving smaller distances. In fact, if the energy is increased further, the distances that can be resolved do not become smaller but larger, since the horizon grows as more energy is pumped into the black hole. This simple consideration puts some lower bound on the distances that can be resolved in scattering experiments, see Fig. 9.1. From this gedankenexperiment, one can deduce that in QG either there must be some fundamental length scale (e.g. of the order of the Planck length) or there is some mechanism at work like in the Veneziano amplitude that renders high energy amplitudes sufficiently soft. The first option is impossible to reconcile with local Lorentz invariance, which provides a way to test/rule out such models, see e.g. [642,643]. The second option is realized in string theory, see e.g. [612,644,645].
- **Quantum gravity correspondence principle.** Our best theory of gravity currently is Einstein gravity, in the sense that all known experiments appear to be compatible with it [17].[1] Thus, we should have a QG correspondence principle:

[1] We are disregarding here the possibility that dark matter or dark energy are consequences of a modification of Einstein gravity since there appears to be no convincing and predictive model available so far.

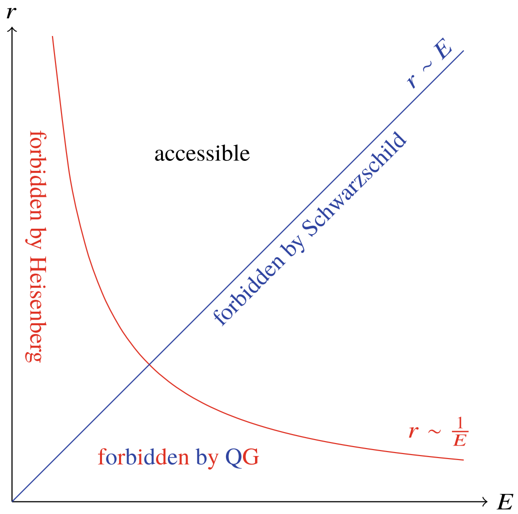


**Fig. 9.1** Distance resolution in high energy scattering as function of energy

any quantum theory of gravity must reproduce Einstein gravity, including its black hole solutions and their smooth and regular horizons, in the classical limit. While this seems like a trivial statement, it is important to bear it in mind when speculating about QG—successfully addressing quantum aspects of gravity makes only sense if the same theory is also correct classically.

- **Semi-classical gravity.** GR may be viewed as a field theory with the metric as the classical field. One may quantize it like any other QFT. This has been carried out by trying various different techniques and methods, yielding that the theory is not renormalizable [124,125]. While this non-renormalizability was the inspiration for some QG proposals, it is not a crucial deficiency once we recall Wilsonian EFT: Regardless of the UV details of the QG theory, all such quantum effects at the semiclassical level, i.e. energies sufficiently lower than the Planck scale, should be captured by diffeomorphism invariant operators with the lowest numbers of derivatives, i.e. the cosmological constant and Einstein–Hilbert terms, with small higher curvature corrections. This perturbative approach allows predicting quantum corrections, e.g. to the Newton potential [126–128]. Whatever the correct UV completion is, it should give a clear prediction about the form of these higher curvature corrections. However, even without an explicit UV completion one can work in a bottom-up way and study perturbatively theories with higher curvature corrections. Black holes are an important part of the vast literature of such higher curvature gravity theories. A fraction of the still-developing literature is concerned with the construction of such black hole solutions and revisiting basic black hole theorems discussed in Chap. 3. In addition, one should examine if the laws of black hole thermodynamics are satisfied for black hole solutions to these theories. While Wald's entropy and the derivation of the first law reviewed in Chap. 5 are manifestly holding for any diffeomorphism invariant theory, the generalized second law should still be studied and checked.

- **Horizons and holography.** Another consequence of black hole horizons and the BH law (9.1) is that the classical black hole entropy is extensive (scales with the volume) in one lower dimension. This observation inspired the holographic principle [85,86,646], which most likely is a key aspect of QG. The most elaborated realization of the holographic principle is the AdS/CFT correspondence deduced from string theory [88–90]. Substantial progress in QG was made after the turn of the millennium by implementing and applying the holographic principle, see our discussion in Chap. 8. It is an open question if/how holography works generically in asymptotically flat, dS, or arbitrary spacetimes.
- **Horizons and causal structure in quantum gravity.** One of the key notions in the (mathematical) definition of black holes (cf. Chap. 3) and their semiclassical behavior (cf. Chaps. 5 and 6) is the notion of horizon. QG is often believed to bring in a notion of "quantum spacetime" and hence a "quantum causal structure". The stretched horizon and the membrane paradigm picture (cf. Sect. 6.8) can be a toy model for a "semiclassical horizon" that may be useful to the definition of a quantum black hole.
- **Quantum gravity and black hole vacuum states.** QG effects can have implications for the possible vacuum state and Hilbert space of fluctuations for quantum fields in a black hole background (see the semiclassical discussion in Chap. 6), especially the UV sector from the near horizon observer viewpoint. All these effects need to be studied and their ramifications for the physics of black holes should be taken into account.
- **Entropy bounds and generalized second law.** In addition to all the reasons why black holes are remarkable, there is an astonishing discrepancy between their classical simplicity and their quantum mechanical complexity. Indeed, classically black holes are as simple as elementary particles, characterized only by a handful of numbers (mass, spin, charges), see the uniqueness and no-hair results in Chap. 3. Quantum-mechanically, their humongous BH entropy (9.1) shows that black holes are extremely complex. Entropy bounds lift this observation to a postulate: black holes are the most complex objects that can possibly exist in our (or any other) universe; see the discussion in Sect. 6.5.2 for the precise formulation of some entropy bounds. If these entropy bounds are genuine, they should be derivable from QG and also be present in its holographic dual (provided the latter exists). The generalized second law (6.47) is a related clue and has led to new concepts in QG that could be useful, such as the notion of quantum extremal surfaces [577].
- **Information loss and how to avoid it.** The semiclassical loss of information induced by black hole evaporation is often presented as the key puzzle to be solved by any approach to QG. While we agree with this attitude, it is a logical possibility that information is lost, which is why this item is not on the top of our list. The one point on which there seems to be rather universal agreement is that the most fruitful approach is to try to be as conservative as possible. However, it is not agreed whether postulating that no information is lost is more conservative than postulating that black holes behave like an open quantum system or vice versa. Thus, while it is expected of any quantum theory of gravity to make a decisive statement concerning information loss, we are not 100% sure what we expect

this statement to be. So unlike the BH law (9.1), we cannot use information preservation/information loss as a template for falsification. For a summary of information preservation see [455]. For the information loss perspective see [647].

- **Absence of global symmetries.** QG is conjectured to not allow for global symmetries (as opposed to gauge symmetries and global parts thereof), see e.g. [648] and refs. therein. Such global symmetries and associated charges do not appear in the first law of black hole mechanics, see Sect. 5.5. A simple way to argue why this is the case is to throw some object with a global charge (like the baryon number) into a black hole and wait until the black hole has evaporated. Unless there is some remnant carrying the global charge, the global charge cannot be conserved. Remnants usually are ruled out since they would have to be far too abundant, see e.g. [649].
- **Weak gravity conjecture.** The conjecture that gravity is the weakest force brought an interesting new twist to the absence of global symmetries [30]: if global symmetries are not allowed, then also arbitrarily weak local symmetries must be forbidden since they are indistinguishable from global symmetries. Moreover, extremal black holes must not be stable (otherwise they would be remnants), so there must be at least one particle whose mass is smaller than its gauge charge (in Planck units); this amounts to saying that the gravitational force is weaker than any gauge force. To accommodate this line of reasoning one cannot neglect the other forces besides gravity, so the most natural place for the weak gravity conjecture is string theory, where QG necessitates the presence of (all) the other interactions.
- **Singularities and their resolution.** If black hole (or big bang) singularities were not screened by horizons they would be excellent sources for QG phenomenology. According to the CCC (see Sect. 3.2.7), there is an "IR-conspiracy" that hides all such singularities/strong curvature regions from asymptotic observers. Concerning this issue, the task of QG is twofold: 1. explain the IR-conspiracy from first principles, and 2. show how singularities get resolved by quantum effects. Following this research avenue, the hope is that once these two issues are solved for some candidate theory of QG, the solution is so compelling that we can conclude to be on the right track.
- **Near horizon and null boundary symmetries.** The relatively recent study of near horizon symmetries and soft hair excitations of black holes, summarized in Sect. 8.5, led to speculations that near horizon symmetries could be crucial for counting, labeling, and constructing black hole microstates. Regardless of whether or not this will turn out to be correct, near horizon symmetries are intriguing properties intrinsic to black hole horizons and are expected to be of some use in QG. We shall elaborate on this in Sect. 9.5 below.
- **Chaos.** Black holes and thermal systems share one other property with other, namely chaotic behavior. Classically, this means that the present determines the future, but the approximate present does not determine the approximate future. In the context of quantum information (and black hole physics) chaotic behavior is referred to as "scrambling". It was conjectured that black holes are the fastest scramblers in the universe [457,650,651], with a scrambling time $t_* \sim \frac{\ln S}{2\pi T}$,

where $T$ is the Hawking temperature (6.29) and $S$ the Bekenstein–Hawking entropy (5.43). Moreover, black holes saturate the conjectured chaos bound on the Lyapunov exponent, $\lambda_L = 2\pi T$ [652,653] (see also Exercise 7.14), which suggests that quantum mechanical systems saturating the chaos bound may have a holographic gravitational interpretation. Thus, exploring chaotic behavior is expedient for scrutinizing the holographic approach to QG.

- **How to define a black hole quantum mechanically?** The classical black hole definition provided in Sect. 3.1 is not suitable in the quantum theory, since black holes evaporate—so there is no event horizon in QG. We have saved this question for the last item since we cannot offer any answer to it. Thus, currently, this point does not provide us directly with any guidelines concerning QG. Still, it is worthwhile to address this question, if only to agree on what we actually mean by a black hole in a QG context.

## 9.2 Black Hole Complementarity, Firewalls, Page Curve and Islands

We discuss now in a bit more detail quantum aspects of black hole complementarity introduced in Sect. 6.9, with particular focus on firewalls and how to avoid them. The essence of the firewall paradox can be expressed in terms of entanglement properties of Hawking quanta [92,654].

Consider three quantum states $A$, $B$, $R$, where $A$, $B$ are a quantum pair created due to the Hawking process, with $A$ being the particle emitted to infinity and $B$ the particle falling into the black hole. The state $R$ denotes earlier Hawking radiation. The assumption that Hawking radiation is pure means that $R$ must be (almost maximally) entangled with $A$ (this leads to correlations that an asymptotic observer could measure to deduce deviations from a mixed state). The assumption of the EP, i.e. a smooth horizon, means that $A$ and $B$ must be (maximally) entangled with each other. Both together imply that the assumption to apply effective QFT slightly inside/outside the horizon cannot hold since in ordinary quantum theories we have entanglement monogamy, i.e. the state $A$ cannot be simultaneously (maximally) entangled with $B$ and $R$. See e.g. [131] for a summary of this discussion.

There are different options to resolve the entanglement ménage à trois and recover monogamy. One is to give up entanglement between $A$ and $B$, which leads to firewalls. The second option is to give up entanglement between $A$ and $R$, which leads to information loss. If neither of these options seems attractive one has to work a bit harder, and there are different possible lines of resolving this issue.

One general idea is to drop the assumption that EFT works. A particular avenue is to drop the implicit assumption that the black hole interior is independent of the black hole exterior. Indeed, a conceptually simple resolution is to postulate/argue/derive that $B$ is identical to $R$, in which case entanglement would be monogamous, despite appearances.[2] This idea that the black hole interior is a 'scrambled version' of the black hole exterior was made more precise by Kyriakos Papadodimas and Suvrat Raju using AdS/CFT as inspiration, see [655] and refs. therein.

A particular way of phrasing the issues with Hawking evaporation is due to Don Page [442,656] and culminates in the Page curve displayed in the figure below.

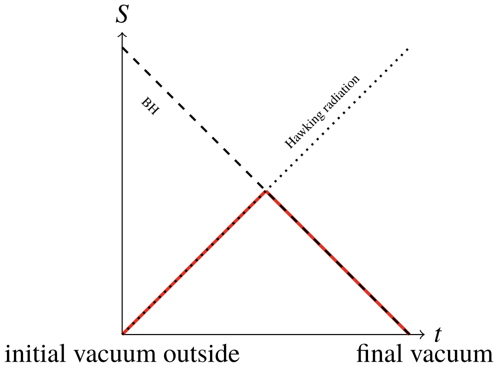


In this figure, the linearly rising curve reproduces Hawking's semiclassical result, i.e. the entropy of Hawking radiation increases linearly as a function of time, until the black hole has evaporated completely. The fact that this curve does not go back to zero means information was lost in the evaporation process. The linearly decreasing curve is the Bekenstein–Hawking entropy of the black hole. The proposal by Page is that the entanglement entropy of the Hawking radiation with the black hole is bounded by these two curves, i.e. loosely follows the thick red curve in the figure. For many QG researchers deriving the Page curve has become a synonym for solving the black hole information puzzle.

A more recent development, known as 'islands' [657–659], is based on a more precise definition of black hole entropy. The essence is as follows. To address the issue of information loss it is important to distinguish the coarse-grained entropy contained in the generalized second law (the BH entropy plus the entropy of the exterior matter) from the fine-grained entropy. The former may well continue to increase monotonically, capturing information loss for all practical purposes, but the latter should follow the Page curve and drop to zero when the black hole has evaporated. The fine-grained entropy $S_f$ schematically is defined as

$$S_f = \min\left(\frac{A}{4} + S_{\text{matter}}\right) \tag{9.2}$$

where one takes an arbitrary area outside the black hole, computes its BH entropy, adds the entropy of matter fields outside this surface, and then minimizes their sum by varying the area. In this process, it is allowed to move the area into the interior of the black hole and to have a multiply connected 'exterior'. A disconnected region in the

[2] In the spirit of this whimsical technical slang, this would be like having an affair with your life partner.

black hole interior is referred to as ‘island’ and emerges when it is more efficient to pay the price for an increased area since $S_{\text{matter}}$ goes down sufficiently. This happens when there are regions far from each other with entangled pairs of quanta, which is precisely what happens in the Hawking effect.

The main claim is that the fine-grained entropy follows the Page curve and drops to zero after the black hole has evaporated. For black holes in their early stage, when there is still collapsing matter in the interior, the minimum occurs when the surface is in the center so that the fine-grained entropy consists just of $S_{\text{matter}}$, evolving unitarily by construction. By contrast, if a black hole has settled down and emitted for a long time the area that minimizes the fine-grained entropy is close to the horizon, essentially because the number of entangled pairs is very large so that moving the area all the way to the center would be too costly. Since in the course of evaporation the horizon area shrinks also the fine-grained entropy goes down and eventually goes to zero (the fine-grained entropy in the Hawking radiation goes down since eventually there will be no entangled partner hidden behind a horizon). See [455] for a review on the entropy of Hawking radiation.

## 9.3 Black Holes in String Theory

String theory claims to provide a unified quantum formulation for all matter fields and their interactions, including gravity. As such, string theory is expected to supply the framework to formulate and address questions and puzzles regarding quantum aspects of black holes. As the name suggests, its “fundamental” degrees of freedom are strings (rather than particles) moving on a $d$-dimensional target space, governed by the worldsheet theory which is a 2-dimensional $\sigma$-model, a $2d$ conformal field theory. In superstring theory, the worldsheet theory is taken to be a supersymmetric $2d$ sigma-model. Cancellation of the Weyl anomaly for the (Euclidean) worldsheet with any given topology, then fixes the number of spacetime dimensions, which is $d = 10$ for a superstring theory. One of the salient features of string theory is its background independence, intuitively meaning that the background over which strings propagate may be viewed as a condensate state of strings themselves. Moreover, string theory is described by two parameters, the string scale $m_s$ and the string coupling $g_s$; string tension is then $2\pi\alpha' = m_s^{-2} := l_s^2$ where $l_s$ is the string length scale.

As implied by various string theory dualities, the theory besides strings has also brane-type states. In string theory one can hence recognize three class of states: F(undamental) strings whose tension parametrically scales like $m_s^2$, $\mathrm{D}_p$-branes whose tension scales like $m_s^{p+1}/g_s$ and $\mathrm{NS}_5$-branes with tension scaling as $m_s^6/g_s^2$. F-strings have a set of massless states, which fall into short representation of $N = 1$ or $N = 2$ 10-dimensional supersymmetry algebras, and also a tower of massive states with mass $M^2 = m_s^2 N$ for any integer $N$ and degeneracy growing like $e^{M/m_s}$. Therefore, the effective degrees of freedom of the weakly coupled theory are those of F-strings while in strongly coupled theory $\mathrm{D}_p$ or $\mathrm{NS}_5$ -branes become light and dominate the dynamics. For more on string theory we refer the reader to the excellent books on the theory, e.g. [517–519,660,661].

For low energy processes with $l_s E \ll 1$ and in the weakly coupled regime $g_s \lesssim 1$, effectively and in leading order only massless string states contribute, which can be described by a field theory. The low energy effective theory (LEFT) of weakly coupled string theory is a (super)gravity theory, plus stringy corrections that appear as higher derivative terms added to Einstein–Hilbert term, see Appendix I for a quick review. The Newton constant of the $10d$ string theories and string parameters are related as

$$10d \text{ Newton constant :} \qquad 16\pi G_{\mathrm{N}} = (2\pi)^3 g_s^2 l_s^8. \tag{9.3}$$

String theory in a lower dimension $d$ may then be generically obtained through compactification of $10d$ theory over a $10-d$ compact manifold, the topological and geometric properties of which determines the characteristics of the lower-dimensional theory [517–519,660,661]. In particular if the volume of compact manifold $V_{\text{10-d}} := L^{10-d}$ is not large, $EL \lesssim 1$ where $E$ is the typical energy of the system, then the LEFT of lower-dimensional string theory is a (super)gravity [521,522,662] with effective Newton constant $(2\pi)^3 g_s^2 l_s^8 / V_{\text{10-d}}$, as implied by the KK theory [514,663].

String theory is proven to be 1-loop renormalizable and is widely believed to be all-loop renormalizable. The appearance of (super)gravity theories as LEFT of strings means that all solutions to these (super)gravity theories may also be viewed as backgrounds over which string theory can be consistently formulated (in a perturbative $\alpha'$-expansion). Among these are black hole/brane solutions discussed in Chap. 7. These solutions typically carry charges of various $p$-form fields, which are abundant in the supergravity theories, F-strings carry the charge of (Neveu–Schwarz-Neveu–Schwarz) 2-form, $\mathrm{NS}_5$-branes carry the charge of the Hodge dual to that of F-strings, a 6-form charge, and $\mathrm{D}_p$-branes carry (Ramond-Ramond) $(p+1)$-form charges. Importantly, D-branes besides being a solitonic (extended) solution of supergravity theories also have a description in terms of weakly coupled open strings: $\mathrm{D}_p$-branes are objects with $(p+1)$-dimensional worldvolume where open strings can attach to by Dirichlet boundary conditions [664]. As we shall discuss in the next section, the existence of the two complementary descriptions for $\mathrm{D}_p$-branes, in string theory and in supergravity, is at the root of black hole microstate counting within string theory.

**> Black hole/string transition**

From a string theory perspective, there are different regimes of relevance in a black hole context. At a sufficiently small temperature (so that the inverse temperature is large as compared to the string length) the semiclassical picture of Chap. 6 is recovered, with small $\alpha'$ corrections that are genuinely "stringy". However, when a critical temperature, known as Hagedorn temperature, is approached the picture radically changes. Model calculations show solutions involving a winding condensate [665], which allows an interpretation as a gas of (hot) strings. Relatedly, already earlier it was speculated that very small black holes turn into highly excited strings at the Hagedorn temperature [666]. For recent results and more literature on the black hole/string transition see [667,668].

Particularly interesting black string/brane configurations are the supersymmetric (BPS) solutions. These BPS solutions are always extremal and have the lowest possible mass (tension) for a given set of conserved $p$-form charge (densities) quantized in integer units. Therefore, BPS configurations are stable and cannot decay. Moreover, being supersymmetric means that they are (generically) protected against quantum corrections: while these are found as solutions/normalizable states for $g_s \lesssim 1$ theory, they remain solutions/normalizable states for $g_s \gtrsim 1$. So, we know a part of the Hilbert space of the strongly coupled theory.

This latter property provides a mechanism to analyze or at least count black hole microstates: Let us consider a BPS configuration at weak coupling comprising an almost free gas of strings and branes. As we increase the string coupling they form a BPS bound state which has the same $p$-form charges. This BPS state can be an extremal black hole of the same charges which has a non-zero entropy. This string theory description, as we will see next, provides a good handle on the black hole microstate problem. In the next two subsections, we discuss two families of BPS string theory black holes. As a useful text, we refer the reader to [543,669].

### 9.3.1 D1-D5-P System

It appears that the supergravity solutions corresponding to BPS brane/string systems with one or two kinds of $p$-form charges have either vanishingly small or a singular horizon and hence are not the best examples for considering simple microstate countings, see e.g. [654]. For these one- or two-charge solutions, the geometries may acquire microscopic horizons once we consider $\alpha'$ corrections. The first non-trivial semiclassical example with a macroscopically large horizon to consider is a three-charge system.

One of the most commonly studied three-charge black hole configurations consists of $N_1$ intersecting D1-branes wrapping an $\mathrm{S}^1$-cycle and $N_5$ D5-branes wrapping $\mathrm{T}^4\times\mathrm{S}^1$, together with $P$ momentum modes (GW) along the $\mathrm{S}^1$. These give rise to a $5d$ black hole background in 10-dimensional type IIB string theory on $\mathrm{T}^4\times\mathrm{S}^1$. Let the $\mathrm{T}^4$ be along $X^a$, $a = 6, 7, 8, 9$ with cycles of radii $R_a$ and volume $V_4$ and the $\mathrm{S}^1$ be along $X^5$ and of radius $R$; hence, D1-branes have their worldvolume along $X^0$, $X^5$ and D5-branes along $X^0, X^5, \ldots, X^9$. The $5d$ spacetime is then spanned by $X^0$, $X^i$, $i = 1, 2, 3, 4$. The Einstein-frame[3] metric corresponding to the $5d$ D1-D5-P black hole system is [543]

$$\mathrm{d}s^2 = -\left(H_1(r)H_5(r)H_{\mathrm{P}}(r)\right)^{-2/3}\mathrm{d}t^2 + \left(H_1(r)H_5(r)H_{\mathrm{P}}(r)\right)^{1/3}\left[\mathrm{d}r^2 + r^2\,\mathrm{d}\Omega_3^2\right] \tag{9.4}$$

$$H_1(r) = 1 + \frac{r_1^2}{r^2}, \qquad H_5(r) = 1 + \frac{r_5^2}{r^2}, \qquad H_{\mathrm{P}}(r) = 1 + \frac{r_{\mathrm{P}}^2}{r^2} \tag{9.5}$$

[3] Readers unfamiliar with the Einstein-frame should consult Appendix I.

where

$$r_1^2 = N_1 g_s l_s^2 \left(\frac{l_s^4}{V_4}\right), \qquad r_5^2 = N_5 g_s l_s^2, \qquad r_{\rm P}^2 = P g_s^2 l_s^2 \left(\frac{l_s^6}{V_4 R^2}\right). \tag{9.6}$$

Some further comments are in order:

- The full supergravity solution also involves a non-trivial profile for the dilaton $\Phi$ and the Ramond-Ramond 2-form field, which we do not present here, as we do not need them for our analysis.
- The above solution corresponds to delocalized (smeared) D1-branes along the $\mathrm{T}^4$ directions. The momentum modes (GW) are moving along the $X^5$ directions while delocalized along $\mathrm{T}^4$.
- The above solution is 1/8 BPS, i.e. it preserves 4 real supercharges (out of the 32 supercharges of the original IIB theory). When one of the charges $N_1$, $N_5$, or $P$ vanishes, the solution becomes 1/4 BPS, and when two of the charges are zero the solution is 1/2 BPS.
- This solution is a marginal bound state of the three ingredients (D1-D5-P) and hence its ADM mass

$$M_{\rm ADM} = \frac{P}{R} + \frac{N_1 R}{l_s^2 g_s} + \frac{N_5 R V_4}{l_s^6 g_s} \tag{9.7}$$

  is the sum of the three individual contributions.
- In general, one may replace $\mathrm{T}^4$ with another 2-dimensional Calabi–Yau manifold, namely K3. In this case the solution becomes 1/16 BPS.
- The above is a solution to supergravity, which in general receives $g_s$ or $\alpha'$ higher derivative corrections. So, as a string theory background one should discuss the validity of supergravity approximation: (i) weakly curved background $r_1, r_5, r_{\rm P} \gtrsim l_s$, (ii) perturbative strings $g_s \ll 1$, (iii) $V_4 \gtrsim l_s^4$, $R \gtrsim l_s$. These imply $N_1 N_5 P \gg 1$.

The $5d$ black hole (9.4) is extremal and its horizon is at $r = 0$. Its surface gravity is zero and its horizon area is

$$A_{\rm H} = 2\pi^2 (r^6 H_1(r) H_5(r) H_{\rm P}(r))^{1/2}\big|_{r=0} = 2\pi^2 r_1 r_5 r_{\rm P}\,. \tag{9.8}$$

Recalling (9.3), the $5d$ Newton constant is

$$16\pi G_{\rm N} = \frac{(2\pi)^3 g_s^2 l_s^8}{2\pi R V_4}\,. \tag{9.9}$$

Therefore, the BH entropy

$$S_{\rm BH} = \frac{A_{\rm H}}{4G_{\rm N}} = 2\pi\sqrt{N_1 N_5 P} \tag{9.10}$$

remarkably is independent of $g_s$ and $V_4$, $R$. It is given by a product of three integers and hence cannot receive (quantum) corrections. This is in contrast to the ADM mass of the solution (9.7). Cancellation of all extra non-integer moduli is in fact a manifestation of BPS-protection discussed above. The entropy of generic black holes is expected to depend also on the moduli and continuous parameters.

**Near horizon geometry**

One may study the metric (9.4) in the near horizon limit $r \to 0$. In this limit, one may drop the 1 in the harmonic functions $H_i$ (9.5) to obtain $H_1(r)H_5(r)H_{\rm P} \simeq (\frac{L}{2\rho})^3$ where $L^3 := r_1 r_5 r_{\rm P}$, $r^2 = 2L\rho$. Since $\rho \lesssim r_i^2/L$, the metric (9.4) takes the form of an $\mathrm{AdS}_2\times \mathrm{S}^3$ geometry.

$$\mathrm{d}s^2 = -\frac{4\rho^2}{L^2}\,\mathrm{d}t^2 + \frac{L^2}{4\rho^2}\,\mathrm{d}\rho^2 + L^2\,\mathrm{d}\Omega_3^2 \tag{9.11}$$

When $N_1 N_5 \gtrsim P$ the geometry may be viewed as a D1-D5 brane system wrapped on an $\mathrm{S}^1$ perturbed by turning on $P$ units of GW on the $\mathrm{S}^1$. The near horizon limit for the D1-D5 geometry in string frame for IIB theory on $\mathrm{T}^4$ is the constant dilaton $\mathrm{AdS}_3\times\mathrm{S}^3$ solution [88]. The geometry (9.4) may then be viewed as the BPS deformation of the $\mathrm{AdS}_3\times\mathrm{S}^3$ by the GW [670,671].

### 9.3.2 Breckenridge–Myers–Peet–Vafa Solution

The D1-D5-P $5d$ black hole solution of the previous subsection is static. One may add two angular momenta along two circles on the $\mathrm{S}^3$, as in usual $5d$ MP black hole discussed in Sect. 7.5.2. A solution with two general angular momenta is not BPS; the BPS solution comes with two equal angular momenta $J$. This solution was first constructed and studied in [672]. The metric for the $10d$ type IIB uplift of the solution is of the form [671,673]

$$\begin{aligned}\mathrm{d}s^2 = \frac{1}{\sqrt{H_1(r)H_5(r)}}\left(-\,\mathrm{d}t^2 + \mathrm{d}y^2 + \frac{r_{\rm P}^2}{r^2}(\mathrm{d}t-\mathrm{d}y)^2 - \frac{\hat{J}}{r^2}\sigma_3(\mathrm{d}t-\mathrm{d}y)\right)\\ + \sqrt{H_1(r)H_5(r)}\,(\sum_{i=1}^{4}\mathrm{d}x_i\,\mathrm{d}x_i) + \sqrt{\frac{H_1(r)}{H_5(r)}}\,\mathrm{d}s_4^2\end{aligned} \tag{9.12}$$

where

$$\sum_{i=1}^{4}\mathrm{d}x_i\,\mathrm{d}x_i = \mathrm{d}r^2 + r^2\,\mathrm{d}\Omega_3^2\,. \tag{9.13}$$

The functions $H_1(r)$, $H_5(r)$ are given in (9.12), $\mathrm{d}s_4^2$ is the metric over a $\mathrm{T}^4$ or $\mathrm{K}_3$, $y$ is a direction along a circle of radius $R$, and $\sigma_3$ is a 1-form on the $\mathrm{S}^3$ defined as,

$$\mathrm{d}\Omega_3^2 = \frac{1}{4}(\mathrm{d}\theta^2 + \sin^2\theta\,\mathrm{d}\phi^2 + \sigma_3^2)\,, \qquad \sigma_3 = \mathrm{d}\psi - \cos\theta\,\mathrm{d}\phi\,, \tag{9.14}$$

with $\theta \in [0, \pi]$, $\phi \in [0, 2\pi]$, $\psi \in [0, 4\pi]$.

This geometry is 1/16 BPS and is specified by four integer parameters $N_1, N_5, P, J$, where $J = \frac{\pi \hat{J}}{4G_{\mathrm{N}}}$ with $G_{\mathrm{N}}$ given in (9.9). For $J = 0$ case this is the $10d$ uplift of (9.4). One may reduce the solution over $\mathrm{T}^4\times\mathrm{S}^1$ to obtain a $5d$ solution. The horizon is at $r = 0$, has zero surface gravity, and the Bekenstein–Hawking entropy

$$S_{\mathrm{BH}} = \frac{A_{\mathrm{H}}}{4G_{\mathrm{N}}} = 2\pi\sqrt{N_1 N_5 P - J^2}\,. \tag{9.15}$$

## 9.4 Microstate Counting

As discussed, typical black holes in string theory, in some string duality frame, may be viewed as a collection of different kinds of intersecting D-branes and/or fundamental strings. The LEFT of the intersecting branes relevant to the black hole microstates typically gives rise to a $\mathrm{CFT}_2$ of a given central charge. Moreover, as discussed in Chap. 3, $\mathrm{AdS}_3$ gravity has BTZ black holes. Recalling the $\mathrm{AdS}_3/\mathrm{CFT}_2$ duality and Brown–Henneaux analysis, these black holes are hence expected to have a microscopic description in a $\mathrm{CFT}_2$. One can then use this general feature to perform microstate counting using the *Cardy formula* and give a microcanonical statistical mechanical description of the BH entropy.

### > Cardy formula and its corrections

The celebrated Cardy formula [674] counts the number of states in a $\mathrm{CFT}_2$, subject to some assumptions, like sparsity of the spectrum, see e.g. [675]. Here we present the statement and the main results; a sketch of the proof may be worked through in Exercises 9.6, 9.7 and a more detailed proof may be found in [676] and references therein.

Consider a *unitary, modular invariant* $2d$ CFT with a *mass gap* and discrete spectrum with left and right central charges $c_{\mathrm{L}}, c_{\mathrm{R}}$. States in this theory are labeled by the eigenvalues of left and right Virasoro generators $L_0, \bar{L}_0$. Let the values of these operators on the vacuum state of the theory on cylinder (torus) be $\Delta_0, \bar{\Delta}_0$. The density of states with left and right excitations $\Delta, \bar{\Delta}$ *in a saddle point approximation* $\Delta \gtrsim c \gtrsim 1$ is given as [676]

$$\rho(\Delta, \bar{\Delta}) \simeq \left(\frac{\pi^2}{3}\right)^2 \rho_0\, \tilde{c}_{\mathrm{L}}\tilde{c}_{\mathrm{R}} \cdot \frac{I_1(S_{\mathrm{L}}^0)}{S_{\mathrm{L}}^0}\,\frac{I_1(S_{\mathrm{R}}^0)}{S_{\mathrm{R}}^0} \tag{9.16}$$

where $\rho_0 = \rho_0(\Delta_0, \bar{\Delta}_0)$ is the degeneracy of the vacuum state,

$$\tilde{c}_{\rm L} = c_{\rm L} - 24\Delta_0\,, \qquad \tilde{c}_{\rm R} = c_{\rm R} - 24\bar{\Delta}_0\,, \tag{9.17a}$$

$$S^0_{\rm L} = 2\pi\sqrt{\frac{\tilde{c}_{\rm L}}{6}(\Delta - \frac{c_{\rm L}}{24})}\,, \qquad S^0_{\rm R} = 2\pi\sqrt{\frac{\tilde{c}_{\rm R}}{6}(\bar{\Delta} - \frac{c_{\rm R}}{24})}\,, \tag{9.17b}$$

and $I_1(x)$ is the modified Bessel function, so that $I_1(x) \sim \frac{1}{\sqrt{2\pi x}}e^x, \quad x \gg 1$.

The entropy in the microcanonical ensemble is then given by

$$S(\Delta, \bar{\Delta}) := \ln \rho(\Delta, \bar{\Delta}) \simeq S^0_{\rm L} + S^0_{\rm R} - \frac{3}{2}\ln S^0_{\rm L} - \frac{3}{2}\ln S^0_{\rm R} + \cdots \tag{9.18}$$

The terms

$$\boxed{S_{\rm Cardy} := S^0_L + S^0_R = 2\pi\sqrt{\frac{\tilde{c}_{\rm L}}{6}(\Delta - \frac{c_{\rm L}}{24})} + 2\pi\sqrt{\frac{\tilde{c}_{\rm R}}{6}(\bar{\Delta} - \frac{c_{\rm R}}{24})}} \tag{9.19}$$

are called Cardy formula. The next terms are logarithmic corrections to the Cardy formula and the ellipsis denotes exponentially suppressed corrections to the Cardy formula.

We conclude with further comments on the Cardy formula:

- In the saddle point approximation the entropy is just sum of entropies of left and right sectors; there are no terms mixing them.
- The temperature in the right and left sectors may be defined using the standard thermodynamical relations, as

$$\ell T_{\rm L} := \left(\frac{\partial S_{\rm L}}{\partial \Delta}\right)^{-1}, \qquad \ell T_{\rm R} := \left(\frac{\partial S_{\rm R}}{\partial \bar{\Delta}}\right)^{-1} \tag{9.20}$$

  where $\ell$ is an arbitrary scale in which we measure energy levels of the CFT. In an $AdS_3/CFT_2$ setup $\ell$ may be taken as $AdS_3$ radius.
- The central charge in the Cardy formula (9.19) appears through the combination $\tilde{c}$ (9.17a). For $CFT_2$ on the plane, $\Delta_0, \bar{\Delta}_0$ are typically zero and hence $\tilde{c} = c$; however, this is not true in general.
- The Cardy entropy and its subleading corrections are only functions of the left and right Cardy expressions (9.17b) and not individual $c$, $\Delta$'s.
- The entropy in the $\Delta \gg c$ case is proportional to the square root of $\tilde{c}\Delta$.
- States of a $CFT_2$ may also be labeled by their energy $E$ and angular momentum $J$, which are related to $\Delta, \bar{\Delta}$ as

$$\Delta - \frac{c_{\rm L}}{24} = \frac{1}{2}(E + J), \qquad \bar{\Delta} - \frac{c_{\rm R}}{24} = \frac{1}{2}(E - J)\,. \tag{9.21}$$

- For the chiral excitations when $E = |J|$, the entropy of the full system is the entropy of the remaining chiral sector.

### 9.4.1 Microstate Counting for BTZ Black Holes

The line element for BTZ black holes is given in (7.3), their mass, angular momentum, and other thermodynamic relations in (7.4)–(7.6). The Brown–Henneaux analysis yields $c_\text{R} = c_\text{L} = c = \frac{3\ell}{2G_\text{N}}$ and for the presumed dual $\text{CFT}_2$

$$\Delta - \frac{c}{24} = \frac{1}{2}(\ell M_\text{BTZ} + J_\text{BTZ}) = \frac{(r_+ + r_-)^2}{16\ell G_\text{N}}, \qquad \bar{\Delta} - \frac{c}{24} = \frac{1}{2}(\ell M_\text{BTZ} - J_\text{BTZ}) = \frac{(r_+ - r_-)^2}{16\ell G_\text{N}}. \tag{9.22}$$

Hence,

$$S_\text{L}^0 = \frac{\pi c(r_+ + r_-)}{6\ell}, \qquad S_\text{R}^0 = \frac{\pi c(r_+ - r_-)}{6\ell} \tag{9.23}$$

and the black hole entropy (neglecting subleading corrections) is of Cardy-type,

$$S_\text{Cardy} = S_\text{L}^0 + S_\text{R}^0 = \frac{\pi c r_+}{3\ell} = S_\text{BTZ} = \frac{2\pi r_+}{4G_\text{N}} = S_\text{BH} \tag{9.24}$$

see (7.5) and [677].

Remarkably, this result does not rely on string theory or supersymmetry. It is only assuming that the BTZ geometry has effectively a dual description in terms of $\text{CFT}_2$ at Brown–Henneaux central charge (7.23). This dual description need not be precise. In other words, the BTZ geometry is effectively like a thermal state in the Brown–Henneaux CFT. A more precise description may reveal small deviations from a thermal distribution.

We also comment on the logarithmic corrections to the Cardy formula. The factor $-3/2$ in (9.18) is required by the modular invariance and is the correction we find in the *microcanonical* description. In the *grand canonical* description, in which temperature and horizon angular velocity, or temperatures in the left and right sectors, are fixed, there is no logarithmic correction, see e.g. [430,678,679]. The details of the derivation are given as an exercise; the final result is [676]

$$S_\text{g.can.} = \frac{\pi^2}{3}(c_\text{L} T_\text{L} + c_\text{R} T_\text{R}) + O(e^{-\frac{\pi^2}{3} c_\text{L} T_\text{L}}) + O(e^{-\frac{\pi^2}{3} c_\text{R} T_\text{R}})\,. \tag{9.25}$$

In particular there is no logarithmic correction once we write the entropy in terms of the temperatures.

### 9.4.2 Microstate Counting for D1-D5-P and Breckenridge–Myers–Peet–Vafa Black Hole

As discussed, within the geometry associated with the near horizon limit of the D1-D5-P system there is an extremal BTZ black hole excitation of $\text{AdS}_3 \times \text{S}^3 \times \text{T}^4$ geometry over an $\text{S}^1$ inside $\text{AdS}_3$ (see Exercise 9.4). The latter geometry is the near horizon limit of the D1-D5 system and dual to a $\text{CFT}_2$ with central charge $c = 6N_1N_5$

[88,554] (see Exercise 9.4). Within this picture, the $P$ units of GW correspond to a chiral excitation of this CFT by $\Delta = P$, $\bar{\Delta} = 0$. Then, using the Cardy formula (9.19) obtains $S_{\rm L}^0 = 2\pi\sqrt{N_1 N_5 P}$, $S_{\rm R}^0 = 0$. Therefore, we recover the BH entropy (9.10) as the leading order contribution to the Cardy formula. To be able to use the Cardy formula we assumed $P \gtrsim N_1 N_5 \gg 1$. Nonetheless, one can argue that what is actually needed is $N_1 N_5 P \gg 1$, since one can use another string duality frame (e.g. via IIB S-duality) if $P$ is not large, where now the central charge is given by $6PN_5$ and $N_1$ is the excitation.

For the Breckenridge–Myers–Peet–Vafa black hole one can perform a similar analysis and finds that (9.12) in the near horizon limit becomes an extremal BTZ$\times$ $\mathrm{S}^3_q \times \mathrm{T}^4$ geometry, where $\mathrm{S}^3_q$ is the squashed three-sphere. That is, turning on angular momentum squashes the three-sphere and hence changes the central charge of the dual CFT$_2$ to $c = 6N_1 N_5\sqrt{1 - \frac{J^2}{N_1 N_5 P}}$, see Exercise 9.4 for more details. The excitation of the CFT$_2$ has $\Delta = \frac{6R^2 r_{\rm P}^2}{c r_1^2 r_5^2}$, $\bar{\Delta} = 0$. Using the Cardy formula (9.19) then recovers the Breckenridge–Myers–Peet–Vafa entropy (9.15).

We close this part with three remarks. In our discussions above we connected the D1-D5-P or Breckenridge–Myers–Peet–Vafa black holes with a CFT$_2$ and used the Cardy formula (9.19) for the microstate counting in which we did not explicitly use supersymmetry or details of string theory. However, the fact that the geometries (9.4) or (9.12) are good string theory backgrounds where stringy corrections are absent or under very good control relies on supersymmetry. Moreover, preconditions of the Cardy formula, i.e. the existence of a dual CFT$_2$ at a given central charge which is unitary, modular invariant, and has a discrete spectrum, are guaranteed through the string theory construction of AdS/CFT. So, string theory was at least implicitly used in microstate counting. In addition, as we shall see in the next section, supersymmetry, and string theory, while not crucial for microstate counting, can be used to provide a picture of what the microstates really are. This stringy picture also provides a method to compute the logarithmic corrections of the black hole as well. They, too, match with the log-corrections to the Cardy formula [430,680,681].

## 9.5 Microstate Identification, Fuzzball and Fluffball Proposals

The Strominger–Vafa idea, while very effective in the counting of certain BPS black hole microstates, sheds little light on what these microstates are in a (strongly coupled) gravitational description where we have the black hole (rather than a gas of uncoupled BPS microstates), nor it is useful in addressing the information puzzle. For the latter, we need to reliably go beyond supersymmetric BPS black holes and have a more detailed microscopic description of the microstates in the range of the coupling where the black hole form (and e.g. not in a weakly coupled regime where we have a free gas of strings/branes). In this section, we review and discuss two proposals for microstate identification/construction, the fuzzball, and fluffball proposals. These two are qualitatively and presumably also conceptually different, in the sense that the former is more within the framework of string theory and what this theory of QG offers and the latter is more within the semiclassical framework and does not rely on any a full QG description.

### 9.5.1 Fuzzball Proposal, Microstate Geometries

According to the fuzzball proposal [654] a black hole is an ensemble of $e^{S_{\rm BH}}$ *horizonless smooth microstate geometries*. The horizon of a black hole is then an effective outcome of the superposition of these microstate geometries. In this framework, QG effects are not confined to the Planck length and typical microstate geometries have non-trivial structures up to the scale of the horizon; these microstates fill up the inside horizon region.

While this proposal and its main idea can be stated without resorting to a specific theory of QG, it is strongly based on string theory observations in which fundamental degrees of freedom are not (quantum) fields but extended objects like strings and branes which besides the "center of mass" degree of freedom also have internal energy levels and winding modes over the compact part of the internal space. Microstate geometries are a gas of such states involving both center of motion (like what we have in ordinary gases) and internal excitations and windings. The effective size associated with each microstate depends on the amount of internal excitation, which can be much larger than the basic length scale in the problem, $l_s$. Therefore, the stringy uncertainties and fuzziness do not remain confined to the string scales $l_s$ but grow with the number of charges (or excitations) [666,682]. A similar intuition and picture is compatible with the Cardy formula and does not rely on every detail of string theory: In a CFT of central charge $c$ the gap between energy levels goes like $1/(lc)$ where $l$ is a fundamental length scale in the problem; in string theory examples $l \sim l_s$ and the fuzziness for a state of energy $E$ is growing like $\sqrt{lc/E}$. For the example of the D1-D5-P system discussed in the previous section, this fuzziness scale is of the order of the horizon size of the associated BTZ black hole.

Within the fuzzball proposal, the information puzzle can be addressed in a rather simple manner: Radiation from non-extremal black holes does not happen by a pair production process from the vacuum, but rather is a result of the (weak) interactions between each microstate geometry with the fields outside. This is much like the blackbody radiation from a usual quantum thermal system, which is the result of interactions of microstates of the system with the electromagnetic field quanta. So the information from the would-be Hawking pair is stored in the microstate geometries. Moreover, this proposal addresses the firewall issue in a simple way: As described, the Hawking process at each and every step is a unitary process and if the original black hole was in a pure state the density matrix of the whole system (black hole+radiation) always remains a pure state with vanishing von Neumann entropy. According to the fuzzball proposal, the firewall (as well as the non-unitarity and the Page curve [442,656]) is an artifact of insisting on a semiclassical picture in which the system is separated into a black hole and outside+radiation subsystems, which is not allowed as quantum (gravity) effects appear on scales as large as the horizon size.

The above ideas and descriptions sound interesting but should be substantiated by explicit constructions and computations. Details may be found in [654,683–688] and references therein. Here we give a short account for the simplest two-charge D1-D5 system. As mentioned, this system does not have a finite size macroscopic horizon. Nonetheless, $\alpha'$-corrections lead to a microscopic horizon with non-vanshing entropy. The string theory construction of this system yields the entropy $S = 2\pi\sqrt{2N_1 N_5}$, e.g. see [654] and references therein. Now let us verify whether we can account for $e^S$ microstate geometries. Consider the D1-D5 system whose basic metric is (9.12) with $r_{\mathrm{P}} = \hat{J} = 0$. One can then promote this basic solution to a general family of BPS solutions to type IIB supergravity. The metric for this microstate geometries in the string frame is [686,687],

$$
\mathrm{d}s^2 = \frac{h}{\sqrt{f_1 f_5}}\left[-(\mathrm{d}t-\mathcal{A})^2 + (\mathrm{d}y-\mathcal{B})^2\right] + \sqrt{f_1 f_5}\,(\sum_{i=1}^{4}\mathrm{d}x_i\,\mathrm{d}x_i) + \sqrt{\frac{f_1}{f_5}}\,(\sum_{i=1}^{4}\mathrm{d}z_a\,\mathrm{d}z_a) \tag{9.26}
$$

where $y \equiv y + 2\pi R$, $z_a$ are periodic coordinates on a $\mathrm{T}^4$, $\mathcal{A} := A_i\,\mathrm{d}x^i$, $\mathcal{B} := B_i\,\mathrm{d}x^i$ are two 1-forms over $x^i$ space, and

$$
A_i = -\frac{r_5^2}{L}\int_0^L \mathrm{d}v\,\frac{F_i'(v)}{|\mathbf{x}-\mathbf{F}(v)|^2}, \qquad C_a = -\frac{r_5^2}{L}\int_0^L \mathrm{d}v\,\frac{G_a'(v)}{|\mathbf{x}-\mathbf{F}(v)|^2}, \tag{9.27}
$$

$$
f_5 = 1 + \frac{r_5^2}{L}\int_0^L \mathrm{d}v\,\frac{1}{|\mathbf{x}-\mathbf{F}(v)|^2}, \qquad h = \frac{f_1 f_5}{f_1 f_5 - C_4^2} \tag{9.28}
$$

$$
f_1 = 1 + \frac{r_5^2}{L}\int_0^L \mathrm{d}v\,\frac{F_i' F_i' + G_a' G_a'}{|\mathbf{x}-\mathbf{F}(v)|^2} - \frac{\sum_{a=1}^{3} C_a^2}{f_5} \tag{9.29}
$$

with $v = t - y$ and

$$
L = \frac{2\pi r_5^2}{R}, \qquad r_1^2 = \frac{r_5^2}{L}\int_0^L \mathrm{d}v\,|\mathbf{F}'|^2\,. \tag{9.30}
$$

Finally, $\mathrm{d}\mathcal{B} = -\star_4\,\mathrm{d}\mathcal{A}$, where $\star_4$ is the Hodge star over the $4d$ $x^i$-space.

This solution is specified by $F_i(v)$, $G_a(v)$, which are, respectively, two $4d$ vector fields over $x_i$ and $z_a$ directions and may be viewed as two curves in these directions. Smoothness of these geometries at $\mathbf{x} = \mathbf{F}(v)$ requires that $F_i'(v)$ and $G_a'(v)$ do not have zero modes [686]. Moreover, these geometries do not have a horizon and we may choose the origin of the $x^i$ space such that $\int_0^L \mathrm{d}v\,\mathbf{F}_i' = 0$. The above eight-function family of solutions are microstate geometries and one may count them using geometric quantization [689], yielding the same counting as in string theory [686]. If we had not considered the $G_a(v)$ functions, we would have missed some of the microstates arriving at $S_{\mathrm{Rychkov}} = 2\pi\sqrt{2N_1 N_5/3}$ [689]. As we see, the internal part of the solution, the $\mathrm{T}^4$ part, plays a crucial role in capturing the microstate geometries. So, a non-trivial test of the proposal is to repeat this analysis for the solution in which $\mathrm{T}^4$ is replaced by $\mathrm{K}_3$ [686,687].

A more critical test of the proposal appears in the construction of microstate geometries for three-charge cases where we have macroscopic classical horizon size. So far we do not have a construction that captures all microstate geometries for this case, see [683] for a recent account. Given the explicit form of (some of) the microstate geometries, one may compute the greybody factors (cf. Sect. 6.4.5) and Hawking radiation rate, and explore black hole evaporation and resolution to the information puzzle in the fuzzball setup. See [654, 683–685, 687] and references therein for more detailed discussions.

We close this part with some recurring questions in the fuzzball program: Can it be implemented consistently within (super)gravity or do we need information beyond this? Does (super)gravity suffice to give a full account of all microstate geometries? How should we superpose microstate geometries to obtain a (super)gravity solution of finite-horizon size? It seems that a full realization of the fuzzball proposal requires information beyond (super)gravity and detailed QG (string theory) information is needed [687]. In cases where we have dual CFT descriptions like D1-D5-P system, this information may be provided through the dual CFT.

### 9.5.2 Soft Hair Proposal and Its Fluffball Realization

Another idea for addressing the information puzzle and microstate identification is the *soft hair* proposal [114, 690]. According to this proposal, a black hole as seen by an outside observer is not completely and uniquely described by the ADM charges. There is additional 'hair' for a black hole of given ADM charges. This hair is 'soft' in the sense that turning it on does not change the ADM charges; the soft hair is labeled by conserved charges that commute with the ADM charges. However, in order for the soft hair to play the role of microstates, there should be a finite set of them for a given value of ADM charges. Moreover, to be relevant for the resolution of the information puzzle they should unitarily interact with non-soft modes (the Hawking radiation quanta) such that the information in the soft modes can also be transferred to the Hawking radiation quanta.

Recalling the basic theorems of Chap. 3, in particular the uniqueness theorems, the crucial question is whether black holes can in principle possess such soft hair in the first place and how to bypass these theorems. To answer it, we note that these theorems are basically a result of the EP, which manifests itself in the diffeomorphism invariance of the theory and the fact that the EOM define well-posed dynamics. So, to accommodate any extra information we need to amend/refine the EP in presence of a horizon that acts as the causal boundary for outside observers, see [691] and references therein. As discussed in Chap. 5, this is a general feature of any generic gauge/diffeomorphism invariant theory in presence of boundaries: there are two kinds of gauge transformations, proper ones that do not change the physical state, and non-proper ones that act non-trivially on the physical state. The latter can be used to label the boundary data. Here, by boundary, we mean a general codimension-1 surface in the spacetime, which may be spacelike (a constant time slice), null or timelike. Examples of these, respectively, are boundaries of asymptotically dS, flat, and AdS spaces. For the case of black holes the horizon can also be viewed as another null boundary [692, 693]. In other words, in presence of boundaries (e.g. a horizon), there are boundary degrees of freedom whose role is to guarantee physically prescribed boundary conditions as well as accounting for the degrees of freedom corresponding to the excised part of the spacetime (behind the boundary). These boundary degrees of freedom only reside at the boundary but can interact with themselves and with the bulk degrees of freedom. These interactions are specified by the gauge invariance of bulk+boundary theory. This picture is very familiar in the context of electromagnetic theory formulated in a box. The boundary conditions are fixed by the electromagnetic properties of the box (e.g. conductance tensor) and boundary degrees of freedom manifest themselves through the boundary currents, see e.g. [694,695]. Also quantum Hall physics applies the concept of boundary excitations due to non-proper gauge symmetries, see e.g. [696].

Even before moving to particular constructions/formulations of the soft hair proposal, already at the level of general ideas, we see some qualitative and conceptual differences between this proposal and the fuzzball proposal. The soft hair idea tries to realize a semiclassical description for black hole microstates and the information puzzle whereas the fuzzball program crucially requires QG features. In the former, the horizon is the distinctive sign of black holes and plays an important role whereas in the latter the horizon is not evidently a special place but merely outcome of microstate superposition. For the soft hair proposal, the region inside the black hole need not play a special role while in the fuzzball it is the region where the microstates reside. It is also instructive to compare soft hair and membrane paradigm: The soft hair may be viewed as a more microscopic description/realization of the membrane fluid [697].

The solution phase space analysis in Sect. 5.3 provides the appropriate framework to formulate the soft hair proposal. As already discussed there, configurations in the solution phase space are labeled by two distinct sets of charges: the exact symmetry charges (like the ADM charges) and those associated with non-trivial gauge transformations, and these two sets of charges commute. This is the basic property we need for the realization of the soft hair idea. The drawback, however, is that the algebra of the latter set of charges is infinite-dimensional and has infinite-dimensional representations. Therefore, we have way too much soft hair. So additionally, we need to provide a haircut consistent with the solution phase space framework. In other words, the soft hair must be rendered slightly non-soft so that one cannot keep adding soft hair excitations ad infinitum. Doing this in a controlled way is not trivial. In the rest of this section, we briefly discuss a specific proposal that does the job.

**> Fluffball proposal, explicit construction of soft hair microstates**

The most precise formulation of soft hair microstates has been constructed for BTZ black holes in pure $AdS_3$ gravity. This construction has three essential parts [698, 699]:

1. **Near horizon algebra and Hilbert space.** The near horizon algebra consists of two $u(1)$ currents [584,585]:

$$[\mathcal{J}_n^{\pm}, \mathcal{J}_m^{\pm}] = \frac{n}{2}\delta_{n+m,\,0}\,, \qquad [\mathcal{J}_n^{\pm}, \mathcal{J}_m^{\mp}] = 0\,, \tag{9.31}$$

with $(\mathcal{J}_n^{\pm})^{\dagger} = \mathcal{J}_{-n}^{\pm}$. The near horizon Hilbert space is constructed by the repeated action of creation operators $\prod_{n_i>0}\mathcal{J}_{-n_i}^{\pm}$ on the vacuum state $|0\rangle$, defined through

$$\mathcal{J}_n^{\pm}|0\rangle = 0\,, \qquad \forall n \geq 0\,. \tag{9.32}$$

We note that $\mathcal{J}_0^{\pm}$, which commute with all the other $\mathcal{J}$, play the role of left and right sectors Hamiltonian of the near horizon observer [584]. Therefore, all states in the near horizon Hilbert space have vanishing $\mathcal{J}_0^{\pm}$ eigenvalues and are soft.

2. **Asymptotic algebra and Hilbert space.** The asymptotic symmetry algebra is the Brown–Henneaux Virasoro charges $\boldsymbol{L}_n^{\pm}$, which may be written in terms of an asymptotic current algebra $\boldsymbol{J}_n^{\pm}$

$$\begin{aligned} \boldsymbol{L}_n^{\pm} &:= in\boldsymbol{J}_n^{\pm} + \frac{6}{c}\sum_{m\in\mathbb{Z}} :\boldsymbol{J}_{n-m}^{\pm}\boldsymbol{J}_m^{\pm}: \\ [\boldsymbol{J}_n^{\pm}, \boldsymbol{J}_m^{\pm}] &= \frac{nc}{12}\delta_{n+m,\,0}\,, \qquad [\boldsymbol{J}_n^{\pm}, \boldsymbol{J}_m^{\mp}] = 0\,, \end{aligned} \tag{9.33}$$

where $c = \frac{3\ell}{2G_{\mathrm{N}}}$ is the Brown–Henneaux central charge. One can show that the $\boldsymbol{L}_n^{\pm}$ generate two Virasoro algebras

$$[\boldsymbol{L}_n^{\pm}, \boldsymbol{L}_m^{\pm}] = (n-m)\boldsymbol{L}_{n+m} + \frac{c}{12}n^3\,\delta_{n+m,\,0}\,, \qquad [\boldsymbol{L}_n^{\pm}, \boldsymbol{L}_m^{\mp}] = 0\,. \tag{9.34}$$

The asymptotic Hilbert space is then constructed by taking $(\boldsymbol{J}_n^{\pm})^{\dagger} = \boldsymbol{J}_{-n}^{\pm}$, $n \neq 0$ and defining the asymptotic vacuum state $|J_0^{\pm}; 0\rangle$ as

$$\boldsymbol{J}_0^{\pm}|J_0^{\pm}; 0\rangle = \frac{c}{6}J_0^{\pm}|J_0^{\pm}; 0\rangle, \qquad \boldsymbol{J}_n^{\pm}|J_0^{\pm}; 0\rangle = 0\,, \qquad \forall n > 0\,. \tag{9.35}$$

The $\boldsymbol{J}_0^{\pm}$ are not necessarily Hermitian and $J_0$ can take imaginary and real values. The asymptotic Hilbert space has two classes of states: (i) Global AdS+conic defects $\mathcal{H}_{\mathrm{CG}}$ for which $J_0^{\pm} = i\nu/2$, $\nu \in (0, 1]$ (with $L_0^{\pm} := (J_0^{\pm})^2 \in [-\frac{1}{24}, 0)$), and (ii) BTZ geometries $\mathcal{H}_{\mathrm{BTZ}}$ for which $J_0 \in [0, \infty)$ ($L_0^{\pm} \geq 0$), as depicted in Fig. 9.2. The value $\nu = 1$ describes global $\mathrm{AdS}_3$ spacetime and $\nu \neq 1$ particles on $\mathrm{AdS}_3$. Of course, these are single particle/black holes states, and in general in the Hilbert space we can have multi-particle states, too. They do not have a straightforward geometric interpretation, but are easily constructed algebraically. A BTZ black hole of mass $M$ and angular momentum $J$, is then a state $|\Delta^{\pm}\rangle_{\mathrm{BTZ}}$

$$\boldsymbol{J}_n^{\pm}|\Delta^{\pm}\rangle_{\mathrm{BTZ}} = J_0^{\pm}|\Delta^{\pm}\rangle_{\mathrm{BTZ}}\,\delta_{n,0}, \qquad J_0^{\pm} := \sqrt{\frac{6\Delta^{\pm}}{c}} = \sqrt{\frac{3(\ell M \pm J)}{c}}. \tag{9.36}$$

3. **Relating asymptotic and near horizon Hilbert spaces to identify microstates.** We have introduced above two Hilbert spaces which are apparently distinct. These two can be (or physically, should be) *identified* by an appropriate matching, which in the fluffball proposal is conjectured to be given by

$$\boldsymbol{L}_n^{\pm} := \frac{1}{c}\sum_{p\in\mathbb{Z}} : \mathcal{J}^{\pm}_{nc-p}\boldsymbol{\mathcal{J}}^{\pm}_{p} : \tag{9.37}$$

See [699] for detailed discussions. A BTZ black hole state $|\Delta^{\pm}\rangle_{\rm BTZ}$ then corresponds to a collection of semiclassical microstates in the near horizon Hilbert space,

$$\boxed{|\Delta^{\pm}\rangle_{\rm BTZ} = \prod_{n_i^{\pm}>0}(\boldsymbol{\mathcal{J}}^{+}_{-n_i^{+}}\cdot\boldsymbol{\mathcal{J}}^{-}_{-n_i^{-}})|0\rangle\,, \qquad \sum_i n_i^{\pm} = c\Delta^{\pm}\,.} \tag{9.38}$$

As pointed out above, all states in the near horizon Hilbert space, including $|\Delta^{\pm}\rangle_{\rm BTZ}$ are soft they have vanishing $\boldsymbol{\mathcal{J}}_0^{\pm}$. We hence have an explicit realization of the soft hair proposal. Nevertheless, the second equality (9.38) provides a cutoff on the soft hair spectrum, since the soft hair excitations are not soft with respect to the Virasoro charges (9.37).

**Counting microstates.** As a check, one may count the microstates for a BTZ black hole of given $\Delta^{\pm}$. Equation (9.38) provides the answer, recalling the Hardy–Ramanujan counting [700]: the number of possible partitions of a given positive integer $N$ into non-negative integers $p(N)$ for $N \gg 1$ is $p(N) = \frac{1}{4N\sqrt{3}}\exp(2\pi\sqrt{\frac{N}{6}})$, see Exercise 9.11. Therefore, the black hole entropy, $\ln(p(c\Delta^{+})\cdot p(c\Delta^{-}))$ for $c\Delta^{\pm} \gg 1$, is given by

$$S_{\rm BTZ} = 2\pi\sqrt{\frac{c\Delta^{+}}{6}} + 2\pi\sqrt{\frac{c\Delta^{-}}{6}} + \cdots \tag{9.39}$$

This, to the leading order, matches perfectly the earlier results (9.18). In addition, a careful analysis taking into account the statistical mechanics ensemble reveals also matching of the log-corrections [699], see also Exercise 9.12.

---

The above construction is based on two mild assumptions. (1) The Brown–Henneaux central charge is quantized in positive integers; (2) The deficit angle $\nu$ is quantized in units of $1/c$: $\nu = r/c,\ r = 1, 2, \ldots, c$. These are Bohr-like quantization conditions and may be an outcome of a full quantum theory, if available. For example, in the D1-D5-P system the central charge is $6N_1N_5$, which is an integer. In the same system, various string dualities also imply quantization of mass of $AdS_3$ particles and hence quantization of the deficit angle $\nu$.

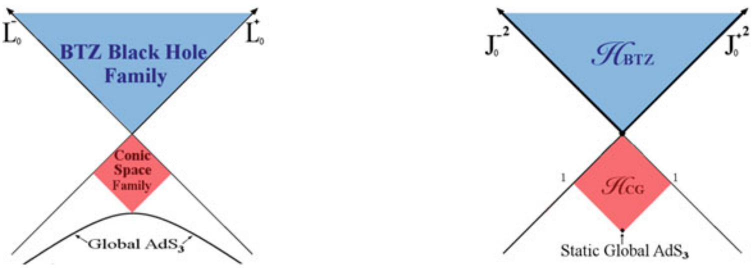


**Fig. 9.2** The asymptotic Hilbert space, in two representations, “Virasoro basis” (left) and “current $J$ basis” (right) [699]

We close this part with some further comments. We have *constructed* BTZ black hole microstates as coherent superpositions of a gas of (weakly interacting) particles on $AdS_3$ in a semiclassical description, without resorting to a full QG formulation. While simple atypical microstates may have a geometric description (e.g. as conical defect geometries), a general microstate, which is a multi-particle state, does not have geometric realization. Thus, even though our construction was inspired by near horizon geometry as a segue to algebraic considerations, typical microstates do not have an obvious geometric interpretation for a near horizon observer. By contrast, an asymptotic observer has a clear geometric interpretation as BTZ black hole, but does not have semiclassical access to the precise microstate. Moreover, there is a “particle-black hole” duality, in the sense that two sectors of the asymptotic Hilbert space depicted in Fig. 9.2 are mapped to each other as described above. All these states belong to the near horizon Hilbert space and are hence soft hair, as discussed above. See [699] for more discussions. Our explicit construction here is for $AdS_3$, but a similar line of ideas may in principle work for more realistic $4d$ black holes. The example of extremal Kerr has been worked out in [701].

## 9.6 Information Puzzle and AdS/CFT

AdS/CFT provides a non-perturbative definition of QG that manifestly preserves unitarity (at least if the dual CFT is unitary—see Chap. 8, or [702, 703] and refs. therein for examples of non-unitary holography). As such the black hole formation and evaporation should in principle admit a unitary description. So the main question here is how to manifestly formulate this “in principle”-description and uncover the missing ingredient in Hawking’s semiclassical derivation.

Conversely, on the CFT side, it can be instructive to show how information can be apparently lost by taking suitable limits that mimic the semiclassical approximation on the gravity side. A particular example along this line was studied in $AdS_3/CFT_2$ in [704] where the collapse of a spherical shell was set up in the dual $CFT_2$. Taking the semiclassical limit amounts to sending the central charge of the $CFT_2$ to infinity. It has been shown that unitarity is indeed violated in the $CFT_2$ in the $1/c$ expansion if non-perturbative corrections are dropped.

As discussed in the previous chapter, we have small black holes in AdS that do not reach thermal equilibrium with their own Hawking radiation. These black holes are similar to asymptotically flat black holes and AdS/CFT is not of practical help. For large AdS black holes, which reach thermal equilibrium and a stationary phase with their own Hawking radiation, AdS/CFT can provide good handles. For these black holes, the main question is not about the unitarity of the description at a fully-fledged quantum level, which is guaranteed by the setup, but whether there is a semiclassical description that respects other basic features like locality and smoothness of the geometry (near the horizon) and if yes, how precisely this semiclassical description is formulated. For eternal black holes that do not evaporate, one needs to reformulate the information puzzle. Here we briefly discuss such a reformulation within the thermofield double [580]. The idea is to perturb a thermofield doubled state and explore what happens to it within time scales $t$ much larger than the temperature $1/\beta$, in $t/\beta \gg 1$.

In a unitary CFT any perturbation around a thermal state should always carry the information that it is a perturbation of a thermal state; it should never "fully thermalize". As discussed in Sect. 8.3.2, in the CFT side this perturbation may be probed by the two-sided correlator $P = \langle \mathrm{TFD}|\mathcal{O}_L(0, \mathbf{x})\tilde{\mathcal{O}}_R(t, \mathbf{y})|\mathrm{TFD}\rangle$, where $\mathcal{O}_L$ and $\tilde{\mathcal{O}}_R$ may encode perturbations on the left or right CFT's around a thermofield double state, respectively inserted at $(0, \mathbf{x})$ and $(t, \mathbf{y})$; see Exercise 9.9 for more analysis. If the cluster decomposition and locality in the *gravity* description holds, then for $t/\beta \gg 1$, $P_{\text{gravity}} \sim e^{kt/\beta}$ where $k$ is some constant. That is, $P_{\text{gravity}}$ exponentially decays and the state becomes arbitrarily close to a thermal state. On the other hand, the same computation within a *unitary thermal CFT* is expected to yield, $P_{\text{CFT}} \sim e^{\tilde{k}S}$ where $S$ is the entropy and $\tilde{k}$ is some constant. While $P_{\text{CFT}}$ is exponentially suppressed by the entropy, it does not decay with time $t$. So, for $t/\beta \gg 1$, $P_{\text{CFT}} \gg P_{\text{gravity}}$.

This apparent puzzle, which may be viewed as a reformulation of the information puzzle, can be remedied if the assumptions yielding the gravity result can be relaxed. One of these assumptions is locality of the gravity description. The other one is overlooking the non-perturbative contributions to the gravity side of order $e^{-1/G_{\text{N}}} \sim e^{-S}$. Indeed, as discussed in Sect. 8.3.3, there exist thermal AdS and eternal AdS black hole saddle points, and the former can contribute to $P_{\text{gravity}}$. There may be other saddle points (Euclidean wormhole type saddles) that can also contribute. This description does not tell us how the information could be retrieved in (quantum) gravity but gives an idea of where to look for it.

Other related issues, like the firewall paradox and the recent discussions of islands in the context of Hawking radiation (see Sects. 6.9 and 9.2) can also be made more precise and addressed using AdS/CFT, see the literature quoted in these sections.

## Further Reading

While string theory is currently the leading candidate for a theory of QG, there are other QG proposals that we did not discuss, e.g. loop quantum gravity [705–707], asymptotic safety [708] or causal dynamical triangulation [709]. See [710,711] for a bird's eye view of various approaches to QG and [712] for a review of options that avoid quantizing gravity and the associated challenges.

For more on black hole microstate counting within string theory see [606,713–715].

For more on subleading corrections to the Cardy formula (the Farey-tail expansion) see [716].

For discussion on fuzzball versus firewall see [717–719].

For AdS/CFT and black hole information puzzle see Thomas Hartman's lecture notes, available at the webpage http://www.hartmanhep.net/topics2021/ or Daniel Harlow's lecture notes [131]. See [626,627] for recent discussions on thermofield double and realization of horizons in the dual CFT description. The Snowmass White Paper on "Quantum aspects of black holes and the emergence of spacetime" [720] provides a comprehensive guide to some of the more recent literature.

## Exercises

**9.1 Ensemble dependence of log corrections.**

Show that the number $N$ in the logarithmic corrections to the entropy (9.1) depends on the thermodynamic ensemble that is used. In particular, show the relation

$$S_{\mathrm{c}} = S_{\mathrm{mc}} + \frac{1}{2}\ln\big(CT^2\big) + \dots$$

where $S_{\mathrm{c}}$ is the canonical entropy, $S_{\mathrm{mc}}$ the microcanonical entropy, $C$ the specific heat and $T$ the temperature.

**9.2 Double-copy for black holes.**

Scattering amplitudes show a remarkable double-copy mechanism that relates (color-stripped) amplitudes in Yang–Mills theory to gravitational amplitudes, see [721] and refs. therein. Convince yourself that this double-copy mechanism can be extended to black holes by considering the following steps.

(1) Take the Maxwell equations $\partial_\mu F^{\mu\nu} = j^\nu$ with the abelian current $j^\nu = -gv^\nu\delta^{(3)}(\boldsymbol{x})$, where $g$ is the magnitude and $v^\nu = (1, \boldsymbol{0})$ the 4-velocity of the point charge in its rest frame. Show that in a suitable gauge the gauge connection is given by

$$A^\mu = \frac{g}{4\pi r}\,k^\mu \qquad r^2 = \boldsymbol{x}^2$$

with the null vector

$$k^\mu = \big(1,\ \frac{\boldsymbol{x}}{r}\big)\,.$$

(2) Make the double-copy replacement

$$g \to \kappa M \qquad\qquad k_\mu \to k_\mu k_\nu$$

in the connection $A_\mu$ to construct a symmetric 2-tensor (the non-perturbative graviton)

$$h_{\mu\nu} = \frac{\kappa M}{4\pi r} k_\mu k_\nu$$

and show that the sum of Minkowski metric plus non-perturbative graviton,

$$g_{\mu\nu} = \eta_{\mu\nu} + h_{\mu\nu}$$

is the Schwarzschild metric for a black hole of mass $M$ in Kerr–Schild form (see also Exercise 2.39; fix the gravitational coupling constant $\kappa$ suitably).

(3) Show that the double-copy mechanism works also for the sources, i.e. show that the distributional energy-momentum tensor

$$T^{\mu\nu} = M v^\mu v^\nu \delta^{(3)}(\boldsymbol{x})$$

plugged into the Einstein equations yields the Schwarzschild metric as a solution (if you have solved Exercise 2.30 this should be straightforward).

Note: This exercise shows that the Schwarzschild black hole is a double-copy of the Coulomb solution. For a discussion of other black holes from a double-copy perspective see [722].

**9.3 No cloning theorem.**

Assume the Hilbert space factorizes, $H = H_E \otimes H_B$, where $H_E$ corresponds to the Hilbert space characterizing the exterior of the black hole and $H_B$ the Hilbert space characterizing the black hole interior. Assume further that black hole complementarity implies $H_E = H_B$. Prepare the system such that the initial state is given by the product state $|\iota\rangle_A \otimes |o\rangle_B$. Using the axioms of quantum mechanics, prove that there is no unitary operator $U$ obeying

$$U\big(|\iota\rangle_A \otimes |o\rangle_B\big) = e^{i\phi}\,|\iota\rangle_A \otimes |\iota\rangle_B$$

for any real number $\phi$ (which may depend on $\iota$ and $o$) and for all normalizable states $|\iota\rangle$, $|o\rangle$. This statement is known as "no cloning theorem".

**9.4 Microstate counting for rotating black holes.**

(1) Starting from (9.12) at $r_\mathrm{p}$, $\hat{J} = 0$, show that in the near horizon limit (dropping 1 in the harmonic functions $H_1$, $H_5$) we obtain $\mathrm{AdS}_3 \times \mathrm{S}^3 \times \mathrm{T}^4$ geometry where $\mathrm{AdS}_3$ and $\mathrm{S}^3$ radii are both equal to $\ell^2 = r_1 r_5$.

(2) Show that the central charge of the dual $2d$ CFT is then

$$c = \frac{3\ell}{2G_\mathrm{N}^{(3)}} = 6 N_1 N_5, \tag{9.40}$$

where $G_\mathrm{N}^{(3)} = \frac{g_s l_s^8}{4V_4\ell^3}$ is the Newton constant of the $3d$ gravity obtained from reduction of the $10d$ theory over $\mathrm{S}^3 \times \mathrm{T}^4$.

(3) One may then turn on $r_{\mathrm{p}}$ while $\hat{J} = 0$. Show that the geometry becomes that of Extremal BTZ$\times$ $\mathrm{S}^3 \times \mathrm{T}^4$, where the horizon radius of the extremal BTZ is $r_{\mathrm{p}} R/\ell$, where $R$ is the radius of the circle in $y$ direction.

(4) Last, one may turn on both $r_{\mathrm{p}}$, $\hat{J}$. Show that the geometry becomes that of Extremal BTZ$\times$ $\mathrm{S}^3_q \times \mathrm{T}^4$ where the radius of $\mathrm{AdS}_3$ is $\ell$ and horizon radius is $r_{\mathrm{p}} R/\ell$ as before and $S_q$ is that of an squashed sphere,

$$\mathrm{d}s_{\mathrm{S}_q} = \frac{\ell^2}{4}(\mathrm{d}\theta^2 + \sin^2\theta \mathrm{d}\phi^2 + q^2\sigma_3^2), \qquad q^2 = 1 - \frac{\hat{J}^2}{\ell^4 r_{\mathrm{p}}} = 1 - \frac{J^2}{N_1 N_5 P}. \quad (9.41)$$

Show that performing the reduction to $3d$, the Newton constant now becomes $G_{\mathrm{N}}^{(3)} = \frac{g_s^2 l_s^8}{4V_4 \ell^3 q}$ and hence the central charge (9.40) becomes $c = 6N_1 N_5 q$.

**9.5 Microstate counting for four-charge 4*d* BPS black holes.**

Consider the $4d$ extremal black hole described by the Einstein-frame metric,

$$\mathrm{d}s^2 = -F(r)^{-1/2}\mathrm{d}t^2 + F^{1/2}(r)\left(\mathrm{r}^2 + r^2\mathrm{d}\Omega^2\right), \qquad F(r) = H_1 H_2 H_3 H_4$$

with $H_i = 1 + \frac{Q_i}{r}$. This is a solution to Einstein-$U(1)^4$ dilaton theory and may be obtained from dimensional reduction of $10d$ type IIA theory (cf. Appendix I), corresponding to configuration of branes consisting of D2,D6, NS5 branes together with KK monopoles. See [543] for more details.

(1) Compute the BH entropy of the above four-charge solution and show it is

$$S_{4-charge} = \frac{\pi\sqrt{Q_1 Q_2 Q_3 Q_4}}{2G_{\mathrm{N}}} = 2\pi\sqrt{N_2 N_6\ N_5 N_w}$$

where $N_2, N_6, N_5$, and $N_w$ are respectively number of D2, D6, NS5, and KK monopoles that constitute the black hole solution.

(2) Given the brane IIA construction mentioned above, repeat Strominger-Vafa counting and obtain the above entropy as the Cardy entropy of a 2d CFT. See [723, 724] for more details.

**9.6 Cardy formula from modular invariance.**

Consider a Euclidean $\mathrm{CFT}_2$ on a torus with coordinates $(\tau, \sigma) \sim (\tau, \sigma + 2\pi) \sim (\tau + \beta, \sigma)$ with a vacuum state that is gapped from the rest of the spectrum. Assume the gap is given by the usual Casimir energy as determined from the central charge $c$. The goal of this exercise is to evaluate the partition function

$$Z[\beta] = \mathrm{Tr}\, e^{-\beta H}$$

in the limit of high temperature, $T = \beta^{-1} \to \infty$.

(1) Consider first the opposite limit, $\beta \to \infty$, and argue that the partition function projects to the ground state

$$\lim_{\beta\to\infty} Z[\beta] \approx e^{-\beta E_0}$$

where $E_0 = -\frac{c}{12}$ is the (free) energy of the gapped vacuum.

(2) Prove the low-high temperature duality $\beta \leftrightarrow 4\pi^2/\beta$ upon exchanging the two cycles $\tau$ and $\sigma$, accompanied by a suitable dilatation.

(3) Combine (1) and (2) to obtain the high-temperature limit of the free energy,

$$\lim_{\beta\to 0} F \approx -\frac{\pi^2 c\, T^2}{3}$$

and show that this result is compatible with the Cardy formula.

**9.7 More on Cardy formula.**

(1) Given (9.18) and properties of Bessel functions verify (9.25).

(2) Show that to leading order for BTZ black hole,

$$T_{\rm R} = \frac{r_+ - r_-}{4\pi\ell}\,, \qquad T_{\rm L} = \frac{r_+ + r_-}{4\pi\ell}\,. \tag{9.42}$$

Note that for the extremal BTZ case with $r_+ = r_-$, $T_{\rm R} = 0$.

(3) Using (9.20) compute corrections to the left and right temperatures (9.42).

(4) Recalling (9.20), show that

$$\frac{2}{T_{\rm BTZ}} = \frac{1}{T_{\rm L}} + \frac{1}{T_{\rm R}}\,, \qquad \Omega_{\rm BTZ} = T_{\rm BTZ}\Big(\frac{1}{T_{\rm L}} - \frac{1}{T_{\rm L}}\Big)\,. \tag{9.43}$$

(5) Compute the microcanonical temperature $T_{\rm MC}^{-1} = \frac{\partial T_{\rm MC}}{\partial E}$ and show $\frac{\pi^2}{3}(c_{\rm L} + c_{\rm R})T_{\rm MC} = \frac{S_{\rm Cardy} I_1(S_{\rm Cardy})}{I_2(S_{\rm Cardy})}$, where $I_1$, $I_2$ are modified Bessel functions.

(6) To define the entropy in canonical formulation one should start from the partition function $Z(\beta_{\rm L}, \beta_{\rm R})$ where,

$$Z(\beta_{\rm L}, \beta_{\rm R}) = \int {\rm d}\Delta\, {\rm d}\bar\Delta\; \rho(\Delta, \bar\Delta)\; e^{-\beta_{\rm L}\Delta} e^{-\bar\Delta\beta_{\rm R}} \tag{9.44}$$

where $\rho(\Delta, \bar\Delta)$ is given in (9.16). Since $\rho$ in the saddle point approximation is product of left and right sectors, $Z = Z_{\rm L}(\beta_{\rm L}) \cdot Z_{\rm R}(\beta_{\rm R})$. That is in the saddle point approximation partition function of any unitary, modular invariant $2d$ CFT is *holomorphically factorizable*.

One can define left and right free energies as $F_{\rm L} = -T_{\rm L} \ln Z_{\rm L}$ and similarly for the right sector, where $T_{\rm L} = \frac{1}{\beta_{\rm L}}$. The total entropy in canonical ensemble is then

$$S_{\rm can} = \frac{\partial F_{\rm L}}{\partial T_{\rm L}} + \frac{\partial F_{\rm R}}{\partial T_{\rm R}}. \tag{9.45}$$

Verify that $S_{\rm can.}$ has the expression given in (9.25).

**9.8 Cardyology for different boundary conditions.**

This exercise investigates the Cardy-type counting for BTZ black holes in 3-dimensional Einstein gravity with different boundary conditions. You may work in the limit $\Delta \gg c_L$ and $\bar{\Delta} \gg c_R$.

(1) Convince yourself that the (holomorphic) microscopic density of states transforms with a Jacobian,

$$\rho(\tilde{\Delta}) = \frac{\partial \Delta}{\partial \tilde{\Delta}}\,\rho(\Delta)$$

where $\Delta$ is the left-moving energy for the theory with the original boundary conditions and $\tilde{\Delta}$ the corresponding quantity for the new boundary conditions. The full density of states is a product of left- and right-moving sectors, $\rho(\Delta, \bar{\Delta}) = \rho(\Delta)\bar{\rho}(\bar{\Delta})$.

(2) Assume the new boundary conditions imply $\tilde{\Delta} \propto \Delta^{(z+1)/2}$ with some $z \geq 0$ (and analogously for the right sector). Calculate the Jacobian in (1) and determine what the Cardy formula looks like for the new boundary conditions. Verify, in particular, that for $z \to 0$ the Cardy entropy scales linearly with $\tilde{\Delta}$.

(3) Verify that the density of states for near horizon boundary conditions ($z = 0$ case),

$$\rho(\tilde{\Delta}) = \frac{e^{2\pi\sqrt{\frac{c}{6}}\,\tilde{\Delta}}}{\sqrt{2\pi\,\tilde{\Delta}}}.$$

(4) Show that the Jacobian factor in (1) with the assumptions stated in (2) changes the log corrections to the entropy in microcanonical ensemble,

$$S(\tilde{\Delta}, \tilde{\bar{\Delta}}) = \ln \rho(\tilde{\Delta}, \tilde{\bar{\Delta}}) = S_L^0 + S_R^0 - \frac{2z+1}{2}\ln S_L^0 - \frac{2z+1}{2}\ln S_R^0 + \cdots$$

**9.9 Perturbing a thermofield double state.**

Consider a thermofield double state $|\mathrm{TFD}\rangle$. Perturb the state with an operator in the left CFT $O_L$.

(1) Argue that the perturbed state is described by $\widetilde{|\mathrm{TFD}\rangle} = (1 + \epsilon O_L)|\mathrm{TFD}\rangle$.

(2) Does $\widetilde{|\mathrm{TFD}\rangle}$ describe a thermal state?

(3) Probe $\widetilde{|\mathrm{TFD}\rangle}$ by an operator in the right CFT $\tilde{O}_R$. Show that the expectation value of this probe in the perturbed state in the leading order in $\epsilon$ is given by the two-point function in the unperturbed original thermofield double state, $\langle \mathrm{TFD}|O_L\tilde{O}_R|\mathrm{TFD}\rangle$.

**9.10 Twisted Sugawara construction.**

Starting with a $u(1)_k$ current algebra, $[J_n,\ J_m] = \frac{k}{2}\,\delta_{n+m,\,0}$, prove that the twisted Sugawara construction

$$L_n = \frac{1}{k}\sum_{p\in\mathbb{Z}} J_{n-p}J_p + in\beta\, J_n$$

yields a Virasoro algebra for the modes $L_n$ with central charge $c = 6k\beta^2$. By calculating $[L_n,\ J_m]$ verify whether or not $J$ is a primary field from a CFT$_2$ perspective.

**9.11 Partitions of integers and Hardy–Ramanujan formula.**

Define $p(n)$ as the number of different partitions of the integer $n$ into positive integers, e.g. $p(5)=7$ because $5=4+1=3+2=3+1+1=2+2+1=2+1+1+1=1+1+1+1+1$. Find a proof that for large $n$ the Hardy–Ramanujan formula,

$$p(n) \sim \frac{1}{4n\sqrt{3}} \exp\left(2\pi\sqrt{\frac{n}{6}}\right)$$

holds. Here is an outline of a proof idea that goes back to Newman [725].

(1) Define the generating function $f(z)=\sum_{n=0}^{\infty} p(n)z^n = \prod_{m=1}^{\infty}(1-z^m)^{-1}$, where $|z|<1$. Define also the auxiliary function

$$\phi(z) = \sqrt{\frac{1-z}{2\pi}} \exp\left(\frac{\pi^2}{12}\frac{1+z}{1-z}\right)$$

and interpret it as another generating function, $\phi(z)=\sum_{n=0}^{\infty} q(n)z^n$.

(2) Prove the inequality

$$|f(z)| < \exp\left(\frac{1}{1-|z|} + \frac{1}{|1-z|}\right)$$

by taking its logarithm and using the identity $\ln f(z) = \sum_{n=1}^{\infty} \frac{1}{n}\frac{z^n}{1-z^n}$.

(3) Prove the estimate $f(z)=\phi(z)[1+O(1-z)]$ for $|z|<1$ and $|1-z|\le 2(1-|z|)$, starting with the exponential map $z=e^{-w}$ such that

$$\ln f(z) = \sum_{n=1}^{\infty} \frac{1}{n(e^{nw}-1)} = \frac{\pi^2}{6w} + \frac{1}{2}\ln\left(1-e^{-w}\right) + \underbrace{w\sum_{n=1}^{\infty}\left(\frac{1}{nw(e^{nw}-1)} - \frac{1}{n^2w^2} + \frac{e^{-nw}}{2nw}\right)}_{O(1)} .$$

The most lengthy part is to show that the last term above is $O(1)$.

(4) Prove that $p(n)=q(n)+\dots$, where the ellipsis denotes term that behave not worse than $O(n^{-5/4}\exp(2\pi\sqrt{\frac{n}{6}}))$. To this end use the identity

$$p(n)-q(n) = \frac{1}{2\pi i}\oint_C \frac{f(z)-\phi(z)}{z^{n+1}}\,\mathrm{d}z$$

where the contour $C$ is the circle $|z|=1-\pi/\sqrt{6n}$.

(5) Finally, compute $q(n)$, starting with the Gaussian integral identity

$$\sqrt{2}\pi e^{\pi^2/12}\phi(z) = (1-z)\int_{-\infty}^{\infty} \exp\left(\pi t\sqrt{\frac{2}{3}} - (1-z)t^2\right)\mathrm{d}t .$$

**9.12 Hardy–Ramanujan and Cardy formula.**

Use the Hardy–Ramanujan formula of the previous exercise.

(1) Show that a partition function $\rho(\Delta, \bar{\Delta}) \sim p(n)\bar{p}(\bar{n})$ obeys the Cardy formula if the energies $\Delta$ ($\bar{\Delta}$) scale like the (large) integers $n$ ($\bar{n}$) in the Hardy–Ramanujan formula above.

(2) Calculate the logarithmic corrections in the Hardy–Ramanujan formula and show how they differ from the logarithmic corrections in the Cardy formula.

# Outlook

# 10

**Abstract**

In this final chapter, we start with a summary of our book in Sect. 10.1, continue with selected open conceptual issues that are the subject of ongoing research in Sect. 10.2 and then finish in Sect. 10.3 with future observational prospects.

## 10.1 Summary of the Book

It is sometimes said that the discovery of today is the tool of tomorrow and the background of the day after. The subject of black holes is currently in a transient phase between the discovery- and tool epochs and has not yet reached the background stage. A lot has happened since John Michell pondered, in 1783, what would occur if the escape velocity of a star exceeded the speed of light. The preceding nine chapters were our attempt to cover the most salient discoveries in black hole physics, as well as the most common tools therein and applications thereof. Before we venture into the unknown future, we briefly take stock of what we covered in our book.

Each chapter was organized similarly, commencing with a brief abstract and concluding with a brief paragraph on further reading, as well as a list of exercises. As mentioned in the introduction, we consider the exercises an integral part of our book. Students who use our book to teach themselves black hole physics are strongly encouraged to solve these exercises—not necessarily all of them, but at least half of them, depending on their specific research interests.

In Chap. 1, besides summarizing basic material like GR, we began with a brief history of black holes that we organized logically, but not necessarily chronologically. We then collected the evidence for black holes prior to any experimental discoveries, based on the collapse of stars. At least in retrospect, the considerations by Chandrasekhar and others provided the rationale for expecting the existence of black holes long before the community understood the physics of accretion disks, the GW emission of black hole mergers, or the intricate gravitational lensing effects leading to black hole shadows. We concluded this chapter by presenting three dif-

 
D. Grumiller and M. M. Sheikh-Jabbari, *Black Hole Physics*, Graduate Texts in Physics,
https://doi.org/10.1007/978-3-031-10343-8_10

ferent schools of thought concerning black holes (or, in fact, anything else), based on the premises ‘everything is geometry and symmetries’ (GR), ‘everything is particles and fields’ (HEP) and ‘everything is information and entanglement’ (quantum information).

In Chap. 2, we introduced the Schwarzschild solution and discussed its geodesics as well as its Carter–Penrose diagram. The later sections generalized these discussions to black holes with charge, angular momentum, black holes in (A)dS, and more exotic black holes, e.g. featuring the gravitational analog of a magnetic monopole. In the very end, we briefly mentioned non-stationary black holes as the first glimpse of time-dependent black hole solutions.

In Chap. 3 we took a more formal perspective than before, starting with the classic(al) definition of black holes for mathematical purposes and discriminating between several notions of horizons. We then summarized some key aspects of black hole theorems and how to prove them, including the Raychaudhuri equation, energy conditions, singularity-, horizon- and uniqueness theorems. We also introduced notions of asymptotic flatness and mentioned cosmic censorship. The final section highlighted the focusing equation and the area theorem, anticipating already aspects of black hole thermodynamics developed in later chapters.

In Chap. 4, we got black holes out of isolation and allowed them to interact with surrounding light, matter, and accretion disks, to be perturbed and ring quasinormally, to emit GW, and to form in the first place. We considered both perturbative and non-perturbative aspects, including black hole stability. These tools are crucial for black hole observations and phenomenology.

In Chap. 5, we introduced notions of (conserved) charges, like the traditional Komar charges or the (Wald-)entropy as Noether charge. This paved the way for the derivation of the four laws of black hole mechanics that describe convexity and conservation equations of these charges. Moreover, these four laws are in one-to-one correspondence with the four laws of thermodynamics, providing a classical incentive to view black holes as thermal states.

In Chap. 6, we studied semiclassical aspects of black holes, i.e. the quantization of fields on a black hole background. We started with general remarks on the variational principle and then summarized the Unruh- and the Hawking-effect. The latter finally established that indeed black holes are thermal systems with a characteristic (Hawking-)temperature and a gigantic (BH-)entropy, given for GR by one quarter of the area $A$ of the event horizon (in units of Newton’s constant $G_{\mathrm{N}}$).

$$\boxed{S_{\mathrm{BH}} = \frac{A}{4G_{\mathrm{N}}}} \tag{10.1}$$

We also re-derived aspects of this thermodynamic description in different ways and discussed the Parikh–Wilczek picture of black hole tunneling, as well as black hole evaporation and the membrane paradigm. The concluding section introduced the information puzzle, a recurring theme of later chapters, including this last one.

Inevitably, every book enjoys (or suffers from) an author’s bias. This may be particularly true for Chap. 7, where we considered black holes in various dimensions, starting with the lower ones. Gravity in three and two dimensions strikes an interesting balance between conceptual wealth and technical accessibility, allowing one to address some issues that are much harder to resolve in higher dimensions. Since research on both subjects is still evolving, we confined ourselves to well-established classical statements, but we stress that one of the main motivations for considering lower-dimensional gravity is its promise to teach us about QG. The final part of the chapter presented results for higher-dimensional black holes, as well as generalizations to black rings, black branes, and other black manifolds, addressing also the limit of GR in a large number of dimensions.

In Chap. 8, we explored the consequences of the holographic principle, in particular, its implementation in the form of the AdS/CFT correspondence. After formulating the basics, including the holographic dictionary for correlation functions and holographic renormalization, we stated the RT formula for holographic entanglement entropy and some of its consequences. We continued with the discussion of AdS black holes as thermal states in a dual CFT and the Hawking–Page phase transition. Asymptotic symmetries, which had featured as a precursor of AdS/CFT in seminal work by Brown and Henneaux, can be extended and applied to the near horizon region, which led to soft hair excitations of black holes. The next sections explored extremal black holes, the attractor mechanism, and the Kerr/CFT correspondence. Since the subject of holography is too rich and broad, we selected black hole-related topics, but to mitigate our inevitable omissions, our final section contained some pointers to key aspects of holography and its applications.

In Chap. 9, we hazarded into quantum aspects of black holes. Naturally, some of the material in this chapter has a different standard than the preceding chapters and the authors' selection bias is even more pronounced here. Our opening gambit consisted of general remarks about black holes and QG, followed by black hole complementarity and firewalls. Next, we focused on black holes in string theory and microstate counting. While counting black hole microstates and recovering the BH entropy is gratifying, eventually, we would also like to explicitly construct all (or at least typical) microstates. To this end, we discussed fuzzballs and fluffballs, but we hasten to add that neither of them is expected to be the last word on black hole microstates. We concluded with broad-brush aspects of the information puzzle in the context of AdS/CFT.

## 10.2 Open Conceptual Issues

There are interesting technical challenges in the theory and mathematics of black holes, which provide numerous worthwhile research avenues. We pointed to some of them in the final paragraphs on further reading in previous chapters, and in particular, in Sect. 9.1. Here we focus on three unresolved conceptual issues, all of which are subjects of ongoing research endeavors.

**Boundary and horizon degrees of freedom**

Sometimes insights are sharply peaked in time and a scientific revolution is imminent, like in the development of GR, quantum mechanics, or AdS/CFT. However, more often, the insights are reached more gradually, like for boundary and horizon degrees of freedom. After the shock provided by the BMS discovery of infinitely many translation-like symmetries in the 1960s [115,116] and the seminal work by Brown and Henneaux in the 1980s [483], it required the AdS/CFT correspondence in the late 1990s [88–90] to get a new perspective on these milestones: the asymptotic symmetries, acting on the classical phase space can be interpreted as global symmetries of the dual field theory.

The asymptotic symmetries generate non-proper diffeomorphisms that change the physical state. Therefore, even in the absence of bulk GW, there can exist boundary gravitons, also known as boundary degrees of freedom or edge states, see e.g. [540, 726,727] (the latter slang is borrowed from Quantum Hall physics, where these edge states feature prominently [696]).

After the turn of the millenium, numerous new insights led to a proliferation of this research avenue. Since then, our understanding of these symmetries has considerably evolved. Some specific topics are generalized asymptotically AdS boundary conditions [484,487,728], the AdS/log CFT correspondence [702,729], flat space holography [492,730,731], relations to memory effect and soft scattering [284,732], celestial holography [733,734] and, more recently, also near horizon symmetries [583,584,735–737] or more generally null boundary symmetries [404,693,738,739] and soft hair [114]. Each of these directions is the subject of ongoing research. In the remainder, we focus briefly on open questions regarding the last two.

In the context of classical black holes, a pressing issue is how the bulk degrees of freedom—the GW and matter—interact with the boundary degrees of freedom and how such interactions affect the charges associated with near horizon symmetries as well as their (non-)conservation. Besides theoretical interest, resolving this issue could be important for phenomenology. At the time of writing this chapter, the most up-to-date analysis is provided by [693].

It is tempting to speculate that near horizon symmetries and soft hair excitations may help to understand the black hole entropy [740] or even to construct semiclassical black hole microstates [698]. Whether or not such constructions work for Kerr black holes is an outstanding open issue.

**Information puzzle**

Despite several claims in the past decades that the information puzzle is finally solved, it remains an active area of research at the start of the 2020s. Holographic correspondences such as AdS/CFT in principle can be considered as solutions to the information puzzle, but just stating that the puzzle is solved and information is not lost does not explain several issues. For instance, what precisely is incorrect with the semiclassical arguments by Hawking, why do they break down, and how to avoid firewalls. Thinking about the information puzzle has engendered a wealth of new concepts and apparent paradoxes, which are spread over our book (see Sect. 1.2.3, 6.9, 9.5, and 9.6).

One of the key observations in this regard is the need to consider the black hole plus its radiation as parts of a single system, e.g. through the ER = EPR proposal [582]. It proposes that entanglement between the black hole and its Hawking radiation is captured by a Euclidean wormhole geometry, as briefly discussed in Sect. 8.3.3. The most recent incarnation of such a setup is the island proposal discussed in Sect. 9.2. The quantum Hilbert space associated with the full system involves various parts that are non-trivially entangled with each other, and the von Neumann entropy associated with this system is the quantity expected to follow the Page curve. If true, this provides a setting in which the quantum evolution of a black hole remains unitary, see [455] for a review.

A potential issue with the island proposal is that it may only work for massive gravity theories, as argued in [741]. See also [742] for a critical review of the island proposal. Thus, the status of the island proposal remains disputed at the time of concluding our book. Not intending to sound flippant, we hope the reader is not too surprised in case they witness at the time of reading this chapter a novel proposal on the market that solves the information puzzle or a new black hole paradox showing an apparent clash between GR and quantum mechanics.

**Black holes as a window to quantum gravity**

In Sect. 9.1, we already discussed some different bearings a theory of QG may have for black holes and their classical and semiclassical analysis. This part is meant to be a complement to the discussions in that section.

The idea that the metric or even the spacetime are not some fundamental objects, but rather emergent quantities is a common thread in numerous approaches to QG, and is inspired by the analogy to hydrodynamics, the effective theory of molecules at low energies. If correct, this idea is relevant for QG, since it indicates that trying to quantize the Einstein equations is as ill-guided as trying to quantize the Euler equations instead of quantizing its fundamental constituents, the molecules. If this line of thinking is pertinent, the obvious question seems ‘what is the analog of the molecules for QG’? Is it conformal bootstrap á la string theory or holographic qubits following RT or a tower of infinitely many Vasiliev-type higher spin-fields or all/none of the above? To make progress on such daunting questions, it is useful to have a simple system available where these issues are relevant. Quantum black holes seem tailor-made for this purpose.

Indeed, it is often said that black holes could play the same role in the development of QG as the hydrogen atom did in the development of quantum mechanics. While this seems a fair metaphor, it highlights a pressing conceptual and technical issue: so far, we do not know precisely how to define a black hole in a quantum mechanical context!

The mathematical definition we gave in Chap. 3 is meaningless since there are no event horizons in the full quantum theory of gravity—at least if information eventually escapes the black hole. So, unless the information is lost, horizons should not be the defining property of quantum black holes.

Thermal properties are a useful ingredient. Therefore, it is tempting to include the property of being a thermal state as part of the definition of a quantum black hole (to reiterate, by thermal state we mean a pure state that is exponentially close to a mixed state and indistinguishable from it through simple experiments). However, our universe has many thermal states that are not black holes, like Planck's photon gas in a box, stars, or the cosmic microwave background radiation. So thermality cannot be the only defining property of black holes.

Similar remarks may apply to other properties, such as the area law for entropy, the fast scrambling of black holes, their saturation of the chaos bound, etc. Every object is defined by the sum of its properties, so we need to figure out more about black holes and how to define them quantum mechanically.

## 10.3 Observational Prospects

As discussed in Chaps. 1 and 4, there are already many observational direct and indirect pieces of evidence for black holes with masses ranging from few solar masses to supermassive black holes of billions of solar masses. The possible mass range is yet wider in theoretical proposals and models, cf. Table 1.1. Our information about their spin and possibly their tidal Love numbers or higher moments [743] is still more limited than their mass [295,298,744–746].

Observational questions regarding black holes are generically aimed at answering three classes of questions: (1) their origins and how they have formed or can form; (2) emissions (electromagnetic or gravity wave) from systems involving black holes, and (3) how they impact their surroundings. These surroundings can be light (shadows, photon-spheres, lensing, and microlensing), accretion disks, other galaxies, or compact massive objects like neutron stars or other black holes in binary systems.

The messengers which carry the information about black holes and their impacts are typically electromagnetic waves with various frequencies, from microwave to X- and $\gamma$-rays, or GWs with frequencies of nano-Hz (in the NanoGrav experiment [747]) to 10–$10^4$ Hz (in the LIGO-VIRGO experiments). Upcoming ground-based advanced LIGO/VIRGO and KAGRA [64,65,748,749] or space-borne experiments such as LISA [750–752] and eLISA [753–757] will greatly advance *GW spectroscopy* in both frequency range and sensitivity of GW detection. This is a quickly evolving field, see e.g. [758–760] for recent reviews. Moreover, in the future, other light particles like axions or neutrinos may also be added to these messengers. We briefly mention some of the upcoming or ongoing searches below (Fig. 10.1).

**Black holes or heavy object mergers**

As discussed, merger of binary systems consisting of two compact stellar objects (white dwarfs, neutron stars, and black holes) typically yield a black hole plus a nearly monochromatic GW which may be accompanied by an electromagnetic emission (in

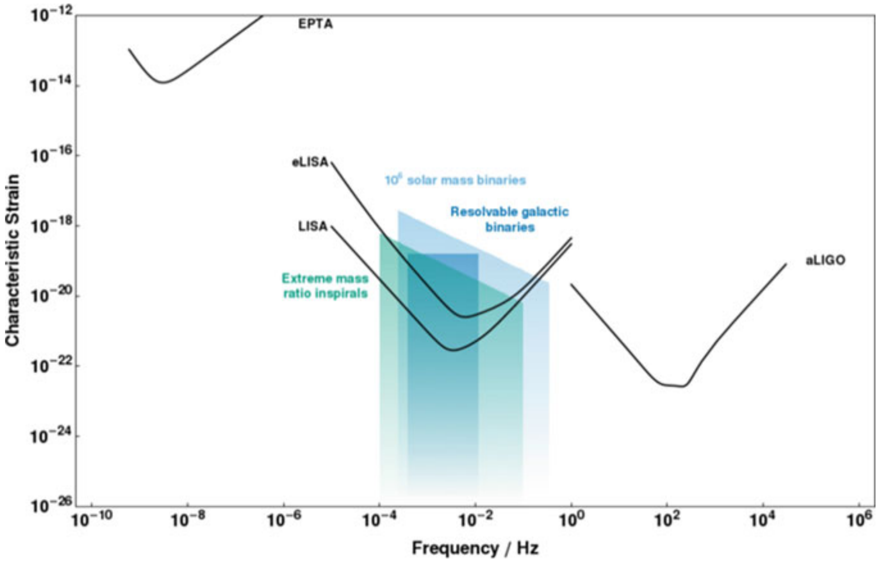


**Fig. 10.1** Sensitivity of LISA, eLISA, and advanced LIGO as a function of frequency. They lie in between the bands for ground-based detectors like advanced LIGO and pulsar timing arrays such as the European Pulsar Timing Array. The characteristic strain of potential astrophysical sources is also shown. To be detectable, the characteristic strain of a signal must be above the noise curve. *Source* Wikipedia

non-black hole-black hole mergers). The merger is then detected through the GW or photon emissions. Such binaries and mergers can be in our galaxy or other galaxies. Advanced LIGO/Virgo/KAGRA and LISA will be able to detect such mergers. Current observations show these mergers yield black holes in a wide mass range from a few $M_\odot$ to $180 M_\odot$ (see Fig. 10.2); the upper range may still increase in future observations.

A merger may involve two intermediate-mass black holes (with masses in a few $100 M_\odot$ range) or two supermassive black holes of masses $\gtrsim 10^6 M_\odot$. According to the most conservative population models, at least a few such supermassive black hole merger events are expected to happen each year. In November 2021, two coalescing supermassive black holes have been reported, where their merger is expected in 250 million years [761]. Mergers can also take place in extreme mass-ratio inspirals, consisting of a light stellar compact object ($< few\ M_\odot$) slowly falling onto more massive black holes of ($\gtrsim 100 M_\odot$) while emitting GWs. Extreme mass-ratio inspirals are expected to occur regularly in the centers of most galaxies and in dense star clusters and will be detectable by LISA.

As discussed, GWs emitted from binary mergers besides a dominant oscillatory signal (predominantly coming from the inspiral and ringdown phases), also have a non-oscillatory component that arises from the nonlinear memory effect [762]. The memory monotonically grows during the late inspiral and merger, modifying the signal by an almost step-function profile [763]. The nonlinear memory, while still

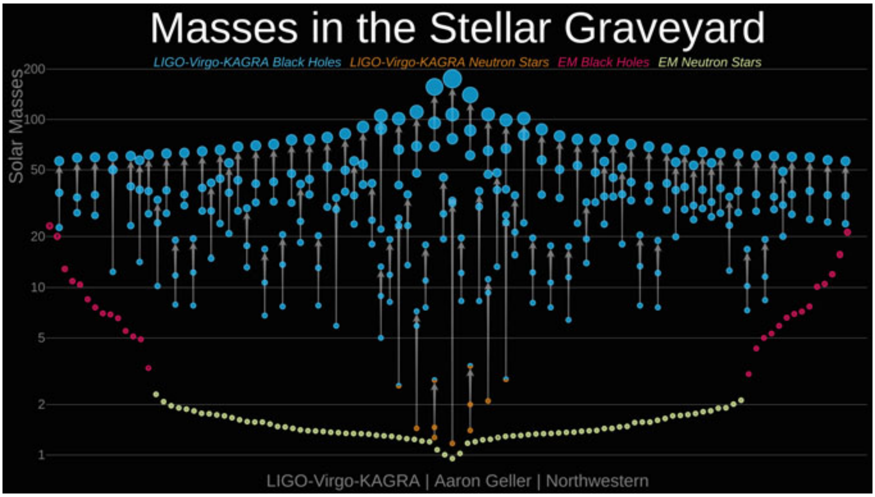


**Fig. 10.2** Masses of detected LIGO/Virgo compact binaries. This plot shows the masses of all compact binaries detected by LIGO/Virgo as of the end of 2021, with black holes in blue and neutron stars in orange. The purple and yellow dots respectively show stellar mass black holes and neutron stars discovered with electromagnetic observations. *Source* LIGO/Virgo-KAGRA collaboration. An interactive version of the plot may be found here

undetected in LIGO/Virgo [764], can be detectable in GW interferometers and pulsar timing array measurements [765,766].

### Primordial black holes

The evolution of the universe during inflation, reheating and through various phase transitions, may yield seeds for sub-solar mass black holes. These seeds (over-densities) can undergo gravitational collapse and form black holes of various sizes, from $10^{-5}$ g to $10^{50}$ g. Those smaller than $\sim 10^{15}$ g have a short Hawking evaporation lifetime and their abundance at formation is constrained by the effects of their Hawking radiation on big bang nucleosynthesis, the cosmic microwave background, the galactic and extragalactic $\gamma$, and cosmic-ray backgrounds [767]. Heavier PBHs are also constrained by their impact on gravitational lensing and imprints on the large-scale structure. PBHs may account for a part of the dark matter in the universe. Current data, including those from NanoGrav [768], and other GW detections [769], yield bounds on the masses of PBH and on the percentage of the dark matter PBH can constitute. The allowed mass ranges are $10^{17}$–$10^{23}$ g and, interestingly, also the stellar mass range 10–100$M_\odot$. In the latter range, PBHs can still account for a large fraction of dark matter. If PBHs exist, they provide a unique probe of the early universe.

### Black hole accretion disks

Accretion disks are one of the observational windows into the black holes that can reveal signatures of event horizons, ISCOs, and ergospheres. Theoretically, there

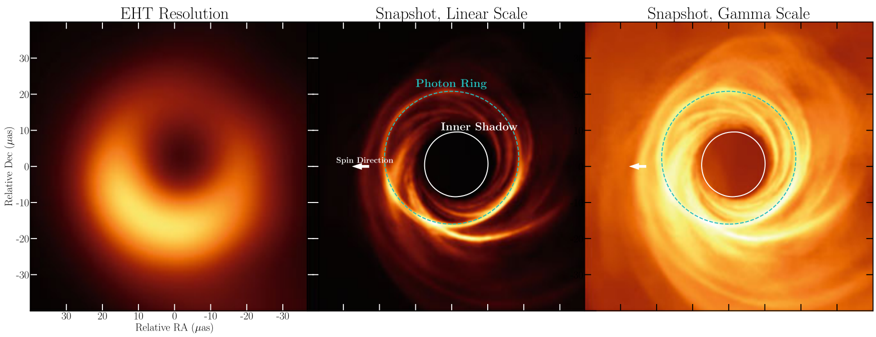


**Fig. 10.3** (Left) Snapshot image from a magnetically arrested radiative simulation of M87* [778], convolved with a circular Gaussian blurring kernel with a full width at half maximum of 15 micro arc-sec ($\mu$as), which at this resolution, qualitatively matches the first images of M87* from the EHT [779]. (Middle) The simulation snapshot at native resolution viewed at an inclination $\theta_o = 163$ deg where the black hole spin vector is oriented to the left and into the page [780]. The filamentary, turbulent structures, a central brightness depression, and a narrow, bright photon ring in this snapshot image closely track the theoretical critical curve (cyan curve). (Right) The same simulation snapshot in a gamma color-scale, accentuating low-brightness features. In this scale, the central brightness depression corresponds to the black hole's *inner shadow*, or the direct lensed image of the equatorial event horizon (white curve). The figure is taken from [777]

are four primary accretion disk models: Polish doughnuts (thick disks), Shakura–Sunyaev (thin) disks, slim disks, and advection-dominated accretion flows. Aspects of these models like stability, jets, spectral states, hardening of X-ray reflections and emissions, quasi-periodic oscillations, and their applications for black hole (or neutron star) mass and spin have been analyzed analytically and numerically [299,301,770,771]. These features and properties have been used to test the Kerr black hole and constrain deviations from Einstein gravity for various galactic and extragalactic black hole candidates. See [772–776] for reviews and recent progress reports.

### Black hole shadows and strong lensing

As discussed in Chaps. 1 and 4, black hole shadows and photon-spheres constitute a unique opportunity to probe black holes in regions very close to their horizon. As the next step, the EHT collaboration is going to extend their results obtained for the black hole in M87* ($M = 6.5 \pm 0.7 \times 10^9 M_\odot$) [26,279], to the supermassive black hole in the center of our galaxy. At the theoretical level, there are several studies on how the addition of matter fields (e.g. scalar hair) or deviations from Einstein gravity affects black hole shadows and photon-spheres. The EHT images released thus far do not resolve features like 'inner shadow' or 'photon ring' of M87* (see Fig.10.3). However, improvement in related observations may detect such features which can teach us more about the black hole mass and spin, see [777] for more analysis.

The era of black hole observations has just begun and will improve our understanding of black holes and the underlying theory of classical and quantum gravity.

# Variational Identities

# A

Consider small variations of the metric $\delta g_{\mu\nu}$ with $\delta^2 g_{\mu\nu} = 0$. Then we have the following variation identities (covariant derivatives are with respect to the reference metric $g_{\mu\nu}$, which is also used to move indices):

| | | |
|---|---|---|
| Inverse metric | $\delta g^{\mu\nu} = -g^{\mu\alpha} g^{\nu\beta}\, \delta g_{\alpha\beta}$ | (A.1) |
| Volume form | $\delta\sqrt{-g} = \frac{1}{2}\sqrt{-g}\, g^{\mu\nu}\, \delta g_{\mu\nu} = -\frac{1}{2}\sqrt{-g}\, g_{\mu\nu}\, \delta g^{\mu\nu}$ | (A.2) |
| Christoffels | $\delta\Gamma^{\lambda}{}_{\mu\nu} = \frac{1}{2} g^{\lambda\tau}\left(\nabla_\mu \delta g_{\nu\tau} + \nabla_\nu \delta g_{\mu\tau} - \nabla_\tau \delta g_{\mu\nu}\right)$ | (A.3) |
| Riemann tensor | $\delta R^{\lambda}{}_{\mu\tau\nu} = \nabla_\tau \delta\Gamma^{\lambda}{}_{\mu\nu} - \nabla_\nu \delta\Gamma^{\lambda}{}_{\mu\tau}$ | (A.4) |
| Ricci tensor | $\delta R_{\mu\nu} = \frac{1}{2}\left(\nabla^\lambda \nabla_\mu \delta g_{\lambda\nu} + \nabla^\lambda \nabla_\nu \delta g_{\lambda\mu} - g^{\lambda\tau} \nabla_\mu \nabla_\nu \delta g_{\lambda\tau} - \nabla^2 \delta g_{\mu\nu}\right)$ | (A.5) |
| Ricci scalar | $\delta R = \nabla^\mu \nabla^\nu \delta g_{\mu\nu} - g^{\mu\nu} \nabla^2 \delta g_{\mu\nu} - R^{\mu\nu}\, \delta g_{\mu\nu}.$ | (A.6) |

While Christoffel symbols are not tensors, their variation $\delta\Gamma^{\lambda}{}_{\mu\nu}$ is a tensor.

If the metric $g$ splits into boundary metric $h$ and normal vector $n$, see (6.4), these additional identities are useful:

| | | |
|---|---|---|
| Normal vector | $\delta n_\mu = \frac{1}{2} n_\mu n^\nu n^\lambda\, \delta g_{\nu\lambda}$ | (A.7) |
| Extrinsic curvature | $\delta K_{\mu\nu} = \frac{1}{2} n^\lambda n^\tau K_{\mu\nu}\, \delta g_{\lambda\tau} + n^\tau\left(n_\mu K^{\lambda}{}_{\nu} + n_\nu K_{\mu}{}^{\lambda}\right) \delta g_{\lambda\tau} - \frac{1}{2} h_\mu{}^\lambda h_\nu{}^\tau n^\sigma \left(\nabla_\lambda \delta g_{\sigma\tau} + \nabla_\tau \delta g_{\lambda\sigma} - \nabla_\sigma \delta g_{\lambda\tau}\right)$ | (A.8) |
| Trace thereof | $\delta K = -\frac{1}{2} n^\mu \left(\nabla^\nu \delta g_{\mu\nu} - g^{\lambda\tau} \nabla_\mu \delta g_{\lambda\tau}\right) - \frac{1}{2} K^{\mu\nu}\, \delta g_{\mu\nu} - \frac{1}{2}\mathcal{D}_\mu\left(h^{\mu\nu} n^\lambda \delta g_{\nu\lambda}\right)$ | (A.9) |

where $\mathcal{D}_\mu := h^\nu_\mu \nabla_\nu$ and $h_{\mu\nu} = g_{\mu\nu} n_\mu n_\nu$ is the induced metric on surface normal to $n^\mu$.



D. Grumiller and M. M. Sheikh-Jabbari, *Black Hole Physics*, Graduate Texts in Physics,
https://doi.org/10.1007/978-3-031-10343-8

Sometimes higher variations are needed. For the metric they vanish by assumption and for the inverse metric they can be deduced from further varying (A.1). All other higher variations can be determined from higher variations of Christoffel symbols.

$$\delta^n \Gamma^{\lambda}{}_{\mu\nu} = \frac{n}{2}\left(\nabla_\mu \delta g_{\nu\tau} + \nabla_\nu \delta g_{\mu\tau} - \nabla_\tau \delta g_{\mu\nu}\right) \delta^{n-1} g^{\lambda\tau}. \tag{A.10}$$

For example, the second variation reads

$$\delta^2 \Gamma^{\lambda}{}_{\mu\nu} = -\left(\nabla_\mu \delta g_{\nu\tau} + \nabla_\nu \delta g_{\mu\tau} - \nabla_\tau \delta g_{\mu\nu}\right) g^{\lambda\alpha} g^{\tau\beta}\, \delta g_{\alpha\beta}\,. \tag{A.11}$$

**Exercises**

**A.1 Verify appendix.**
Show all variation formulas in this appendix.

**A.2 Variational étude.**
Given a hypersurface with normal vector $n^\mu$ (with $n_\mu n^\mu = 1$) calculate the variation of its covariant divergence, $\delta(\nabla_\mu n^\mu)$, up to total boundary derivative terms $\mathcal{D}_\mu(\dots)$, where $\mathcal{D}_\mu := h^\nu_\mu \nabla_\nu$ and all free indices on which $\mathcal{D}_\mu$ acts must be projected to the boundary with $h_{\mu\nu} = g_{\mu\nu} n_\mu n_\nu$. Express the result entirely in terms of variations $\delta g_{\mu\nu}$.

**A.3 Gravitational Chern–Simons term.**
Vary the gravitational CS term $\epsilon^{\mu\nu\lambda}\Gamma^{\alpha}{}_{\mu\beta}(\partial_\nu \Gamma^{\beta}{}_{\lambda\alpha} + \frac{2}{3}\,\Gamma^{\beta}{}_{\nu\gamma}\Gamma^{\gamma}{}_{\lambda\alpha})$ with respect to the metric, where $\Gamma$ is the Christoffel connection, and show that, up to total derivative terms, the result is a tensor (known as 'Cotton-tensor').

**A.4 Maxwell stress tensor.**
Vary the gravitational Maxwell Lagrange-density $\sqrt{-g}\, F_{\mu\alpha} F_{\nu\beta} g^{\mu\nu} g^{\alpha\beta}$ with respect to the inverse metric and show that the resulting expression is proportional to the canonical Maxwell stress tensor.

**A.5 Lovelock equations of motion.**
Lovelock theories in $D$ dimensions are described by the Lagrangian

$$L = \sum_{n=0}^{[\frac{D-1}{2}]} \lambda_n \delta^{\alpha_1\cdots\alpha_n\mu_1\cdots\mu_n}_{\beta_1\cdots\beta_n\nu_1\cdots\nu_n}\; R^{\beta_1\nu_1}{}_{\alpha_1\mu_1} \cdots R^{\beta_n\nu_n}{}_{\alpha_n\mu_n} \tag{A.12}$$

where $\lambda_n$ are constant and $\delta^{\alpha_1\cdots\alpha_n\mu_1\cdots\mu_n}_{\beta_1\cdots\beta_n\nu_1\cdots\nu_n} = \delta^{[\alpha_1}_{[\beta_1} \cdots \delta^{\mu_n]}_{\nu_n]}$.
(1) Show that for $n = 0, 1$ the Lovelock Lagrangian respectively reduces to cosmological constant and Einstein–Hilbert term and for $n = 2$ we get Gauss–Bonnet term.

(2) Compute the EOM for this Lagrangian and show that they are of the form $X_{\mu\nu} := 0$, where $X_{\mu\nu}$ is symmetric and divergence-free, $\nabla^\mu X_{\mu\nu} = 0$.

(3) Show that $X_{\mu\nu} = 0$ are second-order differential equations. In fact, Lovelock has proved [463] that the above Lagrangians are the only ones in the family of $\mathcal{L} = \mathcal{L}(g_{\mu\nu}, R_{\mu\nu\alpha\beta})$ family whose EOM are second order.

(4) Work out the analog of Gibbons–Hawking–York boundary term for the Lovelock theories which guarantees Dirichlet boundary conditions for the metric.

# $p$-Forms

# B

Antisymmetric tensors with $p$ lower indices are also known as $p$-forms. It is common to write them without indices.

$$\Omega_p := \frac{1}{p!}\,\Omega_{\mu_1\mu_2\dots\mu_p}\;\mathrm{d}x^{\mu_1}\wedge\mathrm{d}x^{\mu_2}\wedge\dots\wedge\mathrm{d}x^{\mu_p}. \tag{B.1}$$

The wedge product

$$\mathrm{d}x^1\wedge\mathrm{d}x^2 := \mathrm{d}x^1\otimes\mathrm{d}x^2 - \mathrm{d}x^2\otimes\mathrm{d}x^1 \tag{B.2}$$

ensures total antisymmetry. If taken between a $p$ and a $q$-form it yields a $(p+q)$-form. In $D$ spacetime dimensions, we necessarily have $p \leq D$ due to total antisymmetry. The top-form with $p = D$ is also known as 'volume form'

$$\Omega_D = \frac{1}{D!}\,\Omega_{\mu_1\mu_2\dots\mu_D}\,\tilde{\epsilon}^{\mu_1\mu_2\dots\mu_D}\;\mathrm{d}x^D = \sqrt{-g}\,\frac{1}{D!}\,\Omega_{\mu_1\mu_2\dots\mu_D}\,\epsilon^{\mu_1\mu_2\dots\mu_D}\;\mathrm{d}x^D \tag{B.3}$$

where $\tilde{\epsilon}$ is the totally antisymmetric Levi-Civitá symbol (with values $\pm 1$ and 0), while $\epsilon$ is the corresponding tensor.

Cotangent vectors are 1-forms. A 1-form of particular interest is the de Rahm differential (or exterior derivative)

$$\mathrm{d} = \partial_\mu\;\mathrm{d}x^\mu\,. \tag{B.4}$$

It is common notation to suppress the wedge symbol when we act with the de Rahm differential on a $p$-form, thereby creating a $(p+1)$-form. As long as it acts on quantities that are sufficiently smooth (so that second derivatives commute), we have the identity

$$\mathrm{d}^2 = 0\,. \tag{B.5}$$



D. Grumiller and M. M. Sheikh-Jabbari, *Black Hole Physics*, Graduate Texts in Physics,
https://doi.org/10.1007/978-3-031-10343-8

The de Rahm differential obeys the Leibnitz rule,

$$\mathrm{d}\big(\Omega_p \wedge \Omega_q\big) = \big(\mathrm{d}\Omega_p\big) \wedge \Omega_q + (-1)^p \Omega_p \wedge \mathrm{d}\Omega_q \,. \tag{B.6}$$

The Poincaré lemma states that any closed $p$-form (with $p \geq 1$), $\mathrm{d}\Omega_p = 0$, is exact in a star-shaped region, $\Omega_p = \mathrm{d}\hat{\Omega}_{p-1}$.

The Hodge-star $*$ converts $p$-forms into $(D-p)$-forms.

$$*\,\Omega_p = \frac{1}{p!(D-p)!}\,\Omega_{\nu_1\ldots\nu_p}\epsilon_{\mu_1\ldots\mu_{D-p}}{}^{\nu_1\ldots\nu_p}\;\mathrm{d}x^{\mu_1} \wedge \cdots \wedge \mathrm{d}x^{\mu_{D-p}}. \tag{B.7}$$

It is involutive, $**\,\Omega_p = \pm\Omega_p$, where the sign depends on the form degree $p$, the spacetime dimension $D$, and the signature of the metric.

**Exercises**

**B.1 Maxwell equations in form language.**

Show that the equations $\mathrm{d}F = 0 = *\,\mathrm{d}{*F}$, with the exact 2-form $F = \mathrm{d}A$, are equivalent to the vacuum Maxwell equations.

**B.2 Instanton density.**

Show that in four spacetime dimensions the 4-form $F \wedge F$ is a total derivative term (known as instanton density). Here $F = \mathrm{d}A$ is the Maxwell field strength written as 2-form. Generalize your result to arbitrary even dimensions $D$ by considering $D/2$ wedge products between $F$.

**B.3 Helmholtz–Hodge decomposition.**

Define the adjoint operator $\delta := *\,\mathrm{d}*$ and the Laplacian $\Delta := \mathrm{d}\delta + \delta\,\mathrm{d}$ Show first that $\delta$ reduces the form degree by one while $\Delta$ maintains the same form degree. Then translate in three (Euclidean) dimensions the Hodge decomposition of 1-forms $A$, $A = \mathrm{d}\lambda + \delta\mu$, into traditional vector notation to recover the Helmholtz decomposition of a 3-dimensional vector into a gradient and a curl.

*Note:* In general dimensions and for general $p$-forms the Hodge decomposition, $A = \mathrm{d}\lambda + \delta\mu + h$, includes also a harmonic term $h$ obeying $\Delta h = 0$. The other two terms are called exact ($\mathrm{d}\lambda$) and co-exact ($\delta\mu$).

# Cartan Formulation

# C

According to the EEP, we can locally use a freely falling frame, sometimes called 'elevator frame' or 'orthonormal frame', where the relevant metric is not the spacetime metric $g_{\mu\nu}$ but rather the Minkowski metric $\eta_{ab}$. In order to do the same in tangent space, we introduce a quantity $e^a_\mu$, which allows converting spacetime indices $\mu$ (also known as 'curved' or 'holonomic' indices) locally into Minkowski indices $a$ (also known as 'flat' or 'anholonomic' indices), e.g. $v^a = e^a_\mu v^\mu$. When this is possible also globally the manifold is called 'parallelizable'; in this appendix, we work locally and do not assume anything about the global structure of the manifold.

Using the formalism of Appendix B, we define the 1-form

$$e^a = e^a_\mu(x^\nu)\ \mathrm{d}x^\mu \tag{C.1}$$

and refer to it as 'vielbein'.[1] Its inverse is a vector field, $e_a = e^\mu_a\,\partial_\mu$, and obeys the orthogonality and completeness relations

$$e^a_\mu e^\nu_a = \delta^\nu_\mu \qquad\qquad e^a_\mu e^\mu_b = \delta^a_b\,. \tag{C.2}$$

Curved (flat) indices are raised and lowered with the spacetime metric $g_{\mu\nu}$ (the Minkowski metric $\eta_{ab}$).

Since the norms of vectors should match regardless of whether we contract curved or flat indices, $v^2 = v^\mu v^\nu g_{\mu\nu} = v^a v^b \eta_{ab}$, the spacetime metric must be bilinear in

[1] The naming convention is dimension-dependent. 'Vielbein' is the generic expression ('viel' meaning 'many' and 'bein' meaning 'leg'), while in $D$ dimensions the expression is '$< D >$bein', where $< D >$ is the German word for the number $D$, i.e. 'einbein', 'zweibein', 'dreibein', 'vierbein', ... 'elfbein' for $D = 1, 2, 3, 4, \ldots, 11$. Sometimes the expression 'vielbein' is reserved only for the components of the vector field rather than the 1-form; we shall refer to both of them as 'vielbein', regardless of the index position, since the index position makes it clear whether one is dealing with a 1-form or its dual vector.



D. Grumiller and M. M. Sheikh-Jabbari, *Black Hole Physics*, Graduate Texts in Physics,
https://doi.org/10.1007/978-3-031-10343-8

the vielbein,

$$g_{\mu\nu} = e^a_\mu e^b_\nu \eta_{ab} \,. \tag{C.3}$$

The same logic applies to the inverse metric.

$$g^{\mu\nu} = e^\mu_a e^\nu_b \eta^{ab}. \tag{C.4}$$

The metric has $D(D+1)/2$ independent components in $D$ dimensions, while the vielbein has $D^2$. This means that the vielbein must have $D(D-1)/2$ redundant components from the metric perspective. The origin of this redundancy is local Lorentz invariance, $v'^a = \Lambda^a{}_b v^b$, where $\Lambda^a{}_b$ generates a Lorentz transformation.

Since local symmetries are gauge symmetries there should be a gauge connection 1-form associated with local Lorentz invariance. It is called 'spin-connection' or 'Lorentz-connection' and denoted by

$$\omega^a{}_b = \omega^a{}_{b\mu} \, \mathrm{d}x^\mu \,. \tag{C.5}$$

The gauge-covariant derivative that replaced the de Rahm differential reads

$$D^a{}_b = \delta^a_b \, \mathrm{d} + \omega^a{}_b \,. \tag{C.6}$$

Under local Lorentz transformations, the spin-connection transforms like any other non-abelian gauge connection (for $D > 2$; in $D = 2$ it becomes abelian since the Lorentz group $SO(1, 1)$ is abelian),

$$\omega'^a{}_b = \left(\Lambda^{-1} D \Lambda\right)^a{}_b = \Lambda_c{}^a \, \mathrm{d}\Lambda^c{}_b + \Lambda_c{}^a \omega^c{}_d \Lambda^d{}_b \tag{C.7}$$

while the vielbein transforms like a Lorentz vector

$$e'^a = \Lambda^a{}_b \, e^b \,. \tag{C.8}$$

The full covariant derivative $\mathcal{D}$ (by which we mean Lorentz and spacetime covariant) vanishes when acting on the vielbein.

$$\left(\mathcal{D}e\right)_\mu{}^\nu{}_a = \partial_\mu e^\nu_a + \Gamma^\nu{}_{\mu\lambda} e^\lambda_a + \omega_a{}^c{}_\mu e^\nu_c = 0. \tag{C.9}$$

This statement is known as 'vielbein postulate' and can be derived from the relation $\Gamma^\lambda{}_{\mu\nu} = e^\lambda_a D^a{}_{b\mu} e^b_\nu$, which in turn follows from the definition of the covariant derivative and the requirement $\nabla_\mu X^\nu = (D^a{}_{b\mu} X^b) e^\nu_a$. The statement (C.9) is true regardless of index positions, i.e. $(\mathcal{D}e)_\mu{}^a{}_\nu = 0$. The last equality implies that metricity, $\nabla_\lambda g_{\mu\nu} = 0$, is equivalent to antisymmetry of the spin-connection under exchange of flat indices, $\omega_{ab} = -\omega_{ba}$. In Einstein gravity and most of its generalizations metricity is assumed and hence the spin-connection is antisymmetric.

The fundamental building blocks of the Cartan formulation of gravity are vielbein, spin-connection, and gauge-covariant derivative. Acting with the latter on the former two we obtain interesting 2-forms, namely the torsion 2-form

$$T^a = D^a{}_b e^b = \mathrm{d}e^a + \omega^a{}_b \wedge e^b \tag{C.10}$$

and the curvature 2-form

$$R^a{}_b = D^a{}_c \omega^c{}_b = \mathrm{d}\omega^a{}_b + \omega^a{}_c \wedge \omega^c{}_b\,. \tag{C.11}$$

These two definitions are also known as first and second Cartan structure equations. Like in the previous appendix, we often suppress spacetime indices when presenting $p$-forms and we also suppress the wedge symbol when a derivative acts on a form.

The relation of torsion and curvature 2-forms to Riemannian quantities is as follows. Torsion determines the antisymmetric part of the spacetime connection.

$$e_a^\lambda\, T^a_{\mu\nu} = \Gamma^\lambda{}_{[\mu\nu]}. \tag{C.12}$$

Thus, the absence of torsion implies symmetry of the spacetime connection in the lower index pair. Note, however, that torsion also contributes to the symmetric part of the spacetime connection. This contribution is sometimes called 'contorsion'; to be more precise, the contorsion tensor is the difference between the spacetime connection and the Christoffel connection. If we are interested in Riemannian geometry, we thus have to set torsion to zero in addition to assuming antisymmetry of the Lorentz connection. The Riemann tensor is then determined by contracting the curvature 2-form with vielbeins.

$$R^\lambda{}_{\tau\mu\nu} = R^a{}_{b\mu\nu}\, e_a^\lambda e^{b\,\tau}. \tag{C.13}$$

In some applications, the purely flat-indexed version of the Riemann tensor is useful.

$$R^a{}_{bcd} = R^a{}_{b\mu\nu} e_c^\mu e_d^\nu. \tag{C.14}$$

We have seen that acting once with the gauge-covariant derivative on vielbein and spin-connection leads to interesing 2-forms, torsion, and curvature. However, acting repeatedly with gauge-covariant derivatives does not yield anything new. The relation

$$(D^2)^a{}_b = D^a{}_c D^c{}_b = R^a{}_b \tag{C.15}$$

is known as Bianchi's first identity and implies particularly

$$(DT)^a = (D^2)^a{}_b\, e^b = R^a{}_b \wedge e^b\,. \tag{C.16}$$

Bianchi's second identity (also known as Jacobi identity)

$$(D^3)^a{}_b = (DR)^a{}_b = dR^a{}_b + \omega^a{}_c \wedge R^c{}_b + \omega^b{}_c \wedge R^{ac} = 0 \tag{C.17}$$

shows that no new tensor structures arise when repeatedly acting with gauge-covariant derivatives, besides vielbein, spin-connection, torsion, and curvature.

Thus, constructing gravity actions in the Cartan formulation just requires to build Lorentz-invariant volume forms out of these building blocks, possibly using the Hodge-$*$ defined in the previous appendix. A particular consequence of (C.3) is that the volume form is given by

$$\sqrt{|g|}\,\mathrm{d}^D x = \left|\det e^a_\mu\right|\,\mathrm{d}^D x = \pm e^{a_1}\wedge e^{a_2}\wedge\cdots\wedge e^{a_D}\,\epsilon_{a_1 a_2\ldots a_D} =: \varepsilon \tag{C.18}$$

where the sign depends on the choice of orientation. For example, the Einstein–Hilbert–Palatini action (in dimension $D>2$) is given by

$$\boxed{I_{\mathrm{EHP}}[e^a,\,\omega^a{}_b] = \kappa\int\left(\epsilon_{a_1 a_2 a_3\ldots a_D}\,R^{a_1 a_2}\wedge e^{a_3}\wedge\cdots\wedge e^{a_D}+\lambda\varepsilon\right).} \tag{C.19}$$

The EOM derived from the action (C.19) imply in particular vanishing torsion (from varying the spin-connection) and the Einstein equations (from varying the vielbein and using the on-shell condition of vanishing torsion), which makes the theory defined by the bulk action (C.19) classically equivalent to Einstein gravity (with $\lambda$ being proportional to the cosmological constant $\Lambda$ and $\kappa$ inversely proportional to Newton's constant $G_{\mathrm{N}}$). This classical equivalence no longer holds when spinning matter is coupled to the gravitational theory (C.19) since the matter Lagrangian then depends on the spin-connection so that torsion becomes dynamical. In this Einstein–Cartan theory, where the spin-connection is independent of the vielbein, energy is still the source of curvature and spin the source of torsion. Since gravity is weak and spins tend to average to zero macroscopically (as opposed to energy, which just adds up macroscopically), observing dynamical torsion is quite non-trivial and has not been achieved so far, see e.g. [781,782].

## Exercises

**C.1 Cartan variables in 2*d*.**

Take 2-dimensional metrics in EF gauge, $\mathrm{d}s^2 = -2\,\mathrm{d}u\,\mathrm{d}r - K(u,\,r)\,\mathrm{d}u^2$, and choose the zweibein $e^+ = \mathrm{d}u$, $e^- = -\,\mathrm{d}r - \frac{1}{2}\,K(u,\,r)\,\mathrm{d}u$, with the Minkowski metric in lightcone gauge, $\eta_{\pm\mp} = 1$ and $\eta_{\pm\pm} = 0$. Determine the spin-connection from the condition of vanishing torsion and derive the curvature 2-form as well as the associated Ricci tensor and scalar.

**C.2 Cosmological Einstein–Hilbert–Palatini in 4*d*.**

Vary the action $I_{\mathrm{EHP}}[e^a,\,\omega^a{}_b] = \frac{1}{16\pi G_{\mathrm{N}}}\int\epsilon_{abcd}\big(R^{ab}\wedge e^c\wedge e^d + \frac{1}{2}\,\Lambda e^a\wedge e^b\wedge e^c\wedge e^d\big)$ with respect to vielbein $e^a$ and spin-connection $\omega^a{}_b$. Show that the latter equation yields the condition of vanishing torsion as equation of motion, while the former yields the Einstein equations.

**C.3 Gravitational instanton density and Euler density.**

Vary the action $I_{\text{top}}[\omega^a{}_b] = \int \left(\alpha R^a{}_b \wedge R^b{}_a + \beta\epsilon_{abcd}\, R^{ab} \wedge R^{cd}\right)$ and show that you only get boundary terms, i.e. no contribution to the bulk EOM from this action. Bonus level: consider which boundary and corner terms you have to add to get vanishing variations in presence of boundaries and corners.
*Note:* The term proportional to $\alpha$ is called gravitational instanton density or gravitational Chern–Pontryagin density and the term proportional to $\beta$ Euler density, it is also called the Gauss–Bonnet term.

**C.4 Nieh–Yan form.**

Show that the 4-form $T^a \wedge T_a - e_a \wedge e_b \wedge R^{ab}$, known as Nieh–Yan form, is locally exact in presence of torsion, $T^a \neq 0$, and vanishes in the absence of torsion.

# Teukolsky Equation

# D

In this appendix, we discuss the Teukolsky equation [289,783], which describes perturbations of Kerr black holes, and some of its solution methods. In order to obtain the Teukolsky equation, we need to introduce some formalism that is not part of the main text, namely the Newman–Penrose formalism (for a textbook explaining this formalism in full generality see e.g. [784,785]).

## D.1 Newman–Penrose Formalism Applied to Kerr

Start with the Kerr metric in Boyer–Lindquist coordinates (2.74), (2.75) and introduce the following null tetrad (the component order is $t, r, \theta, \varphi$)

$$l^\mu = \begin{pmatrix} \frac{r^2+a^2}{\Delta} \\ 1 \\ 0 \\ \frac{a}{\Delta} \end{pmatrix}, \quad n^\mu = \frac{1}{2\rho^2}\begin{pmatrix} r^2+a^2 \\ -\Delta \\ 0 \\ a \end{pmatrix}, \quad m^\mu = \frac{1}{\sqrt{2}(r+ia\,\cos\theta)}\begin{pmatrix} ia\sin\theta \\ 0 \\ 1 \\ \frac{i}{\sin\theta} \end{pmatrix} \tag{D.1}$$

with the properties $l_\mu l^\mu = n_\mu n^\mu = m_\mu m^\mu = l_\mu m^\mu = n_\mu m^\mu = 0$, $l_\mu n^\mu = -1$, $m_\mu \bar{m}^\mu = 1$ (bar denotes complex conjugation) and

$$g_{\mu\nu} = -l_\mu n_\nu - n_\mu l_\nu + m_\mu \bar{m}_\nu + \bar{m}_\mu m_\nu\,. \tag{D.2}$$

GW (spin-2 perturbations) can be understood as linearized perturbations of the Weyl tensor $C_{\mu\nu\lambda\kappa}$. They can be parametrized in terms of the Newman–Penrose scalars

$${}_2\Psi_0 = -C_{\mu\nu\lambda\kappa}\, l^\mu m^\nu l^\lambda m^\kappa \qquad {}_2\Psi_4 = -C_{\mu\nu\lambda\kappa}\, n^\mu \bar{m}^\nu n^\lambda \bar{m}^\kappa\,. \tag{D.3}$$



D. Grumiller and M. M. Sheikh-Jabbari, *Black Hole Physics*, Graduate Texts in Physics,
https://doi.org/10.1007/978-3-031-10343-8

Similarly, electromagnetic waves (spin-1 perturbations) can be parametrized in terms of the Newman–Penrose scalars

$$ {}_1\Psi_0 = F_{\mu\nu} l^\mu m^\nu \qquad {}_1\Psi_2 = F_{\mu\nu} \bar{m}^\mu n^\nu \,. \tag{D.4} $$

As shown in [783], also massless spin-1/2 perturbations can be parametrized in terms of scalars ${}_{\frac{1}{2}}\Psi$, and the same is true for scalar (spin-0) perturbations ${}_0\Psi$. Teukolsky realized that all these perturbations for different spins obey the same type of master equation.

## D.2 Teukolsky Master Equation as Heun Equation

Assume there is some perturbation ${}_s\Psi(t,\, r,\, \theta,\, \varphi)$ on a Kerr black hole, where $s = n/2$ is the spin, with $n \in \{0, \pm 1, \pm 2, \pm 3, \pm 4\}$. The quantity ${}_s\Psi(t,\, r,\, \theta,\, \varphi)$ is a Newman–Penrose scalar associated with spin $|s|$, see the previous section.

Teukolsky showed that all such perturbations obey a single master equation that is separable, as consequence of the Kerr Killing tensor. Starting with the separation ansatz

$$ {}_s\Psi(t,\, r,\, \theta,\, \varphi) = e^{-i\omega t + im\varphi}\, {}_sS_{\omega,m,E}(\theta)\, {}_sR_{\omega,m,E}(r) \tag{D.5} $$

with separation constant $E$ yields the Teukolsky angular equation

$$ \left( \frac{1}{\sin\theta} \frac{\mathrm{d}}{\mathrm{d}\theta} \left( \sin\theta \frac{\mathrm{d}}{\mathrm{d}\theta} \right) + {}_sW_{\omega,m,E}(\theta) \right) {}_sS_{\omega,m,E}(\theta) = 0 \tag{D.6} $$

with the effective angular potential

$$ {}_sW_{\omega,m,E}(\theta) = E + a^2\omega^2 \cos^2\theta - 2sa\omega \cos\theta - \frac{s^2 + 2ms \cos\theta + m^2}{\sin^2\theta} \tag{D.7} $$

and the Teukolsky radial equation

$$ \left( \Delta^{-s} \frac{\mathrm{d}}{\mathrm{d}r} \left( \Delta^{s+1} \frac{\mathrm{d}}{\mathrm{d}r} \right) + {}_sV_{\omega,m,E}(r) \right) {}_sR_{\omega,m,E}(r) = 0 \tag{D.8} $$

with the effective radial potential

$$ \begin{aligned} {}_sV_{\omega,m,E}(r) = \frac{\left(\omega(r^2+a^2) - ma\right)^2}{\Delta} & - is\left(\omega(r^2+a^2) - ma\right) \frac{\mathrm{d}\ln\Delta}{\mathrm{d}r} \\ & - E + s(s+1) - a^2\omega^2 + 2ma\omega + 4is\omega r. \end{aligned} \tag{D.9} $$

Solutions to the angular equation (D.6) are generalizations of spherical harmonics (often called 'spin-weighted spheroidal harmonics'); for vanishing frequencies, $\omega = 0$, they are precisely the spin-weighted spherical harmonics ${}_sY_{lm}$, where the angular quantum number $l$ and the spin $s$ determine the separation constant $E = l(l+1) - s(s+1)$.

Both equations reduce to the confluent Heun equation [786,787]

$$\frac{\mathrm{d}^2 H(z)}{\mathrm{d}z^2} + \Big(\alpha + \frac{\beta+1}{z} + \frac{\gamma+1}{z-1}\Big)\frac{\mathrm{d}H(z)}{\mathrm{d}z} + \Big(\frac{\mu}{z} + \frac{\nu}{z-1}\Big)H(z) = 0 \tag{D.10}$$

with suitable choices for the constants $\alpha$, $\beta$, $\gamma$, $\mu$, $\nu$. In the radial case the two regular singular points $z = 0$ and $z = 1$ correspond to the inner and outer horizon of the Kerr black hole, and the irregular singular point $|z| = \infty$ corresponds to $r = \infty$. Thus, either $z = (r - r_-)/(r_+ - r_-)$ or $z = (r_+ - r)/(r_+ - r_-)$.

## D.3 Remarks on the Teukolsky Equation for Vanishing Spin

For vanishing spin, angular and radial Teukolsky equations simplify.

$$\left(\frac{1}{\sin\theta}\frac{\mathrm{d}}{\mathrm{d}\theta}\Big(\sin\theta\frac{\mathrm{d}}{\mathrm{d}\theta}\Big) + a^2\omega^2\cos^2\theta - \frac{m^2}{\sin^2\theta} + E\right){}_0S_{\omega,m,E}(\theta) = 0 \tag{D.11}$$

$$\left(\frac{\mathrm{d}}{\mathrm{d}r}\Big(\Delta\frac{\mathrm{d}}{\mathrm{d}r}\Big) + \frac{\big(\omega(r^2+a^2) - ma\big)^2}{\Delta} - a^2\omega^2 + 2ma\omega - E\right){}_0R_{\omega,m,E}(r) = 0. \tag{D.12}$$

In the low frequency limit, $\omega a \ll 1$, the equations simplify [788]. The angular one, (D.11), is then solved by spherical harmonics, with the separation constant given by $E = l(l+1)$, where $l$ is the angular quantum number of the spherical harmonic. The radial equation (D.12) simplifies from a confluent Heun equation to a hypergeometric equation. Since the hypergeometric function forms representations of $sl(2,\mathbb{R})$ this may be interpreted as indication for hidden conformal symmetry of Kerr black holes, see for instance [789].

In the high frequency limit, $\omega a \gg 1$, the spheroidal differential equation (D.11) simplifies to the Laguerre differential equation. For details on the high-frequency limit, see [790].

## Exercises

**D.1 Kinnersley tetrad and Kerr black hole.**

The null tetrad introduced in Sect. D.1 is known as Kinnersley tetrad. Show that (D.2) with (D.1) reproduces the Kerr metric in Boyer–Lindquist coordinates (2.74), (2.75).

**D.2 Teukolsky and Heun equation.**

Verify that the Teukolsky equation (D.6), (D.7) and (D.8), (D.9) reduce to the confluent Heun equation (D.10) and calculate the constants $\alpha$, $\beta$, $\gamma$, $\mu$, and $\nu$ therein.

# Basics of QFT in Curved Spacetime

# E

In this appendix, we review elementary aspects of QFTs on fixed curved backgrounds. Consider for concreteness a minimally coupled massive scalar field $\phi$ in $D$ spacetime dimensions with Lagrangian

$$\mathcal{L} = -\sqrt{-g}\left(\frac{1}{2}\, g^{\mu\nu}\,\partial_\mu\phi\partial_\nu\phi + m^2\phi^2\right) \tag{E.1}$$

leading to the Klein–Gordon equation on some given background

$$\left(\Box - m^2\right)\phi = \frac{1}{\sqrt{-g}}\,\partial_\mu\left(\sqrt{-g}g^{\mu\nu}\partial_\nu\phi\right) - m^2\phi = 0\,. \tag{E.2}$$

The symplectic inner product on solutions $\phi_{1,2}$ to (E.2),

$$(\phi_1,\,\phi_2) = -i\int_\Sigma \mathrm{d}^{D-1}x\sqrt{\gamma}\,n^\mu\left(\phi_1\partial_\mu\phi_2^* - \phi_2^*\partial_\mu\phi_1\right) \tag{E.3}$$

does not depend on the choice of the spacelike hypersurface $\Sigma$ ($\gamma$ is the induced metric on $\Sigma$, $n^\mu$ the future point unit normal and $*$ denotes complex conjugation). It is convenient to introduce a complete orthonormal set of modes $\psi_i$,

$$(\psi_i,\,\psi_j) = \delta_{ij} \qquad\qquad (\psi_i^*,\,\psi_j^*) = -\delta_{ij} \tag{E.4}$$

in terms of which a generic solution expands as

$$\phi = \sum_i\left(a_i\psi_i + a_i^\dagger\psi_i^*\right). \tag{E.5}$$

According to standard Fock space quantization, the coefficients are replaced by annihilation and creation operators $a_i$, $a_i^\dagger$, obeying the oscillator algebra



D. Grumiller and M. M. Sheikh-Jabbari, *Black Hole Physics*, Graduate Texts in Physics,
https://doi.org/10.1007/978-3-031-10343-8

$$[a_i, a_j^\dagger] = \delta_{ij} \qquad [a_i, a_j] = 0 = [a_i^\dagger, a_j^\dagger]. \tag{E.6}$$

The vacuum state $|0\rangle$ by definition is annihilated by all annihilation operators.

$$a_i|0\rangle = 0 \qquad \forall i. \tag{E.7}$$

For each mode, there is a number operator

$$N_i = a_i^\dagger a_i \tag{E.8}$$

that also annihilates the vacuum, but which has non-vanishing expectation value for excited states. For example, taking a simple descendant of the vacuum,

$$|i\rangle := a_i^\dagger |0\rangle \tag{E.9}$$

leads to expectation values of the number operator that do not vanish in general.

$$\langle i|N_j|i\rangle = \delta_{ij}. \tag{E.10}$$

If we choose a different basis $\chi_i$ using a Bogoliubov transformation,

$$\chi_i = \sum_j \left(\alpha_{ij}\psi_i + \beta_{ij}\psi_i^*\right) \tag{E.11}$$

the vacuum state changes in general, which we shall see in a minute. To preserve the symplectic inner product, the Bogoliubov coefficients must obey the normalization conditions

$$\sum_k \left(\alpha_{ik}\alpha_{jk}^* - \beta_{ik}\beta_{jk}^*\right) = \delta_{ij} \qquad \sum_k \left(\alpha_{ik}\beta_{jk} - \beta_{ik}\alpha_{jk}\right) = 0. \tag{E.12}$$

In the new basis, the field depends on a new set of annihilation and creation operators

$$\phi = \sum_i \left(b_i\chi_i + b_i^\dagger\chi_i^*\right) \tag{E.13}$$

that are related to the old ones by the Bogoliubov coefficients

$$b_i = \sum_j \left(\alpha_{ij}^* a_j - \beta_{ij}^* a_j^\dagger\right). \tag{E.14}$$

Only if all the $\beta$-coefficients vanish the old vacuum is still annihilated by the new annihilation operators. However, if some of the $\beta$-coefficients are non-zero then not all number operators have vanishing expectation value with respect to the old vacuum.

$$\langle 0|b_i^\dagger b_i|0\rangle = \sum_{jk} \beta_{ij}\beta_{ik}^* \langle 0|a_j a_k^\dagger|0\rangle = \sum_j |\beta_{ij}|^2. \tag{E.15}$$

The fact that Bogoliubov transformations with non-vanishing $\beta$-coefficients convert the original vacuum into an excited state is behind numerous physical effects, including Hawking- and Unruh-effects, with applications outside of black hole physics ranging from condensed matter physics (squeezed states, Bose–Einstein condensates) to cosmology (particle generation in the early universe).

Some textbooks and lecture notes that elaborate further on these semiclassical methods include [134,244,459,460].

## Exercises

**E.1 Thermal spectrum from Bogoliubov transformation.**

Consider modes labeled by frequencies $\omega$ and assume the relation

$$\beta_{\omega,\bar{\omega}} = \exp\left(-\pi\omega/\kappa\right)\alpha_{\omega,\bar{\omega}}$$

for the coefficients in the Bogoliubov transformed basis (E.11). Use the normalization conditions (E.12) to show that the number operator (E.13) gives a Planck distribution

$$\langle 0|b_\omega^\dagger b_\omega|0\rangle = \frac{1}{e^{2\pi\omega/\kappa} - 1}$$

for a black body with temperature $T = \frac{\kappa}{2\pi}$.
Bonus: use the results above together with the high-frequency limit of the Regge–Wheeler equation, Exercise 4.7, to argue that for Schwarzschild black holes the Hawking temperature is given by $T = \frac{1}{8\pi M}$. For a derivation of the first displayed equation above see the next exercise.

**E.2 Ray tracing to determine relation between Bogoliubov coefficients.**

In order to obtain the first displayed equation in the previous exercise, one can adopt Hawking's original method of ray tracing, see Sect. 6.4.3. Outgoing positive frequency modes near $\mathfrak{I}^+$ are of the form $\phi_\omega \sim \exp\left(-i\omega u\right)$ with (EF) retarded time $u$.

(1) Show that slightly outside the future event horizon these modes are blue-shifted, $\phi_\omega \sim \exp\left(i\frac{\omega}{\kappa}\ln\epsilon\right)$, where $U = -\epsilon$ is the value of the (Kruskal) retarded time $U$ associated with such a mode, with $\epsilon \ll 1$.

(2) Argue that the rapid oscillations of $\phi_\omega$ justify the geometric optics approximation.

(3) Show that a light ray arriving at Kruskal retarded time $U = -\epsilon$ at $\mathfrak{I}^+$ must have emanated at EF advanced time $v = -\epsilon$, provided the latter is shifted such that an emission time $v = 0$ corresponds to rays traveling exactly along the event horizon.

(4) Combine these results to conclude that within the ray approximation the modes on $\mathfrak{I}^-$ are given by $\phi_\omega(v) = \theta(-v)\exp\left(i\frac{\omega}{\kappa}\ln(-v)\right)$.

(5) Fourier transform this result, $\bar{\phi}_{\bar{\omega}} = \int e^{i\bar{\omega}v}\phi_\omega(v)\,\mathrm{d}v$ and show, using complex analysis, that for positive $\bar{\omega}$ you get $\bar{\phi}_\omega(-\bar{\omega}) = -\exp\left(-\frac{\pi\omega}{\kappa}\right)\bar{\phi}(\bar{\omega})$.

(6) Put all pieces together to conclude that at very late times positive frequency modes at $\mathfrak{I}^+$ match to mixed modes on $\mathfrak{I}^-$ with Bogoliubov coefficients $\alpha_{\omega,\bar{\omega}} = \bar{\phi}_\omega(\bar{\omega})$ and $\beta_{\omega,\bar{\omega}} = \bar{\phi}_\omega(-\bar{\omega})$ obeying the desired relation $\beta_{\omega,\bar{\omega}} = \exp\left(-\pi\omega/\kappa\right)\alpha_{\omega,\bar{\omega}}$.

# ADM $3+1$ Decomposition

F

Consider a scalar time-function $t$ whose isosurfaces $\Sigma$ are (partial) Cauchy surfaces. The timelike unit normal

$$n_\mu = -N\partial_\mu t \tag{F.1}$$

features the lapse function

$$N = \frac{1}{\sqrt{-g^{\mu\nu}(\partial_\mu t)(\partial_\nu t)}} \,. \tag{F.2}$$

The spatial metric on $\Sigma$

$$h_{\mu\nu} = g_{\mu\nu} + n_\mu n_\nu \tag{F.3}$$

by construction projects to zero when contracted with the normal, $h_{\mu\nu}n^\nu = 0$.

The time-flow vector field $t^\mu$ obeying

$$t^\mu \partial_\mu t = 1 \tag{F.4}$$

can be decomposed into tangential and normal parts with respect to $\Sigma$,

$$t^\mu = Nn^\mu + N^\mu \tag{F.5}$$

where $N$ is the lapse function (F.2) and $N^\mu := h^\mu{}_\nu t^\nu$ is the shift vector. It is convenient to adapt the coordinates to a $(3+1)$-split, $x^\mu = (t,\ x^i)$ by defining $\partial_t x^\mu := t^\mu$. This allows to introduce the spatial projector

$$\Pi_i{}^\mu := \frac{\partial x^\mu}{\partial x^i} \tag{F.6}$$



D. Grumiller and M. M. Sheikh-Jabbari, *Black Hole Physics*, Graduate Texts in Physics,
https://doi.org/10.1007/978-3-031-10343-8

and correspondingly projected tensors, $h_{ij} := \Pi_i{}^\mu \Pi_j{}^\nu h_{\mu\nu}$. and $N_i := \Pi_i{}^\mu N_\mu = \Pi_i{}^\mu t_\mu$.

The ADM decomposition

$$g_{\mu\nu}\,\mathrm{d}x^\mu\,\mathrm{d}x^\nu = -N^2\,\mathrm{d}t^2 + h_{ij}\left(\mathrm{d}x^i + N^i\,\mathrm{d}t\right)\left(\mathrm{d}x^j + N^j\,\mathrm{d}t\right) \tag{F.7}$$

splits the (3 + 1)-dimensional metric into the spatial metric $h_{\mu\nu}$, the shift vector $N^\mu$ and the lapse function $N$. The ADM form (F.7) is useful for the canonical analysis of GR. In matrix form, the metric (F.7) is given by

$$g_{\mu\nu} = \begin{pmatrix} -N^2 + N^i N_i & h_{ij}N^j \\ h_{ij}N^i & h_{ij} \end{pmatrix} \tag{F.8}$$

which implies that its determinant

$$-\det(g_{\mu\nu}) = N^2\,\det(h_{ij}) \tag{F.9}$$

is independent from the lapse function $N_i$.

Some textbooks and lecture notes that elaborate further on the ADM 3 + 1 decomposition include [8, 108, 133].

## Exercises

**F.1 Gauss–Codazzi equations.**

Use the spatial metric (F.3) to define projected tensors ${}^\perp T_{\mu\dots}{}^{\nu\dots} = h^\alpha_\mu \dots h^\nu_\beta T_{\alpha\dots}{}^{\beta\dots}$ and intrinsic covariant derivatives, $\mathcal{D}_\mu T_{\nu\dots}{}^{\lambda\dots} = {}^\perp\nabla_\mu T_{\nu\dots}{}^{\lambda\dots}$. Show the Gauss–Codazzi relations

$$\begin{aligned} {}^\perp R_{\alpha\beta\gamma\delta} &= \mathcal{R}_{\alpha\beta\gamma\delta} + K_{\alpha\gamma}K_{\beta\delta} - K_{\beta\gamma}K_{\alpha\delta} \\ {}^\perp\left(R_{\alpha\beta\gamma\delta}n^\alpha\right) &= \mathcal{D}_\delta K_{\beta\gamma} - \mathcal{D}_\gamma K_{\beta\delta} \end{aligned}$$

where $\mathcal{R}$ is the intrinsic Riemann tensor associated with $\mathcal{D}$ and $K$ the extrinsic curvature tensor defined in the main text, (6.7).

**F.2 Double normal component of Riemann tensor.**

In the previous exercise, one component of the full Riemann tensor is missing, namely the double normal component. Show that it obeys a Gauss–Codazzi-like relation

$${}^\perp\left(R_{\alpha\beta\gamma\delta}n^\alpha n^\gamma\right) = K_\beta{}^\mu K_{\mu\delta} - \mathcal{L}_n K_{\beta\delta} + \mathcal{D}_\beta a_\delta + a_\beta a_\delta$$

where $\mathcal{L}_n$ denotes the Lie derivative along the normal vector $n^\alpha$ and $a^\mu := n^\nu\nabla_\nu n^\mu$ is the normal-acceleration.

**F.3 Projected Ricci tensor and Ricci scalar.**

Use the definitions and results of the previous two exercises to derive the projections of the Ricci tensor

$$
\begin{aligned}
{}^{\perp}R_{\alpha\beta} &= \mathcal{R}_{\alpha\beta} + K K_{\alpha\beta} - 2K_{\alpha}{}^{\mu} K_{\beta\mu} + \mathcal{L}_n K_{\alpha\beta} - \mathcal{D}_{\alpha} a_{\beta} - a_{\alpha} a_{\beta} \\
{}^{\perp}\left(R_{\alpha\beta} n^{\alpha}\right) &= \mathcal{D}^{\mu} K_{\mu\beta} - \mathcal{D}_{\beta} K \\
R_{\alpha\beta} n^{\alpha} n^{\beta} &= -K^{\mu\nu} K_{\mu\nu} - \mathcal{L}_n K + \mathcal{D}_{\mu} a^{\mu} + a_{\mu} a^{\mu}
\end{aligned}
$$

and the Ricci scalar

$$
R = \mathcal{R} + K^2 + K^{\mu\nu} K_{\mu\nu} + 2\mathcal{L}_n K - 2\mathcal{D}_{\mu} a^{\mu} - 2a_{\mu} a^{\mu} .
$$

**F.4 Lie derivative of extrinsic curvature.**

Show the equality

$$
\begin{aligned}
\mathcal{L}_n K_{\alpha\beta} &= n^{\mu} \nabla_{\mu} K_{\alpha\beta} + K_{\mu\beta} \nabla_{\alpha} n^{\mu} + K_{\alpha\mu} \nabla_{\beta} n^{\mu} \\
&= -R_{\gamma\alpha\delta\beta} n^{\gamma} n^{\delta} + K_{\alpha\mu} K_{\beta}{}^{\mu} + \mathcal{D}_{\alpha} a_{\beta} + a_{\alpha} a_{\beta}
\end{aligned}
$$

and prove $n^{\alpha} \mathcal{L}_n K_{\alpha\beta} = 0$.

**F.5 Einstein–Hilbert Lagrange density.**

Use the results of the last two exercises to show that up to total derivative terms the Einstein–Hilbert Lagrange density is given by

$$
L_{\text{EH}} = \frac{1}{16\pi G_{\text{N}}} R = \frac{1}{16\pi G_{\text{N}}} \left(\mathcal{R} - K^2 + K^{\mu\nu} K_{\mu\nu}\right) .
$$

**F.6 Canonical momenta in GR.**

Using the previous exercise, determine the canonical momenta in GR,

$$
\pi^{\mu\nu} = \frac{\partial L_{\text{EH}}}{\partial(\mathcal{L}_n h_{\mu\nu})} = \frac{1}{16\pi G_{\text{N}}} \left(K^{\mu\nu} - h^{\mu\nu} K\right) .
$$

**F.7 Hamiltonian and momentum constraints.**

The Einstein tensor $G_{\mu\nu}$ can also be split into intrinsic and normal components. The former are evolution equations and the latter constraint equations from a Hamiltonian perspective, in the sense that they do not involve any normal derivatives acting on the phase space variables $h_{\mu\nu}$, $\pi^{\mu\nu}$. Assuming a spacetime dimension $D > 2$, calculate the Hamiltonian constraint

$$
\mathcal{H} = -2G_{\alpha\beta} n^{\alpha} n^{\beta} = \mathcal{R} + (16\pi G_{\text{N}})^2 \left(\pi^{\mu\nu} \pi_{\mu\nu} - \frac{1}{D-2} \pi^2\right) \approx 0
$$

and the momentum constraints

$$\mathcal{H}_\mu = {}^{\perp}\!\left(G_{\alpha\beta} n^\beta\right) = 16\pi G_{\rm N}\, \mathcal{D}^\mu \pi_{\mu\beta} \approx 0$$

where the notation $\approx 0$ means that these constraints must hold on the physical phase space, but do not hold as general identities on the full phase space.

# Covariant Phase Space Formalism

# G

The *Covariant Phase Space Formalism (CPSF)* provides a systematic way of calculating variations of conserved charges in generic theories with gauge symmetries, in particular generally covariant theories. This method was initiated in [392,791,792] and studied more in [363,373,374,394,793–796]. Wald's approach, reviewed below, is based on the action formulation. There is another way of formulating the CPSF, developed by Barnich et al., based on the EOM (instead of the action) [363,394]. In this appendix, we briefly review the Wald-et al. formulation using their, now standardized, notation. A more extensive and rigorous discussions can be found in the original papers, e.g. in [793], or in pedagogical reviews [396,796].

The key object in this formulation is the construction of the phase space and its symplectic structure. To work out such a phase space one may base the construction on the Lagrangian or action formulation, rather than the Hamiltonian—hence the attribute 'covariant'. This is possible since the symplectic 2-form may be deduced from the surface term in the variation of the action. As a simple illustrative example, consider a multi-particle Lagrangian and its variation

$$L = \sum_i \dot{q}_i^2 - V(q_i), \qquad \delta L = \sum_i \Big[\Big(\ddot{q}_i - \frac{\partial V}{\partial q_i}\Big)\delta q_i + \mathrm{d}(p_i \delta q_i)/\mathrm{d}t\Big] \tag{G.1}$$

where we used the fact that momenta are canonically defined $p_i = \dot{q}_i$. One may then take the second variation of the on-shell action to find $\mathrm{d}(\sum_i \delta p_i \wedge \delta q_i)/\mathrm{d}t$, which is nothing but the time derivative of the symplectic 2-form of the theory computed over the tangent space of the phase space parametrized by $\delta q_i$, $\delta p_i$, for examples see [393].

The above can be extended to field theories that have an infinite-dimensional continuous phase space. In this case, especially in the presence of gauge symmetries, we typically have degenerate directions on the symplectic 2-form, which one needs to tackle. This latter has been studied and analyzed systematically, e.g. for gauge theories [393] or for gravity in a series of papers by Wald and collaborators. After



D. Grumiller and M. M. Sheikh-Jabbari, *Black Hole Physics*, Graduate Texts in Physics,
https://doi.org/10.1007/978-3-031-10343-8

removing the degenerate directions, we have a covariantly defined symplectic form for the theory.

The phase space is a manifold $\mathcal{M}$ that is equipped with a symplectic 2-form $\boldsymbol{\Omega}$. To construct $\boldsymbol{\Omega}$ for a given $d$-dimensional generally invariant theory, we start with the action

$$\mathcal{S}[\Phi] = \int \mathbf{L}, \tag{G.2}$$

where $\mathbf{L}$ is the Lagrangian $d$-form, and $\Phi$ is used to denote collectively all the dynamical fields. Variation of the action leads to

$$\delta \mathbf{L}[\Phi] = \mathbf{E}_\Phi\, \delta\Phi + \mathrm{d}\boldsymbol{\Theta}_{\text{LW}}(\delta\Phi, \Phi)\,, \tag{G.3}$$

where $\delta\Phi$ is a generic field variation and provides the basis for the tangent space of the phase space $\mathcal{M}$. The EOM are given by $\mathbf{E}_\Phi = 0$. The total derivative contribution $\boldsymbol{\Theta}_{\text{LW}}$ is a $(d-1)$-form over the spacetime and a 1-form on the tangent bundle of $\mathcal{M}$, i.e. $\boldsymbol{\Theta}_{\text{LW}}$ is a $(d-1; 1)$-form. We denote on-shell equalities by $\approx$, e.g.

$$\delta \mathbf{L}[\Phi] \approx \mathrm{d}\boldsymbol{\Theta}_{\text{LW}}(\delta\Phi, \Phi)\,. \tag{G.4}$$

The Lee–Wald symplectic 2-form in the CPSF [791] is defined as

$$\boldsymbol{\Omega}^{\Sigma}_{\text{LW}}(\delta_1\Phi, \delta_2\Phi, \Phi) := \int_\Sigma \boldsymbol{\omega}_{\text{LW}}(\delta_1\Phi, \delta_2\Phi, \Phi) \tag{G.5}$$

where $\Sigma$ is a Cauchy surface, $\delta_1\Phi$ and $\delta_2\Phi$ are two arbitrary field perturbations that are members of the tangent bundle of $\mathcal{M}$, and the (pre-)symplectic form

$$\boldsymbol{\omega}_{\text{LW}}(\delta_1\Phi, \delta_2\Phi, \Phi) := \delta_1\boldsymbol{\Theta}_{\text{LW}}(\delta_2\Phi, \Phi) - \delta_2\boldsymbol{\Theta}_{\text{LW}}(\delta_1\Phi, \Phi)\,. \tag{G.6}$$

Therefore, $\boldsymbol{\omega}_{\text{LW}}$ is a $(d-1; 2)$-form. One may show that (G.5) does not depend on the choice of $\Sigma$ (see Exercise G.1 and [791,793]), so we drop the superscript $\Sigma$ on $\boldsymbol{\Omega}^{\Sigma}_{\text{LW}}$ and simply denote it by $\boldsymbol{\Omega}_{\text{LW}}$.

Hereafter, we restrict to solutions of the EOM, with the tangent bundle being variations satisfying the linearized EOM around $\Phi$ for which the symplectic form is closed, $\mathrm{d}\boldsymbol{\omega}_{\text{LW}}(\delta_1\Phi, \delta_2\Phi, \Phi) \approx 0$ and $\boldsymbol{\Omega}_{\text{LW}}$ has no degenerate directions and is conserved. Denoting the set of solutions to the EOM by $\mathcal{F}$, the pair $(\mathcal{F}; \boldsymbol{\Omega})$ constitutes a well-defined phase space. The tangent space of $\mathcal{F}$, spanned by $\delta\Phi$, is denoted by $T_{\mathcal{F}}$.

**Freedom in $\boldsymbol{\omega}$.** The Lee–Wald symplectic form $\boldsymbol{\omega}_{\text{LW}}$ constructed from the boundary term in the Lagrangian (G.4) reveals and therefore inherits a freedom in defining $\boldsymbol{\Theta}$ up to a $(d-2; 1)$-form corner term $\mathbf{Y}$:

$$\boldsymbol{\Theta}_{\text{LW}}(\delta\Phi, \Phi) \to \boldsymbol{\Theta}_{\text{Y}}(\delta\Phi, \Phi) = \boldsymbol{\Theta}_{\text{LW}}(\delta\Phi, \Phi) + \mathrm{d}\mathbf{Y}(\delta\Phi, \Phi)\,. \tag{G.7}$$

As a result, the symplectic current has the following freedom:

$$\begin{aligned}
&\boldsymbol{\omega}_{\rm LW}(\delta_1\Phi, \delta_2\Phi, \Phi) \to \boldsymbol{\omega}_{\rm Y}(\delta_1\Phi, \delta_2\Phi, \Phi)\\
&\boldsymbol{\omega}_{\rm Y}(\delta_1\Phi, \delta_2\Phi, \Phi) = \boldsymbol{\omega}_{\rm LW}(\delta_1\Phi, \delta_2\Phi, \Phi) + \mathrm{d}\big[\delta_1\mathbf{Y}(\delta_2\Phi, \Phi) - \delta_2\mathbf{Y}(\delta_1\Phi, \Phi)\big]\,.
\end{aligned} \tag{G.8}$$

The boundary term $\mathbf{Y}$ is not specified by the theory and may be chosen using physical requirements, e.g. see [380,608,797–799]. From now on we assume this freedom was fixed and drop decorations like 'LW' or 'Y'.

## > Conserved charges on the phase space

The symplectic form $\boldsymbol{\omega}$ may be used to define conserved charges associated with a specific set of transformations generated by $\epsilon$, $\delta_\epsilon\Phi$. The transformations we consider here are among gauge transformations, which also include the exact symmetries (isometries). Since $\mathrm{d}\boldsymbol{\omega}(\delta_1\Phi, \delta_2\Phi, \Phi) \approx 0$ for any two perturbations satisfying the linearized EOM, locally and on the phase space $\mathcal{F}$,

$$\boxed{\boldsymbol{\omega}(\delta\Phi, \delta_\epsilon\Phi, \Phi) \approx \mathrm{d}\boldsymbol{k}_\epsilon(\delta\Phi, \Phi)\,,} \tag{G.9}$$

where $\boldsymbol{k}_\epsilon$ is a $(d-2; 2)$-form. This on-shell relation is called the fundamental identity of the CPSF. One may integrate $\boldsymbol{k}_\epsilon$ over a codimension-2 slice to define the charge variation associated with $\epsilon$ [373]:

$$\not{\delta} Q_\epsilon(\Phi) = \int_\Sigma \mathrm{d}\boldsymbol{k}_\epsilon(\delta\Phi, \Phi) = \oint_{\partial\Sigma} \boldsymbol{k}_\epsilon(\delta\Phi, \Phi)\,. \tag{G.10}$$

The charge variation is a (0; 1)-form and is given by a surface integral, an integral over the codimension-2 spacelike surface at the boundary of $\Sigma$. We have denoted this 'charge variation' by $\not{\delta} Q_\epsilon(\Phi)$, as it is not necessarily the variation of a charge $Q_\epsilon(\Phi)$ over the phase space, i.e. $\delta(\not{\delta} Q_\epsilon(\Phi))$ is not necessarily zero.

The charge variations generated by $\epsilon$, $\not{\delta} Q_\epsilon(\Phi)$ are Hamiltonian generators, as they can be written in terms of the symplectic form,

$$\begin{aligned}
\not{\delta} Q_\epsilon(\Phi) &= \oint_{\partial\Sigma} \boldsymbol{k}_\epsilon(\delta\Phi, \Phi) \approx \int_\Sigma \boldsymbol{\omega}(\delta\Phi, \delta_\epsilon\Phi, \Phi) = \boldsymbol{\Omega}(\delta\Phi, \delta_\epsilon\Phi, \Phi)\\
&= \int_\Sigma \Big(\delta\boldsymbol{\Theta}(\delta_\epsilon\Phi, \Phi) - \delta_\epsilon\boldsymbol{\Theta}(\delta\Phi, \Phi)\Big).
\end{aligned} \tag{G.11}$$

One may show that $\not{\delta} Q_\epsilon(\Phi)$ is conserved in the following sense. If we view $\Sigma$ as a constant time slice at time $t$, then $\not{\delta} Q_\epsilon(\Phi)$ does not depend on $t$, or on the choice of $\Sigma$ (see Exercise G.1).

---

**Proper (trivial) gauge transformations.** If $\not{\delta} Q_\epsilon = 0$ over the whole phase space $\mathcal{F}$, then $\epsilon$ is the generator of a 'proper gauge transformation' [791]. The field configurations related by such coordinate/gauge transformations are physically equivalent as their Hamiltonian generator is trivial and vanishing over the phase space. As is usual in the context of gauge theories or generally covariant theories, one may then define physical states or observables up to gauge equivalent classes.

As an example consider the charges associated with diffeomorphisms and gauge transformations in the Einstein–Maxwell theory. In the presence of $U(1)$ gauge fields $A^a$, labeled by a counting index $a$, besides diffeomorphisms generated by $\xi$, the Lagrangian $\mathbf{L}$ is also invariant under gauge transformations $A^a \to A^a + \mathrm{d}\lambda^a$ for arbitrary scalar generators $\lambda^a$. Our generators $\delta_\epsilon$ now involve both diffeomorphisms and gauge transformations, $\epsilon := \{\xi, \lambda^a\}$ such that $\delta_\epsilon \Phi = \{\mathcal{L}_\xi \Phi, \delta_{\lambda^a}\Phi\}$. We shall come back to this example later, evaluating all the quantities introduced above and below.

**Notation.** Hereafter, we use $\epsilon := \{\xi, \lambda^a\}$ for symmetry generators, which involves a diffeomorphism $\xi$ and some internal gauge transformations $\lambda^a$.

### > Integrability of charges for field-independent symmetries

The charge $Q_\epsilon[\Phi]$ is well defined if $\delta\!\!\!/ Q_\epsilon(\Phi)$ is integrable over the phase space. This condition holds if $(\delta_1\delta_2 - \delta_2\delta_1)Q_\epsilon(\Phi) = 0$, in which $\Phi$ is any field configuration in the phase space $\mathcal{F}$, and $\delta_{1,2}\Phi$ are two arbitrary members of its tangent bundle. For field-independent transformations, i.e. when $\delta\epsilon = 0$, recalling (G.11), the integrability condition is equivalent to [791]

$$\oint_{\partial\Sigma} \xi \cdot \boldsymbol{\omega}(\delta_1\Phi, \delta_2\Phi, \Phi) \approx 0\,, \qquad \forall\Phi \in \mathcal{F}\,,\ \delta\Phi \in T_{\mathcal{F}}\,. \tag{G.12}$$

### > Noether–Wald charges

If the surface integrals of charge variations are finite and non-vanishing, and if $\delta\!\!\!/ Q_\epsilon(\Phi)$ is integrable, we can define the charge $Q_\epsilon(\Phi)$. In this case, (G.11), (G.6), and (G.4) yield

$$\boldsymbol{k}_\epsilon(\delta\Phi, \Phi) \approx \delta\mathbf{Q}_\epsilon - \xi \cdot \boldsymbol{\Theta}(\delta\Phi, \Phi)\,, \tag{G.13}$$

in which the $(d-2; 0)$-form $\mathbf{Q}_\epsilon$ is the *Noether–Wald charge density*, related to the Noether current by $\mathbf{J}_\epsilon := \mathrm{d}\mathbf{Q}_\epsilon$. The latter is defined as

$$\boxed{\mathbf{J}_\epsilon := \boldsymbol{\Theta}(\delta_\epsilon\Phi, \Phi) - \xi \cdot \mathbf{L}\,.} \tag{G.14}$$

One may then evaluate the charge variation density by computing $\boldsymbol{k}_\epsilon$. One may integrate this charge variation density over $\partial\Sigma$ to obtain the charge variation.

**The freedoms.** Given a symmetry generator $\epsilon$, one may use the CPSF or the Noether–Wald charge method to compute the charge. Even if the charge is integrable, the results of the two methods need not necessarily match. The reason is the freedom in either of the methods. These freedoms arise from the use of the Poincaré lemma over the spacetime and the phase space, i.e. $\mathrm{d}X = 0 \Longrightarrow X = \mathrm{d}Z$, $\delta X = 0 \Longrightarrow X = \delta W$ locally. The expressions $Z$ and $W$ are not uniquely determined. The $\mathbf{Y}$-freedom in the definition of $\boldsymbol{\omega}$ (G.7), is an example of such a freedom in the CPSF. As another example, one may readily observe that changing the Lagrangian by a total derivative $\mathbf{L} \to \mathbf{L} + \mathrm{d}\mathbf{W}$, while not changing EOM, modifies the Noether–Wald charge. Interestingly, the $\mathbf{W}$-freedom does not change $\boldsymbol{\omega}$ and hence does not affect the charge computed in the CPSF. Therefore, if the charge associated with a transformation is integrable, matching CPSF and Noether–Wald charges implies a specific fixing of the $\mathbf{W}$-freedom. In any case, in either of the formulations of computation of conserved charges one should address the freedoms.

### > Field-dependent transformations and their charges

So far we assumed that the symmetry generators $\epsilon$ are field independent, i.e. $\delta\epsilon = 0$. However, in general one can relax this assumption but adjust the formulation to account for the field-dependence [799]. Recalling the second line in (G.11), the adjusted charge variations

$$\not{\delta} Q_\epsilon := \int_\Sigma \left(\delta^{[\Phi]}\boldsymbol{\Theta}(\delta_\epsilon\Phi, \Phi) - \delta_\epsilon\boldsymbol{\Theta}(\delta\Phi, \Phi)\right) \tag{G.15}$$

contain field variations $\delta^{[\Phi]}$ that act only on $\Phi$ and not on the $\epsilon$ inside $\boldsymbol{\Theta}$.

One can still compute $\not{\delta} Q_\epsilon$ using the surface integral $\not{\delta} Q_\epsilon = \oint_{\partial\Sigma} \boldsymbol{k}_\epsilon(\delta\Phi, \Phi)$, but the integrability condition is now modified to [799]

$$\oint_{\partial\Sigma} \left(\xi \cdot \boldsymbol{\omega}(\delta_1\Phi, \delta_2\Phi, \Phi) + \boldsymbol{k}_{\delta_1\epsilon}(\delta_2\Phi, \Phi) - \boldsymbol{k}_{\delta_2\epsilon}(\delta_1\Phi, \Phi)\right) \approx 0\,. \tag{G.16}$$

---

### > Symplectic symmetries

By definition, the phase space $(\mathcal{F}; \boldsymbol{\Omega})$ has a non-degenerate symplectic 2-form. It may happen that for a subspace of the tangent space (to a given point $\Phi$) the symplectic density $\boldsymbol{\omega}$ vanishes on-shell, i.e. for a subclass of $\delta_\epsilon\Phi$'s, which will be denoted by $\delta_{\boldsymbol{\omega}}\Phi$,

$$\boldsymbol{\omega}(\delta\Phi, \delta_{\boldsymbol{\omega}}\Phi, \Phi) \approx 0\,, \tag{G.17}$$

for all $\delta\Phi$ satisfying the linearized EOM. Two important properties follow from (G.17): (i) conservation of $\not{\delta} Q_{\boldsymbol{\omega}}$ and that it is independent of $\Sigma$; (ii) independence of the charge on the codimension-2 integration surface $\partial\Sigma$. In this case, the charges may be defined over any compact codimension-2 surface that need not be the boundary of a Cauchy surface [380,796,799]. The transformations generated by $\delta_{\boldsymbol{\omega}}\Phi$ are called symplectic symmetries [380,798].[2]

---

Equation (G.17) may be satisfied for two classes of field perturbations, the non-exact symmetries $\delta_\chi \Phi$ and the exact symmetries $\delta_\eta \Phi$:

1. **Symplectic non-exact symmetries** are the subset of $\delta_{\boldsymbol{\omega}}\Phi$ that are non-zero at least on one point of the phase space. We denote symplectic non-exact symmetry perturbation by $\delta_\chi \Phi \neq 0$. Based on a given solution $\Phi_0$, one may construct a full phase space by the successive action of $\delta_\chi$ on $\Phi_0$ (which is formally denoted as $e^{\int_\gamma \delta_\chi}\ \Phi_0$, where $\gamma$ denotes an arbitrary path in the phase space). The elements in this phase space, denoted by $\mathcal{F}_{\Phi_0}$, are then labeled by conserved charges associated with symplectic non-exact symmetries. These charges are defined by the integration of the symplectic current over a generic smooth, closed, and compact codimension-2 surface $\partial\Sigma$; they fall into the coadjoint orbits of the algebra of symplectic charges. See [377,380,479,799] for a discussion of symplectic charges and their algebra for cases where $\Phi_0$ is a locally $\mathrm{AdS}_3$ geometry or a near-horizon extremal geometry.
2. **Symplectic exact symmetries** are the subset of $\delta_{\boldsymbol{\omega}}\Phi$ that vanish over the whole phase space, $\delta_\eta \Phi = 0$. For symplectic exact symmetries (in short, exact symmetries), (G.17) is obviously satisfied. Exact symmetries are the gauge transformations that do not move us in the solution space. Such $\eta$ are hence in general field-dependent, $\eta = \eta[\Phi]$. If we consider diffeomorphisms, these exact symmetries are the isometries of spacetime generated by the Killing vectors. In the presence of gauge fields, the exact symmetries are not limited to Killing vectors; there could be a subset of internal gauge transformations which do not change a given solution. For example, the Maxwell gauge field corresponding to a set of static charges, in the static gauge, is invariant under gauge transformation generated by $\lambda = \text{const.}$, the global part of the $U(1)$ gauge transformations. These are the set of symmetries for which one may define Komar-type charges, discussed in Sect. 5.3.

### > Example: conserved charges in Dilaton-Einstein–Maxwell theory

As reviewed and explained above, $\boldsymbol{k}_\epsilon$ depends on the details of the theory. As example and to illustrate how our method works, consider Dilaton-Einstein–Maxwell theory with cosmological constant $\Lambda$. The dynamical fields $\Phi$ are the metric $g_{\mu\nu}$, some abelian 1-form gauge fields $A^a$ (with field strength $F^a = \mathrm{d}A^a$) and some scalar

[2] In holographic contexts, symplectic symmetries can be defined for any cutoff surface, i.e. they do not require some asymptotic expansion of the fields. This is in contrast to asymptotic symmetries, see Chap. 7.

fields $\phi^I$ governed by the Lagrangian

$$\mathcal{L} = \frac{1}{16\pi G_{\rm N}}\big(R - 2\mathrm{f}_{IJ}\nabla^\mu\phi^I\nabla_\mu\phi^J - \mathrm{k}_{ab}F^a_{\mu\nu}F^{b\,\mu\nu} - V(\phi)\big)\,. \tag{G.18}$$

The functions $\mathrm{f}_{IJ}$ and $\mathrm{k}_{ab}$ can depend on $\phi^I$. The Lagrangian $d$-form is the Hodge-dual of (G.18), $\mathbf{L} = \star\mathcal{L}$,

$$\mathbf{L} = \frac{\sqrt{-g}}{d!}\,\epsilon_{\mu_1\mu_2\cdots\mu_d}\,\mathcal{L}\;\mathrm{d}x^{\mu_1}\wedge\mathrm{d}x^{\mu_2}\wedge\cdots\wedge\mathrm{d}x^{\mu_d}\,. \tag{G.19}$$

Here $\epsilon_{\mu_1\mu_2\cdots\mu_d}$ is the Levi-Civitá symbol, $\epsilon_{012\cdots d-1} = +1$. The surface $(d-1;1)$-form $\mathbf{\Theta}$ is

$$\mathbf{\Theta} = \frac{\sqrt{-g}}{(d-1)!}\,\epsilon_{\mu\mu_1\cdots\mu_{d-1}}\,(\Theta^{\mathrm{E}\,\mu} + \Theta^{\mathrm{M}\,\mu} + \Theta^{\mathrm{S}\,\mu})\;\mathrm{d}x^{\mu_1}\wedge\cdots\wedge\mathrm{d}x^{\mu_{d-1}} \tag{G.20}$$

in which

$$\Theta^{\mathrm{E}\,\mu}(\delta\Phi,\Phi) = \frac{1}{16\pi G_{\rm N}}(\nabla_\nu h^{\mu\nu} - \nabla^\mu h)\,, \tag{G.21}$$

$$\Theta^{\mathrm{M}\,\mu}(\delta\Phi,\Phi) = \frac{-1}{4\pi G_{\rm N}}\mathrm{k}_{ab}\,F^{a\,\mu\nu}\,\delta A^b_\nu\,, \tag{G.22}$$

$$\Theta^{\mathrm{S}\,\mu}(\delta\Phi,\Phi) = \frac{-1}{4\pi G_{\rm N}}\mathrm{f}_{IJ}\,\nabla^\mu\phi^I\delta\phi^J\,, \tag{G.23}$$

where $h^{\mu\nu} \equiv g^{\mu\sigma}g^{\nu\tau}\delta g_{\sigma\tau}$ and $h \equiv h^\mu_{\ \mu}$. For $\epsilon = \{\xi, \lambda^a\}$, the Noether–Wald $(d-2;0)$-form $\mathbf{Q}_\epsilon$ can be read off from (G.14), yielding

$$\mathbf{Q}_\epsilon = \frac{\sqrt{-g}}{(d-2)!16\pi G_{\rm N}}\,\epsilon_{\mu\nu\mu_1\cdots\mu_{d-2}}\,(\mathrm{Q}^{\mathrm{E}\;\mu\nu}_\epsilon + \mathrm{Q}^{\mathrm{M}\;\mu\nu}_\epsilon + \mathrm{Q}^{\mathrm{S}\;\mu\nu}_\epsilon)\,\mathrm{d}x^{\mu_1}\wedge\cdots\wedge\mathrm{d}x^{\mu_{d-2}} \tag{G.24}$$

with

$$\mathrm{Q}^{\mathrm{E}\;\mu\nu}_\epsilon = \frac{1}{2}\big(\nabla^\nu\xi^\mu - \nabla^\mu\xi^\nu\big)\,, \tag{G.25}$$

$$\mathrm{Q}^{\mathrm{M}\;\mu\nu}_\epsilon = -2\mathrm{k}_{ab}F^{a\;\mu\nu}(A^b_\rho\xi^\rho + \lambda^b)\,, \tag{G.26}$$

$$\mathrm{Q}^{\mathrm{S}\;\mu\nu}_\epsilon = 0\,. \tag{G.27}$$

Next, we compute the $(d-2;1)$-form $\boldsymbol{k}_\epsilon(\delta\Phi,\Phi)$ using (G.13). The calculations are cumbersome but straightforward [795] (e.g. see Appendix C.6 in [796] for the Einstein–Hilbert theory). The final result is

$$\boldsymbol{k}_\epsilon(\delta\Phi,\Phi) = \frac{\sqrt{-g}}{(d-2)!16\pi G_{\rm N}}\epsilon_{\mu\nu\mu_1\cdots\mu_{d-2}}(k^{\mathrm{E}\,\mu\nu}_\epsilon + k^{\mathrm{M}\,\mu\nu}_\epsilon + k^{\mathrm{S}\,\mu\nu}_\epsilon)\mathrm{d}x^{\mu_1}\wedge\cdots\wedge\mathrm{d}x^{\mu_{d-2}} \tag{G.28}$$

where the Einstein part reads

$$\boxed{k_\epsilon^{\mathrm{E}\,\mu\nu}(\delta\Phi,\Phi)=\xi^{[\nu}\nabla^{\mu]}h-\xi^{[\nu}\nabla_\rho h^{\mu]\rho}+\xi_\rho\nabla^{[\nu}h^{\mu]\rho}+\frac{1}{2}h\nabla^{[\nu}\xi^{\mu]}-h^{\rho[\nu}\nabla_\rho\xi^{\mu]}} \tag{G.29}$$

and the Maxwell and scalar parts are given by

$$\begin{aligned}k_\epsilon^{\mathrm{M}\,\mu\nu}(\delta\Phi,\Phi)=&\Big(h\mathrm{k}_{ab}\,F^{a[\nu\mu]}-4\mathrm{k}_{ab}F^{a\rho[\mu}h_\rho{}^{\nu]}-2\mathrm{k}_{ab}\delta F^{a[\mu\nu]}-2\frac{\partial\mathrm{k}_{ab}}{\partial\phi^I}F^{a[\mu\nu]}\delta\phi^I\Big)\\&\Big(\xi^\rho A^b_\rho+\lambda^b\Big)-2\mathrm{k}_{ab}\,F^{a\,[\mu\nu]}\xi^\rho\delta A^b_\rho-2\,\mathrm{k}_{ab}\,F^{a\,\rho[\mu}\xi^{\nu]}\delta A^b_\rho\end{aligned} \tag{G.30}$$

$$k_\epsilon^{\mathrm{S}\,\mu\nu}(\delta\Phi,\Phi)=2\xi^{[\nu}\,\mathrm{f}_{IJ}\,\nabla^{\mu]}\phi^I\,\delta\phi^J\,. \tag{G.31}$$

The results above hold for any value of the cosmological constant $\Lambda$.

---

## > Change of slicing

The CPSF is a systematic way to associate a symplectic structure to the solution space specified by some parameters and functions. The symmetry generators $\epsilon^i$, which are vector fields in the gravity case, take us from one point in the solution space to another close-by point. Thus, they provide a basis on the cotangent space of the solution space and a way to span and label the solution space, if the associated surface charges $Q_i$ are integrable. As in any manifold, one may adapt different slicings. Here we address how this can be done systematically on the solution space, i.e. we study a general coordinate transformation on the solution space. To this end, let us start with the charge variation

$$\delta\!\!\!/ Q_\epsilon=\int\epsilon^i\delta\!\!\!/ Q_i\,\mathrm{d}^{d-2}x\,,\qquad i=1,2,\ldots,N \tag{G.32}$$

and perform a generic change of slicing, i.e. a coordinate change on the solution space, from $Q_i$ to $\tilde{Q}_i$. The expression

$$\tilde{Q}_i=\tilde{Q}_i[Q_j,\partial^nQ_j] \tag{G.33}$$

is a (smooth and real) functional of $Q_i$. Recalling that the charge variation $\delta\!\!\!/ Q_\epsilon$ is a physical observable on the solution space and thus slicing-invariant, fixes how the transformation of the symmetry generators.

$$\tilde{\epsilon}^i=\frac{\delta Q_j}{\delta\tilde{Q}_i}\,\epsilon^j. \tag{G.34}$$

That is, a change of slicing takes a given set of symmetry generators to a field dependent linear combination thereof, while keeping $\delta\!\!\!/ Q_\epsilon$ invariant.

Changes of slicings generically change the charge algebra. More crucially, the very notion of integrability of surface charges is slicing-dependent. Therefore, one can ask if there exist slicings that render a given charge variation $\not\delta Q_\epsilon$ integrable. It has been conjectured [692,739] that in the absence of flux of bulk modes through the boundary, i.e, in the absence of 'genuine flux', there always exist such 'integrable slicings', see Exercise G.4 for an example.

In general, the adjusted Lie bracket [799] of symmetry generators closes onto an algebroid (and not an algebra). Changes of slicings can bring such algebroids into (Lie-)algebra form, see Exercise G.3 for an example. See [376,404,693,737,739, 800,801] for examples and further discussions on changes of slicings.

## Exercises

**G.1 Conservation of symplectic form and charge variations.**

(1) To show that symplectic form (G.5) is independent of $\Sigma$, one may compute it over two different Cauchy surfaces $\Sigma_1$, $\Sigma_2$, find their difference and verify that indeed the difference vanishes. Explore if this requires extra conditions on fluxes at the boundaries of the region between $\Sigma_1$, $\Sigma_2$.

(2) One may repeat the above analysis to show that the charge variation (G.11) is indeed conserved in time, by choosing the two Cauchy surfaces to be two constant time slices at two different times $t_1$, $t_2$ and verifying that once computed on-shell the charge is independent of $t$.

**G.2 More on the integrability condition.**

Prove the field-dependence adjusted integrability condition (G.16).

**G.3 Change of slicing from an algebra to an algebroid.**

Consider the following surface charge (see [737] for more details)

$$Q[\eta, \eta^a] = \int \mathrm{d}^2x \ \left(\eta\mathcal{P} + \eta^a \mathcal{J}_a\right), \qquad a = 1, 2 \tag{G.35}$$

with variations,

$$\begin{aligned} \delta\mathcal{P} &= \eta^a \partial_a \mathcal{P} + \mathcal{P}\partial_a \eta^a, \\ \delta\mathcal{J}_a &= \partial_a \eta\mathcal{P} + \eta^b \partial_b \mathcal{J}_a + \mathcal{J}_b \partial_a \eta^b + \mathcal{J}_a \partial_b \eta^b. \end{aligned} \tag{G.36}$$

(1) Show the charge algebra in the above slicing is

$$\begin{aligned} \{\mathcal{P}(x), \mathcal{P}(y)\} &= 0 \\ \{\mathcal{J}_a(x), \mathcal{P}(y)\} &= \left(\mathcal{P}(y)\frac{\partial}{\partial x^a} - \mathcal{P}(x)\frac{\partial}{\partial y^a}\right)\delta^2(x-y) \\ \{\mathcal{J}_a(x), \mathcal{J}_b(y)\} &= \left(\mathcal{J}_a(y)\frac{\partial}{\partial x^b} - \mathcal{J}_b(x)\frac{\partial}{\partial y^a}\right)\delta^2(x-y). \end{aligned} \tag{G.37}$$

The above is an extension of the $\text{BMS}_4$ algebra, with $\mathcal{P}$ the charge associated with supertranslations and $\mathcal{J}_a$ the charge associated with extended superrotations. The symmetry generators $\eta(x)$, $\eta^a(x)$ also satisfy a similar algebra as (G.37).

(2) Consider the following change of slicing,

$$\eta \to \xi = \eta + \eta^a \mathcal{J}_a, \qquad \eta^a \to \xi^a = \mathcal{P}\eta^a. \tag{G.38}$$

(2-1) Show the charges in the new slicing are $P = \mathcal{P}$, $J_a = \mathcal{J}_a/\mathcal{P}$.

(2-2) Show the charge algebra in $\xi$ slicing is

$$\begin{aligned}
\{P(x), P(y)\} &= 0\\
\{J_a(x), P(y)\} &= \frac{\partial}{\partial x^a}\delta^2(x-y)\\
\{J_a(x), J_b(y)\} &= \frac{1}{P(x)}F_{ba}(x)\delta^2(x-y)
\end{aligned} \tag{G.39}$$

where $F_{ab} := \partial_a J_b - \partial_b J_a$.

(2-3) Show that $\{P(x), F_{ab}(y)\} = 0$ and that (G.39) closes onto an algebra, i.e. it satisfies Jacobi identities. Nonetheless, as one can see it is not a Lie algebra, as the $J_a$, $J_b$ commutator is not linear in the generators.

(2-4) Compute the adjusted Lie bracket of the symmetry generators $\xi, \xi^a$ and show that it is of the form of an algebroid.

### G.4 Change of slicing from non-integrable into integrable charges.

We mentioned that non-integrability of the charge may be an artifact of solution space slicing. Here we take the reader through such example in $2d$ gravity case. The details may be found in [739]. Consider a $2d$ metric and scalar field of the form

$$\begin{aligned}
\mathrm{d}s^2 &= 2\eta(v)\mathrm{d}r\mathrm{d}v - 2r\eta F(v)\mathrm{d}v^2 + \mathcal{O}(r^2),\\
\Phi &= \Phi(v) + \mathcal{O}(r)
\end{aligned} \tag{G.40}$$

where $r = 0$ denote a null surface which is taken to be the boundary of spacetime. The above are the leading expansion terms in powers or $r$ of a $2d$ Einstein-dilaton gravity theory, if

$$F(v) = \frac{\Phi''}{\Phi'} - \frac{\eta'}{\eta},$$

where *prime* denotes derivative with respect to $v$.

(1) Show the vector field

$$\xi = T\partial_v - r(W - T')\partial_r + \mathcal{O}(r)$$

is a generator of symmetry within the solution space (G.40) which is specified by two independent functions $\eta(v)$, $\Phi(v)$.

(2) Compute the Lie bracket of symmetry generators $\xi$ and show they satisfy a $\mathrm{BMS}_3$ algebra.

(3) Find variations of the fields and show

$$\delta_\xi \eta = \eta' T + 2\eta T' - \eta W, \qquad \delta_\xi \Phi = \Phi' T.$$

(4) Compute the charge associated with the symmetry generators $\xi$ and show

$$\not{\delta} Q_\xi = W \delta\Phi + T \not{\delta}\mathcal{A},$$

where

$$\not{\delta}\mathcal{A} = \Gamma\delta\Phi - 2\delta\Phi' + \Phi' \frac{\delta\eta}{\eta}, \qquad \Gamma := -\frac{2\Phi''}{\Phi'} + \frac{\eta'}{\eta}.$$

(5) Consider the following change of slicing

$$W \to \tilde{W} = W - \Gamma T, \qquad T \to \tilde{T} = \Phi' T.$$

Show that the adjusted Lie bracket of symmetry generators vanishes, $[\tilde{\xi}(\tilde{T}_1, \tilde{W}_1), \tilde{\xi}(\tilde{T}_2, \tilde{W}_2)] = 0$.

(6) Write the charge variation in the tilde-slicing and show that the charge becomes integrable with

$$\delta Q_{\tilde{\xi}} = \tilde{W}\delta\Phi + \tilde{T}\delta\mathcal{P}, \qquad \mathcal{P} = -\ln\left(\frac{\Phi'^2}{\eta}\right).$$

(7) Show the charge algebra takes the form of a Heisenberg algebra,

$$\{\Phi(v), \Phi(v')\} = \{\mathcal{P}(v), \mathcal{P}(v')\} = 0, \;\; \{\Phi(v), \mathcal{P}(v')\} = \delta(v - v').$$

# More on Membrane Paradigm

# H

In this appendix, we present more details of derivations associated with the membrane paradigm at the classical level. Take the stretched horizon to be a time-like $(2+1)$-dimensional surface which is at small proper distance $\epsilon$ outside the event horizon, see Fig. 3.9 for a visualization of the stretched horizon. We denote the outward-pointing spacelike unit normal vector to the stretched horizon by $n^\nu$, $n^2 = 1$ and take our *fido*s to follow worldlines with velocity $u^\mu$, $u^2 = -1$, $n \cdot u = 0$. At finite (but small) $\epsilon$ we define $u^\mu = l^\mu - \epsilon\, \Delta^\mu$ and $n^\mu = l^\mu + \epsilon\, \Delta^\mu$ with $l^2 = 0$, $l^\mu \Delta_\mu = 1/(2\epsilon)$ and $\Delta^2 = o(1/\epsilon^2)$. In this Carrollian limit, $\epsilon \to 0$, both $n^\mu$ and $u^\mu$ become null vectors tangent and normal to horizon $\mathcal{H}$.

We take $h_{\mu\nu}$ to be the induced metric on the stretched horizon and $K_{\mu\nu}$ to be its extrinsic curvature

$$h_{\mu\nu} = g_{\mu\nu} - n_\mu n_\nu\,, \qquad K_{\mu\nu} = \frac{1}{2}(\nabla_\mu n_\nu + \nabla_\nu n_\mu)\,. \tag{H.1}$$

For later use we also introduce the metric on the bifurcation surface

$$\gamma_{\mu\nu} = g_{\mu\nu} - n_\mu n_\nu + u_\mu u_\nu\,. \tag{H.2}$$

We denote the directions along the codimension-2 bifurcation surface by $x^a$.

To implement the variational principle we should specify the behavior of the fields at the boundaries, the stretched horizon, and the asymptotic region. Here we only focus on the former since the boundary conditions in the asymptotic region may be fixed independently of those at the horizon. Physically, these boundary conditions should guarantee that the free-fall observers measure finite observables and that they do not see any sources or sinks as they pass through the stretched horizon. Boundary conditions are imposed through the addition of appropriate boundary or surface terms to the action, as discussed in Sect. 6.1. In Maxwell's theory with field strength $F_{\mu\nu}$, the appropriate boundary conditions are to assert that the stretched horizon is a perfectly conducting surface, i.e. $\delta F_{\mu\nu} n^\nu = 0$. For gravity, Dirichlet



D. Grumiller and M. M. Sheikh-Jabbari, *Black Hole Physics*, Graduate Texts in Physics,
https://doi.org/10.1007/978-3-031-10343-8

boundary conditions, $\delta g_{\mu\nu} n^\nu = 0$, are imposed by adding the Gibbons–Hawking–York boundary term. The Einstein–Maxwell theory with appropriate boundary terms is hence

$$I[g_{\mu\nu}, A_\mu] = \frac{1}{16\pi G_{\text{N}}} \int \mathrm{d}^4x \sqrt{-g}(R - F^2) + \frac{1}{8\pi G_{\text{N}}} \oint \mathrm{d}^3x \sqrt{-h}\, (K + 2F_{\mu\nu} n^\mu A^\nu)\,. \tag{H.3}$$

The boundary conditions are chosen such that the boundary terms contribute to the boundary EOM like a boundary source:

$$\mathcal{J}^{\text{H}}_\nu := \frac{\delta I_{\text{b'dry}}}{\delta A^\nu} = \frac{1}{4\pi G_{\text{N}}} n^\mu F_{\mu\nu}\,, \tag{H.4a}$$

$$\mathcal{T}^{\text{H}}_{\mu\nu} := -\frac{2}{\sqrt{-h}} \frac{\delta I_{\text{b'dry}}}{\delta h^{\mu\nu}} = \frac{-1}{8\pi G_{\text{N}}} (K_{\mu\nu} - h_{\mu\nu} K)\,. \tag{H.4b}$$

From now on we refer to the stretched horizon as ‘membrane’.

**Electromagnetic properties of the membrane.** The electric field is normal to the membrane,

$$E_\perp := F_{\mu\nu} n^\mu u^\nu = 4\pi G_{\text{N}} u^\mu \mathcal{J}^{\text{H}}_\mu := 4\pi G_{\text{N}} \sigma \tag{H.5}$$

and is sourced by the local charge density $\sigma$ over the membrane; the total charge on the black hole is its integral over the membrane, taken at some constant universal time, see Exercise H.1. The magnetic field is tangential to the membrane,

$$\mathbf{B}^\mu_\parallel := \epsilon^{\rho\nu\alpha\beta} u_\rho h^\mu{}_\nu F_{\alpha\beta} = 4\pi G_{\text{N}} \epsilon^\mu{}_{\alpha\beta\nu} u^\alpha n^\beta \mathcal{J}^\nu_{\text{H}} \tag{H.6}$$

and is sourced by the local current density at the membrane.

The boundary EOM yield the conservation equation

$$h^{\mu\nu} \nabla_\mu \mathcal{J}^{\text{H}}_\nu = u^\mu \partial_\mu \sigma + \gamma^{ab} \nabla_a \mathcal{J}^{\text{H}}_b = -J_n\,, \tag{H.7}$$

where $J_n = J_\mu n^\mu$ with $J_\mu$ being the external current appearing in the right-hand side of the bulk Maxwell equations outside the horizon, $\nabla^\mu F_{\mu\nu} = 4\pi G_{\text{N}} J_\nu$. Physically, this equation expresses local charge conservation: any charge that falls into the black hole can be regarded as remaining on the membrane; the membrane is an equi-potential surface impermeable to charge. Smoothness of what freely falling observers see at the membrane then relates $\mathbf{E}_\parallel$ to $\mathbf{B}_\parallel$ as (work through Exercise H.2 for the derivation)

$$\mathbf{E}_\parallel = \hat{n} \times \mathbf{B}_\parallel = 4\pi G_{\text{N}} \mathcal{J}_{\text{H}}\,, \tag{H.8}$$

where the spatial vectors are on constant time slices. That is, black holes obey Ohm’s law with vacuum surface resistivity, $\rho = 4\pi G_{\text{N}} \approx 377\ \Omega$. Moreover, (H.8) implies that all radiation in the normal direction is ingoing; a black hole acts as a perfect absorber, consistently with classical intuition. Explicitly, the Poynting-flux is

$$\mathbf{S} = \frac{1}{4\pi G_{\text{N}}} (\mathbf{E} \times \mathbf{B}) = -4\pi G_{\text{N}} \mathcal{J}^2_{\text{H}}\, \hat{n}\,. \tag{H.9}$$

We reiterate that observers falling through the stretched horizon find neither surface sources nor a physical membrane; for them, the stretched horizon is like a red line drawn on some geographic map: helpful for orientation, but not part of the physical world. The membrane paradigm is a useful tool for *fido*s, analogous to the method of image charges in electrostatics, in which a fictitious charge distribution is added to the system to implement, say, conducting boundary conditions.

**Stress and tension of the membrane.** The Israel junction conditions [202] yield the membrane tension $\mathcal{T}^{\text{H}}_{\mu\nu}$ (H.4b). The Einstein equations at the boundary, via the contracted Gauss–Codazzi equations (see Exercise F.1), give the continuity equation,

$$\hat{\nabla}^{\mu}\mathcal{T}^{\text{H}}_{\mu\nu} := h_{\alpha}{}^{\beta}\nabla^{\alpha}\mathcal{T}^{\text{H}}_{\beta\nu} + K^{\alpha\beta}\mathcal{T}^{\text{H}}_{\alpha\beta}\, n_{\nu} + K^{\alpha\beta}\mathcal{T}^{\text{H}}_{\alpha\nu}\, n_{\beta} = -h_{\nu\alpha}T^{\alpha\beta}n_{\beta}\ , \tag{H.10}$$

where $\hat{\nabla}_{\mu}$ is the covariant derivative along the stretched horizon. The above is the Navier–Stokes equation for fluid membrane, which is the analog of (H.7) for the tension of the membrane.[3]

To see this, we first study more closely $\mathcal{T}^{\text{H}}_{\mu\nu}$ and its components, particularly the ones along the $x^a$-directions. Since $\mathcal{T}^{\text{H}}_{\mu\nu}n^{\nu} = 0$, we can decompose the non-zero components as

$$\Sigma^{\text{H}} := \mathcal{T}^{\text{H}}_{\mu\nu}u^{\mu}u^{\nu} \qquad \Pi^{\text{H}}_{a} := \mathcal{T}^{\text{H}}_{\mu\nu}u^{\mu}\gamma^{\nu}{}_{a} \qquad \mathcal{T}^{\text{H}}_{ab} := \mathcal{T}^{\text{H}}_{\mu\nu}\gamma^{\mu}{}_{a}\gamma^{\nu}{}_{b} \tag{H.11}$$

where $\gamma^{\mu}{}_{\nu}$ projects onto the bifurcation surface. As the definitions indicate, $\Sigma^{\text{H}}$, $\Pi^{\text{H}}_{a}$, $\mathcal{T}^{\text{H}}_{ab}$ are respectively tension, momentum flow and stress tensor of the membrane fluid. Next, we take the stretching parameter $\epsilon$ to zero. In the Carrollian limit, $\epsilon \to 0$, $-u^{\mu}u^{\nu}K_{\mu\nu}$ is the surface gravity $\kappa$, $u^{\mu}K^{a}{}_{\mu} = 0$ and the extrinsic curvature of the bifurcation surface $K_{ab} := \frac{1}{2}l^{\mu}\nabla_{\mu}\gamma_{ab}$, where $\gamma_{ab}$ is its induced metric. We can decompose $K_{ab}$ into a traceless part and a trace, $K_{ab} = \sigma_{ab} + \frac{1}{2}\gamma_{ab}\theta$, where $\sigma_{ab}$ is the shear and $\theta$ the expansion of the world lines of nearby horizon surface elements. Therefore,

$$\mathcal{T}^{\text{H}}_{ab} = \frac{1}{8\pi G_{\text{N}}}\left[-\sigma_{ab} + (\frac{1}{2}\theta + \kappa)\gamma_{ab}\right]\ , \tag{H.12}$$

which describes a 2-dimensional viscous Newtonian fluid with pressure $p$, shear viscosity $\eta$ and bulk viscosity $\zeta$,

$$p = \frac{\kappa}{8\pi\ G_{\text{N}}}, \qquad \eta = \frac{1}{16\pi G_{\text{N}}}, \qquad \zeta = -\frac{1}{16\pi G_{\text{N}}}, \tag{H.13}$$

and (H.11) yields $\Sigma^{\text{H}} = -\frac{\theta}{8\pi G_{\text{N}}}$. Note that, unlike ordinary fluids, the membrane has negative bulk viscosity. This would ordinarily indicate an instability against generic

[3] The appearance of the Navier–Stokes equation has led to some confusion in the literature, since it appears to suggest that we are dealing with a Galilean limit, which is not apposite. Rather, we have a Carrollian limit, see the discussion in Sect. 6.8.

perturbations triggering expansion or contraction. It can be regarded as reflecting a null hypersurface's natural tendency to expand or contract, see Sect. 3.2.1.

With the above decompositions, (H.10) yields,

$$u^\mu \nabla_\mu \Sigma + \theta \Sigma = -p\theta + \zeta\theta^2 + 2\eta\sigma_{ab}\sigma^{ab} + T_{\mu\nu}u^\mu n^\nu \ , \tag{H.14a}$$

$$u^\mu \nabla_\mu \Pi_a = -\nabla_a p + \zeta \nabla_a \theta + 2\eta\tilde{\nabla}^b \sigma_{ab} - \gamma^\mu{}_a T_\mu{}^\nu n_\nu \ , \tag{H.14b}$$

where $u^\mu \nabla_\mu$ is the Lie derivative along the proper time, $\tilde{\nabla}^a$ is the covariant derivative with respect to $\gamma_{ab}$ and $\gamma^\mu{}_a T_\mu{}^\nu n_\nu$ denotes the flux of momentum into the black hole. The above then yields the main equations, namely the heat transfer equation (6.78) with membrane temperature and entropy given in (6.79).

## Exercises

**H.1 Charges of a black hole in the membrane paradigm formulation.**

Using (H.4) compute the mass, angular momentum, and electric charge of a KN black hole by integrating over horizon stress tensor or electric field.

**H.2 Derivation of** (H.8).

Using the fact that fields measured by free-fall (inertial observers) at the stretched horizon should be finite, and that *fido*s who make measurements at the membrane, have large Lorentz boost factors with respect to free-fall observers, relate components of electric and magnetic fields free-fall and *fido*s measure. Show that this yields (H.8). You may consult with [802].

**H.3 Membrane paradigm and Einstein–Maxwell-Axion theory.**

Work through membrane paradigm formulation for black hole solutions to Einstein–Maxwell-Axion theory,

# String Theory Low Energy Effective Actions

In Chap. 9, we briefly discussed string theory as a theory of QG. While not a (quantum) field theory, at energies much lower than the string scale $\ell_s^{-1}$, $\ell_s E \ll 1$, the theory admits a LEFT description. For 10-dimensional string theories, this LEFT is supergravity. In accordance with the five 10-dimensional critical string theories, there are four $10d$ supergravities, IIA, IIB, $E_8 \times E_8$ and $SO(32)$ supergravities. The latter is the LEFT of both type I and heterotic $SO(32)$ string theories. Type IIA, IIB theories, respectively, have $\mathcal{N} = (1, 1)$ and $\mathcal{N} = (0, 2)$ supersymmetry and are the only two consistent $10d$ supergravities with 32 supercharges. The $E_8 \times E_8$ and $SO(32)$ theories have 16 supercharges with $\mathcal{N} = (0, 1)$ supersymmetry algebra. Supergravity in $11d$ is unique and has 32 supercharges. This theory is viewed as the LEFT of M-theory.

String or M-theory in lower dimensions is typically obtained from compactifications of the 10- or 11-dimensional theories. Depending on the properties of the compactification manifold, the lower-dimensional theory can have 32 or lower (down to zero) supersymmetries. LEFT of this lower-dimensional string/M-theory is hence typically a lower-dimensional (gauged) supergravity with various supersymmetries. Lower-dimensional supergravities may be classified and specified by their matter bosonic content, supersymmetry, and gauge group. See e.g. [522,662]. There is a general lore that all lower-dimensional supergravities may be obtained from string compactifications. In this appendix, we present the bosonic part of type IIA, type IIB and $11d$ supergravity actions. We use the conventions and notations of [193,518].

## Type II supergravities

The bosonic action for type II theories has a generic form

$$S = \frac{1}{2\kappa^2} \int \mathrm{d}^{10}x \left[\sqrt{-g}\,(\mathcal{L}_{\text{NSNS}} + \mathcal{L}_{\text{RR}}) + \mathcal{L}_{\text{CS}}\right]. \tag{I.1}$$



D. Grumiller and M. M. Sheikh-Jabbari, *Black Hole Physics*, Graduate Texts in Physics,
https://doi.org/10.1007/978-3-031-10343-8

Type IIA, IIB theories share the Neveu–Schwarz-Neveu–Schwarz sector, which in the string-frame is of the form

$$\mathcal{L}_{\text{NSNS}} = e^{-2\phi}\left(R + 4\partial_\mu\phi\partial^\mu\phi - \frac{1}{2}|H_3|^2\right) \tag{I.2}$$

where $R$ is the Ricci scalar, $\phi$ the dilaton field and $H_3 = \mathrm{d}B_2$, with $B_2$ being the Neveu–Schwarz-Neveu–Schwarz 2-form.

The two theories differ in the Ramond-Ramond and CS sectors. For type IIA, the Ramond-Ramond Lagrangian involves a 1-form $C_1$ and 3-form $C_3$ fields,

$$\text{type IIA}: \qquad \mathcal{L}_{\text{RR}} = -\frac{1}{2}\left(|F_2|^2 + \frac{1}{2}|\tilde{F}_4|^2\right), \tag{I.3}$$

where $F_2 = \mathrm{d}C_1$ and $\tilde{F}_4 = \mathrm{d}C_3 - C_1 \wedge H_3$ and

$$\text{type IIA}: \qquad \mathcal{L}_{\text{CS}} = -\frac{1}{2}B_2 \wedge \mathrm{d}C_3 \wedge \mathrm{d}C_3\,. \tag{I.4}$$

For type IIB, $\mathcal{L}_{\text{RR}}$ involves 0-form $\chi$, 2-form $C_2$ and 4-form $C_4$ fields,

$$\text{type IIB}: \qquad \mathcal{L}_{\text{RR}} = -\frac{1}{2}\left(|\mathrm{d}\chi|^2 + |\tilde{F}_3|^2 + \frac{1}{2}|\tilde{F}_5|^2\right) \tag{I.5}$$

where

$$\tilde{F}_3 = \mathrm{d}C_2 - \chi H_3, \qquad \tilde{F}_5 = \mathrm{d}C_4 - \frac{1}{2}C_2 \wedge H_3 + \frac{1}{2}B_2 \wedge \mathrm{d}C_2\,. \tag{I.6}$$

The field strength of the 4-form field in type IIB is self-dual: $\tilde{F}_5 =^* \tilde{F}_5$. One should note that the self-duality condition does not follow from the Lagrangian (I.5) and should be imposed by hand. Finally,

$$\text{type IIB}: \qquad \mathcal{L}_{\text{CS}} = -\frac{1}{2}C_4 \wedge \mathrm{d}C_2 \wedge H_3\,. \tag{I.7}$$

The above theories have a dimensionful parameter $\kappa$ (related to $10d$ Newton constant) and the asymptotic value (expectation value) of the dilaton field $\phi$. There are various form fields in the type II supergravities which as was discussed in Chap. 7, are sourced by various (black) brane solutions, a $p$-brane is sourcing a $(p+1)$-form.

## > 11*d* supergravity

The field content of $11d$ supergravity is a metric, a 3-form, and a 32-component $11d$ Majorana gravitino. The bosonic fields are governed by the action

$$S = \frac{1}{2\kappa^2}\int \mathrm{d}^{11}x\left[\sqrt{-g}\left(R + \frac{1}{2}|F_4|^2\right) - \frac{1}{6}C_3 \wedge F_4 \wedge F_4\right] \tag{I.8}$$

where $F_4 = \mathrm{d}C_3$. This theory has only one dimensionful parameter $\kappa$ related to the $11d$ Newton constant and no other scalar field or parameters.

The type IIA action can be obtained from a dimensional reduction of the $11d$ supergravity action (I.8) over a circle. The radius of the circle is related to the dilaton $\phi$, the Ramond-Ramond 1-form $C_1$ comes from the $11d$ metric, and the Ramond-Ramond 3-form $C_3$ and Neveu–Schwarz-Neveu–Schwarz 2-form $B_2$ from the 3-form in $11d$. See [518] for details of the reduction.

### > String- vs. Einstein-frame

The type II actions above were presented in the string-frame, in which string naturally probes the spacetime. The string-frame is characterized by the $e^{-2\phi}$ factor in front of the Ricci scalar term in the Neveu–Schwarz-Neveu–Schwarz sector (I.2). One may bring the above actions to the Einstein-frame, in which the gravitational part is the Einstein–Hilbert action. This is possible by a dilaton-dependent Weyl rescaling of the metric,

$$g_{\mu\nu} = e^{\phi/2} g^{\mathrm{E}}_{\mu\nu} \tag{I.9}$$

for which $\sqrt{-g}e^{-2\phi}R = \sqrt{g^{\mathrm{E}}}R_{\mathrm{E}} + \cdots$, where $R_{\mathrm{E}}$ is the Ricci scalar computed from the Einstein-frame metric $g^{\mathrm{E}}_{\mu\nu}$ and the ellipsis denotes terms involving the dilaton and its derivatives. The rest of the terms in the Einstein-frame action may be worked out given (I.9), see Exercise I.1.

## Exercises

**I.1 Supergravity in Einstein-frame.**

Starting from (I.9),

(1) work out the kinetic term for the dilaton field in the Neveu–Schwarz-Neveu–Schwarz action (I.2);

(2) show Neveu–Schwarz-Neveu–Schwarz 2-form term in (I.2) takes the form $e^{-\phi}|H_3|^2$.

(3) show the Einstein-frame Lagrangian associated with a $p$-form in the Ramond-Ramond sector takes the form $e^{(2-p/2)\phi}|\tilde{F}_{p+1}|^2$. Therefore the Ramond-Ramond 4-form of the type IIB theory remains invariant.

**I.2 Einstein- and Jordan-frames.**

(1) Consider the $D$-dimensional Brans-Dicke theory,

$$S_{\mathrm{B.D.}} = \frac{1}{16\pi}\int \mathrm{d}^D x\,\sqrt{-g}\left(\phi R - \frac{\omega}{\phi}\,\partial_\mu\phi\partial^\mu\phi\right),$$

where $\omega$ is a constant parameter of the theory. This action is written in the Jordan-frame, as the Ricci scalar term is multiplied by the scalar field $\phi$. Bring the action to the Einstein-frame by a rescaling of the metric,

$$g_{\mu\nu} \to \phi^{\alpha} g^{\mathrm{E}}_{\mu\nu}.$$

(1-1) What is $\alpha$ for any $D > 2$ and show that for $D = 2$ there is no such $\alpha$. This dovetails with the discussion on Chap. 7 on $2d$ gravity.

(1-2) Write the action in the Einstein-frame. What is the Newton constant?

(1-3) Show that the EOM from the $S_{\mathrm{B.D.}}$ upon the same change in the rescaling of metric yields the EOM in the Einstein-frame.

(2) Consider a $D$-dimensional $f(R)$ theory,

$$S = \frac{1}{16\pi} \int \mathrm{d}^D x \sqrt{-g} \mathcal{L}, \qquad \mathcal{L} = f(R).$$

Show that this theory can be recast into an extension of Brans–Dicke theory where scalar $\phi$ has now a non-trivial potential too. That is, $f(R)$ theory is a scalar-tensor theory of gravity. To this end, take the following steps,
(i) $\mathcal{L} = f(\lambda) + \phi(\lambda - R)$, where $\phi$ is a Lagrange multiplier field and $\lambda$ is a scalar.
(ii) Integrate out $\lambda$ by solving its EOM and replacing it back into the action.

# Hints to Some Selected Exercises

J

Each chapter and appendix has some exercises. While most of the exercises already contain some hints and guide the reader toward the answer, a small part of them may require additional information. Here we provide hints (and in some cases full solutions) to a selected subset of the exercises.

## Exercises of Chapter 1

1.1 (1) Eclipse of Jupiter's moon Io happens when Jupiter stands in between Earth and the moon Io. All three objects are moving in orbits around the Sun and the moon also moves around Jupiter. So, the eclip se can happen in a variety of situations when the three objects are aligned. Nonetheless, the upper bound for the time may correspond to when the distance from the Earth to Jupiter–Io system has its maximal difference, i.e. twice Earth's orbit radius. Therefore, $2 \times 1.5 \times 10^{11}/(16.5 \times 60) \sim 3 \times 10^8$ m/sec can give an estimate for speed of light.

(2) Kepler's second law implies angular momentum conservation and hence gravity is a central force. Kepler's first and third laws, on the other hand, imply (i) Newtonian gravity is proportional to the mass of the planet (Galilean or Weak EP), and (ii) it obeys an inverse-square distance law.

1.3 Let $\sim$ denote equality of the two-sides up to dimensions, e.g. $E \sim Mc^2$ and $\hbar \sim EL/c$, where $c, \hbar$ are speed of light and Planck constant and $E, M, L$ respectively denote quantities of dimension energy, mass, time, and length. In the same way, $G_{\text{N}}\hbar/c^3 \sim L^2$ and $G_{\text{N}}M/c^2 \sim L$. With this information, we tackle this problem.

(1) $r_h \sim G_{\text{N}}M/c^2$ and $A_h \sim r_h^2 \sim G_{\text{N}}^2 M^2/c^4$.

(2) $S_{\text{BH}} = A_h/(4G_{\text{N}})$ becomes dimensionless if $G_{\text{N}}$ is replaced with $G_{\text{N}}\hbar/c^3$ which has dimension of length$^2$. Therefore, $S_{\text{BH}} \sim G_{\text{N}}M^2/(\hbar c)$.

(3) $T \sim Mc^2/S_{\text{BH}} \sim \hbar c^3/(G_{\text{N}}M)$. For $M = M_\odot$, $T \sim 10^{-8}$ K.

1.7 (1) Given the expression in the solution to Exercise 1.3, for $M = 10^{31}$ kg we have $r_h \sim 10$ km and $S_{\text{BH}} \sim 10^{80}$. (Note: this is dimensionless entropy, measured in units of Boltzmann constant $k_{\text{B}}$.)



D. Grumiller and M. M. Sheikh-Jabbari, *Black Hole Physics*, Graduate Texts in Physics,
https://doi.org/10.1007/978-3-031-10343-8

(2) To compute the entropy of a Sun-like star, one should have the density and/or temperature profile. Sun-like stars are made of photons and protons, while the mass is dominantly coming from the protons, the entropy is coming from relativistic species present there, namely photons. Moreover, assuming that the system is in a steady state, where some energy is steadily injected from the inner core and is finally radiated out and photons and protons are locally at thermal equilibrium, one can in principle compute the density and temperature profiles. Here, however, our purpose is to estimate the entropy and for the details of star profiles we refer to e.g. [803]. We simply take a relatively simple and realistic temperature profile (as a function of radius $r$), $T(r) = T_0 e^{-\alpha r/R}$, where $T_0 \sim 10^7$ K and $\alpha \sim 2$ and $R$ is the star radius. The entropy density for a gas of photons is $s = CT^3$, $C = \frac{4\pi^2 k_{\rm B}^4}{45\hbar^3 c^3}$ and hence total entropy may be computed as $S = 4\pi C T_0^3 R^3 \int_0^1 \mathrm{d}r\, r^2 e^{-3\alpha r} \sim 10^{-1} C T_0^3 R^3$.

Putting the numbers in, for the entropy of a Sun-like star one obtains $S_{\rm star} \sim 10^{60}$ (in $k_{\rm B}$ units). This value is about 20 orders of magnitude less than a black hole of the same mass. (For comparison note that number of stars in the universe is about $10^{23}$.) This means that the gravitational collapse which yields a black hole produces a huge amount of entropy.

## Exercises of Chapter 2

2.2 For part (1) it is enough to note that $\nabla_{[\nu}\mathbf{n}_{\alpha]} = \partial_{[\nu} N \partial_{\alpha]}$. The condition for hypersurface orthogonality is that $g_{y\mu} = 0$ for $\mu \neq y$.

2.6 The ADM mass and angular momenta, as reviewed in the opening of Chap. 5, was historically among the first formulations to define conserved charged in diffeomorphism-invariant theories like GR. For the details of this method, which is still one of the very commonly used ones, consult with usual GR books mentioned in the Further reading part of Chap. 1. For more recent and advanced discussions see [804, 805] and references therein.

2.8 (1) For $P_\xi$ in (2.123) and $x^\mu(\lambda)$ an affinely parameterized geodesic, $\frac{\mathrm{d}P_\xi}{\mathrm{d}\lambda} = \nabla_\mu \xi_\nu \dot{x}^\mu \dot{x}^\nu$. Note that here $\xi^\mu$ is a Killing vector field which is computed on the geodesic path, therefore $\xi^\mu = \xi^\mu(x^\nu(\lambda))$ and $\frac{\mathrm{d}\xi^\mu}{\mathrm{d}\lambda} = \nabla_\nu \xi^\mu \dot{x}^\nu$. $\frac{\mathrm{d}P_\xi}{\mathrm{d}\lambda}$ vanishes since $\xi^\mu$ is a Killing vector and as such $\nabla_\mu \xi_\nu + \nabla_\nu \xi_\mu = 0$.

(2) Poisson bracket of two conserved charges may be computed as

$$\begin{aligned}
\{P_{\xi_1}, P_{\xi_2}\}_{\text{P.B.}} &= \{\xi_1 \cdot p, \xi_2 \cdot p\}_{\text{P.B.}} \\
&= \{\xi_1^\mu, p_\nu\} p_\mu \xi_2^\nu + \{p_\nu, \xi_2^\mu\} \xi_1^\nu p_\mu \\
&= (\xi_2^\nu \nabla_\nu \xi_1^\mu - \xi_1^\nu \nabla_\nu \xi_2^\mu) p_\mu \\
&= \{\xi_1, \xi_2\}^\mu_{\text{L.B.}} p_\mu = P_{\{\xi_1, \xi_2\}_{\text{L.B.}}}.
\end{aligned} \tag{J.1}$$

2.13 (1) Recalling that $\mathrm{d}r/\mathrm{d}t = \dot{r}/\dot{t} = f(r)\dot{r}/E$, the coordinate time $t$ needed for an infalling radial timelike geodesic which starts at rest from $r_0$ to reach the horizon at $r = r_h$, is given by

$$E(t - t_0) = \sqrt{\frac{r_0}{r_h}} \int_{r_h}^{r_0} \frac{r^{3/2}\mathrm{d}r}{(r - r_h)\sqrt{r_0 - r}}\,, \qquad E^2 = 1 - \frac{r_h}{r_0}.$$

This integral may be computed explicitly. The notable point is that around $r \sim r_0$ the integral goes like $\sqrt{r_0 - r}$ and remains finite, while around $r \sim r_h$, it blows up like $\ln(r - r_h)$. In this respect it is like the null geodesic (2.25).

(2) Analysis of generic time-like geodesics (free particle path) for Schwarzschild geometry may be found in standard GR textbooks like [3,5], see also [806] for some analytic treatment.

2.17 (1) A metric of the form

$$\mathrm{d}s^2 = -f(r)\mathrm{d}t^2 + f^{-1}(r)\mathrm{d}r^2 + r^2\mathrm{d}\Omega_2^2$$

for $f(r) > 0$ region can be brought to the form (2.133) upon the coordinate transformation

$$\ln\rho = \int \frac{\mathrm{d}r}{r\sqrt{f(r)}},$$

where $F(\rho) = (r/\rho)^2$ and $G(\rho) = (1 + \frac{\rho F'}{2F})^2$. Therefore, for generic RN case with horizon radii $r_\pm$, $r_+ \neq r_-$,

$$F(\rho) = \left(\frac{R_h}{\rho} + \frac{\Delta_h}{2}(1 + \frac{1}{\rho^2})\right)^2, \qquad G(\rho) = \left(\frac{\Delta_h(\rho^2 - 1)}{2R_h\rho + \Delta_h(\rho^2 + 1)}\right)^2,$$

where $R_h := (r_+ + r_-)/2$, $\Delta_h := (r_+ - r_-)/2$. For the extremal case with $r_+ = r_-$,

$$F(\rho) = r_+^2(1 + \frac{1}{\rho})^2, \qquad G(\rho) = \left(1 + \frac{1}{\rho}\right)^{-2}.$$

For the Schwarzschild case, $R_h = \Delta_h = r_h/2$ and the above simplifies to, $F = \frac{r_h^2}{8}(1 + \frac{1}{\rho})^4$ and $G(\rho) = (\rho - 1)^2/(\rho + 1)^2$. Note that this coordinate system covers the outside horizon region.

(2) Consider a $2d$ metric of the form $\mathrm{d}s^2 = -f(r)\mathrm{d}t^2 + f^{-1}(r)\mathrm{d}r^2$ and perform the following coordinate transformation $r = F(uz)$, $t = r + G(u/z)$, for some $F$, $G$ functions such that metric in the $u$, $z$ coordinate system takes the form $\mathrm{d}s^2 = 2\mathrm{d}u\mathrm{d}z + g(u, z)\mathrm{d}u^2$, for some function $g$. It is then straightforward algebra to show that absence of $\mathrm{d}z^2$ term in the metric yields to $G' = z^2F'(1 + 1/f(r))$, where $'$ denotes derivative with respect to the argument. This can only be satisfied if $G(u/z) = A + B\ln(u/z)$, for constants $A$, $B$. Requiring $\mathrm{d}z\mathrm{d}u$ term in the metric to be 2, fixes $F'^2 = \frac{1}{2uz}\frac{f}{1-f}$, which yields $F = C - uz/(2B)$ for some constant $C$. With these choices, $g(u, z) = 2z^2\frac{f}{uz}$.

For the rest of the details please see [44].

2.21 $r = 0$ and $r \to \infty$ respectively correspond to $\theta = \pi, 0$ and hence $\theta \in (0, \pi]$. One can readily observe that

$$\mathrm{d}s^2 = \mathrm{d}r^2 + r^2\mathrm{d}\varphi^2 = \frac{1}{4\sin^4\frac{\theta}{2}}\left(\mathrm{d}\theta^2 + \sin^2\theta\mathrm{d}\varphi^2\right).$$

So, the $2d$ flat metric is conformal to the usual metric on $S^2$. One should however note that the conformal factor blows up at $\theta = 0$ (corresponding to $r \to \infty$). Explicitly, $2d$ flat space plus the point at infinity is topologically the same as $S^2$.

2.24 This is a standard exercise and its answer may be found in the literature. For part (1) see [193]. For part (2), see Fig. 8.3. For part (3), gravitational collapse on dS background, see [807]. For part (4), see [808] for charged matter collapse and [809] for collapse of rotating matter.

2.26 There are many papers that explore geodesics in the Kerr geometry. For this specific exercise, one may look at [810] and references therein.

2.27 For more discussions on Zero Angular Momentum Observer in Kerr geometry see [811] and references therein.

2.31 Black holes with generic horizon topology are called 'topological black holes'. While according to Hawking's topology theorem all asymptotically flat Einstein vacuum solutions have spherical horizon topology, for asymptotic $\mathrm{AdS}_4$ cases we have the possibility of topological black holes. See [176,812,813] for more discussions.

Note that the equation in the line below (2.43) can be used to determine surface gravity, where the function $f$ plays the role of the function $K$ in (2.89).

2.34 For an analysis of ISCOs in Kerr-(A)$\mathrm{dS}_D$ black holes see [814].

2.39 Kerr–Schild coordinates was introduced in [201] and since then it has been used and developed in many papers, e.g. see [815], Chap. 28 of [133], [816,817]. For Kerr–Schild double copy of Plebanski–Demianski family see [818] and references therein.

## Exercises of Chapter 3

3.1 (1) Let $l^\mu$ be normal to a null surface with non-affinity parameter $\kappa_l$. The non-affinity parameter of $Nl^\mu$ read from (3.26) is then $\kappa_{Nl} = N\kappa_l + l\cdot\nabla N$.

(2) Requirement of $l$ to be the velocity vector along an affinely parameterized null geodesic fixes $N$ such that $\kappa_{Nl} = 0$. That is, $l \cdot \nabla \ln N = -\kappa_l$, which can be schematically integrated as $N = e^{-\int \kappa_l d\ell}$, where $l \cdot \nabla \int \kappa_l d\ell = \kappa_l$.

(3) Multiplying both sides of (3.1) by $\xi_\nu$ we obtain $\xi^\mu\xi^\nu\nabla_\mu\xi_\nu = \kappa\xi^2$. The left-hand side is zero for any Killing vector $\xi$. So, either $\kappa = 0$ or $\xi^2 = 0$.

(4) For a Killing vector $\nabla_\mu\xi_\nu = -\nabla_\nu\xi_\mu$ and hence the left-hand side of (3.1) may be written as $-\xi^\mu\nabla_\nu\xi_\mu = -\frac{1}{2}\nabla_\nu\xi^2$.

(5) Starting from $\xi_{[\alpha}\nabla_\mu\xi_{\nu]}|_{\mathcal{N}} = 0$ we learn that

$$\xi_\mu\nabla_\nu\xi_\alpha = -\xi_\alpha\nabla_\mu\xi_\nu - \xi_\nu\nabla_\alpha\xi_\mu.$$

Multiplying both sides of the above by $\nabla^\mu \xi^\nu$, using the fact that $\xi$ is a Killing, i.e. $\nabla_\mu \xi_\nu = -\nabla_\nu \xi_\mu$ and (3.1) we find

$$-\xi_\alpha (\nabla_\mu \xi_\nu)^2 - \kappa^2 \xi_\alpha = \kappa^2 \xi_\alpha$$

which readily yields (3.2).

(6) Let us act by $\xi^\mu \nabla_\mu$ on both sides of (3.2). The right-hand side will then be $2\xi^\mu (\nabla_\mu \nabla_\alpha \xi_\beta)(\nabla^\alpha \xi^\beta) = 2R_{\mu\nu\alpha\beta}\xi^\mu \xi^\nu (\nabla^\alpha \xi^\beta) = 0$, where we used (3.28) and antisymmetry of Riemann with respect to the first two indices.

(7) Starting with (3.1), act by $\nabla_\nu$ on both sides. The right-hand side vanishes as showed in (6) above and we hence remain with $\nabla^\nu(\xi^\mu \nabla_\mu \xi_\nu) = 0 = -(\nabla^\nu \xi^\mu)^2 + \xi^\mu \nabla^\nu \nabla_\mu \xi_\nu$. The last term using (3.28) is $R_{\mu\nu}\xi^\mu \xi^\nu$ and one to the last term is $2\kappa^2$ recalling (3.2).

(8) $\xi$ is a hypersurface orthogonal Killing vector that is normal to the Killing horizon, therefore, $\mathrm{d}\xi$ is a 2-form proportional to the binormal to bifurcation surface $\mathcal{B}$, $\mathrm{d}\xi \propto \boldsymbol{\epsilon}$. To fix the proportionality factor, we may square both sides and use (3.2), i.e. $|\mathrm{d}\xi|^2 = -2 \cdot (4\kappa^2)$.

3.4 By definition a Killing horizon $\mathcal{H}$ is generated by a Killing vector field $\xi$ which is null at $\mathcal{H}$ and is hypersurface orthogonal. While for Kerr geometry $\partial_t$ is a Killing and it becomes null at the ergosphere, it is *not* hypersurface orthogonal, as the off-diagonal $g_{t\phi}$ term in the metric does not vanish on the ergosphere. This is how the ergosphere differs from the Killing horizon.

3.6 Let us choose the coordinate system such that the null surface $\mathcal{N}$ sits at $r = 0$, i.e.

$$\mathrm{d}s^2 = -V\mathrm{d}v^2 + 2\mathrm{d}v\mathrm{d}r + g_{ij}(\mathrm{d}x^i + u^i \mathrm{d}v)(\mathrm{d}x^j + u^j \mathrm{d}v)$$

where $V, u^i, g_{ij}$ are coefficients depending on coordinates $r, v, x^i$ such that $V(r = 0) = 0$. The null surface $\mathcal{N}$ is hence spanned by $v, x^i$. $g_{ij}$, which is the metric at constant $r, v$ codimension-2 surfaces, is positive definite.

Consider two generic points on $\mathcal{N}$, $P : (v_1, x_1^i)$, $Q : (v_2, x_2^i)$. The distance between these two points may be easily read from the above metric computed at $r = 0$. These two points are generically space-like separated, and are null separated only if $x_1^i = x_2^i$. That is, the curve along which these two points are null separated is parameterized by $v$ in our adapted coordinate system.

For part (3), using our coordinate system above, one may verify that any vector may be expanded in terms of the null vector $\ell^\mu = g^{\mu r}$, $\xi^\mu$ and $e_i$ such that $\xi^2 = 0$, $\ell \cdot \xi = 1$, $\ell \cdot e_i = \xi \cdot e_i = 0$ at $r = 0$. Then any spacelike vector field $X$ on $\mathcal{N}$ may be written as $\alpha\xi + \beta_i e_i$. With this, one may readily verify what is asked in the exercise.

3.8 (1) Constant $r$ surfaces become null when norm of the normal 1-form $\mathrm{d}r$ vanishes. Since $|\mathrm{d}r|^2 = g^{rr} = 1/g_{rr}$, this happens at roots of $1/g_{rr}$. So, let us assume $1/g_{rr}$ has simple roots, say at $r = r_h$. $\partial_t$ becomes null only if $g_{tt}(r_h) = 0$.

To read the surface gravity, one may expand the geometry around $r = r_h$, by taking $r = r_h + \alpha\rho^2$ and keeping to the leading order in $\rho$. $g_{tt} = \alpha g'_{tt}(r_h)\rho^2$ and

$1/g_{rr} = \alpha\rho^2(1/g_{rr})'(r_h)$, where $'$ denotes derivative with respect to $r$. The near horizon geometry becomes

$$\mathrm{d}s^2 = \alpha g'_{tt}(r_h)\rho^2\mathrm{d}t^2 + (4\alpha)(1/g_{rr})'(r_h)\mathrm{d}\rho^2 + \cdots$$

Upon choosing $(1/g_{rr})'(r_h) = 1/(4\alpha)$, the above metric takes a Rindler form with surface gravity (acceleration) $\kappa$ given by $\kappa^2 = \frac{g'_{tt}}{4(1/g_{rr})'}$ computed at $r = r_h$. If $g_{tt}$, $1/g_{rr}$ have simple roots at $r_h$, $\kappa$ is finite, metric at the horizon is smooth and this expression for $\kappa$ reduces to (3.34).

Alternatively, one may bring the metric to the EF form:

$$\begin{aligned}\mathrm{d}s^2 &= -g_{tt}(r)\left[-\mathrm{d}t^2 + \left(\sqrt{\frac{g_{rr}}{-g_{tt}}}\mathrm{d}r\right)^2\right] + r^2\mathrm{d}\Omega^2\\ &= g_{tt}(r)\mathrm{d}u^2 + 2\sqrt{-g_{tt}g_{rr}}\mathrm{d}r\mathrm{d}u + r^2\mathrm{d}\Omega^2\end{aligned}$$

where $u = t + \int\sqrt{-\frac{g_{rr}}{g_{tt}}}\mathrm{d}r$. This coordinate system is well defined at the horizon if $g_{tt}g_{rr}$ is finite at $r_h$. We also note that $\det g = r^4 g_{rr}g_{tt}\mathrm{vol}(S^2)$. Non-vanishing of $\det g$ also requires $g_{tt}g_{rr} =$ finite at $r_h$.

(2) For a generic stationary and axisymmetric metric, one may start with the form

$$\mathrm{d}s^2 = g(r,\theta)\mathrm{d}t^2 + \frac{\mathrm{d}r^2}{f(r,\theta)} + K(r,\theta)\mathrm{d}\theta^2 + \Phi^2(\theta,r)(\mathrm{d}\phi + \Omega(r,\phi)\mathrm{d}t)^2, \quad \text{(J.2)}$$

we have Killing horizons at root of $f$, $r = r_h$, where $g$ should also vanish to have a smooth metric. One may repeat expanding the metric around $r_h$ and read the surface gravity from the Rindler form of the metric. Some more discussions may be found in Sect. 2 of [819]. The final result for surface gravity for metric (J.2) is the same relation as (3.34).

One may then readily verify that existence of a Killing horizon (generated by a null Killing vector field $\xi$) amounts to the surface gravity $\kappa$ read from the near horizon metric in the Rindler form to be a $\theta$ independent constant.

3.13 The redshift factor for a Schwarzschild black hole is given as

$$\frac{\omega(r)}{\omega_\infty} = \frac{1}{\sqrt{f(r)}}, \qquad f(r) = 1 - \frac{2G_{\mathrm{N}}M}{r},$$

where $\omega(r)$, $\omega_\infty$ are respectively frequencies measured by a *fido* at $r$ and at infinity. If $\omega(r_0) = M_{\mathrm{Pl}}$, $\omega_\infty = \Lambda$ and if $r_0 = 2G_{\mathrm{N}}M(1+\epsilon)$, then

$$\epsilon = \frac{\Lambda^2}{M_{\mathrm{Pl}}^2 - \Lambda^2}.$$

If $\Lambda \lesssim M_{\mathrm{Pl}}$ then, $\epsilon \sim (\frac{\Lambda}{M_{\mathrm{Pl}}})^2$.

3.15 Radial null geodesics for FLRW metric,

$$ds^2 - dt^2 + a(t)^2 \left(dr^2 + r^2 d\Omega^2\right),$$

are given by $dr = \pm dt/a(t)$. Cosmological (event) horizon $r_e$ is then the distance future oriented light rays can travel from where one sits now while particle horizon $r_p$ is the comoving distance light has travel since the big bang. If $a(t) = t^{1+\alpha}$, then for $\alpha > 0$ (accelerating cosmologies), $r_e = t_0^{-\alpha}/\alpha$ while $r_p$ blows up and for $\alpha < 0$ (decelerating cosmologies), $r_p = t_0^{-\alpha}/\alpha$ while $r_e$ blows up.
3.20 Let $x^\mu = x^\mu(s, \tau)$ denote congruence of geodesics where at each given $s$ we have an affinely parameterized time-like geodesic and let $u^\mu := \frac{\partial x^\mu}{\partial s}$ and $t^\mu := \frac{\partial x^\mu}{\partial \tau}$. Note that $t^\mu$ is a timelike vector while $u^\mu$ is typically spacelike. The difference between two close by geodesics at $s, s + ds$, yields the geodesic deviation equation,

$$\frac{d^2 u^\mu}{d\tau^2} = t^\alpha t^\beta \nabla_\alpha \nabla_\beta u^\mu = R^\mu{}_{\alpha\beta\nu} t^\alpha t^\beta u^\nu. \tag{J.3}$$

The geodesic deviation equation concerns the second derivative of a spacelike vector $u^\mu$ along the geodesic, whereas Raychaudhuri equation (3.11) concerns the derivative of a time-like vector $t^\mu$ along the geodesic. Therefore, (J.3) allows probing different components of Riemann than those appearing in the Raychaudhuri equation (namely Ricci tensor along the geodesic).
3.26 (1) For a bifurcate horizon generated by the Killing vector $\xi$, we have the binormal 2-form $\boldsymbol{\epsilon} = d\xi/(2\kappa)$, where $\kappa$ is the surface gravity (see part (8) of Exercise 3.1). Since $\boldsymbol{\epsilon}$ has a definite norm and is well-defined everywhere on $\boldsymbol{\mathcal{B}}$, it is orientable.

(2) $\boldsymbol{\mathcal{B}}$ need not be simply connected, e.g. we can have Mazumdar-Papapedrou multi-centered (extremal) RN solutions (see Exercise 2.36).

(3) In principle $b$ can be non-zero and the horizon can be spindle-like to two spindles attached together. In [260] such solutions with $g = 0, b = 2$ has been constructed. We note that Euler character $\xi = \frac{1}{4\pi} \int_{\boldsymbol{\mathcal{B}}} R$, where $R$ is the Ricci scalar of $\boldsymbol{\mathcal{B}}$.

## Exercises of Chapter 4

4.3 (1) $\xi_H$ is the null vector generating the horizon. The condition for any particle to fall into the hole is that in a Penrose diagram its momentum makes an angle not less than 45° with the horizontal line. Since $\xi_H$ is a future oriented 45° line, therefore, $p_1 \cdot \xi_H \le 0$ is the condition for falling in.

(2) Energy–momentum conservation implies $p_2 = p - p_1$, and therefore, $p_2 \cdot \xi_H = p \cdot \xi_H - p_1 \cdot \xi_H$. Since original particle and $p_1$ are falling into the hole, $p \cdot \xi_H, p_1 \cdot \xi_H \le 0$ but their difference can be positive. So, $p_2$ can in principle fly out.

(3) So, for the Penrose process to work we should have $E = p \cdot k > 0$, $E_1 = p_1 \cdot k < 0$ and $E_2 = p_2 \cdot k > E > 0$, while $p \cdot \xi_H, p_1 \cdot \xi_H \le 0$ and $p_2 \cdot \xi_H > 0$. Let's denote $J = -p \cdot \partial_\phi$ and similarly for the other two particles, then, energy–momentum conservation implies

$$E = E_1 + E_2, \qquad J = J_1 + J_2,$$

and the other conditions for the Penrose process read as

$$E - \Omega J \leq 0, \qquad E_1 - \Omega J_1 \leq 0, \qquad E_2 - \Omega J_2 > 0.$$

These imply that energy extraction $E_2 - E > 0$ is only possible if $J_2 - J > 0$. Maximum extracted energy will happen when $J_1 + J_{\rm BH} = 0$ and when the in-falling equality bound is saturated.

(4) With the emission of $p_2$, black hole loses mass $E_1$ and angular momentum $J_1$, $\delta M = E_1 < 0$, $\delta J = J_1 < 0$ and $\delta M \leq \Omega\delta J$. The process can go on until the above conditions are satisfied. That is, until the hole loses its angular momentum.

(5) Iterating the Penrose process and emission of particles several times a black hole of $(M, J)$ can reach $(m, 0)$ and one can show that the condition for continuation of the process along the way reads as $2M(M + \sqrt{M^2 - J^2/M2}) \leq (2m)^2$. Since $M \geq J$ and $m$ can maximum be $M/\sqrt{2}$ and only up to $1 - \sqrt{2}/2$ percent of the energy of a black hole can be mined. We note that the condition for continuation of the process is that at each stage the area of horizon $A := 8\pi M r_+$ does not decrease, $\delta A \geq 0$.

4.5 By introducing $z_h = r_h\omega$, $z = \omega r$, $z_* = \omega r_*$, the Regge–Wheeler equation (4.4) takes the form

$$\left(\frac{\mathrm{d}^2}{\mathrm{d}z_*^2} - U_l(z)\right)\psi_l = 0, \quad U_l = -1 + (1 - \frac{z_h}{z})(\frac{l(l+1)}{z^2} + \frac{z_h^2}{z^3}).$$

4.6 In large $z$ limit $z_* \sim z$ and the leading term in the potential $U_l$ in the previous exercise becomes $\frac{l(l+1)}{z^2} = W_l^2 - W_l'$ with $W_l = -\frac{l+1}{z}$ or $\frac{l(l+1)}{z^2} = \tilde{W}_l^2 - \tilde{W}_l'$ with $\tilde{W}_l = -\frac{l}{z}$. The Regge-Wheeler equation can then be written as $(\partial_z - W_l)(\partial_z + W_l)\psi_l = 0 = (\partial_z + \tilde{W}_l)(\partial_z - \tilde{W}_l)\psi_l$. This is basically like the usual quantum mechanical harmonic oscillator. The equation $(\frac{\mathrm{d}^2}{\mathrm{d}z^2} - \frac{l(l+1)}{z^2})\psi_l = 0$ can be directly integrated with two basic solutions $\psi_l \sim z^{l+1}, z^{-l}$.

4.12 For the quadrupole moments given, we have

$$\dddot{q}_{ij}\dddot{q}^{ij} = \frac{2 \cdot 16 M^2 R^4}{T^6}(1 + 2\cos^2\frac{2t}{T}).$$

Therefore, $\langle \dddot{q}_{ij}\dddot{q}^{ij}\rangle = \frac{4\cdot 16 M^2 R^4}{T^6}$ and the GW luminosity (4.27) yields, $P \sim M^2R^4/T^6 \sim M^2(MT^2)^{4/3}/T^6 \sim (M/T)^{10/3}$.

4.16 This exercise is basically about conversion of units. Starting from (4.37) we have $M\,\omega^R_{\rm QNM} \approx 0.37367$. For frequency 440 Hz, we get $M \simeq 27.3 M_\odot$ which has a decay time of about 16.4 milliseconds.

4.18 See Chap. 3 of [323].

4.19 See Sect. 2.2.2 of [820].

## Exercises of Chapter 5

5.2 For Einstein vacuum black hole solutions, namely Schwarzschild and Kerr geometries, we have a singularity at which curvature blows up. Therefore, one should take special care in using Stokes' theorem in the derivation of the Komar charge. For Minkowski space, we do not have such an issue. Due to the existence of this subtlety, while the Komar surface integral (5.5) may still be used for Schwarzschild and Kerr, its volume integral yields an incorrect result.

5.4 Starting from the definition of the Noether current (5.35), shifting Lagrangian by $\mathrm{d}\boldsymbol{W}$ shifts $\boldsymbol{\Theta}$ by the $(d-1)$-form $\boldsymbol{W}$ and therefore, the Noether current

$$\mathbf{J}_\xi \to \mathbf{J}_\xi + \mathbf{W}(\delta_\xi \Phi) - \xi \cdot \mathrm{d}\boldsymbol{W} = \mathbf{J}_\xi - \mathrm{d}(\xi \cdot \mathbf{W}(\delta_\xi \Phi)).$$

One may readily check that the shifted Noether current is on-shell conserved and hence on-shell $\mathbf{J}_\xi \approx \mathrm{d}\tilde{\mathbf{Q}}_\xi$. The Noether charge which is a surface integral over the $(d-2)$-form $\tilde{\mathbf{Q}}_\xi$ is then shifted by $-\oint \xi \cdot \mathbf{W}(\delta_\xi \Phi)$.

5.5 (1) Recall that $k_{\mathrm{B}} T$ and $ST$ (where $T$ is temperature) are both of the same dimension as energy. So $S/k_{\mathrm{B}}$ is dimensionless. On the other hand, the (horizon) area is of dimension length$^2$. This may be made dimensionless if it is measured in units of Planck-length$^2$. Recalling Exercise 1.2, therefore, $[S] = k_{\mathrm{B}}[c^3][A]/[\hbar G_{\mathrm{N}}]$. Putting in the numeric factor 1/4, we hence get (5.44).

Regarding the Hawking temperature, it should be proportional to surface gravity $\kappa$ (which is of the dimension of acceleration, length over time$^2$), and also proportional to $\hbar$. $\hbar$ is of dimension of angular momentum and therefore, $\hbar\kappa/c$ is of dimension of energy. These put together yields (5.60).

(2) For a Schwarzschild black hole of mass $M$, entropy and temperature are given as

$$S_{\mathrm{BH}} = 4\pi \frac{G_{\mathrm{N}} M^2 k_{\mathrm{B}}}{\hbar c}, \qquad T_{\mathrm{H}} = \frac{\hbar\, c^3}{8\pi k_{\mathrm{B}} G_{\mathrm{N}} M}.$$

Putting in numbers we get

$$S_{\mathrm{BH}} = 1.6 \times 10^{54} \left(\frac{M}{M_\odot}\right)^2, \qquad T_{\mathrm{H}} = 6 \times 10^{-8}\mathrm{K}\frac{M_\odot}{M}.$$

Energy $E_p$ and entropy $S_p$ of a gas of photons in a volume $V$ and temperature $T$ is given by

$$E_p = \left(\frac{\pi^2 k_{\mathrm{B}}^4}{15\hbar^3 c^3}\right) V T^4, \qquad S_p = \frac{4E_p}{3T}.$$

In the exercise, we are assuming $E_p = Mc^2$ and $V = \frac{4\pi}{3}(2G_{\mathrm{N}} M/c^2)^3$. We hence get

$$T = \left(\frac{45 G_{\mathrm{N}}}{32\pi^3 \hbar c}\right)^{1/4} \left(\frac{\hbar c^3}{k_{\mathrm{B}} G_{\mathrm{N}}}\right) \frac{1}{\sqrt{M}}, \qquad S_p = \frac{8}{3}\left(\frac{2}{45\pi}\right)^{1/4} \left(\frac{G_{\mathrm{N}} M^2}{\hbar c}\right)^{3/4}.$$

As we see, the entropy of the photon system grows like $M^{3/2}$ and that of the black hole like $M^2$. They can become equal when $M \sim M_{\rm Pl}$.
5.8 (1) Starting from (5.63), and recalling that $\xi_{\rm H}$ is a Killing vector, $\mathcal{L}_{\xi_{\rm H}}\Phi_{\rm H} = \xi_{\rm H}\cdot\mathcal{L}_{\xi_{\rm H}}A = 0$. Moreover, similarly to the discussion in Sect. 5.5.1 one can show that $\Phi_{\rm H}$ is a constant over the horizon.

(2) As shown in Sect. 5.4.3, $\mathcal{L}_{\xi_{\rm H}}F = 0$ implies $\mathcal{L}_{\xi_{\rm H}}A = {\rm d}\lambda_{\rm H}$ for some $\lambda_{\rm H}$. Therefore, $\mathcal{L}_{\xi_{\rm H}}\Phi_{\rm H} = \xi_{\rm H}\cdot{\rm d}\lambda_{\rm H} = \mathcal{L}_{\xi_{\rm H}}\lambda_{\rm H}$.

(3) With the above result, integrability of the entropy fixes the gauge transformation part in $\eta_{\rm H}$ (5.50) by the same normalization $\dfrac{2\pi}{\kappa}$ for $\zeta_{\rm H}$, times $\Phi_{\rm H}$.
5.12 The product of inner and outer horizon radii for KN black holes has been shown to be independent of the mass, and depends only on electric charge and angular momentum, see [821,822]. Similar result for KN-Taub-NUT black holes may be found in [823] and references therein.

## Exercises of Chapter 6

6.2 Denote $E < 0$ as $E = -k^2$. The Schrödinger equation becomes $\psi'' = k^2\psi$ and its most general solution is, $\psi = A\sinh kx + B\cosh kx$. For Neumann (Dirichlet) boundary conditions at $x = 0$ we get $B = 0$ $(A = 0)$. At large $x$ in both of these cases $\psi \sim e^{kx}$ and is not normalizable. So, there is no bound state.

For the Robin boundary conditions, $\psi(0) + \alpha\,\psi'(0) = 0$ we learn $B = -Ak\alpha$ and hence the wave function is $\psi = A(\sinh kx - k\alpha\cosh kx)$. To have a normalizable wave function, there should not be an exponential growth at large $x$ and hence $k\alpha = 1$. The energy of the bound state is then $E = -k^2 = -1/\alpha^2$. In the Neumann $(\alpha \to \infty)$ limit $E \to 0$ and $\psi \to 0$. In the Dirichlet case $(\alpha \to 0)$ and $k$ and hence $\psi$ blows up. These two cases are compatible with not having a bound state.
6.6 (1) Metric (6.16) in Euclidean time takes the form

$$
{\rm d}s^2 = e^{2a\xi}\left({\rm d}\tau_E^2 + {\rm d}\xi^2\right) = {\rm d}\rho^2 + a^2\rho^2\,{\rm d}\tau_E^2, \qquad \rho = \frac{e^{a\xi}}{a}.
$$

The second equality shows that absence of conic deficit in the Euclidean $2d$ plane requires $a\tau_E$ to be $2\pi$ periodic.

(2) As we see from the metrics above, Rindler Hamiltonian $i\partial_\tau$ corresponds to rotations in $\tau_E, \rho$ plane. One can make another change of coordinates from the polar coordinates $\tau_E, \rho$ to 'Cartesian coordinates' $(t_E, x)$, in which rotation generator is written as: $-\partial_{\tau_E} = i(t_E\partial_x - x\partial_{t_E})$. One can now Wick rotate back to Minkowski $(t_E \to it)$ where $(t\partial_x - x\partial_t)$ is a boost generator.

(3) At a constant $\rho = \rho_0$, we have a circle of radius $\rho_0$ which may be covered by a coordinate $\tau_{\rho_0}$ with periodicity $2\pi/\rho_0$ and hence the associated temperature is $a\rho_0/(2\pi)$.

(4) Hint: write (6.20), (6.21) in by a shift in $\xi$ and reexamine (6.22) for the shifted creation-annihilation operators.

6.7 Near the horizon at $r = r_{\rm H}$ we may expand metric functions as

$$N(r,\theta) = \frac{1}{4}F'N'\rho^2 + \mathcal{O}(\rho^3), \qquad F(r,\theta) = \frac{1}{4}F'^2\rho^2 + \mathcal{O}(\rho^3),$$

where $r - r_{\rm H} = \frac{1}{4}F'\rho^2 + \mathcal{O}(\rho^3)$ and $F' = \partial_r F(r,\theta)|_{r=r_{\rm H}}$, $N' = \partial_r N(r,\theta)|_{r=r_{\rm H}}$. Inserting the above into the metric and keeping up to $\rho^3$ terms we find a metric like (6.28) with $\kappa^2 = \frac{1}{4}F'N'$. Constancy of $\kappa$ requires that $F'N'$ should be a constant.
6.9 For a Schwarzschild black hole of mass $M$ we have $E = M$, $T = 1/(8\pi G_{\rm N} M)$. Therefore, $8\pi G_{\rm N} E = 1/T$. The specific heat is then $C = \partial E/\partial T = -\frac{1}{8\pi G_{\rm N} T^2} < 0$. Negative specific heat is a sign of thermodynamical instability: the system becomes hotter as it loses energy.
6.17 To compute the emission rate from a rotating black hole, we need to know which particles (with which spin or mass) are available for the emission. The details of analysis may be found in seminal papers by Don Page [438,439].
6.19 Rotating black holes typically lose their spin faster than their energy [439] and hence one would expect that longer lived black holes to be static ones. So, here we focus on the Schwarzschild black holes. Starting from (6.77), requiring $\tau < 13.8$ Gyr we get $M/M_\odot \leq 8.7 \cdot 10^{-20}$.

For the bonus level, see discussions in Sect. 10.3 the PBH part and references given there.
6.23 $\rho(t_1)$ in a diagonal basis may be written as $\rho(t_1) = \sum_i \lambda_i |\psi_i\rangle\langle\psi_i|$, where for a pure state one of $\lambda_i$s is equal to one and the rest are zero. Under a unitary evolution $U(t_2,t_1)$, $\rho(t_2) = U\rho(t_1)U^\dagger = \sum_i \lambda_i|\phi_i\rangle\langle\phi_i|$, where $|\phi_i\rangle = U|\psi_i\rangle$, $\langle\phi_i| = \langle\psi_i|U^\dagger$. Therefore, under a unitary evolution, a pure state evolves only to a pure state. For a non-unitary evolution $|\psi_i\rangle$ and $\langle\psi_i|$ evolve differently (and not necessarily by $U$, $U^\dagger = U^{-1}$ and hence a pure state can evolve to a mixed state.

## Exercises of Chapter 7

7.1 For general construction and discussion see [424,536,542].
7.3 Riemann tensor $R_{\mu\nu\alpha\beta}$ is antisymmetric on its first two and last two indices and therefore, in 3 dimensions, $R_{\mu\nu\alpha\beta} = \epsilon_{\mu\nu\lambda}\epsilon_{\alpha\beta\rho}X^{\lambda\rho}$, where $\epsilon_{\mu\nu\lambda}$ is totally antisymmetric tensor and $X^{\lambda\rho}$ is a symmetric tensor to be specified. To find $X^{\lambda\rho}$ we may multiply both sides of this equation with $g^{\mu\alpha}$, where the LHS reduces to $R_{\nu\beta}$ and the the RHS to $g_{\nu\beta}X - X_{\nu\beta}$, where $X = X^\nu_\nu$. Taking trace of the latter yields $R = 2X$ and therefore, $X_{\nu\beta} = -R_{\nu\beta} + \frac{1}{2}Rg_{\nu\beta}$, i.e. $-X_{\mu\nu}$ is Einstein tensor.

We also note that the above also implies Weyl curvature vanishes in three dimensions.
7.4 and 7.5 See [477] for detailed discussions.
7.6 (1) BTZ black holes are (locally) AdS geometries and as such $|\partial_t|^2 \sim -r^2$ at large $r$. This is in contrast to asymptotically flat black holes, e.g. Kerr, where asymptotically $|\partial_t|^2 \sim -1$. Recalling that $g_{\phi\phi} = r^2$, this means one can corotate with black hole at any $r$. In particular, this means that one can always choose an asymptotically

rotating frame and choose the time like Killing vector to be $\partial_t + \alpha\Omega_{\text{BTZ}}\partial_\phi$ with constant $\alpha < 1$. Therefore, BTZ black holes and typically rotating AdS black holes do not have an ergo-region.

For hints to the other parts of this exercise see [479,480].

7.9 Under the local Weyl scaling (7.27) $D$-dimensional Ricci tensor transforms as [824,825]

$$R_{\mu\nu} \to R_{\mu\nu} - (D-2)(\nabla_\mu\nabla_\nu\Omega - \nabla_\mu\Omega\nabla_\nu\Omega) - (\nabla^2\Omega - (D-2)|\nabla\Omega|^2)g_{\mu\nu}. \tag{J.4}$$

Therefore, in $D = 3$, $S_{\mu\nu} := R_{\mu\nu} - \frac{1}{4}Rg_{\mu\nu}$ transforms as

$$S_{\mu\nu} \to S_{\mu\nu} - \nabla_\mu\nabla_\nu\Omega + \nabla_\mu\Omega\nabla_\nu\Omega - \frac{1}{2}|\nabla\Omega|^2 g_{\mu\nu}.$$

From the above one can show that the Cotton tensor (7.29) is invariant under Weyl scaling. For discussions on Cotton tensor in higher dimensions and their behavior under Weyl scaling see [824,825].

7.10 See [826–828] for the analysis.

7.11 See [513] for more details.

7.14 See [829–831] for more details and analyses.

7.16 See [832].

7.22 (1) Starting from (7.68) one may use either (3.2) with $\xi_{\text{H}} = \partial_t$ or the near horizon expansion and the resulting Rindler metric to read surface gravity $\kappa$. This yields, $\kappa = f'(r = r_h)/2$, where $r_h$ is the root of $f(r)$ in (7.68). Horizon area is $r_h^{D-2}\Omega_{D-2}$, with $\Omega_{D-2}$ given in (7.69). From $f(r_h) = 0$ we learn that

$$r_0^{D-3} = r_h^{D-3}(1 + \frac{r_h^2}{\ell^2}), \qquad r_h\kappa = \frac{D-3}{2} + \frac{D-1}{2}\frac{r_h^2}{\ell^2},$$

and from (7.69) we learn that $\text{d}M = \frac{(D-2)(D-3)\Omega_{D-2}}{16\pi G_{\text{N}}} r_0^{D-4}\text{d}r_0$. One hence readily sees that $\frac{\kappa}{2\pi}\text{d}S = \frac{(D-2)\Omega_{D-2}}{8\pi G_{\text{N}}}\kappa r_h^{D-3}\text{d}r_h = \text{d}M$.

(2) Radial geodesic equations for metric (7.68) read as

$$f(r)\dot{t} = E, \qquad -f(r)\dot{t}^2 + \frac{\dot{r}^2}{f(r)} = \sigma,$$

where *dot* denotes derivative with respect to the affine parameter, $E$ is a constant and $\sigma = 0, -1$ respectively correspond to null and timelike geodesics. We hence obtain

$$\text{Null}: \quad t = \int \frac{\text{d}r}{f}, \qquad \text{Time-like}: \quad t = \int \frac{\text{d}r}{f\sqrt{1 - f/E^2}}.$$

We note that $f(r)$ is a monotonically increasing function and $f(r) > 0$ for $r > r_h$. One may then verify that for future-oriented outward moving null geodesics starting at $r_i > r_h$ it takes $\Delta t = \int_{r_i}^{\infty} \text{d}r/f(r) \lesssim l \tan^{-1}(r/l)$, i.e. outward null geodesics reach asymptotic boundary of AdS in finite coordinate time. For time-like geodesics which have zero velocity at $r_0$, one may rewrite the geodesic equation as

$$\left(\frac{\mathrm{d}r}{\mathrm{d}t}\right)^2 + U(r) = 0, \qquad U(r) = \frac{(f(r) - f_i)f(r)}{f_i}, \quad f_i = f(r_i).$$

The potential $U(r)$ has two zeros at $r = r_h, r_i$ and a turning point in between the two and at large $r$ it grows like $r^4$. That is, at large $r$ the background AdS provides a negative force pushing the particle towards the AdS center and it does not reach AdS boundary at finite time. The particle can oscillate between the two zero of $U(r)$.
7.25 (1) The extremal D3-brane metric is given by

$$\mathrm{d}s^2 = f^{1/2}\left(-\mathrm{d}t^2 + \mathrm{d}x_i\mathrm{d}x_i\right) + \frac{\mathrm{d}r^2}{f(r)^2} + r^2\mathrm{d}\Omega_5^2, \qquad f(r) = 1 - (\frac{r_+}{r})^4,$$

where $i = 1, 2, 3$, dilaton is a constant $e^{2\Phi} = g_s^2$ and the 4-form is $A_4 = (\frac{r_+}{r})^2 \mathrm{d}t \wedge \mathrm{d}x_1 \wedge \mathrm{d}x_2 \wedge \mathrm{d}x_3$. The near horizon expansion may be obtained upon inserting $r = r_+(1 + \rho^4/4)$ and keeping the leading order term in $\rho$:

$$\mathrm{d}s^2 = \rho^2\left(-\mathrm{d}t^2 + \mathrm{d}x_i\mathrm{d}x_i\right) + r_+^2\frac{\mathrm{d}\rho^2}{\rho^2} + r_+^2\mathrm{d}\Omega_5^2, \qquad F_5 = \mathrm{d}A_4 = 2r_+\mathrm{d}t \wedge \mathrm{d}x_1 \wedge \mathrm{d}x_2 \wedge \mathrm{d}x_3 \wedge \mathrm{d}\rho.$$

This is an $\mathrm{AdS}_5\times\mathrm{S}^5$ geometry with equal radii $\ell = r_+$ for $\mathrm{AdS}_5$ and $\mathrm{S}^5$ parts. Upon the coordinate transformation $\rho = r_+/z$ one obtains metric which is $\mathrm{d}s^2 = \frac{r_+^2}{z^2}\left(-\mathrm{d}t^2 + \mathrm{d}x_i\mathrm{d}x_i + \mathrm{d}z^2\right) + r_+^2\mathrm{d}\Omega_5^2$.

(2) In a similar way one may consider near extremal D3-brane metric,

$$\mathrm{d}s^2 = f_-^{1/2}\left(-\frac{f_+}{f_-}\mathrm{d}t^2 + \mathrm{d}x_i\mathrm{d}x_i\right) + \frac{\mathrm{d}r^2}{f_-f_+} + r^2\mathrm{d}\Omega_5^2, \qquad f_\pm(r) = 1 - (\frac{r_\pm}{r})^4,$$

and perform the near horizon expansion as $f_- \sim \ell^4/z^4$, $\mathrm{d}r = \ell^5\mathrm{d}z/z^5$ and $f_+/f_- \simeq \frac{r-r_+}{r-r_-} \simeq 1 - \left(\frac{z}{z_h}\right)^4$, to obtain (7.75).
7.26 (2) Let us explore the near $z_h$ behavior of the geometry. Taking $f(z) \simeq (p+1)(z_h - z)/z_h$, and defining $\rho$ as $\rho^2 = 4z_h(z_h - z)/(p+1)$, the $z - y$ part of metric takes the form $\mathrm{d}\rho^2 + ((p+1)/(2z_h))^2\rho^2\mathrm{d}y^2$. This is smooth if $y$ has $2\pi R$ periodicity with $R = (2z_h)/(p+1)$.

For part (3), see [528].

## Exercises of Chapter 8

8.1 (1) Solve the Killing equation for the domain wall metric. For generic functions $A(\rho)$ you should find translations, $\partial_t$ and $\partial_x$, as well as boosts, $x\partial_t + t\partial_x$, showing compatibility with Poincaré$_2$ expected from a QFT$_2$.

(2) Recall that $A(\rho)$ must tend to a linear function for large positive and negative values of $\rho$ to produce locally $\mathrm{AdS}_3$ behavior, with an arbitrary coefficient in front.

So you can define a local AdS-radius in terms of the derivative of the function $A(\rho)$. Using the Brown–Henneaux result (7.23) that relates AdS radius to the central charge and demanding monotonicity of the central charge establishes the desired condition on the function $A(\rho)$.

8.2 Use Gaussian normal coordinates (8.4), exploit the simple expression for extrinsic curvature (8.5), and calculate $\Gamma^\rho{}_{\mu\nu}$ for the metrics obeying the generalized Fefferman–Graham form in the exercise.

8.3 For the holographic counterterm make an ansatz like in (8.12) (for this exercise, it is sufficient to keep only the two terms displayed explicitly) and determine the coefficients $c_0$ and $c_1$ by demanding that the variational principle is well-defined for a locally asymptotically $AdS_5$ metric. For the latter, you can use a Fefferman–Graham expansion in Gaussian normal coordinates (8.4). If you need a peek at the final result see, e.g. the last (10) in [357].

8.4 Use the holographic dictionary (8.15). This means you have to vary the (full!) action twice and insert for the variations the non-normalizable modes of the metric, i.e. the leading order term in the Fefferman–Graham expansion (8.4). If you need further guidance consult Sect. 4 in [556].

8.5 Follow the rather explicit instructions of the exercise. If you need additional help see Sect. 2 in [538].

8.6 Trace out the $B$-part of your Hilbert space to get the reduced density matrix and then calculate its von Neumann entropy. For the direct product state, you should find a reduced density matrix ($2 \times 2$) with a single non-zero entry, while for the Bell state you should find a reduced density matrix proportional (but not identical) to the unit matrix. Recall (or show) that an expression $\mathrm{Tr}(\rho_A \ln \rho_A)$ for a matrix $\rho_A$ with eigenvalues $\lambda_i$ translates into $\sum_i \lambda_i \, \ln \lambda_i$, and note that all summands vanish when $\lambda_i$ is either 0 or 1.

8.7 The first part should be straightforward since you just need to solve the geodesic equation (1.1) for a rather simple metric, and you have sufficiently many constants of motion to exactly solve the system. The second part is more tricky, and there are various ways to approach it. One approach is to make a uniformization map, i.e. a diffeomorphism of a generic Bañados geometry to Poincaré patch $AdS_3$. It is not at all trivial to construct this diffeomorphism. See [833] for a detailed analysis.

8.8 While probably there is an elegant way of 'seeing' the result immediately, in this case, brute force seems the quickest way to the result, and not a lot of force is needed. For instance, explicitly insert coordinates for the points $A_i$ and determine the various lengths to prove the desired relation.

8.9 You can use as input the anomalous transformation behavior (8.26) of entanglement entropy.

8.10 The instructions are very detailed, so try to follow them. If you need to cross-check intermediate results not displayed in the exercise consult [570].

8.11 If you have not done Exercise 8.5 you need to do this first; alternatively, you can use Sect. 2 of [538]. For the main part of the exercise follow the instructions and compare your results with Sect. 3.10 in [538].

8.15 Use e.g. lightcone coordinates $x^\pm$ for the $2d$ Minkowski metric and solve the asymptotic Killing vector equations, keeping all terms that either blow up or remain $\mathcal{O}(1)$ for large $\rho$. While the order in which you consider various components ultimately does not matter, we find it convenient to consider first the $\rho\rho$-component, next the $\rho\pm$-components, then the $\pm\pm$-components, and finally the $+-$ component. Your result for the asymptotic Killing vectors should feature two free integration functions $\lambda^\pm(x^\pm)$. Their Lie-bracket is then straightforward.

8.16 You need to do the previous exercise first. If you were careful enough to keep all $\mathcal{O}(1)$ terms then the $\pm\pm$-components of the asymptotic Killing equation establish the desired result.

8.18 Once you understand the question asked in the exercise the calculation should be doable in two lines. If you are stuck remember that energy is the eigenvalue of the Hamiltonian.

## Exercises of Chapter 9

9.1 Boltzmann or microcanonical entropy is defined as $S_{\text{mc}}(E) = \ln \omega(E)$ where $\omega(E)$ is number of configurations/states available at the given energy $E$. The canonical entropy $S_{\text{c}}$ is defined as $S_{\text{c}} = -\beta^2 \frac{\partial(\ln Z/\beta)}{\partial\beta}$ where $Z$ is the canonical partition function $Z = \sum_E e^{S_{\text{mc}}(E) - \frac{\partial S_{\text{mc}}(E)}{\partial E} E}$ computed at a fixed temperature, i.e. fixed $\beta = \frac{\partial S_{\text{mc}}(E)}{\partial E}$. One may expand the exponent in the integrand of the partition function $Z$ to the second order in $E$ and perform the sum in this steady phase approximation. To obtain the desired result, one also needs to recall that $C = \partial E/\partial T$, and therefore $\ln(CT^2) = -\ln(\partial^2 S/\partial E^2)$.

9.3 For the proof let's consider two such initial states, $|\Psi\rangle := |\iota\rangle_A \otimes |o\rangle_B$ and $|\Phi\rangle := |\tilde{\iota}\rangle_A \otimes |o\rangle_B$, such that the same unitary operator $U$ acting on $|\Psi\rangle$, $|\Phi\rangle$ yields the same state $|\iota\rangle_A \otimes |\iota\rangle_B$ up to two possible different phases. Next, consider $\langle\Phi|\Psi\rangle$ and use $\langle o|o\rangle = \langle\iota|\iota\rangle = 1$, to obtain

$$\langle\Phi|\Psi\rangle = \langle\tilde{\iota}|\iota\rangle = e^{i\phi(\iota,o)-\phi(\tilde{\iota},o)}(\langle\tilde{\iota}|\iota\rangle)^2.$$

The above yields $|\langle\tilde{\iota}|\iota\rangle|$ is either 0 or 1. However, this can't be true as $|\iota\rangle$ and $|\tilde{\iota}\rangle$ are two arbitrary states. So, there can't be a unitary $U$ which evolves $|\Psi\rangle$ to $|\iota\rangle_A \otimes |\iota\rangle_B$ up to a phase.

9.6 For the rectangular torus with radii $1, \beta/(2\pi)$, the modular parameter is defined as $\tau = i\beta/(2\pi)$. Tori whose $\tau$ are related by Mobius transformations

$$\tau \to \frac{a\tau + b}{c\tau + d},$$

in particular $\tau \to -1/\tau$ ($\beta \to 4\pi^2/\beta$), are equivalent. Modular invariance implies that the partition function does not change under a modular transformation, in particular $Z(\beta) = Z(4\pi^2/\beta)$.

(1) Consider a gapped system with energy spectrum $E_0, E_1, E_2, \cdots$ ($E_0 < E_1 < E_2 < \cdots$) and degeneracies $n_0 = 1, n_1, n_2, \cdots$. In the low temperature ($\beta \to \infty$)

limit in a gapped system, the partition function is well approximated by the contribution from the lowest lying state (ground state):

$$Z[\beta] = \operatorname{Tr} e^{-\beta H} = e^{-\beta E_0} + n_1 e^{-\beta E_1} + \cdots \approx e^{-\beta E_0}. \tag{J.5}$$

(2) At high temperature ($\beta \ll 1$), the dominant contribution to the partition function comes from higher energy states. Suppose the degeneracy of states at energy $E$ is given by $\rho(E) := e^{S(E)}$. The trace in the partition function in this regime can be approximated by an integral:

$$Z(\beta) \simeq \int \mathrm{d}E \; e^{S(E)-\beta E}. \tag{J.6}$$

The main contribution to the above integral is coming from the saddle point $E_s$, where the exponent has a vanishing first derivative. One may consider expansion $S(E) = E^q(S_0 + S_1 E + \cdots)$ for some given $q$. The saddle point is at $E_s^{q-1} \sim \beta/(qS_0)$. Convergence of the partition function and that for lower $\beta$, $E_s$ is expected to be higher imply $0 < q < 1$. Plugging this in the expansion and evaluating (J.6) in the saddle point approximation yields, $Z(\beta) \simeq e^{(1/q-1)\beta E_s} \sim e^{K\beta^{\frac{q}{q-1}}}$ for some constant $K$. In this saddle point approximation analysis, we are not considering log-corrections.

(3) From the above and equating the low and high temperature expansions we learn that $q = 1/2$, $K = E_0$ and $S = 2\pi\sqrt{E|E_0|}$.

9.7 See [676] for the details of the derivation.

9.8 (1) In Exercises 9.6, 9.7 (see also [676]) it has been argued that partition function of a modular invariant $2d$ CFT in all orders in saddle point approximation is holomorphically factorizable,

$$Z(\beta, \bar{\beta}) = Z(\beta)Z(\bar{\beta}), \qquad Z(\beta) \simeq \int \mathrm{d}\Delta \; \rho(\Delta) e^{-\beta\Delta},$$

where $\rho(\Delta)$ is density of states at excitation (energy) $\Delta$. (The $\simeq$ is used because we are assuming that the spectrum is continuous and replaced the sum with integral.) One may change the basis such that $\Delta \to \tilde{\Delta}$, nonetheless, the partition function which involves an integral over all energy states should remain invariant. Therefore, density of states in the new basis should be $\tilde{\rho}(\tilde{\Delta}) = \frac{\partial \Delta}{\partial \tilde{\Delta}} \rho(\Delta)$.

(2) For $\tilde{\Delta} = \Delta^{(z+1)/2}$, then $\tilde{\rho}_z = \frac{2}{z+1} \tilde{\Delta}^{\frac{1-z}{1+z}} \rho(\Delta)$. In the leading (Cardy) order $\rho = \rho_0 \Delta^{-3/4} \, e^{2\pi\sqrt{c\Delta/6}}$ and hence

$$\tilde{\rho}_z(\tilde{\Delta}) = \frac{2\rho_0}{z+1} \tilde{\Delta}^{-\frac{2z+1}{2(z+1)}} \; e^{2\pi\sqrt{c/6}\,\tilde{\Delta}^{\frac{1}{1+z}}}.$$

(3) For $z \to 0$, $\tilde{\rho}_{z=0}(\tilde{\Delta}) = 2\rho_0 \tilde{\Delta}^{-1/2} e^{2\pi\sqrt{c/6}\tilde{\Delta}}$ and hence the Cardy entropy $S = \ln\tilde{\rho} = 2\pi\sqrt{c/6}\tilde{\Delta} - \frac{1}{2}\log\tilde{\Delta}$, is linear in $\tilde{\Delta}$ up to log-corrections.

(4) Given the $\tilde{\rho}_z$ above one may compute entropy in the *microcanonical* ensemble:

$$S_z^{\rm mc} = \ln \tilde{\rho}_z = S_z(\tilde{\Delta}) + S_z(\tilde{\bar{\Delta}}), \qquad S_z(\tilde{\Delta}) = S_z^0 - (z+1/2)\ln S_z^0, \qquad S_z^0 := 2\pi\sqrt{\frac{c}{6}}\,\tilde{\Delta}^{\frac{1}{1+z}}.$$

9.12 See [699] for more details.

## Exercises of Appendix A

A.2 Hint: Note that $\nabla_\mu n^\mu = K$ and use (A.9).

A.4 We start with the definition of energy–momentum tensor (1.5). For the Maxwell case,

$$\begin{aligned} T_{\mu\nu} &= -\frac{2}{\sqrt{-g}}\frac{\delta\sqrt{-g}\,F_{\mu\alpha}F_{\nu\beta}g^{\mu\nu}g^{\alpha\beta}}{\delta g^{\mu\nu}} = -\frac{2}{\sqrt{-g}}\frac{\delta\sqrt{-g}g^{\mu\nu}g^{\alpha\beta}}{g^{\mu\nu}}\;F_{\mu\alpha}F_{\nu\beta} \\ &= 4F_\mu{}^\alpha F_{\nu\alpha} - g_{\mu\nu}F^2. \end{aligned}$$

A.5 (1) For $n=0$, we have just a constant, the cosmological constant. For $n=1$, the $\delta$-tensor reduces to $\delta^\mu_\nu\delta^\alpha_\beta$, this is to be multiplied with Riemann tensor, which yields Ricci scalar. For $n=2$, we have four antisymmetrized $\delta^\mu_\nu$-tensors, which is proportional to $\epsilon^{\mu\nu\alpha\beta}\epsilon^{\gamma\lambda\rho\sigma}$. This is to be multiplied with two Riemann tensors which yields Gauss–Bonnet term.

For parts (2), (3), and (4) see the original Lovelock papers and the review article [834].

## Exercises of Appendix B

B.1 $\mathrm{d}F=0$, recalling Poincaré lemma, may be locally written as $F=\mathrm{d}A$, for a one-form $A$. This equation defines $A$ up to gauge transformations $A\to A+\mathrm{d}\lambda$. The equation $*\,\mathrm{d}{*}F=0$, in $D$ dimensions is a $D-1$-form equal to zero which can equivalently be written as a vector equal to zero. Recalling the definition of the Hodge star (B.7), in terms of components this equation takes the form $\nabla_\mu F^{\mu\nu}=0$.

B.2 In $D$ dimensions $F\wedge F$ is a 4-form. Since $F=\mathrm{d}A$, $F\wedge F=\mathrm{d}(A\wedge \mathrm{d}A)$, hence it is a total derivative. In terms of components, $F\wedge F=\nabla_\mu w^\mu$, $w^\mu = \epsilon^{\mu\nu\alpha\beta}A_\nu\partial_\alpha A_\beta$.

In $D=2n$ dimensions, $\wedge$-product of $n$ field strengths $F$ can be written as $F\wedge\cdots\wedge F=\mathrm{d}(A\wedge F\wedge\cdots\wedge F)$. Also, in $2n$ dimensions one may consider field strength of an $n-1$-form field: $F_n=\mathrm{d}A_{n-1}$. In a similar way, one can show that $F_n\wedge F_n=\mathrm{d}(A_{n-1}\wedge F_n)$.

## Exercises of Appendix C

C.1 Starting from (C.10) vanishing of torsion yields $\mathrm{d}e^a=-\omega^a{}_b\wedge e^b$. In our case $\mathrm{d}e^+=0$, $\mathrm{d}e^-=\frac{1}{2}\partial_r K\mathrm{d}\wedge \mathrm{d}r$. Recalling antisymmetry of the spin-connection $\omega_{ab}=-\omega_{ba}$, we learn that $\omega^-{}_-=-\omega^+{}_+=\frac{1}{2}\partial_r K e^+$ and $\omega^-{}_+=0=\omega^+{}_-$.

One can then use (C.11) to compute curvature 2-form. A simple algebra yields, $R^-{}_- = -R^+{}_+ = \mathrm{d}\omega^-{}_-$, the other two components vanish and $R^+{}_+ = \frac{1}{2}\partial_r^2 K e^+ \wedge e^-$. Therefore, Ricci tensor in $\pm$ basis has $R^+_+ = R^-_- = \frac{1}{2}\partial_r^2 K$ and scalar curvature is $\partial_r^2 K$.

C.4 Let $\mathcal{R} := T^a \wedge T_a - e_a \wedge e_b \wedge R^{ab}$. If $\mathrm{d}\mathcal{R} = 0$, then Poincaré lemma implies locally $\mathcal{R} = \mathrm{d}X$, for some 3-form $X$. So, we first compute $\mathrm{d}\mathcal{R}$:

$$\begin{aligned}\mathrm{d}(T^a \wedge T_a) &= 2\mathrm{d}T^a \wedge T_a \\ &= 2(\mathrm{d}\omega^a{}_c \wedge e^c - \omega^a{}_c \wedge \mathrm{d}e^c) \wedge (\mathrm{d}e_a + \omega_{ad} \wedge e^d) \\ &= 2\mathrm{d}\omega^a{}_c \wedge e^c \wedge \mathrm{d}e_a + 2\mathrm{d}\omega^a{}_c \wedge e^c \wedge \omega_{ad} \wedge e^d - 2\omega^a{}_c \wedge \mathrm{d}e^c \wedge \omega_{ad} \wedge e^d\end{aligned} \tag{J.7}$$

where we used definition of torsion (C.10), (B.6) and $\mathrm{d}e^a \wedge \mathrm{d}e^b \wedge \omega_{ab} = 0$ due to antisymmetry of $\omega_{ab}$. In the same manner, we compute

$$\begin{aligned}\mathrm{d}(e^a \wedge e^b \wedge R_{ab}) &= 2\mathrm{d}e^a \wedge e^b \wedge R_{ab} + e^a \wedge e^b \wedge \mathrm{d}R_{ab} \\ &= 2\mathrm{d}e^a \wedge e^b \wedge \mathrm{d}\omega_{ab} + 2\mathrm{d}e^a \wedge e^b \wedge \omega_{ac} \wedge \omega^c{}_b + 2e^a \wedge e_b \wedge \omega_{ac} \wedge \omega^c{}_b \\ &= 2\mathrm{d}\omega_{ab} \wedge e^b \wedge \mathrm{d}e^a + 2\omega_{ac} \wedge \mathrm{d}e^a \wedge \omega^c{}_b \wedge e^b - 2\omega_{ac} \wedge e^a \wedge \omega^c{}_b \wedge e^b\end{aligned} \tag{J.8}$$

where we used definition of the curvature 2-form (C.11) and (B.6). One can now readily see that (J.7) and (J.8) are equal and hence $\mathrm{d}\mathcal{R} = 0$.

In the absence of torsion, (C.10) implies $\mathrm{d}e^a = -\omega^a{}_b \wedge e^b$ and hence $\mathrm{d}\omega_{ab} \wedge e^b = \omega^{ab} \wedge \mathrm{d}e_b$. Therefore, in this case

$$\begin{aligned}\mathcal{R} = e^a \wedge e^b \wedge R_{ab} &= e^a \wedge e^b \wedge \mathrm{d}\omega_{ab} + e^a \wedge e^b \wedge \omega_{ac} \wedge \omega^c{}_b \\ &= +e^a \wedge \omega^a{}_b \wedge \mathrm{d}e^b + e^a \wedge e^b \wedge \omega_{ac} \wedge \omega^c{}_b \\ &= -e^a \wedge \omega^a{}_b \wedge \omega^b{}_c \wedge e^c + e^a \wedge e^b \wedge \omega_{ac} \wedge \omega^c{}_b = 0.\end{aligned} \tag{J.9}$$

Alternatively, one may directly compute $\mathcal{R}$ using (C.10) and (C.11):

$$\begin{aligned}\mathcal{R} &= \mathrm{d}e^a \wedge \mathrm{d}e_a - \mathrm{d}e^a \wedge e^b \wedge \omega_{ab} + e^a \wedge \mathrm{d}e^b \wedge \omega_{ab} - e^a \wedge e^b \wedge \mathrm{d}\omega_{ab} \\ &= \mathrm{d}\left(e^a \wedge \mathrm{d}e_a - e^a \wedge e^b \wedge \omega_{ab}\right) = \mathrm{d}\left(e^a \wedge T_a\right).\end{aligned} \tag{J.10}$$

The above explicitly shows that $\mathcal{R}$ is an exact 4-form which vanishes for $T^a = 0$.

## Exercises of Appendix D

D.1 Starting from (D.1) and that $g^{\mu\nu} = -l^\mu n^\nu - n^\mu l^\nu + m^\mu \bar{m}^\nu + \bar{m}^\mu m^\nu$ one can readily read inverse metric components as:

$$
\begin{aligned}
g^{tt} &= \frac{1}{\rho^2}[\frac{-(r^2+a^2)^2}{\Delta} + a^2\sin^2\theta] = -\frac{1}{\rho^2\Delta}[(r^2+a^2)\rho^2 + 2ma^2 r\sin^2\theta],\\
g^{t\phi} &= \frac{a}{\rho^2}[-\frac{r^2+a^2}{\Delta} + 1] = -\frac{2mar}{\rho^2\Delta},\\
g^{\phi\phi} &= \frac{1}{\rho^2}[-\frac{a^2}{\Delta} + \frac{1}{\sin^2\theta}] = -\frac{\rho^2 - 2mr}{\rho^2\Delta\sin^2\theta},\\
g^{rr} &= \frac{\Delta}{\rho^2}, \quad g^{\theta\theta} = \frac{1}{\rho^2}
\end{aligned}
\tag{J.11}
$$

and the rest of the components are zero. This is the inverse Kerr metric in Boyer-Lindquist coordinates.

## Exercises of Appendix E

E.1 From (E.11) and the given equation we learn that

$$\int \mathrm{d}\bar{\omega}\; \alpha_{\omega,\bar{\omega}}\alpha^*_{\omega',\bar{\omega}} = \delta(\omega-\omega')[1 - exp(-2\pi\omega/\kappa)]^{-1}.$$

From (E.15), we learn that

$$\langle 0|b^\dagger_\omega b_\omega|0\rangle = e^{-2\pi\omega/\kappa}[1 - exp(-2\pi\omega/\kappa)]^{-1} = \frac{1}{e^{2\pi\omega/\kappa} - 1}.$$

From Exercise 4.7, we learn that $|\beta_\omega/\alpha_\omega|^2 \sim e^{-8\pi\omega/M}$, therefore, $\kappa = \frac{1}{4M}$ or $T = \frac{1}{8\pi M}$.

E.2 This is how originally Hawking derived black hole radiation. For the analysis see discussions in Sect. 6.4.3 and also Sect. 7 of black hole lecture notes by P. Townsend [244].

## Exercises of Appendix F

For hints or derivations on exercises in this appendix see standard GR textbooks like [8,108,133].

## Exercises of Appendix G

G.1 (1) Consider two Cauchy surfaces $\Sigma_1$, $\Sigma_2$ which share the same boundary, such that there is a spacetime volume $V$ enclosed between the two Cauchy surfaces, i.e.

$\Sigma_1 \cup \Sigma_2 = \partial V$. From (G.5), we have

$$\begin{aligned}\boldsymbol{\Omega}_{\rm LW}^{\Sigma_1} - \boldsymbol{\Omega}_{\rm LW}^{\Sigma_2} &= \int_{\Sigma_1} - \int_{\Sigma_2} \boldsymbol{\omega}_{\rm LW}(\delta_1\Phi, \delta_2\Phi, \Phi) \\ &= \int_V {\rm d}\boldsymbol{\omega}_{\rm LW}(\delta_1\Phi, \delta_2\Phi, \Phi) \approx 0.\end{aligned} \tag{J.12}$$

(2) If $\Sigma_i$ is a constant time slice at time $t_i$, then the above yields conservation of symplectic form in time.

G.2 See Appendix A.2 of [799].

G.3 See [737].

G.4 See [739].

## Exercises of Appendix H

For exercises of this appendix see the PhD thesis of Maulik Parikh [802].

## Exercises of Appendix I

I.1 Under Weyl transformation $g^{\rm str}_{\mu\nu} = e^{\phi/2} g^{\rm Ein}_{\mu\nu}$ the 10$d$ Ricci scalar transforms as

$$R_{\rm str} = e^{\phi/2}\left[R_{\rm Ein} - \frac{9}{2}((\partial\phi)^2 + \nabla^2\phi)\right], \qquad \sqrt{-\det g^{\rm str}} = e^{5\phi}\sqrt{-\det g^{\rm Ein}}.$$

Therefore, in the Einstein-frame

$$\mathcal{L}^{\rm Ein}_{\rm NSNS} = \left(R_E + (4 - \frac{9}{2})\partial_\mu\phi\partial^\mu\phi - \frac{1}{2}e^{-\phi}|H_3|^2\right) \tag{J.13}$$

where we dropped the total derivative term $\nabla^2\phi$. For the last term, note that $\sqrt{-\det g^{\rm str}}e^{-2\phi}|H_3|^2_{\rm str} = \sqrt{-\det g^{\rm Ein}}e^{-\phi}|H_3|^2_{\rm Ein}$. Here by $|H_3|^2_{\rm Ein}$ we mean the 3-form $H_3$ is squared using (inverse) Einstein-frame metrics, and similarly for $|H_3|^2_{\rm str}$.

For a $p$-form in the RR sector, $\sqrt{-\det g^{\rm str}}|F_{p+1}|^2_{\rm str} = \sqrt{-\det g^{\rm Ein}}e^{A\phi}|F_{p+1}|^2_{\rm Ein}$, with $A = 5/2 - (p+1)/2 = 2 - p/2$.

# References


1. C. Misner, in *Magic without Magic: John Archibald Wheeler, A Collection of Essays in Honor of his 60th Birthday*, ed. by J. Klauder (Freeman, San Francisco, 1972)
2. R.M. Wald, *General Relativity* (Chicago University Press, Chicago, USA, 1984). https://doi.org/10.7208/chicago/9780226870373.001.0001
3. B. Schutz, *A First Course in General Relativity* (Cambridge University Press, 1985)
4. J. Hartle, *An Introduction to Einstein's General Relativity* (Cambridge University Press, 2003)
5. S.M. Carroll, *Spacetime and Geometry* (Cambridge University Press, 2019)
6. E. Poisson, *A Relativist's Toolkit* (Cambridge, 2004)
7. T. Cheng, *Relativity, Gravitation and Cosmology: A Basic Introduction* (Oxford University Press, 2010)
8. T. Padmanabhan, *Gravitation: Foundations and Frontiers* (Cambridge University Press, 2014)
9. N. Straumann, *General Relativity*. Graduate Texts in Physics (Springer, Dordrecht, 2013). https://doi.org/10.1007/978-94-007-5410-2
10. A. Zee, *Einstein Gravity in a Nutshell* (Princeton University Press, New Jersey, 2013)
11. S. Weinberg, *Gravitation and Cosmology: Principles and Applications of the General Theory of Relativity* (Wiley, New York, 1972)
12. R. d'Inverno, *Introducing Einstein's Relativity* (Clarendon Press, Oxford, 1990)
13. W. Rindler, *Relativity: Special, General, and Cosmological* (Oxford University Press, 2001)
14. M. Hobson, G. Efstathiou, A. Lasenby, *General Relativity: An Introduction for Physicists* (Cambridge University Press, 2006)
15. C. Montgomery, W. Orchiston, I. Whittingham, J. Astron. Hist. Herit. **12**, 90 (2009)
16. C. Will, *Theory and Experiment in Gravitational Physics* (Cambridge University Press, 1993)
17. C.M. Will, Living Rev. Rel. **4**, 4 (2001)
18. C.M. Will, Living Rev. Rel. **9**, 3 (2005)
19. M.P. Haugan, C. Lämmerzahl, Lect. Notes Phys. **562**, 195 (2001). https://doi.org/10.1007/3-540-40988-2_10
20. E. Di Casola, S. Liberati, S. Sonego, Am. J. Phys. **83**, 39 (2015). https://doi.org/10.1119/1.4895342
21. J.W. York Jr., Phys. Rev. Lett. **28**, 1082 (1972)
22. G. Gibbons, S. Hawking, Phys. Rev. D **15**, 2738 (1977). https://doi.org/10.1103/PhysRevD.15.2738
23. B.P. Abbott et al., Phys. Rev. Lett. **116**(6), 061102 (2016). https://doi.org/10.1103/PhysRevLett.116.061102
24. T. Sigfried, Sci. News (2013)




D. Grumiller and M. M. Sheikh-Jabbari, *Black Hole Physics*, Graduate Texts in Physics,
https://doi.org/10.1007/978-3-031-10343-8

25. R.P. Kerr, Phys. Rev. Lett. **11**, 237 (1963)
26. K. Akiyama et al., Astrophys. J. **875**(1), L1 (2019). https://doi.org/10.3847/2041-8213/ab0ec7
27. A. Einstein, Annalen Phys. **49**, 769 (1916)
28. J. Droste, Ned. Acad. Wet, S.A. **19**, 197 (1917)
29. C. Heinicke, F.W. Hehl, Int. J. Mod. Phys. D **24**(02), 1530006 (2014). https://doi.org/10.1142/S0218271815300062
30. N. Arkani-Hamed, L. Motl, A. Nicolis, C. Vafa, JHEP **06**, 060 (2007). https://doi.org/10.1088/1126-6708/2007/06/060
31. L. Flamm, Phys. Zeits. **17**, 448 (1916)
32. P. Painlevé, C.R. Acad, Sci. (Paris) **173**, 677 (1921)
33. A. Gullstrand, Arkiv. Mat. Astron. Fys. **16**(8), 1 (1922)
34. A.S. Eddington, Nature **113**, 192 (1924)
35. G. Lemaitre, Gen. Rel. Grav. **29**, 641 (1997). https://doi.org/10.1023/A:1018855621348
36. H.P. Robertson, Ann. Math. 2 **39 (1)**, 101–104 (1938). https://doi.org/10.2307/1968715
37. J.L. Synge, Proc. Roy. Irish Acad. (Sect. A) **53**, 83 (1950)
38. D. Finkelstein, Phys. Rev. **110**, 965 (1958). https://doi.org/10.1103/PhysRev.110.965
39. G. Szekeres, Publ. Math. Debrecen **7**, 285 (1960)
40. M.D. Kruskal, Phys. Rev. **119**, 1743 (1960). https://doi.org/10.1103/PhysRev.119.1743
41. R. Penrose, Phys. Rev. Lett. **14**, 57 (1965). https://doi.org/10.1103/PhysRevLett.14.57
42. R. Penrose, Gen. Relativ. Gravit. **43**(3), 901 (2011). https://doi.org/10.1007/s10714-010-1110-5
43. E. Kronheimer, R. Penrose, Proc. Cambridge Phil. Soc. **63**, 481 (1967). https://doi.org/10.1017/S030500410004144X
44. W. Israel, Phys. Rev. **143**, 1016 (1966). https://doi.org/10.1103/PhysRev.143.1016
45. S. Hawking, R. Penrose, Proc. Roy. Soc. Lond. A **A314**, 529 (1970). https://doi.org/10.1098/rspa.1970.0021
46. G. Nordström, Proc. Kon. Ned. Akad. Wet. **20**, 1238 (1916)
47. H. Reissner, Ann. Phys. **50**, 106 (1916)
48. F.R. Tangherlini, Nuovo Cim. **27**, 636 (1963). https://doi.org/10.1007/BF02784569
49. E.T. Newman, R. Couch, K. Chinnapared, A. Exton, A. Prakash, R. Torrence, J. Math. Phys. **6**, 918 (1965). https://doi.org/10.1063/1.1704351
50. R. Penrose, R. Floyd, Nature **229**, 177 (1971)
51. S. Chandrasekhar, *The Mathematical Theory of Black Holes* (Clarendon, Oxford, UK, 1992)
52. R. Penrose, Riv. Nuovo Cim. **1**, 252 (1969)
53. R. Penrose, Ann. N. Y. Acad. Sci. **224**, 125 (1973). https://doi.org/10.1111/j.1749-6632.1973.tb41447.x
54. D. Christodoulou, S. Klainerman, Séminaire Équations aux dérivées partielles (Polytechnique) (1989–1990). http://www.numdam.org/item/SEDP_1989-1990____A15_0. Talk:13
55. D. Christodoulou, S. Klainerman, *The Global Nonlinear Stability of the Minkowski Space* (Princeton University Press, 1993)
56. M. Dafermos, G. Holzegel, I. Rodnianski, M. Taylor (2021)
57. C. Bolton, Nature Phys. Sci. **240**, 124 (1972). https://doi.org/10.1038/physci240124a0
58. B.L. Webster, P. Murdin, Nature **235**, 37 (1972). https://doi.org/10.1038/235037a0
59. B. Tetarenko, G. Sivakoff, C. Heinke, J. Gladstone, Astrophys. J. Suppl. **222**(2), 15 (2016). https://doi.org/10.3847/0067-0049/222/2/15
60. W.C. Danchi, M. Bester, C.G. Degiacomi, L.J. Greenhill, C.H. Townes, Astron. J. **107**, 1469 (1994). https://doi.org/10.1086/116960
61. R. Genzel, D. Hollenbach, C.H. Townes, Rep. Prog. Phys. **57**(5), 417 (1994). https://doi.org/10.1088/0034-4885/57/5/001
62. *Event Horizon Telescope*. https://eventhorizontelescope.org
63. *Chandra X-ray Observatory*. https://chandra.harvard.edu
64. *LIGO Gravity Wave Observatory*. https://www.ligo.caltech.edu
65. *VIRGO Gravity Wave Observatory*. https://www.virgo-gw.eu
66. *Gravitational Lensing: Strong, Weak and Micro*

67. L. Wyrzykowski, I. Mandel, Astron. Astrophys. **636**, A20 (2020). https://doi.org/10.1051/0004-6361/201935842
68. N.S. Abrams, M. Takada, Astrophys. J. **905**(2), 121 (2020). https://doi.org/10.3847/1538-4357/abc6aa
69. P.O. Mazur, E. Mottola, ArXiv e-prints (2001)
70. C.B. Chirenti, L. Rezzolla, Class. Quant. Grav. **24**, 4191 (2007). https://doi.org/10.1088/0264-9381/24/16/013
71. N. Sakai, H. Saida, T. Tamaki, Phys. Rev. D **90**(10), 104013 (2014). https://doi.org/10.1103/PhysRevD.90.104013
72. F. Eisenhauer et al., Astrophys. J. **628**, 246 (2005). https://doi.org/10.1086/430667
73. B. Carr, F. Kuhnel, M. Sandstad, Phys. Rev. D **94**(8), 083504 (2016). https://doi.org/10.1103/PhysRevD.94.083504
74. S. Clesse, J. García-Bellido, Phys. Dark Univ. **15**, 142 (2017). https://doi.org/10.1016/j.dark.2016.10.002
75. B. Carr, F. Kuhnel, Ann. Rev. Nucl. Part. Sci. **70**, 355 (2020). https://doi.org/10.1146/annurev-nucl-050520-125911
76. J.D. Bekenstein, Phys. Rev. D **7**, 2333 (1973)
77. J.M. Bardeen, B. Carter, S.W. Hawking, Commun. Math. Phys. **31**, 161 (1973). https://doi.org/10.1007/BF01645742
78. S.W. Hawking, Commun. Math. Phys. **43**, 199 (1975)
79. S.W. Hawking, Nature **248**, 30 (1974)
80. S.W. Hawking, Phys. Rev. D **14**, 2460 (1976)
81. W.G. Unruh, Phys. Rev. D **14**, 870 (1976)
82. G. 't Hooft, Nucl. Phys. **B256**, 727 (1985). https://doi.org/10.1016/0550-3213(85)90418-3
83. L. Susskind, L. Thorlacius, J. Uglum, Phys. Rev. D **48**, 3743 (1993). https://doi.org/10.1103/PhysRevD.48.3743
84. L. Susskind, L. Thorlacius, Phys. Rev. D **49**, 966 (1994). https://doi.org/10.1103/PhysRevD.49.966
85. G. 't Hooft, in *Salamfestschrift* (World Scientific, 1993)
86. L. Susskind, J. Math. Phys. **36**, 6377 (1995)
87. A. Strominger, Nucl. Phys. B **451**, 96 (1995)
88. J.M. Maldacena, Adv. Theor. Math. Phys. **2**, 231 (1998)
89. S.S. Gubser, I.R. Klebanov, A.M. Polyakov, Phys. Lett. B **428**, 105 (1998)
90. E. Witten, Adv. Theor. Math. Phys. **2**, 253 (1998)
91. A. Almheiri, D. Marolf, J. Polchinski, J. Sully, JHEP **1302**, 062 (2013). https://doi.org/10.1007/JHEP02(2013)062
92. A. Almheiri, D. Marolf, J. Polchinski, D. Stanford, J. Sully, JHEP **1309**, 018 (2013). https://doi.org/10.1007/JHEP09(2013)018
93. K. Papadodimas, S. Raju, Phys. Rev. Lett. **112**(5), 051301 (2014). https://doi.org/10.1103/PhysRevLett.112.051301
94. K. Papadodimas, S. Raju, Phys. Rev. D **89**(8), 086010 (2014). https://doi.org/10.1103/PhysRevD.89.086010
95. R.C. Tolman, Phys. Rev. **55**, 364 (1939). https://doi.org/10.1103/PhysRev.55.364
96. J. Oppenheimer, G. Volkoff, Phys. Rev. **55**, 374 (1939). https://doi.org/10.1103/PhysRev.55.374
97. H.Y. Chiu, A. Muriel (eds.), *Stellar Evolution* (MIT Press, Cambridge, Massachusetts, 1972)
98. H.J. Lamers, E.M. Levesque, *Understanding Stellar Evolution* (IOP Publishing, 2017). https://doi.org/10.1088/978-0-7503-1278-3
99. A. Heger, C. Fryer, S. Woosley, N. Langer, D. Hartmann, Astrophys. J. **591**, 288 (2003). https://doi.org/10.1086/375341
100. L. Rezzolla, E.R. Most, L.R. Weih, Astrophys. J. Lett. **852**(2), L25 (2018). https://doi.org/10.3847/2041-8213/aaa401
101. H.T. Cromartie et al., Nature Astron. **4**(1), 72 (2019). https://doi.org/10.1038/s41550-019-0880-2

102. N. Chamel, P. Haensel, Living Rev. Rel. **11**, 10 (2008). https://doi.org/10.12942/lrr-2008-10
103. N. Glendenning, *Compact Stars: Nuclear Physics, Particle Physics, and General Relativity*. Astronomy and Astrophysics Library (Springer New York, 2012). https://books.google.com/books?id=E3YnkgEACAAJ
104. S. Shapiro, S. Teukolsky, *Black Holes, White Dwarfs and Neutron Stars: The Physics of Compact Objects* (Wiley, 2008). https://books.google.com/books?id=CB2kZ-vMhaoC
105. A. Schmitt, ArXiv e-prints **811** (2010). https://doi.org/10.1007/978-3-642-12866-0
106. F.E. Schunck, E.W. Mielke, Class. Quant. Grav. **20**, R301 (2003). https://doi.org/10.1088/0264-9381/20/20/201
107. S.L. Liebling, C. Palenzuela, Living Rev. Rel. **20**(1), 5 (2017). https://doi.org/10.12942/lrr-2012-6
108. C.W. Misner, K. Thorne, J.A. Wheeler, *Gravitation* (W. H. Freeman & Co., San Francisco, 1973)
109. R.M. Wald, *General Relativity* (The University of Chicago Press, 1984)
110. M.W. Choptuik, Phys. Rev. Lett. **70**, 9 (1993)
111. F. Pretorius, Class. Quant. Grav. **23**, S529 (2006)
112. N.I. Shakura, R.A. Sunyaev, Astron. Astrophys. **24**, 337 (1973)
113. T. Baumgarte, S. Shapiro, *Numerical Relativity* (Cambridge University Press, 2010). https://doi.org/10.1017/CBO9781139193344
114. S.W. Hawking, M.J. Perry, A. Strominger, Phys. Rev. Lett. **116**(23), 231301 (2016). https://doi.org/10.1103/PhysRevLett.116.231301
115. H. Bondi, M. van der Burg, A. Metzner, Proc. Roy. Soc. London **A269**, 21 (1962)
116. R. Sachs, Phys. Rev. **128**, 2851 (1962)
117. A. Strominger, *Lectures on the Infrared Structure of Gravity and Gauge Theory* (Princeton University Press, 2018)
118. S. Pasterski, M. Pate, A.M. Raclariu, in *2022 Snowmass Summer Study* (2021)
119. L. Rosenfeld, Eur. Phys. J. H **42**(1), 63 (2017). https://doi.org/10.1140/epjh/e2016-70041-3
120. B.S. DeWitt, Phys. Rev. **160**, 1113 (1967)
121. B.S. DeWitt, Phys. Rev. **162**, 1195 (1967). https://doi.org/10.1103/PhysRev.162.1195
122. B.S. DeWitt, Phys. Rev. **162**, 1239 (1967). https://doi.org/10.1103/PhysRev.162.1239
123. C. Rovelli, in *9th Marcel Grossmann Meeting on Recent Developments in Theoretical and Experimental General Relativity, Gravitation and Relativistic Field Theories* (2000)
124. G. 't Hooft, M.J.G. Veltman, Annales Poincare Phys. Theor. **A20**, 69 (1974)
125. M.H. Goroff, A. Sagnotti, Nucl. Phys. B **266**, 709 (1986)
126. J.F. Donoghue, Phys. Rev. D **50**, 3874 (1994)
127. J.F. Donoghue, Phys. Rev. Lett. **72**, 2996 (1994). https://doi.org/10.1103/PhysRevLett.72.2996
128. N. Bjerrum-Bohr, J.F. Donoghue, B.R. Holstein, Phys. Rev. D **67**, 084033 (2003). https://doi.org/10.1103/PhysRevD.71.069903. [Erratum: Phys. Rev. D 71, 069903 (2005)]
129. D.G. Boulware, S. Deser, Ann. Phys. **89**, 193 (1975). https://doi.org/10.1016/0003-4916(75)90302-4
130. A. Zee, *Quantum Field Theory in a Nutshell* (Princeton University Press, 2003)
131. D. Harlow, Rev. Mod. Phys. **88**, 015002 (2016). https://doi.org/10.1103/RevModPhys.88.015002
132. S. Hawking, G. Ellis, *The Large Scale Structure of Space-Time*. Cambridge Monographs on Mathematical Physics (Cambridge University Press, 2011). https://doi.org/10.1017/CBO9780511524646
133. H. Stephani, D. Kramer, M. MacCallum, C. Hoenselaers, E. Herlt, *Exact Solutions of Einstein's Field Equations* (Cambridge University Press, 2003)
134. V. Frolov, I. Novikov, *Black Hole Physics* (Kluwer Academic Publishers, 1998)
135. L. Susskind, J. Lindesay, *An Introduction to Black Holes, Information and the String Theory Revolution: The Holographic Universe* (World Scientific, 2005). https://books.google.com/books?id=D6B59P8_OE8C

136. J. Navarro-Salas, A. Fabbri, *Modeling Black Hole Evaporation* (World Scientific Publishing Company, 2005). https://books.google.com/books?id=dOK3CgAAQBAJ
137. G.E. Romero, G.S. Vila, Lect. Notes Phys. **876** (2014). https://doi.org/10.1007/978-3-642-39596-3
138. P. Chrusciel, *Geometry of Black Holes*. International Series of Monographs on Physics (Oxford University Press, 2020)
139. R. Ruffini, J.A. Wheeler, Phys. Today **24**(1), 30 (1971). https://doi.org/10.1063/1.3022513
140. L. Barack et al., Class. Quant. Grav. **36**(14), 143001 (2019). https://doi.org/10.1088/1361-6382/ab0587
141. R. Wald, *Space, Time, and Gravity: The Theory of the Big Bang and Black Holes* (University of Chicago Press, 1992). https://books.google.com/books?id=sk5a8ieI91kC
142. K. Thorne, K. Thorne, S. Hawking, *Black Holes and Time Warps: Einstein's Outrageous Legacy*. Commonwealth Fund Book Program (W.W. Norton, 1994). https://books.google.com/books?id=GzlrW6kytdoC
143. L. Susskind, *The Black Hole War: My Battle with Stephen Hawking to Make the World Safe for Quantum Mechanics* (Little, Brown, 2008). https://books.google.com/books?id=f3_rnRVxGIsC
144. S. Gubser, F. Pretorius, *The Little Book of Black Holes* (Princeton University Press, 2018)
145. D. Raine, E. Thomas, *Black Holes: An Introduction* (Imperial College Press, 2005)
146. D. Lüst, W. Vleeshouwers, *Black Hole Information and Thermodynamics*. Springer Briefs in Physics (Springer, 2019). https://books.google.com/books?id=BEKFDwAAQBAJ
147. E. Zakhary, C.B.G. Mcintosh, Gen. Relativ. Gravit. **29**(5), 539 (1997)
148. R.L. Arnowitt, S. Deser, C.W. Misner, Phys. Rev. **116**, 1322 (1959). https://doi.org/10.1103/PhysRev.116.1322
149. R.L. Arnowitt, S. Deser, C.W. Misner, Phys. Rev. **122**, 997 (1961). https://doi.org/10.1103/PhysRev.122.997
150. R.L. Arnowitt, S. Deser, C.W. Misner, Phys. Rev. **117**, 1595 (1960). https://doi.org/10.1103/PhysRev.117.1595
151. R. Park, W. Folkner, A. Konopliv, J. Williams, D. Smith, M. Zuber, Astron. J. **153**, 121 (2017). https://doi.org/10.3847/1538-3881/aa5be2
152. K. Martel, E. Poisson, Am. J. Phys. **69**, 476 (2001). https://doi.org/10.1119/1.1336836
153. G. Ellis, B. Schmidt, Gen. Rel. Grav. **8**, 915 (1977). https://doi.org/10.1007/BF00759240
154. G.F.R. Ellis, B.G. Schmidt, Gen. Relativ. Gravit. **10**, 989 (1979)
155. T. Klösch, T. Strobl, Class. Quant. Grav. **13**, 2395 (1996)
156. M. Spradlin, A. Strominger, A. Volovich, in *Les Houches Summer School: Session 76: Euro Summer School on Unity of Fundamental Physics: Gravity, Gauge Theory and Strings* (2001), pp. 423–453
157. C.W. Misner, J.A. Wheeler, Ann. Phys. **2**, 525 (1957). https://doi.org/10.1016/0003-4916(57)90049-0
158. A. Einstein, N. Rosen, Phys. Rev. **48**, 73 (1935). https://doi.org/10.1103/PhysRev.48.73
159. M. Visser, *Lorentzian Wormholes: From Einstein to Hawking* (AIP, Woodbury, USA, 1995)
160. D. Hochberg, M. Visser, Phys. Rev. D **56**, 4745 (1997). https://doi.org/10.1103/PhysRevD.56.4745
161. K. Bronnikov, Acta Phys. Polon. B **4**, 251 (1973)
162. H. Ellis, J. Math. Phys. **14**, 104 (1973). https://doi.org/10.1063/1.1666161
163. J. Maldacena, X.L. Qi, ArXiv e-prints (2018)
164. B. Bertotti, Phys. Rev. **116**, 1331 (1959). https://doi.org/10.1103/PhysRev.116.1331
165. I. Robinson, Bull. Acad. Pol. Sci. Ser. Sci. Math. Astron. Phys. **7**, 351 (1959)
166. W. Israel, Phys. Rev. **143**, 1016 (1966)
167. T. Klösch, T. Strobl, Class. Quant. Grav. **13**, 1191 (1996). https://doi.org/10.1088/0264-9381/13/5/029
168. B. O'Neill, *The Geometry of Kerr Black Holes*. Dover Books on Physics (Dover Publications, 2014). https://books.google.com/books?id=jHXCAgAAQBAJ

169. S.A. Teukolsky, Class. Quant. Grav. **32**(12), 124006 (2015). https://doi.org/10.1088/0264-9381/32/12/124006
170. P.T. Chruściel, M. Maliborski, N. Yunes, Phys. Rev. D **101**(10), 104048 (2020). https://doi.org/10.1103/PhysRevD.101.104048
171. P.T. Chrusciel, C.R. Olz, S.J. Szybka, Phys. Rev. D **86**, 124041 (2012). https://doi.org/10.1103/PhysRevD.86.124041
172. B. Carter, Phys. Rev. **174**, 1559 (1968). https://doi.org/10.1103/PhysRev.174.1559
173. D. Ahulwalia, D. Grumiller (eds.), *Invited Papers on the Thirring–Lense Effect* (World Scientific, 2005). Special issue of Int. J. Mod. Phys. D
174. H. Nariai, Sci. Rep. Tohoku Univ. Eighth Ser. **34**, 160 (1950)
175. H. Nariai, Sci. Rep. Tohoku Univ. Eighth Ser. **35**, 62 (1951)
176. L. Vanzo, Phys. Rev. D **56**, 6475 (1997). https://doi.org/10.1103/PhysRevD.56.6475
177. D. Birmingham, Class. Quant. Grav. **16**, 1197 (1999). https://doi.org/10.1088/0264-9381/16/4/009
178. J. Plebanski, M. Demianski, Ann. Phys. **98**, 98 (1976). https://doi.org/10.1016/0003-4916(76)90240-2
179. A. Petrov, *Einstein Spaces* (Pergamon, Oxford, 1969)
180. J. Griffiths, J. Podolsky, Int. J. Mod. Phys. D **15**, 335 (2006). https://doi.org/10.1142/S0218271806007742
181. A. Taub, Ann. Math. **53**, 472 (1951). https://doi.org/10.2307/1969567
182. E. Newman, L. Tamburino, T. Unti, J. Math. Phys. **4**, 915 (1963). https://doi.org/10.1063/1.1704018
183. P. Vaidya, Proc. Natl. Inst. Sci. India A **33**, 264 (1951)
184. E. Poisson, *A Relativist's Toolkit: The Mathematics of Black-Hole Mechanics* (Cambridge University Press, 2009). https://doi.org/10.1017/CBO9780511606601
185. J.B. Griffiths, J. Podolsky, *Exact Space-Times in Einstein's General Relativity*. Cambridge Monographs on Mathematical Physics (Cambridge University Press, Cambridge, 2009). https://doi.org/10.1017/CBO9780511635397
186. E. Poisson, A. Pound, I. Vega, Living Rev. Rel. **14**, 7 (2011). https://doi.org/10.12942/lrr-2011-7
187. R.P. Kerr, in *Kerr Fest: Black Holes in Astrophysics, General Relativity and Quantum Gravity* (2007)
188. B. Carter, Commun. Math. Phys. **17**, 233 (1970). https://doi.org/10.1007/BF01647092
189. J.A. Schouten, Proc. Kon. Ned. Akad. Wet. Amsterdam **43**, 449 (1940). https://ci.nii.ac.jp/naid/10011666142/en/
190. A. Nijenhuis, Indagationes Mathematicae (Proceedings) **58**, 390 (1955). https://doi.org/10.1016/S1385-7258(55)50054-0
191. W.E. Couch, R.J. Torrence, Gen. Relativ. Gravit. **16**, 1789 (1984). https://doi.org/10.1007/BF00762916
192. M. Cvetic, C.N. Pope, A. Saha, Phys. Rev. D **102**(8), 086007 (2020). https://doi.org/10.1103/PhysRevD.102.086007
193. D. Sadri, M.M. Sheikh-Jabbari, Rev. Mod. Phys. **76**, 853 (2004). https://doi.org/10.1103/RevModPhys.76.853
194. S. Majumdar, Phys. Rev. **72**, 390 (1947). https://doi.org/10.1103/PhysRev.72.390
195. A. Papapetrou, Proc. Roy. Irish Acad. A **51**, 191 (1947)
196. J. Hartle, S. Hawking, Commun. Math. Phys. **26**, 87 (1972). https://doi.org/10.1007/BF01645696
197. W. Israel, G. Wilson, J. Math. Phys. **13**, 865 (1972). https://doi.org/10.1063/1.1666066
198. J.M. Bardeen, G.T. Horowitz, Phys. Rev. D **60**, 104030 (1999). https://doi.org/10.1103/PhysRevD.60.104030
199. M. Guica, T. Hartman, W. Song, A. Strominger, Phys. Rev. D **80**, 124008 (2009). https://doi.org/10.1103/PhysRevD.80.124008
200. A.J. Amsel, G.T. Horowitz, D. Marolf, M.M. Roberts, Phys. Rev. D **81**, 024033 (2010). https://doi.org/10.1103/PhysRevD.81.024033

201. G.C. Debney, R.P. Kerr, A. Schild, J. Math. Phys. **10**, 1842 (1969). https://doi.org/10.1063/1.1664769
202. W. Israel, Nuovo Cim. **B44S10**, 1 (1966)
203. G. McVittie, Mon. Not. Roy. Astron. Soc. **93**, 325 (1933). https://doi.org/10.1093/mnras/93.5.325
204. V. Faraoni, A.F. Zambrano Moreno, R. Nandra, Phys. Rev. D **85**, 083526 (2012). https://doi.org/10.1103/PhysRevD.85.083526
205. P. Horava, C.M. Melby-Thompson, Gen. Rel. Grav. **43**, 1391 (2011). https://doi.org/10.1007/s10714-010-1117-y
206. I. Booth, Can. J. Phys. **83**, 1073 (2005). https://doi.org/10.1139/p05-063
207. R.M. Wald, V. Iyer, Phys. Rev. D **44**, 3719 (1991). https://doi.org/10.1103/PhysRevD.44.R3719
208. V. Faraoni, G.F.R. Ellis, J.T. Firouzjaee, A. Helou, I. Musco, Phys. Rev. D **95**(2), 024008 (2017). https://doi.org/10.1103/PhysRevD.95.024008
209. R. Penrose, in *Gravitational collapse, Gravitational Radiation and Gravitational Collapse*, ed. by C. DeWitt-Morette (Springer, 1974)
210. M. Dafermos, J. Luk (2017)
211. A. Ashtekar, B. Krishnan, Living Rev. Rel. **7**, 10 (2004). https://doi.org/10.12942/lrr-2004-10
212. R.P. Geroch, G. Horowitz, *Global Structure of Spacetimes* (University Press, United Kingdom, 1979), pp.212–293
213. R.M. Wald, Phys. Rev. D **28**, 2118 (1983). https://doi.org/10.1103/PhysRevD.28.2118
214. E. Curiel, Einstein Stud. **13**, 43 (2017). https://doi.org/10.1007/978-1-4939-3210-8_3
215. T. Faulkner, R.G. Leigh, O. Parrikar, H. Wang, JHEP **09**, 038 (2016). https://doi.org/10.1007/JHEP09(2016)038
216. T. Hartman, S. Kundu, A. Tajdini, JHEP **07**, 066 (2017). https://doi.org/10.1007/JHEP07(2017)066
217. C. Clarke, C.U. Press, P. Goddard, J. Yeomans, *The Analysis of Space-Time Singularities*. Cambridge Lecture Notes in Physics (Cambridge University Press, 1993). https://books.google.by/books?id=aeUADsSiC1QC
218. J.M.M. Senovilla, Gen. Rel. Grav. **30**, 701 (1998). https://doi.org/10.1023/A:1018801101244
219. S. Hollands, A. Ishibashi, J. Math. Phys. **46**, 022503 (2005). https://doi.org/10.1063/1.1829152
220. K. Tanabe, S. Kinoshita, T. Shiromizu, Phys. Rev. D **84**, 044055 (2011). https://doi.org/10.1103/PhysRevD.84.044055
221. S. Hawking, G. Ellis, *The Large Scale Structure of Space-Time* (Cambridge University Press, 1973)
222. S.W. Hawking, Commun. Math. Phys. **25**, 152 (1972)
223. S.W. Hawking, Commun. Math. Phys. **25**, 152 (1972). https://doi.org/10.1007/BF01877517
224. P.T. Chrusciel, R.M. Wald, Class. Quant. Grav. **11**, L147 (1994). https://doi.org/10.1088/0264-9381/11/12/001
225. G.J. Galloway, K. Schleich, D.M. Witt, E. Woolgar, Phys. Rev. D **60**, 104039 (1999). https://doi.org/10.1103/PhysRevD.60.104039
226. R. Emparan, H.S. Reall, Phys. Rev. Lett. **88**, 101101 (2002)
227. R. Emparan, H.S. Reall, Living Rev. Rel. **11**, 6 (2008). https://doi.org/10.12942/lrr-2008-6
228. G. Birkhoff, R. Langer, *Relativity and Modern Physics* (Harvard University Press, 1923). https://books.google.de/books?id=NEpAAAAAIAAJ
229. J. Jebsen, Arkiv för Matematik. Astronomi och Fysik **15**, 1–9 (1921)
230. W. Israel, Phys. Rev. **164**, 1776 (1967). https://doi.org/10.1103/PhysRev.164.1776
231. G. Bunting, A. Masood-ul Alam, Gen. Relativ. Gravit. **19** (1987). https://doi.org/10.1007/BF00770326
232. B. Carter, Phys. Rev. Lett. **26**, 331 (1971). https://doi.org/10.1103/PhysRevLett.26.331
233. D. Robinson, Phys. Rev. Lett. **34**, 905 (1975). https://doi.org/10.1103/PhysRevLett.34.905
234. W. Israel, Commun. Math. Phys. **8**, 245 (1968). https://doi.org/10.1007/BF01645859

235. P.O. Mazur, J. Phys. A **15**, 3173 (1982). https://doi.org/10.1088/0305-4470/15/10/021
236. G.L. Bunting, Proof of the uniqueness conjecture for black holes. Ph.D. thesis, PhD Thesis, University of New England (1983)
237. P.T. Chrusciel, J. Lopes Costa, Asterisque **321**, 195 (2008)
238. P.T. Chrusciel, L. Nguyen, Annales Henri Poincare **11**, 585 (2010). https://doi.org/10.1007/s00023-010-0038-3
239. P.T. Chrusciel, J. Lopes Costa, M. Heusler, Living Rev. Rel. **15**, 7 (2012). https://doi.org/10.12942/lrr-2012-7
240. M.D. Roberts, Gen. Rel. Grav. **21**, 907 (1989)
241. D. Christodoulou, Ann. Math. **140**, 607 (1994). https://doi.org/10.2307/2118619
242. R. Sachs, Proc. Roy. Soc. Lond. A **A264**, 309 (1961). https://doi.org/10.1098/rspa.1961.0202
243. P.T. Chrusciel, E. Delay, G.J. Galloway, R. Howard, Ann. Henri Poincare **2**, 109 (2001). https://doi.org/10.1007/PL00001029
244. P. Townsend, *Lecture Notes on Black Hole Physics* (Cambridge University, 1997). https://arxiv.org/pdf/gr-qc/9707012.pdf
245. H. Reall, *Lecture Notes on Black Hole Physics* (Cambridge University). http://www.damtp.cam.ac.uk/user/hsr1000/black_holes_lectures_2020.pdf
246. H. Friedrich, A.D. Rendall, Lect. Notes Phys. **540**, 127 (2000)
247. A.D. Rendall, Living Rev. Rel. **8**, 6 (2002). https://doi.org/10.12942/lrr-2005-6
248. H. Friedrich, I. Racz, R.M. Wald, Commun. Math. Phys. **204**, 691 (1999). https://doi.org/10.1007/s002200050662
249. A. Ionescu, S. Klainerman (2015)
250. C.A.R. Herdeiro, E. Radu, Phys. Rev. Lett. **112**, 221101 (2014). https://doi.org/10.1103/PhysRevLett.112.221101
251. C.A. Herdeiro, E. Radu, Int. J. Mod. Phys. D **24**(09), 1542014 (2015). https://doi.org/10.1142/S0218271815420146
252. J. Bekenstein, Phys. Rev. D **51**(12), 6608 (1995). https://doi.org/10.1103/PhysRevD.51.R6608
253. M. Isi, M. Giesler, W.M. Farr, M.A. Scheel, S.A. Teukolsky, Phys. Rev. Lett. **123**(11), 111102 (2019). https://doi.org/10.1103/PhysRevLett.123.111102
254. A.E. Broderick, T. Johannsen, A. Loeb, D. Psaltis, Astrophys. J. **784**, 7 (2014). https://doi.org/10.1088/0004-637X/784/1/7
255. R. Wald, Ann. Phys. **82**(2), 548 (1974). https://doi.org/10.1016/0003-4916(74)90125-0
256. S.L. Shapiro, S.A. Teukolsky, Phys. Rev. Lett. **66**, 994 (1991). https://doi.org/10.1103/PhysRevLett.66.994
257. R.M. Wald, ArXiv e-prints pp. 69–85 (1997). https://doi.org/10.1007/978-94-017-0934-7_5
258. V.E. Hubeny, Phys. Rev. D **59**, 064013 (1999). https://doi.org/10.1103/PhysRevD.59.064013
259. J. Sorce, R.M. Wald, Phys. Rev. D **96**(10), 104014 (2017). https://doi.org/10.1103/PhysRevD.96.104014
260. D. Klemm, Phys. Rev. D **89**(8), 084007 (2014). https://doi.org/10.1103/PhysRevD.89.084007
261. M. Mars, Class. Quant. Grav. **26**, 193001 (2009). https://doi.org/10.1088/0264-9381/26/19/193001
262. H.L. Bray, J. Differ. Geom. **59**(2), 177 (2001). https://doi.org/10.4310/jdg/1090349428
263. S. Dain, Class. Quant. Grav. **29**, 073001 (2012). https://doi.org/10.1088/0264-9381/29/7/073001
264. K.S. Thorne, Astrophys. J. **191**, 507 (1974). https://doi.org/10.1086/152991
265. D.N. Page, K.S. Thorne, Astrophys. J. **191**, 499 (1974). https://doi.org/10.1086/152990
266. Y. Tanaka et al., Nature **375**, 659 (1995). https://doi.org/10.1038/375659a0
267. A.M. Ghez, B.L. Klein, M. Morris, E.E. Becklin, Astrophys. J. **509**, 678 (1998)
268. R. Schodel et al., Nature **419**, 694 (2002)
269. A.M. Ghez, S. Salim, S.D. Hornstein, A. Tanner, M. Morris, E.E. Becklin, G. Duchene, Astrophys. J. **620**, 744 (2005). https://doi.org/10.1086/427175
270. A.M. Ghez et al., Astrophys. J. **689**, 1044 (2008). https://doi.org/10.1086/592738
271. R. Genzel, F. Eisenhauer, S. Gillessen, Rev. Mod. Phys. **82**, 3121 (2010). https://doi.org/10.1103/RevModPhys.82.3121

272. N. Yunes, K. Yagi, F. Pretorius, Phys. Rev. D **94**(8), 084002 (2016). https://doi.org/10.1103/PhysRevD.94.084002
273. C. Cutler et al., Phys. Rev. Lett. **70**, 2984 (1993). https://doi.org/10.1103/PhysRevLett.70.2984
274. E. Poisson, C.M. Will, Phys. Rev. D **52**, 848 (1995). https://doi.org/10.1103/PhysRevD.52.848
275. E. Poisson, Phys. Rev. D **57**, 5287 (1998). https://doi.org/10.1103/PhysRevD.57.5287
276. E.E. Flanagan, S.A. Hughes, Phys. Rev. D **57**, 4535 (1998). https://doi.org/10.1103/PhysRevD.57.4535
277. M. Campanelli, C.O. Lousto, Y. Zlochower, D. Merritt, Astrophys. J. Lett. **659**, L5 (2007). https://doi.org/10.1086/516712
278. C.L. Fryer, K.C.B. New, Living Rev. Rel. **14**, 1 (2011)
279. K. Akiyama et al., Astrophys. J. Lett. **875**(1), L6 (2019). https://doi.org/10.3847/2041-8213/ab1141
280. J.P. Luminet, Astron. Astrophys. **75**, 228 (1979)
281. S.E. Gralla, A. Lupsasca, D.P. Marrone, Phys. Rev. D **102**(12), 124004 (2020). https://doi.org/10.1103/PhysRevD.102.124004
282. Y.B. Zel'dovich, A.G. Polnarev, Sov. Astron. **18**, 17 (1974)
283. K.S. Thorne, Phys. Rev. D **45**(2), 520 (1992). https://doi.org/10.1103/PhysRevD.45.520
284. A. Strominger, *Lectures on the Infrared Structure of Gravity and Gauge Theory* (Princeton University Press, 2018)
285. L. Donnay, G. Giribet, H.A. González, A. Puhm, Phys. Rev. D **98**(12), 124016 (2018). https://doi.org/10.1103/PhysRevD.98.124016
286. H. Niikura et al., Nature Astron. **3**(6), 524 (2019). https://doi.org/10.1038/s41550-019-0723-1
287. B.J. Carr, K. Kohri, Y. Sendouda, J. Yokoyama, Phys. Rev. D **81**, 104019 (2010). https://doi.org/10.1103/PhysRevD.81.104019
288. A. Arvanitaki, S. Dimopoulos, S. Dubovsky, N. Kaloper, J. March-Russell, Phys. Rev. D **81**, 123530 (2010). https://doi.org/10.1103/PhysRevD.81.123530
289. S.A. Teukolsky, Phys. Rev. Lett. **29**, 1114 (1972). https://doi.org/10.1103/PhysRevLett.29.1114
290. S.V. Babak, L.P. Grishchuk, Phys. Rev. D **61**, 024038 (2000). https://doi.org/10.1103/PhysRevD.61.024038
291. C.C. Chang, J.M. Nester, C.M. Chen, Phys. Rev. Lett. **83**, 1897 (1999). https://doi.org/10.1103/PhysRevLett.83.1897
292. R. Maartens, B.A. Bassett, Class. Quant. Grav. **15**, 705 (1998). https://doi.org/10.1088/0264-9381/15/3/018
293. R.A. Hulse, J.H. Taylor, Astrophys. J. Lett. **195**, L51 (1975). https://doi.org/10.1086/181708
294. R.A. Hulse, J.H. Taylor, Astrophys. J. Lett. **195**, L51 (1975). https://doi.org/10.1086/181708
295. T. Binnington, E. Poisson, Phys. Rev. D **80**, 084018 (2009). https://doi.org/10.1103/PhysRevD.80.084018
296. A. Le Tiec, M. Casals, Phys. Rev. Lett. **126**(13), 131102 (2021). https://doi.org/10.1103/PhysRevLett.126.131102
297. E.E. Flanagan, T. Hinderer, Phys. Rev. D **77**, 021502 (2008). https://doi.org/10.1103/PhysRevD.77.021502
298. V. Cardoso, E. Franzin, A. Maselli, P. Pani, G. Raposo, Phys. Rev. D **95**(8), 084014 (2017). https://doi.org/10.1103/PhysRevD.95.084014. [Addendum: Phys. Rev. D 95, 089901 (2017)]
299. A.A. Esin, J.E. McClintock, R. Narayan, Astrophys. J. **489**, 865 (1997). https://doi.org/10.1086/304829
300. P.C. Fragile, O.M. Blaes, P. Anninois, J.D. Salmonson, Astrophys. J. **668**, 417 (2007). https://doi.org/10.1086/521092
301. M.A. Abramowicz, P.C. Fragile, Living Rev. Rel. **16**, 1 (2013). https://doi.org/10.12942/lrr-2013-1

302. S.A. Balbus, J.F. Hawley, Rev. Mod. Phys. **70**, 1 (1998). https://doi.org/10.1103/RevModPhys.70.1
303. R.D. Blandford, R.L. Znajek, Mon. Not. Roy. Astron. Soc. **179**, 433 (1977). https://doi.org/10.1093/mnras/179.3.433
304. J. Armas, Y. Cai, G. Compére, D. Garfinkle, S.E. Gralla, JCAP **04**, 009 (2020). https://doi.org/10.1088/1475-7516/2020/04/009
305. A. Kovner, L.D. McLerran, H. Weigert, Phys. Rev. D **52**, 6231 (1995). https://doi.org/10.1103/PhysRevD.52.6231
306. P. Aichelburg, R. Sexl, Gen. Rel. Grav. **2**, 303 (1971). https://doi.org/10.1007/BF00758149
307. D.M. Eardley, S.B. Giddings, Phys. Rev. D **66**, 044011 (2002). https://doi.org/10.1103/PhysRevD.66.044011
308. K.D. Kokkotas, B.G. Schmidt, Living Rev. Rel. **2**, 2 (1999). https://doi.org/10.12942/lrr-1999-2
309. H.P. Nollert, Class. Quant. Grav. **16**, R159 (1999). https://doi.org/10.1088/0264-9381/16/12/201
310. S. Chandrasekhar, S.L. Detweiler, Proc. Roy. Soc. Lond. A **344**, 441 (1975). https://doi.org/10.1098/rspa.1975.0112
311. L. Motl, A. Neitzke, Adv. Theor. Math. Phys. **7**, 307 (2003)
312. E.W. Leaver, Proc. Roy. Soc. Lond. A **402**, 285 (1985). https://doi.org/10.1098/rspa.1985.0119
313. K.S. Thorne, J.R. Klauder, *Magic Without Magic** (San Francisco, 1972)
314. B.S. Kay, R.M. Wald, Class. Quant. Grav. **4**, 893 (1987). https://doi.org/10.1088/0264-9381/4/4/022
315. M. Dafermos, I. Rodnianski, Clay Math. Proc. **17**, 97 (2013)
316. L. Blanchet, Living Rev. Rel. **17**, 2 (2014). https://doi.org/10.12942/lrr-2014-2
317. L. Blanchet, T. Damour, B.R. Iyer, C.M. Will, A.G. Wiseman, Phys. Rev. Lett. **74**, 3515 (1995). https://doi.org/10.1103/PhysRevLett.74.3515
318. L. Blanchet, T. Damour, G. Esposito-Farese, B.R. Iyer, Phys. Rev. Lett. **93**, 091101 (2004). https://doi.org/10.1103/PhysRevLett.93.091101
319. W.D. Goldberger, I.Z. Rothstein, Phys. Rev. D **73**, 104029 (2006). https://doi.org/10.1103/PhysRevD.73.104029
320. D. Christodoulou, Commun. Math. Phys. **109**, 613 (1987)
321. P. Di Francesco, P. Mathieu, D. Senechal, *Conformal Field Theory* (Springer, 1997)
322. D. Christodoulou, Commun. Math. Phys. **93**, 171 (1984). https://doi.org/10.1007/BF01223743
323. C. Gundlach, J.M. Martin-Garcia, Living Rev. Rel. **10**, 5 (2007). https://doi.org/10.12942/lrr-2007-5
324. S. Klainerman, J. Szeftel (2021)
325. T. Regge, J.A. Wheeler, Phys. Rev. **108**, 1063 (1957). https://doi.org/10.1103/PhysRev.108.1063
326. R. Brito, V. Cardoso, P. Pani, *Superradiance: Energy Extraction, Black-Hole Bombs and Implications for Astrophysics and Particle Physics*, vol. 906 (Springer, 2015). https://doi.org/10.1007/978-3-319-19000-6
327. S.W. Davis, C. Done, O.M. Blaes, Astrophys. J. **647**, 525 (2006). https://doi.org/10.1086/505386
328. H.K. Lee, R.A.M.J. Wijers, G.E. Brown, Phys. Rept. **325**, 83 (2000). https://doi.org/10.1016/S0370-1573(99)00084-8
329. J.C. McKinney, Astrophys. J. Lett. **630**, L5 (2005). https://doi.org/10.1086/468184
330. S.S. Komissarov, Mon. Not. Roy. Astron. Soc. **359**, 801 (2005). https://doi.org/10.1111/j.1365-2966.2005.08974.x
331. M. Ruiz, C. Palenzuela, F. Galeazzi, C. Bona, Mon. Not. Roy. Astron. Soc. **423**, 1300 (2012). https://doi.org/10.1111/j.1365-2966.2012.20950.x
332. V. Cardoso, E. Franzin, P. Pani, Phys. Rev. Lett. **116**(17), 171101 (2016). https://doi.org/10.1103/PhysRevLett.116.171101. [Erratum: Phys. Rev. Lett. 117, 089902 (2016)]

333. P.V.P. Cunha, C.A.R. Herdeiro, M.J. Rodriguez, Phys. Rev. D **97**(8), 084020 (2018). https://doi.org/10.1103/PhysRevD.97.084020
334. H.C.D. Lima, Junior., L.C.B. Crispino, P.V.P. Cunha, C.A.R. Herdeiro, Phys. Rev. D **103**(8), 084040 (2021). https://doi.org/10.1103/PhysRevD.103.084040
335. V. Cardoso, A.S. Miranda, E. Berti, H. Witek, V.T. Zanchin, Phys. Rev. D **79**, 064016 (2009). https://doi.org/10.1103/PhysRevD.79.064016
336. V. Cardoso, J.P.S. Lemos, Phys. Rev. D **64**, 084017 (2001). https://doi.org/10.1103/PhysRevD.64.084017
337. G.T. Horowitz, V.E. Hubeny, Phys. Rev. D **62**, 024027 (2000)
338. D. Birmingham, I. Sachs, S.N. Solodukhin, Phys. Rev. Lett. **88**, 151301 (2002). https://doi.org/10.1103/PhysRevLett.88.151301
339. P.K. Kovtun, A.O. Starinets, Phys. Rev. D **72**, 086009 (2005). https://doi.org/10.1103/PhysRevD.72.086009
340. P.S. Joshi, I.H. Dwivedi, Phys. Rev. D **47**, 5357 (1993). https://doi.org/10.1103/PhysRevD.47.5357
341. L. Baiotti, L. Rezzolla, Phys. Rev. Lett. **97**, 141101 (2006). https://doi.org/10.1103/PhysRevLett.97.141101
342. P.S. Joshi, D. Malafarina, Int. J. Mod. Phys. D **20**, 2641 (2011). https://doi.org/10.1142/S0218271811020792
343. P.S. Joshi (ed.), *Gravitational Collapse and Spacetime Singularities*. Cambridge Monographs on Mathematical Physics (Cambridge University Press, 2012). https://doi.org/10.1017/CBO9780511536274
344. F. Cooper, A. Khare, U. Sukhatme, Phys. Rept. **251**, 267 (1995). https://doi.org/10.1016/0370-1573(94)00080-M
345. S.S. Komissarov, in *3rd International Sakharov Conference on Physics* (2002)
346. V.E. Hubeny, M. Rangamani, JHEP **11**, 021 (2002). https://doi.org/10.1088/1126-6708/2002/11/021
347. R. Penrose, in *In Differential Geometry and Relativity. Mathematical Physics and Applied Mathematics*, ed. by M. Flato, M. Cahen, vol 3. (Springer, Dordrecht, 1976), pp. 271–275. https://doi.org/10.1007/978-94-010-1508-0_23
348. E.S.C. Ching, P.T. Leung, W.M. Suen, K. Young, Phys. Rev. D **54**, 3778 (1996). https://doi.org/10.1103/PhysRevD.54.3778
349. A. Komar, Phys. Rev. **113**, 934 (1959). https://doi.org/10.1103/PhysRev.113.934
350. R.L. Arnowitt, S. Deser, C.W. Misner, Gen. Rel. Grav. **40**, 1997 (2008). https://doi.org/10.1007/s10714-008-0661-1
351. T. Regge, C. Teitelboim, Ann. Phys. **88**, 286 (1974)
352. J.D. Brown, J.W. York Jr., Phys. Rev. D **47**, 1407 (1993)
353. S. Hawking, G.T. Horowitz, Class. Quant. Grav. **13**, 1487 (1996). https://doi.org/10.1088/0264-9381/13/6/017
354. A. Ashtekar, A. Magnon, Class. Quant. Grav. **1**, L39 (1984). https://doi.org/10.1088/0264-9381/1/4/002
355. A. Ashtekar, S. Das, Class. Quant. Grav. **17**, L17 (2000). https://doi.org/10.1088/0264-9381/17/2/101
356. R. Aros, M. Contreras, R. Olea, R. Troncoso, J. Zanelli, Phys. Rev. Lett. **84**, 1647 (2000). https://doi.org/10.1103/PhysRevLett.84.1647
357. V. Balasubramanian, P. Kraus, Commun. Math. Phys. **208**, 413 (1999)
358. I. Papadimitriou, K. Skenderis, JHEP **08**, 004 (2005)
359. S. Hollands, A. Ishibashi, D. Marolf, Class. Quant. Grav. **22**, 2881 (2005)
360. S. Deser, B. Tekin, Phys. Rev. D **67**, 084009 (2003). https://doi.org/10.1103/PhysRevD.67.084009
361. V. Balasubramanian, J. de Boer, D. Minic, Phys. Rev. D **65**, 123508 (2002). https://doi.org/10.1103/PhysRevD.65.123508
362. S. Deser, B. Tekin, Phys. Rev. Lett. **89**, 101101 (2002). https://doi.org/10.1103/PhysRevLett.89.101101

363. G. Barnich, G. Compere, J. Math. Phys. **49**, 042901 (2008). https://doi.org/10.1063/1.2889721
364. D. Sudarsky, R.M. Wald, Phys. Rev. D **46**, 1453 (1992). https://doi.org/10.1103/PhysRevD.46.1453
365. D. Sudarsky, R.M. Wald, Phys. Rev. D **47**, R5209 (1993). https://doi.org/10.1103/PhysRevD.47.R5209
366. S. McCormick, Adv. Theor. Math. Phys. **18**(4), 799 (2014). https://doi.org/10.4310/ATMP.2014.v18.n4.a2
367. K. Hajian, A. Seraj, M.M. Sheikh-Jabbari, JHEP **03**, 014 (2014). https://doi.org/10.1007/JHEP03(2014)014
368. K. Prabhu, Class. Quant. Grav. **34**(3), 035011 (2017). https://doi.org/10.1088/1361-6382/aa536b
369. Y. Foures-Bruhat, Acta Mat. **88**, 141 (1952). https://doi.org/10.1007/BF02392131
370. Y. Choquet-Bruhat, R.P. Geroch, Commun. Math. Phys. **14**, 329 (1969). https://doi.org/10.1007/BF01645389
371. O. Sarbach, M. Tiglio, Living Rev. Rel. **15**, 9 (2012). https://doi.org/10.12942/lrr-2012-9
372. B. Carter, Commun. Math. Phys. **10**(4), 280 (1968). https://doi.org/10.1007/BF03399503
373. V. Iyer, R.M. Wald, Phys. Rev. D **50**, 846 (1994)
374. R.M. Wald, Phys. Rev. D **48**, 3427 (1993)
375. K. Hajian, S. Liberati, M.M. Sheikh-Jabbari, M.H. Vahidinia, Phys. Lett. B **812**, 136002 (2021). https://doi.org/10.1016/j.physletb.2020.136002
376. H. Adami, M.M. Sheikh-Jabbari, V. Taghiloo, H. Yavartanoo, C. Zwikel, JHEP **05**, 261 (2021). https://doi.org/10.1007/JHEP05(2021)261
377. K. Hajian, M.M. Sheikh-Jabbari, Phys. Rev. D **93**(4), 044074 (2016). https://doi.org/10.1103/PhysRevD.93.044074
378. G. Barnich, G. Compere, Phys. Rev. **D71**, 044016 (2005). https://doi.org/10.1103/PhysRevD.71.044016, https://doi.org/10.1103/PhysRevD.73.029904, https://doi.org/10.1103/PhysRevD.71.029904 [Erratum: Phys. Rev. **D73**, 029904 (2006)]
379. G.W. Gibbons, M.J. Perry, C.N. Pope, Class. Quant. Grav. **22**, 1503 (2005)
380. G. Compère, K. Hajian, A. Seraj, M.M. Sheikh-Jabbari, JHEP **10**, 093 (2015). https://doi.org/10.1007/JHEP10(2015)093. [JHEP 10, 093 (2015)]
381. S. Hawking, Phys. Rev. D **13**, 191 (1976). https://doi.org/10.1103/PhysRevD.13.191
382. A. Castro, M.J. Rodriguez, Phys. Rev. D **86**, 024008 (2012). https://doi.org/10.1103/PhysRevD.86.024008
383. L. Smarr, Phys. Rev. Lett. **30**, 71 (1973). https://doi.org/10.1103/PhysRevLett.30.71. [Erratum: Phys. Rev. Lett. 30, 521-521 (1973)]
384. J. Bekenstein, Lett. Nuovo Cim. **11**, 467 (1974)
385. J.D. Bekenstein, Phys. Rev. D **9**, 3292 (1974). https://doi.org/10.1103/PhysRevD.9.3292
386. A.C. Wall, JHEP **06**, 021 (2009). https://doi.org/10.1088/1126-6708/2009/06/021
387. A.C. Wall (2018)
388. S. Carlip, Int. J. Mod. Phys. D **23**, 1430023 (2014). https://doi.org/10.1142/S0218271814300237
389. W. Israel, Phys. Rev. Lett. **57**(4), 397 (1986). https://doi.org/10.1103/PhysRevLett.57.397
390. J.W. York Jr., Phys. Rev. D **33**, 2092 (1986)
391. C. Crnkovic, Class. Quant. Grav. **5**, 1557 (1988). https://doi.org/10.1088/0264-9381/5/12/008
392. A. Ashtekar, L. Bombelli, O. Reula (1990)
393. M. Henneaux, C. Teitelboim, *Quantization of Gauge Systems* (University Press, Princeton, USA, 1992), p.520
394. G. Barnich, F. Brandt, Nucl. Phys. B **633**, 3 (2002). https://doi.org/10.1016/S0550-3213(02)00251-1
395. A. Seraj, Conserved charges, surface degrees of freedom, and black hole entropy. Ph.D. thesis, IPM, Tehran (2016)
396. G. Compère, *Advanced Lectures on General Relativity*, vol. 952 (Springer, Cham, Switzerland, 2019). https://doi.org/10.1007/978-3-030-04260-8

397. A. Fiorucci, Leaky covariant phase spaces: theory and application to Λ-BMS symmetry. Ph.D. thesis, Brussels U., Intl. Solvay Inst., Brussels (2021)
398. T. Padmanabhan, Phys. Rept. **406**, 49 (2005)
399. H.W. Braden, J.D. Brown, B.F. Whiting, J.W. York Jr., Phys. Rev. D **42**, 3376 (1990). https://doi.org/10.1103/PhysRevD.42.3376
400. A.C. Wall, Phys. Rev. D **85**, 104049 (2012). https://doi.org/10.1103/PhysRevD.85.104049. [Erratum: Phys. Rev. D 87, 069904 (2013)]
401. W. Donnelly, A.C. Wall, Phys. Rev. D **86**, 064042 (2012). https://doi.org/10.1103/PhysRevD.86.064042
402. A.C. Wall, Int. J. Mod. Phys. D **24**(12), 1544014 (2015). https://doi.org/10.1142/S0218271815440149
403. T. Jacobson, Phys. Rev. Lett. **75**, 1260 (1995). https://doi.org/10.1103/PhysRevLett.75.1260
404. H. Adami, M.M. Sheikh-Jabbari, V. Taghiloo, H. Yavartanoo, Phys. Rev. D **105**(6), 066004 (2022). https://doi.org/10.1103/PhysRevD.105.066004
405. K. Hajian, A. Seraj, M.M. Sheikh-Jabbari, JHEP **10**, 111 (2014). https://doi.org/10.1007/JHEP10(2014)111
406. R. Olea, JHEP **06**, 023 (2005). https://doi.org/10.1088/1126-6708/2005/06/023
407. M. Cvetic, G.W. Gibbons, D. Kubiznak, C.N. Pope, Phys. Rev. D **84**, 024037 (2011). https://doi.org/10.1103/PhysRevD.84.024037
408. B.P. Dolan, Class. Quant. Grav. **28**, 235017 (2011). https://doi.org/10.1088/0264-9381/28/23/235017
409. D. Kubiznak, R.B. Mann, JHEP **07**, 033 (2012). https://doi.org/10.1007/JHEP07(2012)033
410. D. Chernyavsky, K. Hajian, Class. Quant. Grav. **35**(12), 125012 (2018). https://doi.org/10.1088/1361-6382/aac39a
411. K. Hajian, H. Özşahin, B. Tekin, Phys. Rev. D **104**(4), 044024 (2021). https://doi.org/10.1103/PhysRevD.104.044024
412. E. Witten, Phys. Rev. Lett. **38**, 121 (1977). https://doi.org/10.1103/PhysRevLett.38.121
413. L.P. Grishchuk, Y.V. Sidorov, Phys. Rev. D **42**, 3413 (1990). https://doi.org/10.1103/PhysRevD.42.3413
414. R. Kubo, J. Phys. Soc. Jap. **12**, 570 (1957). https://doi.org/10.1143/JPSJ.12.570
415. P.C. Martin, J.S. Schwinger, Phys. Rev. **115**, 1342 (1959). https://doi.org/10.1103/PhysRev.115.1342
416. Y.B. Zeldovich, A.A. Starobinsky, Zh. Eksp, Teor. Fiz. **61**, 2161 (1971)
417. S.W. Hawking, Commun. Math. Phys. **43**, 199 (1975). https://doi.org/10.1007/BF02345020. [Erratum: Commun. Math. Phys. 46, 206 (1976)]
418. J.S. Schwinger, Phys. Rev. **82**, 664 (1951). https://doi.org/10.1103/PhysRev.82.664
419. M.J. Perry (1978)
420. G.W. Gibbons, M.J. Perry, Proc. Roy. Soc. Lond. A **358**, 467 (1978). https://doi.org/10.1098/rspa.1978.0022
421. S.M. Christensen, S.A. Fulling, Phys. Rev. D **15**, 2088 (1977)
422. R.A. Bertlmann, *Anomalies in Quantum Field Theory* (Oxford University Press, 1996)
423. M.J. Duff, Class. Quant. Grav. **11**, 1387 (1994)
424. D. Grumiller, W. Kummer, D.V. Vassilevich, Phys. Rept. **369**, 327 (2002)
425. S.P. Robinson, F. Wilczek, Phys. Rev. Lett. **95**, 011303 (2005). https://doi.org/10.1103/PhysRevLett.95.011303
426. R.A. Konoplya, A. Zhidenko, A.F. Zinhailo, Class. Quant. Grav. **36**, 155002 (2019). https://doi.org/10.1088/1361-6382/ab2e25
427. J.M. Maldacena, A. Strominger, Phys. Rev. D **55**, 861 (1997). https://doi.org/10.1103/PhysRevD.55.861
428. J.A. Wheeler, *A Journey into Gravity and Spacetime* (Freeman, New York, USA, 1990) 257 p. (Scientific American library series, 31)
429. G.W. Gibbons, S.W. Hawking, Phys. Rev. D **15**, 2752 (1977)
430. A. Sen, JHEP **1304**, 156 (2013). https://doi.org/10.1007/JHEP04(2013)156

431. H. Casini, Class. Quant. Grav. **25**, 205021 (2008). https://doi.org/10.1088/0264-9381/25/20/205021
432. R. Bousso, JHEP **07**, 004 (1999). https://doi.org/10.1088/1126-6708/1999/07/004
433. R. Bousso, H. Casini, Z. Fisher, J. Maldacena, Phys. Rev. D **90**(4), 044002 (2014). https://doi.org/10.1103/PhysRevD.90.044002
434. M.K. Parikh, F. Wilczek, Phys. Rev. Lett. **85**, 5042 (2000)
435. M.K. Parikh, Gen. Rel. Grav. **36**, 2419 (2004). https://doi.org/10.1142/S0218271804006498
436. M.K. Parikh, in *10th Marcel Grossmann Meeting on Recent Developments in Theoretical and Experimental General Relativity, Gravitation and Relativistic Field Theories (MG X MMIII)* (2004), pp. 1585–1590. https://doi.org/10.1142/9789812704030_0155
437. P. Kraus, F. Wilczek, Nucl. Phys. B **433**, 403 (1995). https://doi.org/10.1016/0550-3213(94)00411-7
438. D.N. Page, Phys. Rev. D **13**, 198 (1976). https://doi.org/10.1103/PhysRevD.13.198
439. D.N. Page, Phys. Rev. D **14**, 3260 (1976). https://doi.org/10.1103/PhysRevD.14.3260
440. D.N. Page, Phys. Rev. D **16**, 2402 (1977). https://doi.org/10.1103/PhysRevD.16.2402
441. D.N. Page, S.W. Hawking, Astrophys. J. **206**, 1 (1976). https://doi.org/10.1086/154350
442. D.N. Page, New J. Phys. **7**, 203 (2005)
443. K.S. Thorne, R.H. Price, D.A. Macdonald, *Black Holes: The Membrane Paradigm* (Yale University Press, 1986)
444. L. Ciambelli, C. Marteau, A.C. Petkou, P.M. Petropoulos, K. Siampos, Class. Quant. Grav. **35**(16), 165001 (2018). https://doi.org/10.1088/1361-6382/aacf1a
445. L. Donnay, C. Marteau, Class. Quant. Grav. **36**(16), 165002 (2019). https://doi.org/10.1088/1361-6382/ab2fd5
446. S.D. Mathur, Gen. Rel. Grav. **42**, 2331 (2010). https://doi.org/10.1007/s10714-010-1022-4
447. G.W. Gibbons, S.W. Hawking (eds.), *Euclidean Quantum Gravity* (World Scientific, Singapore, 1993)
448. G.W. Gibbons, M.J. Perry, Phys. Rev. Lett. **36**, 985 (1976)
449. M. Srednicki, Phys. Rev. Lett. **71**, 666 (1993). https://doi.org/10.1103/PhysRevLett.71.666
450. J. Callan, G. Curtis, in *29th Rencontres de Moriond: Electroweak Interactions and Unified Theories* (1994), pp. 311–327
451. L. Ciambelli, C. Marteau, Class. Quant. Grav. **36**(8), 085004 (2019). https://doi.org/10.1088/1361-6382/ab0d37
452. A. Bagchi, A. Mehra, P. Nandi, JHEP **05**, 108 (2019). https://doi.org/10.1007/JHEP05(2019)108
453. M. Henneaux, P. Salgado-Rebolledo, JHEP **11**, 180 (2021). https://doi.org/10.1007/JHEP11(2021)180
454. W.G. Unruh, Phys. Rev. Lett. **46**, 1351 (1981)
455. A. Almheiri, T. Hartman, J. Maldacena, E. Shaghoulian, A. Tajdini, Rev. Mod. Phys. **93**(3), 035002 (2021). https://doi.org/10.1103/RevModPhys.93.035002
456. C.R. Stephens, G. 't Hooft, B.F. Whiting, Class. Quant. Grav. **11**, 621 (1994)
457. P. Hayden, J. Preskill, JHEP **09**, 120 (2007). https://doi.org/10.1088/1126-6708/2007/09/120
458. S.D. Mathur, Class. Quant. Grav. **26**, 224001 (2009). https://doi.org/10.1088/0264-9381/26/22/224001
459. V. Mukhanov, S. Winitzki, *Introduction to Quantum Effects in Gravity* (Cambridge University Press, 2007)
460. N.D. Birrell, P.C.W. Davies, (University Press. Cambridge, UK **1982**, 340p (1989)
461. K. Parattu, S. Chakraborty, B.R. Majhi, T. Padmanabhan, Gen. Rel. Grav. **48**(7), 94 (2016). https://doi.org/10.1007/s10714-016-2093-7
462. K. Parattu, S. Chakraborty, T. Padmanabhan, Eur. Phys. J. C **76**(3), 129 (2016). https://doi.org/10.1140/epjc/s10052-016-3979-y
463. D. Lovelock, J. Math. Phys. **13**, 874 (1972). https://doi.org/10.1063/1.1666069
464. R.C. Myers, Phys. Rev. D **36**, 392 (1987)
465. S. Chakraborty, N. Dadhich, JHEP **12**, 003 (2015). https://doi.org/10.1007/JHEP12(2015)003

466. M. Madsen, J.D. Barrow, Nucl. Phys. B **323**, 242 (1989). https://doi.org/10.1016/0550-3213(89)90596-8
467. L. Fatibene, M. Ferraris, M. Francaviglia, Int. J. Geom. Meth. Mod. Phys. **2**, 373 (2005). https://doi.org/10.1142/S0219887805000557
468. A. Guarnizo, L. Castaneda, J.M. Tejeiro, Gen. Rel. Grav. **42**, 2713 (2010). https://doi.org/10.1007/s10714-010-1012-6
469. P. Kraus, F. Wilczek, Nucl. Phys. B **437**, 231 (1995). https://doi.org/10.1016/0550-3213(94)00588-6
470. J. Zhang, Z. Zhao, Phys. Lett. B **638**, 110 (2006). https://doi.org/10.1016/j.physletb.2006.05.059
471. S. Hemming, E. Keski-Vakkuri, Phys. Rev. D **64**, 044006 (2001). https://doi.org/10.1103/PhysRevD.64.044006
472. Q.Q. Jiang, S.Q. Wu, X. Cai, Phys. Rev. D **73**, 064003 (2006). https://doi.org/10.1103/PhysRevD.73.064003. [Erratum: Phys. Rev. D 73, 069902 (2006)]
473. K. Umetsu, Int. J. Mod. Phys. A **25**, 4123 (2010). https://doi.org/10.1142/S0217751X10050251
474. S. Carlip, Spontaneous Dimensional Reduction in Short-Distance Quantum Gravity? ed. by Kowalski-Glikman, Jerzy and R. Durka, and M. Szczachor, AIP Conf. Proc. **1196**(1), 72 (2009) https://doi.org/10.1063/1.3284402
475. S. Carlip, *Quantum Gravity in 2+1 Dimensions*. Cambridge Monographs on Mathematical Physics (Cambridge University Press, 2003). https://doi.org/10.1017/CBO9780511564192. http://www.cambridge.org/uk/catalogue/catalogue.asp?isbn=0521545889
476. M. Bañados, C. Teitelboim, J. Zanelli, Phys. Rev. Lett. **69**, 1849 (1992)
477. M. Bañados, M. Henneaux, C. Teitelboim, J. Zanelli, Phys. Rev. D **48**, 1506 (1993)
478. M. Bañados, ArXiv e-prints (1998)
479. M.M. Sheikh-Jabbari, H. Yavartanoo, Eur. Phys. J. C **76**(9), 493 (2016). https://doi.org/10.1140/epjc/s10052-016-4326-z
480. M.M. Sheikh-Jabbari, H. Yavartanoo, JHEP **07**, 104 (2014). https://doi.org/10.1007/JHEP07(2014)104
481. A. Achucarro, P.K. Townsend, Phys. Lett. B **180**, 89 (1986). https://doi.org/10.1016/0370-2693(86)90140-1
482. E. Witten, Nucl. Phys. B **311**, 46 (1988). https://doi.org/10.1016/0550-3213(88)90143-5
483. J.D. Brown, M. Henneaux, Commun. Math. Phys. **104**, 207 (1986)
484. G. Compère, W. Song, A. Strominger, JHEP **1305**, 152 (2013). https://doi.org/10.1007/JHEP05(2013)152
485. C. Troessaert, JHEP **08**, 044 (2013). https://doi.org/10.1007/JHEP08(2013)044
486. S.G. Avery, R.R. Poojary, N.V. Suryanarayana, JHEP **01**, 144 (2014). https://doi.org/10.1007/JHEP01(2014)144
487. D. Grumiller, M. Riegler, JHEP **10**, 023 (2016). https://doi.org/10.1007/JHEP10(2016)023
488. A. Pérez, D. Tempo, R. Troncoso, JHEP **06**, 103 (2016). https://doi.org/10.1007/JHEP06(2016)103
489. D. Grumiller, W. Merbis, SciPost Phys. **8**(1), 010 (2020). https://doi.org/10.21468/SciPostPhys.8.1.010
490. L. Cornalba, M.S. Costa, Phys. Rev. D **66**, 066001 (2002). https://doi.org/10.1103/PhysRevD.66.066001
491. A. Ashtekar, J. Bicak, B.G. Schmidt, Phys. Rev. D **55**, 669 (1997). https://doi.org/10.1103/PhysRevD.55.669
492. G. Barnich, G. Compere, Class. Quant. Grav. **24**, F15 (2007). https://doi.org/10.1088/0264-9381/24/5/F01, https://doi.org/10.1088/0264-9381/24/11/C01
493. A. Castro, N. Lashkari, A. Maloney, Phys. Rev. D **83**, 124027 (2011). https://doi.org/10.1103/PhysRevD.83.124027
494. H. Afshar, B. Cvetkovic, S. Ertl, D. Grumiller, N. Johansson, Phys. Rev. D **85**, 064033 (2012)
495. S. Deser, R. Jackiw, S. Templeton, Phys. Rev. Lett. **48**, 975 (1982). https://doi.org/10.1103/PhysRevLett.48.975

496. S. Deser, R. Jackiw, S. Templeton, Ann. Phys. **140**, 372 (1982)
497. D.D.K. Chow, C.N. Pope, E. Sezgin, Class. Quant. Grav. **27**, 105001 (2010)
498. S. Ertl, D. Grumiller, N. Johansson, Class. Quant. Grav. **27**, 225021 (2010). https://doi.org/10.1088/0264-9381/27/22/225021
499. K. Hinterbichler, Rev. Mod. Phys. **84**, 671 (2012). https://doi.org/10.1103/RevModPhys.84.671
500. M. Henneaux, S.J. Rey, JHEP **1012**, 007 (2010). https://doi.org/10.1007/JHEP12(2010)007
501. A. Campoleoni, S. Fredenhagen, S. Pfenninger, S. Theisen, JHEP **1011**, 007 (2010). https://doi.org/10.1007/JHEP11(2010)007
502. M.A. Vasiliev, Phys. Lett. B **243**, 378 (1990). https://doi.org/10.1016/0370-2693(90)91400-6
503. V. Didenko, E. Skvortsov (2014)
504. C. Teitelboim, Phys. Lett. B **126**, 41 (1983)
505. R. Jackiw, Nucl. Phys. B **252**, 343 (1985)
506. D. Birmingham, M. Blau, M. Rakowski, G. Thompson, Phys. Rept. **209**, 129 (1991)
507. A.H. Chamseddine, D. Wyler, Phys. Lett. B **228**, 75 (1989)
508. N. Ikeda, K.I. Izawa, Prog. Theor. Phys. **90**, 237 (1993)
509. N. Ikeda, Ann. Phys. **235**, 435 (1994). https://doi.org/10.1006/aphy.1994.1104
510. P. Schaller, T. Strobl, Mod. Phys. Lett. A **9**, 3129 (1994)
511. T. Klösch, T. Strobl, Class. Quant. Grav. **13**, 965 (1996)
512. T. Klösch, T. Strobl, Class. Quant. Grav. **14**, 1689 (1997)
513. D. Grumiller, R. Ruzziconi, C. Zwikel, SciPost Phys. **12**, 032 (2022). https://doi.org/10.21468/SciPostPhys.12.1.032
514. T. Kaluza, Sitzungsberichte der Königlich Preußischen Akademie der Wissenschaften (Berlin), Seite p. 966-972, pp. 966–972 (1921)
515. O. Klein, Zeitschrift fur Physik **37**, 895 (1926). https://doi.org/10.1007/BF01397481
516. O. Klein, Nature **118**, 516 (1926). https://doi.org/10.1038/118516a0
517. J. Polchinski, *String Theory. Vol. 1: An Introduction to the Bosonic String*. Cambridge Monographs on Mathematical Physics (Cambridge University Press, 2007). https://doi.org/10.1017/CBO9780511816079
518. J. Polchinski, *String Theory. Vol. 2: Superstring Theory and Beyond*. Cambridge Monographs on Mathematical Physics (Cambridge University Press, 2007). https://doi.org/10.1017/CBO9780511618123
519. K. Becker, M. Becker, J.H. Schwarz, *String Theory and M-Theory: A Modern Introduction* (Cambridge University Press, 2006)
520. A. Salam, E. Sezgin (eds.), *Supergravities in Diverse Dimensions* (World Scientific, Singapore, 1989). https://doi.org/10.1142/0277. http://www.worldscientific.com/worldscibooks/10.1142/0277
521. T. Ortin, *Gravity and Strings*. Cambridge Monographs on Mathematical Physics (Cambridge University Press, 2015). https://doi.org/10.1017/CBO9781139019750. http://www.cambridge.org/mw/academic/subjects/physics/theoretical-physics-and-mathematical-physics/gravity-and-strings-2nd-edition
522. D.Z. Freedman, A. Van Proeyen, *Supergravity* (Cambridge University Press, Cambridge, UK, 2012). http://www.cambridge.org/mw/academic/subjects/physics/theoretical-physics-and-mathematical-physics/supergravity?format=AR
523. R.C. Myers, M.J. Perry, Ann. Phys. **172**, 304 (1986). https://doi.org/10.1016/0003-4916(86)90186-7
524. R.C. Myers, in *Black Holes in Higher Dimensions*, ed. by G.T. Horowitz (Cambridge University Press, 2012), pp. 101–133
525. M. Johnstone, M.M. Sheikh-Jabbari, J. Simon, H. Yavartanoo, JHEP **04**, 045 (2013). https://doi.org/10.1007/JHEP04(2013)045
526. S. Sadeghian, M.M. Sheikh-Jabbari, M.H. Vahidinia, H. Yavartanoo, Nucl. Phys. B **900**, 222 (2015). https://doi.org/10.1016/j.nuclphysb.2015.09.010
527. A.A. Pomeransky, R.A. Sen'kov (2006)

528. G.T. Horowitz, R.C. Myers, Phys. Rev. D **59**, 026005 (1998). https://doi.org/10.1103/PhysRevD.59.026005
529. G.T. Horowitz, A. Strominger, Nucl. Phys. B **360**, 197 (1991). https://doi.org/10.1016/0550-3213(91)90440-9
530. M.J. Duff, J.X. Lu, Nucl. Phys. B **416**, 301 (1994). https://doi.org/10.1016/0550-3213(94)90586-X
531. M.J. Duff, R.R. Khuri, J.X. Lu, Phys. Rept. **259**, 213 (1995). https://doi.org/10.1016/0370-1573(95)00002-X
532. R. Emparan, R. Suzuki, K. Tanabe, JHEP **06**, 009 (2013). https://doi.org/10.1007/JHEP06(2013)009
533. R. Emparan, C.P. Herzog, Rev. Mod. Phys. **92**(4), 045005 (2020). https://doi.org/10.1103/RevModPhys.92.045005
534. J. Brown, *Lower Dimensional Gravity* (World Scientific, 1988)
535. A. García-Díaz, *Exact Solutions in Three-Dimensional Gravity*. Cambridge Monographs on Mathematical Physics (Cambridge University Press, 2017). https://books.google.com/books?id=vkI4DwAAQBAJ
536. P.H. Ginsparg, G.W. Moore, in *Theoretical Advanced Study Institute (TASI 92): From Black Holes and Strings to Particles* (1993), pp. 277–469
537. D. Grumiller, R. Meyer, Turk. J. Phys. **30**, 349 (2006)
538. D. Grumiller, R. McNees, JHEP **04**, 074 (2007)
539. S. Carlip, Class. Quant. Grav. **12**, 2853 (1995)
540. G. Compère, A. Fiorucci (2018)
541. G. Horowitz, *Black Holes in Higher Dimensions* (Cambridge University Press, 2012). https://books.google.com/books?id=12eGVHojt2UC
542. E. Witten, Phys. Rev. D **44**, 314 (1991)
543. A.W. Peet, in *Theoretical Advanced Study Institute in Elementary Particle Physics (TASI 99): Strings, Branes, and Gravity* (2000), pp. 353–433. https://doi.org/10.1142/9789812799630_0003
544. R. Gregory, R. Laflamme, Phys. Rev. Lett. **70**, 2837 (1993). https://doi.org/10.1103/PhysRevLett.70.2837
545. R. Gregory, R. Laflamme, Nucl. Phys. B **428**, 399 (1994). https://doi.org/10.1016/0550-3213(94)90206-2
546. R. Emparan, D. Grumiller, K. Tanabe, Phys. Rev. Lett. **110**, 251102 (2013). https://doi.org/10.1103/PhysRevLett.110.251102
547. M. Ammon, J. Erdmenger, *Gauge/Gravity Duality* (Cambridge University Press, Cambridge, 2015). http://www.cambridge.org/de/academic/subjects/physics/theoretical-physics-and-mathematical-physics/gaugegravity-duality-foundations-and-applications
548. I. Klebanov, A. Polyakov, Phys. Lett. B **550**, 213 (2002). https://doi.org/10.1016/S0370-2693(02)02980-5
549. E. Sezgin, P. Sundell, Nucl. Phys. B **644**, 303 (2002). https://doi.org/10.1016/S0550-3213(02)00739-3, https://doi.org/10.1016/S0550-3213(02)00739-3
550. L. Susskind, E. Witten (1998)
551. R. Emparan, C.V. Johnson, R.C. Myers, Phys. Rev. D **60**, 104001 (1999)
552. S. de Haro, S.N. Solodukhin, K. Skenderis, Commun. Math. Phys. **217**, 595 (2001). https://doi.org/10.1007/s002200100381
553. K. Skenderis, Class. Quant. Grav. **19**, 5849 (2002)
554. O. Aharony, S.S. Gubser, J.M. Maldacena, H. Ooguri, Y. Oz, Phys. Rept. **323**, 183 (2000)
555. M. Bianchi, Nucl. Phys. Proc. Suppl. **102**, 56 (2001). https://doi.org/10.1016/S0920-5632(01)01536-5. [56 (2000)]
556. H. Liu, A.A. Tseytlin, Nucl. Phys. B **533**, 88 (1998). https://doi.org/10.1016/S0550-3213(98)00443-X
557. G. Arutyunov, S. Frolov, Phys. Rev. D **60**, 026004 (1999). https://doi.org/10.1103/PhysRevD.60.026004

558. A. Bagchi, D. Grumiller, W. Merbis, Phys. Rev. D **93**(6), 061502 (2016). https://doi.org/10.1103/PhysRevD.93.061502
559. A. Belavin, A.M. Polyakov, A. Zamolodchikov, Nucl. Phys. B **241**, 333 (1984). https://doi.org/10.1016/0550-3213(84)90052-X
560. S. Ryu, T. Takayanagi, Phys. Rev. Lett. **96**, 181602 (2006). https://doi.org/10.1103/PhysRevLett.96.181602
561. M.B. Plenio, S. Virmani, Quant. Inf. Comput. **7**, 1 (2007)
562. P. Calabrese, J.L. Cardy, J. Stat. Mech. **0406**, P06002 (2004). https://doi.org/10.1088/1742-5468/2004/06/P06002
563. V.E. Hubeny, M. Rangamani, T. Takayanagi, JHEP **0707**, 062 (2007). https://doi.org/10.1088/1126-6708/2007/07/062
564. M. Headrick, T. Takayanagi, Phys. Rev. D **76**, 106013 (2007). https://doi.org/10.1103/PhysRevD.76.106013
565. H. Araki, E. Lieb, Commun. Math. Phys. **18**, 160 (1970). https://doi.org/10.1007/BF01646092
566. P. Calabrese, J. Cardy, J. Phys. A **42**, 504005 (2009). https://doi.org/10.1088/1751-8113/42/50/504005
567. H. Casini, M. Huerta, Phys. Lett. B **600**, 142 (2004). https://doi.org/10.1016/j.physletb.2004.08.072
568. H. Casini, M. Huerta, J. Phys. A **40**, 7031 (2007). https://doi.org/10.1088/1751-8113/40/25/S57
569. C. Ecker, D. Grumiller, W. van der Schee, M.M. Sheikh-Jabbari, P. Stanzer, SciPost Phys. **6**(3), 036 (2019). https://doi.org/10.21468/SciPostPhys.6.3.036
570. C. Ecker, D. Grumiller, H. Soltanpanahi, P. Stanzer, JHEP **03**, 213 (2021). https://doi.org/10.1007/JHEP03(2021)213
571. R. Bousso, Z. Fisher, S. Leichenauer, A.C. Wall, Phys. Rev. D **93**(6), 064044 (2016). https://doi.org/10.1103/PhysRevD.93.064044
572. R. Bousso, Z. Fisher, J. Koeller, S. Leichenauer, A.C. Wall, Phys. Rev. D **93**(2), 024017 (2016). https://doi.org/10.1103/PhysRevD.93.024017
573. J. Koeller, S. Leichenauer, Phys. Rev. D **94**(2), 024026 (2016). https://doi.org/10.1103/PhysRevD.94.024026
574. S. Balakrishnan, T. Faulkner, Z.U. Khandker, H. Wang, JHEP **09**, 020 (2019). https://doi.org/10.1007/JHEP09(2019)020
575. F. Ceyhan, T. Faulkner, Commun. Math. Phys. **377**(2), 999 (2020). https://doi.org/10.1007/s00220-020-03751-y
576. T. Faulkner, A. Lewkowycz, J. Maldacena, JHEP **11**, 074 (2013). https://doi.org/10.1007/JHEP11(2013)074
577. N. Engelhardt, A.C. Wall, JHEP **01**, 073 (2015). https://doi.org/10.1007/JHEP01(2015)073
578. S.W. Hawking, D.N. Page, Commun. Math. Phys. **87**, 577 (1983)
579. E. Witten, Adv. Theor. Math. Phys. **2**, 505 (1998)
580. J.M. Maldacena, JHEP **04**, 021 (2003). https://doi.org/10.1088/1126-6708/2003/04/021
581. Y. Takahashi, H. Umezawa, Int. J. Mod. Phys. B **10**, 1755 (1996). https://doi.org/10.1142/S0217979296000817
582. J. Maldacena, L. Susskind, Fortsch. Phys. **61**, 781 (2013). https://doi.org/10.1002/prop.201300020
583. L. Donnay, G. Giribet, H.A. Gonzalez, M. Pino, Phys. Rev. Lett. **116**(9), 091101 (2016). https://doi.org/10.1103/PhysRevLett.116.091101
584. H. Afshar, S. Detournay, D. Grumiller, W. Merbis, A. Perez, D. Tempo, R. Troncoso, Phys. Rev. D **93**(10), 101503 (2016). https://doi.org/10.1103/PhysRevD.93.101503
585. H. Afshar, D. Grumiller, W. Merbis, A. Perez, D. Tempo, R. Troncoso, Phys. Rev. D **95**(10), 106005 (2017). https://doi.org/10.1103/PhysRevD.95.106005
586. H.K. Kunduri, J. Lucietti, H.S. Reall, Class. Quant. Grav. **24**, 4169 (2007). https://doi.org/10.1088/0264-9381/24/16/012
587. P. Figueras, H.K. Kunduri, J. Lucietti, M. Rangamani, Phys. Rev. D **78**, 044042 (2008). https://doi.org/10.1103/PhysRevD.78.044042

588. P. Figueras, J. Lucietti, Class. Quant. Grav. **27**, 095001 (2010). https://doi.org/10.1088/0264-9381/27/9/095001
589. H.K. Kunduri, J. Lucietti, Living Rev. Rel. **16**, 8 (2013). https://doi.org/10.12942/lrr-2013-8
590. S. Hollands, A. Ishibashi, R.M. Wald, Commun. Math. Phys. **271**, 699 (2007). https://doi.org/10.1007/s00220-007-0216-4
591. S. Hollands, A. Ishibashi, Commun. Math. Phys. **291**, 403 (2009). https://doi.org/10.1007/s00220-009-0841-1
592. S. Hollands, A. Ishibashi, Ann. Henri Poincare **10**, 1537 (2010). https://doi.org/10.1007/s00023-010-0022-y
593. A.J. Amsel, G.T. Horowitz, D. Marolf, M.M. Roberts, JHEP **0909**, 044 (2009). https://doi.org/10.1088/1126-6708/2009/09/044
594. S. Aretakis, Commun. Math. Phys. **307**, 17 (2011). https://doi.org/10.1007/s00220-011-1254-5
595. S. Aretakis, Adv. Theor. Math. Phys. **19**, 507 (2015). https://doi.org/10.4310/ATMP.2015.v19.n3.a1
596. S. Hollands, A. Ishibashi, Commun. Math. Phys. **339**(3), 949 (2015). https://doi.org/10.1007/s00220-015-2410-0
597. J. Lucietti, K. Murata, H.S. Reall, N. Tanahashi, JHEP **03**, 035 (2013). https://doi.org/10.1007/JHEP03(2013)035
598. J. Lucietti, H.S. Reall, Phys. Rev. D **86**, 104030 (2012). https://doi.org/10.1103/PhysRevD.86.104030
599. D. Astefanesei, K. Goldstein, S. Mahapatra, Gen. Rel. Grav. **40**, 2069 (2008). https://doi.org/10.1007/s10714-008-0616-6
600. D. Astefanesei, R.B. Mann, M.J. Rodriguez, C. Stelea, Class. Quant. Grav. **27**, 165004 (2010). https://doi.org/10.1088/0264-9381/27/16/165004
601. K. Hajian, M.M. Sheikh-Jabbari, Phys. Lett. B **768**, 228 (2017). https://doi.org/10.1016/j.physletb.2017.02.063
602. A. Sen, JHEP **09**, 038 (2005)
603. A. Dabholkar, A. Sen, S.P. Trivedi, JHEP **01**, 096 (2007). https://doi.org/10.1088/1126-6708/2007/01/096
604. K. Goldstein, N. Iizuka, R.P. Jena, S.P. Trivedi, Phys. Rev. D **72**, 124021 (2005). https://doi.org/10.1103/PhysRevD.72.124021
605. D. Astefanesei, K. Goldstein, R.P. Jena, A. Sen, S.P. Trivedi, JHEP **10**, 058 (2006). https://doi.org/10.1088/1126-6708/2006/10/058
606. A. Sen, Gen. Rel. Grav. **40**, 2249 (2008). https://doi.org/10.1007/s10714-008-0626-4
607. J.M. Maldacena, J. Michelson, A. Strominger, JHEP **02**, 011 (1999)
608. G. Compère, K. Hajian, A. Seraj, M.M. Sheikh-Jabbari, Phys. Lett. B **749**, 443 (2015). https://doi.org/10.1016/j.physletb.2015.08.027. [Phys. Lett. B 749, 443 (2015)]
609. V. Balasubramanian, J. de Boer, M.M. Sheikh-Jabbari, J. Simón, JHEP **02**, 017 (2010). https://doi.org/10.1007/JHEP02(2010)017
610. G. Compère, Living Rev. Rel. **15**, 11 (2012)
611. P. Breitenlohner, D.Z. Freedman, Ann. Phys. **144**, 249 (1982). https://doi.org/10.1016/0003-4916(82)90116-6
612. E. Kiritsis, *String Theory in a Nutshell* (Princeton University Press, 2007)
613. G. Policastro, D. Son, A. Starinets, Phys. Rev. Lett. **87**, 081601 (2001). https://doi.org/10.1103/PhysRevLett.87.081601
614. P. Kovtun, D.T. Son, A.O. Starinets, Phys. Rev. Lett. **94**, 111601 (2005)
615. P. Romatschke, U. Romatschke, Phys. Rev. Lett. **99**, 172301 (2007). https://doi.org/10.1103/PhysRevLett.99.172301
616. D.T. Son, Phys. Rev. D **78**, 046003 (2008). https://doi.org/10.1103/PhysRevD.78.046003
617. K. Balasubramanian, J. McGreevy, Phys. Rev. Lett. **101**, 061601 (2008). https://doi.org/10.1103/PhysRevLett.101.061601
618. S.S. Gubser (2008)

619. S.A. Hartnoll, C.P. Herzog, G.T. Horowitz, Phys. Rev. Lett. **101**, 031601 (2008). https://doi.org/10.1103/PhysRevLett.101.031601
620. S. Kachru, X. Liu, M. Mulligan, Phys. Rev. D **78**, 106005 (2008). https://doi.org/10.1103/PhysRevD.78.106005
621. S. Sachdev, Phys. Rev. X **5**(4), 041025 (2015). https://doi.org/10.1103/PhysRevX.5.041025
622. I.R. Klebanov, in *Theoretical Advanced Study Institute in Elementary Particle Physics (TASI 99): Strings, Branes, and Gravity* (2000), pp. 615–650. https://doi.org/10.1142/9789812799630_0007
623. E. D'Hoker, D.Z. Freedman, in Theoretical Advanced Study Institute in Elementary Particle Physics (TASI, Strings, Branes and EXTRA. Dimensions **2002**, 3–158 (2001)
624. I. Papadimitriou, K. Skenderis, I.R.M.A. Lect, Math. Theor. Phys. **8**, 73 (2005). https://doi.org/10.4171/013-1/4
625. N. Beisert, C. Ahn, L.F. Alday, Z. Bajnok, J.M. Drummond et al., Lett. Math. Phys. **99**, 3 (2012). https://doi.org/10.1007/s11005-011-0529-2
626. S. Leutheusser, H. Liu (2021)
627. S. Leutheusser, H. Liu (2021)
628. M. Van Raamsdonk, Gen. Rel. Grav. **42**, 2323 (2010). https://doi.org/10.1142/S0218271810018529
629. T. Hartman, *Lectures on Quantum Gravity and Black Holes* (2015). Lecture notes available at http://www.hartmanhep.net/topics2015/gravity-lectures.pdf
630. L. Susskind, SpringerBriefs in Physics (Springer, 2018). https://doi.org/10.1007/978-3-030-45109-7
631. S. Hartnoll, S. Sachdev, T. Takayanagi, X. Chen, E. Silverstein, J. Sonner, Nature Rev. Phys. **3**(6), 391 (2021). https://doi.org/10.1038/s42254-021-00319-0
632. R. Baier, P. Romatschke, D.T. Son, A.O. Starinets, M.A. Stephanov, JHEP **04**, 100 (2008). https://doi.org/10.1088/1126-6708/2008/04/100
633. J. McGreevy (2009)
634. S. Sachdev, Lect. Notes Phys. **828**, 273 (2011). https://doi.org/10.1007/978-3-642-04864-7_9
635. C. Charmousis, B. Gouteraux, B.S. Kim, E. Kiritsis, R. Meyer, JHEP **11**, 151 (2010). https://doi.org/10.1007/JHEP11(2010)151
636. J. Casalderrey-Solana, H. Liu, D. Mateos, K. Rajagopal, U.A. Wiedemann, *Gauge/String Duality, Hot QCD and Heavy Ion Collisions* (Cambridge University Press, 2014). https://doi.org/10.1017/CBO9781139136747
637. M. Johnstone, M.M. Sheikh-Jabbari, J. Simon, H. Yavartanoo, Phys. Rev. D **88**(10), 101503 (2013). https://doi.org/10.1103/PhysRevD.88.101503
638. K. Godel, Rev. Mod. Phys. **21**, 447 (1949). https://doi.org/10.1103/RevModPhys.21.447
639. S. Hawking, Phys. Rev. D **46**, 603 (1992). https://doi.org/10.1103/PhysRevD.46.603
640. K.A. Khan, R. Penrose, Nature **229**, 185 (1971). https://doi.org/10.1038/229185a0
641. T. Dray, G. 't Hooft, Nucl. Phys. **B253**, 173 (1985)
642. G. Amelino-Camelia, J.R. Ellis, N.E. Mavromatos, D.V. Nanopoulos, S. Sarkar, Nature **393**, 763 (1998). https://doi.org/10.1038/31647
643. D. Mattingly, Living Rev. Rel. **8**, 5 (2005)
644. G. Veneziano, Nuovo Cim. A **57**, 190 (1968). https://doi.org/10.1007/BF02824451
645. D.J. Gross, P.F. Mende, Phys. Lett. B **197**, 129 (1987). https://doi.org/10.1016/0370-2693(87)90355-8
646. R. Bousso, Rev. Mod. Phys. **74**, 825 (2002). https://doi.org/10.1103/RevModPhys.74.825
647. W.G. Unruh, R.M. Wald, Rept. Prog. Phys. **80**(9), 092002 (2017). https://doi.org/10.1088/1361-6633/aa778e
648. D. Harlow, H. Ooguri, Phys. Rev. Lett. **122**(19), 191601 (2019). https://doi.org/10.1103/PhysRevLett.122.191601
649. S.B. Giddings, Phys. Rev. D **49**, 4078 (1994). https://doi.org/10.1103/PhysRevD.49.4078
650. Y. Sekino, L. Susskind, JHEP **10**, 065 (2008). https://doi.org/10.1088/1126-6708/2008/10/065

651. N. Lashkari, D. Stanford, M. Hastings, T. Osborne, P. Hayden, JHEP **04**, 022 (2013). https://doi.org/10.1007/JHEP04(2013)022
652. S.H. Shenker, D. Stanford, JHEP **03**, 067 (2014). https://doi.org/10.1007/JHEP03(2014)067
653. J. Maldacena, S.H. Shenker, D. Stanford, JHEP **08**, 106 (2016). https://doi.org/10.1007/JHEP08(2016)106
654. S.D. Mathur, Fortsch. Phys. **53**, 793 (2005). https://doi.org/10.1002/prop.200410203
655. S. Banerjee, J.W. Bryan, K. Papadodimas, S. Raju, JHEP **05**, 004 (2016). https://doi.org/10.1007/JHEP05(2016)004
656. D.N. Page, Phys. Rev. Lett. **71**, 3743 (1993). https://doi.org/10.1103/PhysRevLett.71.3743
657. G. Penington, JHEP **09**, 002 (2020). https://doi.org/10.1007/JHEP09(2020)002
658. A. Almheiri, N. Engelhardt, D. Marolf, H. Maxfield, JHEP **12**, 063 (2019). https://doi.org/10.1007/JHEP12(2019)063
659. A. Almheiri, R. Mahajan, J. Maldacena, Y. Zhao, JHEP **03**, 149 (2020). https://doi.org/10.1007/JHEP03(2020)149
660. M.B. Green, J.H. Schwarz, E. Witten, *Superstring Theory. Vol. 2: Loop Amplitudes, Anomalies and Phenomenology*. Cambridge Monographs on Mathematical Physics (Cambridge University Press, Cambridge, UK, 1987)
661. M.B. Green, J.H. Schwarz, E. Witten, *Superstring Theory* (Cambridge University Press, 1987). Vol. 1: Introduction
662. A. Salam, E. Sezgin (eds.), *Supergravities in Diverse Dimensions*, vol. 1, 2 (World Scientific, 1989)
663. O. Klein, Z. Phys. **37**, 895 (1926)
664. J. Polchinski, Phys. Rev. Lett. **75**, 4724 (1995). https://doi.org/10.1103/PhysRevLett.75.4724
665. G.T. Horowitz, J. Polchinski, Phys. Rev. D **55**, 6189 (1997). https://doi.org/10.1103/PhysRevD.55.6189
666. L. Susskind, ed. by C. Teitelboim, and J. Zanelli, Some speculations about black hole entropy in string theory, pp. 118–131 (1993)
667. Y. Chen, J. Maldacena, E. Witten (2021)
668. L. Susskind (2021)
669. L. Pieri, Black Holes in String Theory. Ph.D. thesis, Rome U., Tor Vergata (2019)
670. J.P. Gauntlett, R.C. Myers, P.K. Townsend, Class. Quant. Grav. **16**, 1 (1999). https://doi.org/10.1088/0264-9381/16/1/001
671. C. Herdeiro, Nucl. Phys. B **582**, 363 (2000). https://doi.org/10.1016/S0550-3213(00)00335-7
672. J. Breckenridge, R.C. Myers, A. Peet, C. Vafa, Phys. Lett. B **391**, 93 (1997). https://doi.org/10.1016/S0370-2693(96)01460-8
673. L. Dyson, JHEP **01**, 008 (2007). https://doi.org/10.1088/1126-6708/2007/01/008
674. J.L. Cardy, Nucl. Phys. B **270**, 186 (1986)
675. B. Mukhametzhanov, A. Zhiboedov, JHEP **10**, 261 (2019). https://doi.org/10.1007/JHEP10(2019)261
676. F. Loran, M. Sheikh-Jabbari, M. Vincon, JHEP **01**, 110 (2011). https://doi.org/10.1007/JHEP01(2011)110
677. A. Strominger, JHEP **02**, 009 (1998)
678. S. Carlip, C. Teitelboim, Phys. Rev. D **51**, 622 (1995). https://doi.org/10.1103/PhysRevD.51.622
679. S. Carlip, Class. Quant. Grav. **17**, 4175 (2000)
680. A. Sen, Gen. Rel. Grav. **44**(5), 1207 (2012). https://doi.org/10.1007/s10714-012-1336-5
681. A. Sen, Gen. Rel. Grav. **46**, 1711 (2014). https://doi.org/10.1007/s10714-014-1711-5
682. J.G. Russo, L. Susskind, Nucl. Phys. B **437**, 611 (1995). https://doi.org/10.1016/0550-3213(94)00532-J
683. N.P. Warner (2019)
684. B.D. Chowdhury, A. Virmani, in *5th Modave Summer School in Mathematical Physics* (2010)
685. I. Bena, N.P. Warner, Lect. Notes Phys. **755**, 1 (2008). https://doi.org/10.1007/978-3-540-79523-0_1

686. I. Kanitscheider, K. Skenderis, M. Taylor, JHEP **06**, 056 (2007). https://doi.org/10.1088/1126-6708/2007/06/056
687. K. Skenderis, M. Taylor, Phys. Rept. **467**, 117 (2008). https://doi.org/10.1016/j.physrep.2008.08.001
688. O. Lunin, S.D. Mathur, Nucl. Phys. B **623**, 342 (2002). https://doi.org/10.1016/S0550-3213(01)00620-4
689. V.S. Rychkov, JHEP **01**, 063 (2006). https://doi.org/10.1088/1126-6708/2006/01/063
690. S.W. Hawking, M.J. Perry, A. Strominger, JHEP **05**, 161 (2017). https://doi.org/10.1007/JHEP05(2017)161
691. M.M. Sheikh-Jabbari, Int. J. Mod. Phys. D **25**(12), 1644019 (2016). https://doi.org/10.1142/S0218271816440193
692. D. Grumiller, M.M. Sheikh-Jabbari, C. Zwikel, Int. J. Mod. Phys. D **29**(14), 2043006 (2020). https://doi.org/10.1142/S0218271820430063
693. H. Adami, D. Grumiller, M.M. Sheikh-Jabbari, V. Taghiloo, H. Yavartanoo, C. Zwikel, JHEP **11**, 155 (2021). https://doi.org/10.1007/JHEP11(2021)155
694. G. Barnich, Phys. Rev. D **99**(2), 026007 (2019). https://doi.org/10.1103/PhysRevD.99.026007
695. G. Barnich, M. Bonte (2019)
696. D. Tong (2016)
697. D. Grumiller, M. Sheikh-Jabbari, Int. J. Mod. Phys. D **27**(14), 1847006 (2018). https://doi.org/10.1142/S0218271818470065
698. H. Afshar, D. Grumiller, M.M. Sheikh-Jabbari, Phys. Rev. D **96**(8), 084032 (2017). https://doi.org/10.1103/PhysRevD.96.084032
699. H. Afshar, D. Grumiller, M.M. Sheikh-Jabbari, H. Yavartanoo, JHEP **08**, 087 (2017). https://doi.org/10.1007/JHEP08(2017)087
700. G. Hardy, S. Ramanujan, Proc. Lond. Math. Soc. **2**(XVII), 75 (1918)
701. K. Hajian, M. Sheikh-Jabbari, H. Yavartanoo, Phys. Rev. D **98**(2), 026025 (2018). https://doi.org/10.1103/PhysRevD.98.026025
702. D. Grumiller, W. Riedler, J. Rosseel, T. Zojer, J. Phys. A **46**, 494002 (2013). https://doi.org/10.1088/1751-8113/46/49/494002
703. C. Vafa (2014)
704. T. Anous, T. Hartman, A. Rovai, J. Sonner, JHEP **07**, 123 (2016). https://doi.org/10.1007/JHEP07(2016)123
705. C. Rovelli, Living Rev. Rel. **1**, 1 (1998). https://doi.org/10.12942/lrr-1998-1
706. T. Thiemann, Lect. Notes Phys. **631**, 41 (2003). https://doi.org/10.1007/978-3-540-45230-0_3
707. A. Ashtekar, Lect. Notes Phys. **863**, 31 (2013). https://doi.org/10.1007/978-3-642-33036-0_2
708. M. Niedermaier, M. Reuter, Living Rev. Rel. **9**, 5 (2006). https://doi.org/10.12942/lrr-2006-5
709. J. Ambjorn, Z. Drogosz, J. Gizbert-Studnicki, A. Görlich, J. Jurkiewicz, D. Nèmeth, Universe **7**(4), 79 (2021). https://doi.org/10.3390/universe7040079
710. S. Carlip, Rept. Prog. Phys. **64**, 885 (2001). https://doi.org/10.1088/0034-4885/64/8/301
711. S. Carlip, D.W. Chiou, W.T. Ni, R. Woodard, Int. J. Mod. Phys. D **24**(11), 1530028 (2015). https://doi.org/10.1142/S0218271815300281
712. S. Carlip, Class. Quant. Grav. **25**, 154010 (2008). https://doi.org/10.1088/0264-9381/25/15/154010
713. A. Dabholkar, Phys. Rev. Lett. **94**, 241301 (2005). https://doi.org/10.1103/PhysRevLett.94.241301
714. A. Sen, JHEP **03**, 008 (2006). https://doi.org/10.1088/1126-6708/2006/03/008
715. A. Sen, Gen. Rel. Grav. **44**(5), 1207 (2012). https://doi.org/10.1007/s10714-012-1336-5
716. R. Dijkgraaf, J.M. Maldacena, G.W. Moore, E.P. Verlinde (2000)
717. S.D. Mathur, D. Turton, JHEP **01**, 034 (2014). https://doi.org/10.1007/JHEP01(2014)034
718. S.G. Avery, B.D. Chowdhury, A. Puhm, JHEP **09**, 012 (2013). https://doi.org/10.1007/JHEP09(2013)012
719. S.D. Mathur, D. Turton, Nucl. Phys. B **884**, 566 (2014). https://doi.org/10.1016/j.nuclphysb.2014.05.012

720. R. Bousso, X. Dong, N. Engelhardt, T. Faulkner, T. Hartman, S.H. Shenker, D. Stanford (2022)
721. Z. Bern, J.J.M. Carrasco, H. Johansson, Phys. Rev. Lett. **105**, 061602 (2010). https://doi.org/10.1103/PhysRevLett.105.061602
722. R. Monteiro, D. O'Connell, C.D. White, JHEP **12**, 056 (2014). https://doi.org/10.1007/JHEP12(2014)056
723. J.M. Maldacena, A. Strominger, Phys. Rev. Lett. **77**, 428 (1996). https://doi.org/10.1103/PhysRevLett.77.428
724. C.V. Johnson, R.R. Khuri, R.C. Myers, Phys. Lett. B **378**, 78 (1996). https://doi.org/10.1016/0370-2693(96)00383-8
725. D. Newman, Michigan Math. J. **9**, 283 (1962). https://doi.org/10.1307/mmj/1028998729
726. D. Harlow, J.Q. Wu, JHEP **10**, 146 (2020). https://doi.org/10.1007/JHEP10(2020)146
727. M. Geiller, P. Jai-akson, JHEP **09**, 134 (2020). https://doi.org/10.1007/JHEP09(2020)134
728. G. Compère, A. Fiorucci, R. Ruzziconi, Class. Quant. Grav. **36**(19), 195017 (2019). https://doi.org/10.1088/1361-6382/ab3d4b. [Erratum: Class. Quant. Grav. 38, 229501 (2021)]
729. D. Grumiller, N. Johansson, JHEP **07**, 134 (2008). https://doi.org/10.1088/1126-6708/2008/07/134
730. A. Bagchi, S. Detournay, D. Grumiller, Phys. Rev. Lett. **109**, 151301 (2012). https://doi.org/10.1103/PhysRevLett.109.151301
731. A. Bagchi, R. Basu, A. Kakkar, A. Mehra, JHEP **12**, 147 (2016). https://doi.org/10.1007/JHEP12(2016)147
732. A. Strominger, A. Zhiboedov, JHEP **01**, 086 (2016). https://doi.org/10.1007/JHEP01(2016)086
733. S. Pasterski, Eur. Phys. J. C **81**(12), 1062 (2021). https://doi.org/10.1140/epjc/s10052-021-09846-7
734. L. Donnay, S. Pasterski, A. Puhm, JHEP **09**, 176 (2020). https://doi.org/10.1007/JHEP09(2020)176
735. F. Hopfmüller, L. Freidel, Phys. Rev. D **95**(10), 104006 (2017). https://doi.org/10.1103/PhysRevD.95.104006
736. V. Chandrasekaran, E.E. Flanagan, K. Prabhu, JHEP **11**, 125 (2018). https://doi.org/10.1007/JHEP11(2018)125
737. D. Grumiller, A. Pérez, M.M. Sheikh-Jabbari, R. Troncoso, C. Zwikel, Phys. Rev. Lett. **124**(4), 041601 (2020). https://doi.org/10.1103/PhysRevLett.124.041601
738. H. Adami, D. Grumiller, S. Sadeghian, M.M. Sheikh-Jabbari, C. Zwikel, JHEP **04**, 128 (2020). https://doi.org/10.1007/JHEP04(2020)128
739. H. Adami, M.M. Sheikh-Jabbari, V. Taghiloo, H. Yavartanoo, C. Zwikel, JHEP **10**, 107 (2020). https://doi.org/10.1007/JHEP10(2020)107
740. S. Haco, S.W. Hawking, M.J. Perry, A. Strominger, JHEP **12**, 098 (2018). https://doi.org/10.1007/JHEP12(2018)098
741. H. Geng, A. Karch, C. Perez-Pardavila, S. Raju, L. Randall, M. Riojas, S. Shashi (2021)
742. B. Guo, M.R.R. Hughes, S.D. Mathur, M. Mehta, Turk. J. Phys. **45**(6), 281 (2021). https://doi.org/10.3906/fiz-2111-13
743. A.E.H. Love, Nature **89**, 471 (1912). https://doi.org/10.1038/089471a0
744. T. Hinderer, Astrophys. J. **677**, 1216 (2008). https://doi.org/10.1086/533487
745. T. Damour, A. Nagar, Phys. Rev. D **80**, 084035 (2009). https://doi.org/10.1103/PhysRevD.80.084035
746. T. Damour, A. Nagar, L. Villain, Phys. Rev. D **85**, 123007 (2012). https://doi.org/10.1103/PhysRevD.85.123007
747. Z. Arzoumanian et al., Astrophys. J. Lett. **905**(2), L34 (2020). https://doi.org/10.3847/2041-8213/abd401
748. B.P. Abbott et al., Phys. Rev. Lett. **116**(13), 131102 (2016). https://doi.org/10.1103/PhysRevLett.116.131102
749. *Kamioka Gravitational-Wave Detector (KAGRA) Collaboration*. https://gwcenter.icrr.u-tokyo.ac.jp/en/

750. *The Laser Interferometer Space Antenna, LISA Mission*. https://sci.esa.int/web/lisa/-/61367-mission-summary
751. E. Berti, V. Cardoso, C.M. Will, Phys. Rev. D **73**, 064030 (2006). https://doi.org/10.1103/PhysRevD.73.064030
752. E. Barausse et al., Gen. Rel. Grav. **52**(8), 81 (2020). https://doi.org/10.1007/s10714-020-02691-1
753. J. Crowder, N.J. Cornish, Phys. Rev. D **72**, 083005 (2005). https://doi.org/10.1103/PhysRevD.72.083005
754. P. Amaro-Seoane et al., GW Notes **6**, 4 (2013)
755. C. Caprini et al., JCAP **04**, 001 (2016). https://doi.org/10.1088/1475-7516/2016/04/001
756. A. Klein et al., Phys. Rev. D **93**(2), 024003 (2016). https://doi.org/10.1103/PhysRevD.93.024003
757. *The extended Laser Interferometer Space Antenna, eLISA Mission*. https://www.elisascience.org/articles/elisa-mission/elisa-mission-gravitational-universe
758. V. Kalogera, et al. (2021)
759. R. Abbott et al., Phys. Rev. D **104**(2), 022005 (2021). https://doi.org/10.1103/PhysRevD.104.022005
760. B.P. Abbott et al., Living Rev. Rel. **21**(1), 3 (2018). https://doi.org/10.1007/s41114-020-00026-9
761. K.T. Voggel, A.C. Seth, H. Baumgardt, B. Husemann, N. Neumayer, M. Hilker, R. Pechetti, S. Mieske, A. Dumont, I. Georgiev, arXiv e-prints arXiv:2111.14854 (2021)
762. M. Favata, Class. Quant. Grav. **27**, 084036 (2010). https://doi.org/10.1088/0264-9381/27/8/084036
763. D. Pollney, C. Reisswig, Astrophys. J. Lett. **732**, L13 (2011). https://doi.org/10.1088/2041-8205/732/1/L13
764. M. Hübner, P. Lasky, E. Thrane, Phys. Rev. D **104**(2), 023004 (2021). https://doi.org/10.1103/PhysRevD.104.023004
765. P.D. Lasky, E. Thrane, Y. Levin, J. Blackman, Y. Chen, Phys. Rev. Lett. **117**(6), 061102 (2016). https://doi.org/10.1103/PhysRevLett.117.061102
766. E.E. Flanagan, A.M. Grant, A.I. Harte, D.A. Nichols, Phys. Rev. D **99**(8), 084044 (2019). https://doi.org/10.1103/PhysRevD.99.084044
767. B. Carr, K. Kohri, Y. Sendouda, J. Yokoyama, Rept. Prog. Phys. **84**(11), 116902 (2021). https://doi.org/10.1088/1361-6633/ac1e31
768. V. De Luca, G. Franciolini, P. Pani, A. Riotto, JCAP **06**, 044 (2020). https://doi.org/10.1088/1475-7516/2020/06/044
769. B. Carr, F. Kuhnel, in *Les Houches Summer School on Dark Matter* (2021)
770. R.A. Remillard, J.E. McClintock, Ann. Rev. Astron. Astrophys. **44**, 49 (2006). https://doi.org/10.1146/annurev.astro.44.051905.092532
771. J. García et al., Astrophys. J. **782**(2), 76 (2014). https://doi.org/10.1088/0004-637X/782/2/76
772. M.C. Miller, J.M. Miller, Phys. Rept. **548**, 1 (2014). https://doi.org/10.1016/j.physrep.2014.09.003
773. C. Bambi, Rev. Mod. Phys. **89**(2), 025001 (2017). https://doi.org/10.1103/RevModPhys.89.025001
774. C.S. Reynolds, Nature Astron. **3**(1), 41 (2019). https://doi.org/10.1038/s41550-018-0665-z
775. C. Bambi, PoS **MULTIF2019**, 028 (2020). https://doi.org/10.22323/1.362.0028
776. C. Bambi (2021). https://doi.org/10.1007/s40065-021-00336-y
777. A. Chael, M.D. Johnson, A. Lupsasca, Astrophys. J. **918**(1), 6 (2021). https://doi.org/10.3847/1538-4357/ac09ee
778. A. Chael, R. Narayan, M.D. Johnson, Mon. Not. Roy. Astron. Soc. **486**(2), 2873 (2019). https://doi.org/10.1093/mnras/stz988
779. K. Akiyama et al., Astrophys. J. Lett. **875**(1), L4 (2019). https://doi.org/10.3847/2041-8213/ab0e85
780. K. Akiyama et al., Astrophys. J. Lett. **875**(1), L5 (2019). https://doi.org/10.3847/2041-8213/ab0f43

781. F.W. Hehl, P. Von Der Heyde, G.D. Kerlick, J.M. Nester, Rev. Mod. Phys. **48**, 393 (1976)
782. I.L. Shapiro, Phys. Rept. **357**, 113 (2002). https://doi.org/10.1016/S0370-1573(01)00030-8
783. S.A. Teukolsky, Astrophys. J. **185**, 635 (1973). https://doi.org/10.1086/152444
784. R. Penrose, W. Rindler, *Spinors and Space-Time I* (Cambridge University Press, 1984)
785. R. Penrose, W. Rindler, *Spinors and Space-Time II* (Cambridge University Press, 1986)
786. G. Marcilhacy, Lett. Nuovo Cimento **37**, 300 (1983)
787. J. Blandin, R. Pons, G. Marcilhacy, Lett. Nuovo Cimento **38**, 561 (1983)
788. S. Mano, H. Suzuki, E. Takasugi, Prog. Theor. Phys. **95**, 1079 (1996). https://doi.org/10.1143/PTP.95.1079
789. I. Bredberg, C. Keeler, V. Lysov, A. Strominger, Nucl. Phys. B Proc. Suppl. **216**, 194 (2011). https://doi.org/10.1016/j.nuclphysbps.2011.04.155
790. M. Casals, A.C. Ottewill, Phys. Rev. D **71**, 064025 (2005). https://doi.org/10.1103/PhysRevD.71.064025
791. J. Lee, R.M. Wald, J. Math. Phys. **31**, 725 (1990). https://doi.org/10.1063/1.528801
792. A. Ashtekar, L. Bombelli, R. Koul, Lect. Notes Phys. **278**, 356 (1987). https://doi.org/10.1007/3-540-17894-5_378
793. R.M. Wald, A. Zoupas, Phys. Rev. D **61**, 084027 (2000). https://doi.org/10.1103/PhysRevD.61.084027
794. L.B. Szabados, Living Rev. Rel. **7**, 4 (2004). https://doi.org/10.12942/lrr-2004-4
795. G. Compère, Symmetries and conservation laws in Lagrangian gauge theories with applications to the mechanics of black holes and to gravity in three dimensions. Ph.D. thesis, Brussels U. (2007)
796. K. Hajian, On Thermodynamics and Phase Space of Near Horizon Extremal Geometries. Ph.D. thesis, Sharif U. of Tech. (2015)
797. G. Compere, D. Marolf, Class. Quant. Grav. **25**, 195014 (2008). https://doi.org/10.1088/0264-9381/25/19/195014
798. G. Compère, L. Donnay, P.H. Lambert, W. Schulgin, JHEP **03**, 158 (2015). https://doi.org/10.1007/JHEP03(2015)158
799. G. Compère, P. Mao, A. Seraj, M.M. Sheikh-Jabbari, JHEP **01**, 080 (2016). https://doi.org/10.1007/JHEP01(2016)080
800. M. Geiller, C. Goeller, C. Zwikel, JHEP **09**, 029 (2021). https://doi.org/10.1007/JHEP09(2021)029
801. L. Ciambelli, R.G. Leigh, P.C. Pai (2021)
802. M.K. Parikh, Membrane horizons: The Black hole's new clothes. Other thesis, Princeton University (1998)
803. M. Stix, *The Sun: An Introduction*. Astronomy and Astrophysics Library (Springer, Berlin, Heidelberg, 2012). https://books.google.com/books?id=9V7yCAAAQBAJ
804. P.N. Chen, M.T. Wang, Y.K. Wang, S.T. Yau (2021)
805. R. Javadinezhad, U. Kol, M. Porrati, JHEP **04**, 069 (2022). https://doi.org/10.1007/JHEP04(2022)069
806. G.V. Kraniotis, S.B. Whitehouse, Class. Quant. Grav. **20**, 4817 (2003). https://doi.org/10.1088/0264-9381/20/22/007
807. B. McInnes, JHEP **09**, 009 (2003). https://doi.org/10.1088/1126-6708/2003/09/009
808. Y.P. Wang, Class. Quant. Grav. **35**(21), 215007 (2018). https://doi.org/10.1088/1361-6382/aae256
809. E. Poisson, W. Israel, Phys. Rev. Lett. **63**, 1663 (1989). https://doi.org/10.1103/PhysRevLett.63.1663
810. S. Hod, Phys. Lett. B **718**, 1552 (2013). https://doi.org/10.1016/j.physletb.2012.12.047
811. A.V. Frolov, V.P. Frolov, Phys. Rev. D **90**(12), 124010 (2014). https://doi.org/10.1103/PhysRevD.90.124010
812. D.R. Brill, J. Louko, P. Peldan, Phys. Rev. D **56**, 3600 (1997). https://doi.org/10.1103/PhysRevD.56.3600
813. R.B. Mann, Ann. Israel Phys. Soc. **13**, 311 (1997)

814. D. Berenstein, Z. Li, J. Simon, Class. Quant. Grav. **38**(4), 045009 (2021). https://doi.org/10.1088/1361-6382/abcaeb
815. M. Gurses, G. Feza, J. Math. Phys. **16**, 2385 (1975). https://doi.org/10.1063/1.522480
816. C. McIntosh, in *Conference on Mathematical Relativity* (Australian National University, Mathematical Sciences Institute, 1989), pp. 201–206
817. G.W. Gibbons, H. Lu, D.N. Page, C.N. Pope, J. Geom. Phys. **53**, 49 (2005). https://doi.org/10.1016/j.geomphys.2004.05.001
818. A. Luna, R. Monteiro, I. Nicholson, D. O'Connell, Class. Quant. Grav. **36**, 065003 (2019). https://doi.org/10.1088/1361-6382/ab03e6
819. M.M. Sheikh-Jabbari, H. Yavartanoo, JHEP **10**, 013 (2011). https://doi.org/10.1007/JHEP10(2011)013
820. D. Grumiller, Quantum dilaton gravity in two dimensions with matter. Ph.D. thesis, Technische Universität Wien (2001)
821. M. Ansorg, J. Hennig, Phys. Rev. Lett. **102**, 221102 (2009). https://doi.org/10.1103/PhysRevLett.102.221102
822. M. Cvetic, G.W. Gibbons, C.N. Pope, Phys. Rev. Lett. **106**, 121301 (2011). https://doi.org/10.1103/PhysRevLett.106.121301
823. P. Pradhan, Phys. Lett. B **807**, 135521 (2020). https://doi.org/10.1016/j.physletb.2020.135521
824. A. Garcia, F.W. Hehl, C. Heinicke, A. Macias, Class. Quant. Grav. **21**, 1099 (2004). https://doi.org/10.1088/0264-9381/21/4/024
825. J.T. Wheeler, Gen. Rel. Grav. **50**(7), 80 (2018). https://doi.org/10.1007/s10714-018-2401-5
826. S. Deser, R. Jackiw, Commun. Math. Phys. **118**, 495 (1988)
827. S. Deser, B. Tekin, Class. Quant. Grav. **20**, L259 (2003)
828. D. Grumiller, N. Johansson, Int. J. Mod. Phys. D **17**, 2367 (2009). https://doi.org/10.1142/S0218271808014096
829. K. Jensen, Phys. Rev. Lett. **117**(11), 111601 (2016). https://doi.org/10.1103/PhysRevLett.117.111601
830. J. Engelsöy, T.G. Mertens, H. Verlinde, JHEP **07**, 139 (2016). https://doi.org/10.1007/JHEP07(2016)139
831. D. Grumiller, R. McNees, JHEP **01**, 112 (2021). https://doi.org/10.1007/JHEP01(2021)112
832. B.P. Singh, S.G. Ghosh, Ann. Phys. **395**, 127 (2018). https://doi.org/10.1016/j.aop.2018.05.010
833. M.M. Sheikh-Jabbari, H. Yavartanoo, Phys. Rev. D **94**(12), 126006 (2016). https://doi.org/10.1103/PhysRevD.94.126006
834. T. Padmanabhan, D. Kothawala, Phys. Rept. **531**, 115 (2013). https://doi.org/10.1016/j.physrep.2013.05.007